Illinois U Library

Transactions

of the

ASME

The Influence of Shape of Cross Section on the Flexural Fatigue Strength of Steel . . . *T. J. Dolan, J. H. McClow, and W. J. Craig* 469
Hide-Out of Sodium Phosphate in High-Pressure Boilers . . . *F. G. Straub* 479
Chemical Treatment, Demineralization, or Evaporation for Make-Up in High-Pressure By-Product Steam Plants . . . *J. D. Yoder, W. L. Webb, and T. Baumeister* 491
Sulphite and Silica in Boiler Water at Springdale . . . *L. E. Hankison and M. D. Baker* 505
An Automatic Degasser for Steam Sampling in Power Plants . . . *H. M. Rivers, W. H. Trautman, and G. W. Gibble* 511
The Quality of Steam Condensate as Related to Sodium Sulphite in the Boiler Water . . . *R. C. Alexander and J. K. Rummel* 519
Feedwater Treatment During Early Operation of Steam-Electric Stations . . . *R. C. Alexander and J. K. Rummel* 529
Allowable Eccentricity of Spherical Heads Convex to Pressure . . . *R. G. Sturm, L. W. Smith, and H. L. O'Brien* 533
Effect of Welding on Pressure-Vessel Steels . . . *A. F. Scotchbrook, L. Eriv, R. D. Stout, and B. G. Johnston* 539
Some Factors Influencing the Economics of Reheat Installations . . . *R. W. Hartwell and H. A. Wagner* 549
Selection of Steam Conditions for No. 4 Unit—Riverside Generating Station . . . *R. C. Dannettel and G. S. Harris* 557
A Comparison of Costs of Reheat Versus Nonreheat for 100-Mw Units . . . *R. P. Moore* 559
General Discussion of Reheat Papers . . . 561
Analysis of Experimental Data Regarding Certain Design Features of Pressure Vessels . . . *G. J. Schoessow and E. A. Brooks* 567
Experimental Technique in Pressure-Vessel Testing . . . *L. F. Kooistra and R. U. Blaser* 579
Effect of Pressure on the Combustion of Pulverized Coal . . . *T. T. Omori and A. A. Orning* 591
Continuous Gasification of Pulverized Coal With Oxygen and Steam by the Vortex Principle . . . *H. Perry, R. C. Corey, and M. A. Elliott* 599
The Gas-Turbine Regenerator—the Use of Compact Heat-Transfer Surfaces . . . *A. L. London and W. M. Kays* 611
A Perforated-Plate Heat Exchanger . . . *H. O. McMahon, R. J. Bowen, and G. A. Bleyle, Jr.* 623
Effect of Size on the Design and Performance of Internal-Combustion Engines . . . *C. F. Taylor* 633
Influence of Compressibility on Cylindrical Pitot-Tube Measurements . . . *L. W. Thrasher and R. C. Binder* 647
Determination of ASME Nozzle Coefficients for Variable Nozzle External Dimensions . . . *R. G. Folsom* 651
The Response of Thermocouples to Rapid Gas-Temperatures Changes . . . *M. W. Carbon, H. J. Kutsch, and G. A. Hawkins* 655
Crude-Oil Flow Characteristics Experienced in Large-Diameter Lines . . . *L. E. Anderson* 659
Surge Problems in Pipe Lines—Oil and Water . . . *S. L. Kerr* 667
Pressure Losses in Tubing, Pipe, and Fittings . . . *R. J. S. Pigott* 679
Attenuation of Oscillatory Pressures in Instrument Lines . . . *A. S. Iberall* 689
Long-Time Tension and Creep Tests of Plastics . *C. E. Staff, H. M. Quakenbos, Jr., and J. M. Hill* 697
Accelerated-Cavitation Research . . . *W. J. Rheingans* 705

JULY, 1950

VOL. 72, NO. 5

Transactions

of The American Society of Mechanical Engineers

Published on the tenth of every month, except March, June, September, and December

OFFICERS OF THE SOCIETY:

James D. Cunningham, *President*
Joseph L. Kopf, *Treasurer*
C. E. Davies, *Secretary*

COMMITTEE ON PUBLICATIONS:

Ronald B. Smith, *Chairman*
John Haydock
George R. Rich
C. B. Campbell
Paul T. Norton, Jr.
H. G. Wenig
D. R. Thomas } *Junior Advisory Members*
George A. Stetson, *Editor*
K. W. Clendinning, *Managing Editor*

REGIONAL ADVISORY BOARD OF THE PUBLICATIONS COMMITTEE

Kerr Atkinson—I
Otto de Lorenzi—II
W. E. Reaser—III
F. C. Smith—IV
Hendley Blackmon—V
R. E. Turner—VI
R. G. Roshong—VII
M. A. Durland—VIII

Published monthly by The American Society of Mechanical Engineers. Publication office at 20th and Northampton Streets, Easton, Pa. The editorial department is located at the headquarters of the Society, 29 West Thirty-Ninth Street, New York 18, N. Y. Cable address, "Dynamic," New York. Price $1.50 a copy, $12.00 a year for Transactions and the *Journal of Applied Mechanics;* to members and affiliates, $1.00 a copy, $6.00 a year. Changes of address must be received at Society headquarters three weeks before they are to be effective on the mailing list. Please send old as well as new address.... By-Law: The Society shall not be responsible for statements or opinions advanced in papers or ... printed in its publications (B13, Par. 4).... Entered as second-class matter March 2, 1928, at the Post Office at Easton, Pa., under the Act of August 24, 1912.... Copyrighted, 1950, by The American Society of Mechanical Engineers. Reprints from this publication may be made on condition that full credit be given the Transactions of the ASME and the author and that date of publication be stated.

The Influence of Shape of Cross Section on the Flexural Fatigue Strength of Steel

By T. J. DOLAN,[1] J. H. McCLOW,[2] and W. J. CRAIG,[3] URBANA, ILL.

It is not generally known or recognized that the flexural fatigue strength of a beam may be influenced to an appreciable extent by the shape of cross section of the member. In order to obtain further information on the magnitude of this shape effect, flexural fatigue tests were made employing four different shapes of cross section for each of two different steels. The results of these tests are compared and analyzed to clarify or explain some of the shape factors that may be of importance in affecting fatigue behavior. It is concluded that variations in residual stress or alterations of properties due to method of machining the different shapes play only a minor part in affecting the relative endurance limits. The susceptibility to localized inelastic action as governed by the shape of cross section and by the presence of "sore spots," such as outward projecting corners, are tentatively believed to be the primary elements leading to the differences noted in flexural fatigue strengths.

Introduction

A GREAT deal of data is available in the technical literature regarding the effects of the geometrical shape on the fatigue strength exhibited by a metal member. However, the shape factors usually considered by investigators are the abrupt changes of cross section which result in greatly reduced fatigue strengths due to the high localized stresses developed at a notch, fillet, hole, or other change of section. Very little attention has been paid to the possible manner in which the shape of cross section may influence the fatigue properties of a uniform beam.

In studying the effect of type of testing machine on fatigue test results, the ASTM Research Committee on Fatigue of Metals (1)[4] found that a distinct change in fatigue strength seemed to be produced by altering the shape of cross section of a test specimen. In vibratory bending fatigue tests "rectangular" specimens exhibited fatigue strengths as much as 16 per cent lower than the fatigue strength obtained for "round" specimens of the same metal. Furthermore, it has been observed that round specimens tested in vibratory bending developed endurance limits higher than did similar specimens in rotating-beam tests (2, 3).[5]

Based on computations of nominal stress by means of elementary elastic theory (using the flexure formula), there is little reason to suspect that the shape of cross section should have any influence on the fatigue strength of a member. However, materials subjected to repeated stressing do not behave in accordance with the basic assumptions of the theory of elasticity. One possible concept advanced to explain this phenomenon of a shape effect associates the relative amount of material at peak stresses with the propensity toward failure, that is, in a rectangular specimen a larger volume of material in the extreme fiber is subjected to peak stress than in a round specimen, and statistically, there is thus a greater chance for failure to occur. Little data is available to indicate whether factors such as residual stress, variations in machining procedure, or structural readjustments associated with the particular shape of cross section have a definite influence on the fatigue strength of machine parts in service.

Object and Scope of Investigation

The purpose of this investigation was to obtain information regarding the relative magnitude of the effect of shape of cross section on flexural fatigue strength, and to analyze these data in an attempt to determine what factors influenced the fatigue behavior when the shape of the critical cross section was altered.

Flexural fatigue tests were made involving several shapes of specimen from each of two different steels. The size of the critical cross section in specimens of each metal was maintained as nearly constant as possible throughout each series of fatigue tests in order to eliminate as far as possible any size effect.

Four shapes of cross section were chosen for the test, namely, square, diamond, round, and a modified diamond. The techniques of manufacture of each specimen were studied rather critically in order to detect any possible changes in surface conditions and residual stresses which might arise to alter the fatigue properties exhibited by a member.

Materials, Test Specimens, and Method of Testing

The first series of test specimens were made of Mayari-R (a low-alloy structural steel) in a normalized condition and having the chemical and mechanical properties listed in Table 1. The second series of specimens were made of SAE 4340 steel, quenched and tempered to a static tensile strength of approximately 150,000 psi. The static mechanical properties and chemical analysis of this material are listed in Table 2, and a comparison of typical tensile stress-strain curves for the two steels is included in Fig. 1. These metals were selected for the investigation in order to compare the results for two steels having widely different mechanical strength. It was felt that the higher strength exhibited by the SAE 4340 steel would accentuate any shape effects which might be observed with the lower strength Mayari-R steel.

The dimensional details of the flexural-fatigue test specimens are shown in Figs. 2 and 3; these were all cut from $^3/_4$-in-diam bar stock; flats were milled on top and bottom to provide gripping surface for the testing machine.

The modified diamond section, Fig. 3(*d*), was prepared by removing from the extreme fiber of the diamond section the optimum amount to give the theoretically strongest beam. For example, the section modulus for the diamond shape was

$$I/c = 0.1178\, d^3$$

in which d is the width of the side in the diamond section. By removing one eighteenth of the diagonal depth from both the top

---

[1] Engineering Experiment Station, University of Illinois. Mem. ASME.

[2] Cook Research Laboratories, Chicago, Ill.

[3] Engineering Experiment Station, University of Illinois.

[4] Numbers in parentheses refer to the Bibliography at the end of the paper.

[5] Since this paper was written there have been published two articles (11, 12) in which the fatigue data also indicated that rectangular beams were weaker than round beams tested in the same fatigue machine.

Contributed by the Machine Design Division and presented at the Annual Meeting, New York, N. Y., November 27–December 2, 1949, of The American Society of Mechanical Engineers.

Note: Statements and opinions advanced in papers are to be understood as individual expressions of their authors and not those of the Society. Paper No. 49—A-55.

and the bottom, the section modulus for the diamond section became

$$I/c = 0.1243\ d^3$$

which represents approximately $5^1/_2$ per cent increase in elastic flexural strength. For the square section (with the neutral axis of bending parallel to one face) the section modulus was

$$I/c = 0.1667\ d^3$$

in which d represents the length of the side of the square.

Specimens of all four shapes, Figs. 2 and 3, were formed by machining the test section with longitudinal cuts, using a milling cutter having a 3-in. radius. A set of specimens of SAE 4340 steel with the round critical section, Fig. 2(*c*), was also prepared by turning with a single-point tool in a lathe (following the usual procedures for rotating-beam specimens), since the results of the first tests on round specimens seemed to indicate that a difference might exist between the results obtained from milled and from turned surfaces.

All round specimens were polished by means of emery paper wrapped around a rotating cylindrical bar which was moved slowly along the specimen by hand while the specimen was turning slowly in a lathe. For successive grades of polishing paper the direction of rotation of the specimen was reversed to change the direction of abrasive scratches; the final polishing scratches were parallel to the longitudinal axis of the specimen. All other specimens were polished by hand with scratches from successive papers being generated at right angles and finishing with a longitudinal motion with No. 2/0 paper slushed with machine oil.

All fatigue specimens were subjected to completely reversed cycles of flexural stress in Krouse plate-fatigue machines. In operation of these machines one end of the specimen is clamped rigidly in a vise B, and the other end is reciprocated vertically by means of a connecting rod and eccentric crank mechanism,

TABLE 1 CHEMICAL COMPOSITION AND MECHANICAL PROPERTIES OF MAYARI-R STEEL

CHEMICAL COMPOSITION

	Per cent		Per cent
Carbon	0.10	Nickel	0.35
Manganese	0.76	Chromium	0.67
Sulphur	0.028	Copper	0.58
Silicon	0.34	Phosphorus	0.096

MECHANICAL PROPERTIES[a]

Upper yield point, psi	54800
Lower yield point, psi	52600
Tensile strength, psi	75200
Elongation in 2 in., per cent	33.2
Reduction of area, per cent	73.0
Brinell hardness number	147

HEAT-TREATMENT

Normalized at 1600 F

---

[a] Each value represents the average of three tests.

TABLE 2 CHEMICAL COMPOSITION AND MECHANICAL PROPERTIES OF SAE 4340 STEEL

CHEMICAL COMPOSITION

	Per cent		Per cent
Carbon	0.39	Chromium	0.72
Manganese	0.66	Nickel	1.72
Phosphorus	0.012	Molybdenum	0.35
Sulphur	0.018		

MECHANICAL PROPERTIES[a]

Upper yield point, psi	137500
Lower yield point, psi	133000
Tensile strength, psi	148800
Elongation in 2 in., per cent	20.9
Reduction of area, per cent	62.0
Brinell hardness number	322

HEAT-TREATMENT

Quenched in oil from 1525 F, tempered at 1150 F, cooled in air

---

[a] Each value represents the average of five tests.

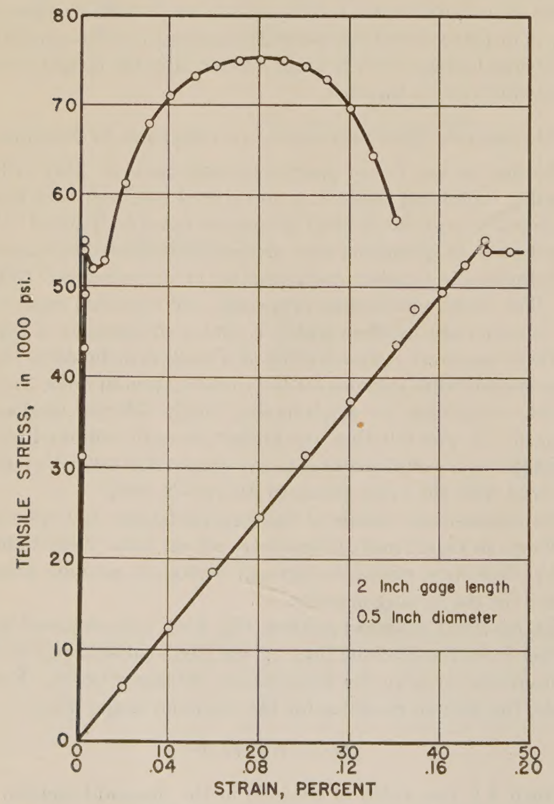

FIG. 1(*a*) STRESS-STRAIN DIAGRAM OF MAYARI-R STEEL

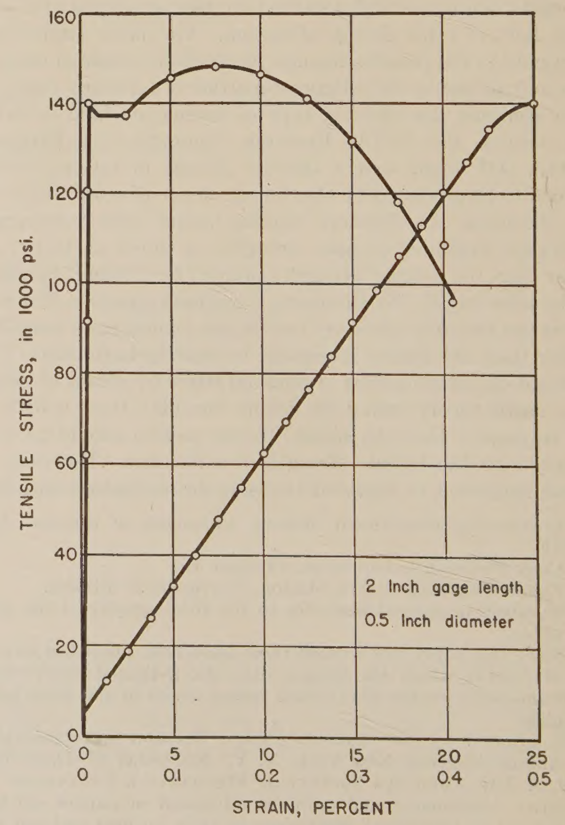

FIG. 1(*b*) STRESS-STRAIN DIAGRAM OF SAE 4340 STEEL

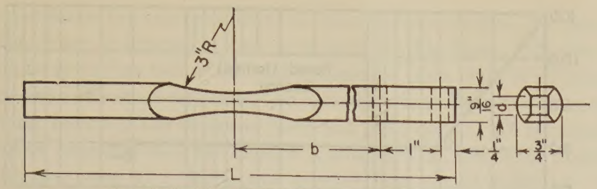

(a) SQUARE SPECIMEN

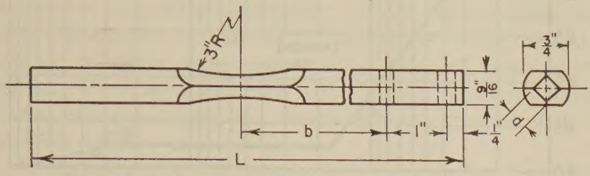

(b) DIAMOND SPECIMEN

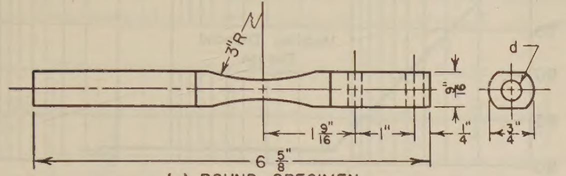

(c) ROUND SPECIMEN

DIMENSION	SAE 4340	MAYARI-R
d	0.32"	0.40
b	6 3/8"	5 3/8"
L	11 1/8"	10 1/8"

Fig. 2 Specimen for Cantilever Bending Machine

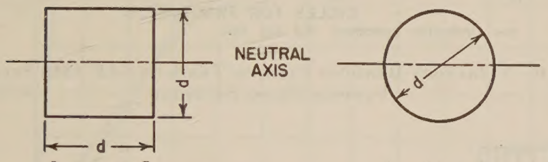

$\frac{I}{c} = .1667\,d^3$ (a) SQUARE SECTION

$\frac{I}{c} = .0982\,d^3$ (b) ROUND SECTION

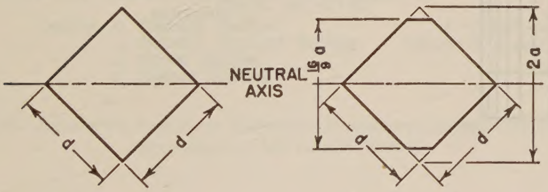

$\frac{I}{c} = .1178\,d^3$ (c) DIAMOND SECTION

$\frac{I}{c} = .1243\,d^3$ (d) MODIFIED DIAMOND SECTION

Fig. 3 Various Cross Sections Used in Tests

Fig. 4. A dead weight required to produce the desired stress in the critical section S, is applied to the pin P, in the clamp C, with the connecting rod AP disconnected and swung out of position. The deflection is noted on the dial indicator D, for both upward and downward loads of the desired amount. The connecting rod AP is then coupled (as shown in Fig. 4), and the eccentric cam A adjusted to provide the same deflections of the dial indicator. For each revolution of the motor a completely reversed cycle of end deflection of the specimen is applied.

In order to check the stability and accuracy with which maximum stresses were reproduced throughout the duration of a test, the machines were stopped periodically and a recheck made of the deflection corresponding to the desired dead weight.

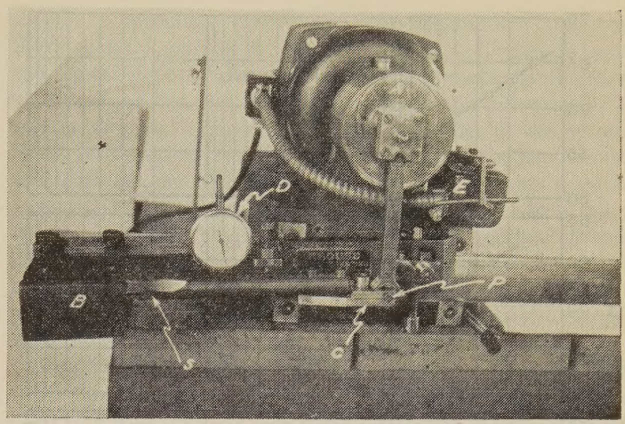

Fig. 4 Krouse Plate-Fatigue Testing Machine

Results of the Investigation

The results of the fatigue tests on Mayari-R and SAE 4340 steels are plotted in the form of S-N diagrams in Figs. 5, 6, and 7. A summary of the fatigue limits obtained for these four shapes of cross section is given in Table 3, for the two steels. It will be noted that for each steel the round specimens exhibited fatigue limits appreciably greater than those obtained for the other three shapes tested. By utilizing the strength of the round specimens of each material as a "par" value, the relative fatigue limits for the various shapes of specimen are compared in the last two columns of Table 3. These ratios indicate that for either steel the general trend of decreasing endurance limits was in the following order: (*a*) round; (*b*) diamond; (*c*) modified diamond and square.

A comparison of the endurance limits for the square and the modified diamond cross sections reveals the fact that their strengths were almost the same, and that their relative order of strength was reversed when comparison is made between the tests on the two different steels. Thus it may be inferred that there was little, if any, difference between the strengths exhibited by the square and the modified diamond beams.

Possible Factors Contributing to a Shape Effect for Beams. In seeking an explanation for these apparently paradoxical differences in fatigue strength, the following concepts have been reviewed in a search for a possible explanation:

1 From a statistical viewpoint, the relative amount of material subjected to stresses greater than a certain percentage of the peak stress may influence the initiation of failure.

2 Possible regions of stress concentration or "sore spots," or the presence of highly stressed fibers that lack lateral support.

3 The presence of varying amounts of residual stresses in the various shapes which may be altered by the differences in manufacturing operations or processing.

4 Alterations in the mechanical properties of the surface fibers caused by differences in the amount of cold-working in the machining operations (and not entirely removed by polishing).

5 The effect of the shape of cross section in controlling the relative extent of "localized" inelastic action occurring on the extreme fibers of the beam.

The possible contributions of each of these items to the various differences in fatigue properties as noted in the tests will be discussed briefly.

By comparing the relative amount of material subjected to the peak stress in each of these cross sections and the sore spots (possible points of stress concentration), one finds that the round shape has a relatively small amount of material at peak stress,

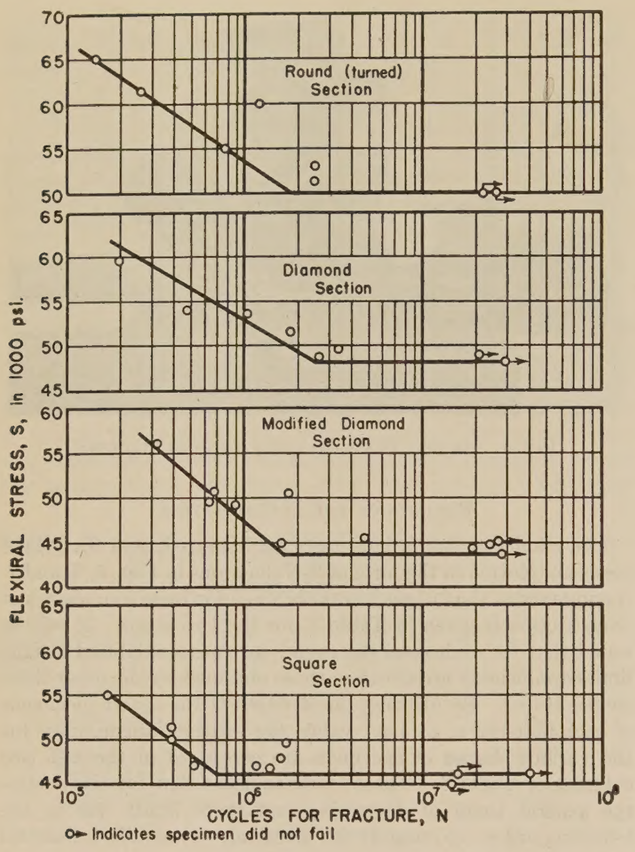

Fig. 5 Vibratory Bending Fatigue Tests of Mayari-R Steel of Various Cross Sections

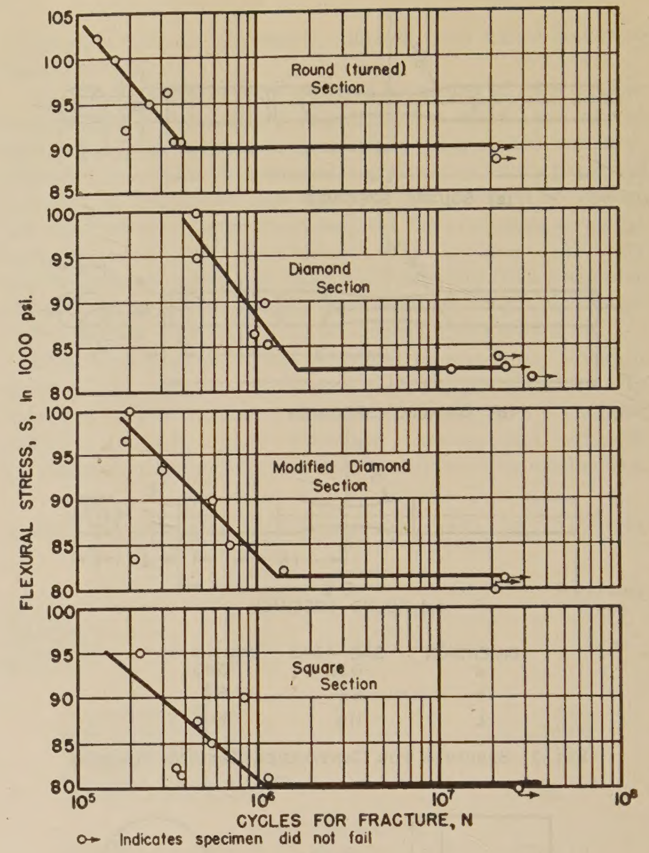

Fig. 6 Vibratory Bending Fatigue Tests of SAE 4340 Steel of Various Cross Sections

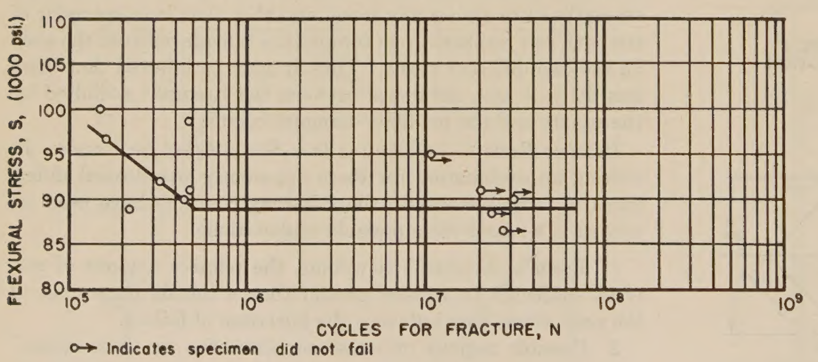

Fig. 7 (*left*) Vibratory Bending Fatigue Tests of SAE 4340 Steel of Milled Round Cross Section

TABLE 3 INFLUENCE OF SHAPE OF CROSS SECTION ON FLEXURAL FATIGUE STRENGTH

(Completely Reversed Cycles of Stress)

Test Results for Mayari-R Specimens

Specimen shape	Fatigue limit, psi	Ratio of fatigue limit to that of round	Per cent reduction in strength (based on round specimen)
Round (turned)[a]	50000	1.00	0
Square (milled)	46000	0.92	8
Diamond (milled)	48000	0.96	4
Modified diamond (milled)	44000	0.88	12

Test Results for SAE 4340 Steel Specimens

Specimen shape	Fatigue limit, psi	Ratio of fatigue limit to that of round	Per cent reduction in strength (based on round specimen)
Round (turned)[a]	90000	1.00	0
Round (milled)	89000	0.99	1
Square (milled)	80500	0.89	10.5
Diamond (milled)	83000	0.92	7.7
Modified diamond (milled)	82000	0.91	8.9

---

[a] Method of machining.

and does not contain sharp corners which may result in localized stresses due to outward projecting fins, or from nicks or scratches crossing the sharp corners. On the other hand, the diamond shape, with the minimum amount of material at peak stress, has one sharp corner which comprises the extreme fiber. This corner may lead to sore spots from which failure may initiate for two reasons, namely, (*a*) it is impossible to produce a sharp corner without some small intersecting scratches which may be effective as stress raisers, and (*b*) the outward projection is entirely unsupported except for the thin layer of metal below it, which in turn is rather highly stressed. Therefore this unsupported edge may be subjected to a localized buckling action during the compressive portion of a stress cycle. On this basis it seems reasonable that round specimens might develop a higher fatigue limit than those of diamond shape or other types with sharp corners.

In order to facilitate comparison of the relative amounts of material in the extreme fibers of these various shapes, the data in Fig. 8 are of interest. The ordinates in this figure indicate the depth in inches below the test surface for each type of specimen, and the abscissas represent the corresponding cross-sectional area lying between the extreme fiber and that depth. It is reasonable to presume that the failure is initiated in the outer fibers of the specimen at a depth not greater than about 0.004 in. For depths less than this amount the square shape has the greatest amount of material at peak stress; the order of decreasing magnitude (for amount of material at peak stress) for the other shapes has the following sequence: modified diamond, round, and diamond. Thus, by comparison with Table 3, the fatigue strength varies in a general manner inversely as the amount of material at peak stress.

In opposition to the thought that the amount of material at peak stress controls the fatigue limit, there are two instances in these tests for which the reverse tendency appeared, namely, (*a*) the round specimens exhibited a higher endurance limit than the diamond shape, and (*b*) the fatigue limits for the square beams and for the modified diamond beams were practically the same, in spite of the fact that there was an appreciable difference in the volume of metal exposed to the peak stresses (in the extreme fibers) for these latter two shapes. It should also be kept in mind that both the modified diamond section and the square section have two sharp corners projecting outward from which failure may be initiated. The exact stress (including residual stresses) in the region of the corner of any of these shapes is unknown and difficult to evaluate, but it seems reasonable to assume that any abrupt change in shape may leave protruding fibers that may initiate fracture in these regions.

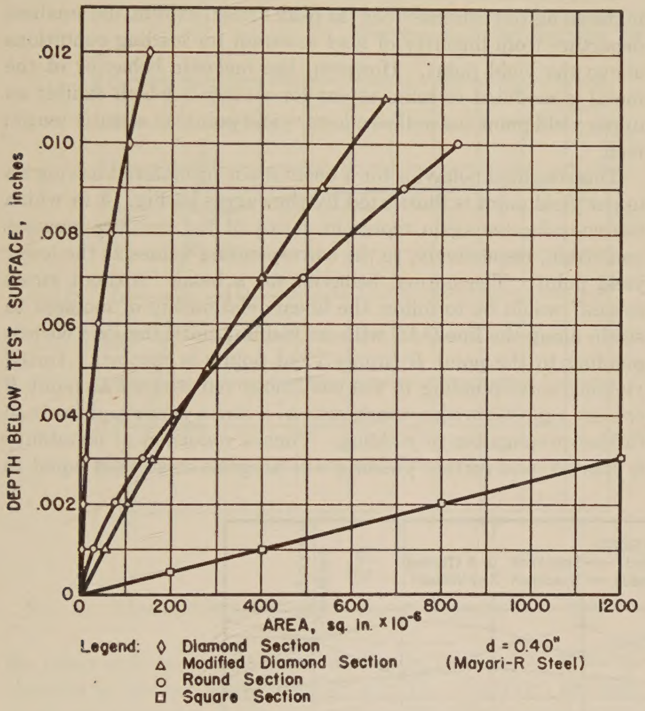

Fig. 8 Relative Areas of Extreme Fibers in Cross Sections of Specimens; Mayari-R Steel

Metallographic examinations of the different specimens indicated that the diamond and modified diamond shapes did not have true sharp corners with flat plane faces. These projecting corners were found to have been rounded slightly in polishing, but this was desirable in order to remove any sharp fins of fragmented material. The cutting operations and cold-working involved in the machining of any specimen develop unknown amounts of residual stress in the surface layers which may be either of a macro (large-scale) or of a micro (small-scale) nature. In polishing a fatigue specimen, the removal of sufficient surface layers will reduce the surface residual stresses (4). However, no suitable methods exist today for measuring these residual stresses or of determining whether they have been removed.

A series of micro-indent (Knoop) hardness surveys were made on a number of test specimens to detect any hardness variations (strain-hardening) which might be a clue to the presence of (accompanying) residual stresses. Specimens with outward projecting corners might be particularly susceptible to the alteration of their physical properties by cold-working (and also to the development of residual stresses) owing to the fact that the pressures of cutting tools were applied in two different directions to the protruding corners. For the round specimens, conversely, this condition would not exist during the machining operations.

The microhardness surveys were made on transverse cross sections with particular attention being given to the material near the surface. However, the Knoop hardness values plotted in Figs. 9, 10, and 11 do not indicate any consistent increase in hardness near the surface. Only a small amount of material is examined at any one indent and hence random variations are to be expected.

The upper shaded area in Fig. 9 indicates the range of hardness found in pearlitic areas in the Mayari-R steel, and the lower shaded area shows the smaller spread of lower hardness found in ferrite grains or colonies of grains. This is in line with pre-

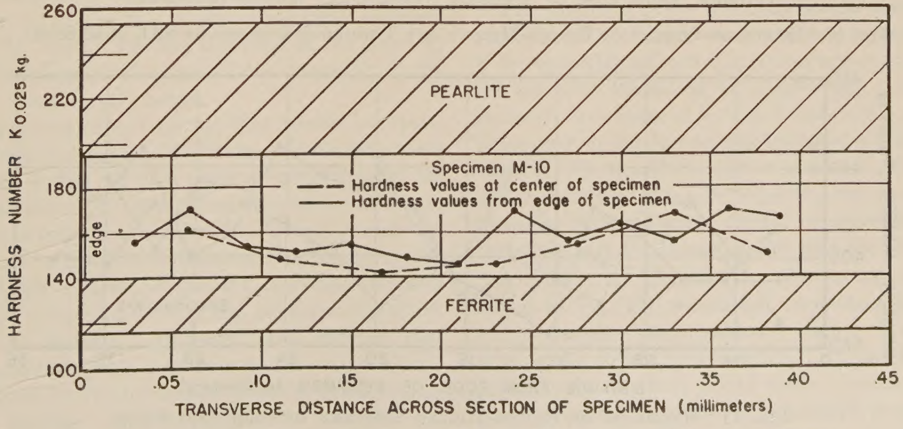

Fig. 9 Hardness Survey of Round-Turned-Specimen of Mayari-R Steel

vious observations that hardness will vary within a material, between different crystals, and also with different orientations and locations within the crystal itself (5). It will be noted that the variations in hardness from the center to the test surface fall entirely between these two bands and show no abnormal increase in the hardness of the surface crystals.

In Fig. 10 is shown a comparison of hardness surveys obtained on round SAE 4340 steel specimens produced by milling and produced by turning in a lathe. No correlation seemed to exist between the minor variations in hardness, and the differences in machining procedure used to form the specimen. In Fig. 11 three parallel surveys of hardness values from the outer surface to the center of a round milled specimen of SAE 4340 steel are plotted. Nevertheless, the random or erratic variations in hardness at each station fall within a fairly consistent band but exhibit no definite change in hardness of surface layers as compared with the material below the surface. Metallographic examination of the edges of transverse sections cut from the critical sections of several specimens did not show visual evidence of appreciable plastic deformation remaining from the machining operations. Thus it was felt that no plausible explanations for this shape effect in fatigue could be based on hardness variations or the presence of residual stresses resulting from cold-working in machining.

Tentative Explanation for Influence of Shape of Cross Section. Several investigators in recent years have supported the hypothesis that initial plastic yield under static loads occurs at a higher stress when a stress gradient exists (as in a beam) than the yield point for the same metal, when subjected to a uniformly distributed stress. Based on this assumption, it has been suggested (8) that a shape factor exists for the determination of yield strength in static flexural tests. However, further evidence indicates (9, 10) that the stress at which general yielding occurs in the extreme fibers of a beam is the same as that for the same metal under a uniform tensile stress, that is, the yield stress is not modified by the presence of a stress gradient.

The extent to which general plastic deformation progresses into a beam at loads above that which initiates yielding is, however, a function of the shape of the beam, Fig. 12. It is therefore probable that the microscopic, heterogeneously distributed inelastic actions that accompany the development of progressive fracture may likewise be influenced to some extent by the shape of cross section (or distribution of metal in the most highly stressed regions of a beam).

As evidence of variations in inelastic action at stresses above the yield point, Fig. 12 illustrates the theoretical curve of Morkovin and Sidebottom (10), in which the ordinates represent the ratio of the actual bending moment on the beam to the bending moment required to initiate yielding, and the abscissas represent the ratio of strain on the extreme fiber to the strain corresponding to the yield point. These curves are applicable to beams made of material with an abrupt yield point (horizontal tangent to the stress-strain curve at the yield point).

It will be observed that beams with the smallest amount of material on the extreme fiber (at peak stress) exhibit the smallest departure from linearity of load to strain for loading conditions above the yield point. However, the inelastic behavior of the metal is modified to some extent for materials which exhibit an upper yield point (as well as a lower yield point) in a static tensile test.

This modified behavior for a beam made of material having an upper yield point is illustrated by the curves in Fig. 13 in which the co-ordinates again represent ratios of the bending moment and strain, respectively, to the corresponding values at the lower yield point. The normal behavior for a beam "without stress raisers" would be to follow the linear relationship of moment to strain along the line *OAC* with no yielding until the load corresponding to the point *B* (upper yield point) is reached. Initial yielding corresponding to the conditions represented at point *B* creates a plastic wedge which acts as a stress raiser and leads to further propagation of yielding. Thus a condition of instability is created, and further yielding will progress at stresses equal to

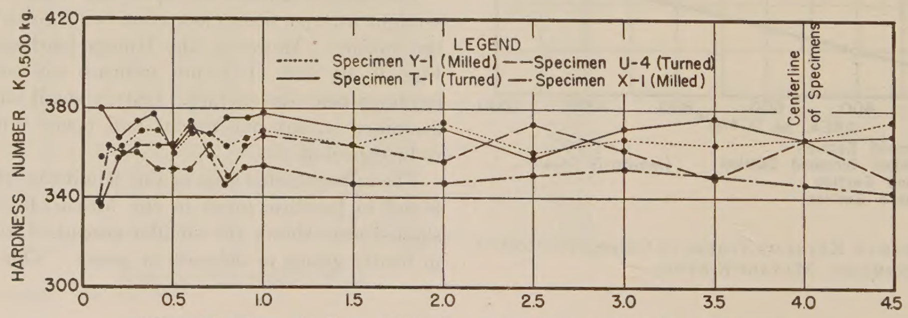

FIG. 10 HARDNESS SURVEY OF ROUND-MILLED AND TURNED-SPECIMENS OF SAE 4340 STEEL

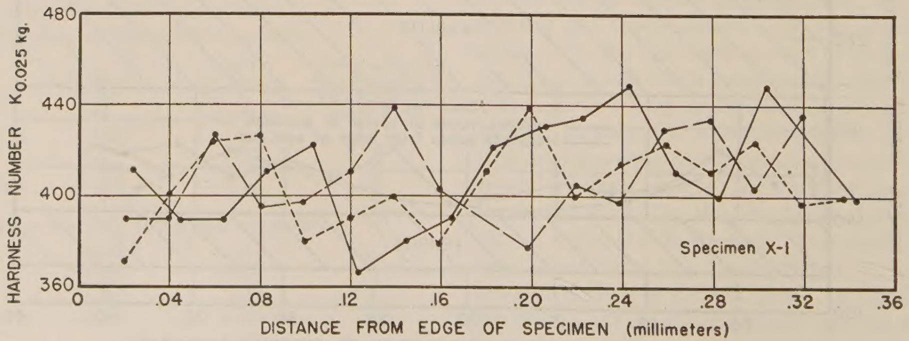

FIG. 11 HARDNESS OF ROUND-MILLED-SPECIMEN OF SAE 4340 STEEL
(Indents made in three parallel lines spaced 0.04 and 0.06 mm.)

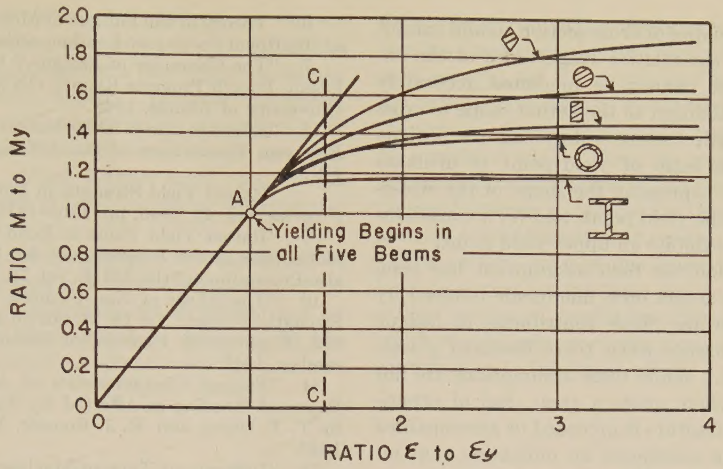

FIG. 12 THEORETICAL DIMENSIONLESS MOMENT-STRAIN DIAGRAM SHOWING EFFECT OF CROSS SECTION ON YIELDING IN MILD-STEEL BEAMS

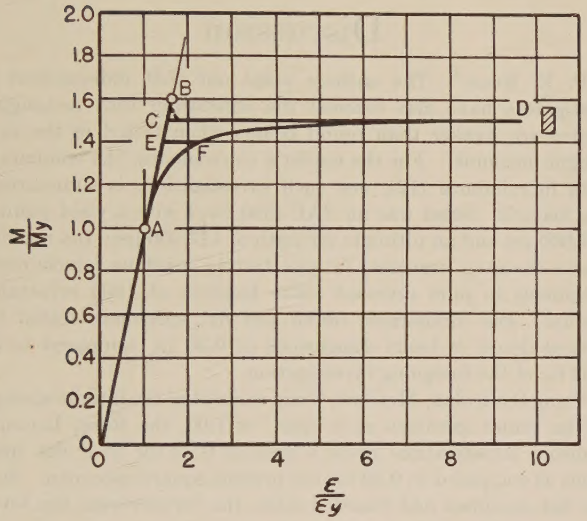

FIG. 13 MOMENT-STRAIN DIAGRAMS FOR RECTANGULAR BEAMS

the lower yield point of the material under constant loads as represented by the horizontal line *CD*, Fig. 13. However, the magnitude of the upper yield point exhibited by the material is controlled by the severity of the localized stresses present which arise from inherent stress raisers, inclusions, surface irregularities, and method of loading. It would be possible for the same beam with stress raisers (such as a roughened surface) to follow the moment-strain curve *OAFD*, or any intermediate curve between lines *ACBD* and *AFD*. Initial yielding will start at the point *A*, corresponding to the lower yield point of the material, if the stress concentration is sufficiently acute.

Morkovin and Sidebottom also reported that outward projecting corners on a beam acted as nuclei from which localized plastic yielding branched out or was reflected along diagonal lines in the outer surfaces of the beam. No similar concentrations of strain or branching of plastic zones was observed for round specimens.

At first hand it may be difficult to visualize how the foregoing discussion applies to the actions progressing in fatigue tests in which the "nominal" computed stresses are considerably below the yield point of the material. However, it is obvious that the nominal stresses do not give a true index of the actual "localized stresses" developed by the individual crystals which are resisting the external loading. In a polycrystalline material, the nominal stress represents only the statistical average; the distribution of stresses on individual crystals will vary over a wide range above and below the nominal computed stress. It is highly probable that a number of the crystals in the surface fibers may either be favorably oriented for inelastic action or subjected to localized high levels of stress with corresponding strain conditions equivalent to the upper portions of the curves in Figs. 12 and 13. Thus localized inelastic actions progressing on a microscopic scale may in turn be influenced by the shape of cross section of the beam.

One might postulate, therefore, that a certain proportion of the crystals could be strained by an amount equivalent to that shown by the vertical line *CC* in Fig. 12. If it be assumed, as has been done by Orowan (6), that the mechanism leading to fatigue fracture is related to a critical amount of localized inelastic deformation, the line *CC* may be used as representative of a criterion for fatigue failure, and corresponds to the strain condition in localized crystals of the beam when repeatedly stressed at the endurance limit of the member.

By applying these observations to the present fatigue tests, it appears probable as a tentative hypothesis that the shape effects as noted in Fig. 12, were of influence in controlling the localized plastic actions, but since the materials employed in the fatigue tests had upper yield points, the modification in action portrayed in Fig. 13 must also be taken into consideration. Based upon these two concepts, the round beams which have little tendency to propagate appreciable inelastic action and which also have no stress raiser of geometric origin on the extreme fiber, should have exhibited the highest fatigue strength.

The diamond shape normally would resist somewhat greater static loads without a corresponding amount of inelastic action if the material did not display an upper yield point. However, for material exhibiting an upper yield point the fatigue limit probably was lowered by the stress-raising effect of the outward projecting corner (promoting inelastic action), and by the greater tendency for this sharp corner to act as a nucleus for the spread and reflection of slip. By following this comparison further, the modified diamond shape should be somewhat stronger than the rectangle, but somewhat weaker than the circle and diamond.

A load-strain diagram for the modified diamond shape (if added to Fig. 12), would fall somewhere between the diamond and the square shape, probably slightly below that curve representing the circular cross section. It also has two outward projecting corners which would make it behave in a manner structurally equivalent to that of the square shape.

On the basis of this reasoning, it appears logical to expect that beams having different shapes of cross section should exhibit different fatigue strengths; the relative magnitudes of the endurance limit for each shape cannot be predicted accurately by any simple formula. In addition to the actual shape of cross section, several other strength factors influencing the fatigue limit might include: (*a*) the ratio of yield point to ultimate strength, (*b*) some parameter expressing the shape of the stress-strain curve in the region of the yield point, and (*c*) a consideration of whether the material exhibits an upper yield point.

In the foregoing explanation the tacit assumption has been made that localized inelastic action on a microscale induced by repeated stressing in the surface fibers contributes to fatigue damage, and that fracture results when these localized plastic actions exceed a certain level. While these assumptions are not susceptible to direct proof, there exists a great deal of experimental evidence that fatigue fracture is preceded or accompanied by plastic slip. This may be considered an indication that inelastic action due to repeated stressing is damaging in fatigue. The concepts of fatigue failure, outlined by Freudenthal and Dolan (7), also emphasize the fact that the first stage of failure in fatigue is that of crystal fragmentation (inelastic action) on a submicroscopic scale.

CONCLUSIONS

Laboratory studies indicated that the flexural fatigue strength of a member was influenced to an appreciable extent by the shape of cross section; steel beams of circular cross section exhibited fatigue limits 8 to 10 per cent greater than the fatigue limits of beams of square cross section. Beams having a diamond cross section (square beams stressed with the neutral axis as a diagonal of the diamond) exhibited endurance limits from 4 to 8 per cent less than the round beams.

The susceptibility to localized inelastic action, as governed by the shape of cross section and by the presence of sore spots, such as outward projecting corners, is tentatively believed to be the primary element leading to the reduction of fatigue strength of the square and diamond shapes to values below that for the round. While the other factors (residual stresses, alterations of properties due to machining, and statistical aspects of the amount of material subjected to peak stress) may have been of some influence in these tests, it is felt that their effect on the fatigue strengths of beams of the shapes studied were of a minor nature.

ACKNOWLEDGMENTS

This investigation has been conducted by members of the staff of the Department of Theoretical and Applied Mechanics as a part of the work of the Engineering Experiment Station of the University of Illinois in co-operation with the Office of Naval Research, United States Navy, under Contract N6-ori-71, Task Order IV, Project NR-031-005. Appreciation is expressed to the Office of Naval Research for its financial assistance in this work.

BIBLIOGRAPHY

1 "The Effect of Type of Testing Machine on Fatigue Test Results," by Research Committee on Fatigue of Metals, Proceedings of the ASTM, vol. 41, 1941, pp. 133–151.

2 "Fatigue Characteristics of Rotating Beam Versus Rectangular Cantilever Specimen of Steel and Aluminum Alloys," by F. D. Fuller and T. T. Oberg, Proceedings of the ASTM, vol. 47, 1947, pp. 665–676.

3 "Certain Mechanical Strength Properties of Aluminum Alloys 25S-T and X76S-T," by T. J. Dolan, NACA Technical Note No. 914, October, 1943.

4 "Work Hardened Surfaces of Fatigue Specimens," by F. C. Hull and H. R. Welton, *Metal Progress*, vol. 48, December, 1945, p. 1287.

5 "The Measured Knoop Hardness of Hard Substances and Factors Affecting Its Determination," by N. W. Thibault and H. L. Nyquist, Trans. ASM, vol. 38, 1947, pp. 271–323.

6 "Theory of the Fatigue of Metals," by E. Orowan, Proceedings of the Royal Society of London, series A, vol. 171, 1939, pp. 79–106.

7 "The Character of Fatigue," by A. M. Freudenthal and T. J. Dolan, Fourth Progress Report, ONR Contract, N6-ori-71, T. O. IV, University of Illinois, 1948.

8 "Effect of Stress Distribution on Yield Points," by F. G. E. Peterson, Proceedings of the ASCE, vol. 72, April, 1946, pp. 445–459:

"Raised Yield Strength in Bend Tests," by G. Brewer, *Metal Progress*, vol. 48, 1945, pp. 1306–1310.

9 "Raised Yield Point in Bend Tests," by T. J. Dolan and O. Sidebottom, *Metal Progress*, vol. 50, October, 1946, pp. 653–657; see also Proceedings of the ASCE, vol. 72, November, 1946, pp. 1275–1283.

10 "The Effect of Non-Uniform Distribution of Stress on Yield Strength of Steel," by D. Morkovin and O. Sidebottom, Bulletin no. 372, Engineering Experiment Station, University of Illinois, December, 1947.

11 "Fatigue Characteristics of Aluminum Alloy 75S-T6 Plate in Reversed Bending as Affected by Type of Machine and Specimen," by T. T. Oberg and R. J. Rooney, Preprint No. 28, ASTM, June, 1949.

12 "Influence of Type of Machine, Range of Speed and Specimen Shape on Fatigue Test Data," by P. K. Roos, D. L. Lemmon, and J. T. Ransom, ASTM Bulletin, May, 1949, pp. 63–65.

Discussion

P. K. Roos.[6] The authors point out that independent investigators have also reached the conclusion that rectangular beams are weaker than round beams when tested in the same fatigue machine. For the reader's convenience, the comparable data in reference (12), one such investigation, is summarized; the material tested was an SAE 4340 steel with a yield point of 107,000 psi and an ultimate strength of 127,000 psi; the machine was a Sonntag universal fatigue testing machine which tested specimens in pure reversed plane bending at 1800 reversals a minute; the comparable round and flat specimens tested had critical depth of beam dimensions of 0.30 in. compared to the 0.32 in. of the foregoing investigation.

Using the Dolan, McClow, Craig concept of the fatigue strength of the round specimen as a "par" of 1.00, the Roos, Lemmon, Ransom investigation[7] gives a ratio of 0.92 for their flat specimens as compared to 0.89 for the present square specimen. Since the flat specimen had rounded sides, the corners were less severe "sore spots" than the corners in the square beam.

This thorough investigation certainly justifies the conclusion that the shape factor is the primary element leading to a reduction of fatigue strength, and, as immediate help to the designer, this is important. However, the concept of the statistical effect of the amount of material subjected to peak stresses as a fundamental part of the fatigue problem needing investigation, should not be forgotten.

AUTHORS' CLOSURE

The authors wish to thank Professor Roos for his contribution to the discussion of this rather intriguing "shape effect" in flexural fatigue tests.

In spite of the fact that the tests quoted by Professor Roos were conducted in a different laboratory, utilizing different types of fatigue machines and heat-treatment of material, it is reassuring to know that they obtained a similar reduction in fatigue strength of the flat or rectangular specimen as compared with the "par" value for a round cross section.

The seriousness of this shape effect is more dramatically emphasized by the pronounced variations in fatigue strength of 75S-T6 aluminum alloy, obtained recently by Oberg and Rooney

---

[6] Associate Professor of Engineering Mechanics, The Pennsylvania State College, State College, Pa.

[7] Influence of Type of Machine, Range of Speed, and Specimen Shape on Fatigue Test Date," by P. K. Roos, D. C. Lemmon, and J. T. Ransom, ASTM Bulletin, No. 158, May, 1949, pp. 63–65.

(11). These authors obtained values of 29,000 psi for the endurance limit of a round specimen as compared with 21,000 psi for a square specimen, and 17,500 psi for a rectangular specimen (whose width was three times the depth). Thus for this aluminum alloy the rectangular specimen exhibited a strength 40 per cent less than the par value obtained for a round specimen tested in the same machine. Much further work needs to be done to appraise the seriousness of (and to enable the designer to predict) these shape effects.

The authors agree that the statistical effect of the amount of material subjected to peak stresses is a fundamental part of all problems involving strength of materials, which should not be neglected in applications to shape effect in fatigue. In the present tests, however, the statistical effect evidently was not the primary controlling factor, or the strengths of the various members tested would have been greatest for the diamond shape, next greatest for the round and modified diamond shapes, and the square cross section would have been by far the weakest of the group. Since the diamond cross section actually proved to be somewhat weaker than the round cross section, it was concluded that other factors of the test condition must have had a greater influence on the results than did the statistical effects of amount of material at peak stress.

The authors hope in the future to be able to conduct similar tests on somewhat the same shapes of cross section but with the critical section of greater size than in the present investigation, which should help to clarify some of our concepts of the factors contributing to this shape effect.

Hide-Out of Sodium Phosphate in High-Pressure Boilers

By F. G. Straub,[1] Urbana, Ill.

A study has been made to explain a type of hide-out of sodium phosphate in steam boilers operating at about 1700 psi. This has shown that an insoluble form of a sodium phosphate is stable at temperatures above 620 F. This type of phosphate is scale-forming and is resistant to heat transfer. This sodium phosphate does not have the properties corresponding to those of the sodium phosphates normally encountered in steam-boiler water. Analyses by chemical means, x rays, and petrographic all indicate that this is a different form of sodium phosphate. Tests indicate that no insoluble potassium phosphate is formed and, if suitable potassium-to-sodium ratio is maintained, this insoluble salt will not form.

Some difficulty has been experienced in boilers operating at a pressure of about 1600 to 1700 psi with loss of phosphate from solution while on steady load. This phosphate reappears in solution when the boiler rating or pressure is reduced. This condition was explained at first as so-called hide-out of phosphate due to conditions of circulation. However, a further study of the problem indicated that this was not the normal hide-out of phosphate. During operation of the boiler the phosphate was added continuously along with sodium hydroxide so as to keep a residual of about 20–40 ppm as Na_3PO_4 and a pH around 11. When the boiler rating was reduced, the soluble phosphate would increase to around 200–300 ppm, but the free hydroxide would be reduced from around 40 ppm to 0 ppm. This loss of phosphate with its subsequent reappearance accompanied by the loss of hydroxide indicated that it was not hiding-out as trisodium phosphate, but as a form more on the acid side, like mono or disodium phosphate.

After 2 or 3 months of operation, difficulty was experienced in the boiler because of failures in wall tubes. These tubes bulged with no indication of corrosion on the water side. Heavy deposits of calcium and sodium phosphate were found on the water side of the tube facing the furnace.

When the boiler pressure was reduced for a short period of operation to around 1300 psi, this peculiar type of phosphate hide out did not take place. The absence of this action at lower pressures indicated that there might be a complex sodium phosphate of low solubility which was forming at the higher temperatures, but which was not stable at the lower temperatures. The possibility was considered that the calcium-phosphate sludge adhering to the wall surface might increase the temperature under the sludge to a point where the insoluble phosphate could form. Conditions were such that a complex sodium-calcium phosphate deposit also might be forming.

Laboratory Investigation

A laboratory investigation was undertaken to determine whether this reaction could be duplicated, and if so, to study the conditions causing the reaction. A small laboratory boiler, as shown in Fig. 1, was used. Heating was accomplished by means of electric resistance wire wound on the heating tube over a thin layer of alundum cement. The tubes were 1 in. ID × $1^3/_8$ in. OD. The wire was wound on the tube for a length of 7 in. The heat input was approximately 50,000 Btu per sq ft per hr calculated on the inside area of the tube. In order to secure circulation in the tube, a smaller tube 0.75 in. OD × 0.68 in. ID was inserted inside it. This inner tube was placed so that it had clearance at the bottom and extended well above the heated area.

The steam-water mixture traveled up the space between the tubes and water traveled down the inside of the inner tube. The presence of circulation in this area was indicated by the fact that the temperature gradient from the outside of the tube to the water in the main part of the boiler remained constant, at a value around 30 to 40 F. A thermocouple was peened into the outer surface of the heating tube at the center of the tube so as to measure the outside temperature of the heating tube. A thermocouple well was placed in the boiler directly above the outlet of the water coming from the heating tube into the main water-storage section. This is referred to as T_1 and that of the outside of the heating tube as T_2.

The boiler held about 8 liters of water when cold. In order to operate at a constant heat input, a fan was directed so as to blow air on a bare steel tube on the top of the test boiler. When the temperature of the boiler water increased above the desired temperature, a temperature controller turned the fan on, and when the temperature was too low, it turned the fan off. This means of control allowed operation which would return the condensed steam without use of a pump. Since no steam was removed from the boiler during the test period, it was not necessary to have any make-up. The chemicals to be added during the test were pumped in solution into the main drum of the boiler.

Boiler Tests

In order to test the boiler a solution of sodium hydroxide (1000 ppm) in distilled water was added to the boiler. The boiler was operated at temperatures from 400 F (250 psi) to 690 F (2900 psi) with constant heat input. The temperature drop ($T_2 - T_1$) was 30 F throughout the test and the concentration of sodium hydroxide also remained constant. This indicated that the hydroxide was evenly distributed throughout the test and that there were no localized spots in which concentration of the chemical might take place.

The inner tube was removed, and the boiler was run with a solution of sodium hydroxide, phosphate, and chloride in the boiler water. Table 1 gives the data collected during this test. After running 2 hr at 500 F, there was but slight temperature increase of the heating tube. When running at higher temperatures there was a slight increase of ($T_2 - T_1$), but a marked decrease in all the chemicals in solution. At the end of the test the heating was stopped and the contents of the boiler removed

---

[1] Research Professor of Chemical Engineering, University of Illinois.

Contributed by the Joint Research Committee on Boiler Feedwater Studies and the Power Division and presented at the Annual Meeting, New York, N. Y., November 27–December 2, 1949, of The American Society of Mechanical Engineers.

Note: Statements and opinions advanced in papers are to be understood as individual expressions of their authors and not those of the Society. Paper No. 49—A-39.

TABLE 1 TEST RUN ON BOILER SHOWN IN FIG. 1, WITH CONSTANT HEAT INPUT AND NO FILLER IN TUBE

($T_2 - T_1$ = temperature differential from outside heating tube to water temperature in boiler)

	Boiler Temp	Heat Input					
Time Hours	° F	$T_2 - T_1$	Amps.	NaOH	PO_4	NaCl	pH
2	500	35	26	85	870	498	11.4
4	525	42	26	43	820	430	11.4
22	550	50	26	55	440	359	11.5
24	610	45	26	18	172	153	11.5
26	610	45	26	3	38	76	11.2
28	610	45	26	12	10	88	10.8

Shut off heat and blow water from boiler while hot. Tube No. 4.

TABLE 2 TEST RUN ON BOILER SHOWN IN FIG. 1, WITH CONSTANT HEAT INPUT

($T_2 - T_1$ = temperature differential from outside heating tube to water temperature in boiler)

Time Hours	Boiler Temp ° F	$T_2 - T_1$	Heat Input Amps.	NaOH	PO_4	NaCl
1	380	35	27	366	750	222
17	550	40	27	372	770	218
20	605	40	26	360	740	222
22	605	40	26	360	750	218
24	650	85	27	415	300	222
40	650	110	27	480	140	218

while the boiler and tube were hot. When the tube was removed and cut in half, a heavy hard deposit was found at the lower end of the heated area of the tube with no deposit at the middle of the tube or above. Since T_2 was measured at the middle of the tube, no appreciable indication of the deposit on the inside of the tube was detected. Analyses of this deposit gave the following results:

Per cent
Fe = 0.11
PO_4 = 60.32
Cl = 0.42
Na = 40.16
Total 101.01

The theoretical composition of Na_3PO_4 is 58 per cent PO_4 and 42 per cent Na. These results indicate that without the inner tube there is very little circulation in the tube, and that the steam leaving the tube causes the material dissolved in the boiler water to concentrate slowly until the solubility point of the salts is reached. At this point the insoluble excess salt crystallizes on the heating surface near the bottom where the concentration is highest. This test indicated that at 610 F, anhydrous trisodium phosphate was the stable phosphate. It also indicated that insertion of the inner tube aided in establishing circulation of boiler water through the heating tube.

The inner tube was replaced and the boiler was operated with a solution of sodium hydroxide, phosphate, and chloride in distilled water at temperatures from 380 to 650 F. Table 2 gives the results of this test. These results show that for water temperatures up to 605 F (1600 psi) there was no appreciable change in ($T_2 - T_1$), or the concentration of the various salts in solution. At 650 F (2200 psi) ($T_2 - T_1$) increased, accompanied by a loss of PO_4, an increase in NaOH, and no change in chloride. This indicated the hide-out of a sodium phosphate salt lower in sodium content than trisodium phosphate.

Table 3 gives the results of a similar test to determine the temperature at which the PO_4 starts to decrease. This test indicated that at 600 F there was no change in ($T_2 - T_1$), PO_4, or NaOH, but at 618 F, ($T_2 - T_1$) commenced to increase, with a loss in PO_4, and an increase in NaOH. At 670 F the phosphate had been reduced from 980 ppm to 40 ppm. The boiler was then cooled to room temperature and reheated to 528 F. The phosphate and the ($T_2 - T_1$) returned to normal. This indicated that the sodium-phosphate compound had formed on the heating surface at a temperature of 618 F (1750 psi) and above, but had redissolved when the boiler was operated at 528 F.

Another test was conducted in which sodium sulphate was added along with the phosphate, hydroxide, and chloride. Table 4 gives the results of this test. The phosphate again began to decrease at 620 F (1790 psi), with an increase in ($T_2 - T_1$). No reduction in the chloride occurred throughout the test, but the sulphate commenced to decrease at a temperature of 638 F with a loss of about 300 ppm at 675 F. When the run was finished, the heat was shut off and the contents of the boiler blown out while the water was still at the higher temperature. The heating tube was removed and cut in half (lengthwise). A deposit of a hard gray-white crystalline material was found evenly distributed throughout the area of the tube subjected to heat input. No deposit was found on the ends of the tubes which were not subjected to any heat input.

About 7.6 grams of this material was present on the heating surface.

A chemical analyses of this material gave the following results:

	Per cent
Sodium (Na)	31.78
Phosphate (PO_4)	41.08
Sulphate (SO_4)......	17.99
Iron (Fe)...........	0.19
Total...............	91.04

TABLE 3 TEST RUN ON BOILER SHOWN IN FIG. 1, WITH CONSTANT HEAT INPUT

($T_2 - T_1$ = temperature differential from outside heating tube to water temperature in boiler)

Time Hours	Boiler Temp °F	$T_2 - T_1$	Heat Input Amps.	NaOH	PO_4	NaCl	pH
1	500	40	27	177	960	435	11.4
3	550	50	26	171	960	427	11.3
5	600	50	26	177	960	438	11.3
19	618	67	26	232	780	438	11.3
23	628	82	26	256	680	427	11.3
26	625	85	26	262	670	427	11.3
27	635	95	26	274	575	427	11.4
43	635	115	26	394	350	427	11.5
46	650	115	26	342	240	427	11.4
50	650	120	26	348	270	427	11.5
71	650	130	26	344	140	427	11.4
76	670	120	25	338	45	427	11.4
78	670	125	26	336	35	427	11.4
95	670	125	26	351	40	450	11.4
2	510	45	26	287	1295	427	11.5
18	528	45	26	207	1250	427	—

TABLE 4 TEST RUN ON BOILER SHOWN IN FIG. 1, WITH CONSTANT HEAT INPUT

($T_2 - T_1$ = temperature differential from outside heating tube to water temperature in boiler)

Time Hours	Boiler Temp. °F	$T_2 - T_1$	Heat Input Amps	NaOH	PO_4	NaCl	Na_2SO_4	pH
1	525	55	26	525	990	415	1670	11.5
21	560	60	26	575	970	405	1685	11.5
23	610	50	25	566	990	392	1730	11.5
24	620	60	26	555	880	398	1685	11.5
41	620	80	25	605	710	398	1670	11.6
46	630	80	25	598	630	392	1670	11.5
49	630	88	25	695	610	400	1650	11.5
66	638	130	25	640	300	405	1480	11.6
68	638	130	25	640	310	405	1470	11.6
70	648	152	25	646	180	410	1420	11.6
73	648	150	25	680	190	405	1450	11.6
90	655	185	25	654	80	400	1360	11.7
92	665	185	25	670	45	400	1345	11.7
94	665	185	25	665	40	408	1360	11.6
97	675	185	25	670	20	410	1330	11.6

Shut off heat and blow water from boiler while tube is hot. About 7.6 grams of scale on heating surface. Tube No. 3.

An x-ray diffraction analysis made by the Allis-Chalmers Manufacturing Company was reported as follows: "The deposit from Tube No. 3 from the laboratory test boiler gave quite a simple x-ray diffraction pattern, but we were not able to make an identification either from our library or from the ASTM card index. An incomplete chemical analysis indicated about 18 per cent sodium sulphate and 52 per cent disodium phosphate. The diffraction patterns, however, for both of these compounds are rather complex and none of the lines for either of these was found in the simple pattern. This would indicate that the two were present in the form of a double salt, crystallizing in rather simple form, perhaps the cubic system."

The sulphate was added in this test, since it is known that sodium sulphate has a decreasing solubility at higher temperatures. The phosphate decreased in concentration and deposited on the tube long before the sulphate began to decrease in concentration.

In order to study further the influence of circulation in the heating tube, the inner filler used in the tests reported in Tables 1, 2, and 3 was changed. The diameter was reduced from $^3/_4$ in. to $^5/_8$ in. OD. This changed the distance between the inner and outer tubes from $^1/_8$ to $^3/_{16}$ in. The phosphate started to decrease and ($T_2 - T_1$) to increase again at 620 F (Table 5), while the sodium chloride remained constant. After 72 hr, when the heat input was reduced from 26 to 23 amp, the phosphate increased some, but did not return to the original value. When the tube was removed and examined the deposit did not cover the entire area of heat input. Deposit occurred on only about the middle two thirds of the heating area.

The deposit appeared to be in two layers. Analyses of these layers gave the following results:

	Top layer, per cent	Layer next to tube, per cent
Sodium (Na).........	28.36	31.30
Phosphate (PO_4)......	56.90	58.62
Iron (Fe)............	14.96	10.24
Total................	100.22	100.16

The amount of sodium present is not sufficient to form trisodium phosphate.

Boiler Modified for Additional Tests

The boiler shown in Fig. 1 was modified to give a different condition of circulation. Fig. 2 shows the modified boiler. The inner tube previously used was removed from the heating tube. The tests reported in Table 6 were made using this boiler. These results indicate that the reduction of the phosphate and the ($T_2 - T_1$) changes were at a lower rate than on the boiler shown in Fig. 1. However, the reduction of the phosphate is evident at temperatures of 620 F and above. The deposit found on this tube at the end of the test was sent to the Victor Chemical Works for examination. The report was as follows:

"A microscopic examination of the scale from the pipe section submitted showed it to be made up of two materials. The greater part was a white amorphous material having a refractive index of 1.526. The balance was a very fine amorphous scale. This is believed to be due to decomposition of the amorphous material.

"The amorphous material, which was estimated to constitute 90 per cent of the scale, was obtained fairly pure by first scraping off the surface deposit. We did not find this to be readily soluble in water. It appears to decompose very slowly in water at room temperature, slightly faster when heated to 70 to 80 deg C. It is readily soluble in dilute acids and decomposes in hot dilute NaOH solutions. The exact composition was not determined, but qualitative tests show sodium, orthophosphate and ferrous iron to be present in appreciable quantities. From these tests the scale is believed to be a sodium ferrous phosphate. Optical properties did not identify the scale."

In order to study the effect of potassium, as compared to sodium, the boiler shown in Fig. 2 was used, and potassium hydroxide, phosphate, and chloride were added. The results of the tests are given in Table 7.

These results indicate that in the absence of sodium, the in-

TABLE 5 TEST RUN ON BOILER SHOWN IN FIG. 1, WITH $^5/_8$-IN-OD FILLER IN TUBE AND CONSTANT HEAT INPUT

($T_2 - T_1$ = temperature differential from outside heating tube to water temperature in boiler)

Time Hours	Boiler Temp ° F	$T_2 - T_1$	Heat Input Amps	NaOH	PO_4	NaCl	pH	
1	500	40	26	-24	820	488	11.4	
18	610	50	26	+48	820	488	11.6	
22	620	70	26	73	740	488	11.6	
25	620	80	26	91	610	488	11.6	
42	620	108	26	116	530	488	11.6	
45	620	105	26	140	495	488	11.6	
49	620	125	26	214	400	497	11.6	
66	620	120	26	195	395	502	11.6	
72	620	120	26	183	395	497	11.6	
90	620	65	23	195	470	497	11.7	
95	620	62	23	202	480	497	11.7	
114	630	120	26	189	315	497	11.8	
119	630	120	26	207	330	502	11.5	
121	640	120	26	226	280	508	11.5	
138	640	135	26	238	175	508	11.6	
142	640	238	26	235	175	508	11.5	
145	650	135	26	238	135	511	——	
162	650	160	26	238	93	511	——	
165	650	160	26	232	90	517	——	
186	650	160	26	226	85	527	——	
190	650	125	23	214	133	527	——	
194	650	125	23	244	143	537	——	
211	650	——	26	226	263	527	——	Intermittent heat input
215	660	160	26	226	60	538	11.5	Constant heat input
218	660	150	26	210	60	538	11.5	Constant heat input

Shut off heat and blow water from boiler while hot. Tube No. 5.

TABLE 6 TEST RUN ON BOILER IN FIG. 2, AT CONSTANT HEAT INPUT

($T_2 - T_1$ = temperature differential from outside heating tube to water temperature in boiler)

Time Hours	Boiler Temp °F	$T_2 - T_1$	Heat Input Amps	NaOH	PO_4	NaCl	pH
3	600	30	25	30	900	434	11.6
5	620	35	25	42	865	444	11.6
22	620	35	25	42	865	448	11.6
29	640	35	25	67	865	448	11.6
47	650	45	25	128	710	458	11.6
55	650	65	25	189	495	___	11.6
73	660	75	25	226	420	458	11.7
96	660	65	25	238	390	488	11.6
120	660	65	25	268	360	488	11.5
144	660	65	25	310	345	488	11.6
156	670	90	25	305	140	___	11.6
168	670	80	25	300	160	493	11.5
176	680	100	25	286	70	___	11.5
190	680	100	25	293	70	565	11.5 Steam leak in boiler

Shut off heat and blow water from boiler while hot. Tube No. 6.

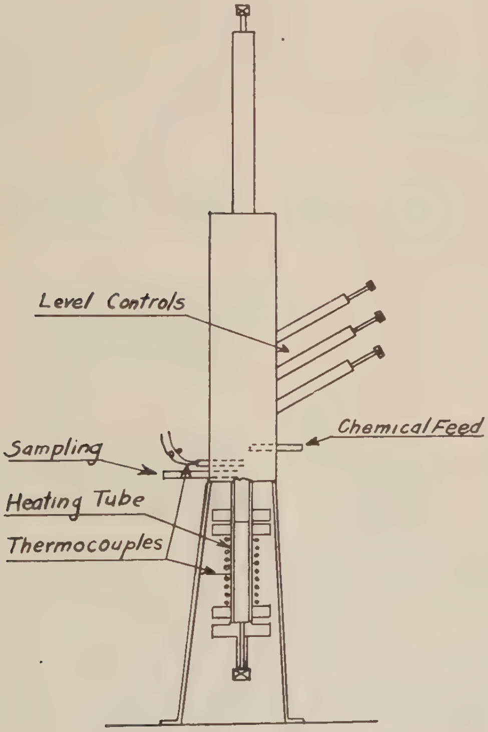

Fig. 1 Test Boiler No. 1

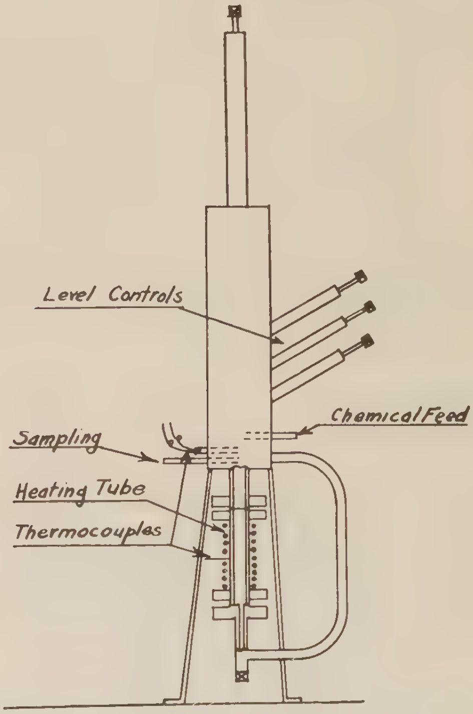

Fig. 2 Test Boiler No. 2

soluble phosphate will not form. Thus with potassium salts present, no appreciable change in PO_4, hydroxide, or ($T_2 - T_1$) was noticed even at a temperature of 680 F (2700 psi). When sodium is added as sodium chloride, so that the total sodium is equal to about 0.2 of the potassium present, hardly any appreciable change in PO_4 or $T_2 - T_1$ was noted. When this was increased to about 0.5 a loss of PO_4 and a change in ($T_2 - T_1$) was observed. A further increase to around 1 made a further reduction in PO_4. This appears to indicate that in a closed-cycle plant, the use of potassium salts in place of sodium would prevent the deposition of the sodium phosphate at the higher temperatures. If there was leakage of sodium salts into the system, the sodium phosphate could form if the ratio of the sodium to the potassium became sufficiently high.

TABLE 7 TEST RUN ON BOILER SHOWN IN FIG. 2, USING POTASSIUM SALTS

($T_2 — T_1$ = temperature differential from outside heating tube to water temperature in boiler)

Time Hours	Boiler Temp. ° F	$T_2 - T_1$	Heat Input Amps.	KOH	PO_4	KCl	Total Cl as NaCl	pH
1	510	30	26	0	1000	457	—	11.7
3	630	43	26	0	1020	—	—	11.6
20	630	45	26	0	1000	453	—	11.6
22	660	45	26	0	1010	460	—	11.6
27	680	45	26	0	1030	—	—	—
45	680	40	26	0	1120	510	—	11.6
Add NaCl to boiler Water 2 grams -								
46	680	45	26	0	1050		1090	—
50	680	45	26	79	1000		1135	—
Add NaCl to boiler Water 4 grams -								
54	680	80	26	158	470		2600	
66	680	80	26	202	470		2770	
Add NaCl to boiler water 4 grams -								
75	680	85	26	183	270		4400	

Shut off heat and blow water from boiler while hot. Tube No. 8.

When the tube was examined, a white deposit was found on the heating surface as expected.

Analysis of this material gave the following results:

	Per cent
Sodium (Na)	10.46
Phosphate (PO_4)	51.91
Chloride (Cl)	0.70
Potassium (K)	1.08
Iron (Fe)	2.87
Total	67.02

Two more tests were conducted with sodium phosphate hydroxide, and chloride in the boiler water in order to obtain more material for analyses. The results of the analyses of the deposit from these tests were as follows:

	Per cent	
	Tube no. 7	Tube no. 9
Sodium (Na)	31.72	30.70
Phosphate (PO_4)	60.32	60.32
Iron (Fe)	8.80	9.36
Total	100.84	100.38

On tube No. 7 the deposit was 0.023 in. thick, and it caused an additional temperature gradient across the heating tube of 160 F. The x-ray diffraction pattern was the same as that obtained from tube No. 3 even though there was no sulphate present in this sample.

The results of examination of the deposit on tube No. 9 by another laboratory were reported as follows:

"Petrographic examination shows about 3/4 of the material to be a glassy isotropic substance with a refractive index of 1.52. The remainder is mostly anisotropic with refractive index values of about 1.595 and 1.68. These results do not correspond to any of the alkali phosphates in our available literature.

RESULTS OF ANALYSIS

	Per cent by weight
Water-soluble material (76.2 per cent by weight):	
Sodium as Na_2O	40.1
Phosphate as P_2O_5	36.0
Insoluble material (23.8 per cent by weight):	
Silica as SiO_2	0.5
Phosphate as P_2O_5	6.4
Iron as Fe_2O_2	12.7
Calcium as CaO	none
Magnesium as MgO	0.1
Sodium as Na_2O	trace

"The insoluble material is apparently composed of a small amount of magnesium silicate, a little silica, some iron phosphate, and some ferric oxide.

"The water-soluble material is evidently a mixture of various sodium phosphates, since the Na_2O ratio is too low for trisodium phosphate and too high for other alkaline phosphates known to exist. Microchemical tests furnish additional evidence in support of this view. A strong alkaline reaction to phenolphthalein indicates the absence of acid phosphates. Silver-nitrate reagent produces specks of both yellow and white precipitate, indicating the presence of orthophosphate (yellow precipitate) and other phosphates (white precipitate). The latter may be metaphosphates, pyrophosphates, or polyphosphates.

"With this possibility in mind, an attempt was made to analyze the sample in accordance with a method given by Loren T. Jones, *Industrial and Engineering Chemistry*, Analytical Edition, Vol. 14, p. 536, 1942. Very poor separations were obtained, as shown by the fact that the summation of the various phosphates determined by this method exceeds the total phosphate found by direct chemical analysis. No explanation is available for this discrepancy which was duplicated on a check run. Results follow:

	Per cent by weight
Orthophosphate as P_2O_5	32.4
Hexametaphosphate as P_2O_5	6.9
Trimetaphosphate as P_2O_5	25.6
Pyrophosphate as P_2O_5	4.9
Polyphosphates as P_2O_5	None
Total	69.8
Total phosphate as P_2O_5	41.2

TABLE 8 TEST RUN ON BOILER SHOWN IN FIG. 3, AT CONSTANT HEAT INPUT

Time Hours	Boiler Temp ° F	NaOH	PO_4	NaCl	pH
16	600	256	900	306	11.5
18	620	305	865	301	11.5
20	620	323	850	306	11.6
23	620	317	800	306	11.6
40	620	390	750	306	11.6
43	620	440	750	306	11.6
45	650	482	660	315	11.6
48	650	530	590	315	11.6
64	650	585	500	301	11.7
68	670	598	240	306	11.7
72	670	585	260	315	11.8
93	600	420	680	301	11.7
113	600	438	660	295	11.8
117	660	560	500	340	11.8
120	660	550	480	335	11.8

"A critical examination of the method used and the results obtained, suggest that the error lies in the determination of the ortho- and trimetaphosphate, since polyphosphates are absent, and the precipitation of hexametaphosphate and pyrophosphate seems quite straightforward. Assuming the latter determinations to be correct, and remembering that polyphosphates are absent, the per cent of ortho and trimetaphosphate may be calculated from the Na_2O to P_2O_5 ratio.

"This calculation gives the following results, which are not capable of analytical proof, but which are considered to be a reasonable approximation of the composition of the sample:

	Per cent by weight
Sodium Hexametaphosphate . . .	9.9
Sodium Pyrophosphate.	9.2
Sodium Orthophosphate.	54.4
Sodium Trimetaphosphate	8.5"

Study of Effect of Rate of Heat Input

To study further the effect of rate of heat input, a different design of boiler was used, Fig. 3. The heat is furnished by means of immersion heaters fitted inside of sealed tubes placed inside a drum. The rate of heat input was 10,000 Btu per sq ft per hr, which was lower than on boiler No. 1. The water passes around the tubes. Table 8 gives the results of the test using this boiler. These results again show that at about 620 F there is a reduction in the PO_4 content with an increase in the hydroxide, and no change in the chloride. The change in the phosphate was less than in the other boiler and there was a higher residual phosphate content at the higher temperatures than found when operating the boiler shown in Fig. 1.

Results of Tests

With the small amount of data collected to date, it is rather difficult to draw very definite conclusions. The general trends may be summarized as follows:

1 At the boiler temperatures encountered in the pressure range of 1700 psi and above, there is present a stable insoluble sodium phosphate which will form as a deposit on the heating surface.

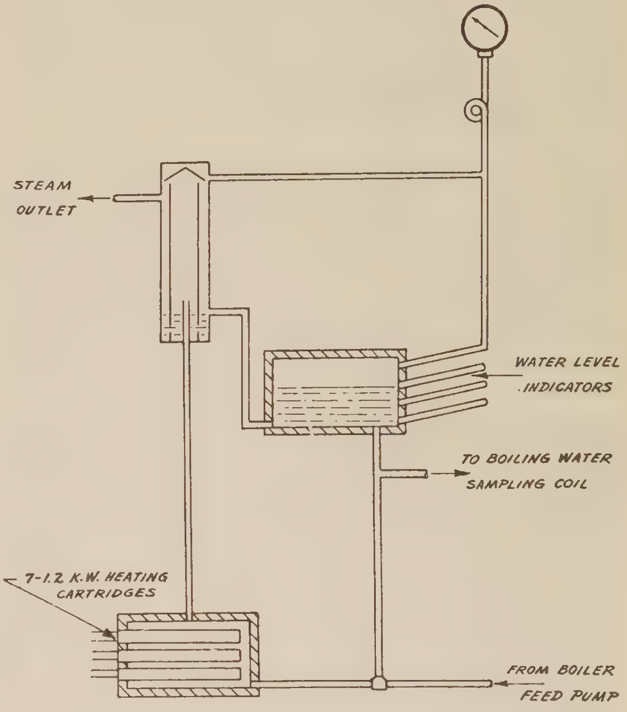

Fig. 3 High-Pressure Boiler Used in Tests

2 Anything which tends to raise the boiler-water temperature will precipitate more of this slightly soluble phosphate from solution. Thus a heavy deposit of calcium phosphate at the heating surface will raise the water temperature at this location and cause precipitation of the insoluble sodium phosphate, which in turn will retard heat transfer and cause still higher temperatures and more deposit. A high rate of heat input may cause temperature increase and start the deposition of the phosphate.

3 The potassium phosphate does not form an insoluble salt at these temperatures. If the ratio of sodium to potassium can be kept low, it is possible to use potassium salts instead of sodium and thus stop the occurrence of this precipitation.

Discussion

Robert C. Adams.[2] The author has disclosed what may be a perplexing problem in operation of high-pressure boilers. Considerably more information may be obtainable from his test results to aid other investigators in the recognition and correction of the condition he describes.

He postulates the formation of an insoluble sodium phosphate having a Na_2O:P_2O_5 ratio less than 3. In both layers of the deposit corresponding to Table 5, and in the deposit on tubes 7 and 9, this ratio was reasonably uniform, ranging between 2.06 and 2.20. This suggests the deposition of a disodium phosphate. Some support for this idea can be deduced from the deposit in the run with added sulphate, corresponding to Table 4. If all the sulphate is assumed to be combined as Na_2SO_4, the molecular ratio of the remaining sodium to phosphate is 2.34—only slightly higher than the above ratio.

This tentative confirmation is canceled, however, by the x-ray diffraction examination of the sodium-sulphate-phosphate deposit. The quoted report implies the formation of a single, crystalline compound, with neither sodium sulphate nor disodium phosphate present in recognizable form.

If the postulated compound exists, it should be possible to isolate and identify it in the deposits. The crystallographic approach should be more effective for this purpose than sole dependence on chemical analysis. The writer would urge the author to employ the petrographic microscope and x-ray diffraction for examination of all such deposits. The data from such examination, even though inconclusive in themselves, if presented systematically, would be most helpful to subsequent investigators. The joint study thus possible should lead to diagnosis and solution of the problem posed by the author.

I. B. Dick.[3] The writer has some knowledge of one of the boilers referred to by Professor Straub in the first paragraph of his paper. It is substantially the same as that described in *Combustion*, August, 1943, pp. 28–34. Designed maximum steam generation is 1,000,000 lb per hr at 1742.5 psig drum pressure. Furnace volume is 54,400 cu ft, and calculated heat liberation at 1,000,000 lb per hr steam flow is 22,100 Btu per cu ft. Water-cooled furnace is formed of bifurcated tubes, 3 in. OD on $3^1/_8$ in. centers.

A hide-out condition was known to exist in this boiler, but no difficulty was experienced in keeping about 30 ppm of Na_3PO_4 in the boiler water. Phosphate, supplied directly to the boiler drum through a separate chemical distributor, was added as a solution of monosodium phosphate. Usage was very moderate, causing no especial concern about the known hide-out condition. The known hide-out amounted to about 100 ppm as Na_3PO_4, which reappeared in the boiler water whenever pressure or rating were decreased about 20 per cent or more.

Following the loss of a wall tube in this unit, samples of boiler water taken while the boiler was dropping off line showed that the phosphate concentration reached a maximum of 800 ppm at about 600 psi and no load, at which point the free caustic soda in the boiler water had completely disappeared, and the water was slightly less alkaline than a solution of Na_3PO_4. Customary limits for free NaOH are from 30 to 50 ppm. It appeared, therefore, that an *acid* phosphate was going back into solution.

This poses several questions:

1 In what manner can an acid phosphate be laid down from a boiler water containing at all times at least 30 ppm free NaOH?

2 Under what conditions of operation can such a phosphate be laid down?

3 What would such an acid phosphate be?

4 Under what conditions would it reappear in solution?

5 How can this condition be corrected?

Professor Straub has contributed toward answering some of these questions. From all available information we construct a picture very much like this:

Acid phosphate cannot be laid down from a strongly alkaline water. Therefore in some manner the phosphate must be out of contact with the boiler water. Since the solubility of TSP is greater at operating temperature than the amount carried in the boiler water, it is evident the first precipitation must have occurred at temperatures in excess of saturation. Somehow this precipitated phosphate, which must at first be crystalline trisodium phosphate, is then converted into an acid phosphate.

There are two theories for the conversion to the acid phosphate, the one which has just been described by Dr. Partridge, and the other that has been alluded to in Professor Straub's paper, involving the formation of pyrophosphates or metaphosphates.

We hold no briefs for either of these two theories.

Since we now have two possible mechanisms for the acid phosphate to have been formed, it is apparent that such a phosphate will go back into solution whenever it is contacted with water at such temperatures that it has definite solubility. Here the observed pressure of about 1300 psi enters the picture, but the limited knowledge of the chemistry of the phosphates at temperatures in the range of 575 F impedes our applying this observation.

The remedy for the condition appears twofold:

1 So operate the unit as to permit frequent removal of precipitated soluble phosphates.

2 So treat the boiler water that the phosphates will not precipitate.

This, however, is another story.

In closing, the writer wishes to say that he believes Mr. Webb, in discussing this paper, is contributing substantially to our knowledge, and so to our food for thought, by reporting on the experiences of the American Gas and Electric Service Corporation in boilers of the 2000 psi class. It is hoped he will continue to do so.

E. P. Partridge and R. K. Scott.[4] It is naturally pleasing to us to have Professor Straub confirm in the laboratory the fact that potassium phosphate does not hide out under conditions simulating a "hot spot" in a high-pressure boiler. We accept his data with gratitude; at the same time we wish to present some interpretations differing in detail from those expressed or implied in his paper.

It might be mentioned that in designing his laboratory boiler, Professor Straub has duplicated faithfully, if unwittingly, a boiler in which gross hide-out of sodium phosphate was observed some fourteen years ago. This was the mercury condenser of the mercury-steam unit at Schenectady. Long nipples, closed at the bottom, projected downward from a horizontal tube sheet. An inner tube within each nipple was intended to act as a downtake. Mercury condensing outside of the nipples boiled the water within them, producing steam at a pressure of 425 psi. Deposits found in these nipples in 1935 were half insoluble sludge, half water-soluble salts, with sodium sulphate predominating over trisodium phosphate. Over week-end shutdowns, the sulphate and phosphate in the boiler water increased markedly.

In an attempt to improve circulation, pairs of nipples were connected together at the bottom to form U-tubes, but not until condensate was used for make-up was satisfactory operation attained. Later, in 1939, deposits found after a period of operation at increased load were essentially trisodium phosphate with less than 10 per cent of insoluble sludge constituents.

---

[2] Superintendent, Chemical Engineering Laboratory, U. S. Naval Engineering Experiment Station, Annapolis, Maryland.

[3] Division Engineer, Consolidated Edison Company of New York, Inc., New York, N. Y.

[4] Hall Laboratories, Inc., Pittsburgh, Pa.

At the temperature of 450 F corresponding to 425 psi, it would have been necessary for the water in the nipples to concentrate until it contained 45 parts of Na_3PO_4 in 100 parts of water before the solid could be deposited (1).[5]

With respect to the changes in concentration of sodium hydroxide accompanying hide-out and redissolving of trisodium phosphate in the water of the experimental boiler, we believe there is an explanation both more simple and more sound than the one implied by the long quotation in the paper by Professor Straub. From the data given in his paper it is evident that concentrated trisodium phosphate actually did react with the steel of his boiler to produce ferrous phosphate, either as such, or combined as sodium ferrous phosphate, at the same time releasing sodium hydroxide. The reaction would be represented in simple over-all form as

$$2Na_3PO_4 + 3Fe + 6H_2O \rightarrow Fe_3(PO_4)_2 + 6NaOH + 6H$$

The ferrous phosphate, stable in contact with the concentrated solution, would, however, hydrolyze as water of the normal low concentration washed over it at lower temperatures, with the resulting reversal of the reaction

$$Fe_3(PO_4)_2 + 6H_2O \rightarrow 3Fe(OH)_2 + 2H_3PO_4$$

$$2H_3PO_4 + 6NaOH \rightarrow 2Na_3PO_4 + 6H_2O$$

in which sodium hydroxide is used up. The ferrous hydroxide would normally be converted further into black magnetic Fe_3O_4.

The suggestion that molecularly dehydrated phosphates were formed from trisodium phosphate in the experimental boiler is based chiefly on the analytical results obtained by the Jones method. However, the report quoted in the paper shows that total P_2O_5 obtained by adding up the various constituents "determined" by this method was 70 per cent greater than total P_2O_5 determined directly. From our fairly comprehensive knowledge of the phosphates as well as of the vagaries of the Jones method for the analysis of sodium phosphates, which would be aggravated in this case by the presence of considerable amounts of iron, we would conclude that metaphosphate and pyrophosphate need not have been present in the deposit.

At the ASME Annual Meeting six years ago, R. E. Hall presented his detailed paper (2) in which he pointed out the several ways in which the substitution of potassium for sodium ion in a boiler water should prove beneficial. With respect to hide-out, he mentioned the favorable experience in one plant where, under conditioning with sodium chemicals, "Both the sulphate and the phosphate skyrocketed when boiler load was reduced." After conditioning with potassium chemicals had been established, successive tests showed "complete absence of sulphate hide-out, and elimination of all but the barest trace of phosphate hide-out."

Subsequently, hide-out of sulphate and phosphate in the 2000-psi forced-circulation boiler at Somerset Station ceased when conditioning with potassium chemicals was commenced, as reported at the Annual Meeting four years ago (3). It was pointed out that the control limits for this boiler since the beginning of 1944 had included the maintenance of a minimum ratio of potassium to sodium in epm of 3:1. This would mean a concentration of sodium (Na) in ppm not exceeding 0.2 times the concentration of potassium (K) in ppm.

Professor Straub may have been influenced by this and by similar reports from the field, not yet published, to undertake the experiments set forth in his paper. Like Kaufman and his associates (4) he has succeeded in confirming in the laboratory the fact that sodium phosphate hides out, while potassium phosphate does not. He has even reached the same conclusion as Hall (5), that 1 epm of Na can be present in the boiler water for each 3 epm of K without losing the improved behavior characteristic of full potassium conditioning.

When Professor Straub discussed the original paper by Hall six years ago, he urged caution and said, "The real importance of the suggested potassium substitution for sodium will depend upon the results obtained in actual operation," a dictum with which we thoroughly agree. With his knowledge of practical operating results in several plants during recent years, reinforced by the results of his laboratory tests, would Professor Straub now recommend potassium conditioning generally for high-pressure boilers afflicted with hide-out?

Hall and his associates continue to feel that potassium conditioning offers considerable promise as a treatment for the boiler disease of which hide-out is a symptom. In mild cases of this disease, an occasional good physic in the form of acid cleaning may suffice; where more severe conditions exist, the continuous mild laxative of potassium conditioning has paid for itself by keeping boilers on the line for longer periods than would otherwise have been possible. But when the disease is organic, surgery may be necessary for a boiler as for a human being. Let us consider some pertinent data.

According to the solubility studies of Schroeder and his associates (1), both trisodium phosphate and sodium sulphate become progressively less soluble as the temperature is increased beyond about 250 and 465 F, respectively. While each is substantially insoluble at the critical temperature of 705 F, nevertheless the amount which can be present in a normal boiler water is far greater than the solubility of most substances which form deposits in boilers. For example, the process of concentration in a boiler water at 1700 psi would have to proceed until 10,000 parts of Na_3PO_4 or more than 100,000 parts of Na_2SO_4 were present in a million parts of H_2O before the first crystal of solid could form. If the original dilute boiler water contained about the same amount of NaOH as of the salt, the limiting values would be even higher.

For trisodium phosphate or sodium sulphate to disappear from solution in boiler water by simple hide-out thus requires the development on some localized area of the boiler heat-transfer surface of a concentrated solution expressed more conveniently in per cent than in parts per million—a brine rather than a boiler water.

If the tube surface is hot enough to cause the concentrating film upon it to become saturated with trisodium phosphate, it is inevitably hot enough to cause continuing deposition of this substance as solid from the boiler water passing through the tube. The main body of boiler water is thus progressively robbed of phosphate as long as the local heat input remains sufficiently high.

The accumulation of solid may cause failure of the tube by simple overheating; wherever the deposit does not completely cover the steel, attack by the concentrated brine would also be likely, according to the experiments of Kaufman and his associates (4) as well as those of Professor Straub reported in the present paper.

What happens if, in a 1700-psi boiler which has consistently developed severe hide-out of sodium phosphate, we substitute potassium ion for sodium ion? The physical conditions which caused the boiler water to concentrate somewhere on strongly-heated tube surfaces remain the same, but instead of automatic deposition of solid when the local concentration attains 10,000 ppm of Na_3PO_4, the amount of K_3PO_4 in the concentrating film can increase without limit to whatever level is determined by the temperature produced in the film. The completely fluid condition maintained at the metal surface is advantageous in several respects. It does not interpose the increasing resistance to heat transfer and to fluid flow of a growing deposit of solid, and it does mingle rapidly with the normal dilute boiler water at every opportunity. The over-all effect in a number of boilers has been to prolong the life of the heat-transfer surfaces. If the local input of heat is high enough, however, the steel will be attacked by the water containing potassium salts just as it would by the water containing sodium salts, or, for that matter, by the purest water ever evaporated in a boiler.

---

[5] Numbers in parentheses refer to the Bibliography at the end of this discussion.

Hall (2) has pointed out how the corrosivity of the concentrating film may be decreased by keeping the chloride high in relation to the hydroxide in the boiler water, or by eliminating free hydroxide altogether and operating with only captive alkalinity. By such expedients much has been done to make the patient more comfortable.

Recently an impressive start has been made on investigations which could lead to prevention of the disease of which hide-out is a symptom. Studies of heat absorption in boiler furnaces, such as those at Tidd Station (6) and at Paddy's Run Station (7) can lead not only to greater efficiency in the utilization of heat, but also to decreased damage to the heat-transfer surfaces when we learn how to distribute the heat more uniformly to them.

BIBLIOGRAPHY

1 "Solubility Equilibria of Sodium Sulfate at Temperatures of 150 to 350° C. I. Effect of Sodium Hydroxide and Sodium Chloride," by W. C. Schroeder, A. Gabriel, and E. P. Partridge, *Journal of the American Chemical Society*, vol. 57, pp. 1539–46 (1935); "III. Effect of Sodium Hydroxide and Sodium Phosphate," by W. C. Schroeder, A. A. Berk, and A. Gabriel, *ibid.*, vol. 59, pp. 1783–1790 (1937).

2 "A New Approach to the Problem of Conditioning Water for Steam Generation," by R. E. Hall, Trans. ASME, vol. 66, 1944, pp. 457–488.

3 "Water Conditioning for the 2000-Psi Boiler at the Somerset Station of Montaup Electric Company," by W. W. Cerna and R. K. Scott, Trans. ASME, vol. 68, 1946, pp. 443–451.

4 "The Behavior of Highly Concentrated Boiler Water," by C. E. Kaufman, V. M. Marcy, and W. H. Trautman, Proceedings of the Sixth Annual Water Conference, Engineers Society of Western Pennsylvania, 1945, pp. 23–49.

5 "Treatment of Steam Boiler Water," R. E. Hall, U. S. Patent 2,476,598, July 19, 1949.

6 "An Investigation of the Variation in Heat Absorption in a Pulverized-Coal-Fired Water-Cooled Steam-Boiler Furnace. I. Variations in Heat Absorption as Shown by Measurement of Surface Temperature of Exposed Side of Furnace Tubes," by L. B. Schueler, Trans. ASME, vol. 70, 1948, pp. 553–567.

7 "Furnace Heat Absorption in Pulverized-Coal-Fired Steam Generator, Using Turbulent Burners at Paddy's Run Station, Louisville, Ky. Part I. Variation in Heat Absorption as Shown by Measurement of Surface Temperature of Exposed Side of Furnace Tubes," by R. I. Wheater and M. H. Howard. Presented at 1949 Annual Meeting, ASME, New York, N. Y., Nov. 27–Dec. 2, 1949. To be published in a later issue of the Transactions of the ASME.

W. L. Webb.[6] The author is to be commended for presenting data showing what may result from endeavoring to maintain high phosphate concentrations in boiler water when conditions are such to permit sodium phosphate hide-out. This paper indicates the inadvisability of feeding chemicals without establishing what becomes of them.

Based on the experience of the company with which the discusser is associated, it is more usual than unusual to find some degree of sodium phosphate hide-out in boilers of the 1200–1400 psi range. In such cases the phosphate feed is rigidly limited to restrict the quantity of hide-out. This results in substantially maintaining equilibrium PO_4 residuals which in the more serious cases may range from less than 1 ppm to perhaps 10 ppm.

Residual phosphate is customarily maintained in the boiler water not only to precipitate the small amount of hardness which normally enters the cycle with evaporator vapor and condenser leakage, but also to properly precipitate unusual surges of contamination, for example, from the priming of an evaporator or from the splitting of a condenser tube. The quantity of water in an operating boiler and the PO_4 residual in the boiler water establishes the number of pounds of phosphate available for precipitating incoming hardness. When this is limited by a low equilibrium PO_4 value by virtue of a hide-out condition, the objective of maintaining residual phosphate is partly defeated.

Disappearance of phosphate due to other than consumption by cycle contamination and losses by blowdown should be distinguished from actual hide-out. For example, following the acid-cleaning of a boiler there may be phosphate consumption in reforming a film on the freshly cleaned boiler metal. The extent of this consumption may be influenced by the type of so-called "conditioning boil" or boiler metal surface treatment which normally follows the rinsing operation after draining the acid solvent.

In case of extensive phosphate disappearance, particularly following acid-cleaning, it is considered good practice to make a careful check of the phosphate which returns to solution upon load reduction to definitely establish the existence of hide-out, and if it exists to limit the quantity hid out. Furthermore, the change in boiler-water alkalinity accompanying the return of phosphate to solution may give some clue to the form of phosphate hide-out. It may be of interest that in several cases boilers in which actual hide-out previously had not been observed have shown hide-out for periods of several months or longer after acid-cleaning. Why this condition should exist is not yet clear.

Following the acid-cleaning in April, 1949, of the Indiana and Michigan Electric Company's 2300-psi boiler at Twin Branch Plant, phosphate consumption was extensive and also hide-out existed to the extent that the equilibrium PO_4 value was less than 2 ppm Previous to this acid-cleaning, hide-out had limited the PO_4 concentration to 8 to 10 ppm. As this new condition still existed in June, it was decided as an experiment, to see if hide-out could be prevented by the use of potassium chemicals. Phosphoric acid and potassium hydroxide were used because of the ease of control of both PO_4 and alkalinity in the boiler water. Potassium chloride was also employed both to assist in the control of the potassium-sodium ratio and to permit the use of the Cl concentration as a measure of the equivalent quantity of water in the boiler and for approximating blowdown.

Upon raising the K/Na epm ratio to about 1.5 (Na:K weight ratio of about 0.4:1) no phosphate returned to solution, presumably because the PO_4 residual of 1 to 2 ppm had been sufficient to prevent hide-out. However, SO_4 increased from 5 to 43 ppm. A further increase in the potassium concentration was accompanied by reappearance of no additional hid-out chemicals.

In a subsequent test just before the 2300-psi boiler was shut down for an extended period, the sodium concentration was progressively increased by the feeding of NaCl in an effort to show at what ratio phosphate and sulphate would start to hide out. At a K/Na epm ratio of about 1.0 (Na:K weight ratio of about 0.6:1), PO_4 decreased from about 24 to 17 ppm but SO_4 remained unchanged at about 29 ppm. A reduction of the ratio to about 0.5 (Na:K weight ratio of 1.2:1) made no appreciable change in either PO_4 or SO_4. By this time the boiler-water dissolved solids were sufficiently high to cause an increase in the conductivity of steam so the ratio was not further reduced.

---

[6] Mechanical Engineering Division, American Gas and Electric Service Corporation, New York, N. Y.

The foregoing experience, as well as that with the 2000-psi boiler at Twin Branch Plant, leads the discusser to suspect that for pressures of this order, possibly 1700 psi and above as indicated by Professor Straub, it may be advisable to employ potassium chemicals for internal treatment solely to prevent phosphate hide-out, particularly if hide-out seriously limits PO_4 residuals. Further data on the 2000-psi boilers shortly to be put into operation at the Philip Sporn Plant may permit conclusions to be more definitely drawn.

Chemical Treatment, Demineralization, or Evaporation for Make-Up in High-Pressure By-Product Steam Plants

By J. D. YODER,[1] W. L. WEBB,[2] and T. BAUMEISTER,[2] NEW YORK, N. Y.

The increased power production obtained by exhausting high-pressure turbines directly to process rather than to coils of evaporators, which in turn produce process steam, is demonstrated. Typical heat balances are presented for systems employing evaporated make-up to the closed cycle and for 100 per cent make-up cycles using water treatments consisting of (*a*) silica removal and sodium-zeolite softening, and (*b*) demineralization and silica absorption. Performance data and costs are given for both evaporated make-up and 100 per cent treated make-up 1400-psi cycles at the Deepwater Operating Company's station.

Introduction

POWER manufactured as a by-product of process steam offers the lowest cost for fuel in mills per kilowatthour obtainable from any type of power plant. The most efficient high-pressure power plant which is devoid of the by-product feature and which delivers only one product—kilowatthours as electric energy—still wastes, as low-grade heat in cooling water of the condenser system, approximately 50 per cent of the heat supplied in fuel. The lowest heat rate as yet anticipated for a central station is 9300 Btu per net kwhr for the Philip Sporn Station.[3]

The lowest heat rate of plants now in operation is of the order of 10,000 Btu per net kwhr which represents a loss of 66 per cent of the heat supplied in the fuel. This waste or loss of heat is chiefly to the condensing water and the remainder is sensible heat of stack gases, combustion imperfections, hydrogen losses, mechanical and electrical losses, auxiliary power requirements, and other incidental and generally unaccounted-for items.

Utilizing Exhaust Steam for Process

The utilization of exhaust steam for process makes possible the avoidance of the heat loss to the cooling water. This is accomplished by using (1) high-pressure turbine exhausting to evaporator coils, which in turn deliver process steam at some practical lower pressure, or (2) high-pressure turbines exhausting directly to the process headers. Either method avoids the Btu loss to the condenser cooling water. The evaporators, however, do not permit the use of the full availability of heat for conversion into work, because the heat delivered to the evaporator coils is degraded by heat exchange to a lower steam pressure for process purposes. This greatly reduces the ratio of available low-cost by-product power to process steam.

When turbines exhaust directly to process, power is generated through the full steam expansion from boiler pressure to process steam pressure. The heat rate approaches the theoretical factor for the conversion of heat into mechanical energy, or 3413 Btu per kwhr.

The major advantage of delivering exhaust steam to an evaporator instead of directly to process is that it permits the return of the condensed steam from the evaporator coils to the boiler feed system without further treatment. The requirements of the power cycle for make-up water are consequently comparable to those of a surface-condensing plant and are of the order of 1 or 2 per cent. This amount is readily supplied by a small-capacity evaporator.

When the turbine exhaust is delivered directly to process, it is necessary to prepare substantially 100 per cent treated make-up water for feed to the boilers. When high-pressure boilers were first installed to supply process steam under these conditions, designing engineers did not believe that the boilers could be operated successfully with 100 per cent treated make-up. With the accumulation of experience, however, it has been demonstrated that 100 per cent treated make-up can be fed even to high-pressure boilers (1400 psi) without operating hazard and with the advantage of the greatly increased by-product power rate.

When an industrial plant installs a high-pressure turbine to exhaust its steam to process, the boiler pressure is generally selected to balance the required power and process-steam demands, thus utilizing the maximum potential by-product power generation. This frequently results in installing 600-psi boilers where more low-cost power could be produced with a higher pressure such as 1400 psi.

When a public utility enters into an agreement to supply both process steam and power to an industrial plant, it is reasonable economy to install boilers to operate at maximum pressures, because any excess power produced by the turbine may be used advantageously by the utility to reduce its over-all cost of generation.

It is the purpose of this paper (1) to emphasize the greater amount of low-heat-rate by-product power which can be generated when turbines are exhausted directly to process rather than to evaporator coils; (2) to present operating data for a 1400-psi plant to substantiate these conclusions, and (3) to demonstrate the satisfactory chemical treatment of water for these conditions.

Fig. 1 illustrates the heat rate in Btu per kwhr, for an efficient condensing plant as compared to the heat rate of by-product power plants when the turbine exhausts (1) to evaporator coils, and (2) directly to process. The plant heat rate with a process evaporator is less than one half of the heat rate for a surface-condensing installation. The heat rate for the case of turbines exhausting directly to process and using softened or demineralized feedwater is, in turn, somewhat less than with process evaporators.

---

[1] Vice-President, The Permutit Company. Mem. ASME.

[2] Mechanical Engineering Division, American Gas and Electric Service Corporation. Mem. ASME.

[3] "The 2000-Psi, 1050 F, and 1000 F Reheat Cycle at the Philip Sporn and Twin Branch Steam-Electric Stations," by Philip Sporn, Trans. ASME, vol. 70, 1948, pp. 287–294.

Contributed by the Joint Research Committee on Boiler Feedwater Studies and Power Division and presented at the Annual Meeting, New York, N. Y., November 27–December 2, 1949, of The American Society of Mechanical Engineers.

Note: Statements and opinions advanced in papers are to be understood as individual expressions of their authors and not those of the Society. Paper No. 49—A-71.

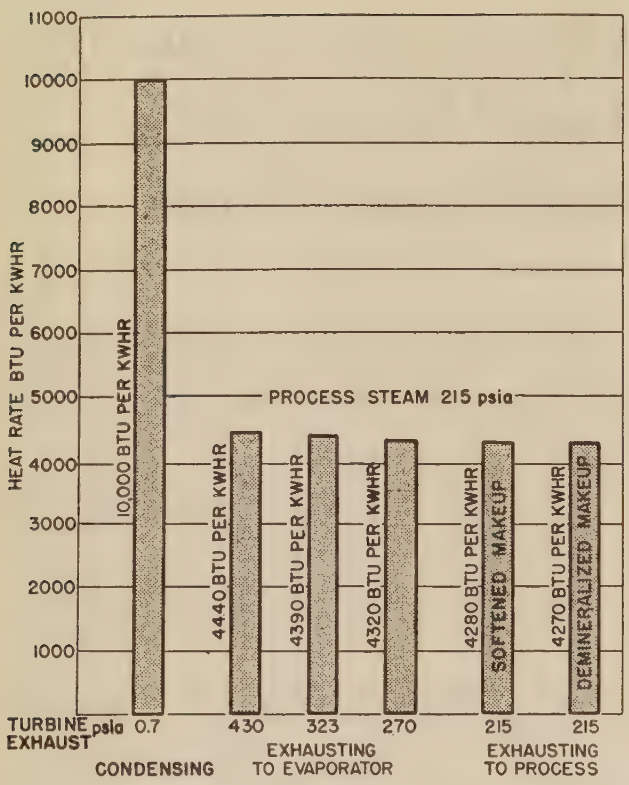

Fig. 1 Plant Heat Rates of 1300 Psia, 760 F Turbine Unit When Exhausting to a Condenser, to Evaporator Coils, or Directly to Process

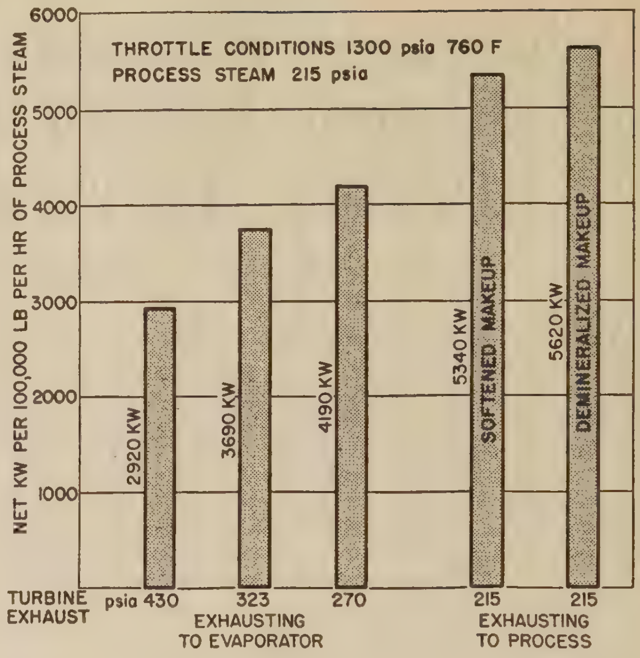

Fig. 2 Comparative Power Outputs for Alternate Types of By-Product Plants

Advantage of Exhausting Directly to Process

The great advantage of exhausting turbines directly to process instead of to evaporator coils is the greater amount of low-fuel-cost power that can be produced. This is illustrated in Fig. 2. Here the relative amounts of by-product power which can be produced with 1400-psi boiler steam for 100,000 lb per hr of 215-psia process steam are shown for (*a*) turbines exhausting to evaporator coils, (*b*) turbines exhausting directly to process and using (1) softened or (2) demineralized make-up.

The power, when using evaporators at a constant vapor pressure, increases as the differential in pressure between evaporator coils and process steam diminishes, or as the mean temperature difference across the evaporator surface is decreased. The amount of heating surface needed in the evaporator coils increases as the pressure or temperature differential becomes less, which correspondingly increases the cost of evaporators.

The chart indicates that when the turbine exhausts at 430 psia to the evaporator coils, the turbine produces 2920 kw of by-product power as compared with 4190 kw when exhausting the turbine at 270 psia. When the turbine exhausts to process and the feedwater is softened, as described later in this paper, the by-product power is 5340 kw, and, if the make-up water were demineralized, the available by-product power would be 5620 kw. The increased power generated, when using demineralized instead of softened make-up, results from less boiler blowoff and therefore less degradation of heat.

The heat-balance diagrams, Figs. 3 through 7, show the basic data for these graphs. The comparative study reflected in these data was greatly simplified by the requirement that process steam under all alternates be delivered at 215 psia and substantially saturated conditions. The heat rates and the amounts of by-product power illustrated in Figs. 1 and 2 were thus determined by the feed cycles and heat balances of Figs. 3 through 7. In the preparation of these figures the following underlying performance estimates were used:

Performance Estimates

1 Process steam conditions, 215 psia dry and saturated.

2 Steam conditions at turbine throttle, 1300 psia, 760 F, and 1347 Btu per lb.

3 (*a*) Internal efficiency of main turbine, 80 per cent.

(*b*) Internal efficiency of heating turbine, 72 per cent.

4 (*a*) Exhaust pressure loss from main turbine shell to evaporator, to heating turbine, to heaters No. 1 and No. 3 or to station wall, 7 per cent.

(*b*) Extraction pressure loss from heating turbine to heater No. 2, 10 per cent.

5 Mechanical and electrical losses, 3 per cent of gross power generated.

6 Gland steam enthalpy, the throttle enthalpy minus 25 per cent of the enthalpy drop in the turbine.

7 Auxiliary power for the generating plant for all conditions, 6 per cent of the gross power generation obtainable with a condensing turbine operating at the given throttle conditions and flow, with a 10 lb per kwhr water rate.

8 Boiler efficiency for power and process steam generation, 87 per cent.

9 Steam losses, 5000 lb per hr.

10 Blowdown losses:

(*a*) From boiler, fed with evaporated make-up, 1500 lb per hr, or approximately $^1/_4$ per cent of boiler output (no heat recovery).

(*b*) From evaporator, 10 per cent of make-up (with heat recovery).

(*c*) From boiler fed with softened water, 21.6 per cent of make-up (with heat recovery).

(*d*) From boiler fed with demineralized water, 2.4 per cent of make-up (with heat recovery).

11 Terminal temperature differences on heat exchanger, closed heaters, and drain coolers taken the same for all conditions and as specified on the diagrams.

12 Cost of process steam computed as the heat in the process steam corrected for boiler efficiency, steam losses, auxiliary power allowance 2 per cent of the heat, and boiler blowoff 10 per cent of make-up (with heat recovery).

Fig. 3 shows a typical cycle diagram for the case of the turbine exhausting to evaporator coils. The heat balance of this figure is based upon operating the turbine at an exhaust pressure of 430 psia, under which condition the amount of by-product power produced per 100,000 lb of process steam was 2920 kw and is so plotted in Fig. 2. Corresponding heat balances for evaporator operation with exhaust pressures of 323 and 270 psia are given in Figs. 4 and 5, respectively.

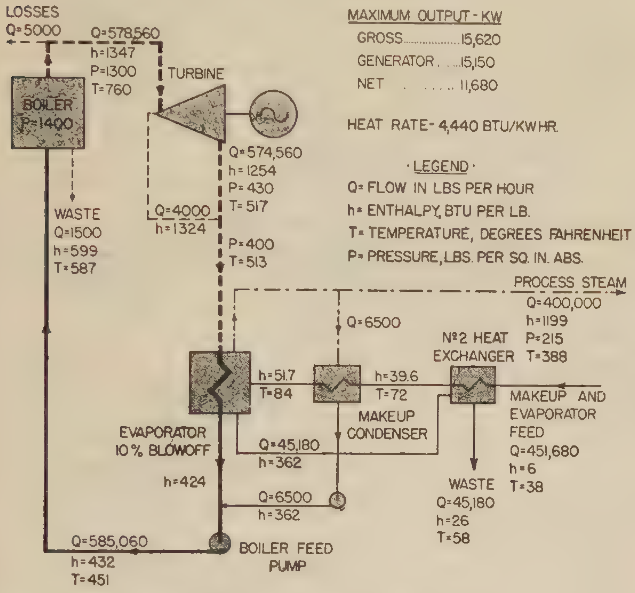

Fig. 3 Heat Balance for High-Pressure Turbine Unit Exhausting at 430 Psia to Evaporator Coils

Fig. 6 is a typical cycle diagram for the delivery of exhaust steam directly from turbine to process and is applicable for the cases of feeding softened or demineralized make-up to the boiler. The heat balance of Fig. 6 is based upon softened make-up water of such analysis as to require a boiler blowdown of 21.6 per cent of make-up. The high-pressure turbine exhausts chiefly to process, but sufficient exhaust steam goes to the heating turbine to complete the heating of the feedwater from 38 F to 390 F. The steam flow through the high-pressure turbine is increased by an amount sufficient to compensate for the inadequacy of boiler blowoff for feed-heating purposes.

Fig. 7 differs from Fig. 6 in that only 2.4 per cent of make-up is blown down from the boiler because of the use of demineralized rather than softened make-up. Since there is less boiler blowoff with demineralized make-up, more steam must pass through the high-pressure turbine to provide the necessary heat in the feedwater. This additional flow increases the by-product power generation. Because less water goes to waste when demineralizing, the heat rate of by-product power is somewhat reduced as illustrated in Fig. 1.

Process-steam installations, similar to those shown in the heat balance, Figs. 3, 4, and 5, in which the high-pressure turbine exhausts to evaporator coils, and in Fig. 6 in which the 100 per cent softened make-up boiler supplies a high-pressure turbine exhausting directly to process, were put into service at the Deepwater Operating Company's Station at Deepwater, N. J., in 1930 and 1942, respectively. Both employ nominally 1400-psi, 725-750 F initial steam conditions at the turbine throttle and supply 215-psia steam to process. No process condensate is returned to the powerhouse from the factory. Raw water separately treated for the two installations is taken from the nearby Salem Canal which is equipped with a valved dam, to prevent salines from the Delaware River from contaminating this surface supply.

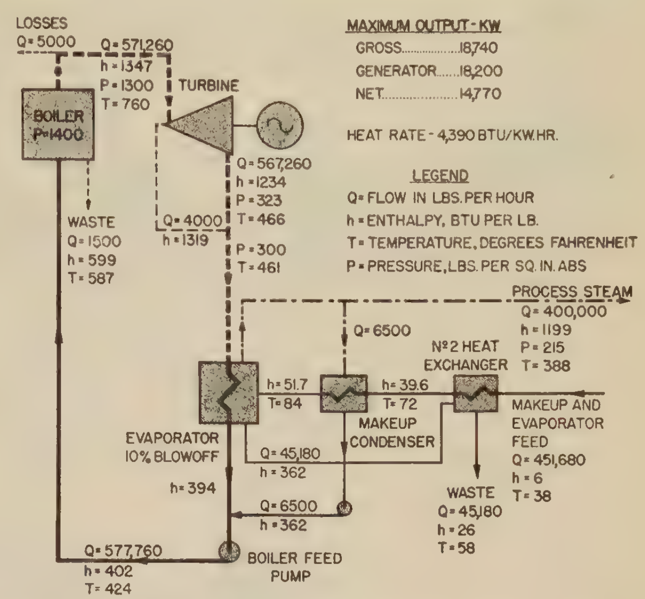

Fig. 4 Heat Balance for High-Pressure Turbine Unit Exhausting at 323 Psia to Evaporator Coils

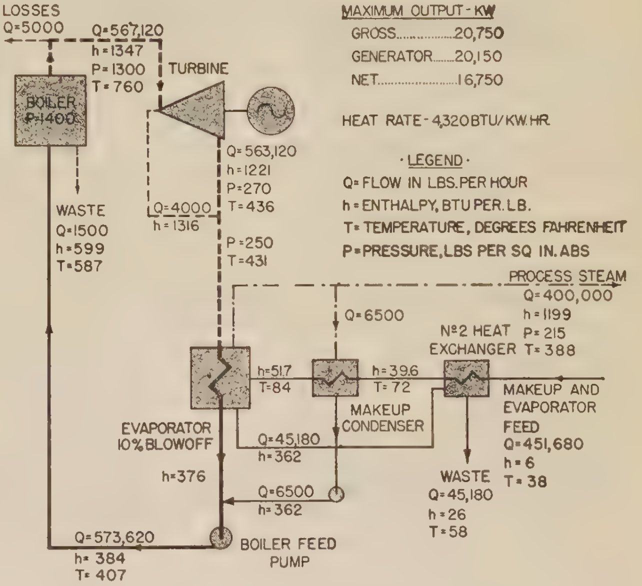

Fig. 5 Heat Balance for High-Pressure Turbine Unit Exhausting at 270 Psia to Evaporator Coils

Deepwater High-Pressure Turbine-Evaporator Unit

The 1930 Deepwater installation consists of two 331,000-lb-per-hr, 725 F cross-drum boilers which supply a 12,500-kw turbine, exhausting to the coils of 7 evaporators, having a combined rated

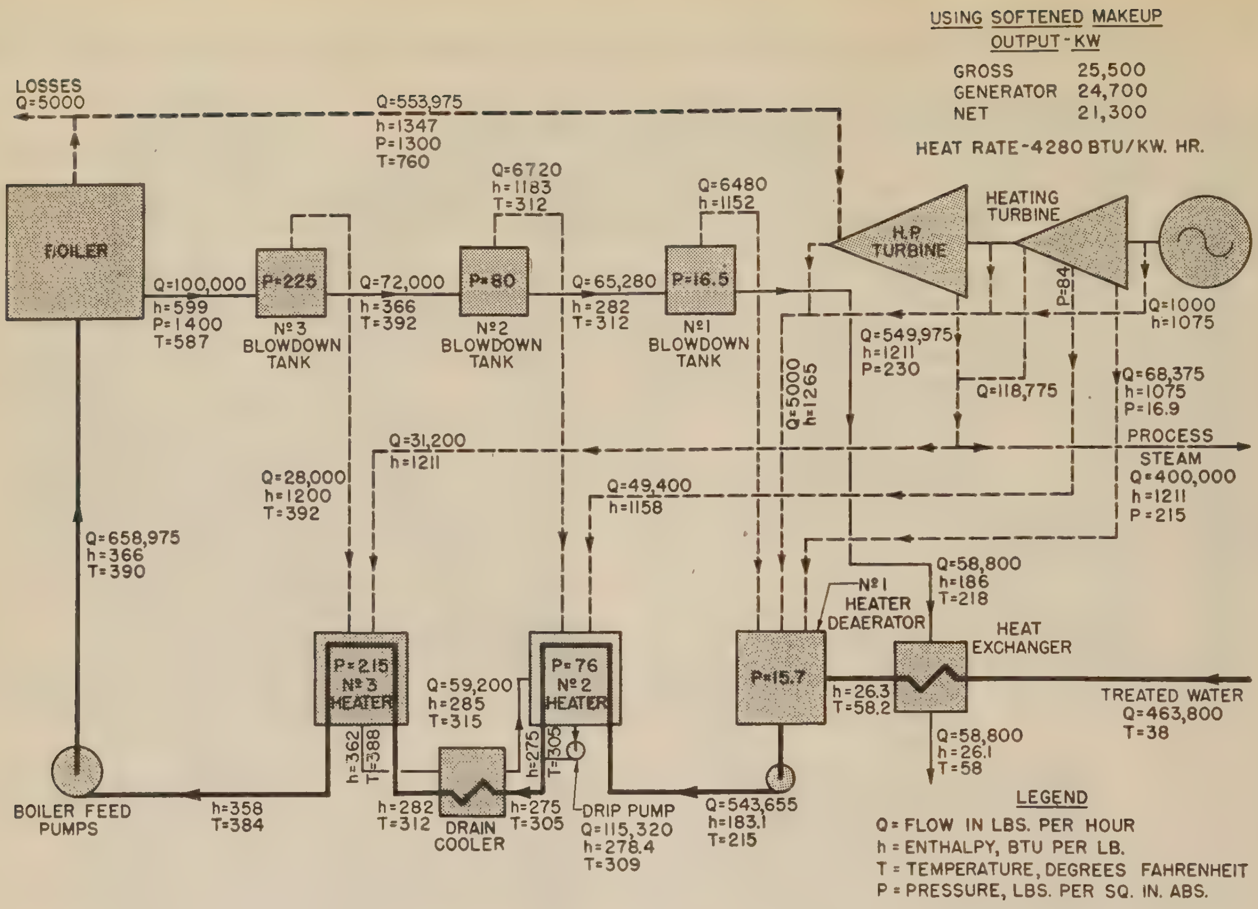

Fig. 6 Heat Balance for 100 Per Cent Softened Make-Up Unit Exhausting Directly to Process

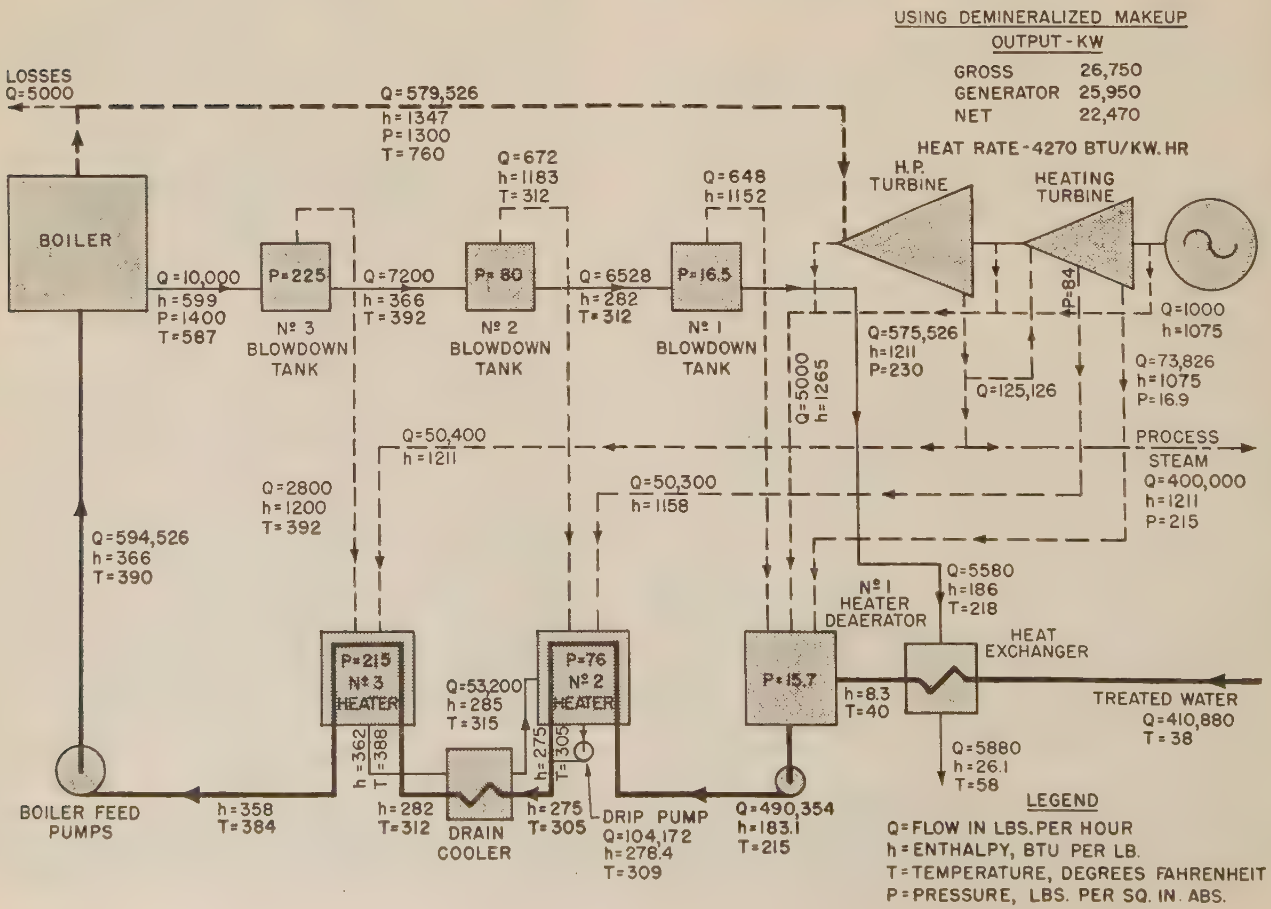

Fig. 7 Heat Balance for 100 Per Cent Demineralized Make-Up Unit Exhausting Directly to Process

TABLE 1 DEEPWATER HIGH-PRESSURE TURBINE—EVAPORATOR UNIT WATER CONDITIONS

Process steam	400,000 lb per hr
Evaporator blowdown	21,000 lb per hr
Blowdown losses	21,000 lb per hr
Evaporator make-up	421,000 lb per hr

	Raw water		Softener effluent		Evaporator shell water	
	(ppm)	(epm)	(ppm)	(epm)	(ppm)	(epm)
Calcium, Ca	19	0.94	1.2	0.06	2	0.10
Magnesium, Mg	7	0.54	0.4	0.04	1	0.08
Sodium, Na	13	0.56	55	2.41	1160	50.50
		2.04		2.51		50.68
Bicarbonate, HCO_3	61	1.00	68	1.11	200	3.28
Carbonate, CO_3	0	0	0	0	540	17.90
Hydroxide, OH	0	0	0	0	0	0
Sulphite, SO_3	0	0	0	0	0	0
Sulphate, SO_4	16	0.34	33	0.69	740	15.40
Chloride, Cl	25	0.70	25	0.71	500	14.10
		2.04		2.51		50.68
Silica, SiO_2	8.6		8.6		124	
Carbon dioxide, CO_2	7		...		...	
Color	25		...		...	
Iron, Fe	1.7		0.2		...	
Total hardness as $CaCO_3$	74	1.48	5	0.10	9	0.18
pH	7.2		8.2		10.4	
Dissolved solids	120		157		3267	
Suspended solids	30		...		113	
Total solids	150		157		3380	

Chemical requirements in terms of treating-plant effluent:

	ppm	¢ per lb	$ per million lb
Ferrous sulphate, 98 per cent $FeSO_4 \cdot 7H_2O$	50	3.0	1.50
Soda ash, 98% Na_2CO_3	25	1.5	0.38
Sodium chloride, 99% NaCl	240	0.6	1.44
Sodium sulphite, 93% Na_2SO_3	6	3.5	0.21
Chemical cost per million lb treated water			$3.53

output of 400,000 lb per hr of 215-psia vapor. Turbine-exhaust pressure varies with load, and with the number of evaporators in service. At rated turbine capacity with 7 evaporators in service, exhaust pressure is approximately 300 psia. Make-up of 1.5 per cent to the 1400-psi cycle is supplied by house evaporators.

Raw water, coagulated and zeolite-softened, is fed to the process evaporators which are continuously blown down. The employment of softened water substantially has eliminated the need for scale-cracking operations. Representative water analyses for this unit are indicated in Table 1.

Deepwater 100 per Cent Softened Make-Up Unit

Prior to undertaking the 1400-psi 100 per cent make-up installation at Deepwater, a pilot-plant test was conducted to establish that the raw water could be treated as contemplated, and that a high-pressure test boiler would operate satisfactorily with only treated-water make-up. This study was described by Carmichael.[4]

In the subsequent 1942 installation the raw water, after treatment for reduction of turbidity, color, silica, and hardness, is fed to a boiler which delivers 550,000 lb per hr of steam at 750 F total temperature. Substantially all the water-cooled surface of this boiler consists of vertical tubes, except the furnace roof and the hopper dry bottom. At full rating, the heat available is 62,000 Btu per hr per sq ft of projected water-cooled furnace area, as compared to 80,000-120,000 Btu per hr per sq ft for boilers of conventional design. Comparative values per cu ft of furnace volume are 13,800 and 18,000-24,000 Btu, respectively. The high-pressure steam is supplied to a 20,000-kw turbine exhausting directly to process.

A schematic diagram of the water-treating plant is shown in Fig. 8. As designed, precipitator No. 1 was for coagulation and color reduction, using ferric sulphate and sulphuric acid at a pH of about 4.5, followed by air agitation for carbon-dioxide removal, and precipitator No. 2 for silica reduction, using ferric sulphate and lime at a pH of 9 to 10. The precipitator effluent flows through gravity filters and is discharged into the clearwell mixing chamber where pH was to have been reduced to 7.5 with sulphuric acid. Pumps transfer water from the clearwell through sodium Zeo-Karb softeners to elevated storage tanks and to the station for boiler make-up. Under this plan of operation, retention in the sedimentation sections of each Spaulding precipitator at rated raw-water flow of 625,000 lb per hr is 170 min.

Operating experience has indicated that sedimentation, and color and silica reduction can be accomplished in one step using ferric sulphate and lime at a pH of 9.2 to 9.6. This permits operating the two precipitators in parallel, thereby doubling the retention time. Because of deposition of slime on precipitator weirs and plugging of filters with organic matter and from carry-over of "wild floc," the raw water is chlorinated. Clay is fed with the lime to assist in weighting the floc.

Contrary to initial expectations that the zeolite material would be subject to attack from waters having pH values of 8 or higher, it has been established that a maximum pH of 10 is satisfactory. Supplementary chemicals consist of caustic soda and sodium sulphite fed at the deaerator discharge, and sodium phosphate and an organic dispersive fed directly to the boiler.

Table 2 indicates representative water conditions of the 100 per cent softened make-up cycle, and the cost of treating chemicals. For comparative purposes, Table 3 presents similar data on the basis of employing demineralization and silica absorption.

During the first 3 years of operation, semiannual outages were necessary for the removal of soft deposits of phosphate sludge and iron oxide from the water-cooled boiler surfaces. Initially this was done mechanically, and later by acid-cleaning. The employment of an organic dispersive in 1945, for maintenance of sludge in suspension, proved to be practically 100 per cent effective. Since 1945 the boiler has been acid-cleaned but once, and then as a precautionary measure. Since feeding the organic material, samples of deposit turbined from selected wall tubes indicated a deposition of some 2 grams per lineal foot of tube, which analyzed about 40 per cent carbon. This seemed to show that there had been some decomposition of the organic dispersive but subsequent examinations showed insufficient deposit to call for any change in treatment.

---

[4] "Experimental Study, Feedwater Treatment for 1400-Lb Boiler Operating Pressure," by D. C. Carmichael, Trans. ASME, vol. 64, 1942, pp. 121–136.

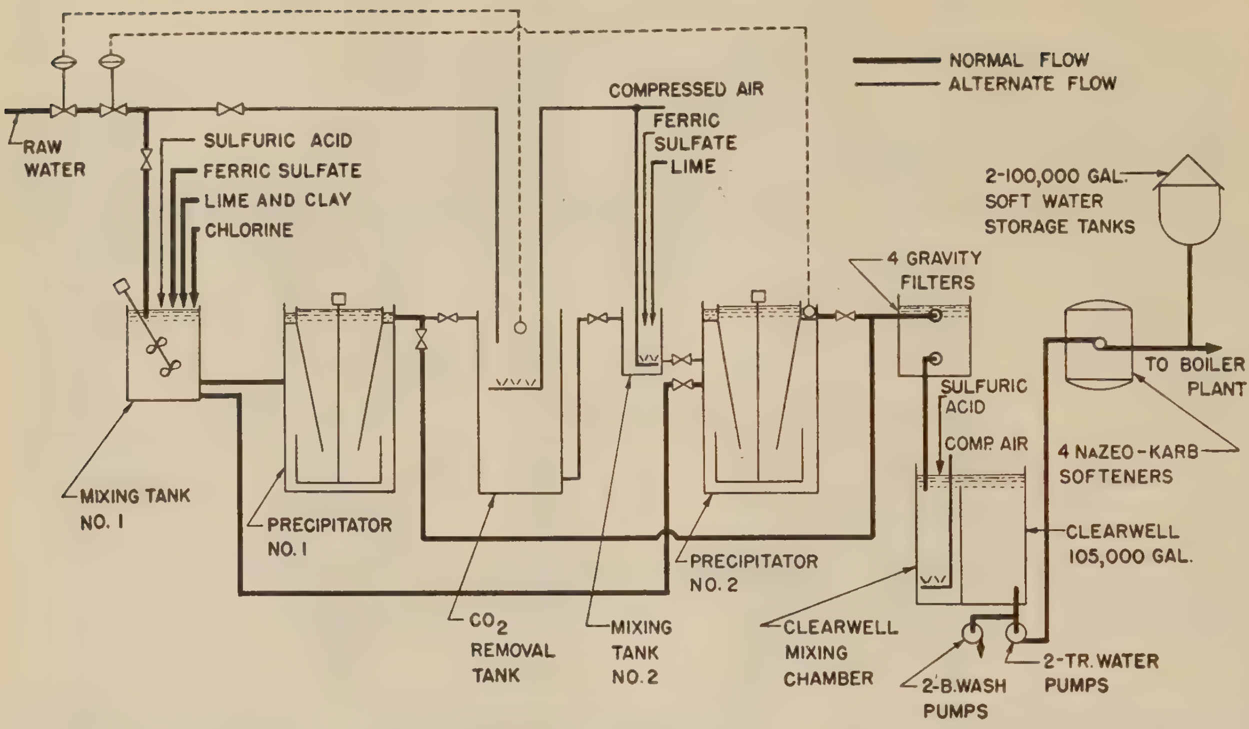

Fig. 8 Schematic Diagram of Water-Treating Plant for the Deepwater 100 Per Cent Softened Make-Up Unit

TABLE 2 DEEPWATER 100 PER CENT SOFTENED MAKE-UP UNIT WATER CONDITIONS

Process steam	400,000 lb per hr
Steam losses	5,000 lb per hr
Boiler blowdown	75,000 lb per hr
Blowdown losses	45,000 lb per hr
Make-up	450,000 lb per hr

	Raw water (ppm)	Raw water (epm)	Filtered precipitator effluent (ppm)	Filtered precipitator effluent (epm)	Softener effluent (ppm)	Softener effluent (epm)	Boiler water (ppm)	Boiler water (epm)
Calcium, Ca	19	0.94	60	3.00	0.6	0.03	0	0
Magnesium, Mg	7	0.54	6	0.52	0.1	0.01	0	0
Sodium, Na	13	0.56	12	0.52	94	4.09	600	26.12
		2.04		4.04		4.13		26.12
Bicarbonate, HCO_3	61	1.00	17	0.28	17	0.28	0	0
Carbonate, CO_3	0	0	2	0.08	2	0.08	8	0.27
Hydroxide, OH	0	0	0	0	0	0	40	2.35
Phosphate, PO_4	0	0	0	0	0	0	15	0.47
Sulphite, SO_3	0	0	0	0	0	0	10	0.25
Sulphate, SO_4	16	0.34	140	2.92	140	2.92	850	17.71
Chloride, Cl	25	0.70	27	0.76	30	0.85	180	5.07
		2.04		4.04		4.13		26.12
Silica, SiO_2	8.6		1.5		1.5		9	
Carbon dioxide, CO_2	7		0		0		...	
Color	25		3		3		...	
Iron, Fe	1.7		0.1		0.1		...	
Total hardness, as $CaCO_3$	74	1.48	176	3.52	2	0.04	...	
pH	7.2		9.2		9.2		11.2	
Dissolved solids	120		257		277		1712	
Suspended solids	30		...		...		38	
Total solids	150		257		277		1750	

Chemical requirements in terms of treating-plant effluent:

	ppm	¢ per lb	$ per million lb
Treating plant			
Ferric sulphate, 78% $Fe_2(SO_4)_3 \cdot 2H_2O$	220	1.5	$3.30
Lime, 90% $Ca(OH)_2$	145	0.6	0.87
Sulphuric acid, 93% H_2SO_4	0	0.9	0
Chlorine, 100% Cl_2	6	9.0	0.54
Sodium chloride, 99% NaCl	700	0.6	4.20
Clay	50	1.0	0.50
Chemical cost per million lb of treated water			$9.41
Supplementary treatment			
Disodium phosphate, 98 per cent Na_2HPO_4	6.0	9.0	$0.54
Caustic soda, 98 per cent NaOH	2.5	2.5	0.06
Sodium sulphite, 93 per cent Na_2SO_3	6.5	3.5	0.23
Organic dispersive	6.0	14.0	0.84
Chemical cost per million lb of treated water			$1.67

TABLE 3 WATER CONDITIONS FOR A 100 PER CENT DEMINERALIZED MAKE-UP UNIT

Process steam	400,000 lb per hr
Steam losses	5,000 lb per hr
Boiler blowdown	10,300 lb per hr
Blowdown losses	6,200 lb per hr
Make-up	411,200 lb per hr

	Raw water		Filtered precipitator effluent		Demineralizer and silica absorber effluent		Boiler water	
	(ppm)	(epm)	(ppm)	(epm)	(ppm)	(epm)	(ppm)	(epm)
Calcium, Ca	19	0.94	34	1.68	0.2	0.01	0	0
Magnesium, Mg	7	0.54	7	0.54	0.1	0.01	0	0
Sodium, Na	13	0.56	13	0.56	1.8	0.08	107	4.66
		2.04		2.78		0.10		4.66
Bicarbonate, HCO_3	61	1.00	65	1.07	4.3	0.07	0	0
Carbonate, CO_3	0	0	6	0.20	0	0	0	0
Hydroxide, OH	0	0	0	0	0	0	40	2.35
Phosphate, PO_4	0	0	0	0	0	0	15	0.47
Sulphite, SO_3	0	0	0	0	0	0	10	0.25
Sulphate, SO_4	16	0.34	39	0.81	0.5	0.01	38	0.79
Chloride, Cl	25	0.70	25	0.70	0.7	0.02	28	0.80
		2.04		2.78		0.10		4.66
Silica, SiO_2	8.6		5.5		0.2		8	
Carbon dioxide, CO_2	7		0		0.5		...	
Color	25		5		5		...	
Iron, Fe	1.7		0.1		0.1		...	
Total hardness, as $CaCO_3$	74	1.48	111	2.22	1	0.02	0	
pH	7.2		9.2		8.0		11.3	
Dissolved solids	120		162		6.5		246	
Suspended solids	30		...		...		40	
Total solids	150		162		6.5		286	

Chemical requirements in terms of treating-plant effluent:

	ppm	¢ per lb	$ per million lb
Treating plant			
Ferric sulphate, 78% $Fe_2(SO_4)_3 \cdot 2H_2O$	59	1.5	$0.89
Lime, 90 per cent $Ca(OH)_2$	39	0.6	0.23
Chlorine, 100 per cent Cl_2	6	9.0	0.54
Caustic soda, 98%, NaOH	458	2.5	11.45
Soda ash, 99 per cent, Na_2CO_3	94	1.5	1.41
Sulphuric acid, 93 per cent H_2SO_4	337	0.9	3.03
Clay	50	1.0	0.50
Chemical cost per million lb of treated water			$18.14
Supplementary treatment			
Disodium phosphate, 98 per cent Na_2HPO_4	1.5	9.0	$0.14
Caustic soda, 98 per cent NaOH	0	2.5	0
Sodium sulphite, 93 per cent Na_2SO_3	0.9	3.5	0.03
Organic dispersive	2.5	14.0	0.35
Chemical cost per million lb of treated water			$0.52

ECONOMICS

In any rational presentation of a subject such as this, it is necessary that some space be devoted to a consideration of the economic aspects of the design as well as to the technical features. It is of course true, here as elsewhere, that any "over-all," "average," "typical," or "representative" costs are bound to be associated intimately with the design details and local conditions. Broadly viewed, however, the alternative designs of by-product power plants using high-pressure turbines exhausting to process evaporators or exhausting directly to process, show an over-all investment requirement which justifies the selection of the latter. Experience has demonstrated that the investment for a high-pressure boiler make-up treating plant, alone, is substantially the same as an evaporator plant alone, for the same process-steam capacity. The complete power plant including boilers, turbines, buildings, and auxiliaries as well as the process-steam equipment is bound to require more investment for the installation exhausting directly to process. The turbine generator is nearly twice the size, and the boiler must be larger. Experience has shown that for a given process-steam output, say, 400,000 lb per hr at 215 psia:

(*a*) The increased by-product power capacity will be obtained at today's prices for an increment of investment in the neighborhood of $100 per kw.

(*b*) The increment of production cost of the electrical energy as produced by the unit exhausting directly to process, as compared to the high-pressure turbine-evaporator unit will be less than the total production cost of a condensing plant using the same fuel.

These are favorable factors, and when it is recognized that the unit exhausting directly to process operates without undue labor or maintenance costs, and without sacrifice of reliability, the over-all economic picture is decidedly favorable to this solution of the problem of the multipurpose steam power plant.

ACKNOWLEDGMENT

Many of the details, figures, and calculations in this paper were prepared by Messrs. A. J. Fiehn and R. H. Marks.

Discussion

R. C. ADAMS.[5] The authors have presented a convincing case for their major thesis, that chemical softening of make-up will produce more power per unit of process steam than evaporation of make-up. A further economic advantage from demineralization of the make-up is less certain.

A complete picture of relative costs cannot be obtained from the limited data of the authors. The only detailed costs they give are those for chemical costs of water treatment in Tables 2 and 3. From these and the comparison in Fig. 2 of the paper, a partial indication of relative expense can be derived.

Table 2, with total chemical costs of $11.08 per million pounds and 450,000 lb per hr of make-up, indicates an hourly cost for chemicals of $4.98. Referring this to the figures for power per unit of process steam in Fig. 2, shows a cost for treating chemicals of 0.023 cent per kwh. Similar calculations from Table 3 for demineralized make-up yield an hourly expenditure of \$7.67, and a chemical cost of 0.034 cent per kwh.

---

[5] Superintendent, Chemical Engineering Laboratory, U.S.N. Engigineering Experiment Station, Annapolis, Md.

Chemical costs for water treatment are a minor, though not negligible, part of the expense of power generation. The hundredth of a cent per kilowatthour increase for demineralization instead of softening looks small. However, it should be recognized as a 50 per cent increase in chemical costs for all power generated.

If the increment in cost is divided by the increment of power, which is a more reasonable basis for appraisal of the process change, the result is even more striking. The 1120 additional kilowatts, attending the standard 400,000 lb per hr of process steam, cost \$2.69 per hr for treating chemicals alone. This means 0.24 cent per kwh. When it is considered that many favorably placed industries can purchase power for about twice this amount the probability of an over-all saving from demineralization shrinks.

This suggests that general application of demineralization for boiler make-up is far from assured. It is more likely that its application will be limited to special cases for some time to come.

S. B. Applebaum.[6] The authors mention two types of water-treating equipment for the make-up water to high-pressure boilers, as follows:

(*a*) Silica removal by contact of the water with precipitates of ferric hydroxide, followed by sodium zeolite to remove the hardness.

(*b*) Demineralization and silica adsorption by ion exchange.

The authors describe an actual installation at Deepwater, N. J., using the first method, and they present hypothetical tables showing what might be expected from a demineralizing plant for the same conditions. However, they do not describe demineralizing-silica removal plants in actual operation or being installed.

The purpose of this discussion is to supplement the paper by supplying information to show that there is a very definite trend toward the installation of plants which demineralize the water and remove the silica by ion exchange.

Case 1 Process Water. One of the earliest plants of this type was installed by the Liquid Conditioning Corporation, now a subsidiary of the writer's company, at a pharmaceutical plant in the Midwest. There had been a two-step demineralizing plant in operation which merely removed the cations and anions but did not remove the silica. However, the USP standards called for a total solids of 10 ppm including the silica and therefore the user purchased a third-step ion-exchange unit for the removal of the residual silica. At the same time, the original demineralizing plant was remodeled by using the most modern resins in the units and by improving the CO_2 removal of the decarbonator.

This plant has been in satisfactory operation for over two years now and Table 4 of this discussion gives the chemical results at various stages of treatment. The plant has a capacity of about 15,000 lb per hr, and it is now being remodeled to make it fully automatic in its operation.

A second plant is being installed by the same user, having a capacity of 20,000 lb per hr of the same general type except that the decarbonator will be of the vacuum type, in order to reduce oxygen as well as free CO_2 between the second and third stages. This plant also will be fully automatic and will contain the most modern resins.

The operation of this plant shows that the silica is reduced to under 0.2 ppm throughout the run and rises to 0.5 ppm at the end of the run. The total electrolytes are reduced from nearly 400 ppm down to under 5 ppm. Therefore the effluent more than meets the USP standard of less than 10 ppm total solids, including the silica.

TABLE 4 CHEMICAL RESULTS FROM TREATMENT

	In ppm expressed as $CaCO_3$				
Constituent	A	B	C	D	E
Cations					
Calcium (Ca^{++})	249	0–1	0–1	0–1	0–1
Magnesium (Mg^{++})	116	0–1	0–1	0–1	0–1
Sodium (Na^{+})	27	0–1	0–1	0–1	0–1
Hydrogen F.M.A. (H^{+})	0	113	0	0	0
Total cations	392	116	0–3	0–3	0–3
Anions					
Bicarbonate (HCO_3^{-})	276	0	0–3	0–3	0
Carbonate (CO_3^{--})	0	0	0	0	0–3
Hydroxide (OH^{-})	0	0	0	0	0
Sulphate (SO_4^{--})	100	100	...	...	...
Chloride (Cl^{-})	16	16	...	...	...
Total anions	392	116	0–3	0–3	0–3[a]
Carbon dioxide, free	15	243	243	2–6	0
Silica	15	15	15	15	0–0.5[b]
pH	7.3	2.5–3.0	4.3–4.8	5.0–5.6	8.0–9.0
Total dissolved solids	...	...	18	8	2–6

[a] 2.5 average throughout run (total electrolytes).
[b] 0.1–0.2 average throughout run (SiO_2).

Notes:
A, Raw.
B, From first step or cation units.
C, From second step or weakly basic anion units.
D, From decarbonator.
E, From third step or silica removal unit.

Although this water is not used for boiler-feed purposes, the continued satisfactory performance of this equipment has been reassuring to boiler-plant operators who were interested in the possibility of applying this system to boiler-feed make-up treatment.

Actually, during the last year there is evidence of a great increase in interest in this new system. A number of installations have been ordered.

Case 2 Central Power Plant. In the spring of 1949, a power plant in the Midwest, which had bought an evaporator for its make-up, decided to install a hydrogen-zeolite unit plus an alkali feed for neutralization plus a degasifier to pretreat the water to the evaporator. While receiving estimates of cost of this pretreating equipment the company also investigated the possibility of adding an anion exchanger for removal of the anions as well as the silica, and finally purchased a two-step demineralizer and silica-removal plant, using the evaporator as an emergency stand-by. The raw water comes from a well. The analysis is given in Table 5 of this discussion. The plant will have a capacity of 20,000#/hr, and is expected to be in operation early in 1950.

Case 3 Industrial Boiler Plant. Another order received was from an industrial plant on the West Coast. This plant previously used evaporators for producing distilled water for make-up purposes for the 420-psig boilers. Due to plant expansion it was necessary to provide for additional make-up. At that time it was decided to discontinue the evaporator and replace it by a demineralizer and ion-exchange silica-removal plant and to install a plant large enough to take care of the expansion.

One of the advantages of the demineralizer is that it permits the boiler to generate steam lower in free carbonic-acid content than the evaporator. This is due to the very low alkalinity of the demineralized effluent and its actual freedom from free CO_2. The pH value of the effluent is usually over 8.5 because the strongly basic anion exchanger absorbs free CO_2 as carbonic acid. The steam from the evaporator, on the other hand, would contain all the CO_2 that is formed by the decomposition of the feedwater alkalinity.

---

[6] Manager of Cold Process Division, Cochrane Corporation, Philadelphia, Pa. Mem. ASME.

TABLE 5 ANALYSIS OF RAW WATER

	Ppm
Total hardness as $CaCO_3$	240
MO alkalinity as $CaCO_3$	247
Sulphates as $CaCO_3$	13
Chlorides as $CaCO_3$	3
Silica as SiO_2	13
Free CO_2 as CO_2	36
Iron as Fe	0.3
Estimated pH value	7.2
Desired Quality of Effluent	
Total hardness as $CaCO_3$	0 to 2
Total cations as $CaCO_3$	2 to 5
Total anions as $CaCO_3$	2 to 5
Silica as SiO_2	under 0.5
pH	under 7.7

The raw water in this case has the following analysis:

		HCO_3	40
Ca	50	CO_2	8
Mg	17	Cl	19
Na	19	SO_4	19
Total cations	86 ppm as $CaCO_3$	Total anions	86 ppm as $CaCO_3$
SiO_2	11		
pH	8.5		

The demineralizing plant, which will have a capacity of 100,000 lb per hr, will consist of three steps, a cation exchanger in the first step, a weakly basic anion exchanger in the second step, then a decarbonator, and finally a strongly basic anion exchanger in the third step which will remove the residual anions and the silica. The quality of the effluent desired in this case is as follows:

	ppm		ppm
Ca	0–1	HCO_3	0–3
Mg	0–1	SO_4	0–1
Na	0–3	Cl	0–1
Total cations	0–5 as $CaCO_3$	Total anions	0.5 as $CaCO_3$
SiO_2	under 0.2 ppm		
pH	over 8.0		

A number of similar installations are being made in the Midwest in central power plants and, judging from the inquiries and specifications that we are receiving calling for bids on this type of equipment, there can be no doubt that boiler users are becoming aware of the advantages of this system and that a definite trend has developed favoring that system instead of evaporators or ferric-hydroxide adsorption of silica.

Demineralizing by two-step ion exchange was in operation for some years, but the anion-exchange resin in the second step was of the weakly basic type which did not remove silica. Obviously, the removal of cations and anions without removing silica did not equal the performance of evaporators, because the boilers would have to be blown off heavily to keep the silica concentration low. It was discovered that by adding fluorides to the raw water, the ordinary demineralizer, using a weakly basic anion exchanger, would be able to remove the silica, and some plants were installed using this system. However, it had disadvantages of high operating cost, and there was a possibility of fluorides going over with the steam into the turbines.

With the advent of the highly basic anion-exchanger material, which removes silica, it is possible to remove silica without adding fluorides. The full advantage of the demineralizing process is, therefore, now available to produce a water of such low electrolyte and low silica content that it is the chemical equivalent of distilled water for boiler-feed purposes.

It is to be hoped that the actual experience with the plants which will be in operation during 1950, will be presented in papers before the Society so that additionl evidence of the good results obtainable with this new process will be available.

D. C. Carmichael.[7] The paper presents a highly interesting subject and one upon which considerable study work was carried out before establishing that a 1400-psi boiler could be operated with 100 per cent make-up.

This work consisted of construction and operation of a 7-gpm water-treatment plant for color and silica removal. The results as to silica removal were much the same as later proved in the plant-size treatment system. The second step of this work was the operation of a 1400-psi boiler with a heating surface of approximately $4^{1}/_{2}$ sq ft. The design of this boiler allowed for operation with a heat input up to and including 100,000 Btu per sq ft per hr. The feedwater for this experimental boiler was 100 per cent make-up from the mentioned water-treatment plant. The experimental boiler was operated for a total period of 120 days, and the prediction at that time was that the plant-size boiler would be operated for at least 6 months between internal cleanings.

The operating results in the Deepwater Operating Company's water-treatment plant may be of interest and are shown in Table 6 herewith. The constituents in the raw water do not vary widely from day to day, although the hardness has increased somewhat during 1948 and 1949. The hardness increase in the feedwater is due to the ferric sulphate and lime treatment. The silica content of the feedwater is fairly constant, irrespective of changes in the raw water. It may be said that the operation of the water-treatment plant is on a routine basis, although some interesting problems arose in the starting of the plant.

Fig. 9 of this discussion is a view of the precipitators, showing the lattice wave arrestors. When the plant was placed in operation, wind action stirred the water to the extent that water of a very unsatisfactory quality resulted. Covering of the tanks was considered but the wave action was overcome by a very low-cost idea—that of floating wood lath interlocked with nails as shown. This wave breaker was cheap and requires little maintenance.

---

[7] Design Division, E. I. du Pont de Nemours and Company, Wilmington, Del. Mem. ASME.

TABLE 6 DEEPWATER OPERATING COMPANY—NO. 7 BOILER —WATER-TREATMENT DATA

	Raw Water		Filter Effluent		Chemical Feed	
	Total Hardness P.P.M.	SiO_2 P.P.M.	Total Hardness	SiO_2 P.P.M.	Ferric Sulphate P.P.M.	Lime P.P.M.
1944						
Min.	44	3.9	114	1.1	121	87
Max.	74	10.6	142	1.9	166	157
Avg.	56	8.5	129	1.8	139	111
1945						
Min.	41	4.0	111	1.2	122	90
Max.	55	10.5	146	1.9	207	156
Avg.	49	8.7	130	1.7	152	113
1946						
Min.	47	6.3	113	1.5	129	103
Max.	69	10.0	149	1.8	184	177
Avg.	54	8.3	126	1.7	155	127
1947						
Min.	46	2.4	115	1.0	105	105
Max.	80	10.6	176	1.8	224	182
Avg.	61	7.9	143	1.5	163	130
1948						
Min.	59	7.1	135	1.1	132	107
Max.	93	11.1	176	1.5	231	179
Avg.	71	9.2	158	1.3	195	141
1949 to date						
Min.	64	4.1	130	1.0	118	193
Max.	93	9.0	171	1.6	194	165
Avg.	75	7.0	152	1.2	168	126

Fig. 10 shows the operating valves of the gravity filters, the valves being located at floor level. They are readily accessible and make for lower investment than when a gallery floor is installed.

Fig. 11 shows the operating valves of the zeolite softeners. The softeners are located across the aisle from the filters, thus making for accessible operation to both the filters and softeners without the operator walking a long distance. In present-day design, only the operating valves and immediate piping would be housed with the shell proper outside, thus decreasing the building investment.

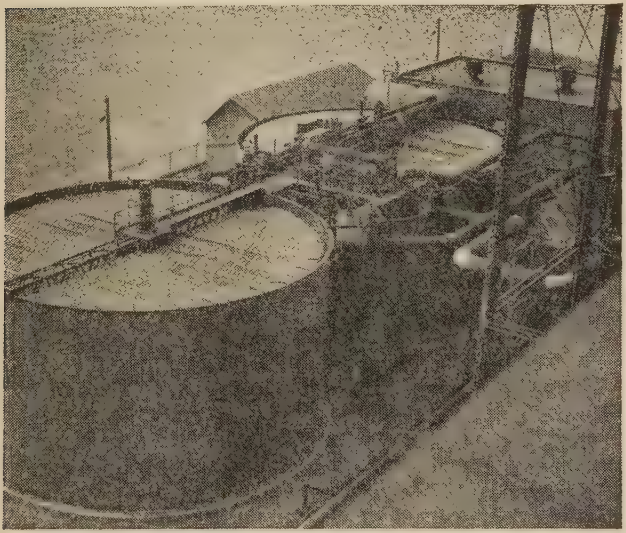

Fig. 9 View of Precipitators Showing Lattice Wave Arrestor

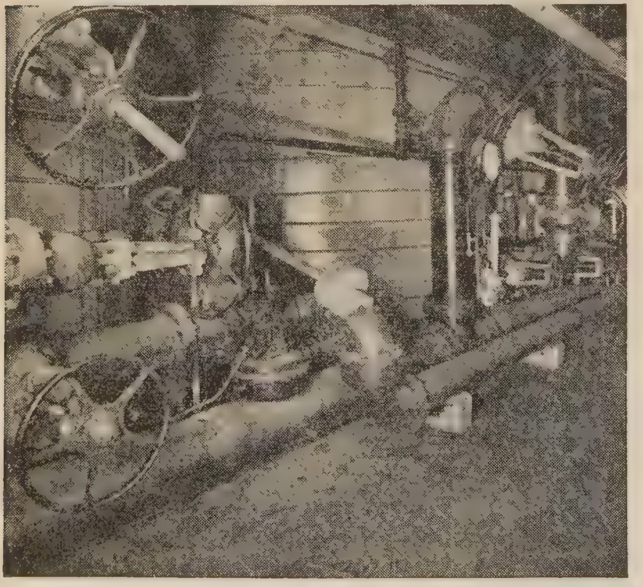

Fig. 10 Permutit Gravity Filters—Deepwater Operating Company

Table 7 of this discussion shows the boiler-water constituents. The blowdown varies from 15 to 20 per cent of the total feedwater, and no turbine-blade deposits have been encountered with the siica and total solid concentrations shown. The final criterion of the feedwater treatment is in the internal condition of the boiler.

TABLE 7 DEEPWATER OPERATING COMPANY—NO. 7 BOILER —BOILER-WATER CONCENTRATIONS

	Alkalinity PHT PPM $CaCO_3$	Hydroxide PPM $CaCO_3$	SiO_2 PPM	PO_4 PPM	Na_2SO_3 PPM	SO_4 PPM	Chloride PPM	Suspended Solids PPM	Total Solids PPM
1944									
Min.	98	87	6.9	11.9	9	624	74	22	1392
Max.	134	119	11.0	12.9	11	843	314	63	1655
Avg.	119	102	10.0	12.5	10	726	168	43	1560
1945									
Min.	112	94	7.0	12.2	9	718	97	60	1509
Max.	132	114	11.1	13.4	21	890	186	99	1686
Avg.	120	102	10.0	12.7	16	796	120	75	1567
1946									
Min.	122	104	9.4	12.8	18	704	90	62	1413
Max.	126	107	10.7	13.8	22	794	199	75	1679
Avg.	124	106	10.1	13.3	20	775	138	66	1606
1947									
Min.	124	105	6.4	13.2	18	662	105	55	1558
Max.	131	114	10.2	16.2	22	872	292	92	1711
Avg.	127	107	9.4	14.2	20	794	152	70	1630
1948									
Min.	125	106	9.5	15.8	18	596	102	50	1512
Max.	130	109	10.2	16.2	21	884	336	98	1694
Avg.	127	107	9.8	16.0	20	800	156	71	1650
1949 to date									
Min.	123	103	7.7	15.8	19	620	101	44	1566
Max.	145	126	10.0	16.4	20	867	354	73	1696
Avg.	131	111	9.2	16.0	20	793	178	60	1640

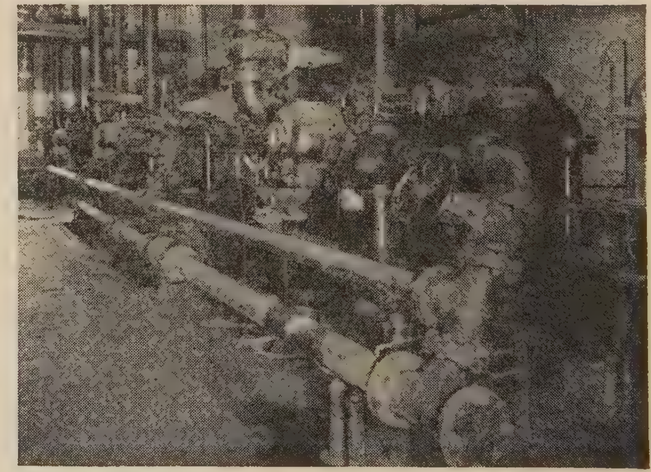

Fig. 11 Permutit Zeolite Softeners—Deepwater Operating Company

Fig. 12 is a side-elevation view of the 1942 boiler installation operating with 100 per cent make-up as mentioned in the paper. The remaining views were taken during the annual inspection of the upper drum and lower drum to show the internal conditions.

Fig. 13 is of the upper drum, which indicates absence of scale or sludge in the drum itself as well as the cyclone separators. Fig. 14 is of the lower drum during the same inspection and likewise shows very little sludge present. These views were taken in June, 1948, after 3 years of operation since the previous cleaning.

The paper gives comparisons on 100 per cent softening versus 100 per cent demineralization. Equipment-cost comparisons between the two methods of treatment would be very enlightening. Likewise, would the boiler manufacturer agree to greater output in pounds per hour with the same unit on 100 per cent demineralized water, as compared to 100 per cent softened water, or would a lower-cost boiler unit be offered for the same output

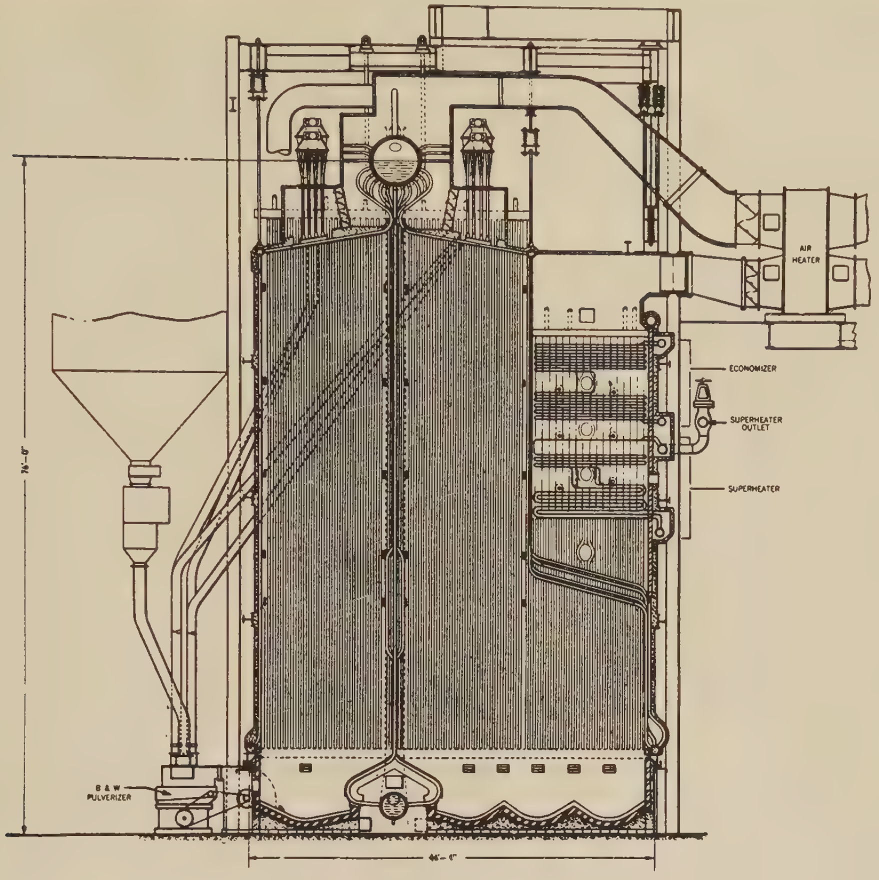

FIG. 12 SIDE ELEVATION OF NO. 7 BOILER

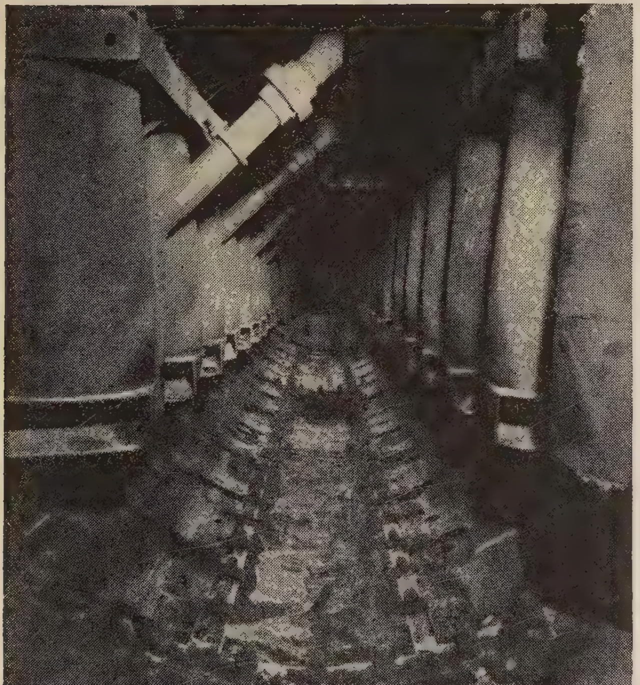

FIG. 13 UPPER DRUM OF NO. 7 BOILER

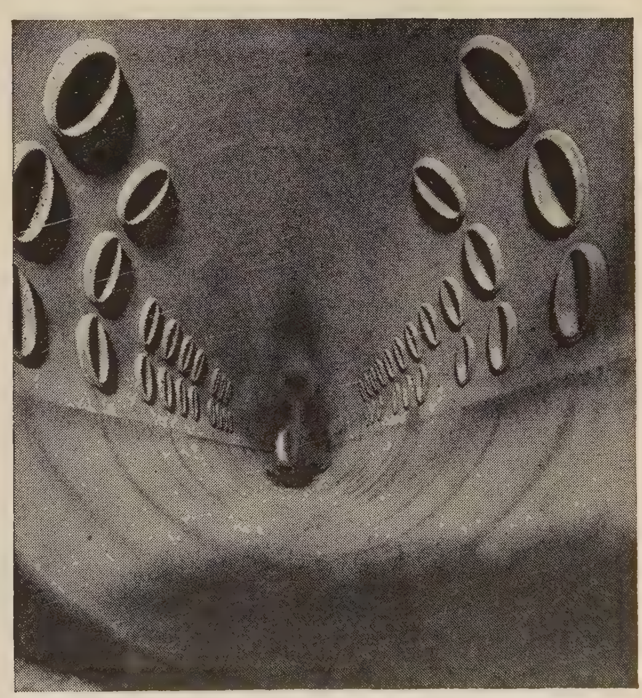

FIG. 14 BOTTOM DRUM OF NO. 7 BOILER

when 100 per cent demineralized water is the source of feedwater? After all, it is the economics of any installation which governs, to a large extent, the type of equipment and design.

In conclusion, it might be stated that the operating results on 100 per cent treated make-up show that the operating difficulties are no greater than have been experienced in many high-pressure boilers operating on low percentages of evaporated make-up.

P. H. Knowlton.[8] The authors correctly emphasize the very high thermal efficiency of electric power production in plants where the power may be generated as a by-product of the generation of steam for other than power purposes. In the case of the Deepwater plant, elimination of the evaporator heat exchangers increases the amount of such high-efficiency power, which represents a gain in useful power output of the plant.

The improvements in feedwater treatment which make possible good operation without the evaporators constitute a valuable contribution to the development of more efficient power plants.

The authors point out that when a public utility and an industrial company co-operate in the design and use of a plant for producing steam and electric power, the tendency is to design a plant giving the largest amount of electric power, in proportion to steam, that can be shown to be economical. This tendency is to be commended, since it means that fuel resources are conserved, as the thermal efficiency at which this power is generated is much higher than by any other available means.

E. A. Pirsh.[9] The authors have presented an interesting study of process steam plants generating by-product electric power. Heat balances are given for systems utilizing high-pressure turbines exhausting either directly to process or to the coils of evaporators, which in turn deliver the steam to process. The low heat rates in these types of plants show that the by-product power can be produced at a much lower fuel cost than is attainable in a central station which wastes heat to the condenser cooling water. The increasing number of plants which are operating successfully in this manner at or near 100 per cent make-up demonstrate the feasibility of such operation even under drastic water-treatment demands.

It is true that when high-pressure boilers were first installed the design engineers were reluctant to believe that they could be operated successfully with 100 per cent make-up. This attitude was in part based upon the knowledge that if excessive blowdown were to be avoided with the poorer quality of feedwater available to the high make-up boiler, it would be necessary to carry the boiler-water concentrations at much higher values. The capacity of the steam-separating equipment available at that time was influenced by increased boiler-water concentrations to a much greater degree than is the case with present-day steam-separating equipment. For this reason the maximum allowable steaming rate per foot length of drum was a more important consideration on over-all boiler design than it is at present.

The improved steam-separation and purification equipment now available permits a plant to carry boiler-water concentrations at higher values and to obtain better steam purity than was formerly possible. This results in a decreased blowdown requirement which is a very significant factor in the operation of high make-up boilers fed with water of relatively high dissolved-solid concentration.

There are now a considerable number of installations operating at or near 100 per cent make-up and at pressures ranging up to 2200 psi which deliver steam with a maximum total dissolved-solids content between 0.5 to 0.8 ppm, when carrying boiler-water concentrations up to 2500 ppm. The absence of tube failures and the long intervals between required cleanings on the waterside in these units is evidence that a properly designed boiler can be operated successfully under conditions of high make-up and high boiler-water concentrations, provided the boiler water is properly conditioned.

The pioneer design and operation of high-pressure boilers, which occurred during the 1920's, were beset with many new problems, and the design engineers, with justification, insisted that these boilers should operate with low make-up so as not to introduce unnecessary complexities through the use of a poorer-quality feedwater. It must be remembered that the science of water conditioning was in its infancy during this period, and the use of phosphates for water conditioning had just been introduced.

The accumulated knowledge obtained from experiences since that time has led to a clearer conception of the objectives to be achieved, a more thorough understanding of the principles involved, and the development of better and more economical means of feedwater- and boiler-water conditioning. Thus the quality of the feedwater for high make-up boilers has improved to the point where it is found economically practical in many instances to produce, by demineralization, a water whose purity approaches that of distilled water.

Proper conditioning of the sludge is of very great importance in a high make-up boiler because of the greater amounts which are present. The sludge must be in such condition that it is nonadherent to the surfaces in the boiler and must be kept in suspension so that it can be blown down from the unit. Sludge-dispersal agents have proved of tremendous value in performing these functions. The advances in the science of water conditioning must receive the major share of the credit for the demonstrated successful operation of high-pressure, high-make-up boilers.

The increasing demand for electric power in this country will stimulate the production of by-product power in process-steam installations, and the success of these plants must be credited in large part to the knowledge disseminated by those who have pioneered this type of operation.

W. C. Woodman.[10] The authors have presented a paper which draws attention to the exceptional opportunities afforded in an industrial plant for obtaining power at fairly low cost where it is possible to generate this power as a by-product of process steam. The economics of the situation, as the authors point out, in the end often dictates the system or cycle to be employed, and present-day production costs require the adoption of pressures and temperatures, and the utilization of heat-saving devices not hereto economically justifiable.

One such device which is particularly applicable to the type of plant chosen by the authors is the thoroughfare desuperheater. By employing this type of heat exchanger, a substantial increase in power may be developed without the generation of additional steam, or conversely, a considerable improvement in economy may be obtained with the same power development. When employing steam for process, that temperature which may be tolerated in the exhaust steam limits the turbine initial temperature to a value less than that which is often economically justifiable. With the use of a thoroughfare desuperheater, which is a wholly practicable heat exchanger, the initial temperature at the turbine inlet may be increased, while the temperature of the exhaust steam supplied to process is reduced on passing through this desuperheater to approximately the value which would be obtained from a turbine having low initial steam temperature. Feedwater forms the cooling medium in the desuperheater. The heat balance, Fig. 15 of this discussion, illustrates the thoroughfare desuperheater applied to the cycle in the authors' Fig. 6. Over 5500 additional kilowatts, representing an increase of 26 per cent, have been obtained with substantially the same boiler output and cycle heat rate. To obtain this additional power, the boiler, turbine, and connecting piping must be designed for the higher temperature, and the thoroughfare desuperheater provided. It is estimated that these modifications can be installed for less than $50 per kw of increased capacity, which is a relatively economical means of obtaining additional power.

---

[8] Thermodynamic Engineer, Turbine Engineering Divisions, General Electric Company, Schenectady, N. Y. Mem. ASME.

[9] Staff Engineer, The Babcock & Wilcox Company, New York, N. Y.

[10] Mechanical Engineer, Stone & Webster Engineering Corporation, Boston, Mass. Mem. ASME.

For industrial plants where power and process-steam demand are not so nicely balanced as in the instances cited by the authors, an extraction-condensing turbine generator can be employed. The use of a thoroughfare desuperheater is equally adaptable for installation in the extraction steam line and permits realizing the added capacity or economy resulting from high initial temperature, without increasing the temperature of the extraction steam to process.

One economic fact in the authors' paper might be given more emphasis and that is the increased construction cost of demineralization over softening equipment. The extra power derived from the demineralization plant, Fig. 7 of the paper, over the softening plant, Fig. 6, is relatively costly. It is estimated that the extra cost of demineralization equipment over the cost of sodium zeolite would approximate the cost of equipping for the high-temperature operation described, and for the conditions assumed by the authors, the purchaser would get greater return on his investment by utilizing high-temperature equipment. The improvement in the cycle resulting from the use of a demineralizing plant develops a net increase of 1170 kw, which we estimate would have an incremental cost of approximately $275 per kw, which seems to us to be more costly than the addition of a condensing end on the turbine.

This apparent advantage of one method of obtaining additional output over the method proposed by the authors serves also to emphasize the need for comprehensive analysis and engineering of each project.

AUTHORS' CLOSURE

The requests for supplementary and more detailed data on costs are natural and numerous. The problem, which confronts the authors, is to prepare such figures so that they will be of use and free of the possibilities of misinterpretation. When any attempt is made to give dollar values, which purport to be "averages" or "representative," they are always subject to misuse because of failure by all parties concerned to be on a common ground. This will occur despite the efforts to resolve differences. We are saddled with the inherent weaknesses of such approaches on the averages.

Mr. Adams correctly states that chemically softened make-up will produce more power per unit of process steam than evaporated make-up. Whether demineralization would be more economical than softening in a specific instance would depend upon many variables including not only water conditions, equipment and installation costs, and expenses for fuel and operating labor, but also upon the judgement of project designing engineers. Mr. Adams' figure of 0.24 cents per kwh obtained by dividing the increment of chemical cost by the increment of power is considerably less than the production cost of most condensing plants. Consequently it might be considered as an argument for demineralization.

As Mr. Applebaum indicates, demineralization is receiving much attention. Undoubtedly the ASME will welcome papers presenting conclusive operating results on this method of treatment.

Mr. Carmichael, because of his direct association with the design and initial operation of the Deepwater 100 per cent Make-up Unit, is well-qualified to discuss experiences with this

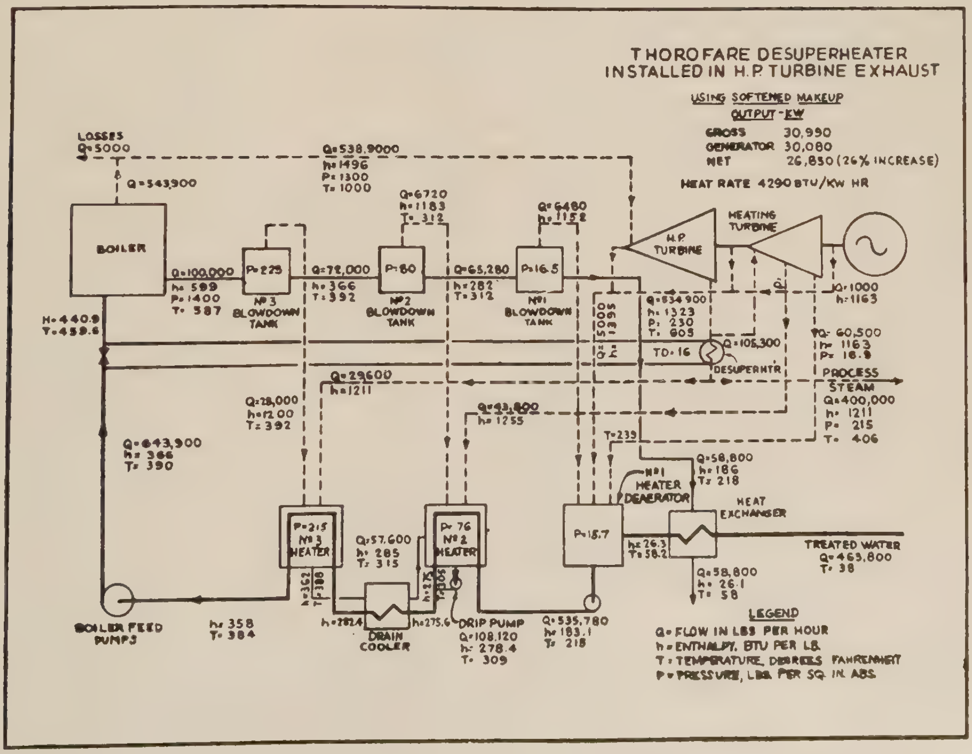

Fig. 15 Thoroughfare Desuperheater Installed in High-Pressure Turbine Exhaust

installation. The authors are most grateful for his contribution. However, as previously indicated, they are reluctant to give comparison of plant-equipment costs involved when employing softened and demineralized make-up. Mr. Carmichael's question concerning boiler design and cost for the two treatments represents only one of the variables which hinges largely on the judgment of the persons concerned. In a case where an existing condensing plant boiler is to be operated such to require high make-up, it probably would reflect good engineering judgment to demineralize rather than soften the make-up water.

It is gratifying to have Mr. Knowlton agree with the thesis of the paper and to emphasize the possibilities in reducing power costs by co-operation of public utilities and the industries requiring large quantities of process steam. Both he and Mr. Pirsh present pertinent observations.

It is most helpful of Mr. Woodman to have prepared a complete heat balance on the use of the thoroughfare heater. The data shown in his Fig. 15 are directly comparable with those contained in the body of the paper and the ASME should be grateful that Mr. Woodman has taken the time to work out such an exact analysis. He cites the gain in power for a given process-steam flow and ventures an estimate of the additional investment. In the case of the Deepwater 100 per cent softened make-up installation, the use of the thoroughfare heater was studied but its installation was not considered to be justifiable on the basis of cost. Other specific cases, coupled with today's prices, could very reasonably lead to different conclusions.

In a similar fashion, any analysis made today should recognize the potentialities of mercury vapor for by-product power generation. Great strides have been made in this field and if a mercury boiler-turbine-condenser-steam unit were postulated instead of the combinations considered in this paper, the ratio of power to process steam would again run to much higher values.

If, for the conditions shown in the heat balances, the output of electric energy in Fig. 3, using a process-steam evaporator, could be considered for comparative purposes as 1.0, then the output with softened make-up, Fig. 6, would be 1.8, and with demineralized make-up, Fig. 7, 1.9. With the thoroughfare heater of Mr. Woodman's Fig. 15, this value for electric power output would climb to 2.4. If mercury vapor were used, then the by-product power would reach a value nearly double that of Fig. 15, actually about 4.4. This high ratio of power to process steam offers one of the real merits of mercury vapor. The disadvantage of the picture is the dollar cost of the increment investment. This, in many instances, is, at present, unfavorable to mercury vapor. But the continually changing prices for fuel and equipment are bound to alter any conclusions on the economic merit of the proposal and a continuing study is justified.

Sulphite and Silica in Boiler Water at Springdale

By L. E. HANKISON[1] and M. D. BAKER,[2] PITTSBURGH, PA.

Hydrogen sulphide was first detected in the gases discharged from the air ejector of the main condenser of No. 7 unit at Springdale Station of West Penn Power Company about 6 months after the unit was placed in service. The story of potassium sulphite and its connection with this unit will form the first part of this paper. Silica deposition on the turbine blades was quite rapid, and after 8 months operation it was necessary to sandblast the silica from the blades. The search for the source of this silica, together with the information found and the corrections applied, will also be discussed.

No. 7 unit at the Springdale Station of the West Penn Power Company is a one boiler - one turbine installation, and is operated independently from the rest of the station. This furnishes an excellent opportunity to make a closely controlled study of the boiler and the turbine as regards water conditions. The unit is fully equipped with instruments as well as what was believed to be a fair complement of sampling facilities for making an investigation.

The boiler is a radiant-heat divided-furnace type furnished by the Babcock & Wilcox Company, and is rated at 800,000 lb per hr of steam at 930 F total temperature, and 1350 psi drum pressure. The turbogenerator is Westinghouse and is usually operated at 85,000 kw. This addition to the Springdale Station was put in regular operating service January 14, 1946.

Sampling Boiler Water

The three original boiler-water sampling points were selected so that the samples obtained would show differences, if any existed, in concentration or chemical constituents at three different parts of the boiler. These are located as follows:

No. 1 This sample is collected from the continuous-blowdown line which extends from the left drumhead to the middle of the drum. It has small intake holes throughout its length. Theoretically, this blowoff pipe should give a representative sample of the water surrounding the length of the pipe, but at best this would be true only when a heavy blowdown was being made. At all other times the sample from this point would be representative of the water surrounding the first few holes in the collecting pipe. It is thought that the No. 1 sampling point gives conditions which exist only at the left end of the drum.

No. 2 This point is located 5 ft from the top end of No. 40 tube in the front wall. The sample obtained was supposed to represent the water in the left half of the boiler and was placed high up in the tube in order to determine if any difference existed in the chemical constituents of the boiler water because of hot spots or faulty circulation. This wall contains 160 three-in-OD tubes 95 ft long.

No. 3 Similar to location of No. 2 sampling point, except this point is in tube No. 119 at the opposite or right half of the front wall.

The boiler water of the unit has always been conditioned with potassium salts. The chemicals used are potassium phosphate, potassium hydroxide, potassium chloride, and potassium sulphite. These chemicals were introduced into the boiler water at the drum in order that the least possible amount of solids would be in the water delivered to the attemperator. The use of potassium salts for boiler-water treatment has been described previously by the authors.[3]

Sulphite. West Penn Power Company considers sulphite an essential conditioning chemical in boiler water. Experience with lack of sulphite was quite expensive and was described by the authors of this paper in a previous presentation.[4] It has been used in No. 77 boiler since it was first put in service, and its use is expected to continue.

It was noted quite early in the operation of the boiler that sulphite analyses of the boiler water were erratic and that the desired concentration was hard to maintain. Also, the water samples contained various quantities of finely divided black iron and copper oxides. The sulphite might vary from 10 ppm excess to none in two consecutive samples from the same sampling point. The day-by-day variations in all constituents in boiler-water analyses except sulphite were in proper proportion, and this gave confidence of correct methods of sampling. The varying results gave reason to question the equipment used to obtain the samples, and the water circulation in the boiler. These conditions, and particularly the unpredictable results of the sulphite analyses were the cause of much concern, and the reason for the boiler-water investigation.

Six months after the boiler was placed in service, intermittent shots of hydrogen sulphide were discharged at the air ejector of the main condenser. As time elapsed, the number and intensity of the shots became greater. The amount of hydrogen sulphide was sufficient to make the air in the turbine room offensive to the operators. The hydrogen sulphide in the 5 cfm of gases discharged from the air ejector was determined colorimetrically, using sodium plumbite. The amount usually found varied from 5 to 25 ppm. The maximum determined was 192 ppm by volume or 229 ppm by weight. This high figure does not represent a large amount of hydrogen sulphide, as 229 ppm by weight in 7200 cu ft of gases per day equals only 6.03 grams. This is equivalent to 1.12 ounces of potassium sulphite. At this time the sulphite feed was varying between 6 and 10 lb per day.

A probable reaction for the decomposition of potassium sulphite in high-pressure-boiler water is as follows

$$4\ K_2SO_3 \rightarrow 3\ K_2SO_4 + K_2S$$

---

[1] Superintendent Efficiency, West Penn Power Company. Mem ASME.

[2] Chief Chemist, West Penn Power Company.

Contributed by the Research Committee on Boiler Feedwater Studies and the Power Division and presented at the Annual Meeting, New York, N. Y., November 27–December 2, 1949, of The American Society of Mechanical Engineers.

Note: Statements and opinions advanced in papers are to be understood as individual expressions of their authors and not those of the Society. Paper No. 49—A-75.

[3] "History of Potassium Boiler-Water Treatment at Springdale," by L. E. Hankison and M. D. Baker, Trans. ASME, vol. 67, 1945, pp. 317–324.

[4] "Corrosion and Embrittlement of Boiler Metal of 1350 Pounds Operating Pressure," by L. E. Hankison and M. D. Baker, Trans. ASME, vol. 69, 1947, pp. 479–486.

This reaction will occur with the dry salt heated to a red heat. It has also been reported to occur in solution in the presence of copper or iron compounds at temperatures above 490 F.[5] At this temperature, with the same catalysts, hydrogen sulphide can be produced from potassium sulphide as in the following

$$K_2S + H_2O \rightarrow KOH + H_2S$$

This reaction was confirmed by the high alkalinity of the boiler water at the time the hydrogen sulphide was most noticeable. During a period of several weeks the pH of the boiler water was in excess of 11.3 without feeding any caustic.

Boiler-water treatment was fed directly into the drum through a chemical feed bottle once each day. While not a constant occurrence, the heaviest discharge of hydrogen sulphide occurred 45 to 90 min after the chemicals were added. The minimum sulphite concentration was set at 3 ppm, and, to prevent going below this value, it was necessary to have 35 to 45 ppm of sulphite in the boiler water immediately after adding the chemical.

A theory that concentrations this high were the cause for the decomposition of sulphite with the resultant formation of sulphide was disproved. Tests were made on three other boilers of the same pressure with sulphite increased by shot treatment to concentrations of 60 to 90 ppm with no detected formation of hydrogen sulphide. The only difference in the chemical conditioning of the four boilers was in the rate of feed from the chemical bottles. The charge of chemicals in the bottle of No. 77 boiler would be emptied in a few minutes, while at least $^1/_2$ hr was required to empty the bottle on each of the other boilers. In all four boilers, the high concentration of sulphite would be reduced to 10 ppm or less in 24 hr. No satisfactory explanation for this reduction or disappearance of sulphite in oxygen-free water is offered or has been found in the literature.

The set minimum concentration of 3 ppm of sulphite in No. 77 boiler was reduced to 1 ppm, but positive tests for hydrogen sulphide were obtained with 1 ppm of sulphite in the boiler water. This seemed to confirm the thought that the boiler had faulty circulation and was developing hot spots with the resultant decomposition of sulphite.

Two plans of action were started immediately, as follows:

1 Purchase and installation of a chemical feed pump that would permit continuous chemical treatment.

2 Installation of additional sampling coils which would permit sufficient samples to be obtained to determine if points of high concentration were occurring.

A Milton Roy pump of 3 gph capacity for continuous treatment was placed in service on April 5, 1947. The chemical treatment is pumped into the discharge line of the Hankison boiler-water recirculator which pumps water continuously from the boiler drum through the economizer for corrosion protection as described by Baker.[6]

Fig. 1 shows where the chemical feed pump discharges into the recirculator line before the water from it enters the main boiler feed line downstream from the attemperator connection. Since this pump was placed in service, continuous low sulphite concentrations have been easily maintained. Following this change in method of treatment there was a reduction in the intensity and frequency of the shots of hydrogen sulphide discharged by the air ejector, but 7 months elapsed before the production of this gas was entirely eliminated.

Fifteen additional sampling points were located on the boiler tubes and headers so that the complete study was made with 18 samples collected as nearly simultaneously as four men could collect them. The lower headers gave water conditions in each wall in accordance with the water supply from the drum. The additional tubes selected for sampling were thought to have the higher rates of evaporation, and consequently would be first to show faulty circulation.

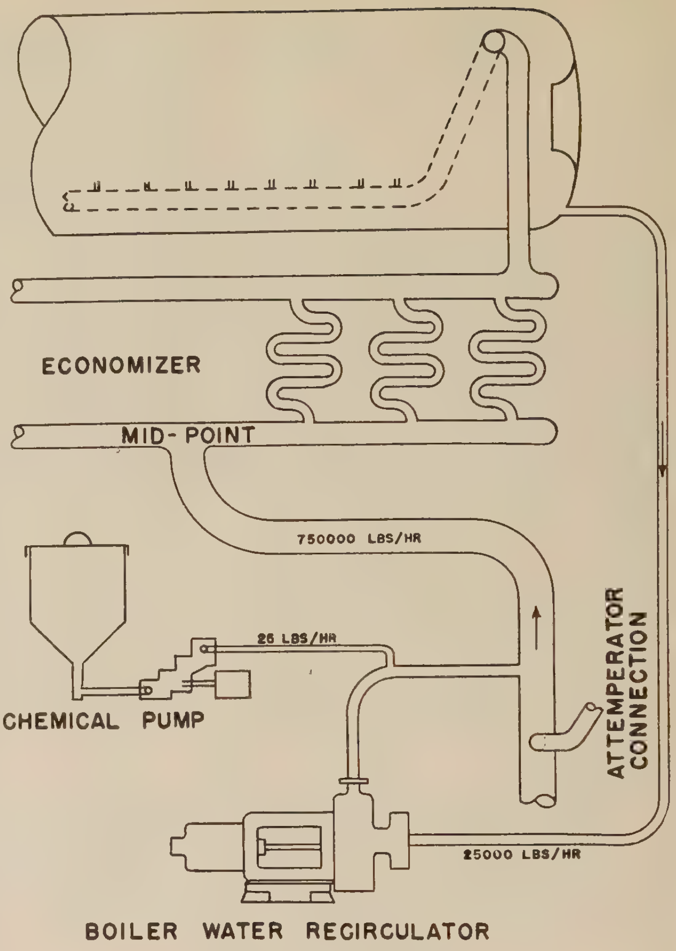

Fig. 1 Boiler Water Recirculator

Table 1 lists the points of sampling and gives a typical set of analyses obtained from the 18 sample points. The variation in ratio of sulphite to the other constituents was typical of the daily analyses made over a period of several months.

The boiler was acid-cleaned in April, 1947, to remove the heavy oxide deposit which was thought might be affecting circulation. It is estimated that the acid-cleaning and the subsequent washing of the drum and headers removed more than 500 lb of deposit. A partial analysis of the material which was removed is given in Table 2.

At the time the boiler was acid-cleaned the turbine was inspected. Severe active corrosion was found on the low-pressure-turbine casing at the discharge throat into the condenser. Also, the metals of the condenser were attacked where the condensed steam rained into the condenser. Subsequent inspections since the hydrogen sulphide disappeared show no active corrosion.

The hydrogen sulphide had attacked the tubes in the air-ejector condenser. The tubes in the inlet section could be broken easily by the hands. The tubes are made of admiralty metal and those replaced in April, 1947, are still giving satisfactory service.

---

[5] "The Behavior of Sodium Sulphite in High-Pressure Steam Boilers," by R. M. Hitchens and J. W. Purssell, Trans. ASME, vol. 60, 1938, pp. 469–473.

[6] "Economy in Boiler Water Recirculation," by M. D. Baker, *Combustion*, vol. 12, October, 1940, pp. 31–34.

TABLE 1 POINTS OF SAMPLING AND TYPICAL ANALYSES OBTAINED

Sample Date - 5/9/47

Sample Points	ppm SO_3	Micromhos Cond.	ppm SiO_2	ppm PO_4	ppm Cl
Drum South End	11	720	5	28	100
South Wall Lower Header	11	708	4	26	96
South Division Wall Lower Header	11	695	3	24	89
South Convection Wall Lower Header	10	665	2	24	92
West Wall Lower Header	11	625	5	24	90
East Wall Lower Header	11	682	3	24	84
East Wall No. 40 Tube Bottom	11	714	4	22	98
East Wall No. 40 Tube Top	13	700	3	24	95
East Wall No. 66 Tube Bottom	7	678	3	24	100
East Wall No. 66 Tube Top	9	636	4	23	88
East Wall No. 119 Tube Bottom	5	650	3	22	85
East Wall No. 119 Tube Top	9	635	2	22	90
Drum Center	6	660	4	26	91
North Convection Wall Lower Header	6	626	3	22	86
North Division Wall Lower Header	10	660	4	24	92
North Division Wall No. X Tube Bottom	7	648	4	23	85
North Division Wall No. X Tube Top	6	645	2	24	92
North Wall Lower Header	11	660	2	24	85

TABLE 2 MATERIAL REMOVED FROM BOILER BEFORE ACID CLEANING

	Per cent
Silica as SiO_2	0.1
Iron oxide as FeO	72.8
Copper as CuO	15.8
Phosphate as P_2O_5	5.2

Theory of Hydrogen-Sulphide Formation. A probable theory for the formation of hydrogen sulphide is that while 45 ppm of sulphite was the maximum found in the boiler water after shot treatment, at the time of injection the concentration was much higher and decomposition occurred. A large proportion of the gas was discharged from the air ejector, but some was absorbed by the condensate and recirculated in the boiler-water cycle. It is quite possible that a large number of cycles were required to discharge all the absorbed gas. The hydrogen sulphide when absorbed by the condensate produced an acid solution which attacked the metals of the system. These dissolved metals when finally concentrated in the boiler would settle out as oxides, but during the conversion from sulphide to oxide, they served as catalysts to break down more of the sulphite. With the removal of deposits by acid-cleaning, and the elimination of large excesses of sulphite, the desired boiler-water condition was slowly established, and the hydrogen sulphide gradually reduced.

The inconsistent sulphite analyses still persisted with the continuous feed of boiler-water chemicals. In the study to determine all inconsistencies it was noted that copper and steel were used in various combinations for sampling lines and inner coils of cooling coils. Table 3 shows the result of this phase of the study. It is to be noted that the samples collected through copper gave erratic sulphite results. Samples collected through steel gave consistent results.

The confirmation that copper reduced the sulphite in the sample was obtained from a series of tests made at the No. 40 tube top sample connection. The steel sample line from the valve was brought out to a tee. Each side of the tee was connected with the same length of steel tubing to sample coils; one with copper inner coil, the other with a stainless-steel inner coil. The flow was regulated at each coil so that the volume of sample was the same. Table 4 is typical of the results that were obtained on numerous tests with a copper coil and stainless-steel coil in parallel; and also with two stainless-steel coils in parallel. In all tests the sample from the copper coil gave a lower sulphite reading than was obtained in the sample from the stainless-steel coil.

Effect of Copper Tubing. Evidence of the effect of copper tubing on the disappearance of sulphite in the boiler water was found at the time of the failure of a section of tubing connecting the source of the sample with the cooling coil. The copper tubing could not be made tight at the fitting and was replaced. The section re-

TABLE 3 RESULTS OF TESTS WITH CONTINUOUS FEED OF BOILER-WATER CHEMICALS

	Sampling Tube Metal	Inner Coil Metal	5/23/47		5/29/47		6/2/47		6/23/47		7/7/47	
			SO_3	Cond.	SO_3	Cond.	SO_3	Cond.	SO_3	Cond.	SO_3	Cond.
Drum South End	S	SS	14	792	2	696	3	762	11	922	9	730
South Wall Lower Header	S	Cu	14	774	2	654	3	750	7	898	5	716
South Division Wall Lower Header	S	Cu	14	762	2	610	3	725	9	875	9	697
South Convection Wall Lower Header	Cu	Cu	11	715	0	610	0	675	6	828	4	666
West Wall Lower Header	S	SS	12	697	2	603	2	658	10	820	8	656
East Wall Lower Header	S	SS	14	728	1	620	2	685	10	847	8	672
East Wall No. 40 Tube Bottom	Cu	Cu	15	773	2	665	2	728	8	900	0	725
East Wall No. 40 Tube Top	S	SS	14	750	2	635	3	715	10	865	8	710
East Wall No. 66 Tube Bottom	Cu	Cu	11	732	0	635	0	682	6	830	2	662
East Wall No. 66 Tube Top	Cu	Cu	9	700	0	592	0	610	6	808	0	658
East Wall No. 119 Tube Bottom	Cu	Cu	9	636	0	545	0	598	5	765	0	635
East Wall No. 119 Tube Top	S	Cu	12	630	2	538	2	585	3	750	3	634
North Convection Wall Lower Header	Cu	Cu	7	616	0	523	0	575	5	735	3	610
North Division Wall Lower Header	S	SS	13	648	4	546	2	610	9	786	7	665
North Division Wall No. X Tube Bottom	Cu	Cu	8	656	1	550	0	610	4	776	4	642
North Division Wall No. X Tube Top	Cu	Cu	8	650	1	545	0	655	4	760	0	642
North Wall Lower Header	S	SS	11	636	3	540	1	602	9	774	8	656

S - Steel
SS - Stainless Steel
Cu - Copper

TABLE 4 RESULTS WITH COPPER ON STAINLESS-STEEL COILS IN PARALLEL, AND STAINLESS-STEEL COILS IN PARALLEL

Coil Metal	SO_3	Conductivity	SiO_2	PO_4	CL
Sample date 7/16/47					
Copper	0	760	3	27	78
Stainless steel	5	808	3	28	83
Sample date 7/22/47					
Stainless steel	4	926	4	28	88
Stainless steel	4	929	4	27	88

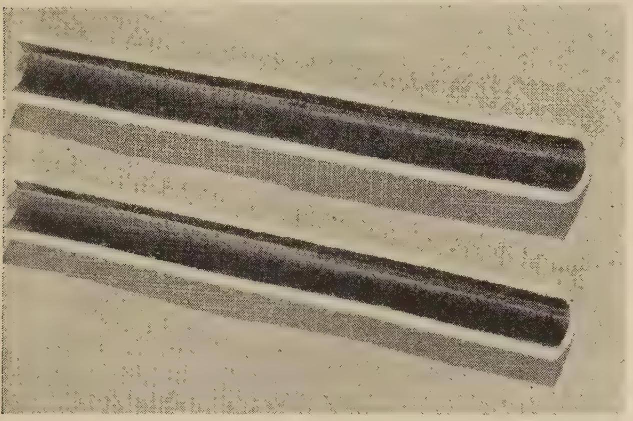

FIG. 2 SPLIT SAMPLING TUBE SHOWING COPPER OXIDE COATING

moved was split lengthwise and the inside was found to be coated with a black enamel-like coating that was badly cracked. In places, little chips of the coating had broken off exposing bare copper. Flakes of the coating removed for analyses were found to be copper oxide. Fig. 2 is a photograph of the split tube showing this oxide. A new section of bright copper tubing was installed. This section of tubing was inspected after a month of normal sampling service and showed definite discoloration. No further testing was done to determine the rate of attack as the copper tubing was replaced as soon as possible. No discoloration or metal attack has ever been found in steel tubing.

Analyses were not made to explain the disappearance of sulphite and the production of the copper-oxide coating. However, bright copper strips were exposed to cold boiler-water samples without discoloration. This would indicate that sulphide was not present in the boiler water. The least trace of sulphide added to these same samples would produce discoloration of the copper strip.

After it was determined that copper would reduce sulphite in boiler-water samples, all permanent boiler-water-sample connections and coils made of copper were replaced with steel. These changes corrected most of the erratic results, but it was found that variations in analyses still persisted and were more pronounced in warm weather than during cold weather. A study was made to determine the effect of temperature of the sample at the time of collection, and it was determined that:

1 Samples collected from an all-steel system at temperatures above 80 F may give low SO_3 results.

2 A sample collected through an all-steel sampling line, a stainless-steel inner cooling coil but with a short copper discharge tube from the coil will be affected if the sample has a temperature above 80 F.

3 A long copper cooling-coil discharge tube can, at any temperature, reduce materially the SO_3 content of the sample.

Some tests were made using monel sampling lines between the valve and cooling coils. Sufficient data were not obtained to arrive at definite conclusions but it was indicated that this metal would reduce the sulphite in the boiler-water sample, but not as much as copper.

Eliminating the erroneous results caused by the effect of copper on the sulphite content of the boiler water, the other data indicated that the boiler was free of circulation trouble.

SILICA DEPOSITION ON TURBINE BLADES

Silica. Silica deposition on turbine blades at Springdale has been mentioned in a previous paper.[3] The rate of deposition on No. 7 unit at Springdale confirms the findings of Straub and Grabowski[7] that silica concentrations above 5 ppm in the boiler water will cause blade deposition. The rate of deposition on the unit at Springdale is measured by the increase in pressure at No. 3 bleed point. With clean blades and at a load of 85,000 kw on the turbine, the pressure at the third-stage bleed point is 128 psi. Any increase in this pressure usually indicates blade deposits.

A definite limit for maximum silica in the boiler water was not established during the period from starting the unit until September 14, 1946. Efforts were made to reduce the silica by blowdown, but no positive program was instituted. During the first 2 months of this period, silica in the boiler water varied between 18 and 25 ppm. During the remainder of the period the silica was gradually reduced to 8 ppm. At the time the unit was taken from service the third-stage pressure had increased to 155 psi. The cover was removed from the turbine and heavy blade deposits were found. The blades were cleaned by sandblasting which restored the turbine to a clean-blade condition. The unit was again placed in service October 1, 1946. During the first week after cleaning, the silica content of the boiler water varied between 13 and 21 ppm. After this the silica content of the boiler water was maintained between 4 and 8 ppm, except for a few short periods. High silica was found after each boiler outage. Blowdown was used to reduce this value to below 5 ppm.

All known sources of silica were investigated and eliminated. Silica due to evaporator carry-over was reduced to a minimum by maintaining the rate of evaporation at or below 50 per cent of rated capacity. Raw-water contamination could not be found. The possibility of silica in the water-conditioning chemicals was investigated and found to be negligible. Analytical procedure was investigated and, after a large amount of work, was found correct. With all these possibilities eliminated, unexplained sudden increases of the silica content of the boiler water were still experienced.

The increase in third-stage bleed pressure confirmed the presence of silica in the boiler water with subsequent vaporization and deposition on the turbine blades. The pressure had increased to 152 psi so that on March 19, 1948, the turbine was caustic-washed to remove this silica. After caustic-washing, the condenser was tested using river water to fill the steam space. The river water was muddy and mud settled on the tube surface and was not drained out with the water. When the condenser was again placed in service a large amount of mud was carried into the boiler. After 20 hr of operation, the silica in the boiler water was found to be 116 ppm. The third-stage pressure was 135 psi and increasing rapidly. Due to load conditions the unit could not be taken out of service.

Heavy blowdowns and vaporization of silica reduced the silica in the boiler water to 12 ppm by March 31, 1948, when the unit was again caustic-washed. By this time the turbine blades had enough deposit to cause the load on the unit to be reduced to 81,000 kw to prevent safety-valve operations on the heaters. With this reduced load the third-stage pressure was 150 psi, and it was estimated that at 85,000-kw load this pressure would be in excess of 165 psi. After the second washing, the third-stage pressure was down to 130 psi when operating at 85,000-kw load.

---

[7] "Silica Deposition in Steam Turbines," by F. G. Straub and H. A. Grabowski, Trans. ASME, vol. 67, 1945, pp. 309–316.

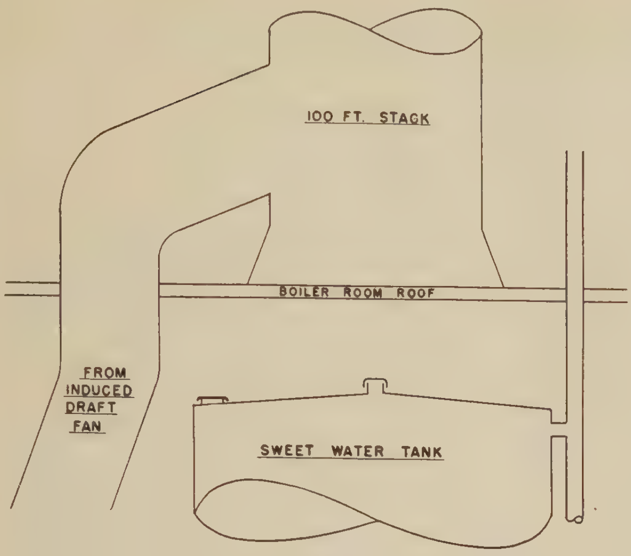

Fig. 3 Diagram Showing Relation of Sweet Water Tank and Vents With Stack

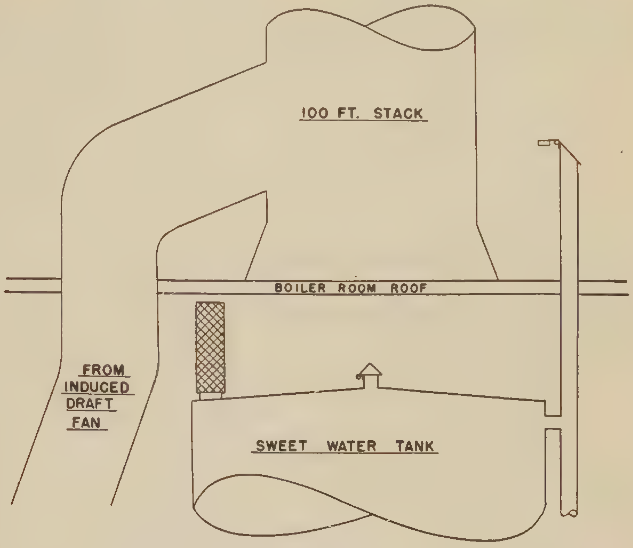

Fig. 4 Showing Changes Made to Exclude Fly Ash From the Sweet Water System and Provide Breathing of the Tank

Fly Ash Cause of Deposits of Silica. With few exceptions the silica content of the boiler water has been maintained at or below 5 ppm since April 1, 1948. Occasional unexplained increases in silica were still experienced. A study of silica in the boiler water showed a relationship between silica increase and the direction of the wind. This apparently absurd observation was investigated and it was found that with a certain wind direction, fly ash from the stacks was blown into an open vent and entered the boiler feedwater system. Further investigation found that certain operations caused the manhole lid on a condensate-water storage tank to blow off. With this lid off, the roof vent caused a positive draft across the tank. This tank is located in the same room with the forced- and induced-draft fans, and the hydromix valves for removing the fly ash from the Cottrell precipitator. At times, the air in this room carries large quantities of fly ash which were drawn into the condensate tank. Correctives were applied, and the unexplained high peaks in the silica content of the boiler water have been reduced but have not disappeared entirely. It is hoped that when all desired changes are made, silica in the boiler water due to fly ash will be eliminated.

Figs. 3 and 4 show these changes in diagrammatic form.

The benefits of the elimination of the fly ash have been shown by the maintenance of the silica in the boiler water below 5 ppm since this source of contamination was discovered. Proof of the reduction in silica contamination is shown by the third-stage pressure on the turbine which has been constant at about 145 psi for the past 5 months. Reduction of silica in the boiler water has been made, but complete elimination is still a problem of the future.

Conclusions

The conclusions of the study are as follows:

1 The water circulation in the boiler is satisfactory.

2 Continuous chemical treatment is needed to obtain satisfactory boiler-water conditioning with the maintenance of minimum concentrations of conditioning chemicals.

3 Copper will remove sulphite from boiler-water samples. Steel should be used for sampling lines, cooling coils, and discharge tubes for collecting boiler-water samples.

4 Sulphite determinations may be in error if the sample is collected at or above 80 F.

5 Hydrogen sulphide in the water-steam circulation cycle of a power-station unit can produce severe corrosion.

6 Silica contamination of the feedwater system may occur because of failure of design engineers to recognize the possibility of contamination by fly ash.

Discussion

C. U. Savoye.[8] This paper is one of those rare exceptions in which anyone, other than the boiler manufacturers, is willing to make the statement that "the water circulation in the boiler is satisfactory."

Long live Mr. Hankison and Mr. Baker!

It takes less than half an hour to read this paper and to understand the results which seem so simple. It was quite a different matter for West Penn Power, looking into the problem from the front end. At that time they questioned everything, including boiler circulation; but instead of taking sides against it, they started out in their typical unbiased fashion to determine just what *was* the true cause and to cherish whatever they found. Obviously this attitude led them to the unexpected.

I do not know whether or not the West Penn people make a better quality of electricity than any other power company, but they should be high up among the electrical lum tums if there is any validity in that little inscription on my package of sodium bicarbonate, i.e., "The priceless ingredient in any product is the character and integrity of its maker."

Authors' Closure

It is indeed hard to present a suitable closure to such a discussion as Mr. Savoye has presented, and it now seems right and proper to simply thank the discusser for his very kind words.

It may be in order to state that the months between the time the paper was written and the present confirm the findings given in the paper in every particular. To those who are still fighting silica, it will be of interest to advise that a period of six weeks has just elapsed (April 20, 1950) during which time no blowdowns were made on the No. 77 boiler and the silica concentration in the boiler water has *not exceeded 3.5 ppm.*

---

[8] Executive Assistant, Babcock & Wilcox Company, New York, N. Y. Mem. ASME.

An Automatic Degasser for Steam Sampling in Power Plants

By H. M. RIVERS,[1] W. H. TRAUTMAN,[2] and G. W. GIBBLE[3]

Electrical conductivity procedures are widely preferred for measuring the purity of condensed steam. Because gases such as carbon dioxide and ammonia contribute to the conductivity as do dissolved salts carried over from the boiler, interpretation of conductivity measurements may be somewhat uncertain. A new degasser has been developed which automatically splits a steam sample into two approximately equal streams of condensate, one containing all solid impurities, the other containing all gaseous impurities in the original sample. Heat-exchange elements are combined in a unique way which guarantees that the weight ratio of one stream to the other will remain substantially constant. Both streams pass through conductivity flow cells so the degree of contamination can be measured continuously by conductometric means.

Because of the accuracy and ease with which the electrical conductivity of steam condensate can be measured (1),[4] conductivity procedures are widely preferred—almost to the exclusion of all other methods—for precise determination of steam purity. Interpretation of the conductivity measured directly on a condensed sample of steam is frequently uncertain, however, because gases such as carbon dioxide and ammonia contribute to the conductivity just as do the dissolved salts which may have been carried over from the boiler. Either these gases must be removed from the sample before conductivity is measured, or they must be determined by chemical analysis so that a suitable correction can be applied. The latter procedure is cumbersome, time-consuming, and unsuitable when steam purity is to be determined continuously. Therefore an efficient steam-sample degasser, automatic in operation, is an essential requirement for continuous determination of steam purity by conductometric means.

Various devices have been developed in recent years to remove gaseous impurities from steam samples (2). In general, these devices operate by first condensing the sample completely. The resulting condensate is then either distilled, aerated, or subjected to vacuum in order to expel the dissolved gases. These techniques are reasonably effective for removing gases present in simple solution. However, all gases which can contribute to conductivity, such as the ammonia and carbon dioxide commonly present in steam, react with water, forming ionized compounds. Only the undissociated fractions of these dissolved gases behave as gases and are relatively easily removable. The dissociated or chemically combined fraction is very much harder to eliminate by customary procedures. Ammonia especially and carbon dioxide to a lesser degree exhibit this behavior.

Ample experience in the past has shown how difficult it is to remove these dissolved gases from steam already condensed. The degasser to be described eliminates this problem altogether, simply by preventing the gases from becoming dissolved to any appreciable extent in the first place.

Operation of Degasser

Fig. 1, a schematic diagram, shows the principal parts of the degasser. Operation is first described briefly and is then explained with additional details.

1 Steam, throttled to between 15 and 100 psig, enters the double reboil coil A immersed in a condensate pool in the separator. Heat exchange takes place between the fluids inside and outside of the coil. Steam in the coils is partially condensed before discharge through orifices, and condensate in the pool around the reboil coils is continuously boiled to eliminate traces of gases.

2 Uncondensed steam passing upward in the separator contacts the outside of the revaporizing chamber B. Partial condensation occurs, with water returning to the pool around the

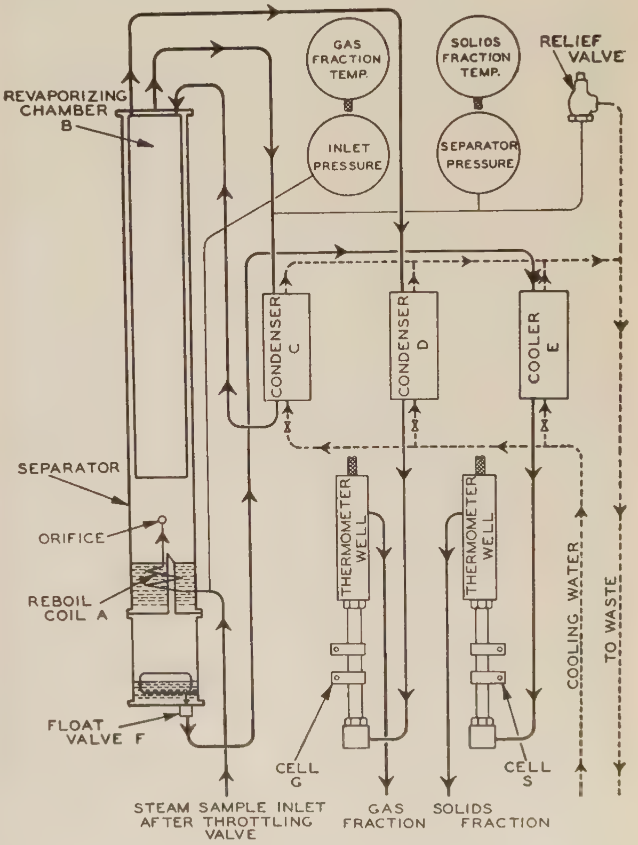

Fig. 1 Schematic Diagram of Degasser

---

[1] Service Department, Hall Laboratories, Inc., Pittsburgh, Pa.

[2] Research Department, Hall Laboratories, Inc.

[3] Formerly with Hall Laboratories, Inc.; now with Arabian-American Oil Company, Ras Tanura, Saudi Arabia.

[4] Numbers in parentheses refer to the Bibliography at the end of the paper.

Contributed by the Joint Research Committee on Boiler Feedwater Studies and the Power Division and presented at the Annual Meeting, New York, N. Y., November 27–December 2, 1949, of The American Society of Mechanical Engineers.

Note: Statements and opinions advanced in papers are to be understood as individual expressions of their authors and not those of the Society. Paper No. 49—A-74.

reboil coil A. The residual steam, containing gases, goes out the top of the separator.

3 The steam containing the gases ("gas fraction"), after leaving the separator, is completely condensed in condenser C.

4 The condensate leaving C is passed into revaporizing chamber B, where it absorbs heat from the steam on the outside and is completely vaporized, effecting the partial condensation in the separator, as mentioned in 2.

5 The gas fraction leaves the revaporizing chamber in the separator, is then condensed and cooled in condenser D, passes through conductivity flow cell G, and overflows to waste.

6 The water in the pool surrounding the reboil coil A contains the solids originally present in the steam but essentially no gases. This "solids fraction" overflows into a float chamber from which it issues continuously through float valve F.

7 The solids fraction is then cooled in cooler E, passes through conductivity cell S, and overflows to waste.

Reboil coil A does three important things: (*a*) Partial condensation of the steam sample provides water in bulk to collect all solid impurities in the original steam. (*b*) Condensation occurs only at boiling temperature; as a result of the low partial pressures of the gases and their lower solubility at higher temperature, they can contaminate the condensate only to a very slight extent. (*c*) Boiling outside coil A removes any traces of gas which may be picked up by condensate dripping down from the revaporizing chamber B. Thus all solid impurities—but practically no gases—remain in the condensate which overflows from the pool at A, and finally leaves through the float valve F. Cooled to room temperature at E, this stream of condensate is the solids fraction.

Heat given up by steam condensing in reboil coil A generates an equivalent amount of steam outside coil A. Condensate formed in coil A passes out of the orifices along with steam and then drops back into the pool, replacing the liquid lost by evaporation there. Thus the steam flow upward through the degasser is equivalent in weight to the total flow of steam sample.

Steam rising through the degasser passes revaporizing chamber B where some condensation occurs. This condensate (also substantially free from gas because it forms at high temperature and under low partial pressure of gases) falls into the pool where it is subjected to further reboiling.

All steam leaving the separator is completely condensed in C. This condensate is revaporized completely in B because of the pressure differential which is maintained between the outside and inside of this revaporizing chamber. In the process, an equivalent amount of steam is condensed outside of B. For each pound of steam leaving the outlet of B, essentially a pound of condensate drips back into the pool and eventually discharges through F. The steam sample is thus split automatically and continuously into two streams flowing at nearly equal rates, the solids fraction, substantially gas-free, and the gas fraction, substantially devoid of dissolved solids.

Since all the solids are concentrated in a fraction comprising about one half of the original weight of steam, and the gases are in a fraction of corresponding size, "magnification" of the two types of constituents is obtained. In each case the measured conductivity is multiplied by a factor which will approximate 0.5 to put the results on an original sample basis. The factor 0.5 can be approached closely if condensation in the steam-sample lines is minimized. This is accomplished by using small sample lines as short as possible, and by insulating thoroughly.

Since the concentration of solids in the solids fraction is about double that of the original sample, the accuracy of steam-purity measurements by conductometric or chemical means is materially improved, particularly when the amount of contamination is slight. For certain special studies such as investigations of "volatile silica" or "selective carry-over," an even further concentration of solids in the solids fraction can be effected by bleeding off a portion of condensed gas fraction after condenser C. If a valve is inserted and used for this purpose, operation is no longer inherently automatic, but still will be reasonably stable.

Often it is desirable to have a continuous indication of total content of gases in the steam. A recording of the conductivity of the gas fraction serves admirably for this purpose. In some cases it may be necessary to determine how much carbon dioxide, ammonia, hydrogen sulphide, or other gas is individually present. While this cannot be done conductometrically, the gas fraction provides a convenient concentrated sample for such analysis by chemical means.

COMMERCIAL UNIT

The degasser[5] is shown completely assembled and ready for use in Fig. 2. Its total weight is about 90 lb with outside dimensions 40 in. × 24 in. × 9 in. The case is made of stainless steel to withstand corrosive atmospheres. All parts which contact steam or condensate flowing to the conductivity cells are fabricated of 18-8 stainless steel, thereby minimizing contamination of the sample. Regulation of cooling-water supply is easily accomplished by means of separate valves to the three coolers. Gages are provided to indicate the pressure of the throttled-steam sample and the operating pressure in the separator. Dial thermometers measure the temperatures of the condensed solids and gas fractions passing through the conductivity cells included with the equipment.

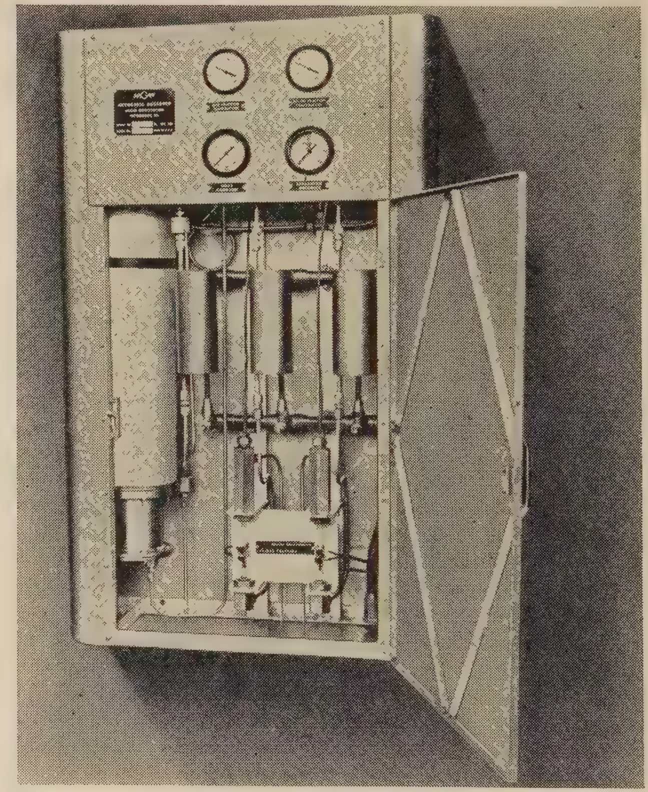

FIG. 2 THE COMMERICAL UNIT

The conductivity cells which are an integral part of the degasser are small in volume, thus minimizing lag in response to any change in sample composition. Cells will ordinarily have a

---

[5] Manufactured by Hagan Corporation, Pittsburgh, Pa.

0.1 constant. However, for very pure steam, it is sometimes advisable to magnify readings, particularly when results are below 1 micromho. Thus if a 0.01 constant cell is substituted, a reading of 0.6 micromho, for example, which may be hard to follow at the edge of some charts, can be brought toward the middle of the charts.

The degasser is quite simple to install and can be moved from place to place with ease.

Factors Producing Dependable Automatic Operation

In any degassing process, some water vapor must be vented away to remove the gaseous contaminants. If only a negligible fraction of the total sample is vented off, the high concentration of gas in the vented vapor tends to prevent complete gas removal from solution. On the other hand, if venting is copious, the volume of the remaining sample will be appreciably smaller, with the result that its solids content will be higher than in the steam undergoing test. These facts are almost universally ignored, with no attempt being made either to measure the vent loss or to control it within any but the widest of limits. Precise control over the rate of venting normally requires painstaking adjustment of cooling-water supply in proportion to rate of sample flow. This requirement for careful adjustment of sample and cooling-water flow rates—which generally must be done by hand—represents a serious shortcoming of most continuous degassers in use at the present time.

In the present degasser, this difficulty has been overcome effectively by the new combination of heat-exchange elements, the heat balance for which is presented in detail in the Appendix. The automatic method of splitting a continuously flowing steam sample into two nearly equivalent fractions depends on the thermal properties of steam and water—and nothing else. Since the total heat content of steam varies but little over the whole range of pressures encountered, the performance of the degasser is virtually independent of original steam pressure and operating pressure in the separator. Changes in rate of sample flow also have little effect. Fluctuations in temperature and pressure of the cooling water will affect the heat content of condensate leaving condenser C, but this variable is insignificant in comparison with the total heat value of steam, which governs the over-all heat balance.

Sample calculations in the Appendix assume certain values which represent extreme irregularities in such operational variables as original steam pressure, operating pressure in the degasser, sample flow rate and cooling-water temperature. It is to be taken for granted that these variables cannot always be held steady under practical plant operating conditions. Yet, in spite of the extreme conditions assumed, the ratio of solids fraction to total sample theoretically should not vary as much as 2 per cent.

This prediction has been consistently verified by field tests under actual plant operating conditions. In a given installation, the ratio of solids fraction to total sample remains substantially constant, varying no more than 1 to 2 per cent over long periods of time. The constancy of this ratio is altered only by virtually complete blockage of the cooling-water supply. On the other hand, to the extent that liquid water is carried over with the steam entering the degasser, the solids fraction will be increased in amount, as well as in conductivity. If gross carry-over occurs, the normal split will be restored when the carry-over ceases.

When the conductivity of a sample is to be measured continuously, it is important that the cell temperature be maintained at a nearly constant value so that the temperature compensator on the conductivity recorder will not have to be reset. The cooling coils D and E are generously designed in regard to heat-exchange surface, and they receive a copious supply of cooling water. As a result, regardless of normal variations in the operation of the degasser, effluent temperatures of the two fractions remain practically constant. While it is desirable to inspect the apparatus daily, adjustments of any kind are seldom necessary. During operation, the degasser requires no more personal attention than any other instrument used continuously as a guide to boiler operation.

To be of greatest value, steam-purity data must correspond, as nearly simultaneously as possible, with records of other conditions of boiler operation, i.e., steam pressure, load, water level, etc. Every effort has been made to keep the liquid retention at a minimum so as to reduce time lag in the degasser. At normal sampling rates of approximately 30 lb per hr, only about 1 min elapses between an incident of steam contamination and the corresponding effect on the conductivity of the solids fraction. With this negligible time lag in the apparatus, momentary changes in steam purity are not blunted or obscured by dilution and the recorded conductivity can be compared readily with other boiler operating data.

Field Experience With the Degasser

The degasser has been field-tested in more than 25 plants to date. In practically all cases the effect of gases in the steam has been eliminated altogether. No measurable amount of carbon dioxide has ever been found in the solids fraction, even when a large quantity of this gas was purposely introduced into the inlet steam. Ammonia concentrations in the range of 2 or 3 ppm have been removed to such an extent that the insignificant residual amount could not be measured accurately by chemical means. In a few severe cases—deliberately chosen because of

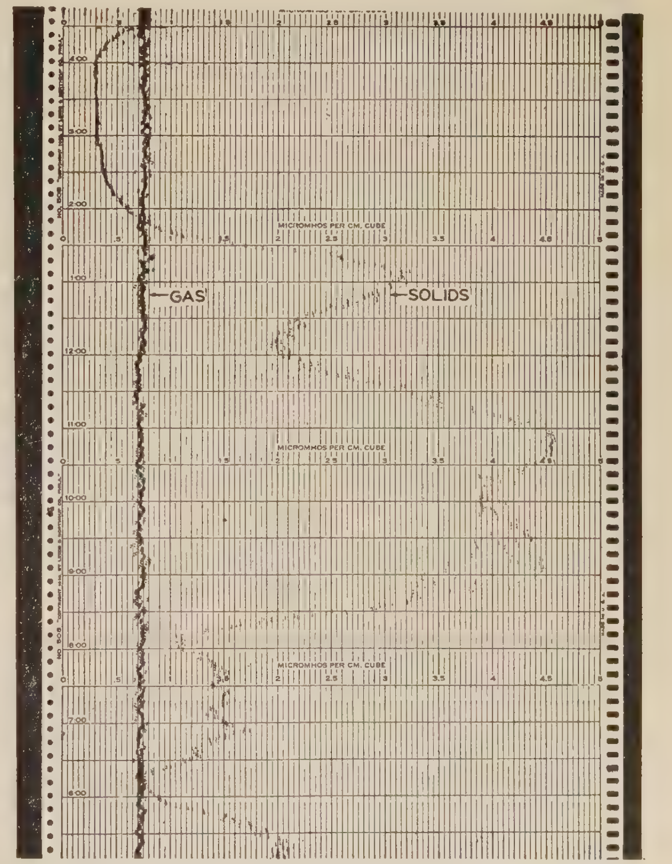

Fig. 3 Conductivity Record From a Chemical Plant, Indicating Constant Gas Fraction and Variable Solids Fraction
(Multiply chart readings by 10.)

extreme ammonia contamination in the range of 10 to 25 ppm—the gas error was reduced to a very low and uniform value which permitted a simple correction to be made by conventional methods (3). Under all circumstances, at least 95 per cent of the ammonia entering has been removed.

The conductivity record shown in Fig. 3 was obtained during steam-purity tests on a 40,000-lb per hr boiler at a chemical plant. Saturated steam at 400 psig was sampled by means of a collecting header between the steam purifiers and inlets to the superheater tubes. The conductivity of the gas fraction remained relatively constant, showing only minor variations which were associated with irregularities in rate of feedwater admission to the boiler. Through most of the time covered by this chart, conductivity of the solids fraction fluctuated widely, revealing a severe carry-over condition. This particular case provided an unusually neat correlation between boiler load and conductivity of the solids fraction, the respective values increasing and decreasing simultaneously and proportionally.

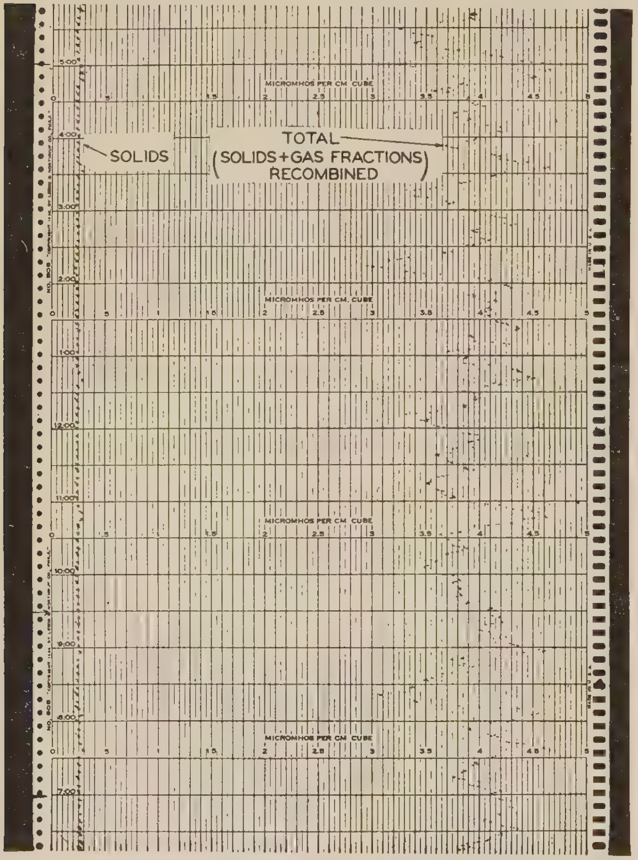

Fig. 4 Conductivity Record From a Steel Mill, Showing Low Constant Solids Fraction and Variable Total Steam Sample
(Multiply chart readings by 10.)

In contrast to Fig. 3, Fig. 4 presents the situation at a steel mill where gas content was extremely high and irregular while solid impurities remained very low and uniform. Conductivity due to solids represents only a small part of the total conductivity of solids and gases combined. Without the degasser, the difficulty in determining whether variations in conductivity were due to gas, to solids, or to both had previously prevented any certain conclusion concerning the extent to which carry-over might be occurring.

At the steel mill the solids fraction was practically constant at about 53 per cent of the total sample flowing. This relationship was determined easily by measuring the volumes of solids-fraction and gas-fraction condensate collected simultaneously for a given interval of time. The ratio of solids fraction to total sample was used as a multiplying factor to convert conductivity to the basis of the original sample. Of course corresponding data for the gas fraction can be converted to an original-sample basis in a similar way.

A single factor is used frequently to interpret the solids-fraction conductivity directly in terms of ppm total solids in the original steam. For example, at the chemical plant where Fig. 3 was developed, the solids fraction represented 56 per cent of the total steam sample. Assuming that 1 micromho of conductivity is equivalent to 0.65 ppm of dissolved and ionized solids, concentration of solid impurities in the original steam was found by multiplying the indicated conductivity by 0.56 × 0.65, or 0.36.

It will be noted that a larger solids fraction flowed from the degasser at the chemical plant than at the steel mill. This came about because of a longer sampling line at the chemical plant. The greater the heat loss and attendant condensation in the sampling line, the larger will be the solids fraction, as shown mathematically in the Appendix.

An incident occurred at one plant which indicates the need for fully automatic conductivity-measuring equipment. Three boilers were operating at maximum capacity. Without warning, the gears driving the induced-draft fan on the boiler next to that attached to the degasser stripped. Although the whole plant was on automatic control, furnace gases, dirt, and the escape of steam from safety valves forced the men observing the test to leave hurriedly. With one boiler off the line, the two remaining were subjected to chaotic operation involving dropping of pressure and of water level in the drum. About 20 min elapsed before conditions were stabilized. On the return of the observers, the degasser was found to be operating normally. Both before and after the disturbance, conductivity of the solids fraction was low, indicating excellent operating conditions. Unfortunately, in this particular instance, only manual conductivity-measuring equipment had been available so that a complete record was not made.

At another plant, a coal fire in a bunker produced very erratic operation of a nearby 600-psig boiler. Personnel were required elsewhere and no attention could be given to the degasser, which, however, continued to function normally. Subsequent inspection of the continuous record showed the boiler had delivered quite pure steam through the whole period.

The degasser has proved very easy to start up. For example, a unit was installed to test the purity of steam generated by a 125-psig evaporator. The evaporator was shut down and drained without touching the degasser. When steaming of the evaporator was resumed, the degasser started to operate automatically. In this case there was no shutting off or opening of valves nor any adjustments.

Even relatively minor physical changes may be reflected in conductivity measurements made with the degasser. A small fire-tube boiler operating at 150 psig has been employed in testing degassers and for providing final design data for certain of the degasser components. The intermittent introduction of feedwater to this boiler showed up very clearly on the conductivity record of the gas fraction. Air introduced with the feedwater flowed through the gas-fraction conductivity cell and, by lessening electrode contact, produced a slight but quite noticeable drop in conductivity.

At one central heating plant, the correlation between load and conductivity was particularly close. In the morning, with increasing demand, conductivities of both solids and gas fractions tended to rise. More carry-over was produced and more gases were introduced into the system per unit time. At the end of the business day, with dropping load, conductivities of both fractions dropped.

By using the degasser in acceptance tests on a new boiler, it was possible to prove rapidly as well as conclusively that negligible carry-over existed even at high loads, high water levels, and high boiler-water concentrations.

Summary

A new degasser has been developed with the following features:

1 Under normal operating conditions substantially all ionizable gases are removed from the solids fraction. Even in extreme cases 95 per cent or more are removed.

2 Because of the inherently stable thermodynamic cycle employed, operation is automatic and cannot be affected materially by even abnormal changes in boiler operation.

3 Since steam and condensate flowing to the cells contact only stainless steel, minimum pickup of contaminants is assured.

4 The time interval from entrance of steam into the degasser to the passage of degassed condensate out of the conductivity flow cell for the solids fraction is of the order of 1 min. The averaging effect of holdup in blunting or spreading out over a period of time momentary conductivity changes is avoided.

5 Since the lag is small, conductivity-recorder charts made in conjunction with the degasser can be compared readily with steam flow, superheat temperature, or other operating charts to obtain a coherent over-all picture of the data.

6 The conductivity of the gas fraction is measured simultaneously by a second cell. The gas fraction can also be easily diverted for chemical analysis.

Acknowledgment

The authors acknowledge with thanks the helpful suggestions of R. E. Hall, E. P. Partridge, C. E. Kaufman, and other associates at Hall Laboratories, Inc.; A. A. Markson and R. R. Donaldson of the Hagan Corporation; and S. Andrews who did much of the detail design work on the commercial model.

The co-operation of the many plants in which the degasser was tested during development is particularly appreciated.

BIBLIOGRAPHY

1 "Electrical Conductance Measurements of Water and Steam, and Applications in Steam Power Plants," by Max Hecht and D. S. McKinney, *Journal of Applied Mechanics*, Trans. ASME, paper no. FSP-53-11, vol. 53, 1931, pp. 139–159.

2 "Design and Development of Apparatus for Measurement of Steam Quality by Electrical Conductivity Methods," by S. T. Powell, H. E. Bacon, Jr., I. G. McChesney, and F. Henry, Trans. AIChE, vol. 33, 1937, pp. 116–138.

"A New Degasifying Steam Condenser for Use in Conductivity Determinations," by F. G. Straub and E. E. Nelson, Trans. ASME, vol. 63, 1941, pp. 645–648.

"Symposium on Problems and Practice in Determining Steam Purity by Conductivity Methods," Proceedings of the ASTM, vol. 41, 1941, pp. 1261–1340. Note especially "The Degasification of Steam Samples for Conductivity Tests," by P. B. Place, pp. 1302–1312; and "A New Type of Conductivity Apparatus for Use With Boiler Waters and Steam Samples," by A. R. Mumford, pp. 1314–1325.

3 "Calculation of Corrections to Conductivity Measurements for Dissolved Gases," by D. S. McKinney, part of Symposium listed in (2), Proceedings of the ASTM, vol. 41, 1941, pp. 1285–1301.

4 "Thermodynamic Properties of Steam," by J. H. Keenan and F. G. Keyes, John Wiley & Sons, Inc., New York, N. Y., 1936.

Appendix

Heat Balance for the Degasser

Heat balance is calculated for a system consisting of the steam-sampling line and of the separator shown in Fig. 1.

The following nomenclature is used in the Appendix:

H_1 = enthalpy of steam sample at sampling point, Btu per lb
H_2 = enthalpy of gas-fraction vapor leaving separator, Btu per lb
h_2 = enthalpy of solids-fraction liquid leaving separator, Btu per lb
h_3 = enthalpy of condensed gas-fraction liquid leaving condenser C, Btu per lb
H_4 = enthalpy of revaporized gas fraction leaving revaporizing chamber B, Btu per lb
L = total heat loss from separator and sampling-line surfaces, Btu per hr
W = flow rate of total steam sample, lb per hr
S = flow rate of solids fraction, lb per hr
G = flow rate of gas fraction, lb per hr

Development of Equations:

$$\text{Total heat entering system, Btu per hr} = WH_1 + Gh_3 \quad\ldots\ldots[1]$$

$$\text{Total heat leaving system, Btu per hr} = Sh_2 + GH_2 + GH_4 + L \quad\ldots\ldots[2]$$

$$G = W - S \quad\ldots\ldots[3]$$

Equating [1] and [2], and substituting [3]

$$WH_1 + (W - S)h_3 = Sh_2 + (W - S)(H_2 + H_4) + L \quad\ldots\ldots[4]$$

$$S(H_2 + H_4 - h_2 - h_3) = W(H_2 + H_4 - H_1 - h_3) + L \quad\ldots\ldots[5]$$

$$(S/W)(H_2 + H_4 - h_2 - h_3) = H_2 + H_4 - H_1 - h_3 + L/W \quad\ldots\ldots[6]$$

Therefore

$$\frac{S}{W} = \frac{H_2 + H_4 - H_1 - h_3 + L/W}{H_2 + H_4 - h_2 - h_3} \quad\ldots\ldots[7]$$

$$G/W = 1 - S/W \quad\ldots\ldots[8]$$

Ranges in Variables. The solids fraction (S/W) and gas fraction (G/W) remain substantially constant in spite of wide fluctuations in the following variables: (*a*) Pressure of original steam at the sampling point; (*b*) steam pressure in the separator; (*c*) cooling-water temperature and rate of flow; (*d*) pressure of steam exhausting from revaporizing chamber B; (*e*) total heat loss from separator and sampling line; and (*f*) sample flow rate. The variations assumed are considerably greater than any likely to be encountered under normal operating conditions.

(*a*) In general, the pressure of saturated steam must vary from about 80 per cent to over 100 per cent to effect a change of 1 per cent in total heat content. Therefore most boilers deliver steam whose enthalpy is substantially constant despite normal fluctuations in pressure. Assume an extreme condition in which drum pressure fluctuates between 300 and 450 psig.

(*b*) Although steam pressure in the separator normally does not vary more than 2 or 3 psi, assume that it may range from a minimum of 5 psig to a maximum of 15 psig.

(*c*) Temperature and volume of cooling water generally can be controlled so as to hold the temperature of condensate leaving coil C within 5 deg F of any desired value. However, assume that this temperature varies from 60 to 80 F.

(*d*) Pressure of exhaust from revaporizing chamber B is not likely to fluctuate as much as 10 psi; but, as an extreme case, assume that it may range from 0 to 10 psig.

(*e*) Heat losses can be kept at a minimum through use of short well-insulated sampling lines and adequate insulation on the apparatus itself. Field tests indicate that the total heat loss can be reduced to about 1500 Btu per hr or less. It remains practically constant, for a given installation, being only feebly affected by reasonable changes in room temperature. Assume that this variable may range from 1425 to 1575 Btu per hr.

(*f*) Although it is difficult to maintain a precisely constant sample flow rate, simple devices (needle valve, orifice, capillary tubing, pressure-regulating valve) may be used to hold this flow reasonably steady. Assume that the sample flow rate may be anything from 25 to 30 lb per hr.

Constancy of Solids Fraction. The independent variables can be arranged according to their minimum and maximum values as in Table 1. The thermal values for steam and water were obtained from tables (4).

TABLE 1 RANGE OF VARIABLES

Variable		Minimum value	Maximum value
H_1	...	(300 psig) 1203.3 Btu per lb	(450 psig) 1204.6 Btu per lb
H_2	...	(5 psig) 1156.3 Btu per lb	(15 psig) 1164.1 Btu per lb
h_2	...	(5 psig) 196.2 Btu per lb	(15 psig) 218.8 Btu per lb
h_3	...	(60 F) 28.1 Btu per lb	(80° F) 48.0 Btu per lb
H_4	...	(0 psig) 1150.4 Btu per lb	(10 psig) 1160.6 Btu per lb
L	...	1425 Btu per hr	1575 Btu per hr
W	...	25 lb per hr	30 lb per hr

By suitable substitution of the values given in Table 1 in Equation [7] minimum and maximum values for the S/W ratio can be readily calculated.

Minimum value for S/W ratio:

$$\frac{1156.3 + 1150.4 - 1204.6 - 48 + (1425/30)}{1156.3 + 1150.4 - 196.2 - 48} = \frac{1101.6}{2062.5}$$

$$= 0.534 \text{ or } 53.4 \text{ per cent}$$

with

$$G/W = 0.466 \text{ or } 46.6 \text{ per cent}$$

Maximum value for S/W ratio:

$$\frac{1164.1 + 1160.6 - 1203.3 - 28.1 + (1575/25)}{1164.1 + 1160.6 - 218.8 - 28.1} = \frac{1156.3}{2077.8}$$

$$= 0.557 \text{ or } 55.7 \text{ per cent}$$

with

$$G/W = 0.443 \text{ or } 44.3 \text{ per cent}$$

Thus the solids fraction varies only from 0.534 to 0.557, and the gas fraction from 0.466 to 0.443, although the controlling variables go through their entire ranges.

Discussion

O. M. Elliott.[6] The authors are to be congratulated for the development of a practical and usable improvement for steam-sampling degasification. It appears that this improvement will make the steam-degasifying and testing technique simple enough for any plant man to obtain reliable steam-contamination data. It is interesting to see how the authors have added to the previous work of Rummel, Gurney, Schwartz, Crosson, Straub, Nelson, Powell, Joos, and many others who have developed practical degasifying equipment for steam-conductivity measurements. Freeing the plant operators from the necessity of frequent adjustment of the degasser is a step in the right direction.

It is to be expected that degasification with this new equipment will be practically complete for most locations where the amount of ammonia in the steam is reasonably low. Where the amount of ammonia in the steam is high, difficulties can be expected with any degasifying equipment. It would be a welcome addition to the paper if in the written closure the authors would present detailed chemical data to show the degasification efficiency of the Hagan equipment for those more difficult conditions where ammonia is a problem. In particular, it would be useful and easy to compare the NH_3 removing efficiency of the degasser to the simple expedient of boiling the totally condensed steam sample to the $^1/_2$ volume in an open flask to remove the gases. Many of us have used this simple $^1/_2$-volume boiling solution to the degasifying problem for quick spot tests for a number of years. The Hagan organization has undoubtedly made this comparison in cases of extreme ammonia contamination, and the observed results would be a most useful addition to this paper.

Those who are less familiar with the Hecht and McKinney steam-conductivity method than the authors, should recall that this method only measures ionized contamination. Suspended solids in the condensate will not be ionized. Also, there are dissolved solids such as silica and iron with such a low order of conductivity that they will not be represented properly by conductivity tests, although they may be present in appreciable concentrations.

P. B. Place.[7] The development of an effective degasser, and particularly one having stable and automatic operational control, is a most welcome addition to the art of steam-sampling and testing.

For many years, inconsistencies in steam-purity test results by conductivity have been evident in that the purity values have not reflected variations in steam output and/or boiler-water concentrations. In practically all cases, except where drum internal leakage has been involved, the measured steam conductivity has remained practically constant when steam flow and/or boiler-water concentration was increased or decreased severalfold. In some cases the conductivity values have been lower at the higher ratings and concentrations.

A possible interpretation of this inconsistency is that the variation in actual steam impurity is so small that it is completely submerged by sample-line contamination and residual gas effects on conductivity. It is gratifying to note that in the author's Fig. 4 the solids-fraction conductivity is in the order of $^1/_4$ micromho, a value that is roughly 4 times the impurity content, in ppm. Such low values have been conspicuously rare in steam-purity tests to date, and it seems possible that a new conception of the purity of commercial steam may be in the making.

It is hoped that further papers on this apparatus will be forthcoming in the near future, in which a comparison will be made with results obtained by some of the current methods such as evaporation and gravimetric determination of impurity, and correction for gases by chemical titrations. It would also be of interest to run gravimetric determinations on a silica-free gas fraction to see whether a solids-free result can be obtained by this method.

The steam-sampling rate of 30 lb per hr for this degasser seems rather low. Sampling rates should be sufficient to reduce any sampling contamination to a minor proportion of the measured conductivity. Low rates of flow are not generally adequate to insure good distribution of sampling with the usual perforated sampling nozzle. Very little reliable data are available along this line, however.

The variations in conductivity of the solids fraction in the authors' Fig. 3, which are assumed to be the result of changes in steam output, are typical of the characteristics of a small leakage carry-over rather than a normal variation due to rating alone. It would be expected that the conductivity of the gas fraction would show some variation, in view of the fact that gas liberation is a function of feedwater flow rather than steam output, and feed flow would change with changes in rating.

The significance and interpretation of steam-purity test results lie more in the manner in which conductivity values vary with changes in operating conditions than in their absolute value. It is therefore important that all such data be accompanied and correlated with such operating conditions as changes in feedwater and steam flow, changes in water level, and changes in boiler-water concentration.

---

[6] Water Conditioning Engineer, Sun Oil Company, Philadelphia, Pa. Mem. ASME.

[7] Research and Development Engineer, Combustion Engineering-Superheater, Inc., New York, N. Y. Mem. ASME.

S. T. POWELL.[8] The fundamental principle upon which the degasser operates is sound and the method described by the authors for sampling steam is a definite improvement over earlier practice. Previous sampling technique was inadequate when ammonia and carbon dioxide were present in the steam in large quantities. The apparatus and its operation are more complex than some other equipment for this purpose but, where critical conditions are expected, such refinements may be justified.

The procedure of actually degassing samples thoroughly rather than trying to analyze chemically and then correct for ammonia and carbon dioxide is less time-consuming and has much merit, since it makes available a continuous record under all conditions and avoids subsequent recalculations to compensate for entrained gases.

The equipment illustrated in Fig. 2 of the paper appears to be well arranged and can be co-ordinated with other control instruments without complicated adjustments. The present trends in power-station design, and especially the trends to higher boiler pressure and temperature make the need for such appliances of growing importance.

W. L. WEBB.[9] Because of the problem of scale formation from the use of surface and well waters for cooling steam and water samples, some plants, including the major stations of the American Gas and Electric System, are employing condensate from the cycles for cooling purposes. This plan commonly results in locating all of the sampling equipment for a unit at one common point both for the operators' convenience and to reduce the cost of cooling water and drain piping. This practice often results in sampling lines 100 ft or more in length.

In employing the Hagan degasser on samples conveyed through long lines, an insulation problem will result if the total heat losses, including those of the sampling line and of the degasser, are to be limited to the order of 1500 Btu per hr. Prospective users of the degasser would be interested in knowing to what extent heat losses in excess of this value affect performance.

In order to permit locating the degasser a considerable distance from the steam-sampling point, might it not be feasible to increase the sample flow rate and by-pass a portion of the sample to waste, provided there can be certainty that the portion entering the degasser is representative of the sample taken. An alternative plan might be to insert the sample tubing inside a line through which steam can be passed, in order to reduce loss of heat from the sample. The authors may wish to express their views on these proposals.

It is understood that the degasser can be used on steam from any source, provided it enters the reboil coil A at 15 to 100 psig, and that its heat content is such as to give an acceptable proportion of solids fraction to gas fraction. Can the authors state the permissible limits of this ratio as influenced by the gas concentrations in the sample?

AUTHORS' CLOSURE

The several discussers have made a valuable contribution to the paper as a whole, and their efforts are sincerely appreciated. Subsequent discussion is confined only to the specific questions which have been raised.

A tremendous amount of analytical data were collected in developing and proving the present degasser. In every instance where degassers of this type have been used in the field, the so-called "gas error" has been eliminated so completely that it no longer affected the reliability of the test data. A tabulation of gas residuals found in the solids fraction—mainly zero or bare-trace values for ammonia, and always zero for carbon dioxide—hardly seemed justified. However, in answer to Mr. Elliott's question regarding efficiency of gas removal under difficult conditions, steam at a certain steel mill contained 26 ppm of ammonia (the highest concentration encountered to date); despite this unusually severe contamination, 98.5 per cent of the total ammonia was carried off in the gas fraction, leaving a concentration of only 0.7 ppm in the concentrated solids fraction. As Mr. Elliott and Mr. Place suggest, many valuable studies can be made, not only to compare the present degasser with other methods of disposing of the gas error, but also to develop and expand our knowledge of steam contamination in general. It is hoped that the results of some of these studies can be presented in subsequent papers by engineers who have been using the degasser for some time in their own plants.

Mr. Place suspects that a sampling rate of 30 lb per hr may be inadequate either to minimize the effects of contamination picked up from the sample line or to insure good sampling. Condensed-steam samples frequently contain appreciable amounts of iron, but it is not safe to assume that all of this iron comes from the sample line. A goodly portion of it may exist as a contaminant in the original steam sample. Of course, when the steam sample flows through a considerable length of bare or lightly insulated pipe, as it does in many cases, hot condensate formed in the line may tend to pick up some iron. The possibility of such contamination is minimized with the present degasser, which uses short, well-insulated sample lines of small diameter. Where warranted, stainless-steel piping could be used to obviate contamination. As Mr. Place states, few reliable data are available concerning optimum steam-sampling rates. The first requirement of any steam sampling and testing procedure is that it provide purity data which can be accurately correlated with all conditions of boiler operation. This requirement has been well satisfied in tests with the degasser in many plants at sampling rates of about 30 lb per hr. While the present apparatus will accommodate flows higher than 30 lb per hr, little is gained by higher sampling rates, so far as actual interpretation of the purity data is concerned. A degasser could be built to any capacity whatever, but one important point should be remembered in this connection. Loss of heat in the steam sample, and the cost of water for cooling set a limit to the sampling rate which can be justified economically. This is especially true of permanent degasser installations.

A moderate amount of scale in the heat exchangers will not disturb the degasser's performance. Where scale-forming tendencies are severe, deposition of scale in the cooling system can be effectively prevented by simple and inexpensive chemical treatment which requires only a few minutes of attention once a month. Nevertheless, condensate is the ideal cooling medium, not only for reasons given by Mr. Webb, but also because the condensate is usually available at fairly constant temperature.

Mr. Webb raises an important question concerning the possible effects of condensation in long steam-sample lines. Condensate thus added to the solids fraction is not subject to automatic control since it does not enter into the basic heat-balance relationships. If the sample flow rate could be held steady, term L/W in Equation [7] of the Appendix would remain constant, and a comparatively high heat loss could be tolerated. It is desirable to keep the heat losses as low as possible so that sample flow rates can vary over a wide range without affecting the solids-fraction percentage. Calculations in the Appendix assume a total heat loss of about 1500 Btu per hr; but that is a typical, not a limiting, figure. In the plants to which Mr. Webb specifically refers, a conventionally insulated sample line 250 ft long should lose heat at the rate of about 6100 Btu per hr. Even under these admittedly extreme conditions, 10 per cent variations in either the total heat loss or the sample flow rate would have no significant effect on the accuracy of the test data. Where practicable, the expedients which Mr. Webb suggests would eliminate or greatly reduce the effects of condensation in long sample lines; obviously, every precaution must be taken to insure that a truly representative sample enters the degasser.

---

[8] Consulting Chemical Engineer, Baltimore, Md. Fellow ASME.

[9] Mechanical Engineering Division, American Gas & Electric Service Corporation, New York, N. Y

Assuming that heat losses are kept at the usual minimum, the solids fraction will be approximately 50 per cent of the total sample. That is assured by the thermodynamic principle upon which the degasser is based. In a few cases, where it has been impossible to lag the sample lines properly, the solids fraction has run as high as 60 or 65 per cent without loss in efficiency of gas removal. No studies have been made to determine the limiting ratio of solids fraction to gas fraction, as this would entail deliberately throwing the degasser out of balance, resorting to manual instead of automatic operation, and setting up conditions not likely to be encountered in actual practice.

The Quality of Steam Condensate as Related to Sodium Sulphite in the Boiler Water

By R. C. ALEXANDER[1] and J. K. RUMMEL[2]

Test data and conclusions are given in this paper which relate to the effect of various concentrations of sodium sulphite on the quality of condensed steam from high-pressure central-station boilers. Increase in sodium sulphite beyond certain limits was found to lower appreciably the pH and to raise the conductivity of the condensed steam. The acid material found in the steam resembles sulphurous acid. Test data, procedures, and equipment are described.

During the course of a research program, which had for its object the reduction of corrosion in the feedwater systems and high-pressure boilers at the Harbor Steam Plant of the City of Los Angeles, Department of Water and Power, efforts were made to increase the pH value of the condensed steam and feedwater, without addition of more than minimum amounts of alkaline materials.

A systematic search for the sources of materials which would promote acid conditions revealed that an appreciable increase in the sodium-sulphite concentration of the boiler water caused a definite decrease in the pH value of the steam condensate and feedwater. Conversely, a decrease in sodium-sulphite concentration caused an increase in pH. It was observed that simultaneously with the lowering of the pH value below 8, the conductivity of the steam condensate was increased. Likewise the amount of reducing material in the condensate increased with increase in sodium sulphite in the boiler water. These data made it evident that if the pH of the steam condensate and the feedwater were to be controlled in a satisfactory manner, it would be necessary first to control the concentrations of sodium sulphite in the boiler water.

With this in mind the authors conducted a joint investigation regarding the desirable limitations of sodium-sulphite concentration and the other effects which have been mentioned. Most of the work was carried out on the Harbor Steam Plant boilers[3] which operate at 1050 psi, but Rummel[4] has investigated separately the effects of sodium sulphite in boilers at other stations which operate at 950 psi and 375 psi, respectively. The operating conditions which relate to the data which are presented for the Harbor Steam Plant are shown in Table 1. Garman and Rowse[3] have given a complete description of the plant.

TABLE 1 OPERATING CONDITIONS HARBOR STEAM PLANT

Boiler pressure	1050 psi
Boiler-water temperature	552 F
Superheated-steam temperature	915 F

Feedwater treatment:

Make-up water. Sodium-hydrogen zeolite softened followed by deaeration and evaporation.

Feedwater—primary. Proportional feeding of sodium sulphite and pH control with caustic soda. Deaeration and venting of gases.

Feedwater—secondary. Sodium phosphate direct to boiler plus caustic soda and sodium sulphite as required. Continuous blowdown to remove suspended matter and control the dissolved solids in boiler water.

In many power stations it is customary to feed sodium sulphite continuously to the feedwater and to maintain certain concentrations of sodium sulphite in the boiler water, in order to remove any residual dissolved oxygen which may be present in the water. The sodium sulphite will react with dissolved oxygen to form sodium sulphate, and the use of sodium sulphite to reduce corrosion, due to dissolved oxygen, is an accepted procedure.

The stability of sodium sulphite in water solution at various temperatures and pressures has been investigated by Taff, Johnstone, and Straub.[5] Their investigation of the decomposition of sodium sulphite in steel bombs at temperatures above 528 F showed that as the temperature was increased up to 600 F, the rate of decomposition increased. At 530 F to 535 F the rate of decomposition, if any, appeared to be very slow. The data which are presented herein are confirming evidence that the sodium-sulphite solutions will decompose at measurable rates, but the principal decomposition product, which was found, differs from that reported by Taff, Johnstone, and Straub.[5] This may be explained by the fact that in the boiler tests, emphasis was placed upon the analysis of the steam condensate whereas in the bomb tests the composition of the liquid in the bomb only was observed.

Hitchens and Purssell[6] have reported on observations dealing with the behavior of sodium sulphite in boilers operating at 625 psi, 1400 psi, and 1775 psi. Tests were made for sulphite and sulphide as equivalent sulphur, in the saturated and superheated steam, and for sulphide in the boiler water. No mention was made of a change in pH or conductivity of the steam with a change in sodium-sulphite concentration of the boiler water, and it is assumed that such tests were not made or were not correlated with the other test data. The lead-acetate indicator-paper method used for the determination of total sulphite and sulphide consumed considerable time and required careful manipulation in order to obtain reproducible results. This procedure was not attempted in securing the data which are reported in this paper.

Analytical Procedures

The analytical tests for the quality of the steam condensate included, pH, conductivity, reducing material as equivalent sulphurous acid, and hydrogen sulphide. The last two tests were not made for all test runs.

The pH value and conductivity were determined on flowing samples taken through stainless-steel sample lines and cooling

---

[1] Mechanical Engineer, City of Los Angeles, Department of Water and Power, Los Angeles, Calif.

[2] Chemical Engineer, Sheppard T. Powell. Consulting Chemical Engineer, Baltimore, Md. Mem. ASME.

[3] "Harbor Steam Plant Goes on the Line," by C. P. Garman and W. C. Rowse, *Power Plant Engineering*, vol. 47, June, 1943, pp. 64–69.

[4] Data Taken by J. K. Rummel at the Redondo Steam Station of the Southern California Edison Company and the Seal Beach Steam Plant of the City of Los Angeles.

Contributed by the Joint Research Committee on Boiler Feedwater Studies and Power Division and presented at the Semi-Annual Meeting, San Francisco, Calif., June 27–30, 1949, of The American Society of Mechanical Engineers.

Note: Statements and opinions advanced in papers are to be understood as individual expressions of their authors and not those of the Society. Manuscript received at ASME Headquarters, January 6, 1950. Paper No. 49—SA-37.

[5] "Decomposition of Sodium-Sulphite Solutions at Elevated Temperatures," by W. O. Taff, H. F. Johnstone, and F. G. Straub, Trans. ASME, vol. 60, 1938, pp. 261–265.

[6] "The Behavior of Sodium Sulphite in High-Pressure Steam Boilers," by R. M. Hitchens and J. W. Pursell, Jr., Trans. ASME, vol. 60, 1938, pp. 469–473.

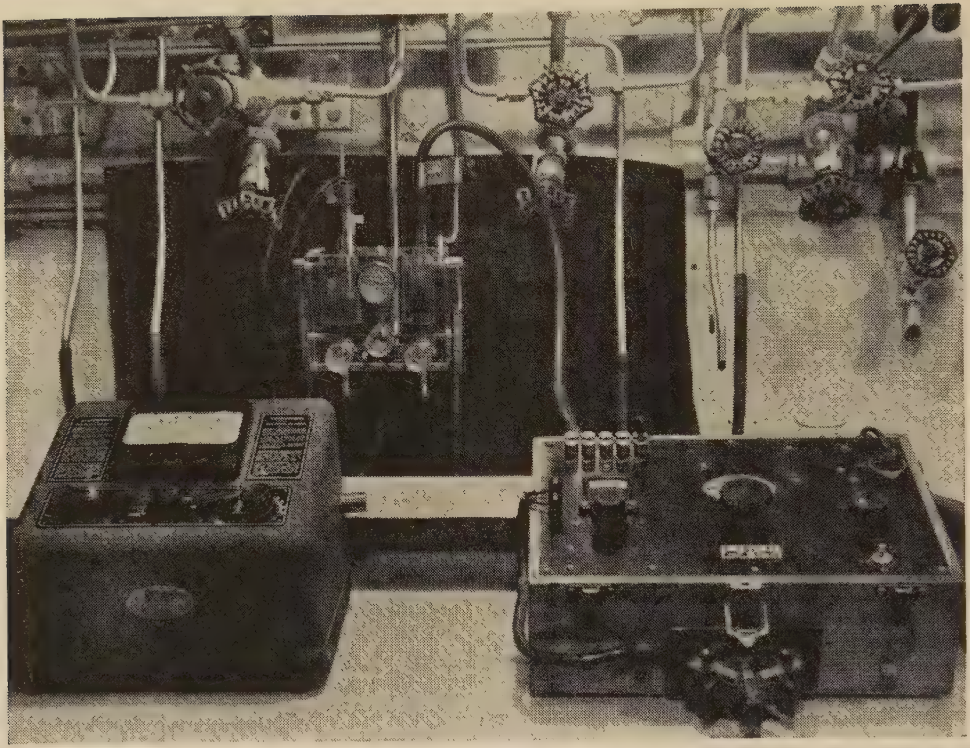

Fig. 1 Flow Cell and Instruments for pH and Conductivity Determinations

coils. A flow cavity, which was made by the authors, for holding the samples and the pH and conductivity cells, and the standard pH and conductivity meters, which were used for the measurements, are shown in Fig. 1.

The reducing material in the steam condensate was determined by direct titration with 0.002 N potassium-iodate solution, after first adding 2 ml of concentrated hydrochloric acid and 1 ml of 2.5 per cent potassium-iodide solution, to each 500 ml of sample. It was not practical to use starch as an indicator for this titration, and the end point was determined by use of an electronic indicator, which consisted of an electronic amplifier coupled to an indicator-ray tube (6E5 type) and a pair of plain platinum electrodes. The apparatus, together with the stirrer and microburette, is in all practical respects the same as that recommended by Ulmer, Reynar, and Decker[7] for "dead stop" end point titrations, as for dissolved oxygen by the modified Winkler method. The indicator tube and platinum cell assembly is sensitive to not more than one drop or 0.05 ml of 0.002 N potassium-iodate solution, which is equivalent to 0.0125 ppm of sodium sulphite, in a 500-ml sample. The test assembly is shown in Fig. 2.

Due to lack of a suitable method, no direct test for sulphurous acid could be made, and its positive identification remains to be completed.

Tests for hydrogen sulphide were made by the sodium-plumbite method recommended by Hitchens and Purssell.[6] Briefly, the method consists of adding 2 ml of 20 per cent sodium hydroxide to each of two 50-ml samples and 1 ml of 1 per cent lead acetate to one of the samples. Comparison is made in matched tall-form Nessler tubes. If a darker color is found in the tube to which the lead acetate has been added, sulphides are present. The amount of sulphide is determined by making up standards from a 0.0005 N sodium-sulphide solution and adding the reagents as already indicated. The method is said to be sensitive to 0.01 ppm of sulphide as equivalent sulphur.

Fig. 2 Titrating Equipment for Measuring Reducing Material

---

[7] "Applicability of the Schwartz-Gurney Method for Determining Dissolved Oxygen in Boiler Feedwater," by R. C. Ulmer, J. M. Reynar, and J. M. Decker, Proceedings of the ASTM, vol. 43, 1943, pp. 1258–1267.

Experimental Procedure

Aside from the data obtained during normal operation of the boilers, a number of tests were made during which the sodium-sulphite concentration was increased rapidly by direct additions to the boiler water, and the quality of the saturated and superheated steam was measured, while gradually reducing the sodium sulphite concentration. The sodium sulphite concentration was raised to 60 ppm or over, in order to note the maximum effect on pH and conductivity of the steam condensate. Both commercial and pure sodium sulphites were used during the tests.

During most of the tests the pH of the boiler water was maintained near 11, and the total alkalinity at about 100 ppm. Several tests were made at a boiler-water pH of near 11.5 and a total alkalinity of 150 ppm or over, in order to determine the neutralizing effect of high boiler-water pH and alkalinity on the acid materials in the steam. One test was made at a boiler-water pH of 10.8 and a total alkalinity of about 60 ppm, in order to show the effect of low alkalinity.

For a good part of each test the boiler load was held to nearly maximum but, due to variable demand for power on the unit, the load was decreased at times to one third normal output. At these times equilibrium conditions were disturbed and there was a temporary change in the relationship between sodium sulphite in the boiler water and the quality of the condensed steam. However, the lowering of boiler load did not have any marked effect on the results.

Since one of the principal materials affecting the pH and conductivity of the steam condensate appeared to be sulphurous acid, several titrations were made in which known amounts of sulphurous acid were added to 2.5 liters of deaerated steam condensate, and the changes in pH and conductivity were recorded. Due to the calomel used in one of the glass electrodes for pH measurements, it was necessary to make separate titrations for conductivity. The apparatus used is shown in Fig. 3.

The sulphurous acid was made by adding strong sulphuric acid to sodium sulphite in a flask, and bubbling the sulphur dioxide gas, which was generated, into steam condensate in a gas-washing bottle. This solution was analyzed and diluted to the required strength for the titrations. In order to avoid errors resulting from oxidation of the sulphurous acid to sulphuric acid it was necessary to make the tests in the minimum time possible. An atmosphere of nitrogen gas was maintained over the water in order to inhibit oxidation of the acid due to contact with air. These data were compared with the results of tests made on the steam condensate which included, as part of the data, the measurement of reducing material, as equivalent sulphurous acid.

Results and Discussion of Boiler Tests

Before the sodium sulphite concentration in the boiler water had been reduced to less than the maximum range of 15 ppm to 45 ppm, the daily routine tests made on samples of steam condensate showed variations in pH of 6.2 to 7.2. The corresponding conductivity readings varied from 0.9 to 0.5 micromhos.

The results of the special tests, during which the sodium sulphite concentrations were purposely raised and lowered, and the effects of boiler water pH, are shown in Figs. 4, 5, 6, and 7.

Typical test results, with a boiler water pH of 11 and a total alkalinity of 100 ppm, are shown in Fig. 4. The sodium sulphite concentration was varied between 3 ppm and 57 ppm. At maximum sodium sulphite concentration, the pH of steam condensate was 5.9, and at the minimum sodium sulphite concentration the pH was 8.3. At nearly the same time the conductivity of the steam condensate varied between 1.1 micromhos and 0.45 micromhos. However, after the conductivity had reached the lowest value, which corresponded to pH 7.8, it rose again to 0.7 micromho for a corresponding pH of 8.3. This is explained by the greater conductivity of the more alkaline materials which were present. These data show that if the boiler water has an alkalinity of about 100 ppm, a pH of 11, and a sulphite concentration of over 7 ppm, the probabilities are that the pH of the steam condensate will be lower than if the sodium sulphite concentration is less than 7 ppm. If the sodium sulphite concentration is as high as 20 ppm, which is a normal value for many boiler waters, the pH of the steam condensate may be less than 7. At sodium-sulphite concentrations in excess of 20 ppm, the pH was definitely on the acid side of 7.

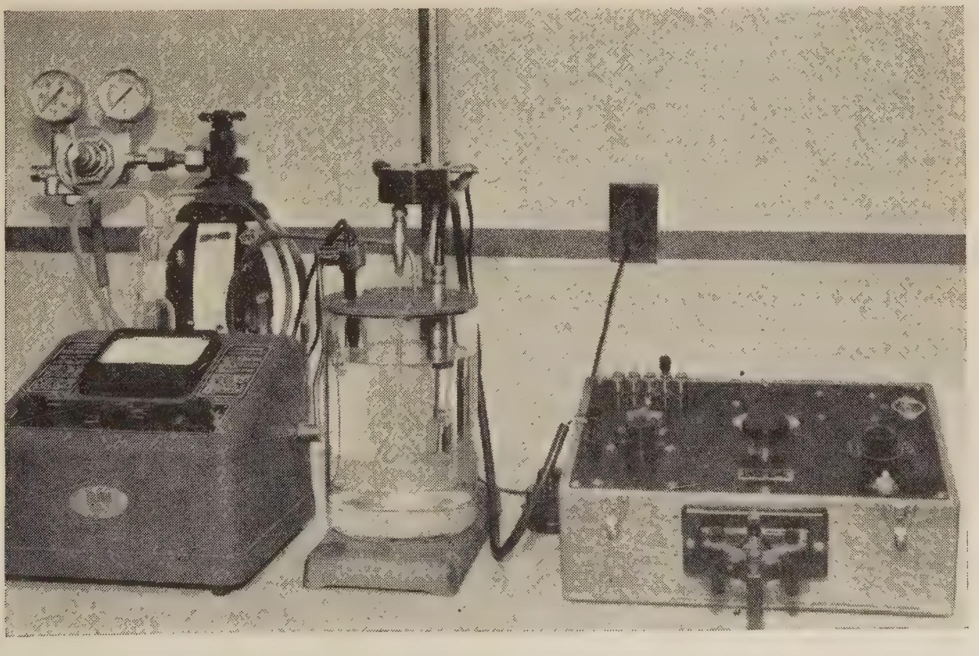

Fig. 3 Equipment for Measuring Change in pH and Conductivity of Steam Condensate With Addition of Sulphurous Acid

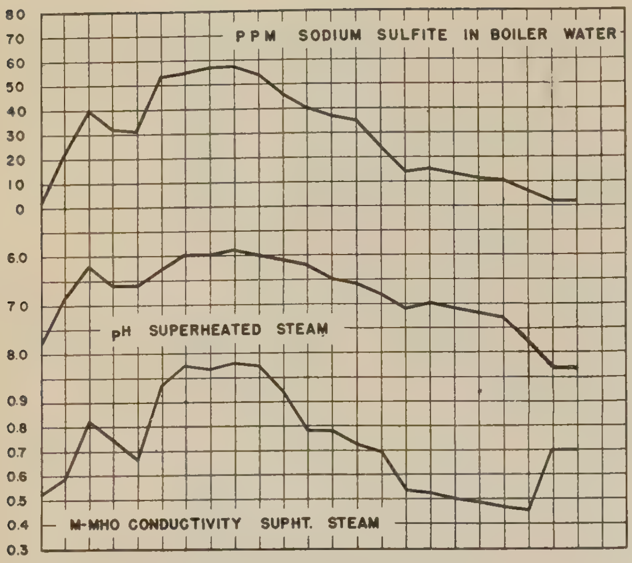

Fig. 4 Test Run to Show Effect of Sodium Sulphite on Steam Quality Boiler Water pH 11 to 11.1

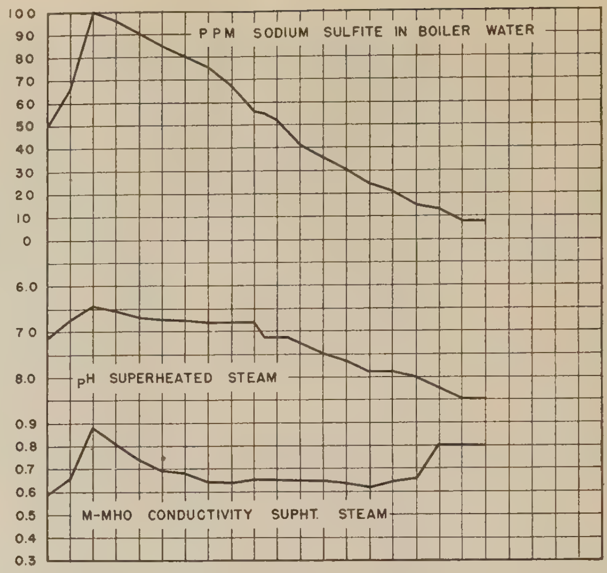

Fig. 6 Test Run to Show Effect of Sodium Sulphite on Steam Quality Boiler Water pH 11.5

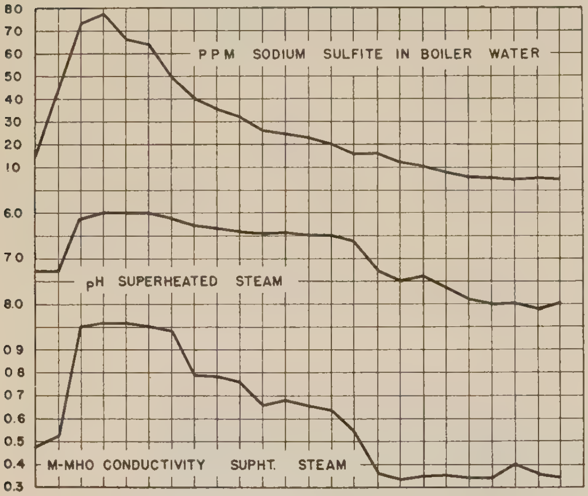

Fig. 5 Test Run to Show Effect of Sodium Sulphite on Steam Quality Boiler Water pH 11

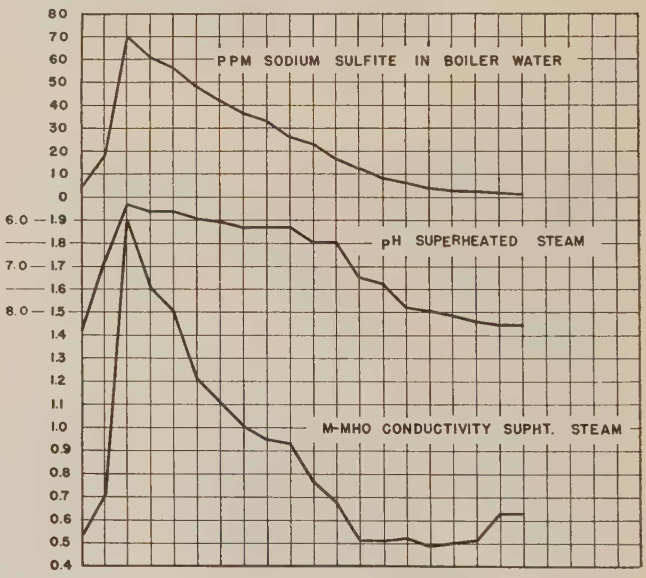

Fig. 7 Test Run to Show Effect of Sodium Sulphite on Steam Quality Boiler Water pH 10.8

It is to be noted that the conductivity data will not show exactly how the quality of the steam is being affected by sodium sulphite. The conductivity, together with the pH of the steam condensate, are required in order to observe the variations in steam quality.

The foregoing pH and conductivity data, for various sodium sulphite concentrations, and a pH of 11 in the boiler water, were confirmed within close limits by the test data obtained for the boilers at the Redondo Steam Station, of the Southern California Edison Company. The data for one test, made during a period of full load, are shown in Fig. 5. At this time the boiler was operated at 950 psi, and the superheated-steam temperature was 900 F. The total alkalinity of the boiler water was approximately 100 ppm, and the pH was near 11.

Of special interest are the data which show that a concentration of sodium sulphite in excess of approximately 60 ppm appears to have little further effect on lowering of the pH and raising the conductivity of the steam condensate. It seems that the pH and alkalinity of the boiler water may at this point retard any further increase in the amount of acid ions which are present in the steam.

As in the case of Fig. 4, the data in Fig. 5 show that if the pH of the steam is to be held at near maximum values, while carrying a boiler water pH of 11 and an alkalinity of 100 ppm, it will be necessary to limit the sodium sulphite in the boiler water to a maximum of 7 ppm.

The test data for the steam condensate show that the pH varied between 6 and 8.1, and the conductivity between 1.0 micromho and 0.3 micromho when the sodium sulphite in the boiler water was varied between 78 ppm and 5 ppm. The slightly lower pH and conductivity values obtained for the steam condensate at Redondo Steam Station are believed to be due principally to the presence of less ammonia. A concentration of not over 0.01 ppm was indicated. At the Harbor Steam Plant the ammonia in the steam condensate was found to vary between 0.02 ppm and 0.03 ppm.

In order to study the effect of boiler water pH and alkalinity on the action of sodium sulphite concentration, a number of test runs were made during which the boiler water pH was increased to 11.5 and 11.6 instead of the normal pH of 11 to 11.1. The results of a typical test are shown in Fig. 6. The pH of the boiler water was held at 11.5, and the total alkalinity was 150 ppm. These data are similar to those obtained at a boiler-water pH of 11.6 and 200 ppm of alkalinity. The boiler was operated at 17 per cent of normal full load.

The data show less change in pH and conductivity with high sodium sulphite concentrations than when the pH of the boiler water was lower, For example, the minimum pH of the condensate was 6.5, instead of 6.0 for a lower boiler water pH. Also, a pH of 7.9 is reached at a sodium sulphite concentration of 24 ppm. However, it will be seen that the pH of the steam condensate continues to increase with decrease in sodium sulphite concentration until, at the maximum of pH 8.5 the sodium sulphite is 8 ppm. Thus a pH of 11.5 in the boiler water was found to have a limited beneficial effect in attaining the maximum pH of the steam condensate.

In order to show the effect of low pH and alkalinity in the boiler water on the action of sodium sulphite, a test was made during which the pH was held at 10.8, and the total alkalinity at about 60 ppm. The results, as given in Fig. 7, show that except for concentrations below about 10 ppm, the sodium sulphite had a definitely greater effect on the pH and conductivity of the steam condensate than when the pH of the boiler water was higher. The amount of reducing material found in the steam was also definitely greater than for higher boiler-water pH.

Each of the foregoing test runs required from 3 to 5 days for completion, during which the condition of the boiler feedwater was maintained as nearly constant as was possible. No large variations in the composition of the feedwater were observed.

The test results for the saturated-steam condensate are not shown, but it is of interest that the saturated steam showed a slightly higher pH than has been reported for the superheated steam. Generally, the difference did not exceed about 0.2 pH.

The tests made at the Seal Beach Steam Plant, on a boiler operating at 375 psi, failed to show any significant changes in pH or conductivity of the steam condensate which could be attributed to the sodium sulphite concentration in the boiler water. Confirming tests should be made under more favorable feedwater conditions, as when a minimum of carbonate is present.

Data Relating to Reducing Material in Steam

Identification of the reducing materials in the steam condensate, which were related to changes in sodium sulphite concentration in the boiler water, the amounts of reducing material in the steam, and the pH and conductivity of the steam condensate, was of interest. This information was not considered to be an essential part of the practical test results obtained, or the main conclusions which were reached in regard to control of the quality of the steam. However, as a matter of interest the data now available are presented. These data and observations may be of use in any further investigation of the decomposition of sodium sulphite in the boiler.

The actual composition of the acid material and the reducing materials in the steam condensate were identified by process of elimination, and by correlation of the reducing material found in the steam condensate with pH and conductivity changes in steam condensate to which reducing material in the form of sulphurous acid was added. The conductivity readings were useful in showing that there were limited amounts of total solids and dissolved gases in the steam condensate.

On numerous occasions, during normal operation, and during several of the experimental runs, tests were made from the presence of sulphides in the steam condensate. In some instances it was believed that a trace of sulphide was present, especially when the condensate had a slight odor resembling sulphide. However, the amount was not sufficient to determine by quantitative analysis, and it was concluded that sulphides represented only minor amounts of the total reducing material found in the steam condensate.

It was assumed that at least part of the reducing material found in the steam was sodium sulphite or other neutral reducing material. During most of the test runs, the increases in reducing materials in the steam condensate corresponded with increases in acidity, decreases in pH, and increases in conductivity. These data have indicated that the amounts of neutral reducing material will vary with the pH of the boiler water and with the alkaline materials present in the steam condensate.

During some of the tests, there was present considerable excess of reducing material over that which can be accounted for by changes in pH of the steam condensate. At high boiler-water pH, the conductivity change was relatively small. These variations have not been explained fully.

The amounts of reducing material found during several of the boiler tests and the corresponding sodium sulphite in the boiler water are shown in Fig. 8. It was observed that within limits, the amount of reducing material in the steam tends to increase with increase in the sodium sulphite in the boiler water, but since each change in boiler water pH, or other condition, gives a different ratio of reducing material to sodium sulphite, it is not possible to show one curve which will apply to all of the boiler tests. Therefore the data shown in Fig. 8 should be checked for each test run that is made. As a matter of convenience, the reducing material is shown as equivalent sulphurous acid.

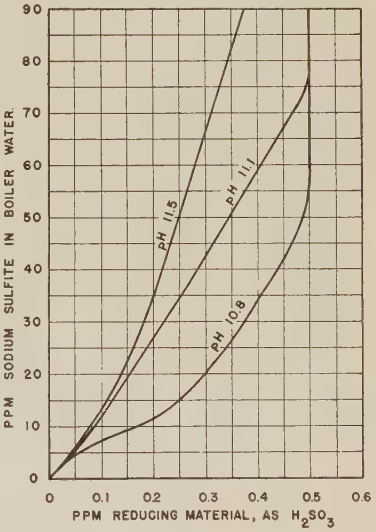

Fig. 8 Variation in Reducing Material in Steam Condensate With Change in Sodium Sulphite Concentration and pH of Boiler Water

The effect of measured additions of sulphurous acid on the pH and conductivity of steam condensate is shown in Figs. 9 and 10. Due to the presence of ammonia and other materials in the condensate, these data are not assumed to be applicable to all boilers. The effect of the alkalinity of the condensate is seen at the start of the pH and conductivity curves. The relationship between pH and sulphurous acid was used in reaching the conclusion that a considerable amount of the reducing material in the steam was sulphurous acid.

In order to compare these data with the test results, it will be necessary to refer first to Fig. 8 which shows the equivalent sulphurous acid found in the steam condensate for different concentrations of sodium sulphite in the boiler water. The sulphurous acid and sodium sulphite values shown may then be used to note whether or not the pH and conductivity results actually obtained for a given sodium sulphite concentration and pH value in the boiler water will parallel the changes in the pH and conductivity values found by additions of sulphurous acid to steam condensate.

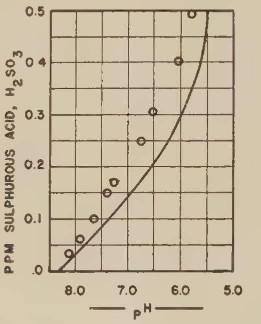

Fig. 9 Change in pH of Steam Condensate With Change in Sulphurous Acid Concentration
(0 Equals pH equivalents for test run shown in Fig. 7.)

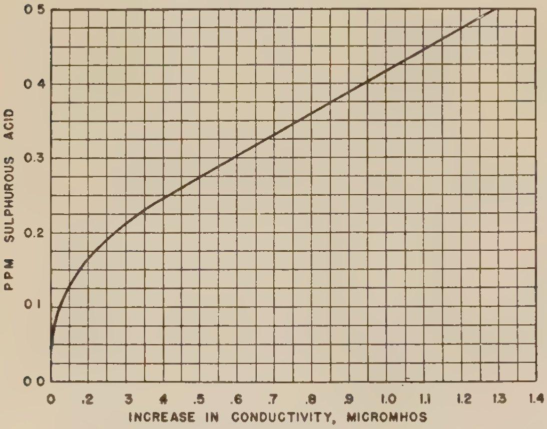

Fig. 10 Change in Conductivity of Steam Condensate With Change in Sulphurous Acid Concentration

By way of illustration, identifying marks have been made in Fig. 9 to show how closely the boiler-test data shown in Fig. 7 parallels the change in pH, when equivalent amounts of reducing material, in the form of sulphurous acid, are present.

Attention is called to the fact that small increases in the amount of acid or alkaline material will cause a considerable change in the pH and conductivity of the steam condensate, and that care is required in obtaining the measurements.

Conclusions

Based on the data obtained from boilers operating at 900 psi and over, the following conclusions have been reached:

It is probable that when more than 5 ppm to 8 ppm of sodium sulphite is present in the boiler water, the quality of the steam will be affected.

The extent to which the composition of the steam is changed will depend largely on the concentration of sodium sulphite, and to some degree on the alkalinity and pH of the boiler water.

The change in steam quality is seen in the lowering of pH, increase in the conductivity and increase in the reducing material of the steam condensate.

A large part of the reducing material found in the steam condensate resembles sulphurous acid.

When the steam contains sufficient ammonia or other alkaline material to overbalance the acid effects of carbon dioxide, it is probable that with small amounts of sodium sulphite in the boiler water, the point of lowest conductivity of the steam condensate will be near a pH of 8. Near this point, increasing the sodium sulphite concentration will lower the pH and raise the conductivity of the condensate, but lowering of the sodium sulphite will increase both the pH and conductivity.

The test data which are presented are of special interest when using conductivity readings to estimate the solid-matter content of the steam condensate and in regulating the amount of solid matter in the form of acid-reducing material.

The quality of the steam from boilers operating at pressures below 900 psi, should be studied further, in order to show the effects of sodium sulphite in the boiler water.

Acknowledgments

To the executive staffs of the City of Los Angeles, Department of Water and Power, the Southern California Edison Company, and to Sheppard T. Powell, appreciation is expressed for the support given to the investigation and for permission to publish the data. Special acknowledgment is given to H. T. Duplice, Harbor Steam Plant Superintendent, and his laboratory staff for the assistance received in arranging and carrying out the tests.

Appendix

After the completion of the foregoing tests, which show the effect of sodium sulphite in the boiler water on the quality of the steam condensate, it was decided to investigate the extent to which the reducing material, expressed as equivalent sulphurous acid, in the steam would carry on through the feedwater system. Accordingly, a test run was made during which the sodium sulphite in the boiler water was raised to 65 ppm by direct injection into the boiler drum, no sodium sulphite was added to the feedwater, and the sodium sulphite in the boiler water was allowed to diminish while testing the steam condensate for pH-value conductivity and reducing material in the condenser hot-well condensate and the feedwater leaving the deaerator for reducing material. The data are shown in Fig. 11. The results of this test confirm some of the previous data and, at the same time, show the rate at which the acid sulphite in the water is oxidized as it passes through the condenser and the various heaters and the deaerator. Furthermore, the test data show the possibility of maintaining a sufficient concentration of sodium sulphite in the boiler water, in order to maintain some reducing material in the feedwater and thus remove dissolved oxygen.

It appears that if the sodium sulphite in the boiler is as great as 10 ppm to 15 ppm, the feedwater before the deaerator will contain a significant amount of reducing material. However, the results found at Harbor Steam Plant are not likely to be duplicated at other plants, and similar tests would need to be made in order to determine the actual condition. It should be noted especially that the rate of reaction of sulphite with oxygen will increase with increase in temperature and, no doubt, to some extent on the concentrations of dissolved oxygen and reducing material. The presence of catalysts also will have a decided effect on reaction rates.

The actual pH value of the steam condensate and feedwater

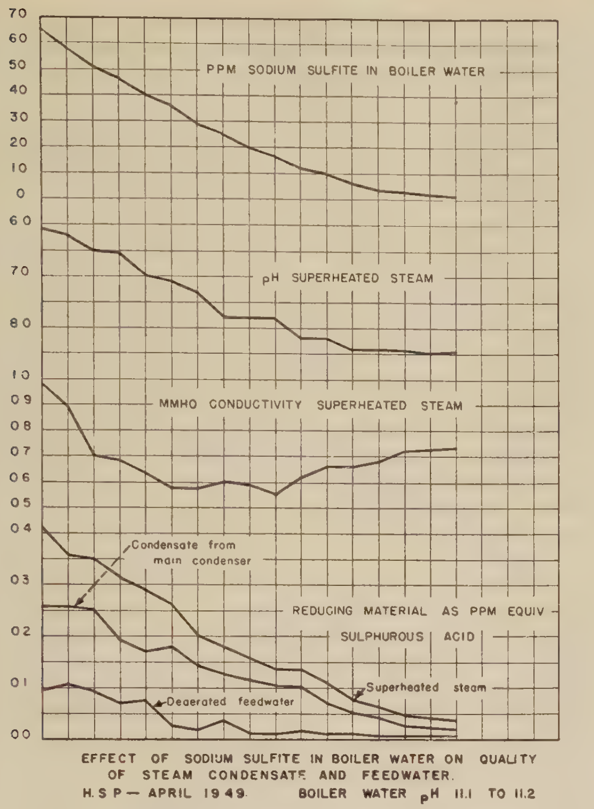

Fig. 11

at Harbor Steam Plant was influenced to some extent by the ammonia naturally present in the water. The ammonia had the effect of neutralizing the acid sulphite and other acid materials in the steam.

These data suggest certain possible advantages in selection of the concentration of sodium sulphite in the boiler water, provided this concentration does not depress unduly the pH value of the steam condensate and the feedwater.

Discussion

M. D. Baker.[8] Mr. Alexander and Mr. Rummel have presented an interesting paper and the data given is a worth-while contribution to the study regarding the behavior of sodium sulphite when used as an oxygen scavenger in boiler water.

The fact that all conclusions are based on superheated-steam condensate and not sufficient data were presented on saturated-steam condensate to make a comparison between saturated and superheated-steam condensate eliminates any conclusions regarding mechanical carry-over with subsequent decomposition of sodium sulphite in the superheater. Some of the results obtained indicate that mechanical carry-over occurred and it would be valuable information if the authors could make any definite comparisons.

The conclusion that sodium sulphite concentrations of 7 ppm or less will not affect the pH of the steam condensate and the data used to obtain the curves in Fig. 5 indicate that the authors have information that should be a worthy contribution in the study of sulphite behavior in boiler water. This leads to several questions. First, do the authors feel that they have sufficient data to make a statement regarding the point of stability of sodium sulphite in boiler water? What is meant; can they state from numerous test data that 7 ppm of sodium sulphite is the minimum concentration at which decomposition due to excess sulphite will occur? When above 7 ppm of sodium sulphite what causes it to decompose and what are the mechanics of the decomposition?

In Fig. 5 does their interpretation of the curves mean that above 50–60 ppm of sodium sulphite the rate of automatic decomposition is constant and continues so until the concentration is lowered to 10–20 ppm of sodium sulphite?

C. E. Kaufman.[9] In the authors' careful investigation of the decomposition of sodium sulphite in boiler water, the emphasis has been on the production of small amounts of sulphurous acid through hydrolysis. Quantitatively, there may easily be some question as to the exact amount of material produced in the steam since the over-all effect is so small. However, the actual fact of SO_2 or H_2SO_3 production would not be unexpected from a physical-chemical standpoint. In fact, substances subject to this sort of behavior might well be listed in a series. For example, in decreasing order of tendency to contribute material to the steam, we might list sodium carbonate, sodium sulphite, and sodium silicate.

In general, with all of these materials, greater amounts of the corresponding acid would be expected to be released as pH of the boiler water is dropped.

In the case of sodium sulphite, the fact of hydrogen sulphide development should not be neglected. The authors found rather negative evidence in this regard but there have been a number of occasions in the experience of the discusser's organization where hydrogen sulphide was a major product.

The difficulty of analyzing for small quantities of sulphur compounds brings up a question. Was it not possible to secure a sampling point where concentration of gases could occur? The aftercondenser on a steam-jet ejector for a turbine condenser will frequently provide rather remarkable and convincing samples. For example, in a number of cases at such a location, "odorific" analysis (rotten-egg smell) alone proved that hydrogen sulphide was an important breakdown product. In like manner, appreciable concentrations of ammonia, far higher than in the over-all steam, have been found.

Ten years ago we investigated the behavior of a 1400-psig boiler which produced steam of increasing conductivity after feed of sodium sulphite. Fig. 12 shows the similarity of this action to that reported by the authors. Only traces of sulphur com-

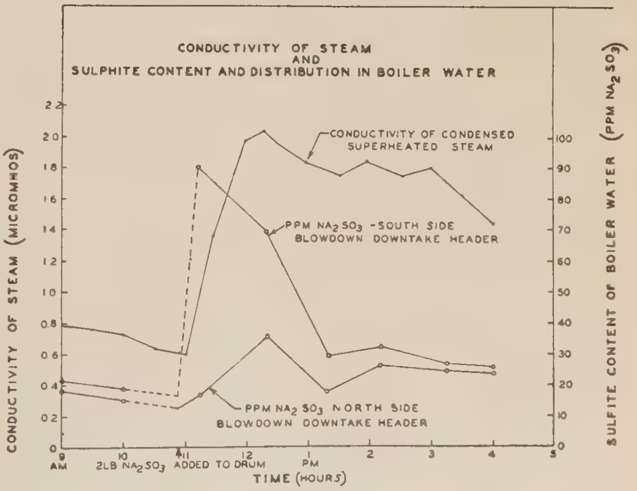

Fig. 12

---

[8] Chief Chemist, West Penn Power Company, Pittsburgh, Pa.

[9] Hall Laboratories, Inc., Pittsburgh, Pa.

pounds were found by field tests in the steam from regular sampling connections. Slower feed of chemical reduced the effect.

What is the significance of sulphur compounds in the steam? The presence of hydrogen sulphide may indicate that hot spots exist in the boiler with attendant auto-oxidation of sodium sulphite to produce sulphate and sulphide. In other words, sulphide production may be a symptom of somewhat critical conditions. Sulphur dioxide or sulphurous acid in the steam may contribute to somewhat lower pH in the condensate but its total effect will be little more conducive to acid corrosion than a small amount of carbon dioxide. In fact, the use of alkaline materials such as ammonia and amines in the steam should undoubtedly be as effective for SO_2 as for CO_2.

The presence of SO_2 (or CO_2) in the steam going to a turbine will be of no concern. Before condensation it is obvious that the dry steam containing gases can have no effect on the metal. Even at a condensing end, solubility relationships dependent on temperature and partial pressures can permit only a trace of gas in solution. In other words, internal corrosion of turbines during operation due to dissolved gases is most improbable.

Thus, although the breakdown of sulphite is of considerable theoretical interest, the small effect which may occur lacks much practical significance. Years of trouble-free experience with boilers at many pressures provide assurance that there is no cause for alarm.

F. G. Straub[10] and H. D. Orgman.[11] Sodium sulphite has been used as an oxygen scavenger in steam boilers for almost twenty years. Taff, Johnstone, and Straub called attention[12] to the possibility of the decomposition of this material in concentrated solutions (4000 ppm) at temperatures above 540 F to form sodium sulphide and sodium sulphate. Hitchens and Purssell[13] reported the results of their study of steam from boilers operating at pressures up to 1400 psi. Their conclusions were that the decomposition to sodium sulphide and sulphate did not take place at concentrations normally carried in the boiler water.

In the intervening years the prevailing opinion appears to have been that in concentrations below 20–30 ppm of sodium sulphite very little, if any, sulphide appears to form. However, if areas in the boiler exist where the sulphite can concentrate, sodium sulphide forms and hydrogen sulphide is found in the steam at steam pressures around 1200 psi.

Some plants have used an excessive amount of sulphite when feeding it intermittently to boilers. This was reduced to a much smaller amount when fed continuously even in cases of practically no blowdown from the boiler. This indicated the possibility of some loss of sulphite at the higher concentrations occurring during intermittent feeding of the chemical.

In order to explain some of the peculiar behavior of the sulphite and to study the limitations of its use, the authors started a study in which a small laboratory steaming test boiler was used. This work is not completed. However, since they have observed the same action that the authors of this paper have, it was deemed advisable to discuss this paper at this time.

The laboratory tests have covered the behavior of sodium sulphite at various concentrations in the boiler water from 250 to 1550 psi. The steam in all cases shows a reduction in pH and an increase in conductance which is almost proportional to the sulphite concentration in the boiler water. The effect is almost proportional to the steam pressure.

The authors' conclusion that sulphurous acid is being distilled from the boiler water appears to be a logical one. In many power plants there has been sufficient ammonia or caustic carry-over from the boiler to mask the pH reducing effect of the small amount of sulphurous acid in the steam. The authors of this paper have been fortunate in having steams with low ammonia content with which they could run their determinations.

The results of these tests should be correlated with the experience in other plants before the power-plant operators become panicky about the effect of sulphite treatment on their preboiler equipment. In many plants sufficient ammonia is present to neutralize the small amount of sulphurous acid in the steam. It indicates the need of control of sodium sulphite in the boiler water to within reasonable limits and at the same time an adequate means of continuously adding the sodium sulphite to the system as to reduce the high peaks of concentrations to a minimum.

W. D. Bissell,[14] W. W. Cerna,[15] E. L. Knoedler,[16] L. G. von Lossberg,[17] and E. B. Powell.[18] The authors have made a very important contribution to boiler-water chemistry, adding valuable, information on the reaction products from sodium sulphite and also contributing constructively to water chemistry, in general, by bringing to attention clearly how sparse and sketchy is the actual knowledge of reactions at moderately high temperatures in this field.

Taff, Johnstone, and Straub in their 1937 paper,[12] as the present authors comment, make no mention of analyses of steam sampled from their bombs but find from analyses of the reacting solutions increasing rates in conversion of sodium sulphite to sodium sulphide and sodium sulphate with temperature increase in the range of about 530 F to 600 F. As reported by Parks[19] it was found in operation of the 2000-psi boiler at Somerset Station that sodium sulphite, when maintained at more than a few parts per million in the boiler water, resulted in considerable contamination of the steam with hydrogen sulphide. As reported by Parks in the paper just mentioned, and by Cerna and Scott,[20] use of potassium-base chemicals in place of sodium-base chemicals was begun at Somerset Station in 1943. As affecting the sulphite radical the change in nature of chemical base apparently brought no very significant change in reactive tendency or essential nature of reaction products. Observations on the 2000-psi boiler at Somerset Station with water temperatures in the range of about 600 F to 625 F have indicated that, for the associated operating conditions, concentrations of sulphite chemical in excess of 4 or 5 ppm SO_3 are accompanied by evolution of hydrogen sulphide and formation of sodium sulphate and some alkali, as evidenced by methyl orange, but scarcely more than a trace of sodium sulphide. Considered together, the observations of the three independent investigating groups suggest that at temperatures of about 530 F and above, sulphites when present in boiler water in excess of some rather small concentrations may be expected to decompose or react with constituents other than dissolved oxygen, and that there exists critical temperature or critical temperatures within the range of 530 F and 625 F above and below which such sulphite reactions are of distinctly different nature, and doubtless other factors are of importance which may even shift the critical reaction temperatures.

---

[10] Research Professor in Chemical Engineering, University of Illinois, Urbana, Ill. Mem. ASME.

[11] Research Assistant in Chemical Engineering, University of Illinois, Urbana, Ill.

[12] "Decomposition of Sodium-Sulphite Solutions at Elevated Temperatures," by W. O. Taff, H. F. Johnstone, and F. G. Straub, Trans. ASME, vol. 60, 1938, pp. 261–265.

[13] "Behavior of Sodium Sulphite in High-Pressure Steam Boilers," by R. M. Hitchens and J. W. Purssell, Jr., Trans. ASME, vol. 60, 1938, pp. 469–473.

[14] Superintendent of Engineering, Montaup Electric Co., Fall River, Mass. Mem. ASME.

[15] Engineer, Hagan Corporation, Pittsburgh, Pa. Mem. ASME.

[16] Chemical Engineer, Sheppard T. Powell, Baltimore, Md. Mem. ASME.

[17] Chemical Engineer, Sheppard T. Powell, Baltimore, Md.

[18] Consulting Engineer, Stone & Webster Engineering Corporation, Boston, Mass. Mem. ASME.

[19] "Experience With Sodium and Potassium Chemicals for Boiler-Water Conditioning at Montaup Electric," by G. U. Parks, Trans. ASME, vol. 67, 1945, pp. 335–338.

[20] Water Conditioning for the 2000-Psi Boiler at the Somerset Station of the Montaup Electric Company, by W. W. Cerna and R. K. Scott, Trans. ASME, vol. 68, 1946, pp. 443–451.

Sheppard T. Powell.[21] In spite of the extensive use of sodium sulphite as a deoxygenating chemical, there is a dearth of quantitative information on the mechanism of the reaction which occurs and the rate and extent of dissociation of sulphites under high-temperature conditions. These phenomena are not particularly significant for low-pressure boiler operation, but the need for such data for high pressure and temperature conditions is urgent. Many operators have concluded that the sulphite salts break down, and have noted the presence of hydrogen sulphite qualitatively in condensate. The authors of these papers have contributed much reliable information, and the data assembled and their extensive investigation have established a sound basis for control of this essential treatment. Other investigators have approached the problem from a somewhat different angle, but their findings generally confirm the authors' conclusions. This paper is a major contribution to the subject and presents definite and reliable data for control of sulphite treatment which, up to the present time, have not been definitely established.

Hydrogen sulphide in steam and condensate has come from sources other than sulphites. The writer has encountered two cases where extensive breakdown of sulphides occurred, which produced heavy concentrations of hydrogen sulphide in the condensate. At both the stations where the difficulty occurred, the feedwater was treated by hot-process softening systems, and the filter material in pressure filters used to filter the effluent was crushed magnetite. The pH value of the water was between 9.0 and 10.5. The sulphides were dissolved from the iron sulphide present in the magnetite ore. An attempt was made to secure magnetite free from sulphide, but no material completely free of iron sulphide could be obtained. It was found necessary to replace the filter material with anthracite coal, after which the presence of sulphide in the condensate was completely eliminated.

Authors' Closure

The authors wish to thank the various commentators for their discussion dealing with the usefulness of the data which have been presented. In answer to Mr. Baker's question on the difference between the quality of the saturated and superheated steam condensates and the effect of carry-over of sodium sulphite into the superheater, it has been stated that we found only a little difference in the quality of the two steam samples. For example, during most of the tests the pH value of the saturated steam was about 0.2 higher than for the superheated steam. Since this difference can be observed with only a trace of sodium sulphite in the boiler water, we have not been able to attribute the changes in pH value of the superheated steam to carry-over of sodium sulphite, followed by decomposition in the superheater. With regard to Mr. Baker's questions on the stability or decomposition levels of various sodium-sulphite concentrations in the boiler water, the conditions of testing were such that the data do not show exact equilibrium conditions. It was indicated that for the boilers under test and the analyses of the boiler water, the pH value and conductivity of the steam condensate would not be changed appreciably when the concentration of sodium sulphite was held at not over 5 ppm to 8 ppm.

In answer to Mr. Kaufman, the authors have on various occasions tested the gas and water leaving the after condenser of the steam jet ejector for the main condenser and have used this data for the control of ammonia in the system. At times we found traces of hydrogen sulphide. However, there are obvious difficulties to be overcome in making quantitative tests of steam quality at this point, and direct tests on the steam samples are recommended.

It was observed that very small amounts of hydrogen sulphide could be detected by smell, but that on a quantitative basis the hydrogen sulphide was of very minor significance during any of the tests which have been described. With regard to the significance of corrosive sulphur compounds in the steam, the authors have been concerned with the amounts of iron oxide and copper found in the water at the condenser hot well and the iron oxide produced in the feedwater systems and the boilers. Concerning the suggested use of amines; an amine which has been used in power plants to raise the pH value of steam condensates decomposed and disappeared rapidly in one of the boiler systems under study and in the absence of a stable material, it is not recommended that amines be used in high-pressure boilers.

In order not to increase the solubility of copper alloys it was not desired to increase the ammonia content of the feedwater and the steam. However, when the acid gases in the system were reduced to a minimum, ammonia in concentrations of as low as 0.02 ppm was found to be effective in maintaining a pH value of 8 or better in the steam condensate.

The authors are very appreciative of information submitted by Drs. Straub and Orgman. Their conclusions, in regard to recent laboratory boiler tests made at various pressures and concentrations of sodium sulphite and pH value, are in confirmation of the conclusions reached by the authors. Due to the broader scope of their studies the completed data and conclusions will be of considerable interest. As has been indicated, the authors are in full agreement with the recommendation that tests be made at individual power plants in order to note the effect of sodium sulphite in the boiler water on the quality of the steam condensate.

The information submitted by Messrs. Bissell, Cerna, Knoedler, von Lossberg, and E. B. Powell have been of interest and we are especially appreciative of the favorable comment which has been offered. Due to limitations in operating pressure for the tests made by the authors, we are unable to verify the indication that hydrogen sulphide is an important product of sodium sulphite decomposition in boilers operated at 2000 psig, but it is suggested that the test methods mentioned in this paper be considered.

In answer to Mr. S. T. Powell's favorable comment, the authors have not been able to confirm the work of others on the production of appreciable amounts of hydrogen sulphide. On the contrary, hydrogen sulphide appeared only as traces and during periods of highest sodium sulphite concentrations in the boiler water. Mr. Powell has mentioned the very interesting possibility that sulphides may be introduced from sources other than sodium sulphite and in this connection the composition of the cooling water to the main condensers should be taken into account.

In closing it is again suggested that the analytical methods which have been presented be considered and that similar quantitative tests on operating boilers be carried out. At this time the decomposition products of sodium sulphite may be measured quantitatively and it should be possible to distinguish between smell and amount of any sulphides which are present.

---

[21] Consulting Chemical Engineer, Baltimore, Md. Fellow ASME.

Feedwater Treatment During Early Operation of Steam-Electric Stations

By R. C. ALEXANDER[1] and J. K. RUMMEL[2]

Based upon the experience with five high-pressure steam-generating units installed at the Harbor Steam Plant of the City of Los Angeles during the last six years, the authors devise some basic practices to follow during early operation of such installations. Their study includes such items as cleaning the feed system, corrosion prevention, chemical control of corrosion, sampling and control tests of the feedwater system, and inspection of equipment.

During the last six years a total of five high-pressure steam-generating units have been installed at the Harbor Steam Plant. The boilers of the first two units operate at 1050 psig drum pressure. The boiler-drum pressure for the last three units varies with load demand. Normally, it varies between 900 psig and 1000 psig. The superheated-steam temperature is 915 F for all units. The first unit was started in 1943, and the last unit began operating on load in July, 1949.

During this time it was found that the items to be considered in preparing the units for service and early operation were not only numerous, but deserved considerable detailed attention.

In general, it has been necessary to study the design, the arrangement of equipment, and the particular local conditions which affected the satisfactory control of the make-up water and the feedwater. Usually the most important single consideration has been the maintenance of minimum corrosion of the feedwater-system equipment, and the disposal of corrosion by-products which lodge in the heaters and the boilers.

These by-products are for the most part iron oxide and copper, which are likely to encourage further corrosion, reduce heat-transfer rates, and cause overheating of boiler tubes.

Due to the highly corrosive harbor water used for cooling in the main condensers, there have been a large number of condenser-tube failures, and contamination of the feedwater with sea water has been a frequent occurrence. This has added considerably to the suspended matter and insoluble solids found in the boilers of units Nos. 1 and 2. At the same time, it has been necessary to maintain a close watch on the condition of the feedwater in order to avoid serious consequences from sea-water leakage. It is fortunate that there have been available the facilities for testing and treatment control, which were installed with each unit, and that satisfactory methods of procedure have been provided or developed as they were required.

Cleaning the Feed System

As shown by past experience, it is highly important that the feedwater system and interconnected equipment be cleaned thoroughly of dirt, grease, rust, and other foreign material which would cause difficulties in operation of the pumps, heat exchangers, and the like, or be carried on to the boilers. When this important step is neglected, the resulting maintenance costs are found to be disproportionate to the probable cost of the preliminary cleaning.

Present practice at Harbor Steam Plant is first to clean by hand all surfaces which can be reached, such as the condenser shell and hot well, the heat exchangers, and the deaerator with its storage tank. Heat-exchanger tubes are cleaned with air and water, and any grease on the tube ends is removed with brushes and a detergent solution. Preliminary cleaning of the unit was followed by circulation of a hot detergent solution through the feed system. This operation simulated the "boiling out" of the boiler. It was effective in removing soluble oil coatings on parts of the equipment and in loosening the dirt for removal by the water flushing which followed. Finally, all traps where dirt collected, such as the bottoms of tanks and the condenser hot wells, were cleaned by hand.

The results of the foregoing cleaning operations have been highly satisfactory, as was reflected in a minimum amount of material carried into the boilers from the feed system, general freedom from clogging of screens used in preliminary operations, and no known damage to pumps or other equipment. After preliminary operation, an examination of one of the boiler units showed that only 2 to 4 grams of deposit could be removed from the tubes, and very little dirt was seen in the feedwater-system equipment. The amount of deposit in the boiler tubes was determined by placing a cloth filter bag over the end of the tube, followed by cleaning with an air-driven rotary wire brush. The bag was then shaken out over a clean paper and the material weighed.

The boiler tubes and drums were washed with water from a hose in order to remove the loose materials, and recently a high-pressure water-washing nozzle has been made for lowering down the tubes in order to clean them more thoroughly.

All of the superheater tubes are washed individually with condensate, flowing at high velocity, in order to remove both insoluble and soluble deposits such as would cause overheating or be carried through the steam turbine and into the feedwater system. A specially designed washing connection is used, which is held in the tube ends with air pressure while the water is flowing through. The washing time is regulated by use of an electronic-eye conductivity indicator and a dip cell. This shows the completion of removal of the soluble material. Visual examination of the wash water shows the removal of insoluble material.

Corrosion Prevention

Returning to the main problem of corrosion prevention, it has been found that both iron and copper are present in the feedwater, and that the deposits found in the feedwater-system equipment and the boilers are composed mostly of iron oxides and copper.

During early operation a large part of the iron oxide comes from the mill scale on the surfaces of the equipment, but after the loose scale has been removed the corrosion process continues to add iron to the feedwater. In the older units the iron in the feed-

---

[1] Mechanical Engineer, City of Los Angeles, Department of Water and Power, Los Angeles, Calif.

[2] Chemical Engineer, Sheppard T. Powell. Consulting Chemical Engineer, Baltimore, Md. Mem. ASME.

Contributed by the Joint Research Committee on Boiler Feedwater Studies and Power Division and presented at the Semi-Annual Meeting, San Francisco, Calif., June 27–30, 1949, of The American Society of Mechanical Engineers.

Note: Statements and opinions advanced in papers are to be understood as individual expressions of their authors and not those of the Society. Manuscript received at ASME Headquarters, January 6, 1950. Paper No. 49—SA-48.

water was about 0.1 ppm and the copper about 0.03 ppm. These data show that appreciable corrosion of the copper alloys in the feedwater system is to be expected, and in this connection it has been realized that there is present a considerably larger area of copper alloy than iron.

Visual inspections of the equipment have shown that corrosive attack has been most rapid where the pH of the water has been lowered by acids and where dissolved oxygen is present. In the deaerator vent condensers, ammonia no doubt has played a part in hastening the failure of brass condenser tubes, but in zones of lower ammonia, acid, and dissolved-oxygen concentrations, no appreciable attack has been seen, and no failures due to corrosion have been experienced.

In some instances erosion has hastened the tendency for corrosion to take place. This was especially noticeable on the turbine-casing surfaces which are in the path of the steam entering the main condenser. However, the attack on the main condenser shell has taken place more rapidly in the air off-take section where the steam condensate contained relatively large amounts of dissolved oxygen and acids.

Another point of local corrosive attack, due to adverse water conditions, has been in the condensate drip-system equipment, which carries the condensate from the evaporator condenser and the stage heaters. This has been noticed in the first unit installed which, during its early operation, carried the vented vapor from the evaporator condenser. This vapor is now vented to atmosphere, and the pH of the water is more favorable. Previously the pH of the water was as low as 5.5 and is now seldom less than pH 7.

Considering the action of carbonic acid alone, it is of interest to note that for an equivalent reduction in pH, much more of this acid is required than if a mineral acid is present. Also, when the acidity of the water has been increased to give a pH of a little less than 5, the carbonic-acid solution is found to be more corrosive than a solution of the same pH to which only hydrochloric acid is added. Whitman, Russell, and Altieri[3] have examined this action experimentally and their results are shown graphically in Fig. 1. It is explained that since at pH 5.4 the carbonic acid is only 6 per cent dissociated and hydrochloric acid is nearly 100 per cent dissociated, the carbonic acid would be about 16 times more concentrated than the hydrochloric acid. It is seen from these data that the corrosion rates may at times depend more largely

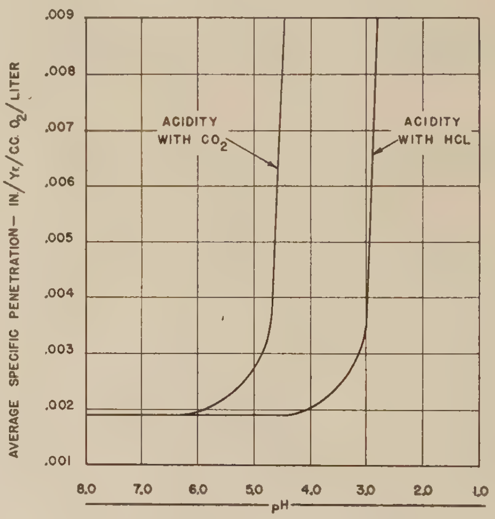

Fig. 1 Comparison of Rates of Corrosion for Carbonic Acid and Hydrochloric Acid

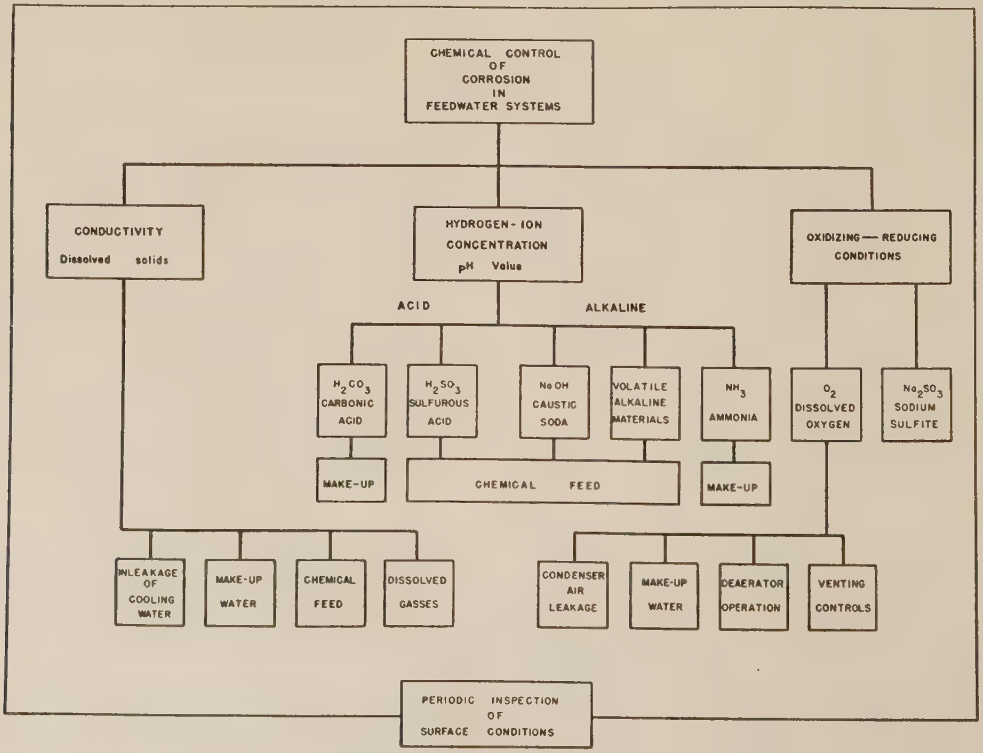

Fig. 2 Items Entering Into Chemical Control of Corrosion

upon the acid concentration than the pH value, and a low pH due to carbonic acid may cause a serious amount of corrosion.

---

[3] "Effect of Hydrogen Ion Concentration of the Submerged Corrosion of Steel," by W. G. Whitman, R. P. Russell, and V. J. Altieri, *Industrial and Engineering Chemistry*, vol. 16, 1924, pp. 665–670.

"The Acid Corrosion of Metals," by W. G. Whitman and R. P. Russell, *Industrial and Engineering Chemistry*, vol. 17, 1925, pp. 348–354.

Chemical Control of Corrosion

For purposes of discussion, the principal items which have entered into chemical control of corrosion in the feedwater systems are shown in Fig. 2. It is indicated here that the principal controls are conductivity, pH, and oxidizing or reducing conditions. Under these are subheadings showing the materials which are present or are added to the feedwater, to counteract any adverse conditions. Other subheadings show sources of feedwater impurities. This type of chart is useful in visualizing the chemical conditions which may exist and the corrective measures which should be taken.

As is indicated, emphasis has been placed upon avoiding high conductivity due to condenser leakage, adjustment of the pH to the highest practical value, and the maintenance of reducing conditions in all parts of the system where such control is feasible.

Dealing with the details of chemical control, it has been realized that all of the factors listed in Fig. 2 are somewhat interrelated and that the corrosion rates may be dependent upon a combination of conditions. This interrelationship is not always clear, but it has required consideration when making adjustments to the treatment control or in evaluating the corrosion found.

The effect of conductivity on corrosion rate has not been shown definitely but it is obvious that the higher the conductivity of the water the better the opportunity for electrochemical corrosion to proceed. Therefore any unnecessary increase in feedwater conductivity has been avoided. This matter has not been considered when adding the chemicals for treatment, since their beneficial effects are assumed to be much greater than any adverse effect due to conductivity. The avoidance of condenser leakage or addition of other high-conductivity water has been given first consideration.

The control of pH in the steam condensate, the feedwater, and the drip returns is considered to be of primary importance and has been given the greatest amount of attention.

As is known, the steam condensate, which is practically the whole of feedwater, is unbuffered, and any small amounts of acid or alkali will make a considerable change in the pH value. Therefore the elimination of dissolved carbon dioxide which forms carbonic acid, and the minimum generation of acids from sodium sulphite in the boiler water, are given close attention. As a first step, the pH value of the steam condensate is maintained in excess of pH 8.2 by careful regulation of the boiler-water alkalinity and sulphite concentrations, and the exclusion of carbonates from the feedwater. The retention of 0.02 ppm to 0.04 ppm of ammonia in the feedwater assists in neutralization of any small amounts of acid elements in the steam and raises the steam condensate above its neutral point of pH 7.

A detailed account of the effects of sulphite in the boiler water on the quality of the steam condensate is given in a separate paper by Alexander and Rummel.[4]

In order to exclude carbonates from the feedwater, close attention is paid to maintaining a low alkalinity in the make-up water to evaporators and in reducing condenser leakage. The elimination of carbonic acid from the system has been given considerable study. It has been found that most of the dissolved gases can be removed by use of the deaerating equipment which was installed, but that adequate venting of the deaerators and evaporator condensers is of great importance to the control. This venting is a necessary part of the pH control and the removal of dissolved oxygen.

The final adjustment of the pH of the feedwater is accomplished by continuous addition of caustic soda, and most of the residual dissolved oxygen is removed by addition of sodium sulphite. The pH value of the feedwater, which was formerly held to pH 8 to pH 8.2, has been raised to pH 8.5 to pH 9. The higher pH is believed to be beneficial in reducing corrosive effects due to dissolved oxygen which is present in measurable amounts in the water leaving the main condenser and probably persists as traces in the water leaving the deaerators.

In units Nos. 1 and 2, the caustic soda and sodium sulphite are added after the condenser hot-well pumps in order to afford further protection of equipment between the hot well and the deaerator. Formerly, these chemicals were added to the deaerator storage tank. The change in the point of feeding has presented some problems in keeping the feed rate constant, but this method of feeding has caused no apparent interference in the removal of carbon dioxide at the deaerator, as was originally feared. Irregular feeding of the chemicals, due to intermittent pump operation, was overcome in part by use of an equalizing tank, but there is some hope of replacing this later with a variable-speed direct-current-motor drive for the pumps.

There has not been sufficient time to determine the effect on corrosion due to the increase in the pH of the water and the further removal of dissolved oxygen, but the amounts of iron and copper in the feedwater are believed to be reasonable for the operating conditions which are experienced. This investigation is being continued and recorders for hydrogen and pH are being used in collecting the data.

TABLE 1 TYPICAL WATER ANALYSIS, UNITS NOS. 1 AND 2 HARBOR STEAM PLANT

—BOILER WATER—

	pH	P-ALK.	M-ALK.	NaCl	Na_2SO_3	Na_2SO_4	PO_4	SiO_2	M. MHOS LAB.	M. MHOS INST.	LOAD M. WATTS
Normal	11.1	60	85	125	7	135	25	2	800		10-60
Max.	11.2	85	110	175	9	175	40	3	1050		10-60
Min.	11.0	45	70	75	3	75	20	1	600		10-60

—FEEDWATER—

	pH	CO_2	NH_3	M. MHOS LAB.	M. MHOS INST.	LOAD M. WATTS
Normal	8.7	0	.02	3		
Max.	9.0	0	.04	5		
Min.	8.5	0	.01	2		

MAIN CONDENSER CONDENSATE—

	pH	CO_2	NH_3	M.MHOS	LOAD M.WATT
Normal	7.9	.2	.02	1.0	
Max	8.1		.03	1.2	
Min.	7.6	.3	.01	0.8	

—JET CONDENSER CONDENSATE—

	pH	CO_2	NH_3	M.MHOS	LOAD M.WATT
Norm.	7.0	0.8	0.4	5.0	
Max.	8.8	0	5.0	30	

—SATURATED STEAM—

	pH	CO_2	NH_3	M. MHOS LAB.	M. MHOS INST.	LOAD M.WATT
Normal	8.4	0	.02	.7		
Max.	8.6	0	.04	.9		
Min.	8.0	.2	.01	.5		

—EVAPORATOR CONDENSATE—

	pH	CO_2	NH_3	M.MHOS	LOAD M.WATT.
Normal	7.0	.4	.03	.65	
Max.	7.4	.3	.04	1.7	
Min.	6.3	.4	.02	.60	

—SUPERHEATED STEAM—

	pH	CO_2	NH_3	M. MHOS LAB.	M. MHOS INST.	LOAD M.WATT
Normal	8.3	0	.02	.65		
Max.	8.5	0	.04	.80		
Min.	7.9	.2	.01	.50		

—EVAPORATOR LIQUID—

	P-ALK.	M-ALK.	Na_2SO_3	PO_4	M.MHOS
Max.	400	550	30	40	4000
Min.	325	400	10	10	3000

—AUX. CONDENSER C'SATE—

TIME	pH	CO_2	NH_3	MHO	LOAD

Results as PPM except as noted.

The analytical results, which are typical of present operating conditions for units Nos. 1 and 2, are shown in Table 1.

Frequency of Sampling and Use of Control Tests

A schematic flow diagram of the feedwater system and the location of various sample points which are available are shown in Fig. 3. The sample points which are used for routine tests are circled by a solid line and the samples which are taken less frequently are shown by dotted lines.

Generally, sufficient chemical-treatment control has been

---

[4] "The Quality of Steam Condensate as Related to Sodium Sulphite in the Boiler Water," by R. C. Alexander and J. K. Rummel, published in this issue of the Transactions, pp. 519–527.

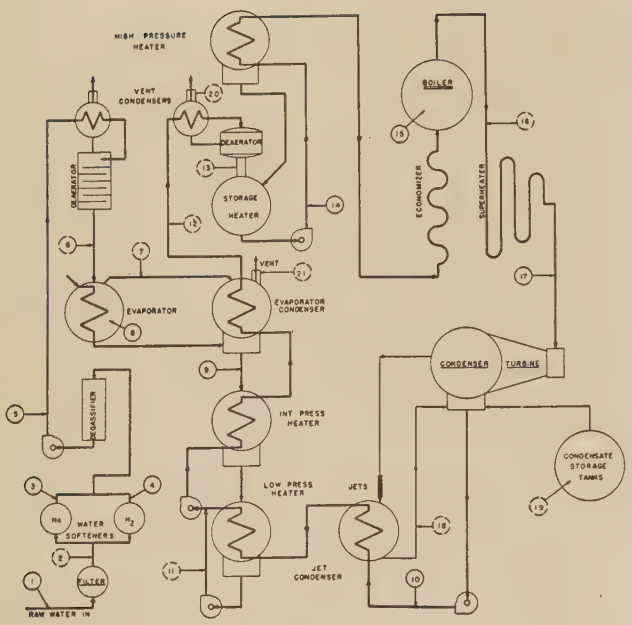

Fig. 3 Flow Diagram Showing Sample Points

maintained by daily tests made on the steam, the feedwater from the deaerator, the condensate from the evaporator condenser, the boiler water, and the effluents from the zeolite softeners.

To determine the minimum vent settings, at times it is necessary to examine the condensed vented vapor for pH and gas content, and to compare the pH of the evaporator condensate or the feedwater with the vent opening.

In order to determine the effectiveness of oxygen removal in the deaerators and the prevention of in-leakage of oxygen in the vicinity of the condenser hot well and condensate pumps, it is necessary to make weekly tests for dissolved oxygen. Indirect tests for dissolved oxygen can be made at any time by determination of the sodium sulphite remaining in the feedwater. This test is much more rapid than the direct method, but, for the present, the direct modified Winkler method is being retained. As a matter of normal routine, the increase and decrease in sodium sulphite demand for maintenance of minimum sulphite concentration in the boiler water can be interpreted as showing the presence of more or less oxygen in the feedwater.

Occasional to frequent tests are made of the water leaving the aftercondenser in the vacuum system of the main condenser. These and related data are used to show when it is advisable to throw the condensate to waste instead of returning it to the system. For example, if the ammonia content of the feedwater is higher than is necessary to maintain the desired pH in the steam condensate, the aftercondenser condensate will run high in ammonia, and a part or all of this condensate may be thrown to waste. In some other system or at another time the free carbon dioxide in the water may be the main consideration.

As has been indicated, the tests most frequently made on the samples of steam condensate are pH value and conductivity expressed as micromhos. Tests for free carbon dioxide and ammonia are made less frequently, but sufficient tests are made to control adequately the venting of deaerators, the evaporator condensate, and to show any need for other adjustments which may be possible.

The determination of iron and copper in the feedwater are being made frequently during investigations of corrosion, and it is likely that these tests will be made occasionally in the future.

Tests for soap hardness, alkalinity, and free chlorine are made on the raw city-water supply, and hardness alkalinity, and free mineral-acid tests are made of the effluents from the zeolite softeners and the blended soft water from the degasifying tower. The alkalinity of this water is maintained at approximately 25 ppm.

At the Harbor Steam Plant it has been found necessary to schedule the minimum amount of test work which should be done, but the laboratory personnel are expected to make such additional tests as may be indicated by the control tests which are made on schedule.

Inspection of Equipment

At times of overhaul, or during other shutdown periods, the opportunity has been taken to inspect the equipment for signs of corrosion and the presence of deposits on the metal surfaces. Inspections now being made by competent personnel are being used as a guide to the effectiveness of corrosion control by feedwater treatment at Harbor Steam Plant. It has been noted that those parts of the system in which the dissolved oxygen has been present and the pH values low, are most likely to show corrosive effects. No severe general corrosion has been found in any of the units, and this is attributed to the care which has been taken in applying the chemical controls which have been recommended. At this time it is believed that satisfactory progress has been made in improving the feedwater conditions so that local corrosive attack may be reduced to a practical minimum.

Finally, it has been shown by tests and inspections that effective deaeration throughout the system for removal of corrosive gases is of prime importance to the success of corrosion control.

Allowable Eccentricity of Spherical Heads Convex to Pressure

By R. G. STURM,[1] L. W. SMITH,[2] and H. L. O'BRIEN[3]

This paper discusses the variables and considerations in the design of spherical heads or shells, initially out-of-round, when subjected to external pressure. A method of calculating charts for design purposes based upon the instantaneous modulus of elasticity is presented herein. Calculations and charts for aluminum 3SO, and charts for stainless steel, 17-7 and "A" nickel are shown.

NOMENCLATURE

THE following nomenclature is used in this paper and is the same as that previously used for similar papers (1, 2, 3):[4]

A = maximum value of deflection, in.
A_0 = maximum initial departure from a perfect sphere, in.
E = modulus of elasticity (Young's Modulus), psi
E' = tangent modulus of elasticity, psi
R = radius of spherical shell, inches.
S = total stress in the shell (direct stress and bending), psi
S_1 = average stress in shell due to pressure only, psi
S_2 = stress in deflected shell due to bending, psi
S_c = stress in shell at collapse, psi
S_u = ultimate strength of material, psi
$\bar{S}$ = modulus of failure, psi
W = actual applied pressure, psi
W_c = collapsing pressure for perfect shell, psi
$\overline{W}$ = collapsing pressure for an out-of-round shell, psi

INTRODUCTION

The design of spherical shells or pressure vessels with heads of spherical contour subjected to external pressure or pressure on the convex side is complicated by the unavoidable initial out-of-roundness of the manufactured shell or head. Beside the basic concepts of the strength of materials, other factors, such as secondary stresses due to bending, must be recognized as contributors to buckling action.

The analysis presented herein leads to curves which may aid designers in the proper selection of spherical shell or head thicknesses when manufacturing tolerances are considered. It is hoped that such curves will be of value to the ASME Code for Unfired Pressure Vessels.

The type of eccentricity is an important factor. Th. von Kármán and H. Tsien (4) point out that a full cup deflection is a stable condition, but a flat deflection is very unstable. The size of the deformed area is also a critical factor.

Investigators have attacked the problem in two general ways. Von Kármán and Tsien (4) have used the theoretical approach as applied to thin shells, whereas Zick and Carlson (5), and Mariner and Keith (6) have approached the problem from the experimental viewpoint.

This paper treats each shell as a departure from a perfect shape in which the bending stress contributes to yielding and collapse. The methods used are primarily analytical and follow similar analytical studies for cylindrical vessels. The analysis for cylindrical vessels has been substantiated by tests and serves as the basis for computing allowable out-of-roundness charts for the present ASME Code for Unfired Pressure Vessels.

ANALYSIS

The basic equation for the buckling of a perfect sphere which is thin enough to buckle elastically is

$$S_c = 0.6\,E\left(\frac{t}{R}\right) \qquad [1]$$

If, however, the head is perfectly spherical but buckling does not occur until the compressive stress in the wall is above the proportional limit, a close approximation of the buckling stress is obtained by using a reduced value for the modulus of elasticity (1). For this case, the tangent modulus of elasticity E' is used. The effective, or tangent, modulus of elasticity is the slope of the tangent to the stress-strain curve at the stress considered. Von Kármán and Tsien corroborate the use of this modulus in preference to the secant modulus (4). The resulting equation is

$$S_c = 0.6\,E'\left(\frac{t}{R}\right) \qquad [2]$$

which is more useful when written as

$$S_c/E' = 0.6\left(\frac{t}{R}\right) \qquad [2a]$$

In Equation [2*a*], the physical properties of the metal (S_c/E') are separated from the geometrical dimensions inherent to the head or shell.

The general expression for the maximum value of deflection for an elastic structure initially out-of-round is given by the equation

$$A = A_0\left(\frac{W}{W_c - W}\right) \qquad [3]$$

At collapse W becomes $\overline{W}$, and this expression gives the value of the moment arm which together with the force in the shell or head wall makes possible the computation of the secondary stresses due to bending.

From the basic laws of statics, the average compressive stress in the wall of a spherical shell under external pressure is given by the equation

$$S_1 = \frac{WR}{2t} \qquad [4]$$

---

[1] Professor, Purdue University, West Lafayette, Ind. Mem. ASME.

[2] Standard Oil (Indiana) Fellow, Purdue University.

[3] Graver Tank and Manufacturing Company, East Chicago, Ind. Jun. ASME.

[4] Numbers in parentheses refer to the Bibliography at the end of the paper.

Contributed by the Special Research Committee on Strength of Vessels Under External Pressure, and Pressure Vessel Research Committee of the Welding Research Council of The Engineering Foundation and presented at the Annual Meeting, New York, N. Y., November 27–December 2, 1949, of THE AMERICAN SOCIETY OF MECHANICAL ENGINEERS.

NOTE: Statements and opinions advanced in papers are to be understood as individual expressions of their authors and not those of the Society. Paper No. 49—A-70.

At the collapsing pressure for a perfect spherical shell, this stress is great enough to cause collapse. In out-of-round shells, the additional stress due to bending must be included in the computation for collapse. From Fig. 1, the moment due to the compressive force in the shell and the total radial deflection of the shell from its true spherical form causes a bending stress of

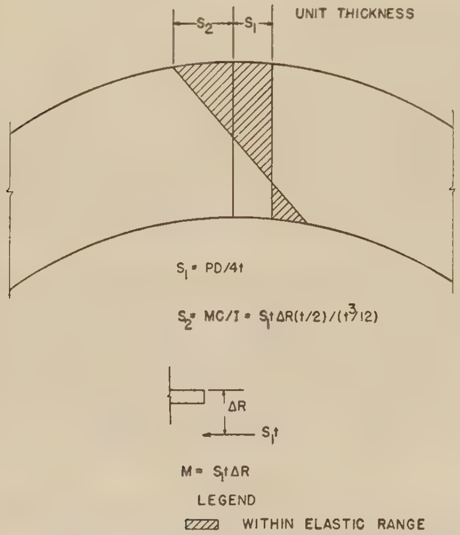

FIG. 1 DERIVATION OF STRESSES IN WALL OF SHELL

$$S_2 = \frac{Mc}{I} = \frac{S_1 t \Delta R \left(\dfrac{t}{2}\right)}{1\left(\dfrac{t^3}{12}\right)}$$

which reduces to

$$S_2 = 6\, S_1 \frac{\Delta R}{t} \quad \text{[5]}$$

Therefore the combined effects of Equations [4] and [5] give the total localized stress in the out-of-round shell or head. Thus the general expression for the maximum total stress in the shell at any pressure is

$$S = S_1 + S_2 = S_1\left(1 + 6\,\frac{\Delta R}{t}\right) \quad \text{[6]}$$

At collapse, the maximum deflection ΔR in Equation [6] is the value of A given by Equation [3]. The stress at collapse is, then

$$S = S_1\left(1 + \frac{6A}{t}\right) \quad \text{[7]}$$

The ratio between the collapsing pressure of an out-of-round shell and the collapsing pressure of a sphere can be defined as a reduction ratio C_R, which may be expressed mathematically as

$$C_R = \frac{\overline{W}}{W_c} \quad \text{[8]}$$

This value of C_R introduced into Equation [3] gives

$$A = A_0\left(\frac{C_R}{1 - C_R}\right) \quad \text{[9]}$$

which gives a measure of the value A at the pressure causing collapse of the out-of-round vessel.

A term often used to predict the maximum load-carrying capacity of beams is the modulus of failure, $\overline{S}$, which is the hypothetical value of stress obtained from the ordinary flexure stress formula $\overline{S} = \dfrac{Mc}{I}$, using the value of M corresponding to the maximum load on a test beam. The value thus obtained is used to predict the maximum value of M for other beams.

From a consideration of a simple rectangular beam, such as a narrow strip of a shell wall (see Fig. 2), a value for this modulus of failure can be arrived at analytically for the case of pure bending. At maximum load, the actual stress distribution will be that indicated by the curved line in Fig. 2, which shows a maximum stress equal to the nominal tensile strength S_u of the material. The hypothetical stress distribution is the straight line which terminates at the modulus of failure $\overline{S}$.

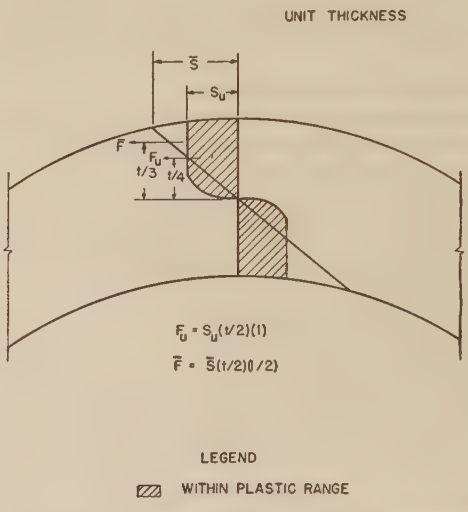

FIG. 2 DERIVATION OF MODULUS OF FAILURE

By equating the moment from the hypothetical stress distribution to that from the actual stress distribution, approximated as constant stress across half of the beam, the following relation is obtained

$$2\,S_u(1)\left(\frac{t}{2}\right)\left(\frac{t}{4}\right) = 2\,\frac{\overline{S}}{2}(1)\left(\frac{t}{2}\right)\left(\frac{t}{3}\right)$$

from which we get

$$\overline{S} = 1.5\, S_u \quad \text{[10]}$$

Numerous tests have indicated that for narrow beams $\overline{S}$ is usually less than 1.5 S_u, and for wide beams or plates $\overline{S}$ is often appreciably greater than 1.5 S_u. For a usable approximation in this paper, however, the relation given by Equation [10] has been used.

At collapse of an out-of-round shell, the maximum localized stress would then be expected to be practically equal to the value of $\overline{S}$. When this value is substituted for the value of S in Equation [7] and the value of A from Equation [9] substituted in Equation [7] the relation becomes

$$\overline{S} = S_1\left(1 + \frac{6A_0}{t}\cdot\frac{C_R}{1 - C_R}\right) \quad \text{[11]}$$

This equation then may be solved for the ratio of A_0/t in terms of the allowable reduction in strength represented by C_R, the ratio of the thickness to the radius (t/R) represented by S_1 and the material in the vessel represented by $\bar{S}$. The resulting equation is

$$\frac{A_0}{t} = \frac{\bar{S} - S_1}{6S_1 \dfrac{C_R}{1 - C_R}} \quad \ldots\ldots\ldots\ldots\ldots\ldots [12]$$

At collapse of an out-of-round vessel, the value of S_1 is $(WR)/(2t)$. For a perfect shell at collapse, the average stress is $S_c = (W_cR)/(2t)$. Therefore

$$\frac{S_1}{S_c} = \frac{W}{W_c} = C_R$$

Now, the right side of Equation [12] may be divided by S_c, the average stress in a perfect shell at collapse, to give

$$\frac{A_0}{t} = \frac{\dfrac{\bar{S}}{S_c} - C_R}{6 \dfrac{C_R{}^2}{1 - C_R}} \quad \ldots\ldots\ldots\ldots\ldots\ldots [13]$$

PROCEDURE

As the first step toward evaluation of the A_0/t values, a range of design characteristics, thickness to diameter ratio, was selected (see Table 1, column 1). This choice made the geometric design conditions the independent variables in the calculations of A_0/t, and all physical properties of the material were later determined from appropriate charts.

The values of C_R for computations are listed in column 2, Table 1, and values of S_c/E', calculated from Equation [2a], are listed in column 3; thus columns 1 through 3 are independent of any physical and metallurgical properties and can be used when constructing tables for all metals.

The figures listed in Table 1 are for 3SO aluminum. The values of S_c for column 4 were obtained (2) from the ordinate of Fig. 3 at the intersection of the S_c/E', (abscissa) value, and the appropriate curve. With proper regard to existing data, the modulus of failure for 3SO aluminum was taken as 21,000 psi (7).

The component parts of Equation [13] were calculated, and listed in Table 1. The resultant values of A_0/t, listed in column 11 do not consider a safety factor. However, any suitable factor may be applied to the resulting curves by dividing the pressures at collapse by that factor.

The results of the foregoing calculations are presented in Fig. 4. This chart was composed by designating the abscissa as the maximum initial departure from a true sphere divided by the head thickness (A_0/t) and the ordinate as the ratio of the collapsing pressure for the out-of-round head to the collapsing pressure for a perfectly spherical head (C_R). The curves were plotted for various ratios of diameter to thickness and for vessels operating under standard temperature conditions.

Charts for ordinary temperatures were also calculated and

TABLE 1 DESIGN CHARACTERISTICS OF 3SO ALUMINUM

(1)	(2)	(3)	(4)	(5)	(6)	(7)	(8)	(9)	(10)	(11)
t/D	C_R	$1.2(\frac{t}{D})$	S_c	$C_R{}^2$	$1-C_n$	$\frac{6C_R{}^2}{1-C_R}$	1.5 S_u	$1.5\,\frac{S_u}{S_c}$	$1.5\,\frac{S_u}{S_c} - C_R$	A_o/t
.0002	.3	.00024	2400	.09	.7	.772	21000	8.85	8.55	11.1
	.4			.16	.6	1.6			8.45	5.21
	.5			.25	.5	3.0			8.35	2.78
	.6			.36	.4	5.4			8.25	1.53
	.7			.49	.3	9.8			8.15	.831
	.8			.64	.2	19.2			8.05	.42
	.9			.81	.1	48.6			7.95	.164
	1.0			1.0	0	0			7.85	0
.001	.3	.0012	3720	.09	.7	.772	21000	5.64	5.34	6.9
	.4			.16	.6	1.6			5.24	3.27
	.5			.25	.5	3.0			5.14	1.71
	.6			.36	.4	5.4			5.04	.933
	.7			.49	.3	9.8			4.94	.504
	.8			.64	.2	19.2			4.84	.257
	.4			.81	.1	48.6			4.74	.098
	1.0			1.0	0	0			4.64	0
.002	.3	.0024	4430	.09	.7	.772	21000	4.73	4.43	5.74
	.4			.16	.6	1.6			4.33	2.71
	.5			.25	.5	3.0			4.23	1.41
	.6			.36	.4	5.4			4.13	.765
	.7			.49	.3	9.8			4.03	.411
	.8			.64	.2	19.2			3.93	.205
	.9			.81	.1	48.6			3.83	.079
	1.0			1.0	0	0			3.73	0
.005	.3	.0060	5570	.09	.7	.772	21000	3.77	3.47	4.48
	.4			.16	.6	1.6			3.37	2.11
	.5			.25	.5	3.0			3.27	1.09
	.6			.36	.4	5.4			3.17	.586
	.7			.49	.3	9.8			3.07	.313
	.8			.64	.2	19.2			2.97	.155
	.9			.81	.1	48.6			2.87	.059
	1.0			1.0	0	0			2.77	0
.010	.3	.012	6540	.09	.7	.772	21000	3.21	2.91	3.77
	.4			.16	.6	1.6			2.81	1.755
	.5			.25	.5	3.0			2.71	.903
	.6			.36	.4	5.4			2.61	.483
	.7			.49	.3	9.8			2.51	.256
	.8			.64	.2	19.2			2.41	.1255
	.9			.81	.1	48.6			2.31	.0476
	1.0			1.0	0	0			2.21	0
.020	.3	.060	7410	.09	.7	.772	21000	2.83	2.53	3.28
	.4			.16	.6	1.6			2.43	1.52
	.5			.25	.5	3.0			2.33	.777
	.6			.36	.4	5.4			2.23	.413
	.7			.49	.3	9.8			2.13	.217
	.8			.64	.2	19.2			2.03	.1065
	.9			.81	.1	48.6			1.93	.0317
	1.0			1.0	0	0			1.83	0

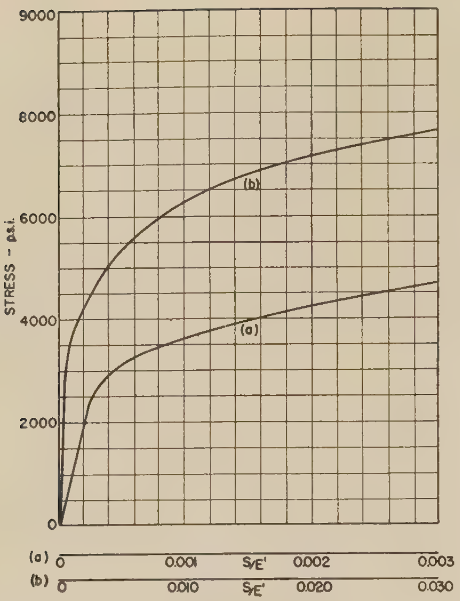

Fig. 3 Curves Used for Determining Modulus of Elasticity of Aluminum, 3SO

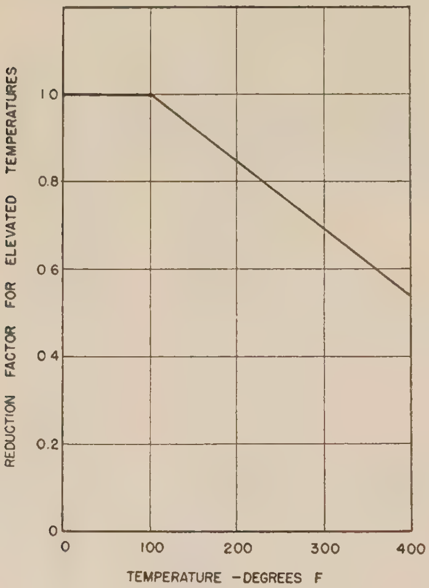

Fig. 5 Chart for Determining Strength Reduction Factor for 3SO Aluminum at Elevated Temperature

drawn for 17-7 stainless steel and "A" nickel, and are represented in Figs. 8 and 9, respectively. The S/E' curves for these materials may be found (2) in Figs. 6 and 7, respectively.

Both the modulus of elasticity and the yield strength of metals operating under elevated-temperature conditions are lower than the same properties at standard conditions. Thus charts similar to those of Figs. 4, 8, and 9, should be drawn for various temperature conditions. However, a strength-reduction factor for aluminum, 3SO, can be obtained from Fig. 5. This chart gives a reduction factor which corrects for both the reduction in modulus of elasticity and yield strength of 3SO aluminum. The factor is applied by multiplying the value of W obtained from Fig. 4 by the correction for the desired temperature to get the reduced value of collapsing pressure at an elevated temperature.

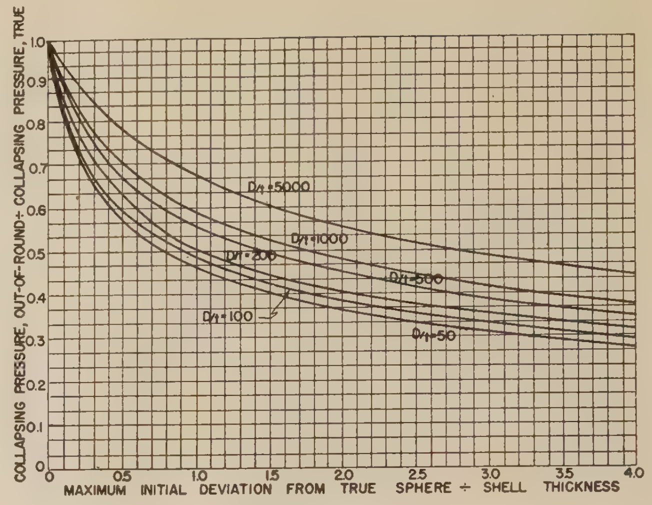

Fig. 4 Chart for Determining Working Pressure for an Initially Out-of-Round Shell Constructed of Aluminum, 3SO

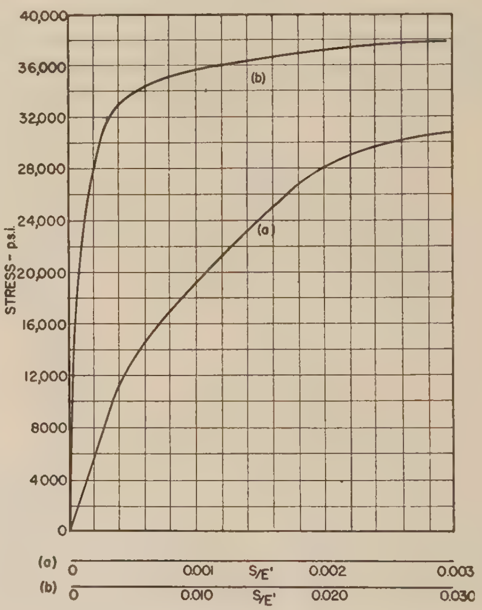

Fig. 6 Curves Used for Determining Modulus of Elasticity of Stainless Steel, 17-7

Summary

1 Unavoidable out-of-roundness incurred in the manufacture of spherical heads or shells necessitates a consideration of the decrease in strength of such vessels due to additional stress caused by the initial deviation from a true sphere.

2 The type and size of deviation from a true sphere is important. A small cup deflection actually stabilizes the shell, but a flat deflection contributes to instability and will give rise to buckling failure.

3 A relation between the collapsing pressure of an out-of-round shell or head, and the value of the initial deviation from a true sphere has been analytically derived, and charts prepared for three representative metals.

4 A method by which similar charts may be constructed is presented herein. This method separates the physical properties of the metal from the geometrical dimensions of the shell.

5 Suitable reduction factors may be applied to determine the

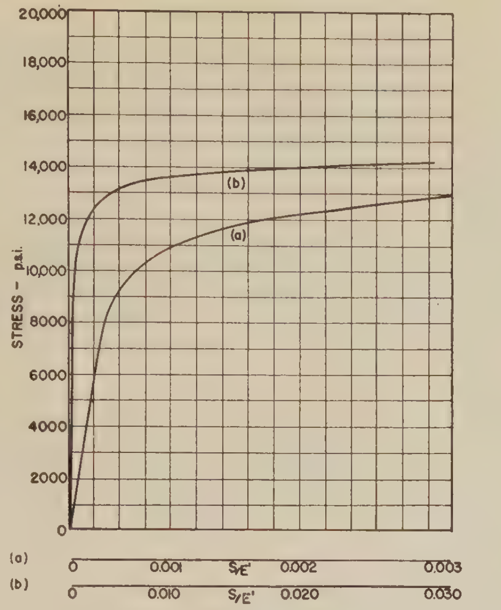

Fig. 7 Curves Used for Determining Modulus of Elasticity of "A" Nickel

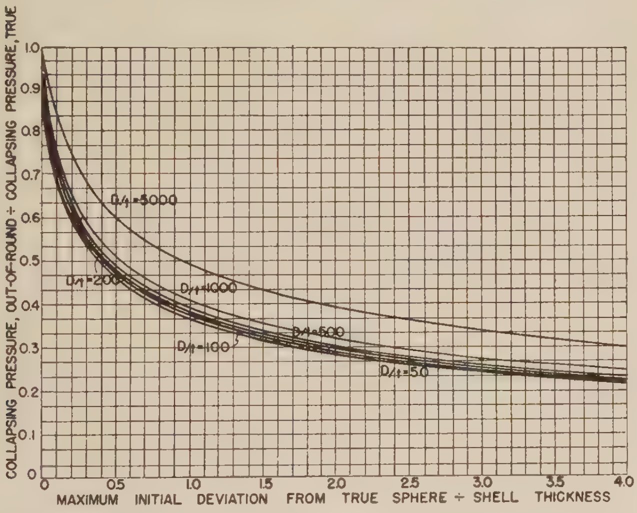

Fig. 9 Chart for Determining Working Pressure of an Initially Out-of-Round Shell Constructed of "A" Nickel

collapsing pressure for 3SO aluminum at an elevated temperature. This may be accomplished by multiplying the collapsing pressure for the out-of-round vessel at standard temperature by the reduction factor for the desired temperature. The reduction factor is less than unity for temperature above standard conditions.

6 Factors of safety may be applied to the results presented here for industrial use. This consideration would not necessitate recalculations of the fundamental relations utilizing the allowable stress, because a suitable factor could be applied directly to the collapsing pressure.

7 Experimental verification of the charts presented herein is desirable.

BIBLIOGRAPHY

1 "A Study of the Collapsing Pressure of Thin Walled Cylinders," by R. G. Sturm, University of Illinois Bulletin, vol. 39, no. 12, November, 1941.

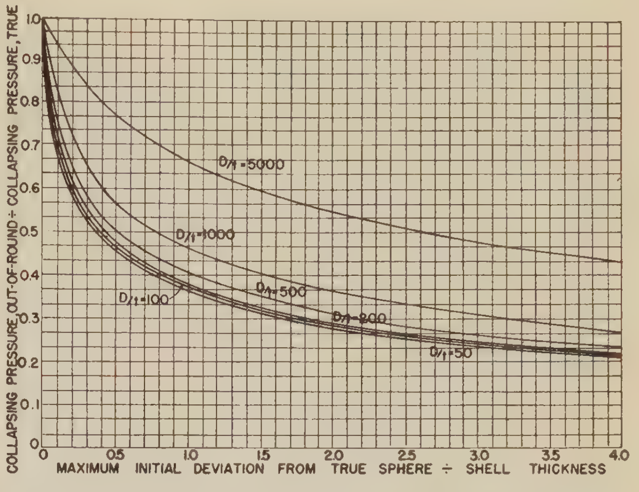

Fig. 8 Chart for Determining Working Pressure of an Initially Out-of-Round Shell Constructed of Stainless Steel, 17-7

2 "Computing Strength of Vessels Subjected to External Pressure," by R. G. Sturm and H. L. O'Brien, Trans. ASME, vol. 69, 1947, pp. 353–358.

3 "Collapsing Strength of Out-of-Round Vessels," by R. G. Sturm and H. L. O'Brien. Paper presented at the Annual Meeting, New York, N. Y., November 29–December 3, 1948, of The American Society of Mechanical Engineers.

4 "Buckling of Spherical Shells by External Pressure," by Th. von Kármán and H. Tsien, *Journal of the Aeronautical Sciences*, vol. 7, December, 1939, pp. 43–50.

5 "Vacuum Tests of Sphere to Failure," by L. P. Zick and C. E. Carlson, *Watertower*, vol. 34, November, 1947, pp. 6–7.

6 "Buckling Tests on Models of the Hemispherical Heads for the 16-Inch by 16-Inch Supersonic Wind Tunnel Vacuum Chamber," by J. Mariner and J. Keith, North American Aviation, Inc., Report.

7 "Spherical Shells Under External Pressure," by M. Holt, Aluminum Research Laboratories Report.

8 "Unfired Cylindrical Vessels Subjected to External Pressure," by F. Hartman, Trans. ASME, vol. 69, 1947, pp. 337–344.

Addendum

In determining the moment arm for the derivation of Equation [5], the initial deflection, A_0, was omitted. Consideration of this value alters Equation [3], since

$$\Delta R = A = A_0\left(\frac{W}{W_c - W}\right) + A_0 = A_0\left(\frac{W_c}{W_c - W}\right)$$

and

$$A = A_0\left(\frac{1}{1 - C_R}\right) \quad \ldots\ldots\ldots\ldots\ldots [9]$$

The value of A thus obtained satisfies the definition of A in the nomenclature, and changes Equation [13] to

$$\frac{A_0}{t} = \frac{\dfrac{\bar{S}}{S_c} - C_R}{\dfrac{6\,C_R}{1 - C_R}}$$

This materially changes column (11) of Table 1, Design Characteristics, with the result that the abscissas for the curves are changed. This is accomplished by multiplying the values of A_0/t by C_R at each value of C_R and t/D. By means of this modification the curves in Figs. 4, 8, and 9 as published can be used for design.

Discussion

Marshall Holt.[5] Coincidently Equation [1] of the paper also applies to the buckling of thin-wall circular cylindrical shells under axial load. Inasmuch as test data and theories of large deflections indicate that the coefficient 0.6 is too large, the question naturally arises as to the validity of this value of the coefficient in the problem of spheres. Von Kármán and Tsien arrive at a value of 0.18[6] for shells which are extremely thin and whose deviation from circularity gives the minimum elastic buckling strength. Although this coefficient does not enter the mathematics of this paper, it will be of great importance to the experimenter who tries to deduce from test results the out-of-roundness that must have existed in his specimens.

In establishing the equation for maximum stress, no consideration is given to the fact that the shell plate is bent in two directions. It would seem that Poisson's ratio should enter this equation. On the other hand, the modulus of failure is deduced from the results of a test under uniaxial stress without consideration of the effects of biaxial loading on the ultimate strength of materials. The authors, no doubt, expect these two effects to compensate for each other.

Authors' Closure

Dr. Holt has raised a very interesting question which should have been covered in the original paper. The work by von Kármán and Tsien deals with extremely thin shells in which the material has an indefinitely high elastic limit. The coefficient 0.18 determined by von Kármán and Tsien represents the reduced value of the classical coefficient, 0.60 for perfectly spherical shells.

This reduced value results from a consideration of an eccentricity sufficient to produce a flat spot over an area which will make the value of the coefficient a minimum. Therefore the coefficient 0.18 cannot be used as a basis for determining the initial out of roundness because it intrinsically includes the effects of out of roundness.

Dr. Holt is correct in expecting the effects of Poisson's ratio and biaxial loading to compensate for each other. A consideration of the maximum distortion energy theory for biaxial bending reveals that when the two bending stresses are nearly equal and the stress normal to the shell is negligibly small the critical stress for inception of plastic action is the same as for unidirectional stress.

For elastic action Poisson's ratio is included in the derivation of the coefficient, 0.60. For plastic action the analysis and derivations may not be as precise as for elastic action but have been found to give reliable results for engineering usage.

---

[5] Aluminum Research Laboratory, New Kensington, Pa.

[6] "The Buckling of Spherical Shells by External Pressure," by Th. von Kármán, and Hsue-Shen Tsien, *Journal of Aeronautical Sciences*, vol. 7, 1939, pp. 43–50.

Effect of Welding on Pressure-Vessel Steels[1]

By A. F. SCOTCHBROOK,[2] L. ERIV,[3] R. D. STOUT,[4] and B. G. JOHNSTON[5]

This paper presents the results of a study using the Lehigh slow notched-bend test to determine the effects of welding on as-received and prestrained plate. It also discusses the effects of different heat inputs in welding, the effects of plate thickness, of carbon content and deoxidation practice, and of heat-treatment after welding.

Introduction

The effect of fabrication processes on steels used in pressure vessels is a subject to which considerable attention has been devoted by the Fabrication Division of the Pressure Vessel Research Committee of the Welding Research Council. It is desired to know which fabrication operations are harmful to the mechanical properties of steels, and to what extent. Eventually this information should lead to materials specifications and to codes of recommended fabrication practice, based upon measured responses of steel to various treatments. With these objectives, the Pressure Vessel Research Committee is sponsoring a project at Lehigh University.

In earlier investigations (1, 2, 3)[6] the effects of various simulated fabrication operations were determined by measuring the changes in transition temperature, strength, and ductility of the material. These fabrication processes included various degrees of plastic strain produced by uniaxial stress, followed by various heat-treatments (3).

This report considers another fabrication process—welding. It was desired to know how different grades of pressure-vessel steels respond to welding, and to observe the effects of plate thickness, of plastic strains before welding, of high and low heat input during welding, and of heat-treatments after welding.

Materials

For the tests reported here, six plain-carbon steels were selected from several mills to cover a range of grades, carbon contents, and deoxidation practices. A complete history is available (2) for two of the steels used, A-201 and A-70, each in two thicknesses, steels A (A-201) and E (A-70) of $^5/_8$-in. thickness, and steels B (A-201) and F (A-70) of $1^1/_4$ in. thickness. These steels were made especially for research purposes. The others came from regular mill stock. Samples for chemical analysis were taken from the steels according to recommended ASTM procedure, and the results of these analyses are given in Table 1. Also included in Table 1 are strength and ductility data for the as-rolled plate, as determined by standard 0.505-in. tensile tests at Lehigh University.

Specimen Preparation and Testing

The transition temperature of each steel was determined for each of the following conditions:

(*a*) Welded.
(*b*) Welded and heat-treated at 500 F.
(*c*) Welded and heat-treated at 1150 F.
(*d*) Elongated 5 per cent and welded.
(*e*) Elongated 5 per cent, welded, and heat-treated at 500 F.
(*f*) Elongated 5 per cent, welded and heat-treated at 1150 F.

This schedule was followed for two heat inputs: 175 amp at 10 ipm with an E6010 $^3/_{16}$-in. electrode (called W1), and 275 amp at 8 ipm with an E6010 $^1/_4$-in. electrode (called W2). To cut down on expensive machining operations, conditions (*b*) and (*e*) were not used for the $1^1/_4$-in. plate (steels B and F).

The longitudinal bead notch-bend test, Fig. 1, was used as developed by a Welding Research Council project at Lehigh University (4). With an automatic welding machine, a weld bead 10 in. long was deposited on a plate surface of the 3-in. × 12-in. specimen. Heat-treating was done one day after welding. The $^5/_8$-in. plate was then notched and tested at plate thickness, while the $1^1/_4$-in. plate was shaped down on the unwelded surface to a thickness of $^5/_8$ in. before notching. Specimens were tested 1 week after welding.

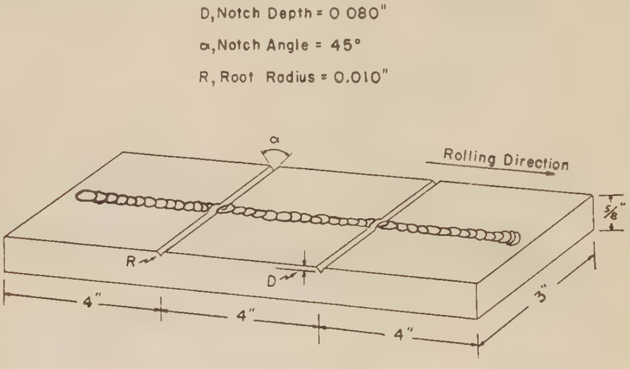

Fig. 1 Lehigh Slow Notched-Bend Specimen With Weld

The 5 per cent prestrain for the foregoing conditions (*d*), (*e*), (*f*) was produced by stretching strips $9^1/_2$-in. × 16-ft in an 800,000-lb testing machine. Gage marks were scribed at 2-ft intervals along the strips, and the distances between marks were measured regularly during the pulling. A 2-ft section from each end of each strip was discarded to avoid using material which had been nonuniformly deformed because of the restraints at and near the testing-machine grips.

The specimens were tested in bending, as in Fig. 2. Three measurements were made on each specimen—per cent lateral contraction, per cent of the fracture area which was cleavage, and energy absorbed by the specimen from the start of the test until the load had passed its maximum and dropped to a value equal to half the maximum. The per cent contraction values were obtained by measuring with a pointed micrometer the width of the

---

[1] Progress Report No. 4 on the Effect of Fabrication Processes on Steels Used in Pressure Vessels, submitted to the Fabrication Division, Pressure Vessel Research Committee of the Welding Research Council of The Engineering Foundation.

[2] Former Research Assistant, Fritz Engineering Laboratory, Lehigh University, Bethlehem, Pa.

[3] Research Assistant, Fritz Engineering Laboratory, Lehigh University, Bethlehem, Pa.

[4] Associate Professor of Metallurgy, Lehigh University.

[5] Director, Fritz Engineering Laboratory, and Professor of Civil Engineering, Lehigh University.

[6] Numbers in parentheses refer to the Bibliography at the end of the paper.

Contributed by the Special Research Committee on Strength of Vessels Under External Pressure, and the Pressure Vessel Research Committee of the Welding Research Council and presented at the Annual Meeting, New York, N. Y., November 27–December 2, 1949, of The American Society of Mechanical Engineers.

Note: Statements and opinions advanced in papers are to be understood as individual expressions of their authors and not those of the Society. Paper No. 49—A-49.

TABLE 1 RESULTS OF ANALYSES

Project Letter	A.S.T.M. No.	Deoxidation	Plate Thickness	C	Mn	P	S	Si	Al	Al_2O_3	N_2	Lower Yield Strength p.s.i.	Maximum Strength p.s.i.	% Red. of Area	% Elongation
I	A-285 Grade A	Rimmed	5/8"	.15	.38	.012	.030	.01	.010	.007	.004	34,650	59,150	63.8	38.0
K	A-285 Grade A	Semi-killed	5/8"	.09	.43	.014	.027	.02	.011	.005	.004	29,600	51,450	73.5	42.3
L	A-285 Grade C	Rimmed	5/8"	.20	.40	.011	.030	.01	.008	.006	.003	32,050	61,400	56.3	37.5
E	A-70 Grade C	Rimmed	5/8"	.22	.37	.019	.028	.02	.010	.002	.004	33,850	64,200	63.2	38.5
F	A-70 Grade C	Rimmed	1 1/4"	.20	.35	.018	.028	.02	.021	.003	.003	26,250	56,300	63.1	39.5
A	A-201 Grade A	Killed	5/8"	.17	.55	.020	.022	.21	.041	.003	.005	35,450	63,150	68.6	38.0
B	A-201 Grade A	Killed	1 1/4"	.15	.55	.020	.019	.20	.041	.006	.004	31,600	63,300	64.6	36.8
P	A-201 Grade A	Killed	5/8"	.12	.41	.015	.027	.19	.018	.007	.003	32,850	57,350	66.7	38.9

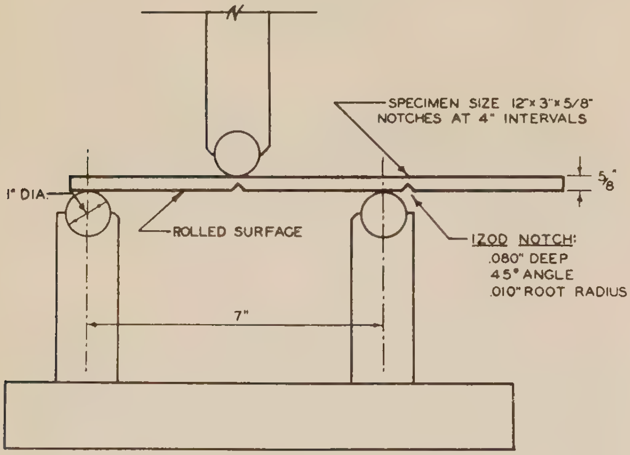

Fig. 2 The Lehigh Slow Notched-Bend Test

specimen 1/32 in. below the notch before and after the test. Per cent cleavage measurements were made on a fractured section with a steel scale. Energy values were determined by measuring with a planimeter the area under a load-deflection curve obtained autographically during the test.

Twelve specimens, or twenty-four notch tests, were used for each condition, four tests at each of six temperatures. The average values at each temperature were connected by straight lines, and the transition temperature was the point at which the per cent contraction, per cent cleavage or energy was equal to half its maximum. When occasionally the transition curve formed a plateau near the transition temperature, a transition range was reported as well as a transition temperature. This range extended from the temperature of —10 per cent to that of +10 per cent of the half-maximum value of contraction, cleavage, or energy which had defined the transition temperature. T_N and T_E, the transition temperatures obtained from per cent contraction and energy curves, respectively, were considered the transition temperatures of the material with the original notch. T_B, obtained from per cent cleavage curves, was considered the transition temperature of the plate when notched by a crack. All three temperatures are listed in Tables 2, 3, and 4.

T_E, as described here, is a transition temperature not previously determined or reported in the earlier papers. T_E was found to agree very closely with T_N for unstrained material, and to be consistently lower than T_N for strained material. Fig. 3 shows typical energy and contraction curves for strained and unstrained material.

To determine the effects of welding, the transition temperatures of welded specimens were compared with those of unwelded specimens from the same material. Although transition curves for the as-received condition have been made earlier for steels B and F (1, 3), they were repeated for use in the present work. It was found that there were some differences between the two sets of curves, which are shown in Figs. 4 to 7. The discrepancies between the curves must be accounted for by variation from plate to plate (2), and by inaccuracy caused by the method of plotting. From these curves it appears that variations in transition temperature as high as 30 F could be intrinsic to plate variations and to the testing and plotting methods, and could not be attributed with surety to the variable being studied.

Discussion of Results

Effect of Welding As-Rolled Plate. Welding increased notch-sensitivity of as-received plate when measured by per cent contraction or energy. The difference between unwelded and welded plate was shown by a significant rise in the transition temperatures T_N and T_E, both of which are affected by the material directly below the machined notch. The rise in T_N caused by welding as-received plate is shown graphically in Fig. 8. The order of transition temperatures after welding was quite different from that before welding.

TABLE 2 EFFECT OF WELDING ON TRANSITION TEMPERATURE—CRITERION—T_N

Steel	As Rolled	Weld w_1^{o} Unstrained	Weld w_2^{oo}	Weld w_1 Post Heat 500°F	Weld w_2	Weld w_1 Post Heat 1150°F	Weld w_2	Strain 5% un-welded	Strain 5% welded w_1	Strain 5% welded w_2	Strain welded w_1 Post Heat 500°F	Strain welded w_2	Strain welded w_1 Post Heat 1150°F	Strain welded w_2
A	-35	33	-18	15	- 8	-30	3	-45	35	20	3	20	-18	6
B	-85	43	47	-	-	7	19	-35	89	93	-	-	-15	0
P	-73	18	30	27[a]	-11	-55	-24	-75	77[b]	11	0	31[c]	-20[d]	-24
I	-28	28	66	41	28	-18	35	-53	45	26	40[e]	15	- 5	-11
K	-53	12	-17	8	-30	-40	-25	10	71	40	53	27	-18	-23
L	-51	63	58	79	59	35	56	- 7	92	88	45	83	-10	48
E	-13	75	68	68	63	30	50	8	80	58	58	40	-13	38
F	-71	81	66	-	-	17	21	48	150	62	-	-	88	18

o w_1 - Welded using 175 amperes at 10 inches per minute with an E6010 3/16" electrode.
oo w_2 - Welded using 275 amperes at 8 inches per minute with an E6010 1/4" electrode.
a - Temperature Range - 5 to 32
b - Temperature Range 45 to 82
c - Temperature Range 0 to 43
d - Temperature Range -26 to 32
e - Temperature Range 0 to 50

TABLE 3 EFFECT OF WELDING ON TRANSITION TEMPERATURE—CRITERION—T_E

Steel	As Rolled	Weld w_1^{o} Unstrained	Weld w_2^{oo}	Weld w_1 Post Heat 500°F	Weld w_2	Weld w_1 Post Heat 1150°F	Weld w_2	Strain 5% un-welded	Strain 5% welded w_1	Strain 5% welded w_2	Strain welded w_1 Post Heat 500°F	Strain welded w_2	Strain welded w_1 Post Heat 1150°F	Strain welded w_2
A	-36	29	-34	-11	-16	-80	- 3	-59	7	- 5	-18	-18	-59	- 8
B	-96	45	55	-	-	-18	5	-58	90	88	-	-	-24	-25
P	-74	17	22	20	-35	-41	-23	-67	49	-18	-28	-36	-41	-46
I	-33	29	61	27	5	-68	-15	-84	0	- 2	-18	-13	-13	-33
K	-54	11	-27	2	-31	-50	-21	-39	46	18	33	15	-28	-29
L	-58	52	51	75	40	13	53	-20	26	38	-26	18[a]	-25	25
E	-13	65	50	33	2	-52[b]	30	-13	14	13	3	8	-21	12
F	-75	100	69	-	-	7	33	-11	136	3	-	-	30	22

o w_1 - Welded using 175 amperes at 10 inches per minute with an E6010 3/16" electrode.

oo w_2 - Welded using 275 amperes at 8 inches per minute with an E6010 1/4" electrode.

a - Temperature Range - 3 to 60

b - Temperature Range - 58 to 15

TABLE 4 EFFECT OF WELDING ON TRANSITION TEMPERATURE—CRITERION—T_B

Steel	As Rolled	Weld W_1° Unstrained	Weld W_2°° Unstrained	Weld W_1 Post Heat 500°F	Weld W_2 Post Heat 500°F	Weld W_1 Post Heat 1150°F	Weld W_2 Post Heat 1150°F	Strain 5% unwelded	Strain 5% welded W_1	Strain 5% welded W_2	Strain welded W_1 Post Heat 500°F	Strain welded W_2 Post Heat 500°F	Strain welded W_1 Post Heat 1150°F	Strain welded W_2 Post Heat 1150°F
A	65	68	53	35	53	45	25	50	90	108	115	111	84	68
B	81	78	70	-	-	67	64	83	95	118	-	-	91	94
P	-50	13	30	13	-11	28	-16	-10	57	65	56	44	48	38
I	45	80	75	83	74	84	61	79	114	85	113	86	88	57
K	55	66	47	55	38	60	75	79	117	97	103	86	80	61
L	87	97	93	92	108	110	100	108	156	148	153	142	131	107
E	110	95	98	109	119	133	113	118	153	150	175	127	125	115
F	180	157	158	-	-	156	164	163	163	212	-	-	158	166

o W_1 - Welded using 175 amperes at 10 inches per minute with an E6010 3/16" electrode.

oo W_2 - Welded using 275 amperes at 8 inches per minute with an E6010 1/4" electrode.

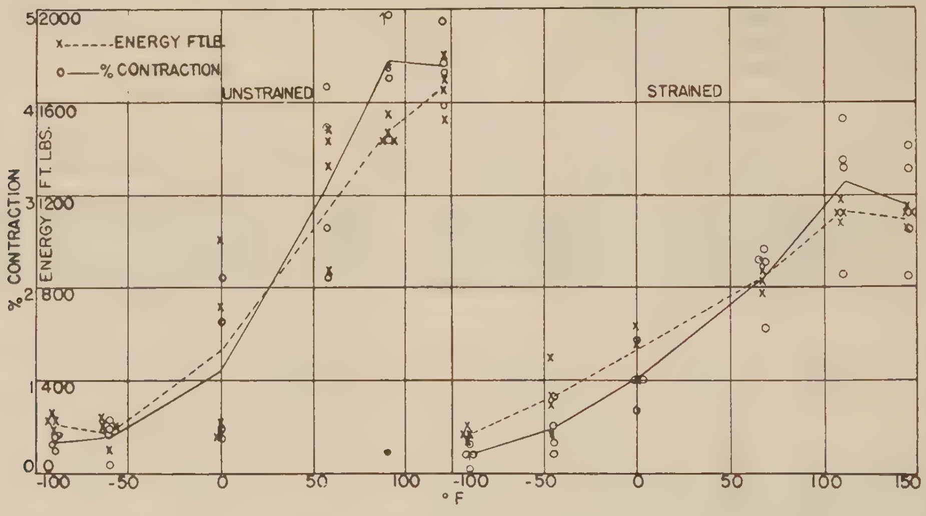

FIG. 3 COMPARISON OF PER CENT CONTRACTION AND ENERGY CURVES FOR WELDED A-201, $^5/_8$-IN. MATERIAL

The notch sensitivity measured by fracture appearance was little affected by welding. This is shown in Fig. 9 by a small rise, or even a drop, in T_B values from unwelded to welded plate.

Effect of Welding Prestrained Plate. As seen in Fig. 10, prestraining often but not always raised somewhat the transition temperatures of as-received plate. The effect of welding this plastically prestrained plate is shown in Figs. 11 and 12. As in the case of as-rolled plate, the T_N for strained plate was significantly raised by welding, Fig. 11. The T_N level after welding strained metal was a little higher than that after welding unstrained metal, Fig. 13.

When the effect of welding prestrained steel is considered in the light of the transition temperature T_B in Fig. 12, it can be seen that T_B for strained steel was raised up to 75 F by welding. T_B for strained and welded plate was, in most cases, appreciably higher than that for unstrained and welded plate, Fig. 14.

Effect of Heat Input. In comparing the differences in level between W1 and W2 in Figs. 8, 9, 11, and 12, it may be noted that, except in two cases, the two heat inputs resulted in about the same transition temperature for these plain-carbon steels.

Effect of Plate Thickness. It can be seen from Figs. 8 to 11 that welding usually caused greater increases in T_N for steels B and F, which were welded at $1^1/_4$-in. thickness, than it did for the other steels, welded at $^5/_8$ in. thickness. Since all the steels were tested in $^5/_8$ in. thickness, this indicates that the increased cooling rate after welding, imposed by the thicker plate, resulted in a higher T_N transition temperature. The T_B transition temperature, Figs. 9 and 12, was changed by welding to about the same degree for $1^1/_4$-in. and $^5/_8$-in. plate.

Effect of Carbon Content and Deoxidation Practice. There appeared to be some correlation between carbon content and transition temperatures, both before and after welding, as shown in Fig. 15. This figure contains only the values for the steels of $^5/_8$ in. thickness.

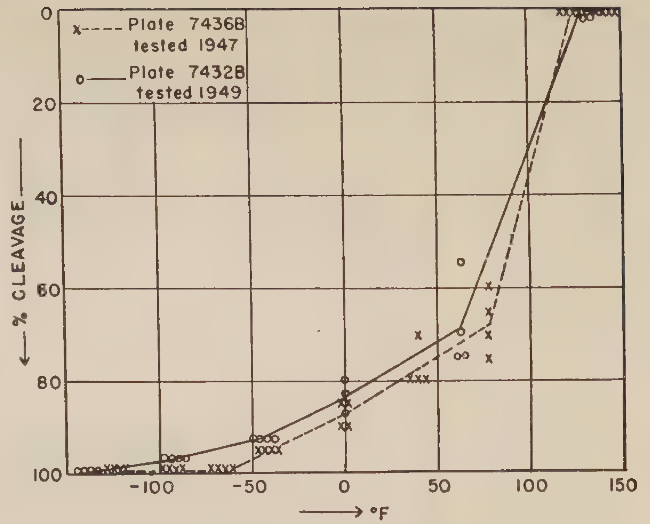

Fig. 4 Transition Curves for Same A-201, 1¼-In. Material Determined in 1947 and 1949
(Lehigh slow notched-bend test. Criterion: Per cent cleavage.)

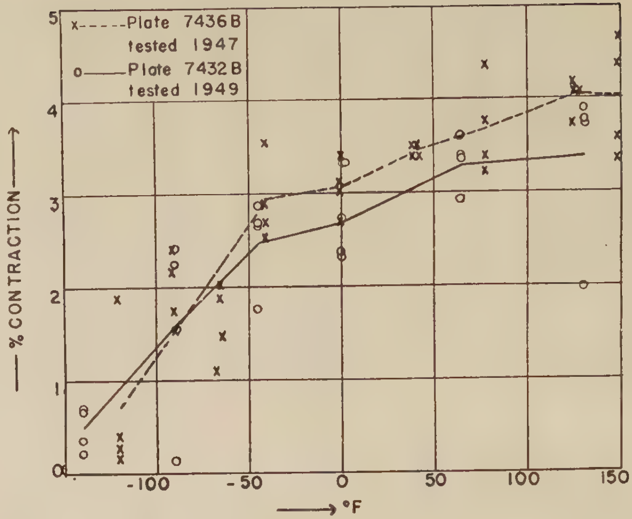

Fig. 5 Transition Curves for Same A-201, 1¼-In. Material Determined in 1947 and 1949
(Lehigh slow notched-bend test. Criterion: Per cent contraction.)

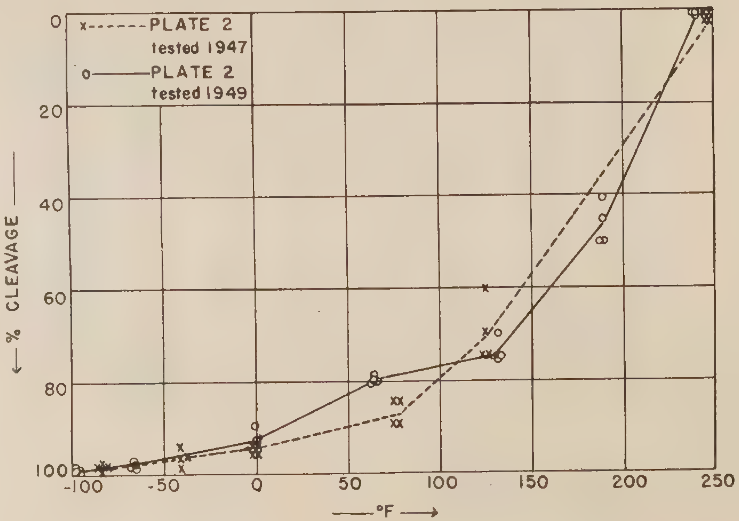

Fig. 6 Transition Curves for Same A-70, 1¼-In. Material Determined in 1947 and 1949
(Lehigh slow notched-bend test. Criterion: Per cent cleavage.)

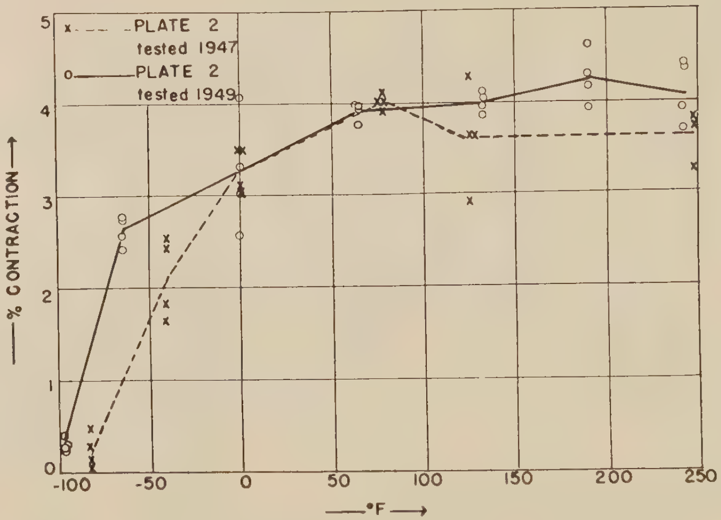

Fig. 7 Transition Curves for Same A-70, 1¼-In. Material Determined in 1947 and 1949
(Lehigh slow notched-bend test. Criterion: Per cent contraction.)

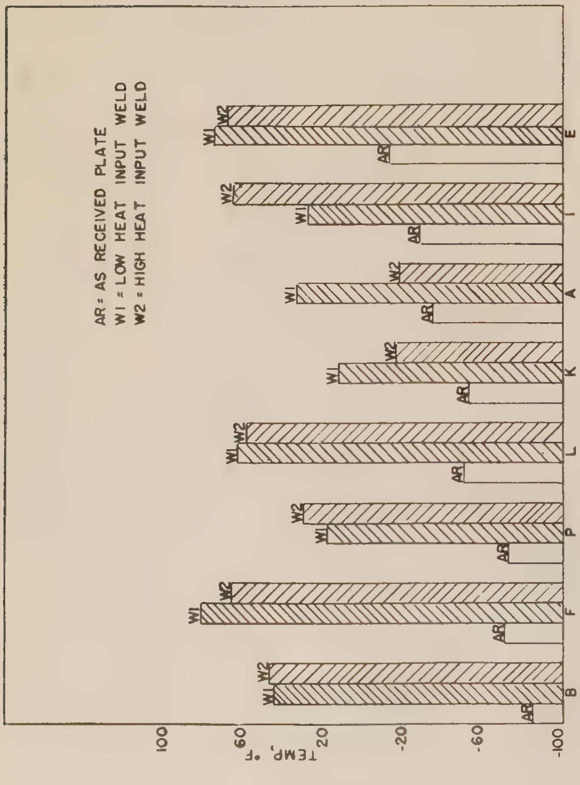

Fig. 8 Effect of Welding on T_N of As-Received Plate

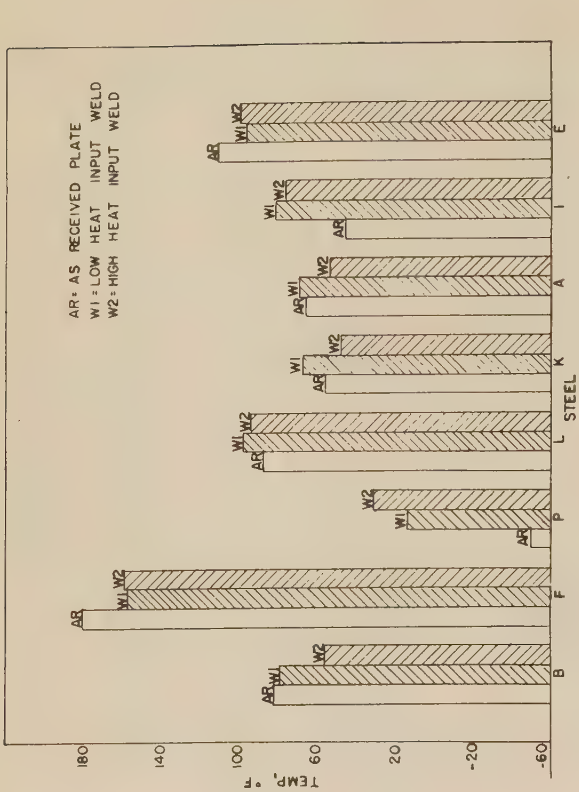

Fig. 9 Effect of Welding on T_B of As-Received Plate

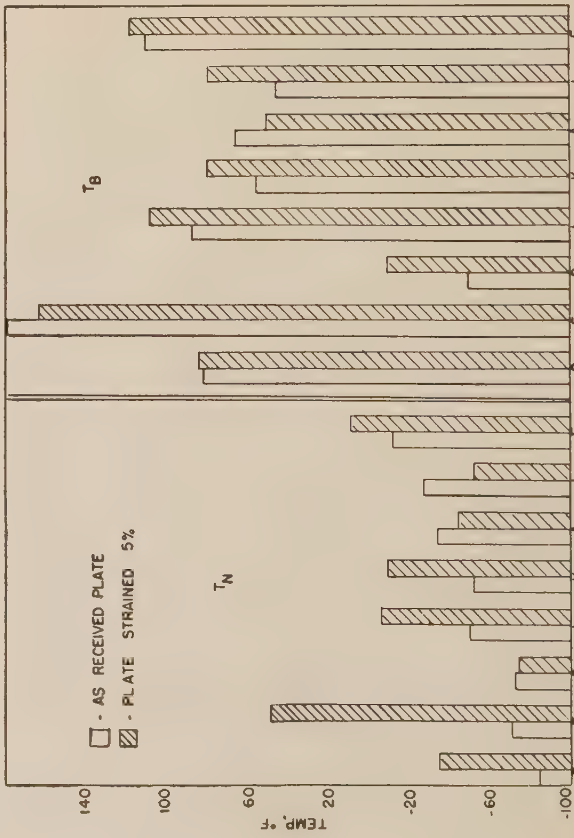

Fig. 10 Effect of Prestrain on T_N and T_B of Unwelded plate

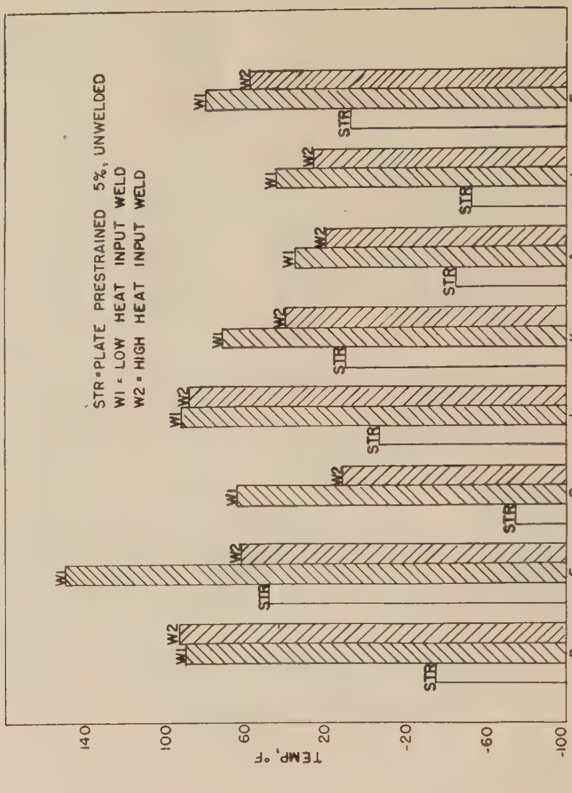

Fig. 11 Effect of Welding on T_N of Strained Plate

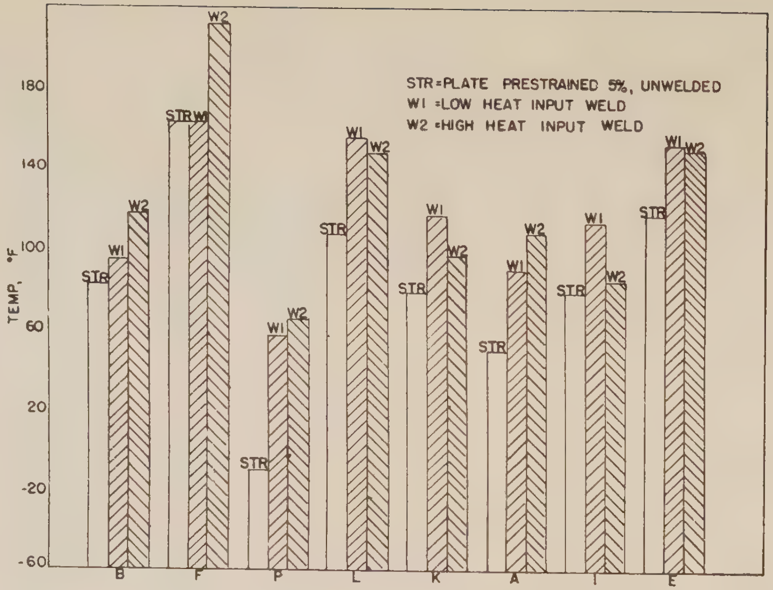

Fig. 12 Effect of Welding on T_B of Strained Plate

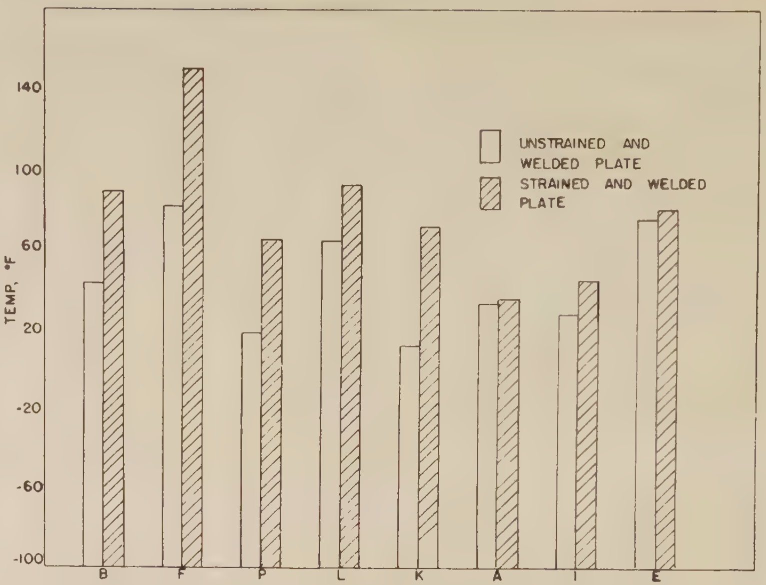

Fig. 13 Comparison of T_N for Unstrained and Welded Plate With Strained and Welded Plate

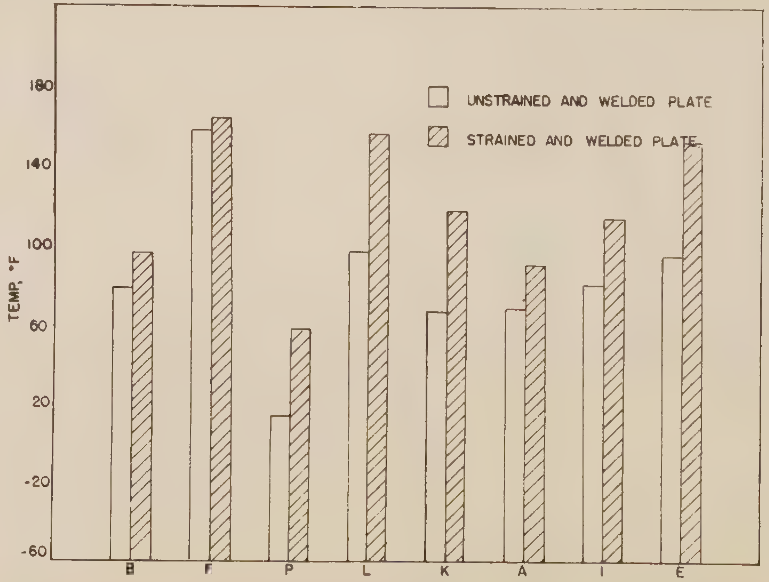

Fig. 14 Comparison of T_B for Unstrained and Welded Plate With Strained and Welded Plate

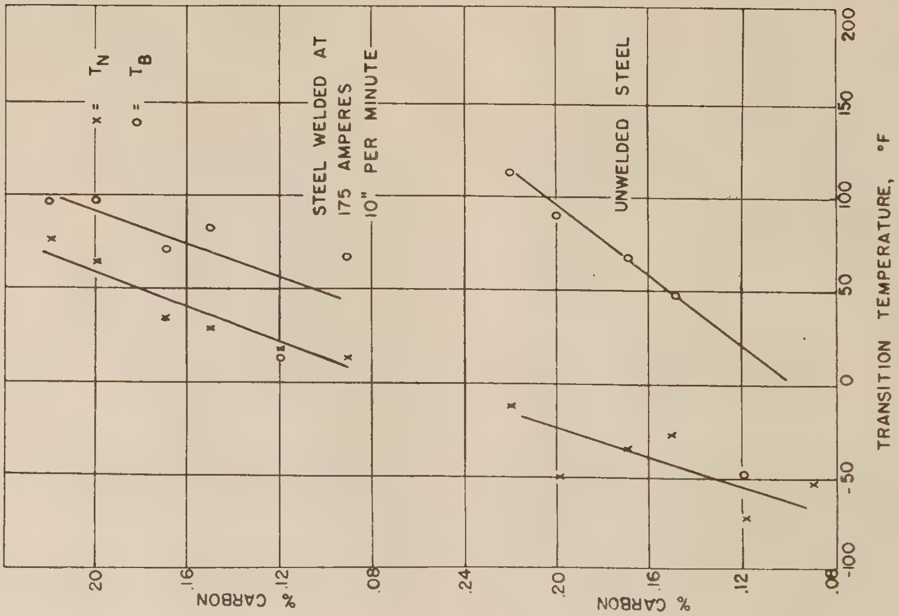

Fig. 15 Relation Between Carbon Content and Transition Temperature

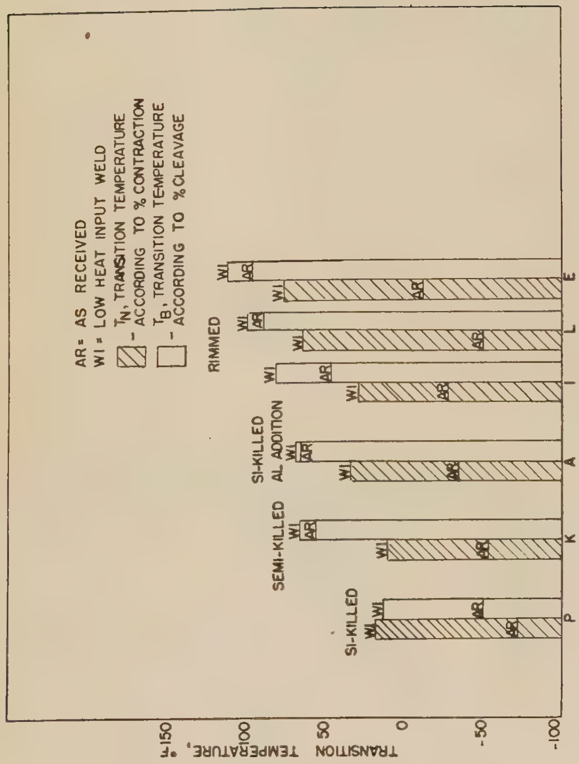

Fig. 16 Relation Between Deoxidation Method and Transition Temperature

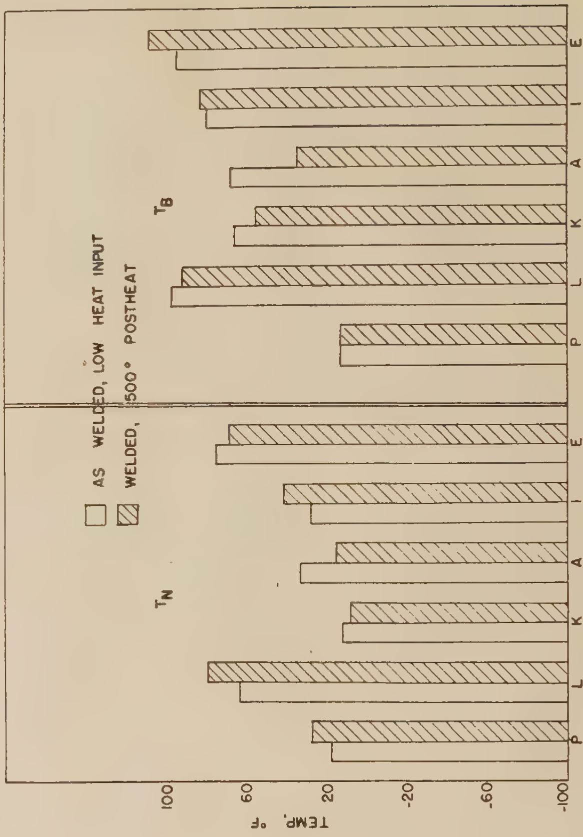

Fig. 17 Effect of 500 Deg Postheat on Unstrained and Welded Plate

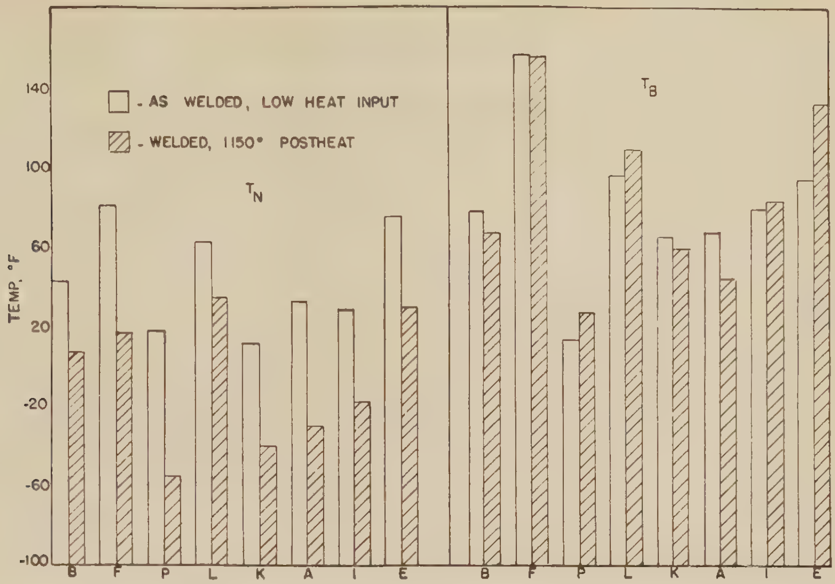

FIG. 18 EFFECT OF 1150 DEG POSTHEAT ON UNSTRAINED AND WELDED PLATE

In Fig. 16 the steels are grouped according to deoxidation practice. According to either T_N or T_B, the rimmed steels had the highest transition temperatures after welding, the killed steel with aluminum addition next, followed by the semikilled, and straight silicon-killed steels. It is interesting to note that the four steels selected at random from mill stock compared favorably with the two pedigreed steels prepared especially for research purposes.

Effect of Heat-Treatment After Welding. The effect of a 500 F heat-treatment after welding unstrained metal at the lower heat input is illustrated in Fig. 17. The heat-treatment has little effect—it sometimes lowered T_N and T_B slightly and sometimes raised them. The 1150 F postheat, however, Fig. 18, lowered T_N by as much as 70 deg, while T_B was unaffected.

Strained and welded metal, however, responded more readily to heat-treatment. In Fig. 19 it can be seen that even the 500 deg postheat lowered T_N somewhat, and it left T_B unchanged. The 1150 deg postheat, as shown in Fig. 20, resulted in a lowering of T_N by as much as 100 deg, and also a consistent lowering of T_B.

The same responses were found after the higher-heat-input weld.

Effect of Welding on Hardness. A study was made of the hardness of the material immediately below the weld in all conditions. It revealed little beyond the fact that welding increased the hardness in this area, and that the 1150-deg postheat had a very slight softening effect.

SUMMARY

1 Welding appreciably increased the notch sensitivity of the material. The increase could not be predicted from the transition temperature of the unwelded plate.

2 Welding prestrained material resulted in a T_N and T_B of slightly higher level than welding unstrained plate.

3 Welding raised the T_N transition temperature of thick plate more than thin plate.

4 The level of transition temperature was apparently a function of carbon content and deoxidation practice.

5 An 1150 F heat-treatment after welding greatly improved the material affected by the weld. A 500 F postheat improved strained and welded material, but not unstrained welded material.

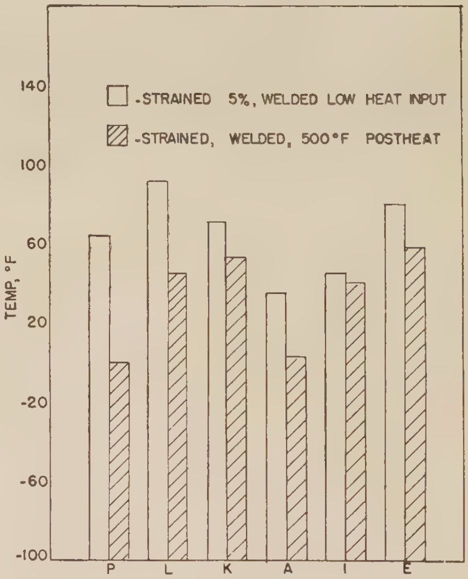

FIG. 19 EFFECT OF 500 DEG POSTHEAT ON STRAINED AND WELDED PLATE

ACKNOWLEDGMENTS

This work was sponsored by the Pressure Vessel Research Committee of the Welding Research Council, which is directed by William Spraragen. Walter Samans is chairman of the Pressure Vessel Research Committee and Boniface E. Rossi is executive secretary. Harry Boardman is chairman of the Fabrication Division of the Pressure Vessel Research Committee, which guided the project staff in this work.

The project was carried on jointly by the Fritz Engineering Laboratory of the Civil Engineering Department, and the Metallurgy Department of Lehigh University.

The execution of work was made possible by the co-operation of Kenneth R. Harpel, laboratory foreman, and the entire laboratory staff.

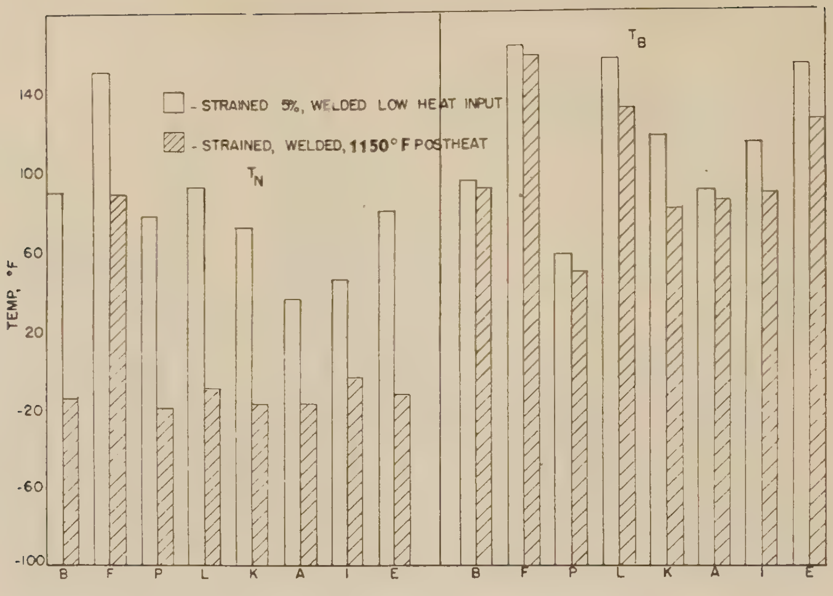

Fig. 20 Effect of 1150 Deg Postheat on Strained and Welded Plate

BIBLIOGRAPHY

1 "Comparison of Notch Tests and Brittleness Criteria," by C. J. Osborn, A. F. Scotchbrook, R. D. Stout, and B. G. Johnston, *The Welding Journal*, vol. 28, 1949, Research Supplement, pp. 24s–33s.

2 "Composition and Property Variation of Two Steels," by C. J. Osborn, A. F. Scotchbrook, R. D. Stout, and B. G. Johnston, *The Welding Journal*, vol. 28, 1949, Research Supplement, pp. 227s–235s.

3 "Effect of Plastic Strain and Heat Treatment," by C. J. Osborn, A. F. Scotchbrook, R. D. Stout, and B. G. Johnston, *The Welding Journal*, vol. 28, 1949, Research Supplement, pp. 337s–353s.

4 "Effect of Welding on Ductility and Notch Sensitivity of Some Ship Steels," by R. D. Stout, L. J. McGeady, C. P. Sun, J. F. Libsch, and G. E. Doan, *The Welding Journal*, vol, 26, 1947, Research Supplement, pp. 335s–357s.

Some Factors Influencing the Economics of Reheat Installations

By R. W. HARTWELL[1] and H. A. WAGNER,[1] DETROIT, MICH.

This paper presents a discussion of some economic factors concerned with choosing between a battery boiler system as compared to a unit boiler-turbine system, and a reheat as compared to a nonreheat plant. Annual costs are compared for four power plants containing the several basic design features. Emphasis is placed upon the difference in average availability of capacity of the four plants, effect on availability of two maintenance schedules, and result of assigning capital charges based upon difference in average available capacity.

In any study concerned with economics of a new power plant, there are numerous factors which require consideration. Basic assumptions in each case must suit the characteristics of the particular power system involved, hence a study made for one plant will not necessarily fit the requirements for another.

This paper covers only certain of the economic factors believed to be pertinent in choosing between (1) a battery boiler system and a unit boiler-turbine system; (2) a reheat and a nonreheat installation.

Special consideration was given to the effect on over-all cost of:

(*a*) Availability of capacity in each of the schemes.

(*b*) The result of different maintenance schedules on availability.

(*c*) Assignment of capital charges resulting from the difference in average capacity available.

It is not the intent of the paper to prove that any one of the four plant schemes studied is the preferred arrangement since this paper represents only a part of a study now being made. Selection of one or two schemes from this analysis should be the starting point for further investigation as to other throttle conditions, different sizes and types of turbine-generators, and other design characteristics such as outdoor or semioutdoor construction, heat-cycle arrangement, and so on. It is believed, however, that an analysis of the effect of some of the foregoing factors will be of interest to those concerned with power-plant economics.

Basic Design Features of Plants Studied

Four plant designs were selected for study to provide a means for investigating the economic desirability of (1) the unit boiler-turbine systems as compared to a battery boiler system; and (2) resuperheating or reheat as compared to a nonreheat installation. Each plant has an installed capacity of 400 mw in four 100-mw tandem-compound double-flow 1800-rpm turbine-generators. Plant A, the battery boiler system, consists of five interconnected boilers; plant B has four boilers, each connected directly to its own turbine; plant C has four boilers, one for each turbine, which are connected by a crossover; plant D is the unit system as for plant B, but provided with reheat. These plants have totally enclosed boiler rooms and pulverized-fuel-burning boilers equipped with unit coal-pulverizing mills.

The estimated total cost for each of the four types of plants considered, and the cost per kilowatt which was based upon nameplate turbine-generator capacity, are given in Table 1. The better thermal economy of the reheat installation is reflected in smaller boilers, condensers, boiler feed pumps, piping, etc., all of which have been evaluated in arriving at the total cost of the reheat plant.

Throttle Conditions. Plants A, B, and C were assigned the 1300-psi 950 F throttle condition in comparing the battery boiler system with the unit system, since use of higher steam conditions would have increased piping costs to a disproportionate extent, and unduly penalized the battery boiler system. Detroit Edison installed two 100-mw 1300-psi 950 F turbine-generators and four boilers at Trenton Channel power plant during 1949, for which accurate cost data are available. Also, two similar machines with the same steam conditions, together with four boilers, will be installed for service at the Connors Creek plant in 1951.

In setting up the reheat installation, plant D, an effort was made to choose conditions which were high enough to favor a reheat cycle and yet which were somewhat comparable with the nonreheat condition. The 1450-psi operating steam pressure seems to be popular because the cost of turbine-generators for 1450 psi apparently is no more than for 850 psi, assuming the same temperature for both pressures. Subsequent studies may investigate the economic advantages of reheat and nonreheat installations with equivalent throttle conditions.

Boiler Capacity and Arrangement. Of the 970,000-lb per hr boilers in plants A and B, each has approximately 10 per cent excess steam-generating capacity over the maximum steam requirements of one 100-mw turbine-generator. In the battery boiler system of plant A one spare boiler was provided, and all boilers supply steam to a common main steam header. Provision of more boilers of a smaller size in the battery boiler scheme was not included since it was determined that more boilers would involve a higher cost with no compensating economic return. Plant B has four entirely separate unit boiler-turbine combinations, while plant C is laid out as a unit system with sufficient crossover piping so that any of the four boilers can supply steam to any of the four turbines. The 1,100,000-lb per hr boilers were sized so that any three boilers can supply sufficient steam to carry rated load, 100 mw, on each of the four turbine-generators. The larger boilers are desirable to secure a higher average plant availability made possible by the crossover.

The reheat boilers in plant D are comparable with those in plant B in that about 10 per cent excess steam-generating capacity over maximum turbine requirements is provided and the four boiler-turbine units are entirely separate.

Pump and Heater Arrangement. The arrangement of the pumps and heaters for all plants is essentially the same. Each turbine has two full-size condenser pumps and three half-size combination boiler feed and heater feed pumps. Five feedwater

---

[1] Engineering Department, The Detroit Edison Company. Mem. ASME.

Contributed by the Power Division and presented at the Annual Meeting, New York, N. Y., November 27–December 2, 1949, of The American Society of Mechanical Engineers.

Note: Statements and opinions advanced in papers are to be understood as individual expressions of their authors and not those of the Society. Paper No. 49—A-100.

TABLE 1 COMPARISON OF NEW PLANT BOILER-TURBINE ARRANGEMENTS; NAME-PLATE CAPACITY 400 MW
(Four 100-mw turbine generators)

Plant Designation	A	B	C	D
	Battery Boiler System 5-970,000 lb per hr boilers	Unit System - No Crossover 4-970,000 lb per hr boilers	Unit System - With Crossover 4-1,100,000 lb. per hr boilers	Unit System - Reheat No Crossover 4-800,000 lb per hr boilers
Throttle Conditions	1300 psi - 950 F	1300 psi - 950 F	1300 psi - 950 F	1450 psi - 1000 F - 1000 F
Total Plant Cost	$ 72,000,000	$ 65,751,000	$ 67,805,000	$ 67,612,000
Cost per kw	$ 180.00	$ 164,40	$ 169.50	$ 169.05
Annual fixed charge per kw based on a 10 per cent fixed charge rate	18.00	16.44	16.95	16.91
Availability, per cent				
Maintenance Schedule A - Single Shift 5 week tri-annual turbine overhaul 2 week annual boiler overhaul 1 1/2 week annual boiler inspection	95.2	90.4	93.8	90.4
Maintenance Schedule B - Double Shift on Overhauls 2 1/2 week tri-annual turbine overhaul 1 week annual boiler overhaul 1 week annual boiler inspection	96.9	94.2	96.0	94.2
Average annual available capacity based on a maximum net turbine capability of 113,000 kw				
Maintenance Schedule A, kw	430,300	408,600	424,000	408,600
Maintenance Schedule B, kw	438,000	425,800	434,000	425,800

heaters are provided for the turbines in plants A, B, and C whereas six heaters are provided for the reheat turbines in plant D.

PLANT AVAILABILITY

The scheduling of Detroit Edision turbine-generator overhauls has become increasingly difficult during the postwar years because summer peak loads have shown a pronounced upward trend and are now about 88 per cent of the previous winter peak loads.

The 12 per cent difference between the summer and winter peak loads represents the theoretical amount of capacity available to accommodate equipment maintenance and overhaul in the summer. All of this margin is not available, however, as higher circulating-water temperatures during the summer months cause a reduction in machine capacity of about 4 per cent. The remaining 8 per cent of the winter peak, which is about 120 mw, is available for summer maintenance. Overhaul scheduling for a system which includes 28 turbine generators, many of which are 75 and 100 mw capacity, is seriously affected, therefore, by the anticipated availability of the various machines.

Maintenance Schedules. In establishing a new plant-maintenance schedule, it is necessary to forecast the average maintenance time for the boilers and turbines for a minimum 35-year period. Operating records for equipment in the system and reports of other companies provide a basis for assuming maintenance schedules. For the purposes of this analysis, two schedules have been used: one based upon single-shift maintenance, and the other on double-shift maintenance (Table 2). Each schedule provides approximately the same number of man-hours for the equipment overhauls and inspections.

TABLE 2 MAINTENANCE SCHEDULES, BASED UPON 35 YEARS OF OPERATION

	Schedule A single shift	Schedule B double shift
Scheduled outages:		
Turbine overhaul, triannual	5 weeks	$2^1/_2$ weeks
Boiler overhaul, annual	2 weeks	1 week
Boiler inspection, annual	$1^1/_2$ weeks	1 week
Unscheduled outages:		
Turbine forced outage, annual	2 days	2 days
Turbine maintenance, annual	2 days	2 days
Boiler forced outage, annual	$^1/_2$ day	$^1/_2$ day

The annual boiler-inspection period gives the maintenance personnel an opportunity to check thoroughly the condition of the boiler and to make necessary repairs. With an inspection period scheduled about 6 months after a boiler overhaul, it is anticipated that no other boiler outages will occur, except the $^1/_2$-day forced outage per year. In setting up the lifetime boiler-maintenance schedules, it was assumed that all boilers would be acid-cleaned, and that a spare coal-pulverizing mill would be installed so that no boiler outage will result from mill maintenance.

The allowance thus made for unscheduled turbine-maintenance outage is to cover minor repairs, or adjustments, or other troubles of such a nature that immediate outage is not caused but which require correction within a reasonable length of time.

These two schedules represent possible practice on the part of one company. Other maintenance practices in force in other utilities[2] will have an important bearing upon availability as is indicated by the difference between schedules A and B.

Availability Calculation for a Four Turbine - Four Boiler Plant. A four turbine - four boiler plant arranged on a unit-system basis, operating with a single-shift maintenance schedule, such as schedule A, would have availability over a typical 3-year period, assuming best coincidence of boiler and turbine repairs as given in Table 3.

TABLE 3 AVAILABILITY OF FOUR TURBINE-FOUR BOILER PLANT

Scheduled outages:		
1st year	One turbine and one boiler overhaul	5 weeks
	Three boiler overhauls	6 weeks
	Four boiler inspections	6 weeks
	Total for 1st year	17 weeks
2nd year	Same as 1st year	
	Total for 2nd year	17 weeks
3rd year	Two turbine and two boiler overhauls	10 weeks
	Two boiler overhauls	4 weeks
	Four boiler inspections	6 weeks
	Total for 3rd year	20 weeks
	Average scheduled outages per year	18 weeks
Unscheduled outages, per year:		
Boiler forced outage		2 days
Turbine forced outage		8 days
Turbine maintenance outage		0 days
	Average unscheduled outage per year	2 weeks
	Total outage per year	20 weeks

$$\text{Availability} = 100\left[1 - \frac{20}{52 \times 4}\right] = 90.4 \text{ per cent}$$

In these calculations, the effect of increase in frequency of forced outage due to addition of forced boiler outage to the forced turbine outage in the unit system is minimized, since average capacity of the several plants is based only upon availability. If the total reserve against forced outage were computed by probability methods, the increase in reserve required by the greater frequency of outage of the unit system would be a significant amount.[3] The extra reserve capacity so determined would be added to the increase in reserve needed for summer maintenance for the unit system as indicated herein, to make all plants equivalent in average available capacity.

The availability figures for all plans under consideration and for both maintenance schedules are shown in Table 1.

CAPACITY CHARGES

In studying the merits of the four plant designs shown in Table 1, it is desirable to make each design comparable with the other from a capacity standpoint. As is shown in Table 1, plant A with its battery boiler system, has the best availability and hence the highest average available capacity. Conversely, plants B and D, designed as unit systems without crossover piping, have the poorest availability and the lowest average available capacity. The difference in the average available capacity should be considered if, as pointed out heretofore, maintenance schedules require that summer peak loads must be met with reserves no better than under winter peak-load conditions. During the latter, it is assumed in all schemes that full capacity is available. The capacity charge is determined by applying fixed charges on the investment required to provide the difference in average available capacity, as indicated by the following example:

Method of Calculation. With maintenance schedule A in effect, plant A has a 430,300-kw average available capacity, which is 21,700 kw more than the 408,600-kw average capacity of plant B. One means of making these two plants equivalent would be to install 21,700 kw of additional capacity in plant B. The cost of this capacity at $164.40 per kilowatt for plant B would be about $3,570,000. Annual fixed charges on this investment, which include taxes, insurance, depreciation, and interest, would be $357,000. As is demonstrated in this simple calculation, the amount of the capacity charge is influenced by equipment availability, the cost of the new capacity involved, and the fixed-charge rate.

Partial Capacity Charges. The annual capacity charge of $357,000 computed in the foregoing represents a 100 per cent capacity charge. This assumes that each year plant B is in service will be one during which a close maintenance schedule is in effect wherein careful consideration must be given to peak loads during the summer months as well as during the winter months. Furthermore, it is assumed that added system capability correctly matches load growth, and only a minimum amount of reserve capacity is available at all times.

---

[2] Turbine and Boiler Overhaul Practice, EEI Publication No. R-13, August, 1949.

[3] "Outage Expectancy as a Basis for Generator Reserve" by H. P. Seelye, Trans. AIEE, vol. 66, 1947, pp 1483–1488.

The likelihood that all of the years in the life of a power plant will be prosperous ones, during which power loads remain high, is remote. Past experience indicates that there will be depression years, during which peak loads tend to fall off, and with these lower loads machine availability becomes less important. In depression years, capacity reserves are high, and therefore capacity charges do not seem justified. Because of this condition, it is postulated that a partial charge should be made against the plant designs which have poorer machine availability.

In many cases reserve capacity might be bought from interconnected systems during the close maintenance years, thereby saving the charges during depression years. Then too, a company interconnected to a system which generates hydropower might arrange the purchase of excess power during the summer months. It is recognized, however, that reserve capacity or power purchase agreements are often on a short-term basis, and may not cover the life of a plant.

The contention that capacity charges should be made only when the amount of capacity involved is influential in deciding when to install an additional machine, should be considered. Actually, many factors are involved in establishing the amount of capacity which has sufficient effect on the system to warrant installation of a new machine, and hence to require a special capacity charge. Some of these factors are matters of policy, such as reserve allowance and equipment maintenance, while others pertain to conditions under which a company is operating, i.e., system size, interconnections, machine sizes, load characteristics, etc. In one case the deficiency of 21,700 kw of capacity, which is the difference between that provided by plants A and B, could require the installation of new capacity, while in some other case the deficiency of this amount of capacity might not affect the expansion policies of the company.

Thus it is evident that conditions may require a full 100 per cent capacity charge, whereas others require none at all. This study therefore includes capacity-charge rates of 0, 50, and 100 per cent.

ANNUAL OVER-ALL COSTS

In developing the annual costs for the plants, four basic cost items were considered. These were (1) the fixed charges on the investment, (2) coal costs, (3) labor costs, and (4) capacity charges.

Fixed Charges. Annual fixed charges which include property taxes, insurance, depreciation, and interest were computed at 10 per cent on the investments.

Income taxes were not included as a fixed-charge item since they are associated with revenue rather than with investment. The economics of one plant design over another is not necessarily subject to income taxes as these savings might be considered applied to rate reductions, for averaging out with less profitable phases of the business, or to offset increasing costs without rate increases. It would appear that income taxes should be considered on completion of the analysis, so that the effect of such items as coal and labor costs can be included. No deductions for income taxes have been applied in this study.

Coal Costs. The basic coal cost assumed in this study was 25.8 cents per million Btu, representing a coal having 11,800 Btu per lb heating value and a long-range cost of $6.10 per ton delivered.

Since it is extremely difficult to forecast long-term coal costs, one of the annual operating-cost comparisons was made holding the annual plant factor constant while varying coal costs from 16 to 32 cents per million Btu.

In computing the coal costs for the various plants, it was assumed that for a specific annual plant factor the same number of kilowatthours would be required by the system. The base generation therefore would be equal to the net plant capability times per cent availability of the battery boiler system times annual plant factor. It is assumed that the net plant capability is 113 mw per machine, or 452 mw for the plant. A plant with a poorer availability would be unable to produce all of the required generation and therefore some kilowatthours would be supplied by less efficient machines on the system. The foregoing does not include a capacity charge. With a 50 per cent capacity charge, only one half of the generation deficiency need be transferred to the less efficient capacity. If a 100 per cent capacity charge is made, it may be assumed that all of the required kilowatthours will be generated on high economy capacity. The charge against plants with poorer availability will depend upon the heat rates of the machines to which the generation is transferred.

Labor Costs. In a new plant with centralized control features, modern coal-handling equipment, and large turbines and boilers, the number of men per megawatt of capacity is considerably less than found in many existing plants. It was estimated that the labor complement, including operating and maintenance personnel, for plant A would be about 210 men. Plant C, with its unit system and crossover, has one less boiler to overhaul each year and therefore requires fewer maintenance personnel. It was assumed that more boiler-maintenance overtime or additional maintenance personnel would be required in plants B and D, as compared to plant C, as boiler outage means turbine outage in plants B and D.

Based upon the foregoing, the assumed labor costs, including wages and such items as social security, pensions, insurance, etc., for each plant are given in Table 4.

TABLE 4 ASSUMED LABOR COSTS

Plant		Annual labor cost	
Designation	Description	Maintenance schedule A	Maintenance schedule B
A	Battery boiler system	$830000	$830000
B	Unit system—no crossover	813000	843000
C	Unit system—crossover	802000	802000
D	Unit system—reheat	813000	843000

Capacity Charges. Operating cost data are presented for three different capacity charge rates, 0, 50, and 100 per cent. The method of computing these charges and a brief discussion of the reasons for including them in an economic analysis which involves equipment with different availabilities was presented earlier in the paper.

Annual Operating-Cost Comparisons. Table 5 presents the annual operating-cost comparisons for the four plants under consideration, assuming a 70 per cent annual plant factor and a coal cost of 25.8 cents per million Btu. The annual plant factor is the ratio of the kilowatthours generated on the machine in a year to the product of the kilowatt name-plate rating × 8760 hr. Total operating costs are shown for both maintenance schedules and the three selected capacity charge rates, 0, 50, and 100 per cent. In all cases the cost of operating the battery boiler system that is, plant A, was found to be the highest and therefore this arrangement was used as a basis for comparison. The savings over the cost of operating plant A are shown for the other three plants.

COMPARISON OF PLANT OPERATING COSTS

The curves drawn in Figs. 1, 2, and 3 offer a means of comparing the plants from the standpoint of total operating costs. These

TABLE 5 COMPARISON OF NEW PLANT BOILER-TURBINE ARRANGEMENT; NAME-PLATE CAPACITY 400 MW
(Four 100-mw turbine generators)

Plant Designation		A Battery Boiler System 5-970,000 lb per hr boilers	B Unit System - No Crossover 4-970,000 lb per hr boilers	C Unit System - With Crossover 4-1,100,000 lb per hr boilers	D Unit System - Reheat No Crossover 4-800,000 lb per hr boilers
Annual Cost of Operation - Maintenance Schedule A 70% APF - No Capacity Charges	Fixed Charges	$ 7,200,000	$ 6,575,000	$ 6,780,000	$ 6,762,000
	Coal Cost	6,518,000	6,672,000	6,562,000	6,359,000
	Labor Cost	830,000	813,000	802,000	813,000
	Capacity Charge	0	0	0	0
	Total Annual Cost	$ 14,548,000	$ 14,060,000	$ 14,164,000	$ 13,934,000
	Saving over Battery Boiler System	-	$488,000	$404,000	$614,000
Maintenance Schedule A 70% APF - 50% Capacity Charges	Fixed Charges	$ 7,200,000	$ 6,575,000	$ 6,780,000	$ 6,762,000
	Coal Cost	6,518,000	6,595,000	6,539,000	6,274,000
	Labor Cost	830,000	813,000	802,000	813,000
	Capacity Charge	0	178,000	54,000	183,000
	Total Annual Cost	$ 14,548,000	$ 14,161,000	$ 14,175,000	$ 14,032,000
	Saving over Battery Boiler System	-	$387,000	$373,000	$516,000
Maintenance Schedule A 70% APF - 100% Capacity Charges	Fixed Charges	$ 7,200,000	$ 6,575,000	$ 6,780,000	$ 6,762,000
	Coal Cost	6,518,000	6,518,000	6,518,000	6,189,000
	Labor Cost	830,000	813,000	802,000	813,000
	Capacity Charge	0	357,000	107,000	367,000
	Total Annual Cost	$ 14,548,000	$ 14,263,000	$ 14,227,000	$ 14,131,000
	Saving over Battery Boiler System	-	$285,000	$341,000	$417,000
Annual Cost of Operation - Maintenance Schedule B 70% APF - No Capacity Charges	Fixed Charges	$ 7,200,000	$ 6,575,000	$ 6,780,000	$ 6,762,000
	Coal Cost	6,518,000	6,604,000	6,546,000	6,284,000
	Labor Cost	830,000	843,000	802,000	843,000
	Capacity Charge	0	0	0	0
	Total Annual Cost	$ 14,548,000	$ 14,022,000	$ 14,148,000	$ 13,889,000
	Saving over Battery Boiler System	-	$526,000	$420,000	$659,000
Maintenance Schedule B 70% APF - 50% Capacity Charges	Fixed Charges	$ 7,200,000	$ 6,575,000	$ 6,780,000	$ 6,762,000
	Coal Cost	6,518,000	6,561,000	6,532,000	6,237,000
	Labor Cost	830,000	843,000	802,000	843,000
	Capacity Charge	0	100,000	34,000	103,000
	Total Annual Cost	$ 14,548,000	$ 14,079,000	$ 14,168,000	$ 13,945,000
	Saving over Battery Boiler System	-	$469,000	$400,000	$603,000
Maintenance Schedule B 70% APF - 100% Capacity Charges	Fixed Charges	$ 7,200,000	$ 6,575,000	$ 6,780,000	$ 6,762,000
	Coal Cost	6,518,000	6,518,000	6,518,000	6,189,000
	Labor Cost	830,000	843,000	802,000	843,000
	Capacity Charge	0	201,000	68,000	206,000
	Total Annual Cost	$ 14,548,000	$ 14,137,000	$ 14,188,000	$ 14,000,000
	Saving over Battery Boiler System	-	$411,000	$380,000	$548,000

Coal cost assumed at 25.8 cents per million Btu.

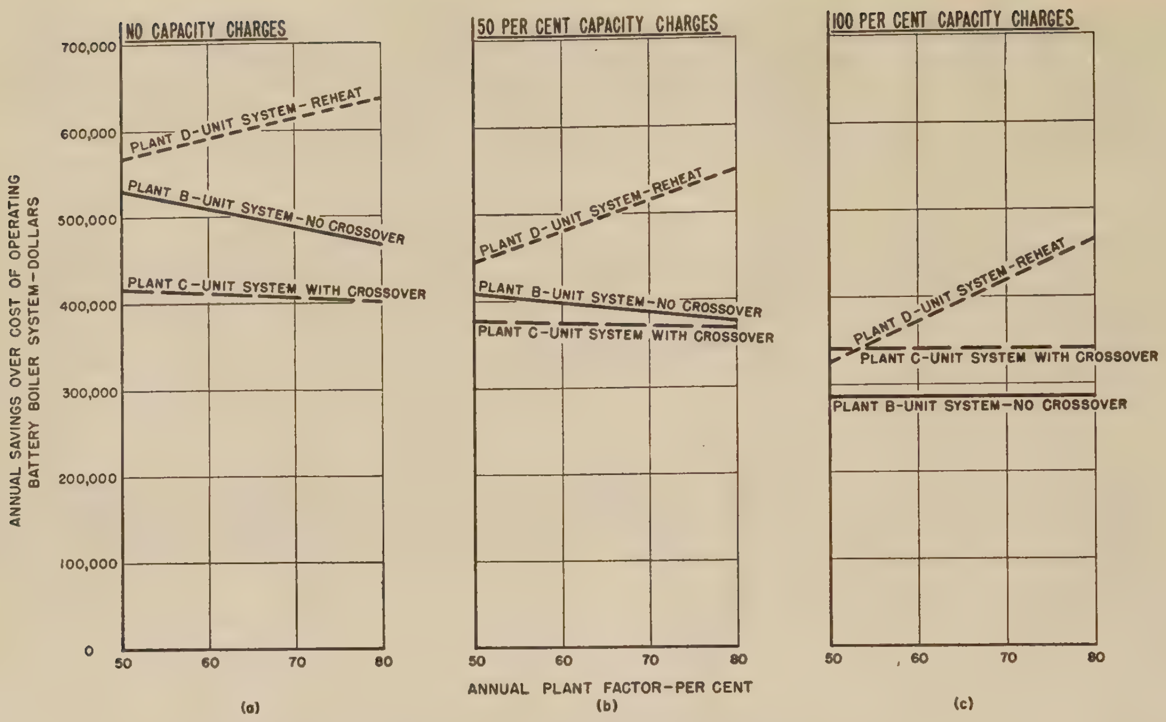

Assumed maintenance Schedule A—5-week triannual turbine overhaul
Using only single shift 2-week annual boiler overhaul
$1^1/_2$-week annual boiler inspection

FIG. 1 BOILER-TURBINE ARRANGEMENT COMPARISON—MAINTENANCE SCHEDULE A
(Each arrangement has four 100-mw turbines and boiler capacity as shown in Table 1. Assumed coal cost 25.8 cents per million Btu.)

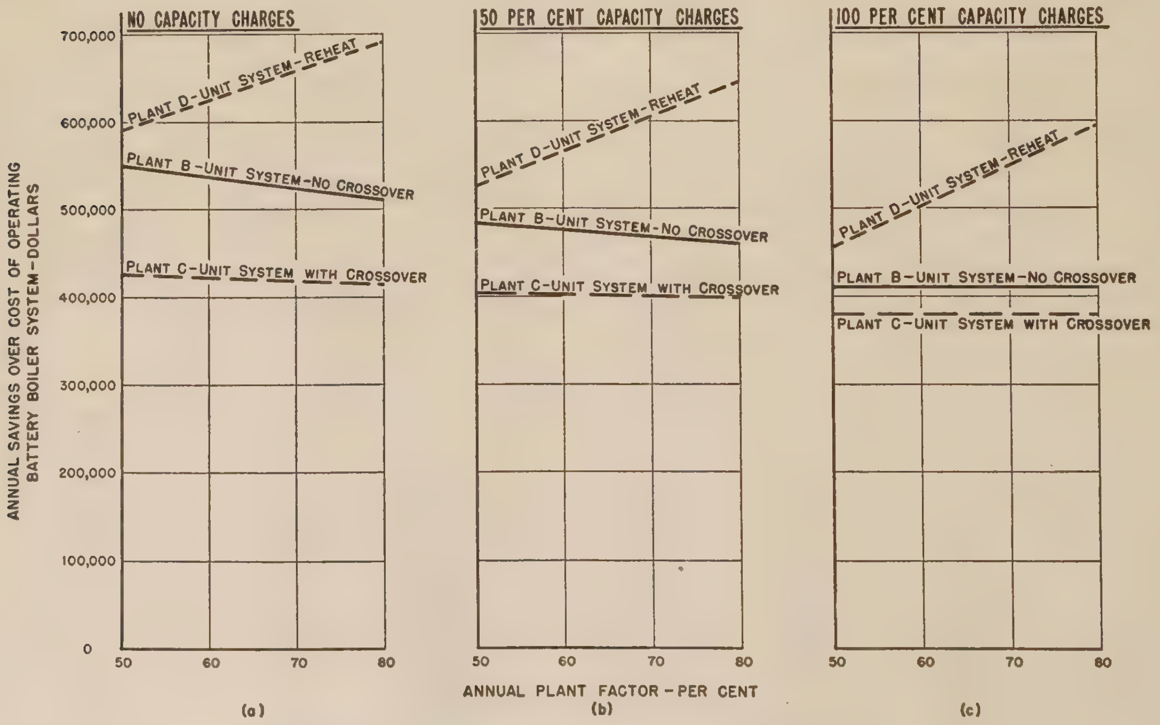

Assumed maintenance Schedule B—$2^1/_2$ week triannual turbine overhaul
Using double shift on overhauls 1-week annual boiler overhaul
1-week annual boiler inspection

FIG. 2 BOILER-TURBINE ARRANGEMENT COMPARISON—MAINTENANCE SCHEDULE B
(Each arrangement has four 100-mw turbines and boiler capacity as shown in Table 1. Assumed coal cost 25.8 cents per million Btu.)

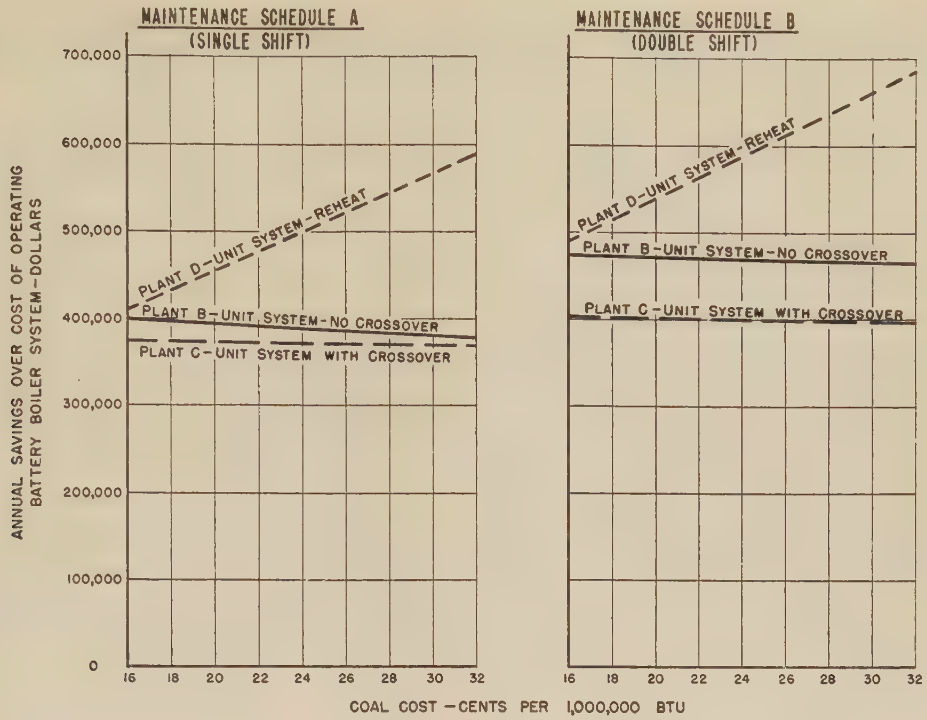

Fig. 3 Boiler-Turbine-Arrangement Comparison; Effect of Coal Costs on Relative Positions of Arrangements Under Consideration

(Assumptions: 50 per cent capacity charges; 70 per cent annual plant factor.)

curves show the effect of including capacity charges, of varying the annual plant factor, of shortening the maintenance time on boilers and turbine generators, and of varying the coal costs. In drawing these curves, the unit-system plants, with and without the crossover, and with reheat, are compared with the cost of operating a battery boiler plant.

For example, it might be concluded that the new plant would operate under the following conditions over its useful life:

1 Maintenance schedule A.
2 Capacity charge, 50 per cent.
3 Annual plant factor, 70 per cent.
4 Coal cost, 25.8 cents per million Btu.

Fig. 1(*b*), which presents curves based upon these assumptions, shows that the operating costs for a reheat installation would be $135,000 less per year than the annual costs for a 1300-psi 950 F unit system with no reheat. Over a 35-year period, which might represent the minimum life of the equipment from an obsolescence standpoint, this saving would amount to $4,725,000. In comparing the costs of plants B and C, which should reflect the added cost of the crossover and larger boilers, it appears that the installation of a unit system could not necessarily be justified on the basis of economics alone, as the saving is only about $13,000 per year. The choice between these two designs might be decided on the basis of operating flexibility, or possibly the difference in the total investment.

Effect of Capacity-Charge Variation. Including capacity charges in the comparison of two plant designs favors the plant with the highest availability. This relationship is clearly shown in Fig. 1 wherein plants B and C are compared for 0, 50, and 100 per cent capacity-charge rates. When no capacity charges are assessed, plant B, unit system without crossover, has a significant advantage over the unit system with a crossover installation, plant C. The relative position of the curves for these two plants is reversed, however, when 100 per cent capacity charges are included. In Fig. 2, where maintenance schedule B is in effect, the savings curves for plants B and C tend to come together as capacity charges are included, but do not reverse positions. The variation in the effect of including the capacity charges results from the difference in availability under the two maintenance schedules.

The curves for plant B, for instance, tend to become horizontal as the capacity-charge rate is increased, because the amount of generation transferred to low-economy equipment varies inversely with capacity charges.

Effect of Annual Plant-Factor Variation. As the annual plant factor for a comparatively low-availability installation, such as has been assumed in plants B and D, is increased, the amount of generation transferred to low-economy machines must be increased. This means that increasing the annual plant factor reduces the savings for unit-system plants. In the case of the high-economy reheat plant, the loss of savings due to generation transfer is more than offset by fuel savings at high load factors. This accounts for the divergence of the curves for plants B and D in Figs. 1 and 2.

The reheat machines would probably have higher annual plant factors than the 1300-psi 950 F machines in the other plants, since the lower heat-rate capacity would carry more of the off-peak loads. A credit which would reflect the added coal savings made possible by a higher-use-factor reheat plant could be computed and included in the coal-cost calculations. This factor is not included, however, since the amount involved is relatively small and is dependent upon the questionable accuracy of long-term load growth and daily load-curve assumptions. On the other hand, if reheat machines are operated over any considerable part of their life at loads below 75 per cent of their name-plate rating, consideration should be given to possible reduction in thermal economy at such loads.

Effect of Changing the Maintenance Schedule. Reducing the number of days the boilers and turbines are out of service for general maintenance, improves the savings rate of all unit-system plants. This improvement is more pronounced in the case of plants B and D where equipment availability is low. The amount of time required for boiler overhauls and inspections has more effect on the operating expenses of the unit-system plants than the time required for turbine maintenance. This conclusion is based upon an analysis of a third maintenance schedule which required double-shift boiler maintenance and single-shift turbine maintenance. Detailed calculations on this schedule have been omitted from this analysis to avoid complicating the presentation.

The schedules for general maintenance of boilers and associated auxiliaries are matters of individual preference resulting from operation of a variety of equipment. This is another of the factors on which a single value acceptable to the industry cannot be specified.

Effect of Coal-Cost Variation. A change in cost of coal has a pronounced effect on the savings made possible in a reheat plant. Fig. 3, drawn for a 70 per cent annual plant factor and a 50 per cent capacity-charge rate, shows that the savings from a reheat plant increase sharply as the cost of coal increases. This increase occurs under both maintenance-schedule assumptions. The heat-rate savings in the reheat plant offset the loss of savings which is common to each of the unit-system plants. These small reductions in savings which result in a slight negative slope of the curves for plants B and C are caused by the increased cost of generating the kilowatthours transferred to low-economy machines.

CONCLUSIONS

In so far as conclusions can be reached on a partial study, it is evident that assignment of fixed charges where justified by minimum reserve capacity, may have a pronounced effect on the cost of operation of the four types of plants considered. Likewise, variation in annual plant factor, single or double-shift maintenance, and increase in coal cost all have a significant influence on the annual operating cost.

Figs. 1, 2, and 3 are based upon the substantial savings to be realized by the unit system, the unit system with crossover, or the reheat installation as compared with the battery boiler system. It is believed that the trend toward the unit system can be explained in part at least by this comparison.

The reheat installation appears favorable economically in all cases, although if 100 per cent capacity charges are assigned, and annual plant factors of 60 per cent or lower are used, the savings in favor of reheat are considerably reduced. In this case, any extra complexity in operation, possible reduction in coal cost, or long-time partial-load operation at less than 75 per cent nameplate rating, would militate against a reheat installation.

Selection of Steam Conditions for No. 4 Unit—Riverside Generating Station

By R. C. DANNETTEL[1] and G. S. HARRIS,[2] BALTIMORE, MD.

In the summer of 1948, the Consolidated Gas Electric Light and Power Company of Baltimore ordered a 75,000-kw-capability, 3600-rpm, straight-condensing unit for installation as No. 4 Unit in its Riverside Generating Station. This selection was made after consideration of units both for straight-condensing and reheat cycles and was based upon judgment that the nonreheat unit should be more economical in total dollar costs to the company during the life of the unit.

IN THE summer of 1948, the Consolidated Gas Electric Light and Power Company of Baltimore ordered a 75,000-kw-capability, 3600-rpm, straight-condensing unit for installation as No. 4 Unit in Its Riverside Generating Station. It is expected that this machine will be placed in operation in the fall of 1951. Design throttle steam conditions of 1450 psig, 1050 F were selected after consideration was given to the following sizes of units and operating conditions:

66,000-kw capability, 850 psig, 900 F
75,000-kw capability, 1250 psig, 950 F,
  with reheat to 950 F
75,000-kw capability, 1450 psig, 1000 F,
  with reheat to 1000 F
75,000-kw capability, 1450 psig, 1050 F

In the study leading to the final selection, the 850-psi unit was used as a measuring stick. The company has in operation four 60,000-kw, 850 psi units which were ordered in the period from 1939 to 1946, and which represented the economic selection for the coal market and equipment market of that period. When the first of this series of units was placed in service at Westport Station in 1941, the fuel cost per million Btu and construction costs were such that it was not economical to spend additional money for improvement in heat rate. By 1948, however, the cost per million Btu had practically doubled, and construction costs had increased sufficiently to warrant a careful reconsideration of the most economical steam conditions.

As a unit with 75,000-kw maximum capability could be accommodated by the system, the study centered around a "preferred standard" 60,000-kw unit with 66,000-kw capability for 850-psig 900 F steam conditions, and three alternative arrangements embodying 60,000-kw, nominally rated, 75,000-kw, maximum-capability units both for straight-through condensing and reheat cycles.

Construction-Cost Estimates

The first step involved the preparation of construction-cost estimates. These were carefully made by bringing up to date the actual costs of preceding units in the station and substituting current bids for those items affected by change in size and heat balance. The result was somewhat surprising since it indicated a spread of less than 2 per cent in the cost per kilowatt of capability. The 1250-psig 950/950 F unit showed the lowest installation cost per kilowatt of capability with the 1450-psig, 1050 F, straight-condensing unit a very close second. The 1450-psig 1000/1000 F design showed the highest installation cost. Fixed charges were of course in the same order. Computation of fixed charges included consideration of return on the investment, depreciation, property taxes, and income taxes based upon three methods of financing the project, that is, by bonds, by stock, and from surplus.

Operating Costs

The next step was an investigation of operating costs. The heat rates showed a wide range with the 1450-psig 1000/1000 F design about $12^1/_2$ per cent better than the 850-psi unit. There were, however, a number of corollary problems to be disposed of before operating costs could be set down in terms of dollars per year.

The question of operating labor proved to be easy to solve since it is not planned to augment the operating force at the station to take care of this unit, regardless of its size or steam conditions.

Perhaps the most difficult problem in the determination of operating costs was the selection of annual generation on which to base fuel costs. It was realized that load-duration curves would be of little value since, with units differing somewhat in capability, the load-duration curves would have corresponding differences. The matter was settled by arbitrarily using 6000 hr operation at 66,000 kw for all units.

The cost per ton of fuel is of course a variable and was handled by computing the annual fuel cost for each unit over a wide range of fuel prices.

In order to combine all of these factors and find a parameter for comparison of the units, a curve sheet, Fig. 1, was prepared with the cost to "own and operate" plotted as ordinates and with the cost of coal in dollars per ton as abscissas. The cost to own and operate was, for the purpose of this study, considered to be the sum of fixed charges and fuel costs. Because of the annual generation selected, the fixed charges for the 75,000-kw units were re-

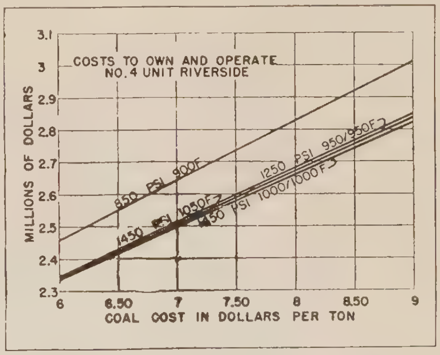

Fig. 1 Costs to Own and Operate No. 4 Unit Riverside

---

[1] Senior Engineer, Consolidated Gas Electric Light and Power Company of Baltimore. Mem. ASME.

[2] Assistant Electrical Engineer, Consolidated Gas Electric Light and Power Company of Baltimore. Mem. ASME.

Contributed by the Power Division and presented at the Annual Meeting, New York, N. Y., November 27–December 2, 1949, of The American Society of Mechanical Engineers.

Note: Statements and opinions advanced in papers are to be understood as individual expressions of their authors and not those of the Society. Paper No. 49—A-62.

duced proportionately to 66,000 kw for comparison purposes. The coal cost in dollars per ton can be interpreted as the cost of coal delivered to the bunker The cost of coal at the time the study was made amounted to about $8.50 per ton. It was found that with the cost to own and operate approximately $3,000,000 per year, there was a spread of about $180,000 or about 6 per cent, Fig. 2. The highest cost was for the 850-psig 900 F unit; the lowest cost was for the 75,000-kw, 1450-psig 1000/1000 F unit. The annual cost to own and operate the 75,000-kw, 1450-psig, 1050 F straight-condensing unit was computed to be about $24,000 above that of the 1000 F reheat unit.

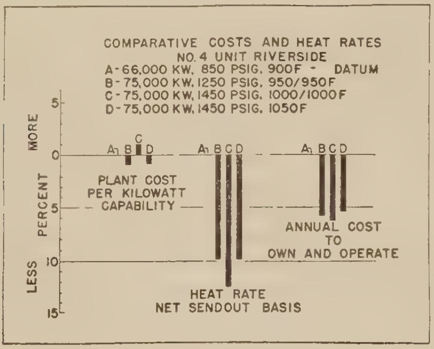

Fig. 2 Comparative Costs and Heat Rates No. 4 Unit Riverside

The difference in cost to own and operate was considered to be within the limits of accuracy of estimating and led to the opinion that the 1450-psig 1050 F, straight-condensing unit, and the 1450-psig 1000/1000 F unit could be considered on the same basis in so far as total expense for fuel and fixed charges was concerned. The final selection then rested on judgment as to availability, reliability, and maintenance.

Availability, Reliability, and Maintenance

The control gear for a reheat unit is sufficiently complicated to lessen reliability somewhat; the unit could not so readily adapt itself to the sudden changes in load which may be expected with system disturbances; and the unit could not be used to regulate frequency on the system. The multiplicity of piping and controls to and from the reheat turbine might well add to station maintenance. Two superheaters and superheat controls would be needed. For the Riverside unit, where the selection of the boiler was influenced by the obvious savings in engineering costs made possible by duplicating the furnace and mill arrangement of other units in the station, one of these controls would be a spray desuperheater which has undesirable features. The gains from reheat are doubtful during the light-load operation which can be expected as the unit ages. Steam and fuel would be wasted at times to protect the reheater from overheating.

The nonreheat unit has a single superheater and control and a minimum of high-temperature piping and valves. The use of 1050 F presents no serious metallurgical problems. This plant should require less maintenance than a reheat unit and should therefore be less expensive to operate.

In comparison with reheat units, the 1450-psig, 1050 F-straight-condensing unit should be simpler to install and operate; with less controls should be more reliable and available; should be more adaptable during system disturbances and for frequency regulation; and, considering maintenance and probable light-load operation, should be more economical in total dollar costs to the company during the life of the unit.

A Comparison of Costs of Reheat Versus Nonreheat for 100-Mw Units

By R. P. MOORE,[1] BUFFALO, N. Y.

This paper analyzes the differences in cost of the various elements of a steam-electric power plant, as affected by choice of the reheat or nonreheat cycle applied to units of about 100,000-kw capability.

Any economic study, the object of which is to ascertain whether or not the use of the reheat cycle in a proposed steam-power-plant development is justified, necessarily must start with differences in capital investment. These then can be compared to the improvement in plant efficiency to be expected from the use of reheat.

The author does not attempt, in this study, to cover all possible combinations of size of unit, plant arrangement, pressures, temperatures, and the like. The data contained herein, while presented in as general a form as possible, are based upon units of 100-mw capability in a single boiler-single turbine arrangement with throttle steam at 1450 psig, superheated and reheated to 1000 F. The reheat turbines are reverse-flow, double-flow, single-shaft, tandem-compound units for 3600 rpm, with bleeding for regenerative heating. They are compared to nonreheat units of similar arrangement, except that the steam passes straight through from throttle to condenser. The fuel is pulverized bituminous coal. Mechanical dust collectors are used.

Cost Elements of Reheat Cycle

The use of reheat affects the original cost of various parts of a steam-electric power plant in different ways. If it is assumed that the capability of the plant is to be the same whether the cycle is reheat or nonreheat, then the boiler plant and parts pertaining to it, excepting the boiler itself, would cost less. This is a direct result of the improved fuel economy. Certain other parts would cost even less than is indicated by the improvement in cycle efficiency. These are the parts carrying the cycle fluid, such as the feedwater system and the condensing system. The generator and the main bus and switch structure are unaffected by the choice of cycle. Finally, there are parts that cost more. Table 1 divides the main items of a plant into these four categories.

Opinions will differ as to the category in which some of the items should be placed. Certainly all of the items in any one of the groups will not follow exactly the same formula in figuring differences in the cost of equipment for the two cycles. A few examples will serve to illustrate.

1 Most pieces of equipment are built in standard sizes. Reducing the fuel requirements by adopting reheat may or may not permit the use of a smaller-size pulverizer, for instance. If it does, the step in cost may be greater than the step in required capacity. It is believed that plus and minus errors of this nature will essentially balance each other.

2 If the plant or unit under consideration is an extension of existing facilities, there may be a number of items which, though they otherwise might be reduced in cost, must be extended as previously installed, without having advantage of savings possible in a new project.

3 Table 1 shows the condenser in the category, the size of which varies approximately with the heat rejection. However, the flow of steam through the last wheels of a reheat turbine is so much less than that through the corresponding nonreheat machine (if the same-size wheels are used) that the reheat turbine possibly can make better use of improved vacua and thereby justify a larger condenser than indicated by the flow. This, however, would seem to be a subject for a separate study involving, in addition, triple versus double flow.

TABLE 1 PLANT COMPONENTS FOR COST ESTIMATING

I Parts of a plant which vary in size generally inversely with cycle efficiency

- Coal storage
- Coal handling
- Fuel-burning equipment
- Fans and ducts
- Dust collectors
- Ash disposal
- Boilerhouse structure
- Auxiliary electrical equipment

II Parts of a plant which vary more in size than efficiency would indicate:

(*A*) Generally directly with the flow of cycle fluid:

- High-pressure steam pipe
- Condensate and boiler feed pumps
- Condensate and feedwater piping
- Bleeder heaters and piping

(*B*) Generally directly with heat rejection to condenser:

- Condenser
- Circulating water pumps
- Intake and discharge flumes
- Screening equipment

III Parts of a plant which are affected little, if any, by cycle efficiency:

- Land and improvements
- Generator and main transformer and connections
- Metering and controls
- Turbine hall
- Electrical structures
- Evaporators
- Feedwater treatment
- Offices, locker rooms, shops, and administration space

IV Parts of a plant which cost more for reheat than for nonreheat, capability of unit remaining the same:

- Turbine
- Boiler
- Reheat piping

Gain in Economy of Reheat

Messrs. E. E. Harris and A. O. White[2] have shown that, for reheat pressures below 500 psia, the per cent gain in economy of reheat over nonreheat is 5 or better. Their figure[2] can be used for the purposes of this paper. The reduction of cycle fluid flow at full capacity is 16.4 per cent and of the heat rejection to the condenser 8.7 per cent, all other conditions, except for reheat remaining the same.

An examination of cost data on plants of the size described, both under construction and recently completed, reveals that at the present time the cost of those items listed in category I, Table 1, totals about \$22.50 per kw of capability. For category II(*A*), Table 1, the total cost is \$8, and for II(*B*) \$7.50 per kw of capability. These figures apply to nonreheat units. The cost of items in category III have no effect upon this discussion. For category

---

[1] Mechanical Engineer, Buffalo Niagara Electric Corporation. Mem. ASME.

Contributed by the Power Division and presented at the Annual Meeting, New York, N. Y., November 27–December 2, 1949, of The American Society of Mechanical Engineers.

Note: Statements and opinions advanced in papers are to be understood as individual expressions of their authors and not those of the Society. Paper No. 49—A-99.

[2] "Development in Resuperheating in Steam Power Plants," by E. E. Harris and A. O. White, Trans. ASME, vol. 71, 1949, pp. 685–691, Fig. 11.

IV, the difference in cost between reheat and nonreheat units is approximately $3.88 per kw of capability.

The cost of power-plant equipment does not vary directly as its size, generally speaking. A machine having 10 per cent greater capacity than another does not cost 10 per cent more. Experience shows that a factor of about 0.7 applied to the difference in capacity will express the difference in cost. In other words, the machine having the 10 per cent greater capacity should cost approximately 1.07 times as much. This factor varies from 0.65 to 0.75, but experience indicates that 0.7 is a good figure for estimating purposes. Authority for it is not readily found outside of price books and quotations, but an article by Alfred Iddles[3] substantiates the figure.

Applying these data to the difference in cost between reheat and nonreheat the ledger stands as follows:

Credits:

For items in category I (Table 1)
22.50 × 0.05 × 0.7 = $0.79 per kw
For items in category II(*A*)
8.00 × 0.164 × 0.7 = 0.92
For items in category II(*B*)
7.40 × 0.087 × 0.7 = 0.45
Total credits for reheat........................ $2.16 per kw

Debits:

For items in category IV $3.88
Total charges for reheat........................ $3.88
Net charge for reheat.......................... $1.72 per kw

These figures apply only to new locations where presumably all possible savings can be made.

With coal costing $7.50 per ton of 2000 lb, and a coal rate of 0.8 lb per kwhr and 5000 hr per year use (57 per cent capacity factor), the saving per year using reheat instead of nonreheat would be $0.75 per kw per year. After allowing 10 per cent for interest, insurance, and taxes, there remains $0.58 which would write off the additional cost in 3 years. Even if coal cost only one half as much, the writeoff can be accomplished in 8 years if the capacity factor averages 57 per cent. No allowance is made for additional operation or maintenance as the author feels that none will be required.

---

[3] "Planning New Capacity," by Alfred Iddles, *Electrical World*, vol. 105, 1935, pp. 983–986.

General Discussion of Reheat Papers

Louis Elliott.[1] Noting the decisions reached as to reheat versus regenerative cycle, in designing steam plants, and without knowing detailed conditions and special methods of reasoning, it sometimes appears that one engineer wants reheat and recommends it, for a relatively small turbine and moderate fuel costs, and another does not like reheat and rejects it, although the turbine in question is a large unit and fuel costs are relatively high. However, in most or all cases, a careful study is given to the economics of the cycle to be selected, as is evidenced by the three papers on this subject.[2,3,4]

Considering that the use of reheat is one of the most important methods of improving steam-plant efficiency, aside from utilization of higher steam temperatures, the decision as to cycle is an important one, and warrants the closest attention. It is necessary, in arriving at a rational conclusion, to determine with some completeness the character of major equipment that would be used for the regenerative- or reheat-cycle plant, and obtain close estimates of cost. These estimates should of course include all elements in which there is a significant difference in investment. Similarly, careful study must be given to relative efficiencies, again taking into consideration all elements showing significant differences, and making sure that for each cycle the plant design and operation are quite thoroughly worked out.

It happens that no recommendation to a client, in which this discusser has been involved, has specified a reheat installation. It may be that this results from the fact that most of the turbine units have been in the moderate or smaller sizes, and that fuel costs on clients' properties have frequently been much lower than those prevailing in the North and East. Recommendations as to plant cycle have been made for a large number of turbines of the magnitude of 60 mw nominal rating—which have indeed been bought for clients in larger numbers than any other one size.

Ordinarily, the estimated saving in production costs, effected by the use of reheat, is expressed as a percentage of incremental investment for the reheat design. To justify reheat, percentage return on increase in investment should be somewhat higher than the normal assigned for charges on cost of station as a whole. In the first place, depreciation of a boiler plant is higher than the average on the entire station. In addition, a reheat plant involves greater complication, perhaps slightly greater expense for operation and maintenance, and possibly some little penalty in reliability.

With respect to magnitude of fixed charges, the papers under discussion show a wide range in allowances made—from 10 to 15 per cent—for all elements of fixed charges and taxes applying to power-station investment. It is now general practice to include, as an element of fixed charges and taxes, an allowance for federal income tax, and state income tax, if any, which must be earned before net return. Federal income tax may frequently be figured, conveniently, as a percentage of investment. It is usually necessary to obtain from management estimates or information on the following: Cost of money, or desired return; average proportion of total capital that will be borrowed; average interest rate to be paid on borrowed capital; method of accounting for depreciation or amortization; life of plant or period of amortization to be assumed; ad valorem or other local taxes. Some of these data can be obtained from annual financial reports, but as the percentages required are those that may obtain through life of property or period of amortization, a new approach is desirable. With such basic values established, an equivalent constant percentage may be taken from annuity tables, covering cost of money plus allowance for depreciation or amortization.

The general subject of station design as affecting magnitude of reserve or system reliability, together with the economics of reheat, were discussed in the Wagner-Hartwell paper.[2] Engineers should appreciate the careful analysis of the influence of plant design on system reserves and reliability. The mathematical process, based upon a mass of outage data and the long and consistent history of operation in large cities, certainly give interesting results, developing the effect of such elements as cross-connection of steam generators and provision of reserve boiler capacity in a large installation.

However, the writer is inclined to feel that, for the usual power system, the long-time influence of differences in design on magnitude of reserves required may be exaggerated. Indeed, it appears that in a good many cases undue stress is laid upon the highest reliability of utility plants, and that continuity of service is "oversold." While New York and other great cities doubtless do call for special treatment, for the smaller cities and for interconnected systems covering large territories, it appears that adherence to a mathematical standard for reliability may be unwarranted.

Almost all the recommendations for plant design in which the writer has been involved have called for one steam generator per turbine generator, with no interconnection between boilers; this has applied to units up to 100 mw in size. There are tangible and intangible values in simplicity, and, aside from saving in investment cost, there is an element of ruggedness and reliability in the avoidance of steam and water interconnections.

G. A. Taylor.[5] We have given a great deal of study to the Hartwell-Wagner paper[2] and have found that study very well worth while. The writer, with others, has set up a method of evaluating power-plant equipment that is very complete and has many unique features. We believe that this method can be used advantageously by all of us, but we must keep in mind that there are many conditions peculiar to each system. Care must be taken to evaluate these conditions properly.

The authors state that better thermal economy of the reheat installation is reflected in smaller boilers, etc. The boilers are smaller when rated in pounds of steam per hour. The boilers are about 5 per cent smaller when rated by heat input. We have found that the size of the reheat boiler is almost the same as the size of a nonreheat boiler for the same pressure and temperature, other conditions being equal. Since the heat input to the reheat boiler is about 5 per cent less than the heat input to the nonreheat boiler, the firing equipment can be slightly smaller, the furnace can be 5 per cent smaller, but the superheater and reheater require much more space than the superheater on a nonreheat boiler. With all other design factors being equal, our experience shows that the cost of a reheat boiler is about 5 per cent more than the cost of a nonreheat boiler. This was brought out previously by Messrs. Rowand, Raynor, and Gilg.[6] We believe it is very important when comparing reheat to nonreheat boilers to keep all other design factors the same.

---

[1] Consulting Mechanical Engineer, Ebasco Services Incorporated, New York, N.Y. Mem. ASME.

[2] "Some Factors Influencing the Economics of Reheat Installations," by R. W. Hartwell, and H. A. Wagner, published in this issue of the Transactions, pp. 549–556.

[3] "Selection of Steam Conditions for No. 4 Unit, Riverside Generating Station," by R. C. Dannettel, and G. S. Harris, published in this issue of the Transactions, pp. 557–558.

[4] "A Comparison of Costs of Reheat Versus Nonreheat for 100-Mw Units," by R. P. Moore, published in this issue of the Transactions, pp. 559–560.

[5] Project Manager, The Babcock & Wilcox Company, New York, N. Y.

Boilers are being bought today for comfortable operation with a minimum of man power. It appears that for schemes "A" and "C" of the paper consideration should be given to the possibility of using the short-time overload capacity of the boilers when one boiler is out of service. The use of this overload capacity might mean that more man power would be required to keep the heating surfaces clean but it might be worth while.

The 12 per cent difference between the summer and winter peak loads is an interesting bit of data and certainly makes it evident that more spare capacity on the system will be required now than in the past. This condition of course would be most troublesome to those systems that use old and inefficient generating equipment as stand-by for the modern equipment. We believe it will be necessary for the engineers making a study similar to this on any specific system to estimate the cost of power generated by the old equipment. On many systems the "capacity-charge" method of calculation would result in error because of the very high cost of stand-by power. It also can be true when power is purchased. We have observed that depending upon purchased power can be very dangerous because when one power system is operating at high load the power systems from which power can be purchased are also operating at high load and may not have any surplus available.

One feature of the battery boiler system is disturbing to us, that is, the thermal stresses set up in the main steam header whenever a boiler is cut into service. We can visualize 650 F steam being turned into a header, the temperature of which is between 950 F and 1050 F. We would like to suggest that the designers provide some protection against such thermal shocks.

This paper[2] brings out very forcibly the fact that rating boilers in thousands of pounds of steam per hour is no longer satisfactory. Not many years ago the practice of rating a boiler in "horsepower" was satisfactory until increased pressures and steam temperatures made this method inadequate and caused us to go to rating boilers in thousands of pounds of steam per hour. The popularity of reheat cycles with high pressures and temperatures has now made it necessary for us to start using another yardstick. We should begin to think of "heat input," "heat output," or "megawatts" when thinking of the capacities of modern boilers.

E. E. **Harris.**[7] R. P. Moore's paper[4] states, "This paper analyzes the differences in cost of the various elements of a steam-electric power plant, as affected by choice of the reheat or nonreheat cycle applied to units of about 100,000-kw capability."

It appears that the author's approach is a more logical method for determining the costs between a reheat and a nonreheat station. He attempts to evaluate only the differences between two such plants.

In his Table 1 various parts of a power station have been placed in different classifications, depending upon how the cost of these parts varies. Some equipment changes cost due to a change in heat consumption, while other equipment changes cost due to a change in liquid flow. Other parts do not change cost by changing heat consumption or cycle flow. There is an increase in cost for the turbine and boiler, with an additional charge for reheat piping.

In Table 1, Section II-A, Bleeder Heaters and Piping, it would be inferred that the cost of these would be reduced directly with the flow of the cycle fluid. The heater and the extraction piping next below the reheat point may increase in cost due to higher-temperature steam to this heater than would be obtained for a nonreheat unit. This additional cost may be of small magnitude.

Table I, Item III—Metering and Controls—probably would cost more for the reheat installation. The turbine hall, depending upon the arrangement, may cost more due to the increase in length of a reheat machine over a nonreheat unit. Evaporators may cost less, as well as the feedwater-treatment apparatus. If these items in Section III balance out to zero differential in cost, then they do not enter into a cost difference between reheat and nonreheat.

The paper states, "Net charge for reheat $1.72 per kilowatt." This addition is based upon costs assigned to the various items in Table 1. If they represent average costs, then $1.72 per kilowatt corresponds to between 1 and 2 per cent additional cost for a reheat station over a nonreheat station. Such an increase in cost for the reheat station compared with the gain in economy obtained by reheating makes reheating appear very favorable.

E. H. **Krieg.**[8] At the 1948 Annual Meeting of the Society, an outstanding group of papers was presented which discussed the engineering aspects of the reheat cycle quite completely, with the exception of its economic aspects. Desiring to present a few thoughts on the economics of reheat from the stockholders' or management's viewpoint while interest was still warm, and to supplement the data given in "Comparative Costs of Resuperheating Installations,"[9] Mr. Stanley Stokes and the writer prepared a paper, "Union Electric Finds Attractive Return in Reheat."[10] Some of the points therein bear reiteration when discussing the present papers.[2,3,4] Engineers will welcome these good papers on economics, for no engineering study can be complete without justification of the proposed investment.

We agree with the conclusion reached in R. P. Moore's paper,[4] that, although a plant designed for the reheat cycle costs more, its adoption is justified in many cases. This discussion is intended to amplify that conclusion.

The Hartwell-Wagner paper[2] mentions the often forgotten concept that to justify interconnected boilers, extra capacity is required either in the form of an extra boiler or larger boilers. The hours per year when the interconnection would be used may prove to be too small to justify the interconnection otherwise. The paper[2] does not mention that availability of battery boilers is sometimes adversely affected by the sectionalizing valve (or its by-pass) in the interconnecting steam and water lines. When a boiler or turbine is down and steam or water leaks into it from the adjacent active unit, a total of two units must come off. The writer wonders if Mr. Steinberg assumed[11] that valves always remain tight and never need maintenance, with consequent outage of two boilers instead of one, or possibly two turbines instead of one. The question is: Won't the valves in the several interconnections cause almost as many lost kilowatthours over 30 years as they will save? We have many data on turbine availability, but little on the effect of valve tightness on availability other than the recollection of operators of specific cases. There is a need for some factual data on such cases.

Messrs. Dannettel and Harris[3] state: "When the first of these series of units was placed in service at Westport Station in 1941, the fuel cost per million Btu and construction costs were such that it was not economical to spend additional money for improvement in heat rate. By 1948, however, the cost per million Btu had practically doubled, and construction costs had increased sufficiently to warrant a careful reconsideration of the most economical steam conditions." It is admittedly difficult to do so, but power-station design should not be concerned with present fuel costs but with the cost of fuel 16 years from now, that is, the average of the 3 to 33-year period hence.

---

[6] "High-Pressure Boilers With Reheaters," by W. H. Rowand, A. E. Raynor, and F. X. Gilg, Trans. ASME, vol. 71, 1949, pp. 719–727.

[7] General Electric Company, Schenectady, N. Y.

[8] Consulting Engineer, Stone & Webster Engineering Corporation, Boston, Mass. Fellow ASME.

[9] *Electrical World*, vol. 132, Sept. 10, 1949, pp. 87–91.

[10] *Electrical World*, vol. 132, Dec. 17, 1949, pp. 93–96.

[11] "Relation of Thermal Plant Design to Reserve Capacity," by M. J. Steinberg, *Electrical Engineering*, vol. 69, January, 1950, pp. 64–67.

Metallurgically, there are such meager long-term data on the characteristics of certain steels at 1050 F and over that some speculation attends their use at the present time. The incremental dollar savings do not always appear to balance the incremental headaches.

In the paper by Messrs. Dannettel and Harris,[3] could not a more direct comparison between reheat and nonreheat costs be made for approximately the same thermal performance, e.g., 1450 psi, 1050 F compared with 1250 psi, 950 F/950 F reheat? The paper admirably presents the small cost difference between reheat and nonreheat: "The result was somewhat surprising indicating a spread of less than 2 per cent in the cost per kilowatt of capability."

Availability might be better served with 950 F reheat cycle than for a 1050 F straight-through cycle, because in one study it was noted that the former enjoyed a lower furnace-gas exit temperature which should give less slagging. This is especially important with strip coal.

It is regretted that the effect of system interconnections seems to be omitted from many studies. Load factor of a unit is a function of how that unit serves an integrated group of systems on which there are usually some low-efficiency units for taking low load factors, giving new units better load factors. When engineers expect the load factor of a new unit to decrease in the future, that decrease will not take place unless more efficient units are installed.

Reviewing the issues developed thus far, the enigma of reheat is not the mere estimation of investment costs nor return on the investment. Rather, much of the problem or the enigma appears to be one of "futures" in coal and labor. The present price of coal has no bearing on the problem because the proposed plant does not begin to burn coal until some 3 years after the decision has been made to build the plant. Then, if the amortization period is 30 years, the coal price between 3 and 33 years from now is all that is significant—similarly for labor costs. What fuel will cost in the future has a greater effect on the choice of cycle than whether one cycle is 5 per cent more efficient than another. It seems too bad that, relatively, so little attention is focused on actual past and probable future fuel costs in journals devoted to power plants. Perhaps some enterprising power-industry publication will favor us with regular fuel-cost forecasts needed by power-plant engineers. A great deal of attention, perhaps too much, is given to calculating the difference a few Btu may make, using existing costs without proportionate attention being given to what future fuel costs may be.

Even this is not the whole story, for the effect of a higher coal price during the early years is of far greater significance than during its later years. During the first 5 years the load factor of the plant will certainly be high, and a high fuel cost then will produce a large return. But during the 25 to 30-year-old period when a low load factor may well be the case, a low fuel cost means little, for the earnings made during "boyhood" will support its "old age." If an inefficient plant is built today, its future fate inevitably will be low load factor; interconnection contracts will take care of that. The better the performance that is designed into today's plant, the less will it be backed off by future plants.

No two people can agree on what coal prices will be during the next 33 years, and it is anybody's right to estimate or speculate on what they will be. At the risk, or rather with the certain knowledge that others will disagree, this slant on future coal prices may have some guidepost value.

W. F. Ryan.[12] No matter which set of assumptions is used, the Messrs. Hartwell and Wagner[2] find an annual saving of about $130,000 for a unit system with reheat (Plan D) compared with a nonreheat unit system (Plan B). The maximum differential is $137,000 and the minimum $126,000 per year. This is the net return, before income taxes, on an increment investment of $1,861,000.

A factor which should not be overlooked is that, assuming regulated and limited net profits for the utility, the $130,000 more or less reduction in annual production expense represents an ultimate saving to the customer on his energy charge, while the $1,861,000 added investment represents an increase in his demand charge.

Some of us can remember the "great depression" when power customers whose markets had evaporated, and whose gross income had shrunk in proportion to sales, refused to understand why the power company demanded so much money for such small amounts of energy. Those of us who remember those days might hesitate to accept this return on what is ultimately an increase in demand charge. We remember that when a customer is using a lot of energy, he is prosperous and can pay for it. When he is not using much energy, he is hard up, and complains bitterly about paying for his previously established demand.

The savings which accrue from the use of a unit system are assignable to the demand factor, exclusively. Therefore it is not only a substantial saving, but it is a saving in the right place. We are indebted to the authors for so clear a demonstration of the advantage of unit installation.

Under other conditions the case for reheat may be more convincing. For example, in dealing with larger units, the lowest cost undoubtedly will be obtained by installing the greatest capacity economically feasible on a single-shaft 3600-rpm machine. In this case capacity may be increased several thousand kilowatts by the use of reheat, effecting a substantial saving comparable to that shown in this paper[2] in production expense, and also in the unit capital cost of the plant.

Sabin Crocker.[13] The authors are to be congratulated on contributing an excellent paper on a timely subject that warrants careful analysis. They have done well in offering an objective presentation of data concerning the relative availability of boiler-turbine units installed with and without crossovers. The paper affords a variety of factual data from which the reader can select the set that best suits his own conception of availability and what share of capital charges should be assessed against any loss thereof.

One of the important facts brought out by the paper is the reduction in outage time obtained by using two-shift maintenance instead of one shift. For the straight unit system without crossovers, this represents a gain in availability of 3.8 per cent as shown in Table 1. This gain in availability can be obtained at little expense for premium pay since only the controlling jobs of longest duration need to go on double shift; other jobs can be finished in time on one shift with a normal crew or by putting extra men on the one shift where more can work to advantage simultaneously.

With two-shift maintenance the authors show the difference in availability of the unit system with and without crossovers to be something less than 2 per cent which agrees with the experience of operating companies that have had unit systems in use for some time. In fact, the engineers of some operating companies contend that there is less outage without crossovers than with because the extra valves and other items associated with the crossovers and with operating the boilers in battery constitute an added source of outage. In any event the operation of a boiler and turbine on the straight unit system without crossovers permits omitting the nonreturn valve as well as two or more gate valves per unit. This results in a considerable reduction in pressure-drop losses and perhaps an ensuing saving in boiler cost together with the saving in cost of the valves and piping omitted. Furthermore the straight unit system permits a simplification of steam and feedwater controls and metering which both facilitates operation and reduces cost. Inasmuch as the authors have shown a difference in investment of $5.10 per kw changeable to the crossovers plus some extra boiler capacity, the writer concludes that they have made due allowance for differences in piping, controls, and metering. Nevertheless, more details concerning estimated differences in investment would be helpful.

---

[12] Engineering Manager, Stone & Webster Engineering Corporation, Boston, Mass. Fellow ASME.

[13] Mechanical Engineer, Ebasco Services Incorporated, New York, N. Y. Mem. ASME.

Granting for the purposes of discussion that the authors were right in assigning about 2 per cent in round figures less availability without the crossovers (see Table 1 for 96.0–94.2 = 1.8 per cent), the writer would like to apply this figure in trying to analyze what it means as applied to an actual system. Assuming an existing name-plate rating of 1,700,000 kw for units installed on the electrical system, the addition of 400,000 kw would bring the installed capacity up to 2,100,000 kw. The last 400,000 kw, by assumption, would have an availability 2 per cent less without crossovers than if such had been provided. Thus for an addition of 400,000 kw, the loss of availability would be diluted to the following extent:

$$\frac{400{,}000 \times 2 \text{ per cent}}{2{,}100{,}000} = 0.38 \text{ per cent}$$

A loss in availability of less than 0.4 per cent when spread over the system as a whole seems within the capability of existing reserves to carry without installing more capacity on this account. Continuing the reasoning on this basis, it would be perhaps 15 to 20 years before the further dilution of availability due to adding successive units without crossovers could approach 1 per cent loss in availability for the electrical system as a whole. This still remains a small figure with respect to other uncertainties to be considered in determining what constitutes reasonable reserve.

Theoretically, on an electrical system having aggregate nameplate ratings of 2,100,000 kw, a difference, 0.4 per cent represents only 8400 kw which is a relatively small amount to obtain by way of assistance over an interconnection or, in a pinch, by temporarily reducing voltage or dropping nonessential load. From a practical operating standpoint, a loss in availability of this order is apt to mean that one of the new large boiler-turbine units without crossovers would be off the system at some remote time when full reserve for backing it up is not available. On a system having units of various sizes it is to be expected that a smaller unit would be in reserve for this contingency which, plus about 8000 kw aid from a tie line, or as otherwise noted above, would tide things over.

Closure by R. W. Hartwell and H. A. Wagner

The authors believe that Mr. Elliott is quite right in his statement that the reliability standards indicated in the paper may not be applicable to small power systems where continuity of service and other factors may differ materially from those considered suitable for large systems. Such variables make it impractical to apply the results of our analysis directly to another power system.

Mr. Taylor has raised an interesting point with reference to rating of boilers in terms of heat input or output rather than steam output. He is, of course, correct. To many engineers, however, the capacity of a boiler in terms of steam output conveys a better appreciation of size, even though not strictly accurate, than heat input or output in million Btu. The authors agree, however, that we should begin to think in terms of heat rather than pounds of steam.

Mr. Krieg's discussion concerning the cost of coal over the life of the equipment is certainly pertinent. In stating, however, that the fuel cost over the first five years of a plant is the more important, some of the uncertainty of speculating on long-time coal costs is removed. Whereas the fuel purchaser will be extremely hesitant about predicting the cost of coal for a 30 to 40-year period, he probably would not be too hesitant in giving a figure for the next five years. The authors feel sure that Mr. Krieg would agree that the inability to predict the long-time coal cost should not be considered a reason to stop the quest for more efficient power plants.

Mr. Ryan makes a very good point that the amounts of money involved in the several schemes differ greatly. It is entirely possible that a somewhat less efficient plant might prove a much better choice depending on future business and load conditions.

Mr. Crocker correctly points out that small differences in availability are difficult to evaluate in terms of capacity. Whereas an increment of capacity considered individually might be considered too small to warrant a capacity charge, several of such increments, however, could add up to a capacity which could not be overlooked. Again, numerous factors require consideration as to whether a charge for small capacity differences is warranted on a particular system.

The authors appreciate the comments made by the discussers of this paper. These comments represent an important addition to the information presented in the symposium on the economics of reheat power plants.

Closure by R. C. Dannettel and G. S. Harris

The authors appreciate the helpful suggestions of the discussers and, in general, agree with them. The importance of some of these points justifies further discussion for clarification.

Mr. Elliott emphasizes that estimates should include "all elements in which there is a significant difference in investment." The surprising result in the authors' investment studies was the small difference when all elements were considered as contrasted with the much larger spread of costs indicated by consideration of a few major elements. With respect to magnitude of fixed charges, the constant percentage used by the authors was determined by a staff member of the Company's Economic Planning Committee who was familiar with the taxes, interest rates, and amortization rates mentioned by Mr. Elliott and who also was in a position to weigh the effects of stock-bond-surplus financing of the project. There is full agreement with Mr. Elliott's comment "To justify reheat, percentage return on increase in investment should be somewhat higher than the normal assigned for charges on cost of station as whole."

Mr. Krieg is correct in saying, "It is admittedly difficult to do so, but power-station design should not be concerned with present fuel costs but with the cost of fuel 16 years from now, that is, the average of the 3 to 33-year period hence." The authors based their computations on a study of the estimated average cost of coal for a 30-year period prepared by the Company's purchasing agent. Mindful of the severe changes in fuel costs between 1941 and 1948, and acknowledging the difficulty of predicting future prices, the authors graphed their results with coal costs as abscissas (Fig. 1 in paper) to permit evaluation with wide latitude in estimates of future coal cost.

The authors agree with Mr. Krieg's statements that the "problem of reheat" appears to be one of "futures" in coal and labor with the further complication of future load factor. The graphs plotted against coal cost offer a partial solution to the first part of this problem by predicting in advance the effect of a wrong guess in estimating fuel cost. The second part is best answered by a composite load-duration curve including estimated effects of system interconnection and the progress of the manufacturers and the central-station industry in producing more efficient units in the future. A curve of thermal rates plotted against years shows clearly the achievements to date and promises better efficiency for future units; sound engineering dictates that each improvement be weighed as it becomes available and incorporated in the system whenever a study of all elements of cost shows that its selection would result in greater over-all return to the stockholders over the life of the unit. It may be of interest that a study conducted along these lines one year later than the one reported confirms the assumptions made for No. 4 Unit at Riverside and indicates similar general conclusions.

Mr. Krieg is correct in stating that the 1450 psi, 1050 F, and the 1250 psi, 950 F/950 F cycles would have approximately the same thermal performance and should offer a more direct comparison than 1450 psi, 1050 F compared with 1450 psi, 1000 F/1000 F. The results of this comparison are shown in the graphs and indicate that the cycles with approximately the same thermal performance differ very slightly from each other in costs.

The authors frankly admit that their computations show a small saving by use of the reheat cycle but are in full agreement with Mr. Krieg that "the incremental dollar savings do not always appear to balance the incremental headaches."

Analysis of Experimental Data Regarding Certain Design Features of Pressure Vessels

By G. J. SCHOESSOW[1] and E. A. BROOKS,[2] BARBERTON, OHIO

This paper presents an analysis of data obtained by strain-gage experimental stress analysis on drum heads and nozzle openings in drum shells. This analysis, while referred particularly to power boilers, is also applicable to other types of pressure vessels. The data obtained are reduced to dimensionless form so that they may be applied to drums of other size and thickness but geometrically similar, and to illustrate more clearly the action of the drum in resisting pressure. The relationship between operating-stress level and the life of the vessel in service is discussed with particular reference to a drum that has given over 40 years of satisfactory service with an operating-stress range over a considerable area of the vessel of approximately the ultimate strength of the material. The effect of prestress created in the vessel by overpressuring, such as applying the $1^1/_2$-times working-pressure hydrostatic test, is discussed.

IN A vessel of complicated shape subjected to internal pressure, the simple membrane-stress concepts do not suffice to give an adequate idea of the stress situation. Cylindrical shells are somewhat out of round, vary in thickness, and are pierced by openings. Their end closures tend to dilate radially at a rate different from that of the shell, they deviate from a true spherical shape, often markedly, and are themselves pierced with openings. These deviations from a true membrane shape set up bending in the vessel wall and cause the direct loading to vary from point to point.

In the series of experimental stress analyses on pressure vessels whose technique has been reported by L. F. Kooistra and R. U. Blaser,[3] resistance strain gages were bonded in opposite pairs to the inner and outer walls of the test drums. From the readings of these gages may be computed the stresses at the inner and outer walls. The direct stress on the wall at that point is given by one half the sum of the stresses inside and outside, while the bending stress is given by one half their difference. These direct and bending stresses, plotted over the vessel wall, give an excellent idea of how the vessel behaves under pressure. A somewhat better conception is obtained if, instead of stress, the actual loads and moments be plotted. The direct load is obtained by multiplying the direct stress by the vessel thickness; the bending moment, by multiplying the bending stress by one sixth the thickness squared.

A plot of the distribution of direct loading and moment over the vessel surface would show how the vessel takes the loading due to its internal pressure. The direct loading is diverted from the more flexible to the more rigid portions of the vessel, the deviations setting up bending in the shell. The information so obtained is instructive, but applies only to the specific vessel tested. It is necessary further to interpret the data to apply the test results to prototype vessels.

The direct load at any point of a vessel is proportional to the internal pressure and to the inside radius, so that if we divide the load per inch of shell (T) by the pressure and by the inside radius, we obtain a dimensionless value showing the relative loading at each point, the value of unity corresponding to the simple membrane stress in a cylinder, the value 0.5 to the simple membrane stress in a sphere. The bending moment at any point is proportional to the direct load and to a geometric eccentricity, which latter is proportional to the inside radius. If then we divide the moment per inch of shell (M) by the pressure and by the inside radius squared, we obtain a dimensionless value showing the relative bending at each point, the value zero corresponding to a direct loading without bending. The values so obtained are independent of the size of the vessel, depending only on its shape.

To use these charts in finding the actual stresses in a prototype vessel, the foregoing procedure is reversed. The dimensionless value for direct load is multiplied by the pressure and by the inside radius to give the load (T) per inch of shell, which is divided by the shell thickness to give direct stress. The value for bending is multiplied by the pressure and by the inside radius squared to give moment (M) per inch of shell, which is divided by one sixth the thickness squared to give bending stress. The direct and bending stresses are added algebraically to give the stresses at the inside and outside surfaces of the prototype vessel.

Heads

The results obtained for dished heads of different shapes are shown in Figs. 1 to 8, inclusive. In each case the radius shown is the inside radius of the cylindrical skirt of the head. The circumferential direction is parallel to the circumference of the skirt. The meridional direction is perpendicular thereto, lying in a plane containing the axis of the drum. A positive load value corresponds to tensile load, a positive moment value corresponds to tension on the inside surface of the vessel, both with internal pressure applied.

Figs. 1 to 8 show the loading distribution in dished heads. In general, the dished heads tend to move toward the spherical shape giving circumferential compression and rapid changes of bending moment, indicative of large shears, at the knuckle. This circumferential compression carries well into the cylindrical portion of the shell. At the crown of a blankhead, the curvature increases under pressure, producing compression inside. At the opening in a manhead there is found a high circumferential tension with local bending in the flued-in manway.

Figs. 6 and 7 show an ellipsoidal blankhead and a similar head with an opening so reinforced as to dilate at the same rate as the portion of the blankhead crown replaced. During fabrication the reinforcement was displaced axially, causing the bending shown near the reinforcement. Otherwise the reinforcement is seen to perform satisfactorily. The unreinforced hemispherical manhead, Fig. 8, is seen to perform about as would be predicted

---

[1] Manager and Chief Engineer, Engineering Department, The Babcock & Wilcox Company. Mem. ASME.

[2] Engineer, The Babcock & Wilcox Company.

[3] "Experimental Technique in Pressure-Vessel Testing," by L. F. Kooistra and R. U. Blaser, published in this issue of the Transactions, pp. 579–589.

Contributed by the Power and Applied Mechanics Divisions and presented at the Fall Meeting, Erie, Pa., September 28–30, 1949, of The American Society of Mechanical Engineers.

Note: Statements and opinions advanced in papers are to be understood as individual expressions of their authors and not those of the Society. Paper No. 49—F-19.

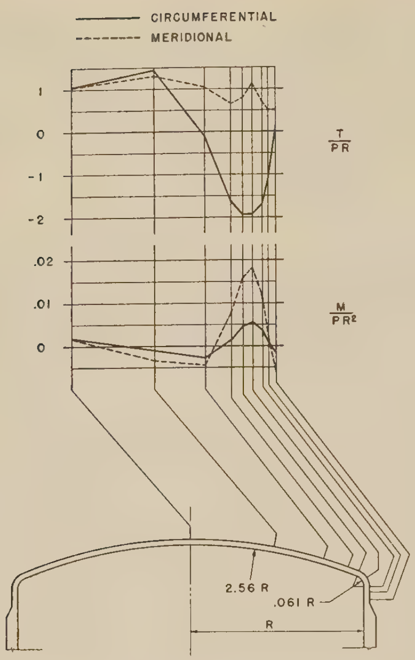

Fig. 1 Loading Distribution in Shallow Blankhead of Type Used Prior to 1915

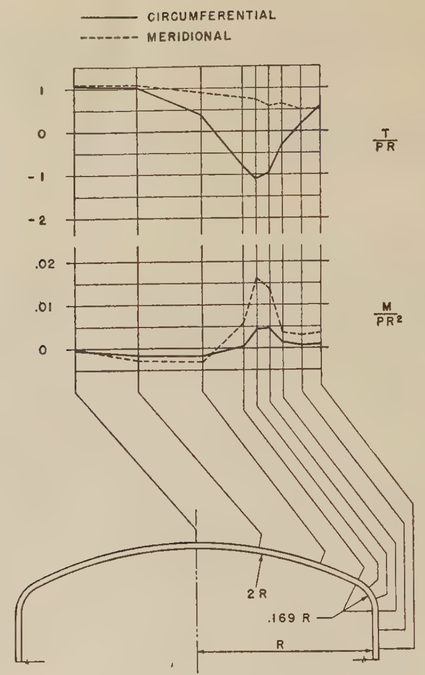

Fig. 3 Loading Distribution in Shallow Blankhead of Type in Current Use

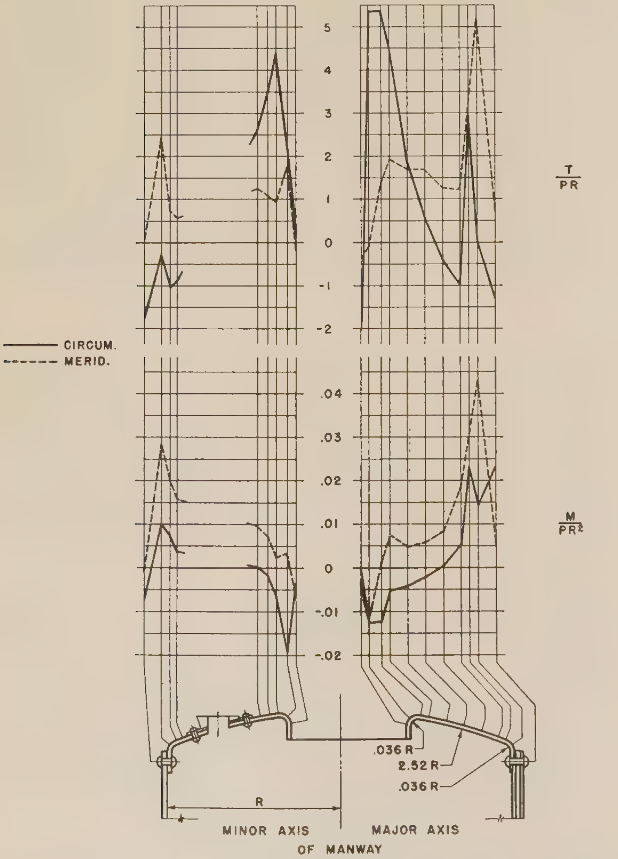

Fig. 2 Loading Distribution in Shallow Manhead Fabricated in 1906

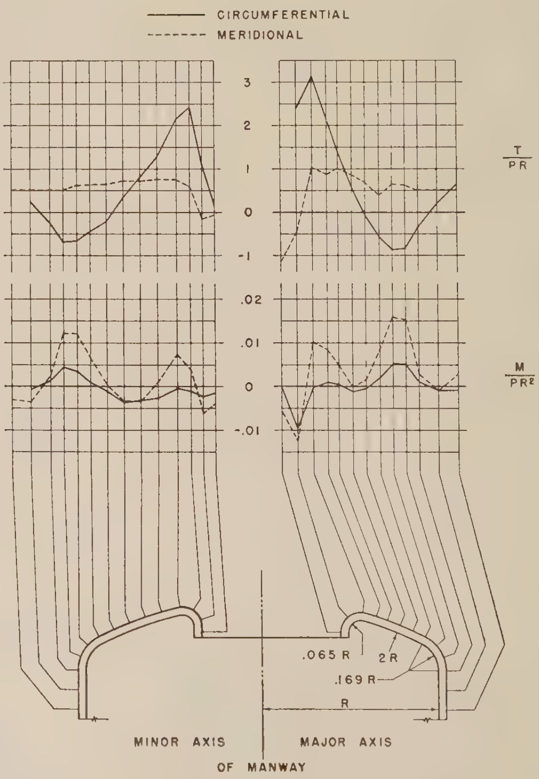

Fig. 4 Loading Distribution in Shallow Manhead of Type in Current Use

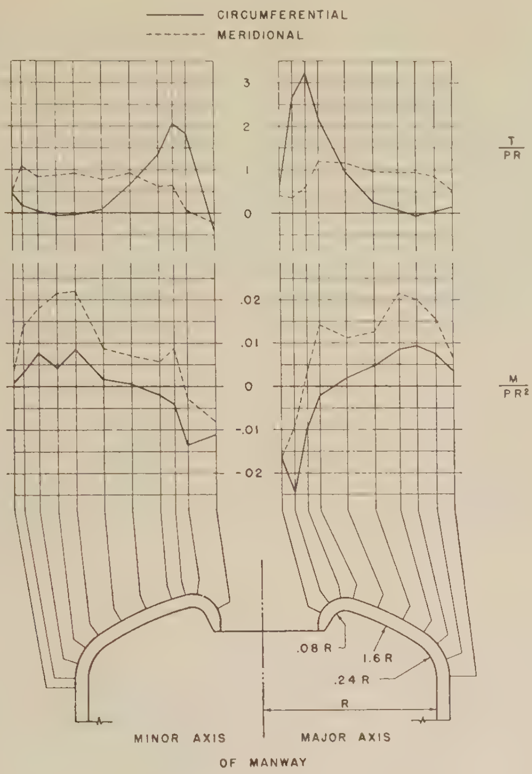

FIG. 5 LOADING DISTRIBUTION IN MARINE-TYPE MANHEAD

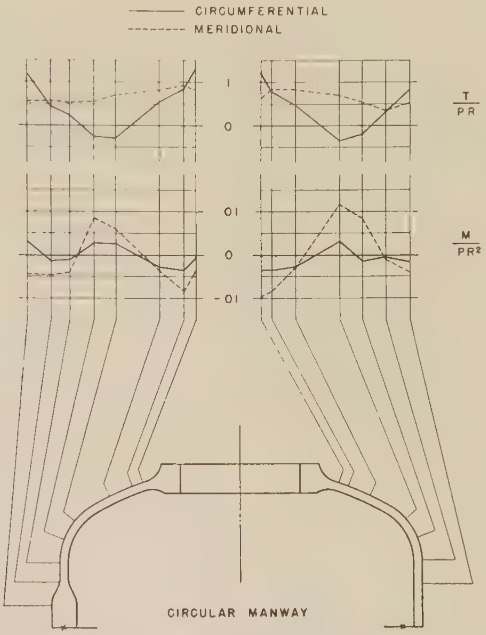

FIG. 7 LOADING DISTRIBUTION IN 2:1 ELLIPSOIDAL REINFORCED MANHEAD

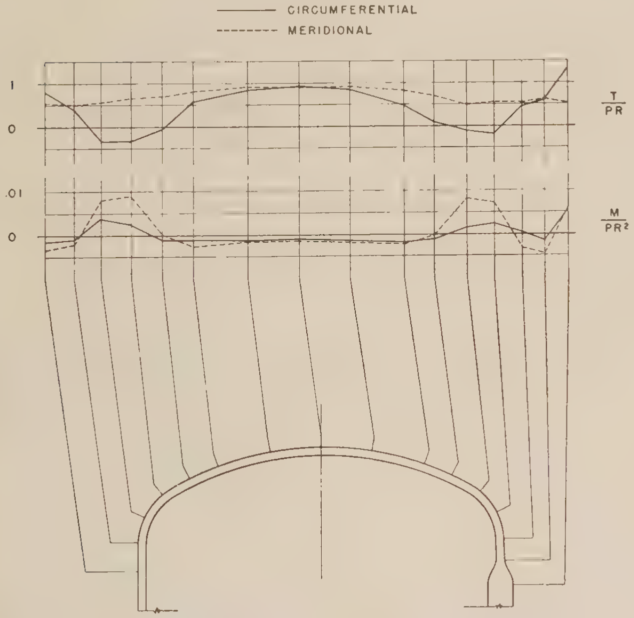

FIG. 6 LOADING DISTRIBUTION IN 2:1 ELLIPSOIDAL BLANKHEAD

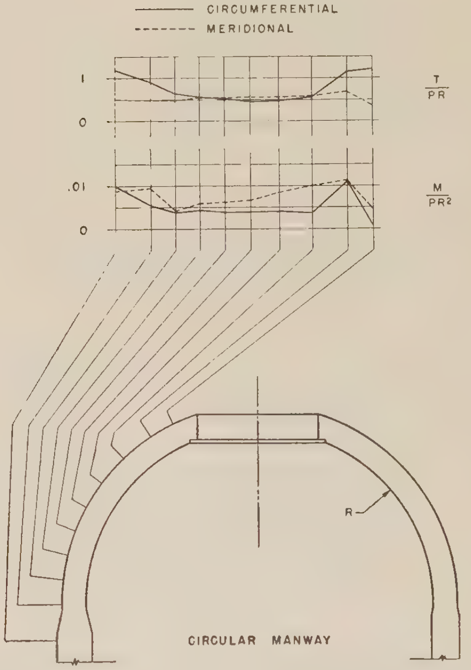

FIG. 8 LOADING DISTRIBUTION IN HEMISPHERICAL MANHEAD

from theoretical considerations. The circumferential stress at the edge of the opening is twice that in the head elsewhere. The increased deflection near the opening causes a reduction in the curvature of the head, with positive bending throughout.

OPENINGS

Round Openings. Openings in a cylindrical shell are focal points for the initiation of failure, particularly when operating at high stress levels in services involving frequent pressure changes. The designer will seek to reinforce such openings by adding metal locally around the hole. Each such addition of metal reduces the stress at the opening but as more metal is added the reinforced area becomes more rigid. If this be carried on sufficiently, the stresses at the outside edge of the reinforcement will rise to values higher than at the opening, and the opening becomes over-reinforced.

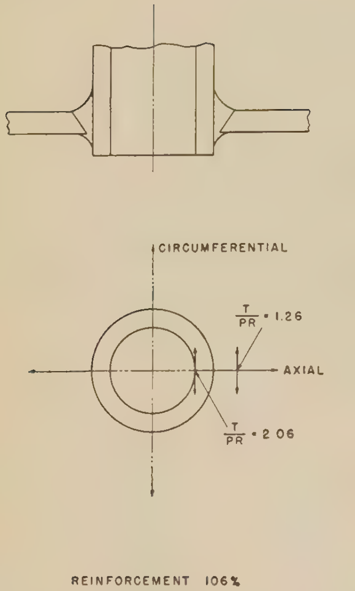

Fig. 9 Maximum Loadings at Inserted Circular Nozzle

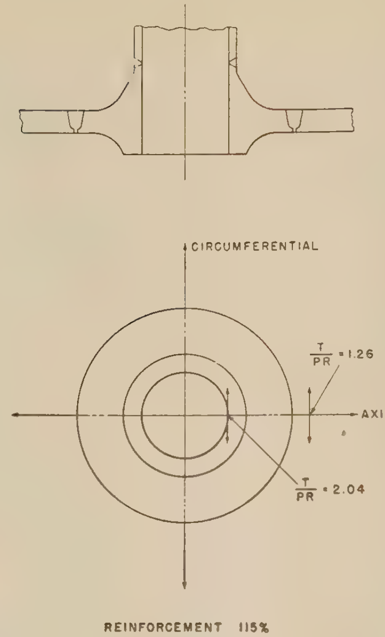

Fig. 10 Maximum Loadings at Circular Nozzle Opening With Integral Reinforcement

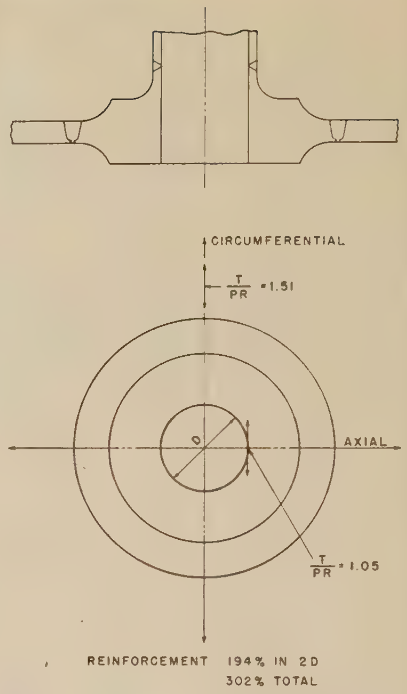

Fig. 11 Maximum Loadings at Circular Nozzle Opening With Thick Integral Reinforcement

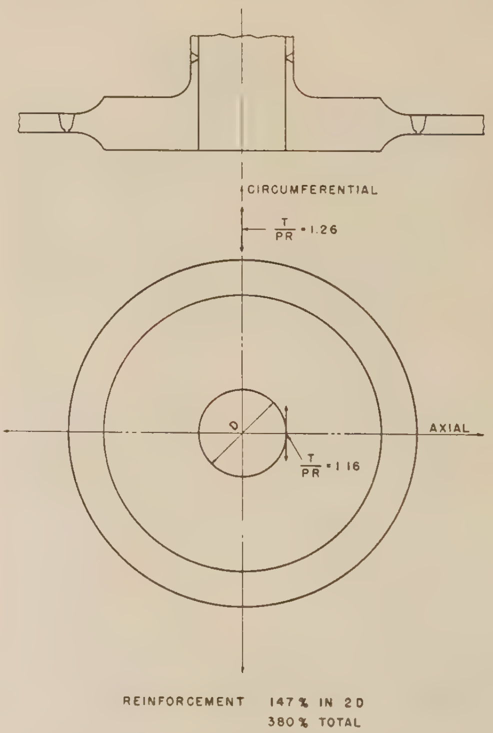

Fig. 12 Maximum Loadings at Circular Nozzle Opening With Large-Diameter Integral Reinforcement

Figs. 9 to 12, inclusive, show the effect of adding reinforcement in various degrees at the opening.

Fig. 9 shows a heavy inserted nozzle. Counting only that part of the nozzle and weld that is symmetrical about the center of the vessel shell, the added reinforcing area is 106 per cent the area cut out in the opening. This is considerably more than required by present design rules, and a little more than would be required if the provision allowing 2-in. free opening without reinforcement were removed from the present rules. It is seen that the maximum stress at the bore has been dropped to 2.06 from the 2.50 times the average shell stress that is found at an unreinforced round opening. This is a relatively minor improvement.

Fig. 10 shows an inserted nozzle with welds that are readily radiographed. The changes in thickness are less abrupt, while the total reinforcing area is only slightly increased to 115 per cent. The maximum stress at the bore is only slightly reduced to 2.04 times the average shell stress, corresponding to the slight increase in area of reinforcement over the nozzle of Fig. 9.

Fig. 11 shows the effect of increasing considerably the reinforcement by adding metal close to the opening. The added reinforcement within one opening diameter as specified by present rules is 194 per cent, and the total added area is 302 per cent. The maximum stress at the bore is 1.05 times the average shell stress but the stress in the shell just outside the reinforcing area is now 1.51 times the average shell stress, showing the rigidity of the thick reinforcement.

Fig. 12 shows the effect of increasing the diameter of the reinforcement and reducing the thickness so as to maintain reinforcing area while reducing rigidity. Here the added reinforcement is 147 per cent within one opening diameter either side of the opening, 380 per cent total. The maximum bore stress is now 1.16 times the average shell stress and the maximum shell stress is 1.26 times the average.

Further experimentation with reinforcement shape can yield forms of still better performance. All the reinforcements tested were essentially the same shape in both circumferential and meridional sections. Tapering to a different shape in the circumferential direction will be most effective in reducing the rigidity of the reinforcement, while keeping down the stress at the bore. All such designs are expensive to fabricate and are bulky, occupying shell surface needed for functional drum attachments. As openings are usually for the flow of fluids, there is no necessity that the opening be round. The virtue of the round opening lies in its simplicity. If this virtue is to be lost in reinforcement to give uniform stress levels throughout the vessel, then it becomes permissible to examine the performance of openings having more advantageous shapes.

Elliptical Openings. The wall of a cylindrical vessel is loaded in two principal directions, the major load circumferential, the minor axial and of a little less than one half the magnitude. The minimum stress concentration at an opening in a plate so loaded is obtained by making the opening elliptical with the lengths of the axes proportional to the plate loadings in the same directions. So designed, the tangential stress is uniform around the periphery of the hole and is equal to the sum of the unpierced plate stresses in the major and minor directions. In drums this means that the opening is an ellipse with axis ratio 2:1, and with peripheral stress 1.5 times the average circumferential stress in the drum shell. Several such elliptical nozzles were built and tested with results shown in Figs. 13 to 16, inclusive.

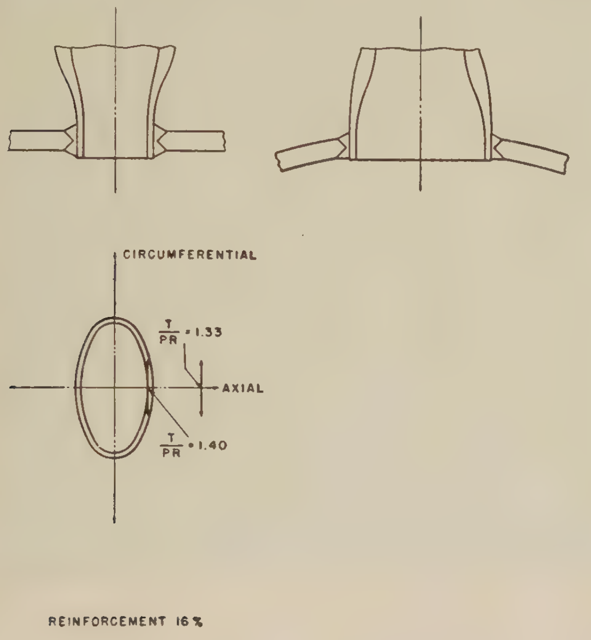

Fig. 13 Maximum Loadings at Elliptical Nozzle Opening With Minimum Reinforcement

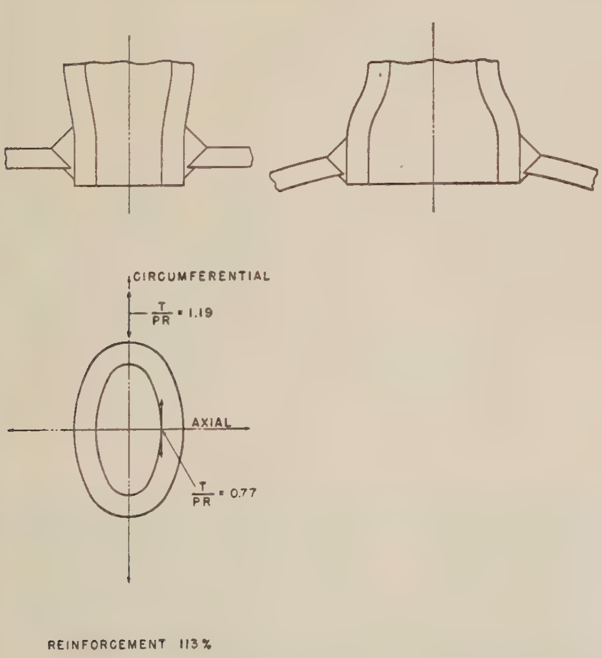

Fig. 14 Maximum Loadings at Heavy Inserted Elliptical Nozzle

Fig. 13 shows a thin-walled nozzle designed to give minimum reinforcement. In the longitudinal section, the area added that is symmetrical about the vessel wall is 16 per cent of the area lost in the opening. The maximum stress is found in the inside of the nozzle, equal to 1.40 times the average circumferential stress in the vessel. Here even a small amount of reinforcement has produced an appreciable reduction in maximum stress from the 1.50 factor expected without reinforcement.

Fig. 14 shows a nozzle with a thick wall, the reinforcing area symmetrical about the vessel wall being 113 per cent the area cut out. This is seen to be too heavily reinforced, for the stress inside the opening is 0.77 the stress in the vessel wall, while the stress factor in the plate outside the nozzle has risen to 1.19.

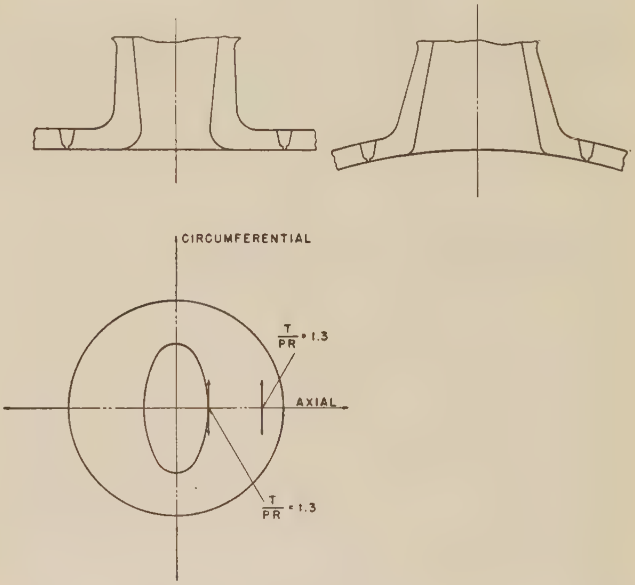

Fig. 15 Maximum Loadings at Cast Elliptical Nozzle Inserted into Circular Opening in Drum

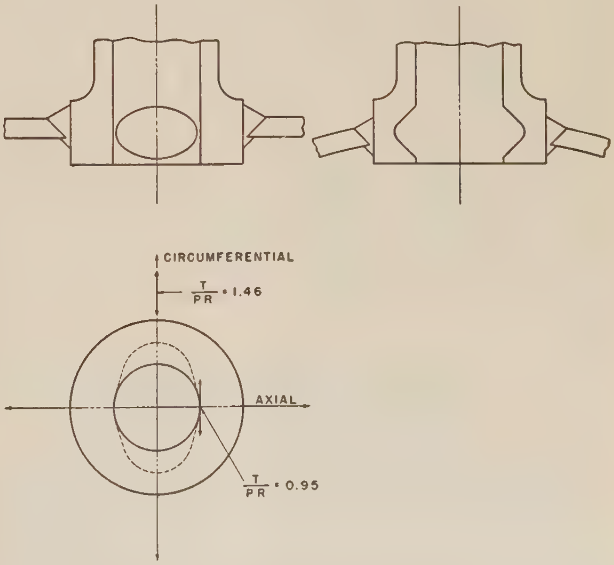

Fig. 16 Maximum Loading in Circular Inserted Nozzle With Section of Oval Shape in Plane of Shell

With an optimum design of intermediate thickness, a stress level but slightly above that in the unpierced plate can be achieved.

The designs in Figs. 13 and 14 occupy an absolute minimum of area of drum shell, often a very valuable consideration. They do, however, require the cutting of an elliptical hole in the shell which may be objectionable, and do not permit of ready x-ray examination of the welds.

Fig. 15 shows a cast nozzle with elliptical opening which inserts into a round hole in the shell. This proved to be a little light in design with a stress factor of 1.3. A somewhat heavier version of this nozzle should prove to be a near perfect nozzle.

Fig. 16 shows a heavy nozzle with a round hole machined to an oval shape at the vessel wall. It performed about as might have been expected for the same amount of reinforcement on a round opening, so that the oval shaping made little difference.

Design Methods

In the past the design of many boiler parts has been on an arbitrary rule-of-thumb basis. In the case of dished heads and reinforced holes, for example, there has been available no adequate theory nor any method of determining experimentally the behavior of these parts. The experimental techniques of Kooistra and Blaser[3] have now filled the latter deficiency, so that a re-examination of the methods of design of heads and openings is in order.

The general method of design of boiler parts has been to set up a reasonable appearing formula involving the pressure, the dimensions of the part, and one or more arbitrary constants relating to the material used, and to experience with the part obtained from service or from proof-pressure test. It is unfortunate that one of these constants has had the dimensions of stress, for this practice has given the impression that such a stress level actually existed in the vessel, with the corollary that these stress levels were the maximum desirable. It is significant that in the case of complicated pressure-vessel elements, such as stay bolts, stress factors are not used. If we are to apply our new knowledge of the behavior of boiler parts to design, we must be prepared to alter our ideas concerning permissible stresses, or our new knowledge will do us a disservice.

Allowable Stress

With the means available to determine stress levels throughout a vessel, we must find a reliable method of determining allowable stresses in a vessel for a given service. The service test is the most reliable test of a design, but it takes a long time to complete. Safety considerations make it impractical to determine limiting stresses in this manner.

The test to destruction by overpressure is quickly accomplished, but has the serious difficulty that often the shape just before failure is much different from that of the vessel in operating condition, and the properties of the material have changed markedly, so that the vessel at failure is quite different from the vessel it was desired to test. The overpressure test will not usually show the effect of high local stresses, as at notches, which may cause failure in service.

The fatigue test, produced by the cyclic application of pressure, does not distort the vessel and may be relied upon to show the existence of any important stress raisers. It simulates in a short time the variations of pressure which the prototype will experience in service, and can be run to failure without hazard so that limiting stress values can be obtained. It is, however, open to the objection that the fast cycling of the fatigue test may not produce the same effect in the vessel as the slow cycling in service, with long periods at nearly constant pressure. The validity of this objection can be established only by service tests.

The fatigue test, generally performed with cold water as a pressure medium for safety and convenience, does not reproduce the effect of temperature on the vessel. Temperature does affect the physical properties of the vessel material, so must affect the life of the vessel. Up to the saturation temperatures of high-pressure boilers, the change in short-time physical properties of steel is small.

The work of Kooistra and Blaser[3] on fatigue of pressure vessels at elevated temperatures shows no significant effect of temperature on the fatigue life of steel in the saturation-temperature range. It appears unnecessary to perform fatigue tests at temperatures in the saturation range. The fatigue test is also open to the objection that it does not reproduce the effect of corrosive media on the vessel material. The validity of this objection must also be determined by service tests.

In the past, due to insufficient knowledge, vessels containing parts operating at high stress levels were fabricated and operated. A study of the history of such vessels may prove a valuable aid in determining allowable stress levels. There are a large number of such vessels available. If we determine the stress levels actually obtaining in such vessels by experimental stress analysis when the vessel is retired, we will be better able to assess the validity of the fatigue test.

Prior to 1915 boiler-drum heads were of the shallow dished-and-flanged type shown in Figs. 1 and 2. Recently, in the course of a modernization program at a district steam-heating plant, a drum with a satisfactorily long life at full design pressure became available. The boiler was first installed in 1906 and was removed from service in 1948. Design pressure was 200 psi, with 175 psi being maintained on the main steam headers, so that the actual drum pressure was between those values. A 300-psi test pressure was applied on starting up each fall, and at other times after opening up the boiler. No accurate log of boiler operation was kept; however, all boilers of the plant were required during the colder periods of winter, some boilers were banked or shut down during milder weather, and all were laid up dry each summer.

Such service is in many ways more severe than steady operation, for it involves many more stress cycles, and exposes the drum to corrosion while cold and in contact with moist air. No close estimate can be given of the number of stress cycles applied during the 42 years of operation, but it would appear that the cycles of 300-psi test pressure would number about 75, while the cycles of operating pressure would number several thousand.

The high stress level is clearly portrayed in Fig. 17, showing the pattern of Lüders' lines formed on a head of this drum. This pattern was so fully developed that it showed up clearly even after sandblasting the scale from the surface. This drum was made from 55,000 UTS open-hearth steel plate. Extensive sectioning and testing of the highly stressed regions of the head showed no significant change in physical properties over those given in the original mill tests of the plate. The interior surface in contact with boiler water was covered with a smooth coating of scale, but showed no signs of corrosive attack. The exterior surface showed a few deep pits, apparently at points where the boiler brickwork was in contact with the drum shell. From any visible evidence this drum was in good shape and ready for another extended period of service.

Fig. 18 shows the stresses actually measured in this drum at 200 psi pressure. These of course represent stress range at this pressure after a preceding 300-psi test pressure. It appears that the stress range at any point did not much exceed twice the yield point of the material at design pressure. At test pressure the stress range exceeded twice the yield point over limited areas.

From the foregoing data on this drum we are in a position to draw some tentative conclusions concerning the relative importance of the various factors in drum life.

We do not have any data as to the fatigue strength of the ma-

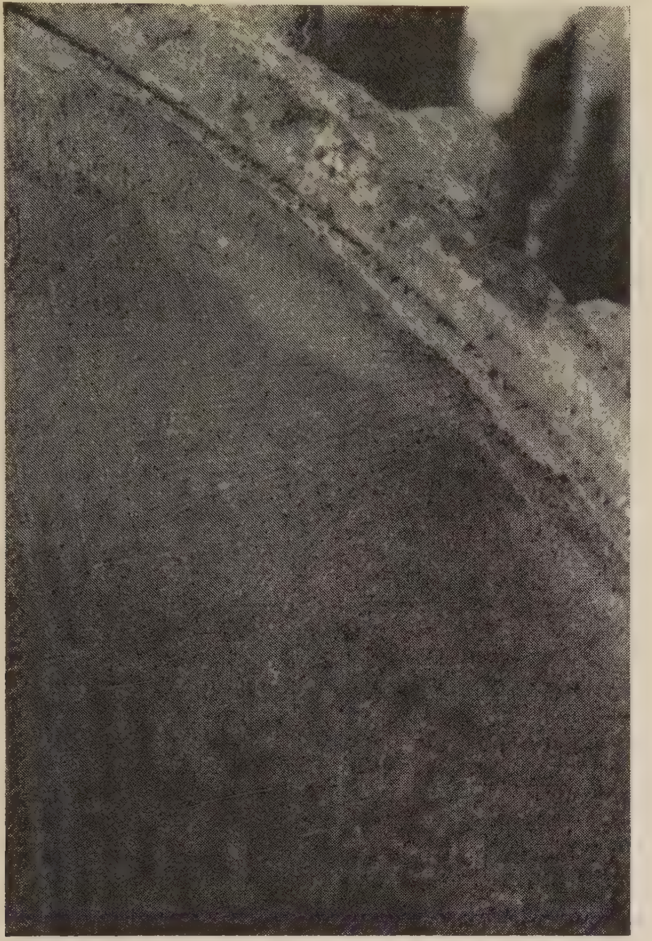

Fig. 17 Lüders' Lines on Outer Surface of Knuckle of Shallow Dished Manhead Fabricated in 1906

terial of this drum, but, considering the severity and probable number of the stress cycles, we may assume safely that a considerable portion of the fatigue life of this drum has been spent. Neither time nor exposure to boiler water has greatly accelerated the failure, for the drum was to all appearances in good condition. It would then appear that the fatigue test is a reliable test of service life for boiler drums.

There is a general relationship between stress range and number of cycles to failure, expressed in the conventional S-N curve. The desirable maximum stress range in a vessel is that range which will produce a service life of the vessel which shall exceed the desired service life, expressed in number of service cycles, by a safe margin. In the determination of stress range all contributing factors should be considered, such as thermal stresses, not merely pressure stresses alone. We now have available or obtainable sufficient information to design vessels on such a basis.

Prestress

The application of an initial overpressure, as by a pressure test, will so prestress a vessel as to reduce the stress at working pressure in various portions of the vessel. This may have a beneficial effect on the life of the vessel.

Consider a vessel so constructed that when the pressure is raised from zero to design pressure, the growth of various localized portions of the vessel corresponds to a stress range varying from zero stress to over twice the yield point of the vessel material. If the vessel pressure is simply raised to design pressure without any initial overpressure, then the stress picture is that indicated in Fig. 19. Those portions with stress ranges between once and twice yield point operate at yield point with no yielding on subsequent pressure applications. With pressure off, these same portions have prestresses varying down to negative yield point. Those portions of the vessel with a stress range of over twice the

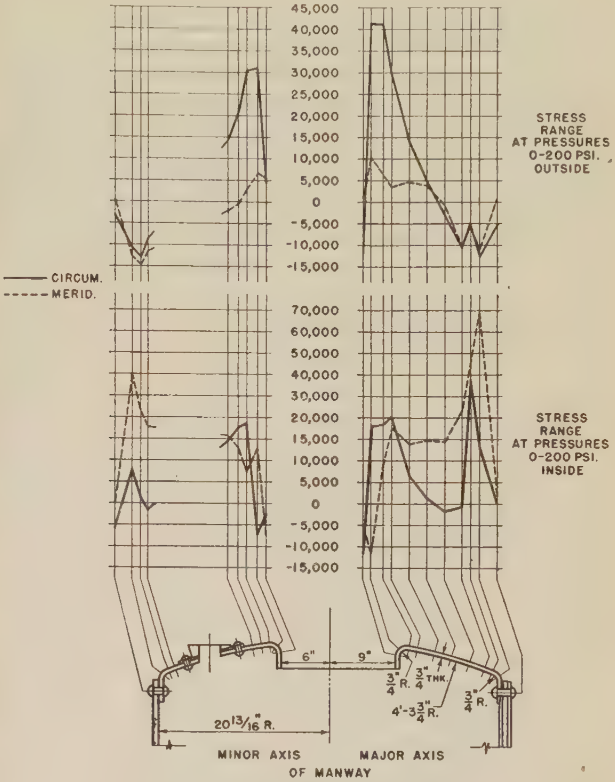

Fig. 18 Stress Range at 200 Psi in Manhead Fabricated in 1906

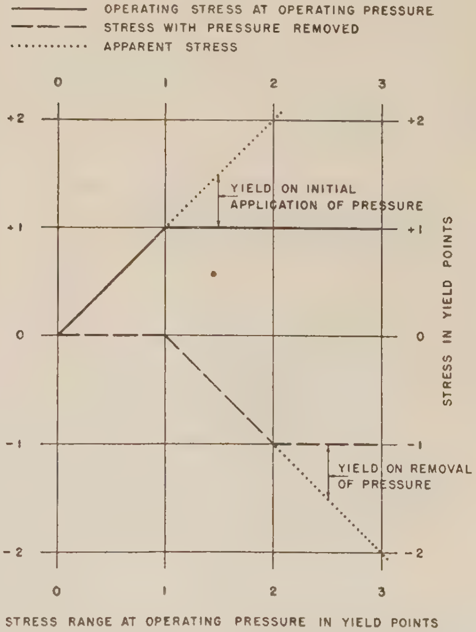

Fig. 19 Behavior of Vessel at Locally High Stressed Points With no Initial Overpressure

yield point must yield with each application and release of pressure.

If an initial overpressure is applied, Figs. 20 and 21 show that the operating stress is lowered for portions with an operating stress range of less than twice the yield point. If an overpressure of 3/2 working pressure is applied, then the operating stress for those portions of the vessel with an operating stress range less than 5/3 yield point does not exceed 2/3 yield point. If an overpressure of 2 times working pressure is applied, then the operating stress for those portions of the vessel with an operating stress range less than 3/2 yield point does not exceed 1/2 yield point. Similar relationships apply for other values of initial overpressure. No initial prestress can benefit those portions of the vessel which have an operating stress range of over twice the yield point, for these portions must yield with each application and release of operating pressure.

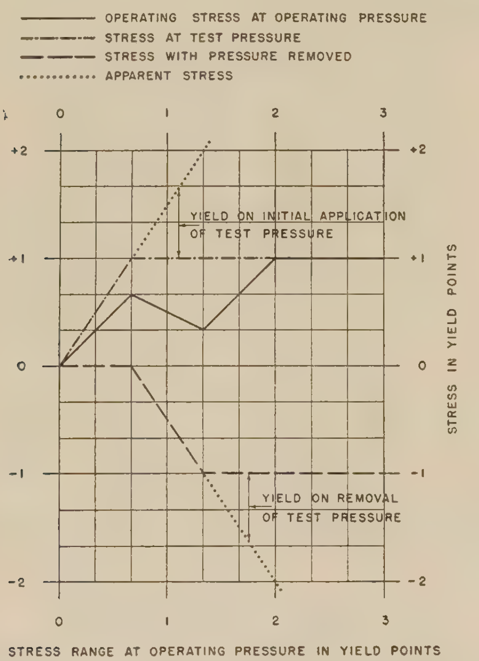

Fig. 20 Behavior of Vessel at Locally High Stressed Points With Initial Overpressure 1.5 Times Working Pressure

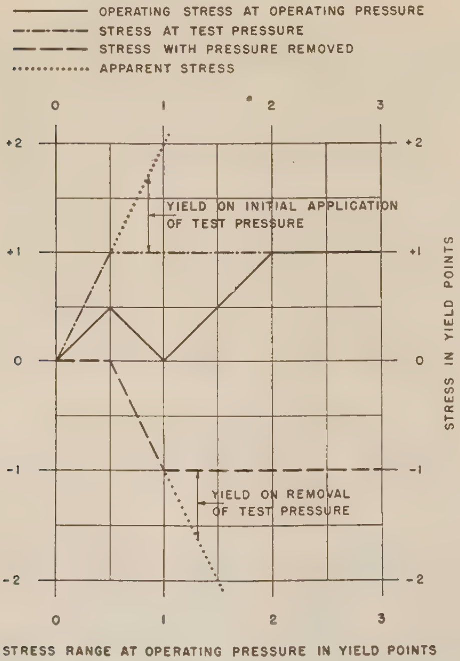

Fig. 21 Behavior of Vessel at Locally High Stressed Points With Initial Overpressure 2.0 Times Working Pressure

The foregoing discussion assumes that only limited portions of the vessel have these high stress ranges so that their yielding will not affect appreciably the general stress level of the vessel. To the extent that this assumption is not justified, that yielding of the higher stressed portions does increase the general stress level, then to that extent is the amount of prestress obtainable restricted. A vessel with a uniform stress range throughout cannot be prestressed.

It has also been assumed that yield point is a simple, definite stress. Actually, the yield point is not a clearly defined value in any case, and is considerably influenced by previous cold-working of the material, and by the stress conditions in the perpendicular directions. The effect of these considerations is to round off the sharp corners of the curves in Figs. 19, 20, and 21, and to alter the value of yield point selected, but does not change the general relationship.

It has been shown that the effect of prestress is limited to portions of the vessel having stress ranges within certain limits as set forth. Whether this prestressing will increase vessel life depends upon whether corrosion resistance or fatigue life is improved. Experience with older drums, such as the case already cited, would indicate that corrosion due to contact with properly treated boiler water is negligible for boiler plate at any stress level. There may, however, be benefits in services using other media. Fatigue-test data indicate that there may be some improvement in fatigue life of mild steel by prestressing at ranges below twice yield point, but that this improvement is in a life already many hundred times the number of pressure cycles possible in boiler service.

We may conclude that prestressing is not significantly beneficial to the life of boiler drums. The pressure test is of course of value in boilers to show up safely incipient failures in parts weakened by erosion or other cause. The value of prestress in other services should be determined by the effect on corrosion and fatigue life in that service.

Conclusion

The results of many experimental stress analyses of boiler drums have been given in a form permitting their ready application to other vessels of the same general shape.

The significance of these results is discussed with particular reference to allowable stress levels in design. It is shown that in power-boiler service there is no selective corrosive attack of boiler plate at stress ranges of twice the yield point. It is also shown that present design rules are not correct as regards dished heads and reinforced openings.

Discussion

H. C. Boardman.[4] This paper is timely because it treats of problems now of great interest to the ASME Boiler Code Committee and to the Design and Fabrication Divisions of the Pressure Vessel Research Committee of the Welding Research Council. It brings out into the open stress factors which present codes for pressure vessels either conceal or only mention in cautionary phrases. Surely it will stir code writers to a keener awareness of the deficiencies of their work, and of their obligation to keep rules of design as close to the forefront of knowledge as considerations of safety will permit.

---

[4] Director of Research, Chicago Bridge & Iron Company, Chicago, Ill. Mem. ASME.

The technique and interpretation of electric-strain-gage surveys are well established and understood; the authors' company has contributed much both to this technique and this understanding. Such surveys, complemented by mathematical analyses, should be accepted as a basis for the design of pressure vessels, as already they are officially accepted for the design of storage tanks. The Standard Specifications for Elevated Steel Water Tanks, Standpipes and Reservoirs states:

> "It is recognized that no specifications for the design of elevated tanks can be sufficiently specific and complete to eliminate the necessity of judgment on the part of the designer. It is also recognized that strain gage surveys are a proper source of design information."

A similar statement could well be made with reference to pressure-vessel design.

Presumably "direct load," "direct loading," and "load per inch of shell" are synonymous; also "bending moment" and "moment per inch of shell."

Aptly descriptive of how connections upset the membrane stress system is the statement: "The direct loading is diverted from the more flexible to the more rigid portions of the vessel, the deviations setting up bending in the shell." These words convey to the mind a picture of "direct-load" contours bunching up near nozzles and supports and correspondingly thinning out elsewhere to keep their sum total equal to the bursting pressure. The moments established in this way are of two kinds—those in planes perpendicular to and tangent to the shell. The latter are due to the cited shifting of direct loadings because of vessel attachments and other geometric irregularities.

In calculating their dimensionless values for "relative loading and bending" the authors have assumed that, at any point in the shell, the "load per inch of shell" is proportional to the pressure and the shell radius, and that the "moment per inch of shell" is the product of the "direct load" times a "geometric eccentricity" which is proportional to the shell radius only. How is it known that the geometric eccentricity is not a function of pressure too, just as the eccentricity of a column is a function both of the load on the column and the geometry of the unloaded column? As another example, the moment per inch of shell at a cylinder to a conical-head connection varies approximately as the product of the three-halves power of the pressure and the square of the cylinder radius, and inversely as the square root of the unit stress used in designing.

The authors' dimensionless values for a cylinder are the direct load and moment per inch of shell for a cylinder having a radius of 1 in., under a pressure of 1 psi, assuming that the geometric eccentricity for this small cylinder is the eccentricity for the actual cylinder divided by the radius of the actual cylinder. Is this probable? What is meant by: "The values so obtained are independent of the size of the vessel depending only on its shape"? Is not a given set of the authors' dimensionless numbers precisely applicable only to vessels which, including the shell thickness, are photographic enlargements or reductions of each other? Nevertheless, such dimensionless numbers should be quite useful when applied to vessels departing from photographic similarity; doubtless the authors intend that they be so used.

Dished Heads. The reported results for the heads tested are believed to be in line with the results of crude mathematical analysis and with intuitive knowledge of how heads behave. It is gratifying to observe that properly reinforced circular openings in spheres change little the normal stresses in adjacent shell plates.

Openings. This section is a real contribution because it shows how shape refinements, commonly known as streamlining, can reduce stress concentrations. Although elliptical openings have been used for some time, it is probable that this paper for the first time demonstrates their advantages quantitatively. Are not such openings amenable to fairly accurate mathematical analysis?

Incidentally, there is now being conducted at the Chicago plant of the writer's company, a strain-gage survey of a large rectangular clean-out door, installed in the bottom ring of a section of an oil storage tank 100 ft diam, with the bottom of the opening flush with the upper surface of the horizontal tank bottom plate. To carry the normal ring-tension stresses in the shell around the opening, without causing bending in the tank shell and tank bottom, there is provided a continuous bar with its width perpendicular to the shell, which bar forms the top and bottom of the opening, and is shaped to a parabola around each end of the opening. Of course this bar is welded to the shell. In this case the parabola is the equilibrium curve for the shell loads on the bar. However, in the case of a cylindrical pressure vessel, the 2:1 ellipse is not the equilibrium curve for the shell loads upon it and therefore is subject to bending as well as direct stresses. The 1.414:1 ellipse in a cylindrical shell is free of bending moments but is subject to a variable direct stress.

Design Methods and Stresses. This portion of the paper is very stimulating and helpful. The authors truly state: "If we are to apply our new knowledge... to design we must be prepared to alter our ideas concerning permissible stresses, or our new knowledge will do us a disservice." The same thought has been expressed many times in meetings of the ASME Boiler Code Committee, and really is an indirect way of saying that the inevitable changeover, from the crude idea that the nominal stresses of simple design formulas are the actual stresses in the vessel, to the idea that the working stress at points of stress concentration may safely be practically at the yield point, must involve a period of education and conditioning to make acceptance possible. Such education and conditioning result in one of the greatest products of the Pressure Vessel Research Committee and in papers such as the one under discussion.

The service history of the boiler-drum heads built in 1915 is most encouraging and gives assurance that the heads of the 1950 ASME Unfired Pressure Vessel Code are quite safe for the services intended.

It is startling to read "It appears that the stress range at any point did not much exceed twice the yield point of the material at design pressure," and "The desirable maximum stress range in a vessel is that range which will produce a service life of the vessel which shall exceed the desired service life, expressed in number of service cycles, by a safe margin." The first statement arouses a bit of doubt as to whether the stress range did really exceed twice the yield point; perhaps the tensile and compressive yield points were sufficiently raised by the straining to keep the stress range between them. The second statement, extended to the limit, appears to mean that, if a vessel were so streamlined as to be free of stress concentrations, it could for most services be operated safely at general stress levels practically up to the yield point in tension. This is plenty of food for thought.

The writer questions the reasoning by which the authors reached the conclusion that "the fatigue test is an accurate test of service life for boiler drums." How the fact that a boiler drum, poorly designed by present standards, withstood service conditions for over 40 years, and then appeared to be in good condition, leads to the conclusion that the fatigue test is an accurate test of service life for modern boilers, is rather obscure.

Prestress. The questions of prestress and the hydrostatic test are inseparable, especially for vessels not thermally stress-relieved. In such vessels cold-forming and welding lock up very complex stress systems which, in a sense, are prestress systems.

These the hydrostatic test modifies by plastic-straining, particularly in the welds and in regions where there are fabricating misalignments and design discontinuities such, for example, as the direct connection of a conical head to a cylindrical shell.

The real question is whether the residual-stress system after the hydrostatic test is more favorable to vessel service than the locked-up stress system which would develop in service if the hydrostatic test were omitted.

Since the major stresses induced by pressure are tensile, it seems that the highest tensile prestrain short of general yielding is the most beneficial because it most reduces misalignments and, in regions of design discontinuities, results in the lowest subsequent "pressure-on" tensile stress in service. Furthermore, should the latter effect be overdone, to the extent that plastic compressive yielding occurred upon release of pressure, such secondary yielding would again modify the residual-stress system so that thereafter the pressure-on tensile stress in service would be the lowest possible, and the "pressure-off" stress would be the compression yield point. Of course the extreme tolerable stress cycle is between the highest possible compressive and tensile yield points short of failure.

On the other hand, if no overpressure were applied prior to service, the pressure-off compressive stresses at regions of stress concentrations would be the lowest possible, and the pressure-on stress would be the tensile yield point if plastic yielding occurred when the working pressure was first applied.

Does the Bauschinger effect in any way change this reasoning? Does embrittlement due to cold-working?

The concluding statement: "It is. .shown that present design rules are not correct as regards dished heads and reinforced openings" cannot be denied in an absolute sense. However, the burden of proof is on him who claims that the dished heads of the 1950 ASME Unfired Pressure Vessel Code are inadequate for boiler and other pressure-vessel services. Although in theory these heads could be improved by providing a transition spiral (like a railroad transition spiral), between the cylinder proper and the head proper, such refinement and complication seem inadvisable in view of the practically perfect performance of modern dished heads, both torispherical and ellipsoidal.

Commendation is due the authors for this most stimulating, instructive, and forward-looking paper.

D. S. Jacobus.[5] The authors should be commended for showing the way in which advances may be made in designs and constructions.

The advantage of diminishing stress concentrations is well known but, as shown by the tests and data given in the paper, such concentrations exist in some of the usual constructions.

If models of new designs were tested in the way described in the paper, progress could be made in formulating rules to provide the necessary safety with a minimum amount of material.

Let us hope that the work of the authors will cause such a movement to be started and perpetuate their efforts.

Authors' Closure

It is indeed gratifying to the authors of a paper to find their work has been to some avail, that their paper has been read thoroughly and with discernment, and that it has evoked searching discussion. The original paper, being necessarily limited in length, passed lightly over much experience and analysis that influenced the conclusions drawn. Mr. H. C. Boardman has pointed out several significant gaps in the paper which we will endeavor to fill in this closure.

In connection with the dimensionless constants set up to assay the behavior of a shell or dished head, it has been pointed out that the geometric eccentricity implicit in the moment constant is a function of pressure as well as vessel size for a given vessel shape. We have found this to be only a minor factor. The doubly curved surface of a drum head is so rigid that its shape changes only slightly with pressure unless the pressure is carried so high that a large portion of the head material has yielded. In such a case a new head shape is formed which behaves somewhat differently. We have had only a few opportunities of checking heads of similar shape but varying ratios of thickness to diameter. In each case the load and moment coefficients have checked to within the geometric accuracy of the vessels.

The testing so far has been confined to vessels of the proportions in general use. As our company uses progressively deeper heads with increasing pressure, there has been no opportunity to test any shape over a wide range of thicknesses. We would expect, however, that in very thick heads there would be a nonlinear stress distribution through the wall at places where the curvature is high in relation to the thickness, much as in a curved beam. Properly evaluated, the same loading and bending constants might well still hold for thick heads.

The elliptical openings were designed from the analysis of C. E. Inglis as given by Timoshenko.[6] In high-pressure drums, the addition of material to form a reinforcement for an opening is sometimes undesirable, both for fabrication and for service life. Reinforcement is then best provided by increasing the shell thickness. The optimum opening shape without local reinforcement is an ellipse whose axes are parallel and proportional to the principal stresses. The local tangential stress around the opening is the sum of the principal stresses. This is predicted from the analysis and closely verified experimentally. If local reinforcement is added to further reduce local stresses, then the optimum opening shape becomes less elongated, until, in the limit, for no disturbance in the shall plate, the optimum opening shape becomes an ellipse whose axis ratio is the square root of the ratio of the principal stresses. This result is important in the design of efficient low-pressure vessels, and we are much indebted to Mr Boardman for his analysis of the latter condition.

In the case of the old-type drum which was strain-gage tested, the metallurgical examination showed only normal 55,000-psi UTS plate. There was no elevation of the yield point or abnormal corrosive attack even in the zone showing extensive Lüders' lines. The physical properties checked the original mill-test reports to the usual accuracy of such tests. The strain gages definitely showed a stress range at working pressure of at least twice yield point, and proportionally more at test pressure. A measured yield point is a function of the shape as well as the material of the specimen, and actual yielding in the direction of load is also affected by the stresses in the perpendicular directions, so that we cannot say that an operating stress range of twice the the yield point of a standard 0.505 specimen means actual yielding in the vessel. Nor can it be determined from the behavior of any gage that yielding has taken place at that gage, for yielding at an adjacent location at another stress level will increase the load on the metal under the gage to show an apparent yielding.

In applying strain gages to a vessel, it is unlikely that the gage will be applied exactly to the highest stressed location. The gage indicates average strain over its gage length so that the peak stress is always larger than indicated. All these factors add so that it may be stated confidently that the peak-stress range in the head of the old drum tested was well over twice the nominal yield point of the material as given by a standard 0.505 specimen.

---

[5] Past-President, ASME.

[6] "Theory of Elasticity," by S. Timoshenko, McGraw-Hill Book Company, Inc., New York, N. Y., 1934, p. 175.

The extensive and well-formed system of Lüders' lines shows that there was much plastic action during the drum life.

Service tests have shown no definite upper limit for allowable stress in boiler drums. Given the usual good water conditions, local stress ranges at working pressure of twice the nominal yield point seem to operate with complete satisfaction. As it is manifestly impractical to operate a vessel with the general stress level at yield point, it is seen that isolated stress raisers may have a concentration factor of at least 2.

This of course applies to boiler drums and present boiler plate. Contact with other fluids and the use of high-strength steels may alter these conclusions markedly and will require a separate evaluation.

Certain features of design are not susceptible to stress analysis, either mathematical or experimental. Examples are the fillet at a gasket seat and the built-in crack at the root of a fillet weld. For such cases, an accelerated service test is desirable. The simplest such test is the room-temperature fatigue test. This fatigue test can be invalid on three counts: (1) Its results may be unrelated to service life; (2) they may be overly optimistic, or, (3) pessimistic in predicting service life.

1 A room-temperature fatigue test, using water as the pressure fluid, will certainly not predict performance under corrosive conditions or at high temperatures in the creep range. However, our tests have revealed no invalidating evidence in the range of saturation temperatures in boiler work up to 650 F.

2 The speed of cycling is necessarily much higher in a fatigue test than in boiler service, and there is an observed small increase in fatigue strength with increase of cycling frequency. It is possible that very slow cycling might show some lowering of fatigue strength. However, we may note that fatigue strength is unaffected by testing frequency from the slowest normally run up to about 5000 cycles per min. An increase to 1,000,000 cycles per min will raise the endurance limit by a factor of the order of 30 per cent. We would not expect to find any serious lessening of fatigue strength at very slow cycling rates. Our service experience shows no corrosive attack from boiler water during these slow cycles.

3 Several factors apply which may make service life greater than that predicted from fatigue-testing. If the fatigue life is determined by the number of cycles at peak or test pressure, then the cycling at lower operating pressures may raise the endurance limit appreciably. If the service life is predicted from number of cycles at working pressure, properly weighted for the damage caused by occasional overpressuring, then the effect of the mild heat-treatment at saturation temperature may be underestimated.

The amount of information available from service experience, concerning operation at stress ranges higher than twice yield point, is very small. Feed nozzles have developed cracks when quenched with cold water. Fired mud drums have cracked when insulated from the water inside by scale or oil. Boiler sectional headers have cracked when intermittently quenched by improper use of the water lance. All of these cases have involved estimated thermal stress ranges of 100,000 psi or more and at least several hundred cycles. The service life obtained under such conditions is about what could be predicted from fatigue-test data. Certainly, if the service life were very much less than might be predicted from fatigue data, the old drums built prior to 1915 would not have the long service life actually afforded. If we require that a design when submitted to fatigue test, shall exhibit a life, measured in number of cycles that shall exceed the desired service life by a wide margin, say by a factor of 10, then the safety of the design is certainly assured. There are several commonly used details of current boilers that may not meet such a test.

The stress ranges in blankheads designed in accordance with the ASME Power Code are shown in Fig. 22 of this closure. It is seen that the stress range is high in the thinner low-pressure heads and very low in high-pressure heads. This is inherent in any head-design formula which specifies a thickness proportional to pressure. The company with which the authors are connected has no service experience with the thin low-pressure heads.

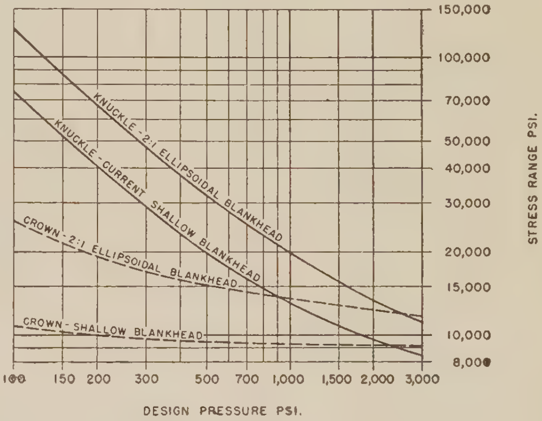

Fig. 22 Actual Operating Stress Range in 2:1 Ellipsoidal and Shallow Dished Blankheads Similar to Figs. 6 and 3. Designed in Accordance With ASME Power Code: $S = 14{,}000$ Psi

For many years, long before these tests were conducted, it has been our practice to use shallow dished heads at pressures below 300 psi, 2:1 ellipsoidal heads from 300 psi to about 1000 psi, and hemispherical heads at higher pressures. Heads designed for 160 psi are used at lower pressures. This practice, it is now seen, has kept operating stress ranges under 50,000 psi. Dished heads might well be used at much higher pressures than is now the practice, if the Code were modified to permit a reasonable stress range at such pressures.

Experimental Technique in Pressure-Vessel Testing

By L. F. KOOISTRA[1] and R. U. BLASER,[2] ALLIANCE, OHIO

The latest designs of pressure vessels for high-pressure boiler service have been investigated by means of experimental stress analysis and hydraulic fatigue tests. Methods have been developed to measure strain on the inside as well as on the outside of pressure vessels under internal pressure. Pulsating hydraulic fatigue tests were conducted on full-scale high-pressure drums. Scale-model vessels of about one tenth actual size were similarly tested in a saturated-steam and water atmosphere of 2000 psi. The technique used in these tests, and the special apparatus built for the purpose are described.

Introduction

Experimental development of pressure vessels has been carried on for many years during which various testing techniques and procedures have been used. This paper will discuss certain phases of this development that have taken place in the authors' company during the past 10 years. It has long been felt that the use of a design factor of 5 was unnecessarily large, and that more appropriately it could be called a factor of ignorance rather than a factor of safety. The very considerable amount of work herein described was undertaken to reduce the number of unknown factors in pressure-vessel design.

In the earlier stages, experimental stress analysis was conducted by means of Berry strain gages and somewhat later by using DeForest scratch gages. These tools were later replaced by the Baldwin-Southwark SR-4 gages. The SR-4 gages were so much more accurate and sensitive and could be used with so much greater facility that the art of experimental stress analysis came into its own with the use of this tool. This paper, therefore, will deal largely with the development and the technique employed for experimental stress analysis starting with the use of the SR-4 gage.

Besides the use of SR-4 gages, which tell the designer what stress levels are reached in the various parts of the structure under internal pressure, other methods for determining stress concentrations were employed, such as room-temperature and high-temperature fatigue tests. The room-temperature fatigue tests were conducted on full-size drums, and the high-temperature fatigue test on scale-model cylindrical specimens. The room-temperature full-size drums were subjected to hydraulic pulsations by means of apparatus specially built for this purpose. The high-temperature specimens were placed inside of a steam drum in an atmosphere of saturated steam and water and were similarily tested by means of hydraulic pulsations. The methods used in this kind of testing and the special apparatus built for this purpose will be described.

The results of the experimental stress analysis, and the merit of various design features are discussed in a companion paper by Schoessow and Brooks.[3]

Problems in fabrication of fusion-welded pressure vessels, and the inspection and control of the materials entering into this type of product, are described in another companion paper by O. R. Carpenter.[4]

Early Considerations

For a great many years it has been accepted practice to subject pressure vessels to a hydrostatic proof test. Sometimes a procedure of hammer testing was also included. Test measurements in the early days were limited to visual observations, linear measurements by rule, or tape measure, and mechanical gages. Such mechanical gages became more refined as dial indicators, Berry gages, and Huggenberger tensometers became available for measuring strain due to pressure loading. All these were restricted to readings on the outside of pressure vessels. Strain determinations on the inside of vessels under pressure first became practical through the advent of the DeForest scratch gage.

Requirements of such extensometers and strain-measuring devices are small size, sensitivity, ease of multiple application, reliability, low cost, little or no damage to specimens, and stability. Slightly more than 10 years ago the resistance-wire strain gage, combining all these requirements, was introduced. This measuring tool has done much to further the art of experimental analysis. It has made possible a clearer understanding of the distribution of stress, both on inside and outside surfaces of pressure vessels. Because of the advantages mentioned. the SR-4 electric-resistance strain gage has been used in most of the work herein described.

At various times brittle coatings, such as whitewash, and later "Stresscoat" have been used to determine the locations of maximum stress. Stresscoat is particularly useful in many cases where the location and direction of maximum stresses is obscure. In this application it serves as an excellent detective measure to determine critical or maximum stress points.

Experimental Stress Analysis

In testing pressure vessels under internal pressure, a problem immediately arises as to the choice of pressure medium to be used. For the regular hydrostatic tests, water is generally used for this purpose. When stress measurements were made on the outside of the vessel, water was entirely satisfactory. Even later, when DeForest type scratch gages were used for internal-stress measurements, water was not objectionable. The SR-4 gage, being an electrical device, is naturally sensitive to moisture. Consequently, a great deal of development work has been done by several experimenters toward waterproofing SR-4 gage setups.

For atmospheric work, a Petrosene wax coating proved very satisfactory. Waterproofing for internal hydraulic pressure, however, was not available at the time of the earlier SR-4 tests

---

[1] Assistant Director, Materials Laboratory, Babcock & Wilcox Company, Research and Development Department. Mem. ASME.

[2] Head, Engineering Physics Section, Babcock & Wilcox Company, Research and Development Department.

Contributed by the Power and Applied Mechanics Divisions and presented at the Fall Meeting, Erie, Pa., September 28–30, 1949, of The American Society of Mechanical Engineers.

Note: Statements and opinions advanced in papers are to be understood as individual expressions of their authors and not those of the Society. Paper No. 49—F-20.

[3] "Analysis of Experimental Data Regarding Certain Design Features of Pressure Vessels," by G. J. Schoessow and E. A. Brooks, published in this issue of Transactions, pp. 567–577.

[4] "Fabrication of Pressure Vessels," by O. R. Carpenter (not printed).

(1942) and for that matter is still not reliable for high-pressure work.

For the first test in which internal stresses were determined, compressed air was chosen as a pressurizing medium. For this purpose the drum was set up on end, which was permissible in this case since only the stresses in the manhead on one end were to be measured.

Fig. 1 shows the upper end of the drum with the SR-4 gage arrangement. After filling the drum with air at 200 psi, water from the hydraulic line was admitted at the bottom. The rising water column then compressed the air further until the desired test pressure was reached. Maximum pressures of 1268 psi were obtained without the water level touching the lowermost gage wires. No particular difficulties were experienced in obtaining consistent data.

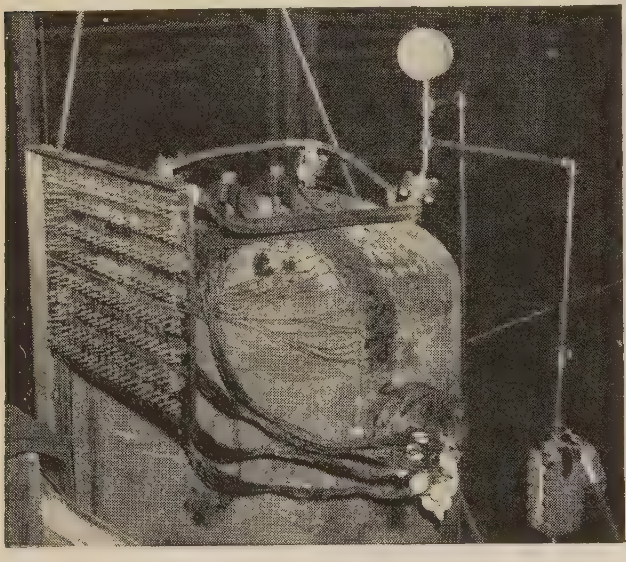

Fig. 1 View of Test Setup of Steam Drum in Vertical Position Using Compressed Air as Pressure Medium

Using a compressible gas in high-pressure vessels, sometimes at double the working pressure, was considered dangerous, particularly for experimental vessels. Therefore a method having less energy storage was highly desirable.

In searching for a dry, high-resistance pressurizing liquid, the choice naturally falls on transformer oil. After testing several oils for this purpose, an inexpensive light lubricating oil proved equally satisfactory. The next problem was to bring the necessary gage wires through the pressure shell, electrically insulated and pressure-tight. A special plug was designed for this purpose.

This multiwire plug is shown in Fig. 2 as it looks in the process of assembly. Once put together, several feet of wire are left on either side of the plug so that rewiring the plug is not necessary since soldered connections are made at the end of the leads. Construction details of this plug are shown in Fig. 3. This plug has been used with pressures up to 3750 psi and has been completely satisfactory both with respect to the absence of leaks as well as electrical insulation.

To check the reliability of strain gages under pressure, a separate test was conducted with a weighted cantilever beam inside a small pressure chamber. This pressure chamber could be taken to whatever pressure was desired up to a maximum of 5000 psi, Fig. 4. It could be rotated about a central point so that the cantilever beam would be horizontal, vertical, or at any intermediate angle. Near the fixed end the cantilever beam was provided with machined flats, top and bottom, on which the SR-4 strain gages were applied. Since the cantilever was surrounded on all sides by the high-pressure atmosphere in which it was placed, the gages registered a compression strain as expected. By rotating the assembly, bending stresses independent of internal pressure could be induced in the cantilever beam so that strains due to bending could be isolated from those due to internal pressure. Some variations between gages resulted. Further investigation revealed that these variations were due to differences in technique of application, such as, variation in thickness of the cement layer between metal and gage, air bubbles, etc.

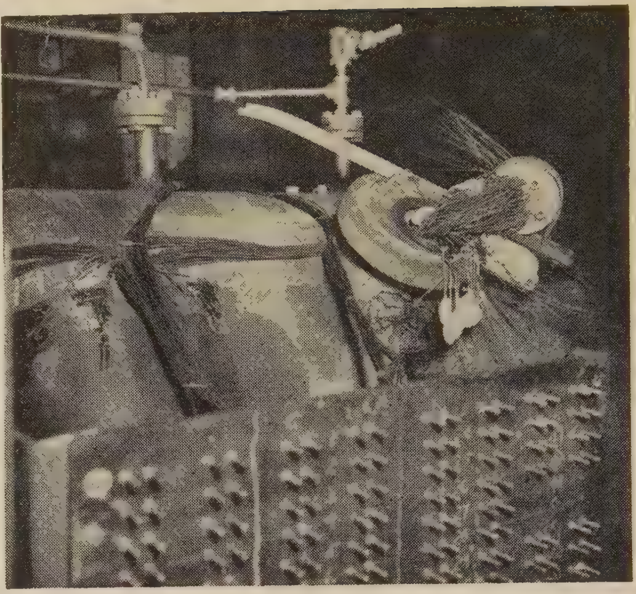

Fig. 2 View of SR-4 Gage Setup Showing Multiwire Pressure Seal in Process of Assembly

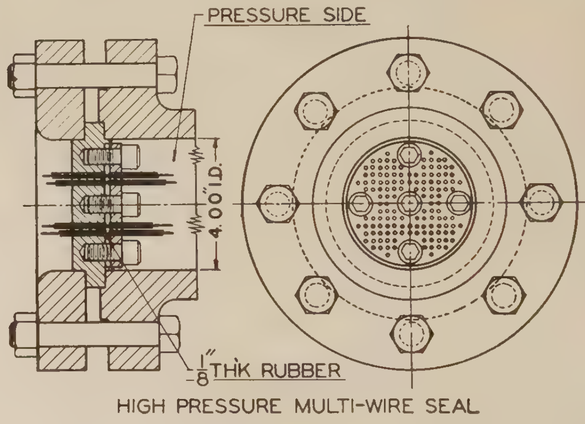

Fig. 3 High-Pressure Multiwire Seal

Fig. 5 shows results obtained using an inside reference gage. Briefly, the conclusion is that SR-4 strain gages are reliable at least up to the maximum test pressure of 5000 psi if applied correctly.

For the large vessel tests it is customary to use a dummy gage to correct for temperature changes. When measuring stress under hydraulic pressure, this dummy gage is placed inside the vessel for the inside gages. The dummy-gage specimen is of course in compression on all sides and will show a compression strain. Gages on the inside surface of the vessel have pressures radial to the surface, and a Poisson's ratio effect is present for both dummy

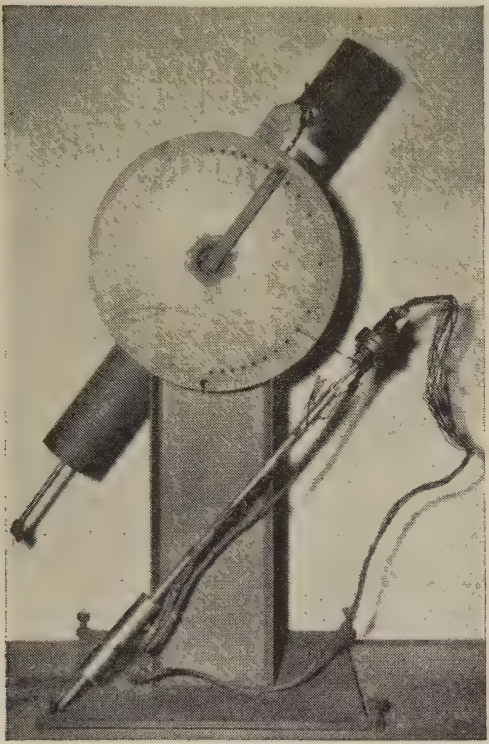

Fig. 4 Apparatus for Calibrating SR Gages Under Hydraulic Pressure

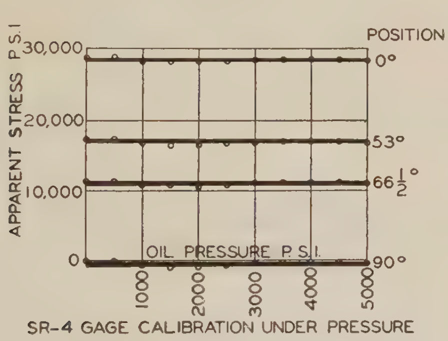

Fig. 5 Effect of Hydraulic Pressure on SR-4 Gage Readings

and test gages. The theoretical correction for pressure on a dummy block will be as follows

$$\text{Apparent strain } \epsilon_z = \frac{P(1 - 2\mu)}{E}$$

$$\text{Stress correction} = E\,\epsilon_z = P\,(1 - 2\mu) \text{ psi}$$

in which:

P = internal pressure, psi
E = modulus of elasticity
μ = Poisson's ratio
ϵ_z = apparent strain

These corrections are negligible in the testing of drums and pressure vessels at comparatively low pressure, and in most cases have been neglected.

Instrumentation

SR-4 strain gages from $^1/_8$ in. to 6 in. gage length, and rosettes of various types have been used. The original tests were made with the Baldwin-Southwark galvanometer-type control box. Later, the electronic SR-4 strain indicator greatly increased the facility of taking strain data. The latest-type K strain indicator is now used. A six-channel Brush Development Company pen-and-ink recorder and amplifier setup is now in use on some dynamic measurements. These are also applicable to measuring stresses during fatigue tests which will be described later.

Although from an electronic point of view stranded lead wire for the multiwire plug may be desirable, solid wire is essential to prevent leakage. Consequently, solid wire of sizes from No. 22 to No. 18 gage have been used in all high-pressure work.

For switching from one gage to another in a multiple setup, plugs similar to those used on household appliances, such as toasters, irons, etc., have proved quite satisfactory. These double-terminal plugs were very simple and enabled rapid manual changing from gage to gage. With two men, several hundred gage locations can be read in one hour. The hydraulic pressure is of course held constant during this interval.

Figs. 6, 7, and 8 show arrangements of representative jobs. The outside views show the terminal board in place. It has been found that the material from which this terminal board is made is critical. It should be of a moistureproof material. This requirement also applies to more modern switching arrangements including multipoint tap switches and automatic switching units.

Fatigue Testing

There are many cases on record and in the literature where pressure vessels have been tested to destruction under hydraulic pressure. These vessels usually fail at pressures from 3 to 5 times the allowable working pressure. In those instances where the pressure vessel was made of one of the regular boiler-plate materials, the failure generally occurred after very considerable distortion of the original shape. The relatively large amount of plastic deformation, which of necessity occurs in the weakest section of the design, goes so far beyond the operating strain range in these locations that the final values have very little bearing on the behavior of such a vessel in regular operation. It has been argued successfully that in the final stages of a static-pressure destruction test, one will not be testing the same shape nor the same material as that of the original vessel. Therefore it would be more to the point to test the design in a shape and condition similar to actual service.

It is for this reason that considerable work has been done on testing pressure vessels under conditions of pulsating fatigue from zero to a maximum internal pressure. Although this type of test does not simulate the service conditions of many types of pressure vessels either, it does bring out points of severe stress concentration, or is a means of demonstrating that such stress concentrations do not exceed those that are unavoidable in pressure-vessel design. Where a boiler drum, for example, may be subjected to but a few hundred major cycles during its service life, a pulsating fatigue test of 100,000 cycles at or above working pressure will establish confidence that the design does not contain regions of severe strain which could result in premature failure. Although a more pertinent test is desirable, none has so far been devised except for the high-temperature fatigue test described later, where operating temperature is taken into consideration.

As long as the test pressure did not exceed the hydraulic line pressure available, the pulsation fatigue tests were conducted by means of a motorized valve. This device admits water from the hydraulic system to the test drum and discharges the volume expansion after a certain predetermined maximum pressure has been reached.

When drums with a design pressure of over 1000 psi had to be tested, the 1500-psi hydraulic pressure was insufficient to produce pulsation for $1^1/_2$ times working pressure. Hence it was decided

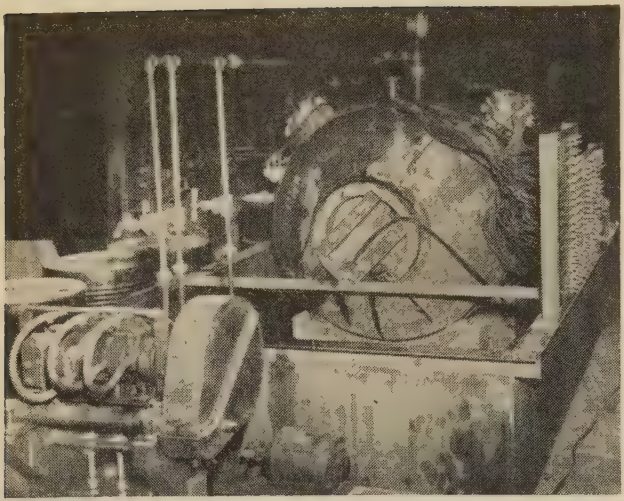

Fig. 6 External View of Drum Specimen With Reinforced Manhole and Various Nozzle Designs

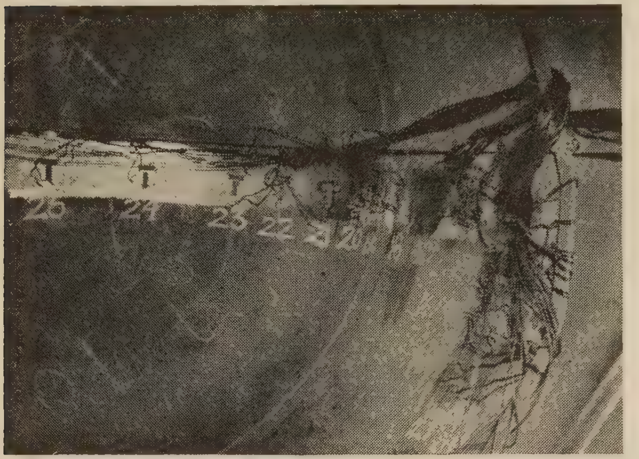

Fig. 7 Inside View SR-4 Test Setup Showing Gage-Wiring Arrangement and Nozzle Opening

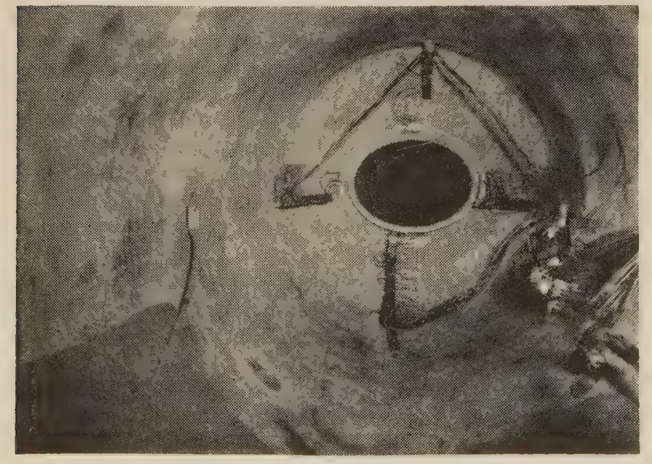

Fig. 8 Inside View Showing SR-4 Gage Test Setup in Stirling Boiler Mud Drum

(This drum had been subjected to severe overpressure.)

to build an apparatus that would extend the pressure range up to 6000 psi.

The energy required to pump water at the rate necessary for testing full-size specimens up to a pressure of 6000 psi and then release it, amounts to about 450 hp. This not only would be a sizable piece of apparatus but would become quite expensive for continuous testing in so far as power is concerned. It was therefore thought economical to build a balanced apparatus in which only the frictional forces would have to be overcome. This apparatus consists of two opposed plungers actuated by a central cam, as shown diagrammatically in Fig. 9. Each plunger is connected to a closed hydraulic system completely filled with water. In many tests two drums will be tested simultaneously, one on each plunger. When only one specimen is to be tested the opposing piston is connected to a balance or "dummy" drum to form the elastic counterpart.

When a plunger is pushed into the cylinder, the water in the system is compressed up to the end of the stroke, and on the return stroke the plunger is forced outward by the elastic action of the compressed water. Disregarding friction, the work done by forcing the piston in is equal to the work delivered when it is pushed out. By opposing two plungers and actuating them with a suitable cam, the actual energy input can be reduced to frictional losses only. The shape of the cam, however, has to be designed so that the torque required by the ingoing plunger is equal to the torque delivered by the outgoing plunger.

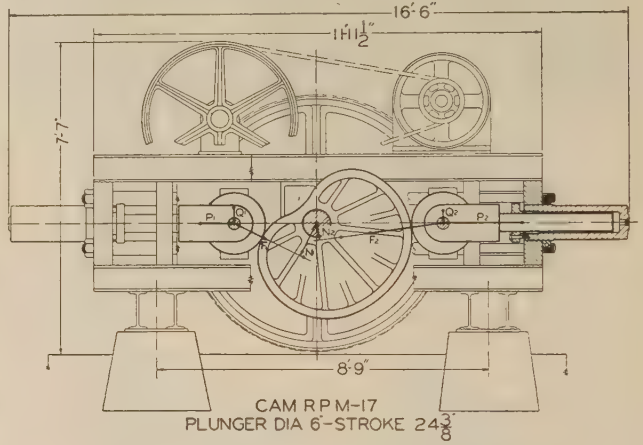

Fig. 9 Diagram Showing Cam and Roller Mechanism of Pulsator

Referring to Fig. 9, the shape of the cam must satisfy the following relationship

$$F_1 \times N_1 = F_2 \times N_2$$

where

F = resultant of P and Q
N = radius on which F operates
P = proportional to plunger travel
Q = vertical reaction on crossheads

Although there is a theoretical solution for the shape of the cam when the stroke and the diameter of the roller are known, the shape had to be approximated with four sections of circles to avoid making the machining of the cam too costly. A torque analysis of the final shape shows that the simultaneous torque curves very nearly overlap one another, see Fig. 10.

The apparatus was equipped with a 75-hp motor. Only a fraction of this power has been necessary to drive it. The cyclic speed is about 17 pulsations per min for each plunger. Plungers are 6 in. diam and have $24^3/_8$ in. stroke, providing a displacement of 687 cu in.

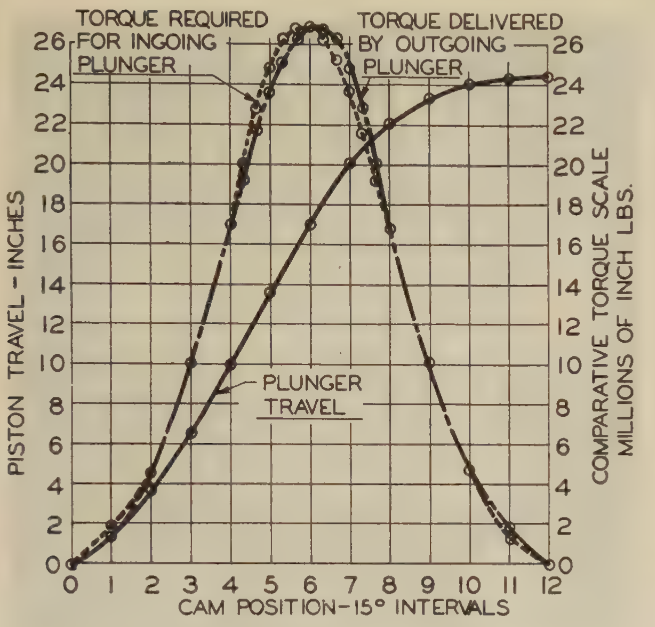

Fig. 10 Torque-and-Plunger Travel Diagram for Pulsator-Cam Mechanism

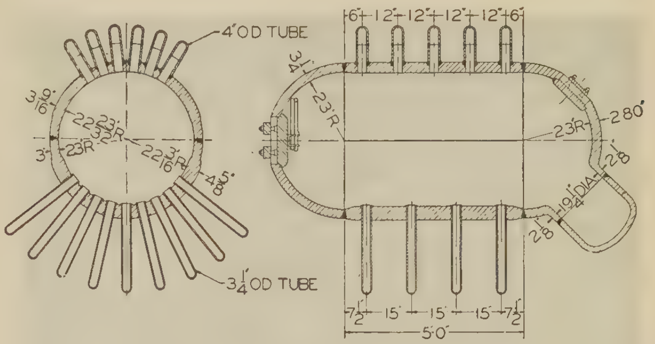

Fig. 11 Full-Size-Drum Fatigue Specimens

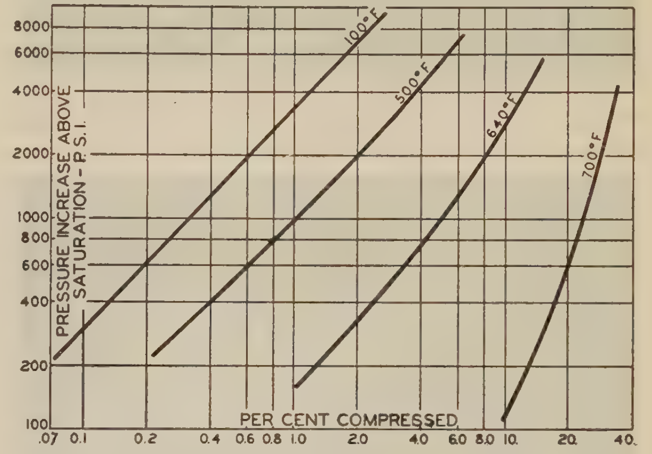

Fig. 12 Compressibility of Water at Various Temperatures

In order to avoid injury to operating personnel, test drums have been protected by heavy blasting mats made of $^3/_4$-in-diam steel cables.

The heaviest vessel tested on this apparatus is that shown in Fig. 11, having an inside diameter of 46 in. and shell thicknesses of $3^9/_{16}$ and $4^5/_8$ in. The maximum testing pressure used to date is $1^1/_2$ times the working pressure of the specimens, or 3750 psi. The compressibility of water for room-temperature operation (100 F) is shown in Fig. 12. For large-size high-pressure specimens, the volume expansion still is several times the total displacement of the pulsator plunger. It is therefore necessary to displace the major part of the water volume in the specimen drum by a much less compressible solid. In the beginning pig iron was used for this purpose but when even this became a critical material during the war, it was found that dense paving brick made an excellent substitute.

The elastic displacement during a pressure cycle is due, for the major part, to the compressibility of the water and to a lesser degree is a result of the dilation of the vessel under the action of internal pressure. These values can be calculated from known equations as long as the physical constants of the material are known.

In most tests the pulsator was operated only during working hours, with rest periods at night and over week ends. One run would consist of 100,000 cycles, after which the specimen drum was carefully inspected, visually and with magnetic-particle technique. The first run is usually conducted at working pressure, others at higher pressure up to 1.5 times working pressure.

In so far as boiler service is concerned, the first run would demonstrate that, from the point of view of cyclic loading, the drum is good for many times its natural service life. The second and third run are superimposed to obtain additional information as to its margin of strength and its ability to withstand considerable overpressure on infrequent occasions.

It is realized that the stepwise increase in cycle pressure will result in somewhat better fatigue life than would be obtained on a straight run. This procedure was followed only as a matter of economy in testing time. If the cycle pressure is chosen too low, a test to failure would last indefinitely at the slow speed of 17 rpm, and if chosen too high the number of cycles to failure might be so few that the test could be considered insignificant and not justify the high cost of the specimen. The extra number of cycles that may have been obtained from the "coaxing" effect can easily be discounted in the large margin of fatigue life obtained on a properly designed vessel. Failures like those shown in Fig. 13 bring out stress-concentration points at which design improvements are required.

The pulsation test on all important specimens is preceded by an experimental stress analysis, as shown in Fig. 14. Lately the experimental stress analysis in turn has been preceded by a brittle-lacquer test cycle to determine points of maximum stress, and to indicate the best location for the SR-4 gages for measuring maximum stresses.

Slow Cycle Test

When observing a vessel that is being subjected to fairly rapid cycles of pulsating pressure, there appears to be a difference in response to this type of cycle compared to bringing the pressure up to the maximum and then holding it there. In heavy vessels, a time factor or a brief period of readjustment seems to enter. This is particularly noticeable when the drum contains a multiplicity of closely spaced expanded tubes.

In testing the specimen drum shown in Fig. 15, this observation led to a change in the pressure cycle. For this specimen, which contained six $4^1/_2$-in-diam, four $3^1/_4$-in-diam, twenty 2-in-diam, and ninety-four 1-in-diam tube holes, the pressure cycle was as follows:

After opening the hydraulic valve, the pressure was allowed to rise to the maximum test pressure, was kept there for $2^1/_2$ minutes, and then released by opening the discharge. After $2^1/_2$ minutes at

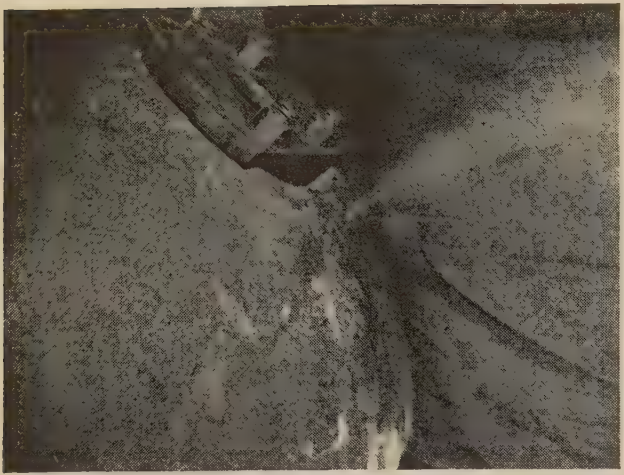

FIG. 13 VIEW SHOWING FATIGUE FAILURE IN HIGH-PRESSURE-DRUM SPECIMEN

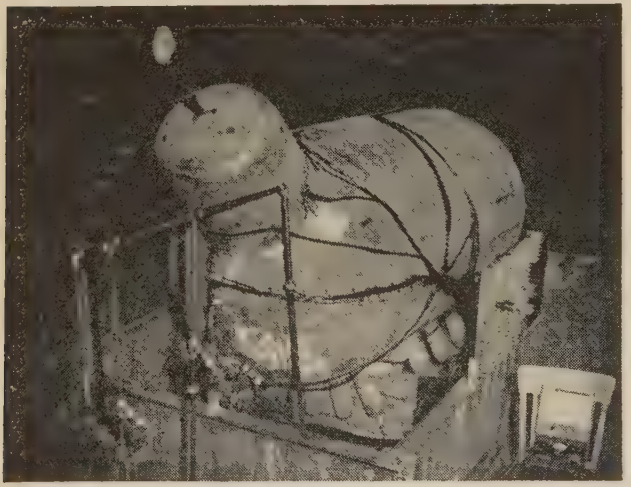

FIG. 14 OUTSIDE VIEW OF HIGH-PRESSURE-DRUM SPECIMEN SHOWING PUSHOUT DOWNCOMER CONNECTION ON NEAR HEAD

zero pressure, the cycle was repeated. This cycle seemed to be more severe than the continuous cycle without rest periods. At $1^1/_2$ times working pressure, several leaks were developed on the expanded tube seats. This was particularly true on the small-diameter tubes and provided an opportunity to improve the method of expanding this size tube. Fig. 16 is an inside view of the tube ligaments.

HIGH-TEMPERATURE FATIGUE TEST

All the tests described were conducted at room temperature. Under actual service conditions, however, the metal of the drum is exposed to saturated steam and water. It was therefore desirable to investigate the effect of temperature as well as the contact with steam and boiler water. An apparatus to perform a pulsating fatigue test under simulated service conditions was designed to investigate this phase.

Although this apparatus went through a few evolutionary stages, only the final arrangement will be considered here. The test was performed on scale models, since compressibility of high-temperature water is such that plunger displacement for full-size specimens is beyond the scope of practical possibilities. Compressibility values for water at elevated temperatures are given in Fig. 12.

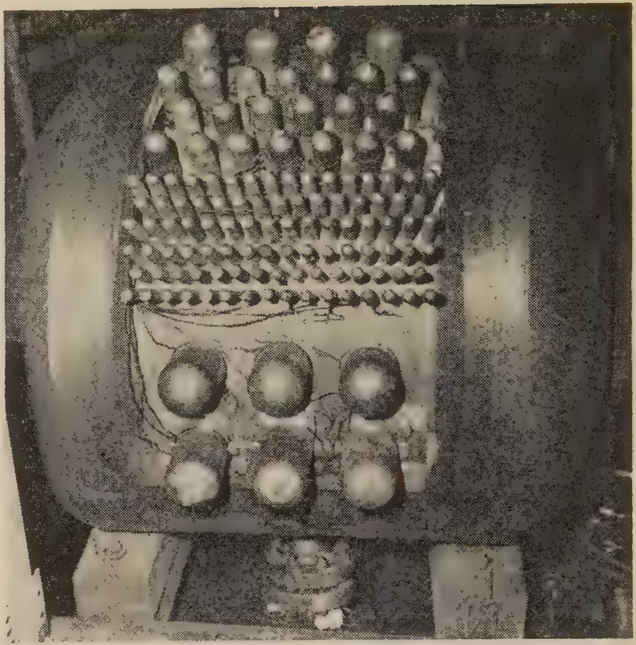

FIG. 15 EXTERNAL VIEW OF FULL-SIZE DRUM SPECIMENS SHOWING TEST SETUP ON TUBE LIGAMENTS

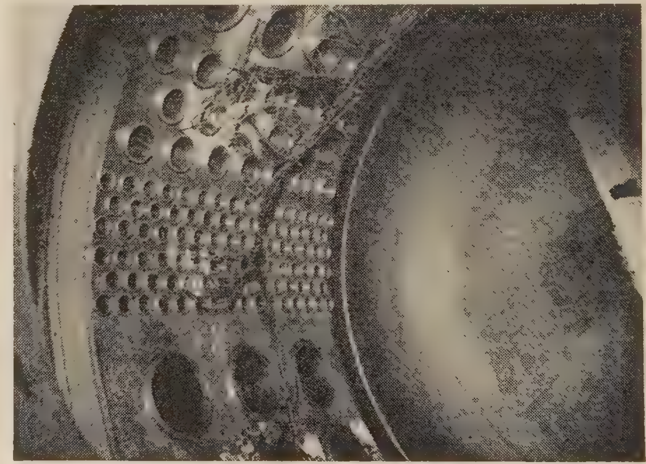

FIG. 16 INSIDE VIEW OF TEST SETUP ON TUBE LIGAMENTS

A diagrammatic arrangement of the test apparatus is shown in Fig. 17. Since the hydraulic pulsations were provided by a high-pressure triplex pump, only three specimens or pairs of specimens could be tested at any one time. The inlet and discharge valves were removed from the pump so that the plungers only pulsated the water without actual pumping action.

The specimens were placed in a 24-in. ID × 5-ft-long steam drum which was operated at a pressure of 2000 to 2500 psi. The location of the specimens was such that approximately one half was above the water line and the other below it. The water in the drum was representative of average boiler-water conditions, namely, a pH of 10.5–11, a $NaSO_4$ to NaCl ratio of 3 to 1, and a total solids concentration of 1500–2000 ppm.

The inside of each specimen is connected to one of the three plunger bodies of the triplex pump. The maximum pressure of the fatigue cycle was 7500 psi so that the pressure difference between inside and outside of the specimens was 5000 psi. In parallel with the specimens in the steam drum, three similar

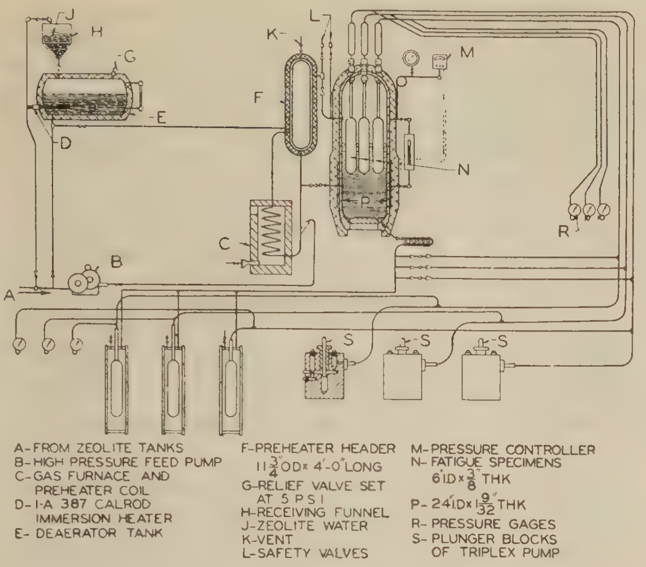
J
H
G
K
L
M
F
E
D
N
P
R
C
B
A
S
S
S
A-FROM ZEOLITE TANKS
B-HIGH PRESSURE FEED PUMP
C-GAS FURNACE AND PREHEATER COIL
D-I-A 387 CALROD IMMERSION HEATER
E-DEAERATOR TANK
F-PREHEATER HEADER 11 3/4" OD × 4'-0" LONG
G-RELIEF VALVE SET AT 5 PSI
H-RECEIVING FUNNEL
J-ZEOLITE WATER
K-VENT
L-SAFETY VALVES
M-PRESSURE CONTROLLER
N-FATIGUE SPECIMENS 6" I.D × 3/8" THK
P-24" I.D × 1 9/32" THK
R-PRESSURE GAGES
S-PLUNGER BLOCKS OF TRIPLEX PUMP

Fig. 17 Diagrammatic Arrangement of High-Temperature Fatigue-Test Apparatus

specimens were tested simultaneously under exactly the same conditions, except that their temperature was maintained at room temperature. They were paired with the three specimens in the steam drum on the same pulsing circuit and placed in individual headers. These headers were connected directly with steam drum so that the cold specimens were subjected to the same boiler water as those located in the steam drum.

Leakage from the plunger packing is made up from the steam drum through three cooled make-up connections. They are provided with a check valve, allowing water to flow from the drum to each of the pulsing circuits. This arrangement provides that the pressure in the pulsing circuits can never fall below the steam-drum pressure, thereby preventing flashing of the water in the hot specimens.

Specimens were 6 in. ID and $^3/_8$ in. thick with heavy hemispherical ends and about 24 in. long on the straight cylindrical part, as shown in Fig. 18. The cylindrical sections were made of regular $1^1/_4$-in-thick boiler plate bent to a semicylindrical shape, welded together, and then machined inside and out.

Pressure-Cycle Control

The maximum pressure reached in the pulsing circuit depends upon the total water content of the circuit, the temperature of this water, the dilation of circuit and specimens, and the plunger displacement.

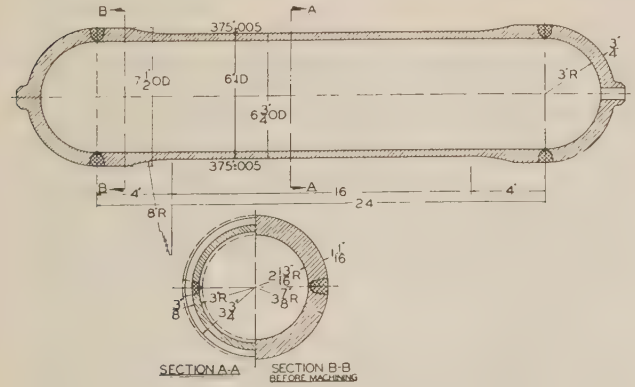

Fig. 18 High-Temperature Fatigue Specimen

(One-tenth scale model.)

At the operating temperature of the hot specimens, the compressibility of the water is so great that a large percentage of the space in the specimen has to be displaced by a solid metal core.

This core was made of such size that the maximum cycle pressure would rise above that necessary for this test. Some additional water volume was then provided on the outside of the steam drum by connecting to each circuit a high-pressure buffer vessel somewhat smaller than the specimen itself. By regulating the temperature in the buffer vessels, the compressibility of the water contained in them could be varied at will, and thus the over-all compressibility of the circuit controlled.

Operation

Great care has to be exercised in the operation of this test apparatus. When starting, the steam drum and all parts of the pulsing circuits containing high-temperature water have to be brought up to full temperature to insure maximum compressibility. The by-pass valves in the small lines short-circuiting between the three plunger blocks are opened, after which the pump is started. While watching the maximum pressure on the pressure indicators, the by-pass valves are closed gradually. After the by-pass valves are closed, and the pulsing circuits are on their own, the cycle pressure is brought up to the maximum desired pressure by reducing the temperature of the buffer vessels.

Considerable trouble was experienced due to leakage of high-pressure valves, particularly check valves and high-pressure relief valves. These troubles were gradually overcome by proper design, and operation settled down to a watchful routine.

The speed of the pump is only about 17 rpm so that testing proceeds at rather a slow pace.

Results of Fatigue Tests

Full-Size Specimens. Quite a large number of pressure vessels have been tested by the authors' company using techniques similar to those described. Some of the early tests were reported by Prof. H. F. Moore.[5] The work reported was continued to include various drum designs with and without tube holes. Later tests included banded vessels as well as many pressure vessels covering the range of thicknesses from $^1/_2$ in. to $4^5/_8$ in. Details of several of these test vessels and the results will be included here.

Stirling Boiler Mud Drum. This drum had been rejected because of laminated plate which caused difficulties in producing a satisfactory weld. It was made of SA-212 plate but no detailed physical data are available on the material. The design pressure was 200 psi for the completed drum with tube holes. It was tested before any tube holes had been drilled and therefore a pressure of 700 psi was used. Previous pressures up to 850 psi in preliminary testing had resulted in an amount of plastic yielding on the head which changed the manhead shape to one which approximated a cone instead of the original dished shape. This drum underwent 100,000 cycles of pressure at 700 psi, which corresponded to an average stress range in the shell of 15,700 psi. A later strain-gage test on the head indicated that there were locations having a stress range of 77,000 psi at this pressure. Notwithstanding the high stresses, this drum showed no failure after the test.

Test Drum, Fig. 15. The test drum, shown in Figs. 15 and 16, was also made of SA-212 plate and included a total number of 124 expanded tube nipples ranging from 1 in. diam up to $4^1/_2$-in. diam. This drum was designed for a pressure of 980 psi at a stress of 22,500 psi in the shell proper. The drum was given 100,000 cycles at 1078 psi pressure and 1400 slow cycles at 1470 psi pressure as described previously. Strain-gage tests have indicated stresses at various locations, as given in Table 1.

---

[5] "Tests of the Resistance to Repeated Pressure of Forged Riveted and Welded Boiler Shells," by H. F. Moore, Trans. ASME, vol. 53, 1931, pp. 55–60.

TABLE 1 STRESSES IN TEST DRUM, FIG. 15

Cycles	Pressure, psi	Stresses, psi Tube ligaments	Manhead	Blank head
4	980	23600	39400	35600
100000	WP 1078	26000	43300	39200
1400	1470	34500	57500	51700

The results of this fatigue test were leaks at some of the tube seats. This development resulted in changes in tube-expanding methods which will not be discussed here. There were no indications of incipient failure in any of the other locations, such as the shell proper or in the head knuckles.

Drum With Intentionally Faulty Welds. For another vessel a piece of rimmed steel, SA-70 plate, having laminations and nonmetallic inclusions, was used for the shell and the blank head. The manhead was SA-212 plate. The thicknesses of shell, blank head, and manhead were $^{1}/_{2}$ in., $^{5}/_{8}$ in. and $^{13}/_{16}$ in., respectively. This test was conducted to determine the effect of welding defects on the fatigue life of a vessel and both submerged-arc welding and automatic multipass welding were used. The final failure was in a highly stressed section of the manhead knuckle, although incipient cracks also appeared in the defective longitudinal weld seam. The conditions of failure are described in greater detail in the companion paper by Carpenter.[4] The physical properties and chemistry of some of the parts of this drum are given in Table 2.

TABLE 2 PROPERTIES OF PARTS OF TEST DRUM

	Blank head	Shell	Manhead	Manhead
	MILL REPORTS	0.505 IN.	(AFTER TEST)	
Tensile, psi	56700	56600	79900	82900
Yield point, psi	36900	37200	42400	43300
Elongation, per cent	32.5	32.0	30.7	28.8
	CHEMISTRY,	PER CENT		
C	0.21	0.21	0.28	
Mn	0.41	0.41	0.69	
P	0.015	0.015	0.012	
S	0.040	0.040	0.027	
Cu	0.32	0.32	0.22	
Si			0.20	

The stresses and cycles in the shell proper are given in the following tabulation, but due to stress concentration, the inside of the knuckle of the head has probable stresses as high as 35,000 psi. The series of cycles follows:

100000 cycles at 560 psi pressure	13750 hoop stress
100000 cycles at 615 psi pressure	15000 hoop stress
161000 cycles at 840 psi pressure	20600 hoop stress

Even under these adverse conditions the vessel withstood a number of pressure cycles far beyond actual service requirements both in number and magnitude.

High-Pressure Drum. This drum, shown in Fig. 11, was designed for a working pressure of 2500 psi, and tested at pressures up to 3750 psi. The average ligament stress in the upper shell was 23,585 psi calculated in accordance with the 1943 ASME Codes. This drum was made of SA-212 steel with the physical properties given in Table 3.

TABLE 3 PHYSICAL PROPERTIES OF TEST DRUM

	Upper shell	Lower shell
Plate thickness, in.	3 $^{9}/_{16}$	4 $^{5}/_{8}$
Tensile strength, psi	70820	68250
Yield point, psi	36750	37500
Elongation in 2 in., per cent	35	33
Reduction of area in 2 in., per cent	56	55.7

The first point of stress concentration located was a failure in the sharp corner of the manhole-cover seat shown in Fig. 13. This occurred after 100,000 cycles at 2500 psi pressure and 57,240 additional cycles at 3000 psi pressure. This point in the original construction was improved by a change in design. During the pulsating fatigue test this drum was subjected to the series of pulsations given in Table 4.

TABLE 4 PULSATIONS ON TEST DRUM

Cycles	Pressure psi	Calculated average ligament stress, psi	Maximum stress range in tube hole, psi
100000 at working pressure (WP)	2500	23585	41800 test
100000 at 1.2 WP	3000	28300	51200[a]
100000 at 1.4 WP	3500	33000	59730[a]
12000 at 1.5 WP	3750	35380	65500 test

[a] Values calculated from the average measured stress-concentration factor for this location of 1.81.

The test was terminated after the cycles indicated, owing to a fatigue failure which resulted in a leak at a welded-tube stub in the upper shell. This was a radial crack starting at the inside of the tube hole on the longitudinal center line. Further inspection revealed 13 such failures in the upper shell tube sheet. The test was dismantled and metallurgical inspection of these failures will be made.

Model Tests. In the high-temperature fatigue tests, 15 specimens were tested, 9 of which were of the type shown in Fig. 18, and will be reported here. Of the latter, 4 were tested at room temperature and 5 in direct comparison in the steam drum at 2000-psi saturated-steam and water atmosphere. All failures occurred in the weld or weld-affected zone, and all of them were in a longitudinal direction, i.e., transverse to the maximum stress. The test data are given in Table 5, and are plotted on logarithmic co-ordinates in Fig. 19. As a means of comparison an S-N curve for full-size welded specimens is also shown.[6] The stress range of the cycle is not exactly alike, however, since the latter specimens were tested from zero to a maximum tension, and the model specimens were tested from a hydraulic compressive stress of the steam-drum atmosphere of 2000 psi to a maximum biaxial cylinder stress resulting from internal pressure.

This comparison brings out the following:

1 The test results of the cylindrical specimens are lower than those of the flat-plate specimens.

2 In the scatter band there is no particular preference between the points of the hot specimens and the cold specimens. There is apparently no significant change in the endurance limit resulting from the high-temperature steam-drum environment.

CONCLUSION

The foregoing testing techniques are the outgrowth of many years of pressure-vessel development work. They do not in every case result in data leading to absolute conclusions but are, rather, several approaches to the problem of reducing the wide margin for unknown factors in this field of engineering. By measuring stresses, by subjecting both model and full-size specimens to static as well as cyclic loading, and at room temperature as well as under simulated service conditions, the background of knowledge has been extended. The results attained are as follows:

1 A reliable method of measuring stress on the inside surface of heavy vessels under high internal pressure has been developed.

---

[6] Bulletin no. 27, University of Illinois, Engineering Experiment Station.

TABLE 5 DATA ON CYLINDRICAL MODELS IN HIGH-PRESSURE STEAM-AND-WATER ATMOSPHERE

Specimen description	No.	Tensile strength, psi	Yield point, psi	Weld metal[a]	Stress relief	Average hoop stress, psi	Number of cycles	Location of failure[b]
Series A × made of bent $^3/_8$-in. plate, not polished, welds ground flush (hot)	1	77090	43390	A	No	38000	49267	1 in. from longitudinal weld seam and parallel
	2	77090	43390	A	No	43000	34289	Junction of long and girth weld
	3	77090	43390	B	No	41700	31360	Longitudinal weld seam
Series D ● specimens made of bent $^3/_8$-in-thick plate, medium polish inside and outside (hot)	1	70000 to 74600	40600 to 48700	A	No	31700	269000	Edge of longitudinal weld seam
	2			A	Yes	32800	340000	Girth weld seams
	3			B	No	34500	76000	Longitudinal weld seam
Series F ⊙; hot specimen made of SA-212 plate, machine inside and outside (see Fig. 18)	1			A	Yes	35000	105212	Longitudinal weld steam space
	2			A	Yes	35000	192085	Longitudinal weld steam space
	3	74700	52160[c]	A	Yes	33600	306018	Longitudinal weld steam space
	4			A	Yes	34000	186221	Longitudinal weld steam space
	5			A	Yes	33200	242123	Longitudinal weld water space
Series G ⊡; room temperature, specimens same as Series F	1	72180	46090[c]	A	Yes	33700	54942	Longitudinal weld
	2			A	Yes	35200	219611	Longitudinal weld
	3			A	Yes	34400	247958	Longitudinal weld
	4			A	Yes	33600	268550	Longitudinal weld
Weld metal................		71500	79990 on test plate longitudinal and transverse are approximately equal					

[a] Electrode designation: A, Carbon-moly coated electrode (0.33 C, 0.5 Mo); B, 25 Cr 20 Ni coated electrode.

[b] All failures were longitudinal cracks; i.e., transverse to the maximum stress, starting at small mechanical weld defects.

[c] These physical properties were determined on one hot and one cold specimen after test.

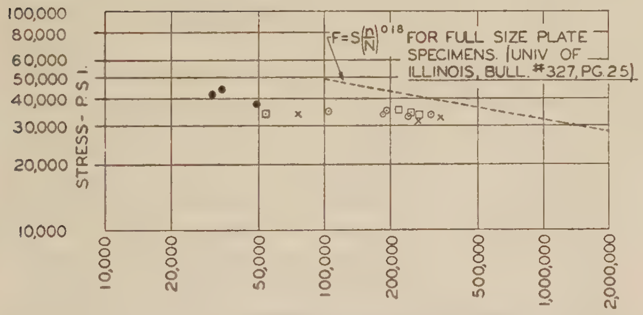

FIG. 19 SOME RESULTS ON CYLINDRICAL SPECIMENS SUBJECT TO CYCLIC PULSATION

× = Specimens in series A of Table 1
● = Specimens in series D of Table 1
⊙ = Specimens in series F of Table 1
□ = Specimens in series G of Table 1

This work resulted in the use of oil as a pressurizing medium.

2 A simple and reliable device for bringing a multiplicity of gage wires through the wall of a pressure vessel in a manner suitable for accurate strain-gage measurements was designed and successfully used.

3 A method has been developed to isolate the effect of hydraulic pressure on SR-4 gages and to calibrate them in a setup employing an inside "dummy."

4 An apparatus has been designed and built for pulsating full-scale pressure vessels economically up to a maximum pressure of 6000 psi at room temperature.

5 A method of pulsating model vessels in an atmosphere of saturated steam and water at elevated pressure and temperature has been built and operated, and a limited check made to determine the effect of such an environment compared to that of room-temperature water.

As the problem of pressure-vessel design at the present time is under intensive investigation, it is hoped that this work will contribute in some small measure to developing the optimum design from an economic, engineering, and service point of view.

Discussion

Henry Liessenberg.[7] The authors stated that in applying the slow cycle test, which had proved more severe than the first pulsation test, leaks developed on the expanded tube ends, particularly on the small-size tubes. It would be helpful if the authors would state whether tube expansion was controlled by the elongation method, or what other method for control in expanding was applied; also the amount of expanding before test and additional amount of rerolling required to eliminate leakage.

The authors are to be congratulated on the brilliant conception of their high-temperature fatigue test, even if small models had to be used. It is interesting that the test indicated practically no difference in number of cycles between hot and cold specimens. It is the writer's belief that if the shell is exposed to furnace gas, which is of much higher temperature than the inside water temperature as used in model test, different results would be encountered. To conduct such a test would require considerable expenditure. It would be helpful if the authors would state to what percentage failures occurred between longitudinal and circumferential welds, or if all failures occurred in longitudinal welds only, as well as type of failures. Did any failures occur in the attachment weld of the tube nipples?

The statement that endurance-limit tests on cylindrical specimens are considerably lower than on flat-plate specimens is in agreement with previous conclusions, i.e., that in a curved plate, as used in drums, initial residual stresses due to rolling, pressing, or forming are never fully eliminated by annealing.

Were microphotographs taken of weld and adjacent plate before test and after failure to indicate possible change in grain structure under fatigue test? If so, will the authors supply such photographs for study?

H. L. O'Brien[8] and E. Wetterstrom.[9] The discussion which follows has a twofold purpose: Primarily, the mathematical development of experimental techniques for analyzing biaxial-stress conditions is directed toward the end of illustrating that the authors' assumptions are accurate within the limits of their test. Nevertheless, it is to be pointed out that appropriate corrections must be made when the SR-4 electrical resistance strain gage is utilized under certain conditions of loading.

---

[7] Combustion Engineering-Superheater, Inc., New York, N. Y.

[8] Research Engineer, Graver Tank and Manufacturing Company, East Chicago, Ind. Jun. ASME.

[9] Graver Research Fellow, Purdue University, Lafayette, Ind. Mem. ASME.

The nomenclature resorted to in this development is as follows:

$\bar{\epsilon}_0, \bar{\epsilon}_1, \bar{\epsilon}_2$ = strain as read, in./in.
$\epsilon_0, \epsilon_1, \epsilon_2$ = actual strain, in./in.
P = hydrostatic pressure, psi
E = modulus of elasticity, psi
μ = Poisson's ratio
S = stress, psi

The basic equation of biaxial stress is[10]

$$S_1 = \frac{E}{(1-\mu^2)} (\epsilon_1 + \mu\epsilon_2) \ldots\ldots\ldots\ldots\ldots [1]$$

From this relationship it is apparent that the stress in any direction can be determined if the strain in that direction and the strain at 90 deg are known. When these strains are being evaluated by an SR-4 strain-gage circuit, there is no assurance that the strains are correct "as read," owing to the difference in loading the active gage and the dummy gage. The former is subjected to pressure in one direction only, whereas the dummy gage is under pressure from all sides. These conditions are illustrated in Figs. 20 and 21, herewith, along with the co-ordinate system.

Writing the equation for strain in the stressed body, we obtain

$$\epsilon_1 = \frac{P}{E}\mu - \frac{S_2}{E}\mu + \frac{S_1}{E} \ldots\ldots\ldots\ldots\ldots [2]$$

$$\epsilon_2 = \frac{P}{E}\mu + \frac{S_2}{E} - \frac{S_1}{E}\mu \ldots\ldots\ldots\ldots\ldots [3]$$

A solution to simultaneous Equations [1] and [2] is obtained by multiplying Equation [3] through by μ and adding

$$\epsilon_1 = \frac{P}{E}\mu - \frac{S_2}{E}\mu + \frac{S_1}{E}$$

$$\mu\epsilon_2 = \frac{P}{E}\mu^2 + \frac{S_2}{E}\mu - \frac{S_1}{E}\mu^2$$

$$(\epsilon_1 + \mu\epsilon_2) = \frac{P}{E}(\mu + \mu^2) + \frac{S_1}{E}(1-\mu^2)$$

Then $$\frac{S_1}{E}(1-\mu^2) = (\epsilon_1 + \mu\epsilon_2) - \frac{P}{E}(\mu + \mu^2) \ldots\ldots\ldots [4]$$

Introducing the argument $\epsilon_1 = \bar{\epsilon}_1 - \epsilon_0$ Equation [4] may be rewritten as

$$\frac{S_1}{E}(1-\mu^2) = [{}_1\bar{\epsilon} - \epsilon_0 + \mu(\bar{\epsilon}_2 - \epsilon_0)] - \frac{P}{E}(\mu + \mu^2)$$

$$\frac{S_1}{E}(1-\mu^2) = [\bar{\epsilon}_1 + \mu\bar{\epsilon}_2 - \epsilon_0(1 + \mu)] - \frac{P}{E}(\mu + \mu^2)$$

Substituting $\epsilon_0 = (P/E)(1 - 2\mu)$ we obtain

$$\frac{S_1}{E}(1-\mu^2) = \bar{\epsilon}_1 + \mu\bar{\epsilon}_2 - \frac{P}{E}(1-2\mu)(1+\mu) - \frac{P}{E}(\mu + \mu^2) \ldots\ldots [5]$$

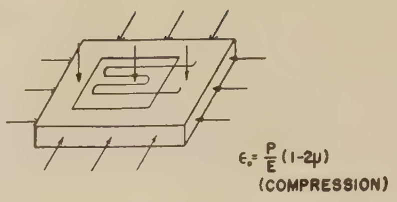

FIG. 20 DUMMY GAGE BLOCK SUBJECT TO PRESSURE FROM ALL DIRECTIONS

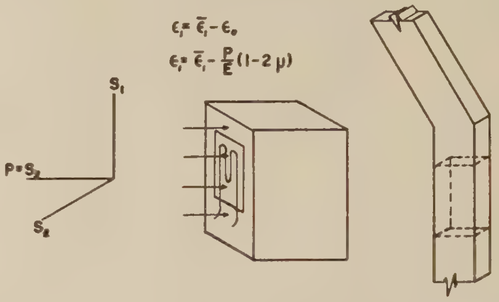
$\epsilon_1 = \bar{\epsilon}_1 - \epsilon_0$
$\epsilon_1 = \bar{\epsilon}_1 - \frac{P}{E}(1-2\mu)$
S_1
$P = S_2$
S_2

FIG. 21 ACTIVE GAGE SUBJECT TO PRESSURE FROM ONE DIRECTION ONLY

Clearing Equation [5] results in a stress relation

$$S_1 = \frac{E}{(1-\mu^2)}\left[(\bar{\epsilon}_1 + \mu\bar{\epsilon}_2) - \frac{P}{E}(1-\mu^2)\right] \ldots\ldots [6]$$

A more useful form of Equation [6] may be expressed when each side of the equation is divided by P

$$\frac{S_1}{P} = \frac{E}{P(1-\mu^2)}(\bar{\epsilon}_1 + \mu\bar{\epsilon}_2) - 1 \ldots\ldots\ldots\ldots [7]$$

and

$$\frac{S_2}{P} = \frac{E}{P(1-\mu^2)}(\bar{\epsilon}_2 + \mu\bar{\epsilon}_1) - 1 \ldots\ldots\ldots\ldots [8]$$

The ratio $S/P:D/t$ illustrates that thick-wall cylinders have a low S/P value. For this reason the constant "1" becomes increasingly significant as the shell thickness increases.

Example: A cylinder of 46 in. ID is 4 in. thick. The theoretical Lamé stress at 2000 psi internal pressure is 24,100 psi. The corresponding S/P ratio is approximately 12 units. If this same stress is determined experimentally by using the SR-4 strain-gage readings in Equation [1] of this discussion, the ratio of S/P will be 13 units; the discrepancy is accounted for only when Equation [8] is utilized. An error of $^1/_{13}$ = 7.7 per cent is encountered in the use of Equation [1].

L. P. ZICK.[11] If the G-E magnetic gage were substituted for the DeForest scratch gage, the history described could very easily pass as a description of our own early activities in this field. The SR-4 strain gages and equipment now dominate our work. However, our techniques and methods and those of the authors' company have taken quite different paths, the chief difference being that we have used water (with all its troubles), as the pressure medium because of the size and the corresponding lower pressures of the vessels tested.[12]

Experimental Stress Analysis. The method of keeping the liquid level below the gage locations should surely save some difficulties. However, one word of caution—if separate leads of any length are used they, too, should remain above the liquid.

---

[10] "Theory of Elasticity," by S. Timoshenko, McGraw-Hill Book Company, Inc., New York, N. Y., 1934, p. 162.

[11] Research Engineer, Chicago Bridge & Iron Company, Chicago, Ill.

[12] "Strain Gage Survey Around the Supports of a 48-Foot Diameter Hortonsphere," by L. P. Zick and C. E. Carlson, Proceedings of the Society for Experimental Stress Analysis, vol. VI, no. II, pp. 41–60.

The cantilever bar tests showing the reliability of the strain gages under very high pressures is certainly encouraging.

Fatigue Testing. The method and test ranges for the fatigue tests gain additional merit in that the authors realize that the values of the various ranges vary. On the other hand, the statement, "After the initial proof test of $1^1/_2$ or 2 times working pressure there will be no further plastic deformation in the vessel during its entire service life," rightly or wrongly, seems to ignore the Bauschinger effect and strain-aging. The observations during the slow-cycle testing also seem contrary to this statement.

The use of double balanced plungers with the activating cam combined with the use of noncompressible ballast is an ideal example of a method revelation which will probably save someone else time, trouble, and expense.

High-Temperature Fatigue Test. The high-temperature fatigue tests are very interesting and have required considerable planning. The statement that all the specimens to date have failed in or near the weld does not agree with the results found by Professor Wilson. Has the possibility of a difference in welding technique been studied as a source of reduced fatigue strength?

AUTHORS' CLOSURE

We greatly appreciate the favorable comments of many engineers and acknowledge that our techniques may not apply in many applications which we did not cover. We will attempt to answer some of the detailed questions which have been submitted.

Mr. Liessenberg has asked for details on the tube-expansion method. Most of these tubes, especially the small size, were ball drift-expanded and, since the ball has a specific size, the amount of expansion does not need control by additional means. As to the amount of expansion before test and any additional rerolling, it is true that some repetition of expanding was necessary. In fact, the complete set of smaller tubes was replaced during tests of various tube seat designs.

Exposure of the high-temperature specimens to hot gases undoubtedly would have an effect on the results, but this effect becomes of real importance only on the heavier walled vessels. Our particular interests were in applications where this contact with hot gases is not present, since most of our high-pressure boiler drums are either outside the furnace proper or have adequate protection against the hot gases. In order to give a more complete record on the high-temperature tests, Table 5 was added to the final paper. The last column in this table and note (*b*) show that all of the failures were longitudinal cracks resulting from circumferential stresses. Out of fifteen failures, only one was at a girth seam, and one at the junction of a girth and longitudinal seam, but even these were in a longitudinal direction.

A metallurgical investigation of some of the failures indicated that they were initiated at minute, mechanical, weld defects, such as entrapped slag or small gas pockets. There were no failures in the tube-nipple connection welds. We regret that no microphotographs of the weld and plate were taken before the test for the comparison of grain structure. Such photographs of this location after failure are available, however, and we will be pleased to supply them for study.

Messrs. O'Brien and Wetterstrom have contributed a satisfactory algebraic combination of the strain-gage correction and the effect of pressure radial to the inside surface.

This combined formula is not applicable in at least two cases. Of first importance in this is the study of the actual unit strains which are present with relation to yield points, plastic flow, and residual stresses. Another case is where an external dummy gage must be used with inside gages. In the latter case the radial pressure inside must still be evaluated without the "dummy" block correction. In studying true-strain values, the dummy strain correction alone must be made since the effect of radial pressure at the test location is part of the study.

For the tests in which they are applicable, the formulas of Mr. O'Brien and Mr. Wetterstrom give the same stress result as our procedure. However, we believe it is highly desirable to consider stresses in a three-dimensional system and not to confuse corrections with actual stresses. Our interpretation is then as follows:

1 The compression of the inside dummy gage block due to pressure results in a false strain reading for the test gage. This is, therefore, a true correction which must be made, and the value for this "apparent strain ϵ_x" was given in the original paper.

2 The effect of pressure on the test location is not a correction but a true stress which must be included in the triaxial stress system. This evaluation must then be made by use of the basic strain equation as follows:

$$\epsilon_1 = \frac{1}{E}\,(S_1 - \mu\, S_2 - \mu\, S_3)$$

in which S_3 becomes the pressure. This should not be interpreted as a correction, but is a true existing stress radial to the surface.

3 Our usual approach then is to make the strain correction, caused by the dummy compression, on all the strain readings in inside gages. This is a true correction, similar to those made for gage factor resistances outside the instrument range, temperature differences, etc. The pressure is then evaluated as an existing stress in a three-dimensional system.

We agree that for the particular purpose of plotting the S/P ratio for inside gages, as is done in some of the PVRC projects, for example, the formula proposed by Messrs. O'Brien and Wetterstrom is a useful short cut. It must be used with considerable caution, however, in the applications described above.

Mr. Zick cautioned about keeping the leads out of the water, which we agree is necessary. In the case of the vertical vessel, the leads were definitely kept above the water. The drum in Fig. 1 of the paper was provided with a gage glass at a location that made it possible to observe the water level if it should rise above a maximum allowable level.

Concerning the Bauschinger effect, we believe that a properly designed pressure vessel would not have stress ranges equal to the range between tension and compression yield points. We believe any strain-aging effect will be insignificant because of insufficient deformation occurring in the pressure vessel.

The particular application of the slow cycles and the time element required involved expanded tubes where there was relative motion between surfaces held together primarily by friction. We believe it is more important in this study than in the major part of the pressure vessel. The statement regarding the behavior of a vessel after the initial proof test only appeared in the first draft and after due consideration was deleted, but not in time to correct the preprints.

Mr. Zick also mentions that the fatigue data do not agree with those obtained by Professor Wilson and asks whether differences in technique can be the answer.

This is quite likely since the weld deposit and basic weld rod may be considerably different from the tensile plate investigations of Professor Wilson. An additional effect of a difference in environment is also a possibility. Other differences of course include the biaxial stress condition in the cylindrical specimens as well as size effect and speed of testing.

Effect of Pressure on the Combustion of Pulverized Coal[1]

By T. T. Omori[2] and A. A. Orning[3]

A theoretical study of heat transfer to a sphere suspended in cold air and suddenly exposed to radiation from a high-temperature source indicated an effect of air pressure which had not been disclosed by previous theoretical studies relating to the ignition of pulverized coal in air suspension. Experimental investigation, in the absence of an extended flame so that the source of radiant heat could be independently controlled, showed an adverse effect of elevated pressures upon completeness of combustion which was much larger than a beneficial effect of increased partial pressures of oxygen. It appeared that increased pressure, through a lower initial heating rate, produced less reactive combustion residues which lost ignition before combustion was complete. Complete combustion could be obtained only by increasing the radiant intensity responsible for ignition.

Introduction

With the appearance of the gas turbine as an economical prime mover, considerable interest has been aroused in the combustion of fuels under pressure. Experience with gas turbines has shown that liquid fuels can be burned under pressure with good efficiency at extremely high burning rates in terms of heat release per unit volume. While pulverized coal can also be burned in such units at very high combustion rates, at least as compared to steam-boiler practice (1),[4] it has appeared more difficult to avoid high combustible losses in the fly ash. It might seem that such losses could be reduced by the simple provision of more combustion space. However, it will appear that added space will not improve combustion unless proper attention is given to flame conditions.

A study of the ignition and combustion of individual particles of pulverized coal under atmospheric pressure (2) showed that the temperature responsible for ignition, presumably through its effect upon the initial heating rate of the fuel as it entered the furnace, had a marked effect upon the ability of residual particles to maintain ignition. Maintenance of ignition was found to be dependent upon the ability of the burning particles to maintain sufficiently high temperatures, certainly higher than 1000 and possibly on the order of 2000 C. Accordingly, except possibly in hot slagging furnaces, burning residues must maintain temperatures considerably above those of their surroundings if good combustion of such particles is to be maintained as they move out of the flame into cooler parts of the furnace.

Since subsequent loss of ignition appears somehow related to the conditions under which ignition occurs, the various theoretical studies of the ignition of pulverized coal are of particular interest. These studies involve the calculation of the temperature history, prior to ignition, of a particle suspended in air and suddenly exposed to a high-temperature source of radiant heat.

Nusselt (3) calculated theoretical ignition times of various fuels on the assumption that a spherical particle received heat by radiation from the furnace walls and lost heat by conduction into the particle and into surrounding gases. However, some of the basic assumptions made were of doubtful validity. An infinite thermal conductivity of the particle, a simplifying assumption facilitating solution, was implied though not explicitly stated. Further, the heating of a particle to its ignition temperature is a transient phenomenon; the assumption of a steady-state heat-transfer coefficient between particle and surrounding gas is subject to question. Nusselt gave his heat flow equation in the form

$$(4/3)\pi a^3 \rho c \frac{dt_s}{d\theta} = \phi\sigma \left[\left(\frac{T_w}{100}\right)^4 - \left(\frac{T_s}{100}\right)^4 \right] 4\pi a^2 - 4\pi a k (t_s - t_0) \qquad [1]$$

where

a = particle radius
c = specific heat per unit weight of particle
σ = radiation constant
ϕ = radiation-angle factor
t_s = particle temperature, deg C (T_s, deg K)
t_w = radiation temperature of furnace walls, deg C (T_w, deg K)
t_0 = temperature of air and of particle at θ equal zero; also, temperature of air at infinite radius
k = thermal conductivity of air
ρ = particle density
θ = time

The term to the left of the equality is the rate of heat absorption, assuming infinite thermal conductivity for the particle. The first term on the right is the rate at which heat is received by the particle due to radiation from the furnace walls, while the second represents loss by conduction from the particle to surrounding air. The second term can be derived by assuming that heat flow to the surrounding air is given by the steady-state equation

$$-4\pi r^2 k \frac{dt}{dr} = 4\pi a k (t_s - t_0) \qquad [2]$$

which integrates to the form

$$t = \frac{a}{r}(t_s - t_0) + t_0 \qquad [3]$$

where

r = distance from center of sphere
t = air temperature at distance r

This indicates that the temperature distribution in the surrounding air was assumed to be proportional to $1/r$.

---

[1] Abstract from a thesis by T. T. Omori in partial fulfillment of the requirements for the degree of Doctor of Science in Chemical Engineering at Carnegie Institute of Technology.

[2] Formerly Member of Staff, Coal Research Laboratory, Carnegie Institute of Technology, Pittsburgh, Pa.; present address: California Institute of Technology, Pasadena, Calif.

[3] Member of Staff, Coal Research Laboratory, Carnegie Institute of Technology, Pittsburgh, Pa. Mem. ASME.

[4] Numbers in parentheses refer to the Bibliography at the end of the paper.

Contributed by the Fuels Division and presented at the Annual Meeting, New York, N. Y., November 27–December 2, 1949, of The American Society of Mechanical Engineers.

Note: Statements and opinions advanced in papers are to be understood as individual expressions of their authors and not those of the Society. Manuscript received at ASME Headquarters January 9, 1950. Paper No. 49—A-72.

Neglecting heat loss due to back radiation, Nusselt simplified his original equation to

$$\frac{c\rho a^2}{3}\frac{dt_s}{d\theta} + k(t_s - t_0) - \phi\sigma a\left(\frac{T_w}{100}\right)^4 = 0 \ldots\ldots\ldots [4]$$

which integrates to

$$t_s = t_0 + \frac{\phi\sigma a}{k}\left(\frac{T_w}{100}\right)^4(1 - e^{-3k\theta/c\rho a^2}) \ldots\ldots\ldots [5]$$

For sufficiently small times this equation may be approximated as

$$t_s = t_0 + \phi\sigma\left(\frac{T_w}{100}\right)^4\frac{3\theta}{c\rho a} \ldots\ldots\ldots\ldots\ldots [6]$$

This indicates an initial rate of temperature rise inversely proportional to the particle radius and to the heat capacity per unit volume of solid but independent of the thermal properties of the gas.

For sufficiently large times the equation may be approximated as

$$t_s = t_0 + \frac{\phi\sigma a}{k}\left(\frac{T_w}{100}\right)^4 \ldots\ldots\ldots\ldots\ldots [7]$$

indicating final temperatures directly proportional to the particle radius and to the intensity of radiation, but inversely proportional to the thermal conductivity of the gas, a quantity which is essentially independent of pressure.

Starting with a heat-balance equation which was essentially the same as Nusselt's, Traustel (4) introduced a correction for the effect of a finite amount of excess air. This was accomplished by assuming that the average air temperature to which the particle was losing heat could be expressed as a function of time and a dimensionless quantity N, the ratio of heat capacities of the associated quantities of air and coal. The constant term t_∞, was replaced by a function of θ and t_s. Integration led to the form

$$\frac{1}{D} = \frac{1 - e^{-n}}{2\left(1 + \frac{1}{N}\right)^2} + \frac{2Z}{(N + 1)D^2} \ldots\ldots\ldots\ldots [8]$$

where

$$D = \frac{2a\phi\sigma}{k(t_s - t_0)}\left(\frac{T_w}{100}\right)^4 \ldots\ldots\ldots\ldots\ldots [9]$$

$$Z = \frac{3\phi^2\sigma^2\theta}{c\rho k(t_s - t_0)^2}\left(\frac{T_w}{100}\right)^8 \ldots\ldots\ldots\ldots [10]$$

$$n = \left(1 + \frac{1}{N}\right)\frac{3k\theta}{c\rho a^2} \ldots\ldots\ldots\ldots\ldots\ldots [11]$$

The limiting forms of Equation [8] are of particular interest. For sufficiently small times, such that the exponential may be replaced by the first two terms of its binomial expansion, the result is identical with that obtained for Nusselt's equation, indicating an initial heating rate independent of the excess amount as well as of the thermal properties of the air. For sufficiently large times, such that the exponential may be neglected, the equation becomes

$$t_s = \phi\sigma\left(\frac{T_w}{100}\right)^4\left[\frac{N^2a}{(N + 1)^2k} + \frac{3\theta}{(N + 1)c\rho a}\right] + t_0 \ldots [12]$$

With infinite excess air, this is identical with the final limiting form of Nusselt's equation, while with finite excess air it indicates a final rate of temperature rise proportional to the ratio of the heat capacity of the coal to the heat capacity of the coal plus the air.

Traustel's analysis involves all of Nusselt's assumptions, both failing to find any dependence upon pressure if proper account is taken of the ratios of heat capacities. Accordingly, it would appear desirable to examine the heat-transfer system more rigorously. The coal particles, suspended in relatively cold gas initially at the same temperature as the coal, are suddenly introduced into a hot furnace. Heat transfer to the particle surface from the furnace can be assumed to be by radiation through transparent gas. Over the interesting range of surface temperatures, the fourth power of the absolute surface temperature can be neglected as compared to that of the source of radiant heat. The rate of heat transfer by radiation to the surface depends only upon the radiation temperature and the extent and character of the particle surface. Under these conditions, the surface can be considered as a heat source of constant strength. Heat loss from the surface is by conduction into the particle and into the surrounding gas.

Though general solutions of the problem as posed have not been found, the solution for a spherical heat source of constant strength with heat diffusing both inward and outward, the two regions having the same thermal properties, has been given by Carslaw (6)

$$t = \frac{Q}{8ark\pi^{3/2}}\int_{(1/2)\sqrt{\rho c/k\theta}}^{\infty}[e^{-(r - a)^2\tau^2} - e^{-(r + a)^2\tau^2}]\frac{d\tau}{\tau} \ldots . [13]$$

where Q is the strength of the spherical source (Carslaw's $q\rho c$).

Integration by parts followed by expansion in a power series, and omission of all but the leading terms leads to an approximation valid within 1 per cent when

$$\frac{(r + a)}{2}\sqrt{\frac{\rho c}{k\theta}}$$

is less than 0.2

$$t = \frac{Q}{4\pi kr} - \frac{Q}{4\pi k}\sqrt{\frac{\rho c}{k\pi\theta}} + t_0 \quad \text{for} \quad r > a \ldots\ldots . [14]$$

and

$$t = \frac{Q}{4\pi ka} - \frac{Q}{4\pi k}\sqrt{\frac{\rho c}{k\pi\theta}} + t_0 \quad \text{for} \quad r < a \ldots\ldots\ldots [15]$$

where t_0 is arbitrarily added as the air temperature at $r = \infty$. For large times the temperature outside the sphere varies as $1/r$ as assumed by Nusselt. With air at 100 C and r slightly greater than a, the minimum time at which the expressions are valid is

$$\theta_m = (79.1)a^2P \ldots\ldots\ldots\ldots\ldots\ldots [16]$$

where P is expressed in atmospheres, and a in centimeters. For a 100- and 200-mesh particle, each in air at 1 atm pressure, these times are 0.0043 and 0.0011 second, respectively.

Accordingly, after a few milliseconds, the inward heat flow becomes comparatively negligible and the outward flow becomes

$$Q_0 = \frac{4\pi ka(t_s - t_0)}{1 - a\sqrt{\frac{\rho c}{k\theta}}} \ldots\ldots\ldots\ldots\ldots\ldots [17]$$

Comparison with the assumption made by Nusselt

$$Q_N = 4\pi ka(t_s - t_0) \ldots\ldots\ldots\ldots\ldots\ldots [18]$$

shows that Nusselt underestimated the outward heat flow by failing to include the factor

$$1 - a\sqrt{\frac{\rho c}{\pi k\theta}} \qquad [19]$$

This factor applies to a system having the same thermal properties within and without the sphere. With dissimilar materials, coal and air, the system may be assumed to have reached a quasi-steady state after a few milliseconds, and the estimate of outward heat flow as a function of the density and thermal properties of, and the temperature drop through, the air is probably fair. Estimated corrections to be applied to Nusselt's assumption are shown in Fig. 1. The corrections are strongly dependent upon pressure and indicate considerably larger values for the smaller times where estimates are not available.

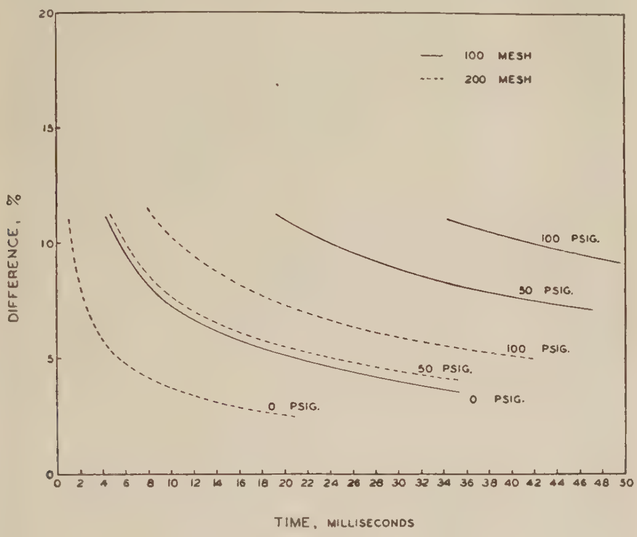

Fig. 1 Corrections to Be Applied to Nusselt's Estimates of Outward Heat-Flow Rate

These estimates have taken no account of relative velocities between coal and air. Rigorous solutions for the simultaneous conduction and convection problem are not available. An approximate solution by Johnstone, Pigford, and Chapin (7) leads to an estimate of outward heat flow

$$q = 0.714\ D_p^{3/2}\ (t_s - t_0)\sqrt{kV\rho c} \qquad [20]$$

where D_p is the particle diameter and V the relative velocity. The rate of convective heat loss appears proportional to the square root of the gas density and hence proportional to the square root of the total pressure.

If there is any appreciable relative velocity between the particle and surrounding gas, an increase in pressure will tend to increase the rate of heat loss from the surface. Owing to the dependence upon temperature drop, this effect starts at zero and increases with time. A pressure effect arising out of the transient character of the heat-flow system should be superimposed. Since the latter, as shown in Fig. 1, is greatest at the start, the combined effect would be a continued influence of pressure upon the rate of heat loss from the particle into the surrounding atmosphere. This loss concerns only part of the heat-transfer system responsible for the initial temperature history of the coal particle. However, it is only this part which should depend upon pressure. Any other dependence must arise out of mechanical action such as restraint of particle swelling or cenosphere (2) formation.

Since the solution for the heat-transfer problem, though not rigorous, indicated a decreased initial heating rate with increased pressure and, since there was a possibility of direct mechanical action, an experimental investigation of the effect of pressure upon ignition seemed highly desirable. The investigation required such "thin" streams of coal particles that ignition resulted from heat transfer from controlled wall temperatures rather than from a flame. Use of various partial pressures of oxygen was indicated to determine any pressure effects resulting from increased availability of oxygen. Provision had to be made for collection of combustion residues in order to determine the effect of ignition conditions upon ensuing combustion.

Apparatus and Procedure

The furnace used for the study of the ignition and combustion of pulverized coal under pressure is shown in Figs. 2 and 3. The furnace was built in a 24-in. length of Shelby tubing, 6 in. ID and $^1/_4$ in. wall thickness. A water-cooling jacket covered the central 13 in. of the tube. The tube was mounted horizontally and provided with a window along the center of the bottom side. A sheet of single-strength window glass was inserted about 1 in. above the pyrex-glass pressure window. A stream of secondary air, introduced between the two glasses and passed through nozzles around the upper glass, further protected the window

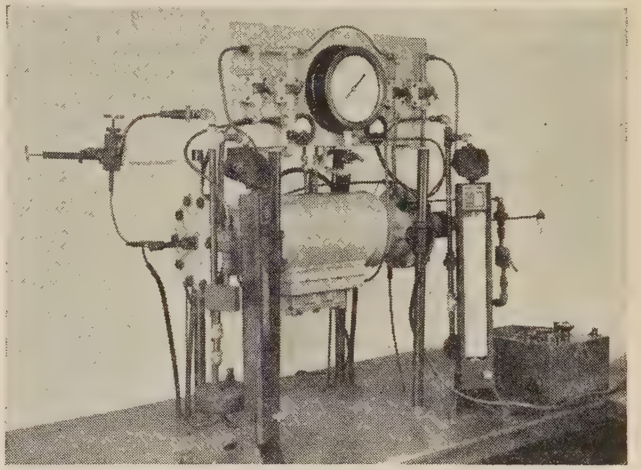

Fig. 2 View of Apparatus

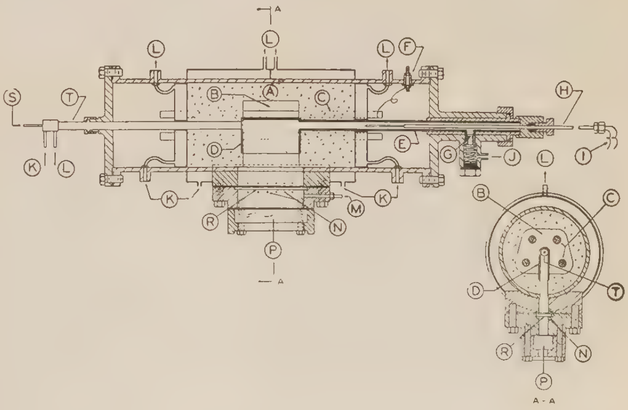

A	Fire-Crete
B	Furnace cavity
C	Globars
D	Alundum shape
E	Retractable refractory tube
F	Insulated lead
G	Filter
H	Retractable thermocouple
J	Gas outlet
K & L	Cooling-water connections
M	Secondary-air inlet
N	Air orifices
P	Pressure window
R	Secondary window
S	Coal inlet
T	Water-cooled tube

Fig. 3 Sections of Pressurized Furnace

from the furnace heat and provided some upward air flow through the combustion space.

The furnace insulation was cast from "Hi-Temperature Fire-Crete" to provide support for the "Globar" heating elements, the water-cooled feed tube, the ceramic outlet tube, and the alundum tunnel which limited the combustion space. Water-cooled end plates held the furnace elements in place and protected the electrical connections in the end compartments. A power input of 4 kw brought the furnace to 1300 C, as indicated by an optical pyrometer sighted upon the inside of the alundum tunnel, but this temperature could not be maintained with full air flow.

The coal was fed from a removable brass cartridge into the primary-air stream by a screw-feed plunger assisted by a vibrator. Suitable isolation valves permitted reloading without depressuring the furnace. Any gas leakage through the plunger packing gland had to be by-passed around the cartridge to keep the coal from packing against the plunger. Orifice meters were used to measure the air-flow rates. The volume flow rates at furnace pressure and room temperature were held constant, 0.0053 cfm for the primary, and 0.177 cfm for the secondary air admitted past the window. These flow rates appeared to be optimum values for carrying the coal through the 5-in. distance across the top of the tunnel and into the outlet tube. The transit time for the coal particles was somewhat uncertain. Based upon jet conditions it was 0.015 sec, while exit conditions would indicate 0.065 sec, varying somewhat with exit-gas temperature. The removable outlet tube, $^1/_2$ in. ID and 18 in. long, had a side opening placed just over a filter plate ahead of the throttling valve used for pressure control. While some combustion residues fell to the observation window, the greater portion was always found in the outlet tube or on the filter plate.

The percentage combustion was determined on the basis of ash analyses. Residues from the filter plate, from the outlet tube, and from the window, if any, were collected and analyzed individually. Any residues falling upon the hot surface of the outlet tube near the furnace cavity had to be discarded and ignored. While such residues had ample time for complete combustion in a temperature-controlled reaction on the hot surface, no appreciable further combustion would have occurred had they been promptly carried out of the hot zone.

A retractable thermocouple was placed in the outlet tube. The thermocouple indication agreed with the optical pyrometer sighted through the window onto the inside of the alundum tunnel when no gas was flowing, but showed substantially lower temperatures with gas flowing. The optical pyrometer indication was taken as the temperature for correlation with percentage combustion.

Experimental Results

The proximate analyses of the coals studied are given in Table 1. The degree of combustion of these coals in various atmospheres as a function of furnace temperature is shown in Figs. 4 through 10. Fig. 4 gives data for 100–140 mesh Pittsburgh seam coal in air at zero, 50, and 100 psig. Figs. 5 and 6 show similar data for Illinois No. 6 and Pocahontas No. 3 seam coals, respectively. The curves, relating the degree of combustion to furnace radiation temperature at constant pressure, show a progressive change in form as the pressure is increased and, to a lesser extent, as the rank of the coal increases. The curve for the Illinois coal at atmospheric pressure is displaced furthest to the left and is everywhere concave downward. The Illinois coal at intermediate pressure and the Pittsburgh and Pocahontas coals at atmospheric pressure show curves with points of inflection within the temperature range explored. The steepest points of the curves for the Pittsburgh and Pocahontas coals occur at temperatures which had previously been shown to be the minimum for uniform ignition of these coals (2). The remaining curves must become concave downward as combustion reaches completion with furnace temperatures above 1100 C. Whatever the significance of this change in the form of the curves, it appears that higher furnace temperatures were necessary to obtain the same percentage combustion with higher furnace pressures or higher rank coals.

TABLE 1 PROXIMATE ANALYSES OF COALS STUDIED

Seam	County	Moisture per cent	Volatile matter, per cent	Fixed carbon, per cent	Ash, per cent	Btu
Pittsburgh	Fayette, Pa.	1.9	33.6	57.0	7.5	13,910
Pocahontas No. 3	McDowell, W. Va.	0.8	15.3	78.3	5.6	14,760
Illinois No. 6	Franklin, Ill.	6.7	33.9	50.3	9.1	12,270

Fig. 7 shows curves for 170–200 mesh as compared to 100–140 mesh Pittsburgh seam coal. While the curve for atmospheric pressure is shifted upward and its point of maximum slope shifted somewhat to higher temperatures, the curves at the higher pressures are not appreciably different from those found for the coarser-sized coal. Similar studies at 50 psig showed insignificant changes for the Pocahontas coal and an upward shift of 5 to 10 percentage points for the Illinois coal. Minus 200-mesh Pittsburgh seam coal was also studied, Fig. 8. It was difficult to obtain reproducible results with this size coal. Based upon a number of duplicate points for the atmospheric-pressure curve, large circles were drawn representing probable error limits. These show that a more involved curve than that shown is not justified. These curves all show points of inflection but the maximum slopes occur at higher temperatures than those found for coarser sizes of this coal.

Figs. 9 and 10 show the effect of higher partial pressures of oxygen with the Pittsburgh seam coal. Proceeding to 50 per cent and 90 per cent oxygen in nitrogen mixtures, the curves, at each total pressure, move somewhat upward and to the left with increasing partial pressure of oxygen. However, the effect is not so marked as the depressive effect of increasing total pressure. The difference would be even greater if the pressure effect was taken at constant partial pressure of oxygen rather than at constant composition. Only at 90 per cent oxygen and 50 psi pressure was the effect great enough to make a substantial change in the form of the curve.

Interpretation of Data

In order to interpret the experimental data, it is necessary to

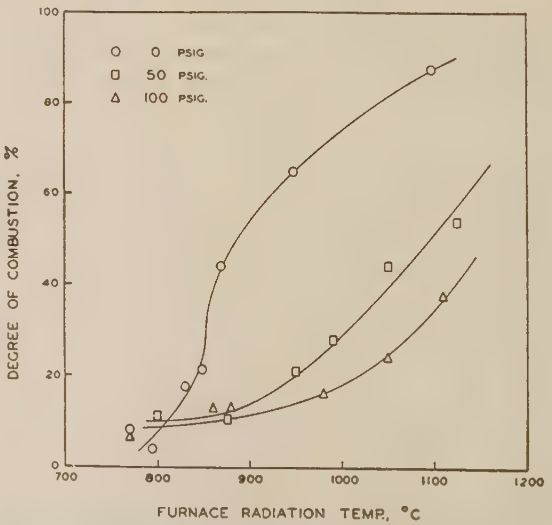

Fig. 4 Degree of Combustion of Pittsburgh Seam Coal
(100–140 mesh. Gas composition: 20 per cent oxygen, 80 per cent nitrogen.)

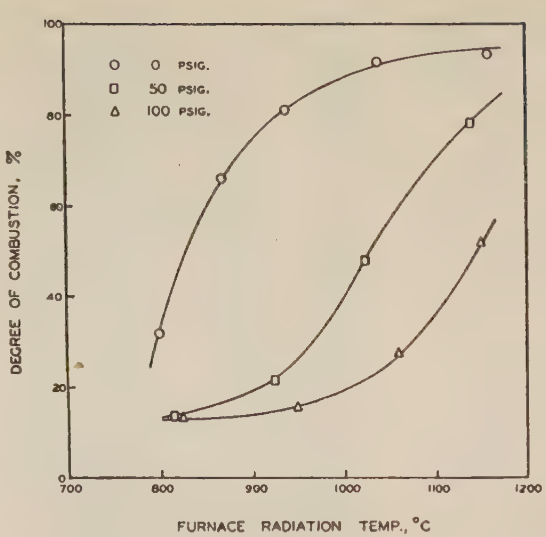

FIG. 5 DEGREE OF COMBUSTION OF ILLINOIS NO. 6 SEAM COAL

(100–140 mesh. Gas composition: 20 per cent oxygen, 80 per cent nitrogen.)

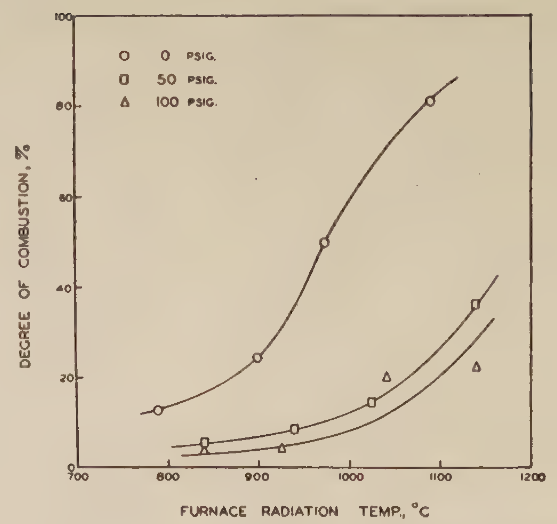

FIG. 6 DEGREE OF COMBUSTION OF POCAHONTAS NO. 3 SEAM COAL

(100–140 mesh. Gas composition: 20 per cent oxygen, 80 per cent nitrogen.)

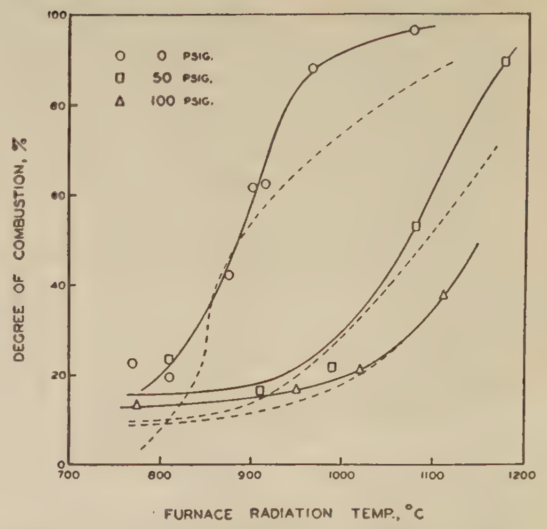

FIG. 7 DEGREE OF COMBUSTION OF PITTSBURGH SEAM COAL

(Solid lines, 170–200 mesh; dashed lines, 100–140 mesh. Gas composition: 20 per cent oxygen, 80 per cent nitrogen.)

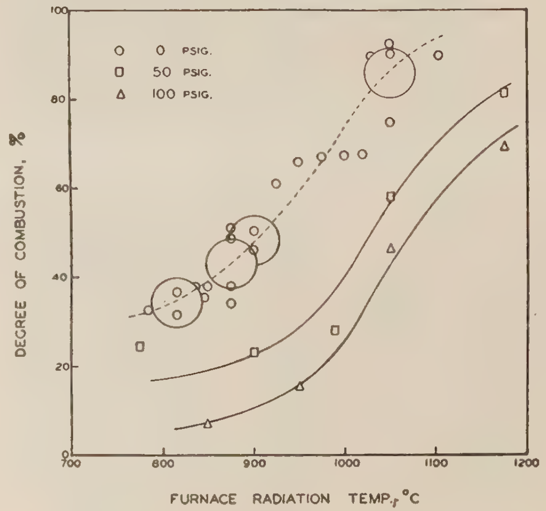

FIG. 8 DEGREE OF COMBUSTION OF PITTSBURGH SEAM COAL

(Minus 200 mesh. Gas composition: 20 per cent oxygen, 80 per cent nitrogen.)

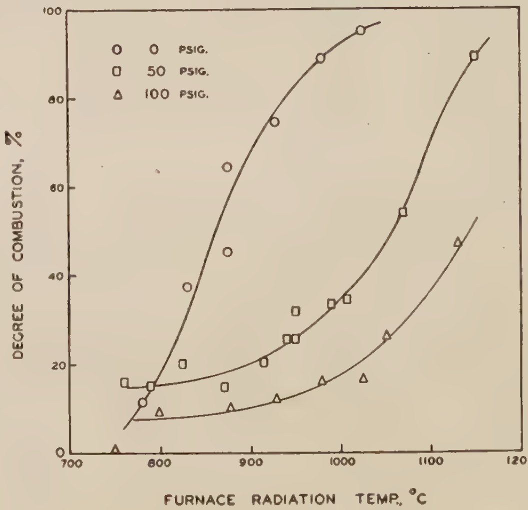

FIG. 9 DEGREE OF COMBUSTION OF PITTSBURGH SEAM COAL

(100–140 mesh. Gas composition: 50 per cent oxygen, 50 per cent nitrogen.)

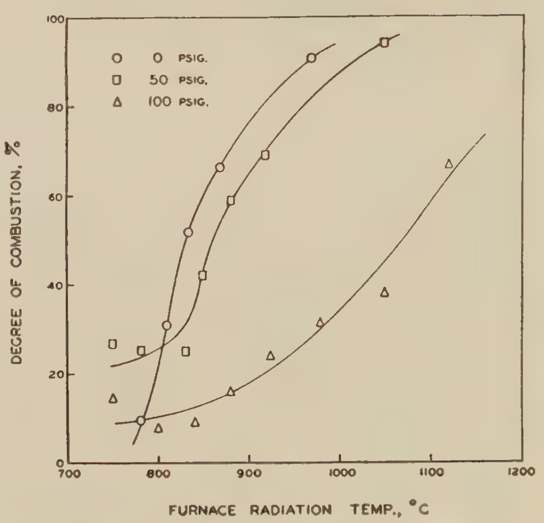

FIG. 10 DEGREE OF COMBUSTION OF PITTSBURGH SEAM COAL

(100–140 mesh. Gas composition: 90 per cent oxygen, 10 per cent nitrogen.)

recognize the conditions under which the coal was ignited. The coal and the primary-gas stream entered together at the water-cooling temperature. The primary air entered as a jet moving through the secondary air which had some opportunity to approach furnace temperature. The coal probably remained within the jet long enough so that the hotter secondary gas had little chance to influence the ignition process. The two gas streams ultimately mixed but never reached the radiation temperature of the furnace walls. Thermocouple indications were always lower than the furnace radiation temperature and, with the furnace at 1200 C, fell to 600 C in the outlet tube where the thermocouple probably came nearest to measuring the gas temperature.

In all instances the active burning times were less than the transit times across the furnace. The burning particles generally were incandescent for only a small portion of the total distance of travel across the combustion chamber. Nevertheless, the degree of completeness of combustion, even at temperature levels giving uniform ignition, increased strongly with increasing temperature, increased moderately with partial pressure of oxygen, but was strongly depressed by increasing total pressure.

It would seem evident that these variables influenced the degree of combustion through an effect upon loss of ignition. The burning particles, failing to consume the oxidizing gas as rapidly as it can be transported by convection and diffusion to the burning surface, fall to a temperature somewhere between that of the immediately surrounding gases and the radiation temperature of the furnace. At the lower temperature the rate of burning is so low as to contribute practically nothing during the limited time of transit through the furnace.

The ability to consume the oxidizing gas as rapidly as it can reach the burning surface depends upon the particle temperature. Since the heat capacity of the particle is relatively small, as compared to its heat of combustion, this temperature is such as to obtain a balance between the rates of heat release and heat dissipation to the surroundings. Heat loss to the immediately surrounding gas should depend upon pressure, but these gases have been heated to a high temperature by the combustion process reducing any heat loss to such a level that it would seem that increasing the partial pressure of the oxygen, making it more readily available to combustion, should easily offset any such effect. This is contrary to the relative effects found. Changing pressure and gas composition should have little effect upon heat loss by radiation. Further, the burning-particle temperatures probably were so high that back radiation from the furnace was not an important factor. The previous studies at atmospheric pressure showed a marked effect of furnace temperature with little difference whether the active burning period ended within the furnace or in an environment at room temperature (2).

However, the temperature required to maintain ignition does depend upon the reactivity of the burning residue; the more reactive the surface the lower the temperature at which the oxidizing gas will be consumed as rapidly as it can reach the surface and the more completely the particle will be expected to burn out before it loses ignition. While the arguments relating the different variables to the balance between heat release and heat dissipation are not rigorous, it appears that these variables could exert their influence through an effect of the initial heating rate of the coal as it enters the furnace upon the reactivity of the combustion residues.

The alternate suggestion that the effect might have been due to an influence upon cenosphere size (8) seems not to be correct, since it was observed qualitatively that the cenosphere size decreases with increasing pressure, while previous work showed that, within the temperature ranges giving uniform ignition, the cenosphere size also decreases with increasing furnace temperature.

Failure to find a marked effect of coal size is of particular interest. Traustel's (4) analysis indicated an optimum size, giving most rapid initial rates of temperature rise; the finer sizes heat less rapidly owing to more intimate contact with the heat capacity of the surrounding air. This is not in contradiction to large furnace practice. Increasing coal fineness produces a shorter and more intense flame, favoring increased rates of heat transfer to the incoming fuel. Any effect of higher resistance to heat flow with finer coal would be overpowered by the increased flame intensity.

Such interplay between the influence of various factors upon ignition with a controlled igniting source and the influence of these factors upon the ability of a flame to supply heat transfer for ignition should be the basis for further experimental investigation. The controlled source with low-density suspensions leads to particulate ignition, each particle igniting independently. Increasing the density of suspension beyond some critical value, collective ignition occurs with the appearance of a definite flame front (2). The influence of fuel character, size distribution, coal-to-air ratio, and aerodynamic factors upon this limit should be investigated. The influence of such factors upon the intensity of radiation from flames should be studied, in order, for instance, to determine to what extent the more intense radiation from a short flame of fine coal can offset the more difficult ignition of a finer coal particle.

Such information will be particularly useful in the development of combustion systems for gas-turbine cycles where good combustion is much more difficult to obtain than in large furnaces. High gas velocities and early introduction of high excess air tend to reduce the rate of heat transfer into incoming fuel. The adverse effect of pressure upon the rate of temperature rise further decreases the reactivity of combustion residues. Corrective measures must involve increased flame intensity held close to the point of entry of fuel into the combustion chamber. Increasing volumes available for combustion will be of no avail unless the wall temperatures are high enough, probably in the slagging range, to avoid loss of ignition.

Summary and Conclusions

1 A theoretical study of heat transfer indicated an adverse effect of pressure upon the ignition of pulverized coal, the rate of heating falling with increased pressure.

2 Apparatus and procedures were devised for studying the effect of total as well as oxygen partial pressure with controlled igniting conditions upon the resulting combustion process. The resulting data confirmed the indication from earlier work at atmospheric pressure that decreased initial heating rates under pressure would lead to less complete combustion.

3 Particularly in application to gas-turbine cycles, good combustion demands high rates of heat transfer to incoming fuel. Increased volume for combustion cannot replace inadequate ignition intensity.

BIBLIOGRAPHY

1 "Experimental Combustion of Pulverized Coal at Atmospheric and Elevated Pressures," by H. R. Hazard and F. D. Buckley, Trans. ASME, vol. 70, 1948, pp. 729–737.

2 "Combustion of Pulverized Coal," by A. A. Orning, Trans. ASME, vol. 64, 1942, pp. 497–508.

3 "Der Verbrennungsvorgang in der Kohlenstaubfeurung," by W. Nusselt, *Zeitschrift Verein deutscher Ingenieure*, vol. 68, 1924, pp. 124–128.

4 "Verbrennung in der Schwebe," by Sergei Traustel, *Feuerungstechnik*, vol. 29, 1941, pp. 1–6, 25–31, 49–60.

5 "Chemistry of Coal Utilization," H. H. Lowry, editor, chapt. 34—"The Combustion of Pulverized Coal," by A. A. Orning, John Wiley & Sons, Inc., New York, N. Y., 1945, pp. 1522–1567.

6 "Mathematical Theory of Conduction of Heat in Solids," by H. S. Carslaw, Macmillan and Company, London, England, 1921, pp. 149–152.

7 "Heat Transfer to Clouds of Falling Particles," by H. F. Johnstone, R. L. Pigford, and J. H. Chapin, University of Illinois Bulletin, vol. 38, No. 43, June 17, 1941.

8 "The Mechanism of the Combustion of Pulverized Fuel," by A. A. Orning—"Papers to Be Discussed at a Conference on Pulverized Fuel," Harrogate, England, June, 1947, Pulverized Fuel Conference Committee, The Institute of Fuel, London, England, pp. 45–64.

Discussion

H. R. Hazard.[5] The authors have done an excellent piece of experimental work in which they have controlled the environment of individual particles of burning coal to determine the influence of pressure, temperature, and oxygen concentration on completeness of combustion. However, the conditions under which the tests were run were far removed from conditions existing in practical combustion chambers, and therefore data must be interpreted carefully if they are to be of practical value.

One factor which may have had an important bearing on the results was the use of constant volumes of primary air and secondary air at all pressures. Thus at 115 psia, the mass flow of air through the test combustion chamber was 7.8 times that at 15 psia, though the coal-firing rate was probably unchanged. This increased the Reynolds number by a factor of 7.8, thus increasing convection heat transfer from the particle to some degree not discussed in the paper. This probably would reduce completeness of combustion, because air temperatures were always considerably below wall temperatures. If the extremely high air/fuel ratios used at 115 psia also resulted in very low exit-gas temperatures, they might account in part for poor combustion at 115 psia. Thus the poor combustion found at 115 psia was not necessarily the effect of pressure alone, but probably reflects the very large increase of air flow with pressure.

The manner in which the authors discuss partial pressure of oxygen suggests that oxygen is more readily available for combustion at higher static pressures because partial pressure of oxygen is higher. Actually, while the mass rate of diffusion is directly proportional to the partial pressure, it is inversely proportional to density, and is, therefore, independent of static pressure. The availability of oxygen can thus be increased only by increasing the proportion of oxygen in the mixture.

The value of the method used was that it isolated and amplified small combustion effects which might have passed unnoticed in combustion chambers designed for practical operation. In the test furnace, a definite effect of pressure was shown which was probably much greater than mathematical analysis would indicate. The effect shown can be regarded as a qualitative demonstration that, under temperature conditions where ignition is barely maintained, and where gas temperatures are below both particle temperatures and wall temperatures, pressure will affect combustion adversely because of heat loss by convection from the particle.

The final completeness of combustion is not necessarily related to the initial heating rate in all equipment, though such a relation did exist in the authors' test equipment for obvious reasons. In that equipment, the radiation temperature to which a particle was exposed was essentially constant throughout its combustion history. Low furnace temperatures thus resulted in early loss of ignition as well as slow ignition, while high furnace temperatures would delay loss of ignition as well as accelerate ignition. Two combustion chambers operated at Battelle have demonstrated that ignition intensity and loss of ignition need not be related. In one, a gas-turbine combustor 30 in. in diam, ignition was extremely rapid, with flame temperatures above 2600 F within 6 in. of the point of coal admission. However, the flame passed close to very cold walls, and was quickly diluted by large quantities of excess air, and combustion efficiency was only 60 per cent. In another investigation, low-volatile coal was burned in a tubular refractory furnace 18 in. diam and 8.5 ft long. Ignition was so slow that at distances of 1 ft, 2 ft, and 3.3 ft from the burner, flame temperatures were only 1935, 2060, and 2240 F, respectively; however, at 6 ft from the burner, both gas temperature and refractory temperature were 2570 F, and at 8.5 ft from the burner 97 per cent of the coal had been burned. In this test, rate of heating was much lower than in the gas-turbine combustor, but combustion took place under nearly adiabatic conditions so that loss of ignition did not occur until burning had practically run its course.

In gas-turbine practice the combustor-inlet and combustor-outlet temperatures, and the volume rate of air flow would be nearly constant over a wide range of pressures. Mass rate of air flow and fuel flow would vary in almost direct proportion to pressure. Because of higher flame density and higher firing rates at higher pressures, it would be expected that flame temperatures would be considerably higher than at low pressures. This would result in higher radiating temperatures for ignition, which might be expected to compensate to a great degree any adverse convection effect. At the end of combustion, gas temperatures in an air-cooled combustor would be higher than wall temperatures by perhaps 1000 F, so that increased convection at high pressures actually should benefit combustion rather than cause early loss of ignition noted under the authors' test conditions.

At Battelle, as referred to by the authors,[6] tests have been run to determine the effect of pressure on combustion in a pulverized-coal flame. Conditions differed from gas-turbine practice in that firing rate was not proportional to pressure, but was nominally constant for all tests, at 120 lb of coal per hr. Flame temperatures of about 2800 F were obtained near the burner. Under these conditions no large effect of pressure was found. If ignition was retarded by pressure, the effect on practical operation was negligible.

Inspection of the authors' curves, Figs. 7 through 10, suggests that if the tests had been run at temperatures of 2500 to 3000 F (1370 to 1650 C), complete combustion might have been obtained at all pressures.

The data presented are of interest principally because they point out that not all the combustion effects resulting from use of high pressures are favorable, and care must be exercised to minimize the unfavorable effects which might be expected.

AUTHORS' CLOSURE

The questions raised by Mr. Hazard involve interpretation of the data presented as an alternative to that presented in the paper. His analysis requires extension of empirical correlations from large-scale experiments to the microscopic scale involved in these studies of combustion of pulverized coal. This requires caution in the absence of rigorous mathematical solutions for either mass or heat-transfer rates in processes involving both convection and diffusion.

Some confusion appears between these attempts to explain loss of ignition and the demonstration of effects of pressure, acting through the initial heating rate, upon the ease of maintaining ignition. Ignition is easily maintained in a hot furnace in the slagging range, but is increasingly difficult with high excess air and rapid cooling of the burning particle by radiation to cold walls. Under the latter conditions the data show that ignition must be effected by a more intense source of radiant heat with increased pressure than at atmospheric pressure in order to maintain ignition. Otherwise, combustion will be less complete and increased combustion space alone will not be adequate.

---

[5] Assistant Supervisor, Battelle Memorial Institute, Columbus, Ohio. Jun. ASME.

[6] Reference is to authors' bibliography (1).

Continuous Gasification of Pulverized Coal With Oxygen and Steam by the Vortex Principle

By H. PERRY,[1] R. C. COREY,[2] and M. A. ELLIOTT[3]

This progress report presents the preliminary results of the gasification of pulverized coal by steam-oxygen mixtures in a vortex reactor. The basic principles of reactor design, and an illustrative example of their application are given. A method of calculating the composition of the gas produced in this reactor is presented and has been checked experimentally. The carbon conversion and the limits of operation have been found to be closely related to the type and uniformity of the coal distribution. A method of improving the operation of the equipment and the quality of the gas by a change in the type of coal distributor appears to be promising.

Introduction

THE manufacture of synthetic liquid fuels by the Fischer Tropsch process, which appears to be a future commercial possibility in this country, requires approximately 30,000 scf of hydrogen and carbon monoxide (synthesis gas) for each barrel of product. Although synthesis gas can be made from oil, natural gas, or coal, it is obvious that if synthetic fuels are to supplement a substantial percentage of the liquid fuels consumed in the future, coal must be looked to as the primary source.

Established gasification processes in this country could supply the synthesis-gas requirements, but since they depend for successful operation on coke, or classes of coal found only in certain geographical areas, there is an urgent need for a process that will operate with any class of coal, thereby removing fuel costs and sources as restrictions.

Many methods have been proposed for the gasification of coal for the production of synthesis gas, and since several excellent reviews of these methods have been published[4,5,6,7] they will be only summarized here for the purpose of showing the advantages and disadvantages of each, and the basis for the present investigation. The methods have been classified by Newman[4] into the four following groups:

1 Fine fuel gasified in a fluidized bed.
2 Fine fuel gasified in a fixed bed.
3 Lump fuel gasified in a fixed bed.
4 Fine fuel gasified in suspension.

The fluidized-bed processes, of which the Winkler is typical, require a highly reactive and noncoking coal or char, a large reactor volume, and a relatively large consumption of oxygen per pound of fuel gasified. The dust loading and the carbon dioxide in the gas produced are high. Where cheap fines of a highly reactive fuel are available, this process might be suitable for use in the United States.

The processes in which fine fuel is gasified in a fixed bed at atmospheric pressure are an extension of the use of air-blown gas producers. The necessity of using either sized coke or anthracite severely limits these processes both economically and from the viewpoint of available raw materials. The Lurgi process, which involves a fixed-bed operation at 20 to 30 atm with small-sized fuel, suffers the same limitations from the standpoint of coal requirements, and, in addition, produces substantial quantities of methane, which is a diluent in the Fischer Tropsch process and would require an expensive reforming process if the product were to be used for synthesis gas.

The fixed-bed processes using lump fuel have the advantage of requiring only a modification in design and operation of existing water-gas generators, and thus the years of accumulated experience with such equipment could be used. However, from a commercial standpoint, high-temperature coke is the only suitable fuel, and this imposes a serious limitation on the use of the conventional water-gas process.

One of the most promising methods appears to be the gasification of pulverized coal in suspension in a stream of oxygen and steam. Favorable characteristics inherent in such a process appear to be: (1) Relatively high specific rates of gasification due to the high specific surface of the fuel; (2) the advantages of a continuous process in ease of control and the need of a small plant size for large throughputs; and (3) the use of any class of coal.

Suspension gasification of pulverized coal may be classified, in general, in two ways, depending upon the path of the coal particle with respect to the gas: (*a*) The coal may flow with one or both of the reacting gases; (*b*) the coal may have relative motion with respect to the reacting gases, thereby making use of the fact that the speed of the diffusion-controlled phases of the gasification reactions is increased.

Early in 1947, when this investigation was under consideration, the latter classification appeared to merit further experimental work. The Fuel Research Board in England,[8] and the Loco-

---

[1] Chemical Engineer, Research and Development Branch, Office of Synthetic Liquid Fuels, Bureau of Mines, Pittsburgh, Pa.

[2] Supervising Engineer, Combustion Research Section, Coal Branch, Bureau of Mines, Pittsburgh, Pa. Mem. ASME.

[3] Assistant Chief, Research and Development Branch, Office of Synthetic Liquid Fuels, Bruceton, Pa. Mem. ASME.

[4] "Oxygen in the Production of Hydrogen or Synthesis Gas," by L. L. Newman, *Industrial and Engineering Chemistry*, vol. 40, 1948, p. 559.

[5] "Future Possibilities in Methods of Gas Manufacture," by A. R. Powell, *Gas Times*, vol. 52, 1947, pp. 164, 167–168, 233–234 and 237.

[6] "Recent Trends in Gas Producer Practice," by T. J. Brozozowski, British Coal Utilization Research Association, Monthly Bulletin, vol. 12, 1948, p. 237.

[7] "Gasification Methods," by M. W. Thring, British Coal Utilization Research Association, Monthly Bulletin, vol. 8, 1948, p. 69.

Contributed by the Fuels Division and presented at the Annual Meeting, New York, N.Y., November 27–December 2, 1949, of The American Society of Mechanical Engineers.

Note: Statements and opinions advanced in papers are to be understood as individual expressions of their authors and not those of the Society. Paper No. 49—A-73.

[8] "Complete Gasification of Pulverized Coal in a Vortex Chamber," Report of the Fuel Research Board for Year ending March 31, 1938, p. 141.

motive Development Committee[9] had investigated the use of a vortex reaction chamber as a combustor. This reactor appeared to have special advantages for use as a gasifier. One other method of suspension gasification had been tried in the Ruhr, Germany. A pilot plant was operated during the war using a process developed by the Heinrich Koppers Company, which used pulverized coal with oxygen and steam under turbulent conditions. It was claimed to be superior to the Winkler process, but sufficient design details and operating data were not available to the Bureau of Mines to evaluate completely its applicability to commercial operation in this country. In April, 1949, the Bureau placed into operation a synthetic-liquid-fuels demonstration plant in Louisiana, Mo., using a modified Heinrich Koppers unit, designed to gasify 25 tons of coal a day for the Fischer Tropsch plant.

The original work on the vortex reactor was done by the Fuel Research Board in England[8] and was used for the production of producer gas with encouraging results. A few tests were also made using steam-air mixtures, and a typical gas composition was as follows: Analysis, per cent by volume, nitrogen free; CO_2 45.1 per cent, O_2 0.8 per cent, CO 20.5 per cent, H_2 30.3 per cent, CH_4 3.3 per cent, carbon conversion approximately 50 per cent.

It was thought that the high carbon dioxide in the gas resulted from high heat losses because of the small size of the unit. The same principle was studied in 1946 at Battelle Memorial Institute for the Locomotive Development Committee[9] with the objective of developing a combustor for pulverized coal. In these tests heat releases up to 4,000,000 Btu per cu ft were observed.

Careful study of the theory and the results of each of these applications of the vortex principle led to the conclusion that it might be adapted to the gasification of pulverized coal with oxygen and steam. Accordingly, the Research and Development Branch of the Office of Synthetic Liquid Fuels, in cooperation with the Combustion Research Section of the Coal Branch, each of the Bureau of Mines, designed and built a pilot plant at the Pittsburgh Station to gasify 100 lb of coal per hr. This size was selected because it was thought to be large enough to have low heat losses and to be small enough to be operated with reasonable quantities of materials.

THEORY OF THE VORTEX

The design of the vortex required a mathematical analysis of the aerodynamics of the unit and of the forces on the particles. The approximate feed conditions are established by the requirements for making a gas of desired composition. To avoid slagging of ash on the walls, the vortex should be designed so that the largest particles do not reach the wall. The outlet radius must be selected such that the ash and unburned carbon will leave at the exit pipe before reaching the floor of the vortex.

The basic law of the free vortex is the conservation of angular momentum. The fluid is introduced tangentially at the wall and its angular momentum is $M_1V_1R_1$, where V_1 is the tangential velocity at radius R_1 (wall radius), and M_1 is mass of the gas. At any other radius R_2 within the vortex the angular momentum must be the same as at the wall, so that $M_1V_1R_1 = M_2V_2R_2$, or $V_2 = V_1R_1/R_2$. Thus since $R_2 < R_1$, as the gas moves toward the outlet in the center of the chamber the tangential velocity increases. Since the fluid also moves radially toward the outlet, its resulting path is a spiral. If a solid particle is introduced into this moving stream, it is accelerated rapidly to the velocity of the stream, and the forces acting on the particle are (1) centrifugal force due to the circular path of the particle, (2) viscous drag of the gas stream, (3) and gravity. If the particle size is such that the centrifugal force and the viscous drag on the particle are equal at some radius within the vortex, and if the particle does not react and change size, it will move downward in a helical path.

If the coal particles are gasified they continually change size. For each size of the coal particle there is a new equilibrium radius—the smaller the particle the nearer the equilibrium radius to the center of the chamber. Thus a reacting particle not only moves in a circular path with the gas stream but also moves across the gas stream seeking new equilibrium radii. This movement of the particle across the gas stream sweeps the products of the reaction from the coal surface, leaving a fresh surface for the reaction to take place.

The method of application of these principles to the design of a vortex for a particular set of feed conditions is shown in the Appendix.

GAS COMPOSITION FROM EQUILIBRIUM CONSIDERATIONS

In the absence of methane in the make gas, the chemical reactions in a mixture of carbon, oxygen, and steam at elevated temperatures are

$$C + O_2 \rightleftarrows CO_2 \quad [1]$$

$$C + H_2O \rightleftarrows CO + H_2 \quad [2]$$

$$C + 2H_2O \rightleftarrows CO_2 + 2H_2 \quad [3]$$

$$C + CO_2 \rightleftarrows 2CO \quad [4]$$

$$CO + H_2O \rightleftarrows CO_2 + H_2 \quad [5]$$

At atmospheric pressure and at the temperatures involved in these calculations, Reaction [1] is assumed to go to completion and the dissociation of steam and carbon dioxide is assumed to be negligible. In the vortex reactor, Reaction [4] was found to take place so slowly as not to influence the final make-gas composition. Equation [5] (water-gas shift reaction) is the only remaining independent equation since Equation [5] = Equation [3] — Equation [2].

The equilibrium composition of the gas produced has been calculated for a variety of conditions from a knowledge of the following:

1 Coal feed rate and ultimate analysis.
2 Gross heating value of coal.
3 Oxygen feed rate and analysis.
4 Steam feed rate and preheat temperature.
5 Heat loss from the unit.
6 Per cent of carbon gasified.

In addition, the following assumptions have been made:

1 Water-gas shift equilibrium is reached (Equation [5]).
2 Boudouard reaction Equation [4], does not influence the final gas composition.
3 The oxidation of C to CO_2 goes to completion.
4 No dissociation of CO_2 and H_2O.
5 No methane is formed.
6 All sulphur in the coal appears as H_2S in the make gas.

The first four assumptions have been found to be essentially correct for the vortex reactor. Small amounts of methane (2–3 per cent) appear in the make gas, but affect the equilibrium calculations only slightly. The form in which the sulphur appears in the make gas has not been determined, but for the low-sulphur coals used in these tests it could appear in any form without changing the equilibrium calculations appreciably.

The per cent of CO_2 in the dry make gas, the per cent steam

---

[9] "Progress Report on Pressurized Combustion of Pulverized Coal," by J. I. Yellott and C. F. Kottcamp, presented by the Fuels Division, Annual Meeting, New York, N. Y., 1946, of THE AMERICAN SOCIETY OF MECHANICAL ENGINEERS.

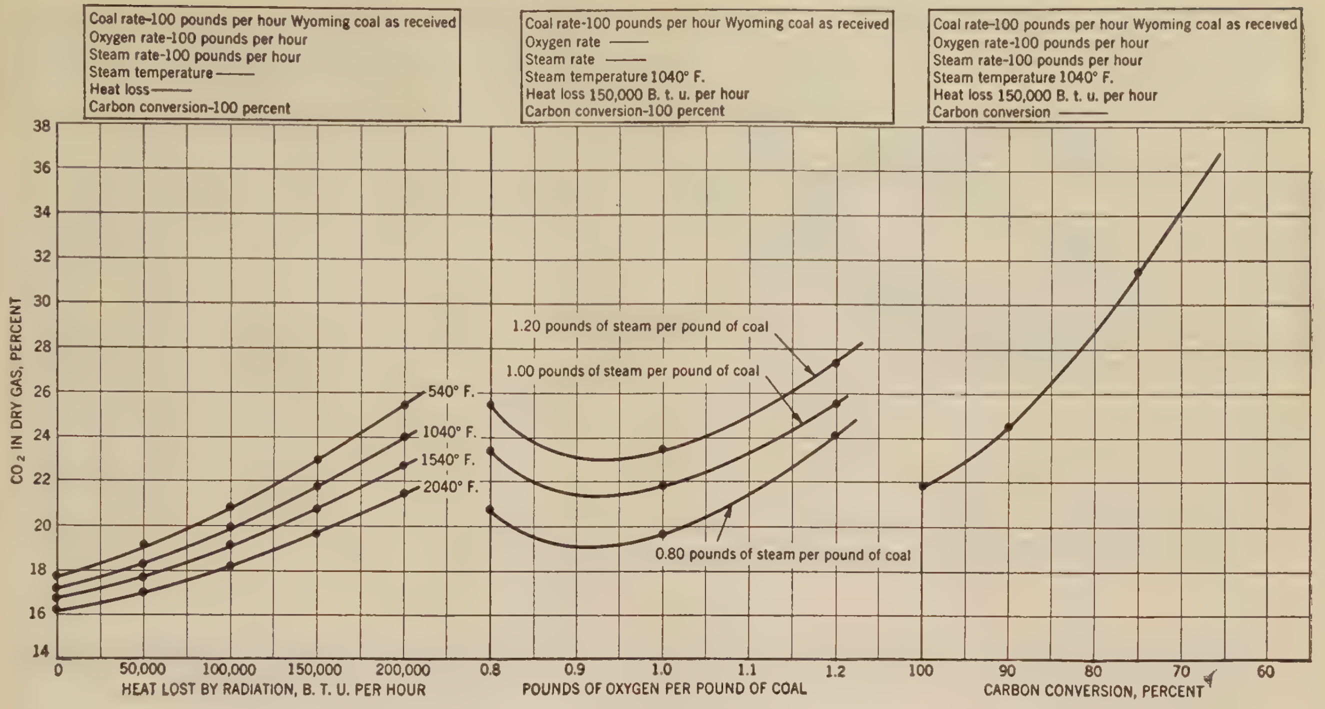

Fig. 1 Calculated Values of Per Cent CO_2 in Dry Make Gas as Function of Process Variables

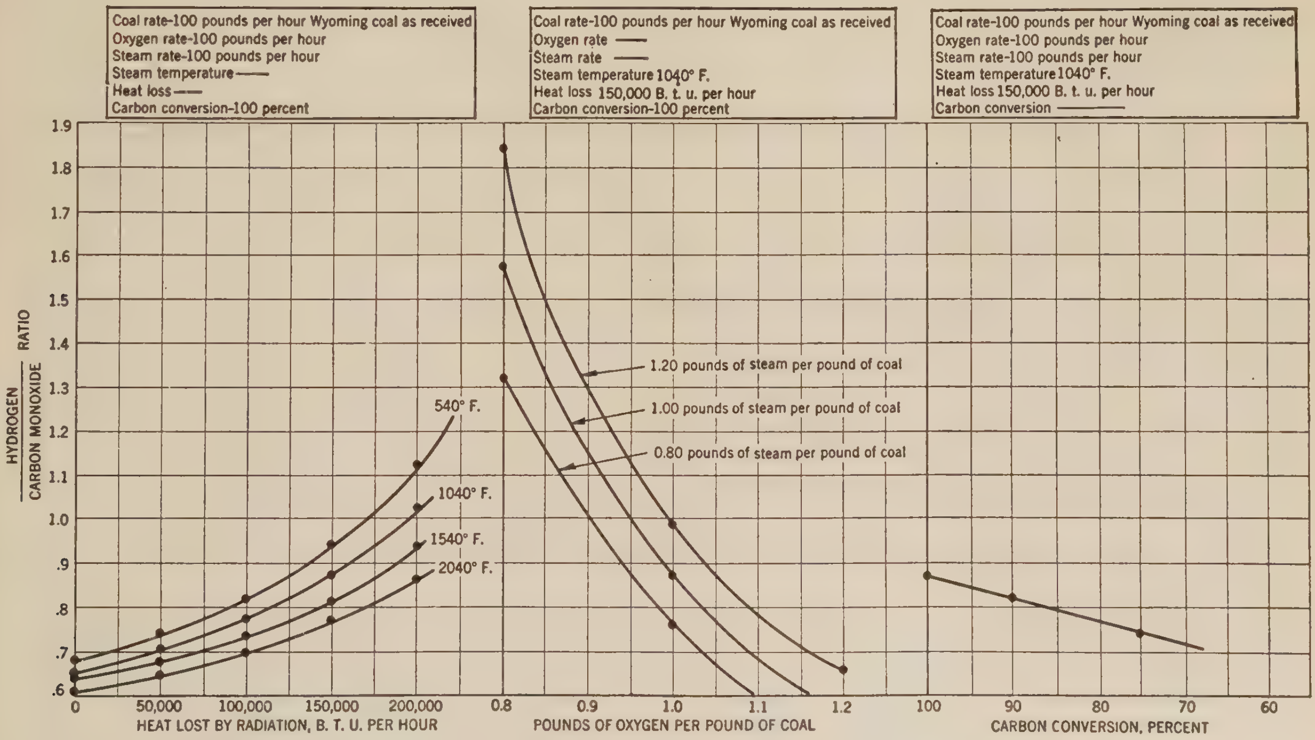

Fig. 2 Calculated Values of H_2-to-CO Ratio in Dry Make Gas as Function of Process Variables

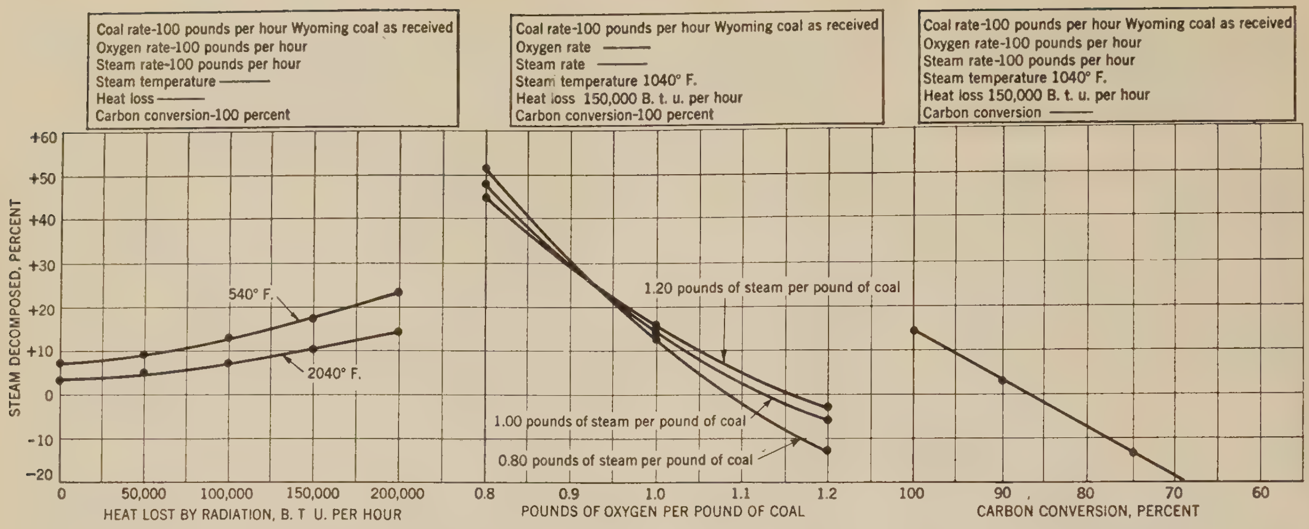

Fig. 3 Calculated Values of Per Cent Steam Decomposed as Function of Process Variables

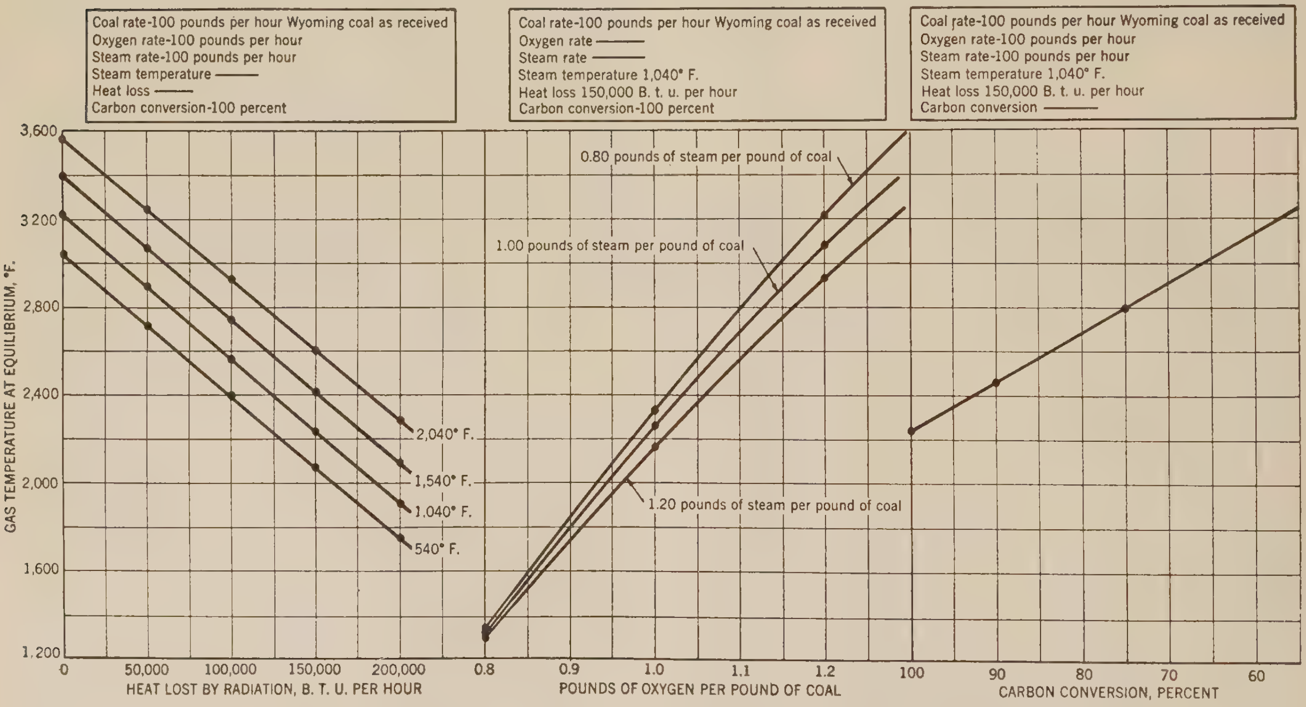

Fig. 4 Calculated Values of Equilibrium Temperature of Gas as Function of Process Variables

decomposition, and the ratio of hydrogen to carbon monoxide have been calculated as a function of the following:

1 Heat lost by radiation.
2 Steam preheat.
3 Oxygen to coal ratio.
4 Steam to coal ratio.
5 Per cent carbon gasified.

The coal used for these calculations was a Rock Springs No. 9, Wyoming coal, the composition of which is given in Table 1.

In the calculations in which the carbon gasified was assumed to be less than 100 per cent, the residue was assumed to be entirely carbon and ash. This agrees with the experimental results.

TABLE 1 ULTIMATE ANALYSIS (3.5 PER CENT MOISTURE), PER CENT

H_2	5.3	O_2	15.4
C	71.6	S	0.9
N_2	1.5	Ash	5.3

Gross heating value = 12,620 Btu per lb

The results of these calculations are shown on Figs. 1, 2, 3, 4. Fig. 1 indicates that the production of CO_2 is a minimum for a weight ratio of oxygen to coal of approximately 0.9. For this feed, therefore, the CO + H_2 is at a maximum. The position of the minimum CO_2 is affected slightly by the steam-to-coal ratio. As the percentage carbon gasified decreases, the CO_2 in the dry make gas increases rapidly.

Fig. 2 shows that as the O_2-to-coal ratio decreases, the H_2-to-CO ratio increases rapidly.

Fig. 3 shows that the percentage of steam decomposed is almost independent of the steam-to-coal ratio, at an oxygen to coal ratio of 0.9.

Fig. 4 shows the effect of the process variables on the exit gas temperature. Increasing heat losses decrease the exit gas temperature, while increasing the oxygen-to-coal ratio in the feed and decreasing the carbon conversion cause the exit gas temperature to increase.

APPARATUS

A flow diagram of the apparatus is shown in Fig. 5. The steam superheater was gas-fired and the heat-transfer surface consisted of two stainless-steel coils. The oxygen, obtained from a Linde Cascade unit, was mixed with the superheated steam and split into four feed lines to the reactor. Pulverized coal was fed from an aerated hopper by a star-wheel feeder to a distributor, and then to the vortex reactor. The gases produced, ash, and unburned carbon, left the reactor at the bottom and passed through a 4-in. refractory-lined pipe. Gas-sampling and temperature measurement were made in this section. The gases and solids were then cooled by a water spray to about 500 F, and part of the solids was recovered with the excess spray water. In the first tests, multiple cyclone separators were used in an attempt to remove the remaining solids, but these proved unsatisfactory and their use was discontinued.

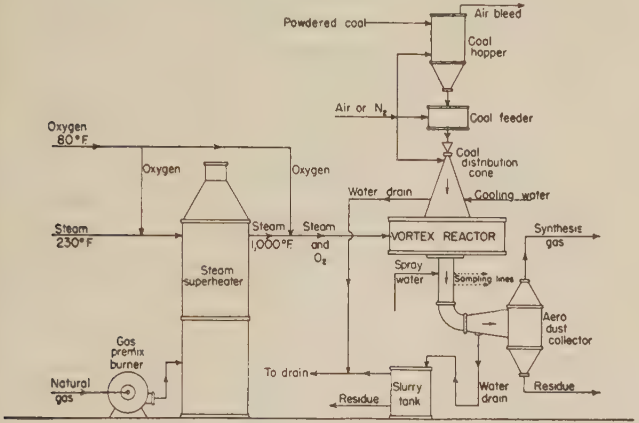

Fig. 5 Flow Sheet for Vortex Gasifier

The construction of the vortex reactor is shown in Fig. 6. Babcock & Wilcox Bafflemix refractory was used to line the outer steel shell, while the slots, top, and bottom of the reaction chamber were cast from B & W Kaocast. Provision for two sight holes and a gas burner was made in the top of the reaction chamber. Movable Pt-PtRh thermocouples were placed in the top and side of the reactor.

The steam and oxygen were measured by means of calibrated sharp-edged orifices. Steam from the service line was throttled to the desired pressure and preheated before measurement at the orifice. The steam temperature leaving the superheater was measured with a Pt-PtRh thermocouple.

The coal hopper held approximately 150 lb of coal and was aerated by an air distributor at the base of the hopper. Mechanical agitation of the coal was tried and resulted in packing of the coal in the hopper. The hopper was connected to the feed mechanism by a standpipe 31 in. high and $4^1/_2$ in. diam. The fluidized coal fell from this standpipe through two openings in the bottom of the pipe (180 deg apart), was picked up by a rotating impeller wheel, carried through 90 deg around the plate and dropped through two outlets to the two feed pipes. A small stream of air was injected into the impeller teeth at both outlet pipes to dislodge the coal. Calibration of the feeder indicated that the coal rate was proportional to the speed of the impeller wheel and varied, at constant speed, by approximately ±3 per cent over 5-min intervals. The feeder and hopper were mounted on scales and connected to the distributor with rubber tubing so that coal-feed rates could be checked regularly.

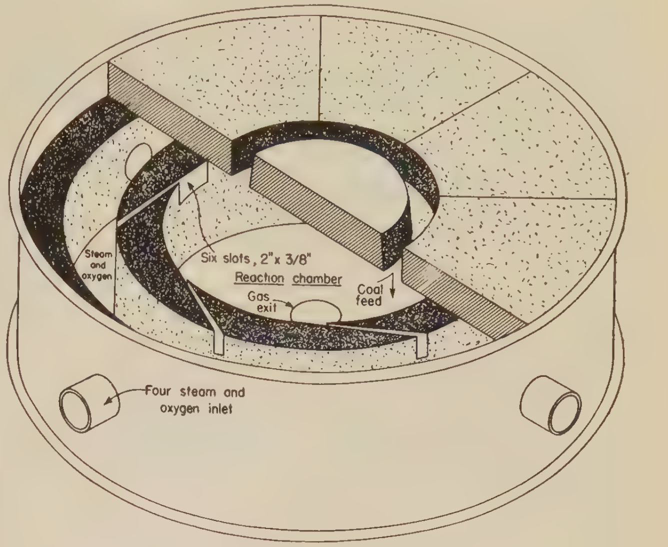

Fig. 6 Schematic Drawing of Vortex Gasifier

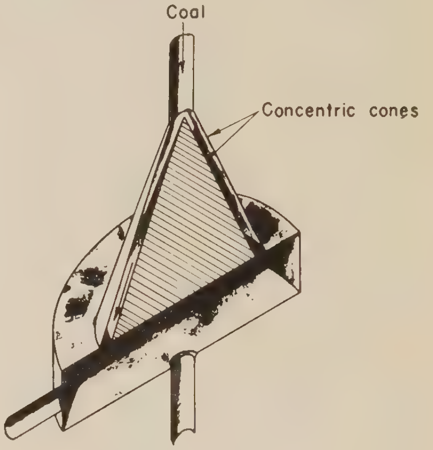

Fig. 7 Cone Distributor

The metered coal fell by gravity to the coal distributor, shown diagrammatically in Fig. 7. The streams of coal were split by the inner cone and passed down the annulus between the two cones into the reaction chamber. The bases of both the inner and outer cones, which were level with the top of the reaction chamber, were water-cooled. A Syntron vibrator was fastened to the distributor to insure steady flow of the coal down the cone. The coal entered the reaction chamber around the entire circumference at a distance 3 in. from the wall of the reactor.

A second type of distributor has been used. In this distributor, the coal, metered as described, falls on a water-cooled spinning plate at the top center of the reactor and is thrown toward the walls in an umbrellalike pattern by the rapidly rotating plate.

EXPERIMENTAL PROCEDURE

Before admitting coal, the reactor was preheated to about 2000 F with a natural gas - air mixture. Primary air was mixed with the gas, and secondary air, preheated in the superheater, was introduced through the slots in the reactor. When the temperature in the reactor reached 1000 F, the secondary air was replaced gradually with the steam-oxygen mixture required for gasification, and heating was continued to 2000 F.

The coal hopper was charged through a $^1/_2$-in. × $^1/_2$-in. screen, with the fluidizing air turned on to prevent packing of the coal while charging. After filling, the charged hopper and standpipe were fluidized for about 30 sec with an air stream introduced at the star wheel.

When the chamber was preheated to the desired temperature, the coal was started into the vortex, and as the temperature of the exit gases rose sharply, the gas-fired burner was removed from the chamber, and the gas and primary air shut off.

A continuous record of the exit-gas temperature was made, and readings of steam flow, oxygen flow, speed of coal feeder, and the weight of the coal hopper were taken periodically. At regular intervals gas samples were taken at the exit pipe with a water-cooled probe.

RESULTS

Limits of Operation. Approximately 45 tests have been made on the unit with the conical coal distributor. In the first eleven tests Bruceton (coking) coal was used and the coal distributor became coked in every test. When Wyoming (noncoking, 70 per cent through 200 mesh) coal was used and when the optimum slot sizes were determined the unit was operated continuously at coal rates between 45 and 85 lb per hr. At both higher and lower rates, unburned coal accumulated on the vortex floor. At the lower rates the small quantities of steam and oxygen required for gasification produced such low tangential velocities in the reactor that the incoming coal stream was not picked up by the gas. At the higher coal rates the density of the incoming coal stream was such that even at the high tangential velocities part of the coal reached the vortex floor before being picked up by the gas.

An attempt to use the same Wyoming coal at rates of 50 lb per hr but with a larger size consist (only 30 per cent through 200 mesh) resulted in an accumulation of unburned carbon in the vortex. One further attempt to use coking coal, under the optimum conditions of slot size and coal-feed rate, also failed.

The limits of operation are a function of the type of coal distributor. In all of the tests in which unburned carbon accumulated on the vortex floor, it was found in irregular piles. At times one side of the vortex was completely clean while the other side was partially filled with coal, indicating uneven feed. With a coking coal, in the cone type of distributor, bridging of coke occurs across the outlet of the distributor, and all of the coal must then be fed through the remaining open area. With a noncoking coal this irregular accumulation of unburned carbon indicates improper design of the distributor. It appears probable that if a noncoking coal were fed uniformly around the circumference by the distributor, the vortex could be operated at both lower and higher coal rates than are now possible.

There is some evidence that this nonuniformity of coal distribution not only affects the operational limits of the unit, but also the composition of the make gas and the gasification efficiency. One test was run for a period of $1^1/_2$ hr without accumulation of unburned coal, but with a known poor distribution of the coal feed. The resulting gas was extremely high in carbon dioxide, and the gasification efficiency was low, when compared to tests with the same feed conditions but with better coal distribution. This nonuniformity of feed also may be the cause of the variation in results for similar feed conditions.

Size Consist of Coal. The vortex was designed so that particles of approximately 325 mesh have an equilibrium radius equal to that of the outlet pipe. The coal actually used in these tests contained 55 per cent by weight of particles smaller than this. For commercial use it is impractical to grind coal with 1 or 2 per cent on 100 mesh and have much less than 45–55 per cent through 325 mesh. To approach practical operating conditions, the usual commercial grind of pulverized coal was used, even though it was realized that the unburned carbon might be high. To reduce the carbon loss caused by the high percentage of fines the outlet diameter of the vortex would have had to be reduced below 4 in., causing a pressure rise in the vortex and excessive velocities in the exit pipe (see Appendix).

Calculation of Results. All of the data have been calculated from an elemental balance on the unit using the feed rates of steam, coal, and oxygen, and the composition of the dry make gas. The residue from all tests consisted essentially of carbon and ash, and if the small amounts of hydrogen and oxygen in the residue are neglected, the calculations are affected by less than 0.5 per cent. From the elemental balance, the moles of dry gas per hour, moles of steam per hour, and the amount of unburned carbon per hour can be calculated. To check the calculated values, it would have been desirable to determine one of these streams experimentally, and some attempts were made to measure the humidity of the make gas and to collect and weigh all of the residue. Both determinations proved to be rather difficult, and, because of the multitude of other problems, were deferred until a gas approaching the desired composition is produced. However, even without a check on the absolute values of these calculated quantities, certain trends appear and are reported.

Data. In the equilibrium calculations, made to determine the composition of the make gas that could be expected with this reactor, the assumption was made that the water-gas equilibrium shift would be satisfied. In Fig. 8 the values of the equilibrium constant, calculated from the make-gas composition, are plotted against the values of the constant corresponding to the measured exit-gas temperature. About one half of the points agree almost exactly, and the remainder are scattered almost equally above and below the line. Considering the errors in temperature measurement and the errors possible in calculations, based on an experimentally unchecked elemental balance, this agreement is excellent.

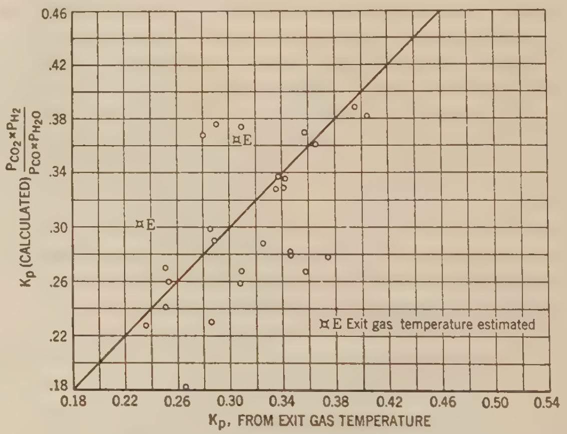

FIG. 8 COMPARISONS OF CALCULATED AND THEORETICAL WATER-GAS EQUILIBRIUM CONSTANTS

The other assumption made concerning equilibrium in calculating the theoretical gas composition was that the rate of the $CO_2 + C \rightleftarrows 2CO$ reaction would be slow enough not to influence the final gas composition. The equilibrium constant for this reaction was calculated as described and is plotted in Fig. 9.

There is considerable scatter of the experimental values but they are roughly $^1/_{60,000}$ of the equilibrium values corresponding to the exit-gas temperature, indicating that the rate of this reaction is such as to influence only slightly the final gas composition.

Thus the major assumptions made in calculating gas compositions, i.e., the water-gas-shift equilibrium is reached, and the effect of the Boudouard reaction is negligible, have been justified for this reactor. It was shown, in the calculation of the equilibrium gas composition, that if the foregoing assumptions are correct, and if the amount of carbon gasified and the heat losses are known for a given set of feed conditions, the make-gas composition can be calculated. Estimate of the heat losses can be made for any size of unit. The per cent of carbon gasified is a characteristic of the type of reactor and is the variable which will determine the practicability of the reactor for gasification purposes.

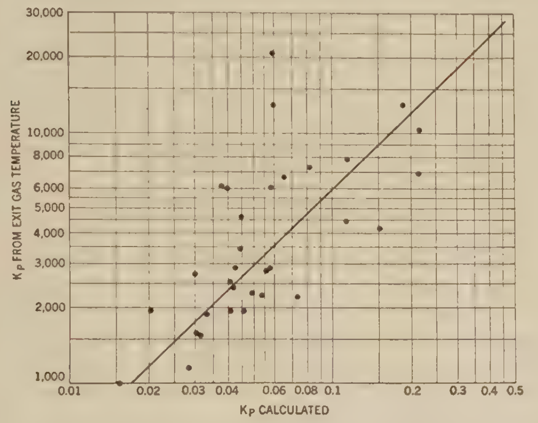

FIG. 9 COMPARISON OF CALCULATED AND THEORETICAL EQUILIBRIUM CONSTANTS FOR THE $CO_2 + C \rightleftarrows 2CO$ REACTION

The data for the test with the cone-type distributor are presented in Table 2. For this table the percentage heat loss is defined as

$$\frac{\text{Heat lost by radiation, convection, etc.}}{\text{Enthalpy in feed — heat of combustion of unburned carbon}}$$

The high percentage of carbon dioxide in the synthesis gas appears to be a result of the excessive heat losses occurring in this small unit. Figs. 10 and 11 show the effect of percentage heat loss on the production of carbon monoxide plus hydrogen, and carbon dioxide per pound of coal gasified. At higher throughputs, the percentage heat loss was reduced and the carbon monoxide and hydrogen produced per pound of coal increased, while the carbon dioxide produced per pound of coal decreased. The dotted curves in these figures are for those tests in which the steam-to-coal ratio was low, and in which the gas produced had a carbon monoxide-to-hydrogen ratio of 2:1 instead of the 1:1 ratio observed in other tests. The relatively high yield of carbon

TABLE 2 DATA FROM TESTS ON CONE-TYPE DISTRIBUTOR

Test No.	S No.	Coal Rate pds/hr	pds O_2 per pd coal	pds H_2O pd coal	% C gasified	Exit gas temp.	Gas made cuft/hr	GAS ANALYSIS			% heat loss
								CO_2	CO	H_2	
43	4	44.8	.905	.800	49	2240	724	50.3	19.5	20.6	36.1
43	3	49.2	.931	.742	52	2320	818	48.0	23.6	18.8	35.9
28	3	53.8	.995	1.222	63	2270	1050	49.6	20.8	24.4	31.1
28	5	52.0	1.023	1.277	66	2340	1070	48.0	22.6	24.4	29.4
28	4	50.3	1.059	1.280	70	2330	1089	47.8	22.4	23.4	30.0
43	2	49.2	1.063	.408	57	2495	888	49.6	23.4	14.8	41.3
43	7	48.0	1.075	.785	62	2375	931	49.2	25.0	19.5	37.3
43	6	48.0	1.077	1.152	65	2370	1027	46.9	22.7	21.2	27.2
30	2	48.0	1.096	1.375	67	2285	996	48.8	24.6	22.6	29.4
30	1	46.8	1.128	1.390	67	2235	942	53.0	21.6	20.2	32.4
30	3	46.0	1.137	1.440	74	2315	1065	46.6	25.2	23.0	29.8
18	AV	46.3	1.157	1.378	70	2360	962	53.7	20.9	22.3	31.3
16	4	46.0	1.197	1.165	74	2180	1030	53.2	19.0	19.6	37.8
43	1	42.0	1.245	.881	73	2410	966	50.2	21.6	15.2	38.0
16	2	50.0	1.292	1.580	76	2150	1130	58.4	15.8	18.2	39.4
16	3	46.0	1.405	1.717	86	2285	1202	55.2	17.2	18.4	35.9
16	5	46.0	1.452	1.165	90	2540	1207	54.4	21.8	17.6	36.7
30	4	48.0	1.452	1.373	85	2860	1173	55.8	23.6	16.6	30.8
38	2	67.0	1.157	.963	69	2570	1442	47.2	26.6	20.4	30.9
38	4	60.0	1.280	.453	83	2680	1345	44.0	40.4	14.0	35.5
35	3	65.0	1.304	1.232	80	2880	1553	50.6	26.4	20.8	27.2
42	5	84.0	.804	.787	47	2360	1326	43.4	24.2	26.2	27.5
42	6	82.0	.823	.326	50	2465	1328	38.8	32.6	25.6	31.7
42	7	82.0	.912	.843	56	2400	1533	40.6	28.8	25.6	26.9
42	4	84.0	.910	.325	55	2570	1387	38.0	38.8	19.8	31.8
42	1	82.0	.916	.864	50	2555	1220	53.4	23.6	22.2	31.[illegible]
33	1	80.0	.989	.970	61	2315	1537	44.2	27.8	24.0	28.5
42	2	84.0	1.000	.772	59	2750	1442	49.6	26.6	20.2	29.6
42	3	84.0	1.012	.318	60	2750	1433	43.2	38.4	17.6	34.1
35	2	76.0	1.015	1.047	63	2480	1480	48.8	23.0	24.6	31.0
37	4	76.0	1.035	.905	67	2595	1660	42.5	27.0	24.7	25.8
33	2	78.0	1.100	.994	73	2470	1730	41.8	32.2	23.2	26.2
33	3	76.0	1.142	1.055	75	2620	1791	40.9	31.7	23.3	25.1

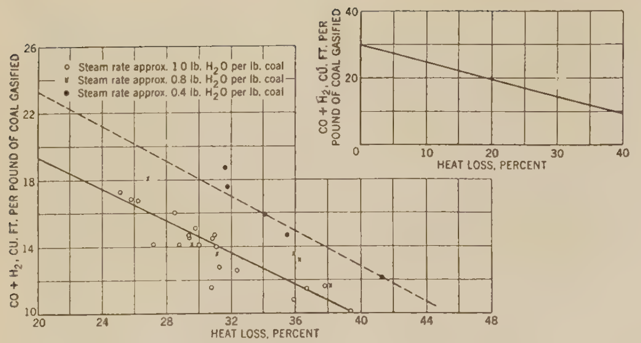

Fig. 10 Effect of Heat Loss on Production of CO + H_2

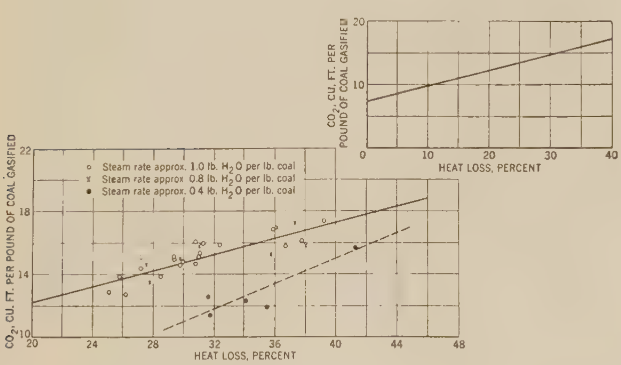

Fig. 11 Effect of Heat Loss on Production of CO_2

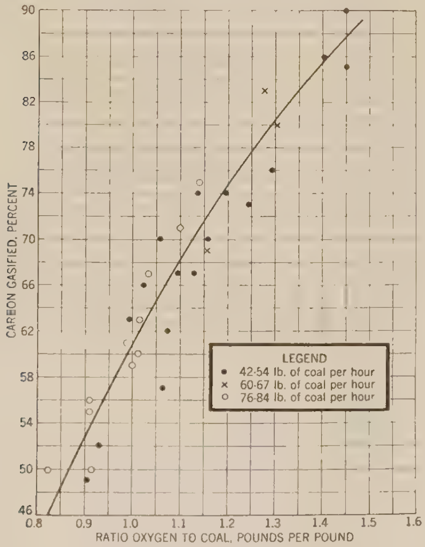

Fig. 12 Per Cent Carbon Gasified as Function of Coal Rate and Oxygen-to-Coal Ratio

monoxide and hydrogen per pound of coal at these conditions probably resulted from the higher temperatures in the reaction zone in the presence of low steam concentrations, and the formation of a higher carbon monoxide-to-carbon dioxide ratio in the initial oxidation step.

In the inserts in Figs. 10 and 11 the data are replotted and extrapolated to zero heat loss. Under adiabatic conditions, it appears that a yield of 30 to 40 cu ft of hydrogen and carbon monoxide per lb of coal gasified would be obtained, which compares favorably with other gasification processes, and the synthesis gas would contain 15 to 20 per cent carbon dioxide. Thus in large units, where the heat losses are small, the vortex may be expected to produce a satisfactory yield and quality of synthesis gas.

Fig. 12 indicates that for the conditions tested and with the cone distributor, the per cent carbon gasified is independent of the coal rate and almost directly proportional to the pounds of oxygen per pound of coal in the feed. The proportionality between the oxygen in the feed and the carbon converted is evident, since the oxygen concentrations in the make gas were always less than 1 per cent regardless of the quantity of oxygen fed to the reactor. The nearly constant percentage of carbon gasified for different throughputs is probably a function of the hydrodynamics of the unit. As the coal rate was increased the steam and oxygen were increased proportionately and, since the same slot sizes were used in all tests, the tangential wall velocity increased with the increasing throughputs. Increased values of the tangential wall velocity result in smaller carbon particles having an equilibrium radius within the vortex. However, the radial velocity of the fluid in the vortex also increases with increasing throughputs and causes a larger-sized particle to leave the vortex. Calculations indicate that by keeping constant the steam-coal-oxygen ratio, increasing the throughput from 40 to 80 lb of coal per hr should decrease the carbon conversion between 2 and 4 per cent, for the inlet slot conditions used in these tests. This is within the experimental error of measurement.

The carbon conversions range from 50 to 75 per cent for the oxygen-to-coal ratios that are feasible for gasification, and this value is low when compared to the 95 per cent reported for the German Koppers dust process. However, as was noted previously, the vortex was tested with a size consist of coal such that low carbon conversions would be expected. With the cone-type distributor, it was found impossible to operate with a coarser coal.

In some tests, gas samples were taken at different radii within the vortex in an attempt to study the order in which the chemical reactions take place. These data are plotted in Figs. 13, 14, 15, and 16. Although the data were taken for varying feed conditions, the differences in results cannot be explained by this alone, and probably were caused by irregular distribution of the coal in the vortex by the cone distributor. Despite these differences, however, it appears that:

1 The oxygen reacts with volatiles in the coal and with the carbon to form CO_2 and H_2O, thereby minimizing tar formation.

2 Only when the oxygen has been consumed does the steam-carbon reaction begin.

There are several possible methods of increasing the carbon conversion in the vortex. A constant coal-feed rate and a uniform distribution of the coal appear to be effective, and increasing the tangential velocity for the same throughput also should increase the carbon conversion. Since the reaction of carbon with oxygen is extremely rapid and apparently goes to completion, any method of increasing the rate of the steam-carbon reaction will increase the carbon conversion, and this can be accomplished by having a higher density of carbon in the zone of the steam-carbon reaction. To accomplish this the coal must be fed near the center of the vortex and be thrown out toward the walls. One other possible method of increasing the carbon conversion appears to be increasing the depth of the vortex chamber. From Equation [29] (Appendix), which considers only the aerodynamics of the reactor, as the depth of the reaction chamber, h, is increased the size of the particle, a, which will remain in the vortex becomes smaller, and the carbon conversion should be increased. In addition, increasing h increases the time available for gasification and should aid in increasing the carbon conversion

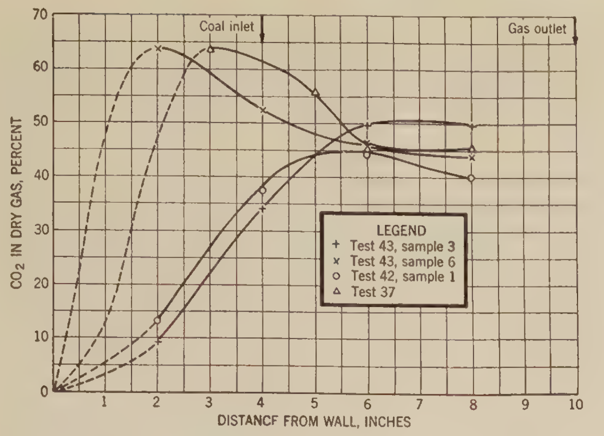

FIG. 13 PER CENT CO_2 IN DRY GAS AT VARIOUS POSITIONS IN VORTEX

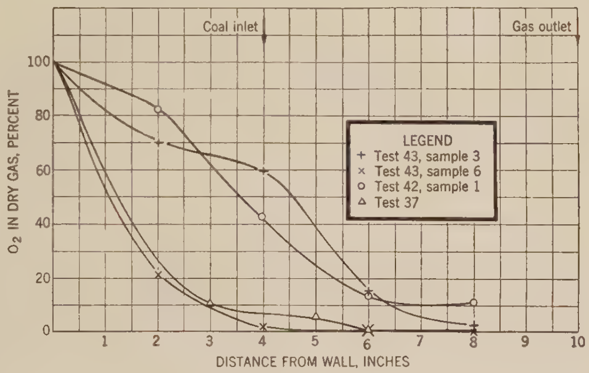

FIG. 14 PER CENT O_2 IN DRY GAS AT VARIOUS POSITIONS IN VORTEX

Several preliminary tests were made with the spinning-plate coal distributor in which the coal is introduced near the center of the reaction chamber. This distributor was designed to increase the carbon density near the center of the reactor, to increase the total path of the carbon particle, and to give more uniform coal distribution. Mechanical difficulties with the driving mechanism caused early shutdowns in every test, but the composition of the gas was much improved over that obtained with the conical coal distributor. Further tests are planned when the mechanical problems are overcome.

CONCLUSIONS

These tests confirm the assumption that from the knowledge of the feed conditions, heat losses, and the per cent carbon gasified, the approximate composition of the gas produced can be predicted for this reactor. In these tests the carbon conversions were low, and the resulting make gas was high in carbon dioxide. For a given set of feed conditions any means of increasing the carbon conversions will improve the quality of the gas. In order for this reactor to be commercially feasible the carbon conversions must be increased.

The results of these initial tests show that the uniformity and the method of coal distribution strongly influence the amount of carbon conversion, the quality of the gas produced, and the maximum and minimum throughputs. The conical coal distributor was unsatisfactory in that the coal was fed nonuniformly near the outer perimeter of the vortex. The few preliminary tests with the spinning-plate distributor suggest that these difficulties have been overcome.

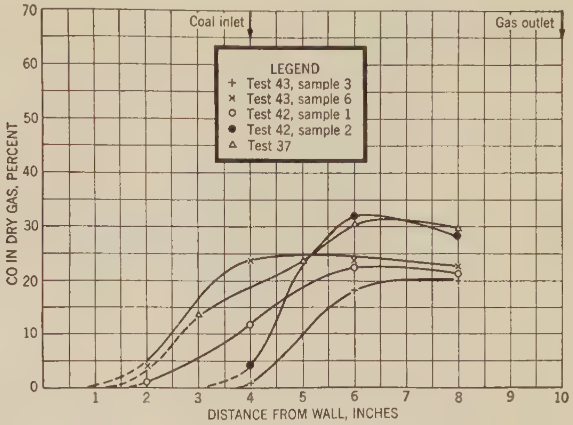

FIG. 15 PER CENT CO IN DRY GAS AT VARIOUS POSITIONS IN VORTEX

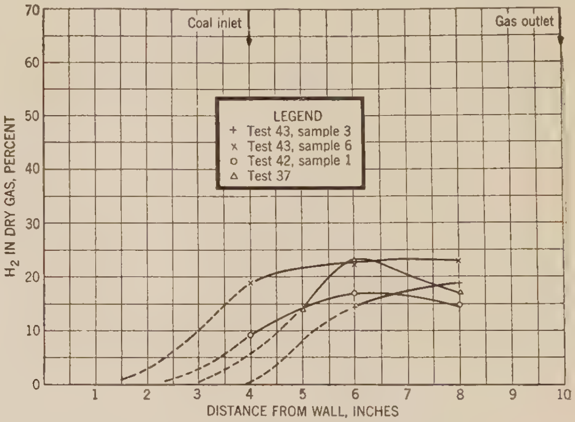

FIG. 16 PER CENT H_2 IN DRY GAS AT VARIOUS POSITIONS IN VORTEX

Other possible methods of increasing the carbon conversion are available, i.e., (1) using a coarser size consist of coal with the spinning-plate distributor, (2) increasing the height of the reaction chamber, and (3) increasing the tangential velocities at constant coal rates. Further tests are planned with the new distributor when the mechanical difficulties have been overcome, and the effect of the foregoing variables on the carbon conversion will also be investigated.

Appendix

NOMENCLATURE

a = particle radius, ft
b = settling velocities of particles, fps
h = depth of vortex chamber, ft
M_1 = mass of inlet gas, lb per hr
M_2 = mass of inlet gas plus coal, lb per hr
r = radius at any point in vortex, ft
R_1 = radius of vortex at inlet, ft
R_2 = radius of vortex at outlet, ft
t = gasification time, sec
u = radial velocity of gas at any radius r, fps
U_1 = radial velocity at R_1, fps
U_2 = radial velocity at R_2, fps
v = tangential velocity of gas at any radius r, fps
V_1 = tangential velocity at R_1, fps
V_2 = tangential velocity at R_2, fps

Z_1 = volume of gas at R_1, cfs
Z_2 = volume of gas at R_2, cfs
η = viscosity of gas in vortex, $\dfrac{\text{lb}}{\text{sec-ft}}$
ρ = density of coal, lb per cu ft

Problem Considered

The following treatment is an extension of the analysis by Hurley[10] of the forces on a particle in a vortex. To illustrate the application of the theory to the design of a vortex, a particular set of feed conditions will be considered as follows:

$$\left.\begin{array}{l}\text{100 lb per hr of oxygen}\\ \text{100 lb per hour of steam}\end{array}\right\}\ \text{600 F}$$

100 lb Wyoming coal per hr—as received
Size consist of coal, 70 per cent through 200 mesh, 1–2 per cent on 100 mesh

Inlet Conditions. The basic law of the ideal free vortex is the conservation of angular momentum

$$M_1V_1R_1 = M_2V_2R_2 \qquad [6]$$

The horizontal forces on a particle at any radius, r, in the vortex are

$$\text{Centrifugal force} = \frac{(4/3\pi a^3\rho)v^2}{r} \qquad [7]$$

$$\text{Viscous drag} = 6\pi a\eta u \qquad [8]$$

When the forces are balanced

$$v^2 = \frac{9\eta u r}{2a^2\rho} \qquad [9]$$

From Equation [6] and for ρ = 130 lb per cu ft

$$V_1{}^2 = 3.46 \times 10^{-2}\,\frac{\eta u r^3}{R_1{}^2a^2}\left(\frac{M_2}{M_1}\right)^2 \qquad [10]$$

Using a viscosity which is the average for the inlet and outlet conditions: η = 0.043 centipoises = 2.89×10^{-5} lb/sec-ft. For the selected feed $M_1 = 200$, and $M_2 = 200 + 100 = 300$ lb and Equation [10] becomes

$$V_1{}^2 = 2.25 \times 10^{-6}\,\frac{ur^3}{a^2R_1{}^2} \qquad [11]$$

If no change in temperature or total number of moles of gas occurred in the reactor, by a material balance across cylinders with radii r and R_1

$$ur = U_1R_1 \qquad [12]$$

For this feed there are 8.7 moles of gas per hr at the inlet and 14.1 moles of gas per hr at the outlet. The average is 11.4 moles per hr. The temperature change is from 1060 R to 2960 R, therefore

$$ur = \frac{2960}{1060} \times \frac{11.4}{8.7}\,U_1R_1 = 3.66\,U_1R_1 \qquad [13]$$

This correction for the change in the number of moles will be approximately the same for any set of feed conditions suitable for gasification, and the correction for temperature change will depend largely upon the amount of steam preheat.

From Equations [11] and [13]

$$V_1{}^2 = 8.24 \times 10^{-6}\,\frac{U_1r^2}{a^2R_1} \qquad [14]$$

If the maximum-size particle permitted in the feed is 100 mesh then a = 0.000246 ft, and Equation [14] becomes

$$V_1{}^2 = 1.362 \times 10^2\,\frac{U_1r^2}{R_1} \qquad [15]$$

But U_1 is equal to the inlet feed volume divided by the wall area

$$U_1 = \frac{Z_1}{2\pi R_1h} \qquad [16]$$

Substituting in Equation [15]

$$V_1{}^2 = 21.7\,\frac{r^2Z_1}{R_1{}^2h}$$

or

$$V_1 = 4.66\,\frac{r}{R_1}\sqrt{\frac{Z_1}{h}} \qquad [17]$$

To keep a 100-mesh particle off the wall $r < R_1$, and this is true for any value of R_1. For the limiting case of $r = R_1$, Equation [17] becomes

$$V_1 = 4.66\sqrt{\frac{Z_1}{h}} \qquad [18]$$

This equation is approximately true for any throughput if the ratio of steam to coal to oxygen is 1:1:1, and the steam-oxygen mixture is at 600 F. The values of V_1 required at different throughputs and for different chamber depths are shown in Fig. 17.

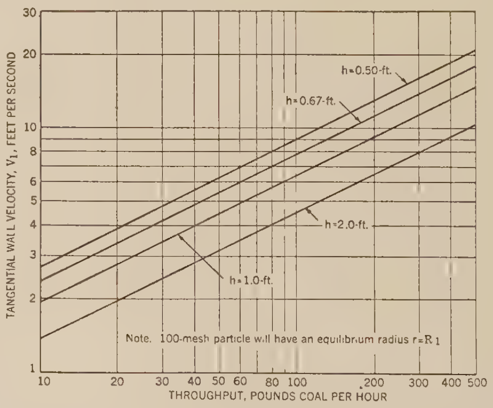

Fig. 17 Required Tangential Wall Velocity as a Function of Throughput at Different Chamber Depths

For the feed conditions selected, i.e., 100 lb per hr each of coal, oxygen, and steam, and with the steam and oxygen at 600 F, Z_1 = 1.865 cfs, and from Equation [18]

$$V_1 = \frac{6.36}{\sqrt{h}} \qquad [19]$$

The value of R_1 cannot be determined from this relation, but a value can be established if the outlet conditions are considered (to be mentioned).

Any value of h may be chosen for the selected feed conditions if the tangential velocity at the wall, V_1, required to satisfy Equation [19] can be obtained with the reactor. However, other physical factors determine h. The depth of the chamber must be such that the particle will leave the chamber before it reaches the vortex floor. The settling velocities of the particle and the gasification time must be known since then

---

[10] "Some Factors Affecting the Design of a Small Combustion Chamber for Pulverized Fuel," T. F. Hurley, *Institute of Fuel*, vol. 4, 1931, p. 243.

$$h = bt \quad \ldots\ldots \quad [20]$$

The settling velocities, b, of coal particles of various sizes can be calculated from Stokes' law if the particles are assumed to be spheres and the viscosity of the fluid is known. These values are plotted in Fig. 18 for a viscosity of 0.043 centipoise.

The estimation of gasification time is more difficult. From the little available data a value of 0.5 to 1.0 sec appeared to be adequate. The design figure actually used was 0.70 sec. From Fig. 18 the settling velocity of a 100-mesh particle is approximately 1 fps, and, using a gasification time of 0.70 sec, the height of the chamber becomes

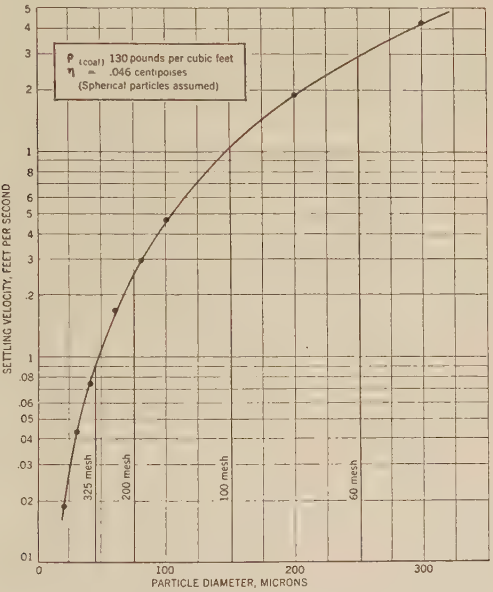

FIG. 18 SETTLING VELOCITY OF COAL PARTICLES

$$h = (1)\ (0.70) = 0.70 \text{ ft} \backsimeq 8 \text{ in.} \quad \ldots\ldots \quad [21]$$

The required value of V_1 can now be calculated from Equation [19]

$$V_1 = \frac{6.36}{\sqrt{0.67}} = 7.8 \text{ fps} \quad \ldots\ldots \quad [22]$$

A series of tests were made to determine the values of V_1 for different throughputs and for various arrangements of the inlet slots. These data were required since it was found that different slot arrangements resulted in markedly different tangential wall velocities even at the same throughput.

A vortex with $R_1 = 1$ ft, $h = {}^2/_3$ ft, and $R_2 = {}^1/_6$ ft was used in these tests. The values obtained for different slot sizes and shapes and at different throughputs are plotted in Fig. 19. If the loss in energy in the fluid expanding from the slot into the vortex chamber were a pure expansion loss then it would be directly proportional to the throughput. In this case other variables must be involved since the tangential wall velocity is proportional to $Z_1^{0.75}$ for all ${}^3/_8$-in-wide slots, $Z_1^{0.27}$ for ${}^1/_4$-in-wide slots, and $Z_1^{0.35}$ for the ${}^1/_8$-in-wide slot. Sufficient data were not obtained to develop an empirical equation to fit all of the experimental data, but enough information was obtained to design the slots for the V_1 values used in these tests.

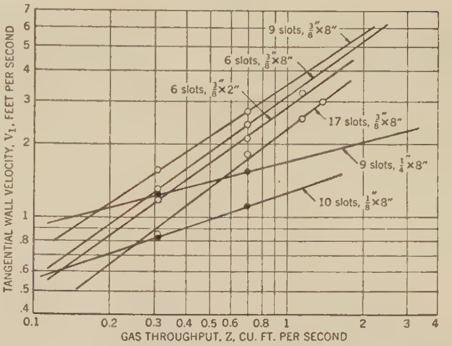

FIG. 19 TANGENTIAL WALL VELOCITY AS FUNCTION OF GAS THROUGHPUT

Outlet Conditions. For the feed conditions selected there are approximately 14 moles of gas leaving the reactor at 2500 F. To calculate the particle size that will just leave the reactor, i.e., $r = R_2$ from Equation [6]

$$V_2 = \frac{200}{300}\,\frac{V_1R_1}{R_2} \quad \ldots\ldots \quad [23]$$

and since

$$Z_2 = 8.4 \text{ cfs} \quad \ldots\ldots \quad [24]$$

therefore

$$U_2 = \frac{8.4}{2\pi R_2 h} = \frac{1.337}{R_2 h} \quad \ldots\ldots \quad [25]$$

At the outlet $\eta = 0.06$ centipoise $= 4.03 \times 10^{-5}$ lb/sec-ft. A particle at the outlet is subject to the same forces as a particle at the inlet so that from Equation [9]

$$V_2^2 = \frac{9}{2}\,\frac{\eta U_2 R_2}{a^2 \rho} \quad \ldots\ldots \quad [26]$$

or

$$a^2 = \frac{9}{2}\,\frac{(4.03 \times 10^{-5})}{130}\,\frac{1.337}{hV_2^2} = \frac{1.863 \times 10^{-6}}{hV_2^2} \quad \ldots\ldots \quad [27]$$

and from Equation [23]

$$a^2 = \left[\frac{1.86 \times 10^{-6}}{(h)\ (0.667)^2\ V_1^2}\right]\frac{R_2^2}{R_1^2} \quad \ldots\ldots \quad [28]$$

or

$$a = \left[\frac{2.05 \times 10^{-3}}{\sqrt{h}\ V_1}\right]\frac{R_2}{R_1} \quad \ldots\ldots \quad [29]$$

From Equation [19], $\sqrt{h}V_1 = 6.36$ so that

$$a = 3.22 \times 10^{-4}\,\frac{R_2}{R_1} \quad \ldots\ldots \quad [30]$$

Thus the smaller the ratio R_2/R_1 the smaller will be the particle that will just leave the vortex, and the higher will be the carbon conversion. To operate the vortex at atmospheric pressure, a value of R_2 greater than 1 in. is required, and a value of 2 in. was found to be more satisfactory. Thus when $R_2 = {}^1/_6$ ft then when

$R_1 =$	0.5 ft	1.0 ft	1.5 ft
$a =$	1.072×10^{-4} ft	0.537×10^{-4} ft	0.358×10^{-4} ft

Since the weight of carbon leaving the reactor is proportional to a^3, increasing the value of R_1 to greater than 1 ft decreases the weight per cent of carbon leaving only slowly. Thus a value of $R_1 = 1$ ft was selected.

From the use of both inlet and outlet conditions, the vortex designed for feed conditions of 100 lb per hr each of coal, oxygen, and steam had

$$R_1 = 1 \text{ ft}$$
$$R_2 = {}^1/_6 \text{ ft}$$
$$h = {}^2/_3 \text{ ft}$$

and required $V_1 = 7.8$ fps. The final slot arrangement, 9 slots each $^3/_8$ in. × 8 in., was selected to give the maximum values of V_1. For the feed conditions selected and at the temperatures at which the steam-oxygen mixture pass through the slots, V_1 should be approximately 6.5 fps. Although this value is slightly lower than that required by the calculations, it was the maximum value obtainable using any of the slot arrangements tested, and it appeared to be satisfactory in view of the factors of safety in design used in calculating the values of V_1 required.

The Gas-Turbine Regenerator—the Use of Compact Heat-Transfer Surfaces

By A. L. LONDON[1] and W. M. KAYS,[2] STANFORD, CALIF.

This paper illustrates the application of high-rating compact surfaces of the plate-fin-type to the regenerator-design problem for typical gas-turbine cycles. Comparisons are made with designs employing circular tube surfaces one inch and one-quarter inch in diameter.

Nomenclature

The following nomenclature is used in this paper:

A = heat-transfer area, sq ft
A_c = free-flow area, sq ft
a = nonflow dimension of heat exchanger, ft
a = plate-metal thickness or tube wall thickness, ft
b = gas-flow dimension of heat exchanger, ft
b = plate spacing, ft
C = air or gas capacity rate, $C = Wc_p$ Btu/(hr)(deg F)
c = air-flow dimension of heat exchanger, ft
c_p = specific heat at constant pressure, Btu/(lb deg F)
D_i = inside diameter of tubes, ft
D_o = outside diameter of tubes, ft
f = Fanning friction factor, dimensionless
G = mass velocity, $G = \dfrac{W}{A_c} = V\rho$ lb/(hr)(sq ft) of A_c
g = proportionality factor in Newton's second law, g = 32.2 lb ft/#-sec²
h = unit conductance for thermal convection heat transfer, Btu/(hr ft² deg F)
K_c = contraction loss coefficient for flow at heat-exchanger entrance, dimensionless
K_e = expansion loss coefficient for flow at heat-exchanger exit, dimensionless
k = thermal conductivity, Btu/(hr sq ft deg F/ft)
L = flow length used in the definition of hydraulic radius, ft
n = number of passes in multipass cross flow heat exchanger, dimensionless
P = pressure, psi, psf
$\mathbf{R}$ = Reynolds number, dimensionless
r_h = hydraulic radius, $r_h = \dfrac{A_c L}{A}$, ft
T = temperature, deg R
t = temperature, deg F
U = unit over-all thermal conductance, Btu/(hr ft² deg F)(sq ft) of A_g
V = heat exchanger total volume, cu ft
V = velocity, fps
v = specific volume, cu ft/lb
W = specific flow rate, lb/(1000 shp-hr)
x_l = longitudinal tube-bank pitch, dimensionless
x_t = transverse tube-bank pitch, dimensionless
α = ratio of total transfer area of one side of exchanger to total volume of exchanger, ft²/ft³
β = ratio of total transfer area of one side of exchanger to volume between the plates of that side, ft²/ft³
δ = fin metal thickness, ft
Δ = with P denotes inlet minus outlet pressure difference
ϵ = heat-exchanger effectiveness, a function of (NTU, C_a/C_g, flow arrangement), dimensionless
η = over-all temperature effectiveness of plate-fin heat-exchanger surface, dimensionless
ρ = density, lb/ft³
σ = ratio of free flow to frontal area, dimensionless
μ = viscosity, lb/(hr ft)

Dimensionless Groupings

N_{St} = Stanton's number, (h/Gc_p), a heat transfer modulus
N_{Pr} = Prandtl's number, $(\mu c_p/k)$, a fluid-properties modulus
$N_{St}N_{Pr}^{2/3}$ = generalized heat-transfer grouping. This factor versus R defines the heat-transfer characteristics of the surface
$\mathbf{R}$ = Reynold's number, $(4r_hG/\mu)$, (D_oG/μ)
f = Fanning friction factor. This factor versus **R** defines the friction characteristics of the surface
NTU = Number of heat-transfer units, (A_gU/C_a)
ϵ = heat-exchanger effectiveness, a function of (NTU C_a/C_g, flow arrangement)

Subscripts

a = air-side condition
g = gas-side condition
f = film average condition
l = fluid entrance condition to heat exchanger
avg = average fluid condition

Miscellaneous

lb = pounds mass in distinction to
# = pounds force
$\cong$ = approximate equivalence

Introduction

The high-efficiency gas-turbine plant, unlike other prime-mover systems, requires a design philosophy of close attention to details in all respects. This insistence on optimum design is mandatory because operation at temperatures approaching metallurgical limits, large specific flow rates (lb/shp-hr) of the working substance, the high "back-work" input to the compressors multiplying the cost of flow-friction power, are all coupled with the requirement of a compact machinery arrangement. The requirement of compactness is a major consideration in the transportation application of the gas-turbine plant if its basically lightweight aspect is to be capitalized upon.

During the present pioneering development of the gas-turbine system, relatively little attention has been devoted to the heat-

---

[1] Professor of Mechanical Engineering, Stanford University, Mem. ASME.

[2] Acting-Instructor of Mechanical Engineering, Stanford University. Jun. ASME.

Contributed by the Gas Turbine Power and Aviation Divisions and presented at the Semi-Annual Meeting, San Francisco, June 27–July 1, 1949, of The American Society of Mechanical Engineers.

Note: Statements and opinions advanced in papers are to be understood as individual expressions of their authors and not those of the Society. Paper No. 49—SA-9.

exchanger components—primarily the regenerator. However, for a gas-turbine plant having a specific fuel consumption over a fairly wide load range comparable to that of a steam plant, a regenerator of considerable specific transfer area is required. For instance, in an open-cycle plant such as described by Soderberg, Smith, and Scott (7),[3] a transfer area of the magnitude of 3 to 4 sq ft/shp rating is needed. This requirement is several times that of the boiler plus condenser of a steam power plant. It is evident, therefore, that if compactness and lightweight are to be realized, boiler or condenser-type surfaces cannot be used. As an illustration of a practical result of the application of such surfaces, reference (8) describes a 5000-kw gas-turbine plant for central-station application. The regenerator of 75 per cent effectiveness, consisting of 1-in-diam tubes providing about 3.9 sq ft/shp, has a weight of the order of 21 lb/shp plant rating. While this massiveness and its concomitant cost and bulk may be admissible in a conservatively designed central-station-type plant, it cannot be extended to the transportation-type prime mover.

This discussion emphasizes the ultimate necessity of the development of types of heat-transfer surfaces for the regenerator having substantially higher area-to-volume ratio characteristics than conventionally used boiler and condenser-tube banks. Thus attention is directed to the use of either small, circular, or flat tube surfaces of the order of $^1/_4$-in. hydraulic diameter, or else extended surfaces. In the latter case it will be necessary to have a type of construction allowing extended area on both the hot and cold gas sides since each heat-transfer film resistance is of the same order of magnitude, and the coefficients are sufficiently low to permit satisfactorily high "temperature effectiveness" for the fin surfaces.

To illustrate the wide variance in inherent compactness of different surfaces, Table 1 compares the area-to-volume ratio of the several types of surfaces described in Fig. 1. The 10:1 difference for plate-fin surfaces as compared to the 1-in-diam tubes and the 2.3:1 comparison even with $^1/_4$-in. tubes is striking and demonstrates the basic advantages of the extended surface.

The aircraft intercooler application is somewhat akin to that of the regenerator, as gas-to-gas heat transfer exists and the requirements of compactness and lightweight are paramount. Here, both the extended plate-fin and tubular direct surfaces are competitive, but it has been necessary to resort to $^1/_4$-in-diam tubes and smaller to match the over-all performance of extended surfaces. This experience is probably indicative of the competition that will exist in the regenerator application for the open-cycle gas-turbine plant.

While manufacturing methods are available for constructing tubular surfaces into high-temperature heat exchangers, such is not the case for extended surfaces. Heretofore, these have been used primarily in the aircraft intercooler and/or air-conditioning fields, and the production methods for low-temperature service cannot be directly extrapolated to the high-temperature regenerator application. Therefore there is a question as to whether or not the development of methods of high-temperature fabrication is worth the major effort it will undoubtedly require. A response to this question requires the prior technical answer to the following:

1 What are the advantages in shape, size, and weight of the extended as compared to the direct-surface regenerator?

2 Can extended surfaces be cleaned, and will the fouling rates be excessive?

3 Will the extended surface be less expensive assuming that manufacturing methods can be developed?

It is the objective of this paper to answer the first question by comparison of extended and direct-surface exchanger cores designed for the same performance. The other two questions can not be answered categorically at this stage, but several points of interest will be considered.

TABLE 1 COMPARISON OF AREA-VOLUME RELATIONS FOR SOME HEAT-EXCHANGER SURFACES

	Area/volume (ft^2/ft^3)	
	Outside	Inside
1-in-OD circular tubes ($x_t = 2$, $x_l = 1$, $D_i/D_o = 0.9$)	18.85	16.96
$^1/_4$-in-OD circular tubes ($x_t = 2$, $x_l = 1$, $D_i/D_o = 0.9$)	74.3	67.9
Plate-fin surface (see Fig. 1) (12 fins/in., $^1/_4$-in. plate spacing)	175.8	

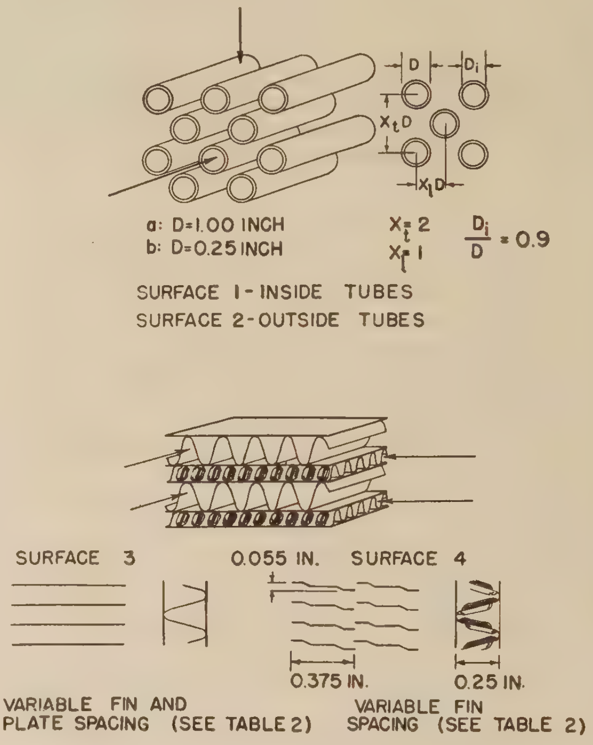

Fig. 1 Description of Four Heat-Exchanger Surfaces
(Refer to Table 2 for further details of geometry and Fig. 4 for basic heat-transfer and flow-friction data.)

Heretofore, comparative studies of this character were impossible because of the lack of basic heat-transfer and flow-friction data for surfaces other than circular tubes. Under the sponsorship of the U. S. N. Bureaus of Ships and Aeronautics, and the Office of Naval Research, however, basic data have recently been made available for a number of variations of the plate-fin type of surface of Fig. 1 (1, 2, 3, 4, 5, 6).

Regenerator Design Considerations

The primary considerations influencing regenerator design may be summarized as follows: (1) manufacturing and cost limitations, (2) maintenance and cleaning requirements, (3) mechanical-design problems including a thorough consideration of thermal stresses, (4) weight, space, and shape limitations, (5) allowable flow-friction limitations, and (6) desired exchanger heat-transfer effectiveness.

As indicated in the introduction, only items 4, 5, and 6 will be considered in any detail in this paper. This will be accomplished in the following manner:

1 Several gas-turbine cycles will be selected for consideration.

2 Several different types of the extended and direct surfaces will be specified along with their basic heat transfer-flow friction characteristics.

---

[3] Numbers in parentheses refer to the Bibliography at the end of the paper.

3 A nominal per cent pressure drop for hot-side plus cold-side flow friction will be specified for each cycle under consideration.

4 A heat-transfer effectiveness also will be specified for each cycle.

On this basis estimates will be made of the size, shape, and weight of regenerators utilizing the different surfaces. A critical comparison will then follow.

Heat-Transfer and Flow-Friction Equations

The exchanger-flow arrangement, the heat-transfer area, flow rates, exchanger effectiveness, and over-all conductance for heat transfer from the hot to cold gas sides are related by heat transfer and thermodynamic considerations. The resulting relations for a particular flow arrangement may be expressed in a form using the following dimensionless groupings

$$\epsilon = \phi\left(NTU, \frac{C_a}{C_g}\right) \qquad \ldots\ldots\ldots\ldots\ldots\ldots [1]$$

where ϕ denotes a functional relation.

The exchanger effectiveness ϵ compares the actual heat-transfer rate in the exchanger to the maximum possible rate as limited by thermodynamic considerations. This is equivalent to the ratio of actual cold-air temperature rise to the difference between inlet-hot-gas and inlet-cold-air temperatures, that is, the effectiveness compares the actual to the maximum possibility for air heating.

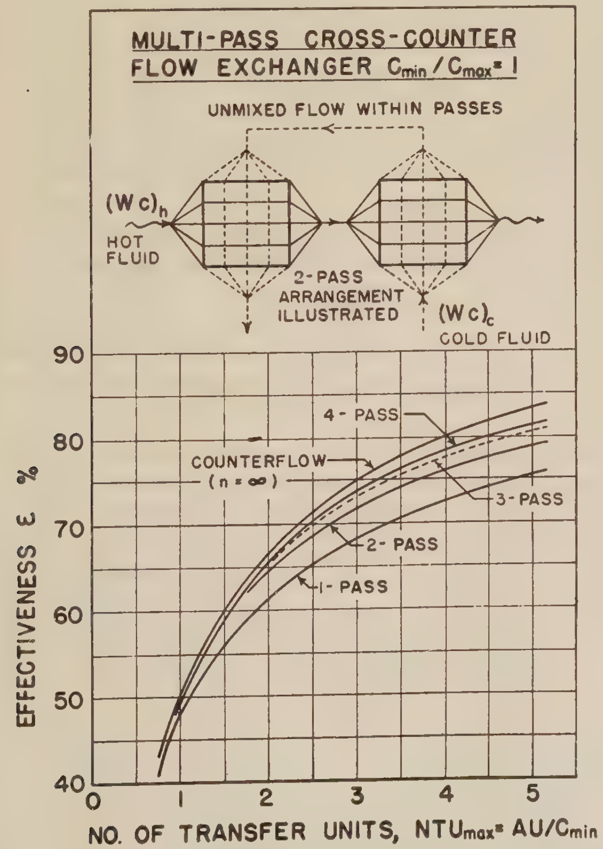

Fig. 2 Regenerator Effectiveness—Number of Heat-Transfer Units Relation

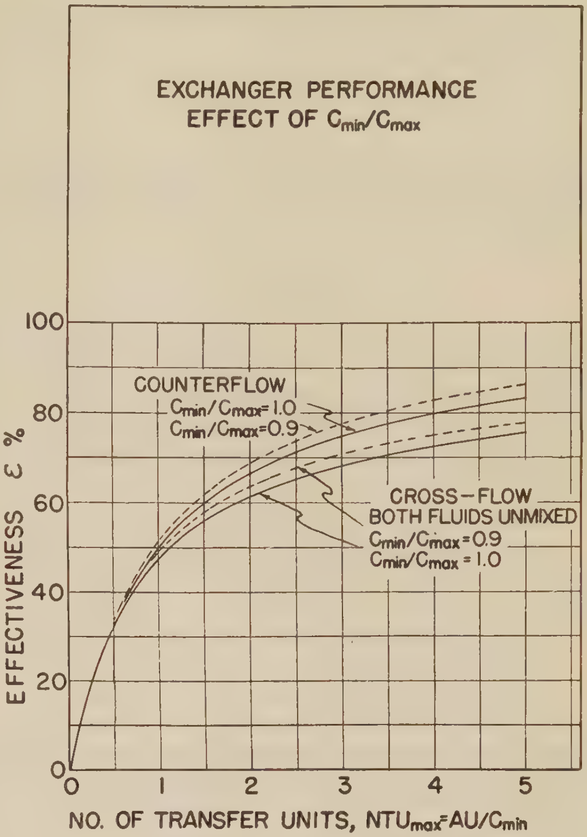

Fig. 3 Influence of Capacity-Rate Ratio on Regenerator Effectiveness

(For the gas-turbine system $C_{air}/C_{gas} = C_{min}/C_{max} = 0.95$ to 0.98.)

The capacity-rate ratio, C_a/C_g, compares the mass-flow rate times specific-heat capacity product of the cold and hot streams. For the regenerator application, because of the small contribution of fuel to the hot-gas rate and the slightly higher specific heat with temperature, C_a/C_g is of the order of 0.96 to 0.98.

The number of heat-transfer units, $NTU = AU/C_a$, is a dimensionless expression of the "heat-transfer size" of the exchanger. Note that the NTU is defined in terms of the minimum capacity rate ($C_a < C_g$).

Fig. 2 gives Equation [1] in graphical form for a number of flow arrangements, and the condition that C_a/C_g = unity, a condition approximately satisfied in the regenerator. The influence of capacity-rate ratio is shown in Fig. 3 for C_a/C_g both unity and 0.90. Any intermediate condition can be established by interpolation.

Flow pressure drop through the exchanger can be determined from the following relation

$$\frac{\Delta P}{P_1} = \frac{G^2}{2g}\frac{v_1}{P_1}\Bigg[\underbrace{(K_c + 1 - \sigma^2)}_{\text{entrance effect}} + \underbrace{2\left(\frac{v_2}{v_1} - 1\right)}_{\text{flow acceleration}} + \underbrace{f\frac{A}{A_c}\frac{v_{avg}}{v_1}}_{\text{core ``skin'' friction}} - \underbrace{(1 - \sigma^2 - K_e)\frac{v_2}{v_1}}_{\text{exit effect}}\Bigg] \ldots [2]$$

The terms associated with the flow contraction on entrance to the core, the flow acceleration or deceleration due to the heat-transfer influence on density, the friction within the core, and the pressure recovery on flow expansion at exit are all indicated in Equation [2]. For multipass arrangements, losses in return headers must be accounted for separately.

The correct average specific volume to be used in the indicated skin-friction component is

$$v_{\text{avg}} = \frac{1}{A}\int_{o}^{A} v dA \ldots\ldots [3]$$

For the sensibly unity magnitude of C_a/C_g in the regenerator, flow temperatures vary linearly with transfer area, A. Thus to a good approximation

$$\frac{v_{\text{avg}}}{v_1} \cong \frac{P_1}{P_{\text{avg}}}\frac{T_{\text{avg}}}{T_1} \ldots\ldots [4]$$

where T_{avg}, P_{avg} are the arithmetic average of the terminal magnitudes.

For the heat-exchanger comparisons of this paper, a simplification of Equation [2] is employed by using nominal magnitudes for K_c, K_e, σ, and v_2/v_1 terms in the brackets. The result is for the hot-gas side

$$\left(\frac{\Delta P}{P_1}\right)_g \cong \frac{G^2}{2g}\frac{v_1}{P_1}\left[f\frac{A}{A_c}\frac{P_1}{P_{\text{avg}}}\frac{T_{\text{avg}}}{T_1}\right] \ldots\ldots [5]$$

and for the cold-gas side

$$\left(\frac{\Delta P}{P_1}\right)_a \cong \frac{G^2}{2g}\frac{v_1}{P_1}\left[2 + f\frac{A}{A_c}\frac{P_1}{P_{\text{avg}}}\frac{T_{\text{avg}}}{T_1}\right] \ldots\ldots [6]$$

For the hot side, the entrance effect tends to cancel the influence of both the flow exit and flow deceleration pressure rises, but for the cold-gas side, flow acceleration on heating adds to the entrance pressure drop. This consideration accounts for the difference between Equations [5] and [6]. In any event, as the core friction term $\left(f\frac{A}{A_c}\frac{P_1}{P_{\text{avg}}}\frac{T_{\text{avg}}}{T_1}\right)$ is of the order of 15 to 50, the over-all pressure drop is not markedly influenced by the other flow effects.

The total regenerator flow-friction work expenditure is proportional to

$$\left(\frac{\Delta P}{P_1}\right)_{\text{total}} = \left(\frac{\Delta P}{P_1}\right)_a + \left(\frac{\Delta P}{P_1}\right)_g$$

for a given cycle and a given operating pressure ratio. This fraction pressure drop is simply related to either the additional compressor work requirement or the diminution of turbine work arising from flow friction. A one per cent pressure drop on the air side causes just as much "loss" as one per cent on the gas side.

With respect to the distribution of friction losses on the air and gas sides, the following general comments can be made:

If the plant is to be operated primarily at full load, an approximately equal distribution of flow-friction work is desirable, i.e.

$$(\Delta P/P_1)_a/(\Delta P/P_1)_g = 0.7 - 1.5$$

as it tends to result in minimum regenerator volume. Should high part-load efficiencies for the plant be desirable, however, the regenerator designs should tend toward

$$(\Delta P/P_1)_a/(\Delta P/P_1)_g < 0.25$$

at full load. This conclusion stems from the fact that while the hot-side density is relatively constant with load for the open-cycle plant, the air-side density decreases markedly as pressure ratio is decreased. The consequence is, while the gas-side loss in terms of plant specific fuel consumption tends to remain fairly constant, the air-side loss increases strongly as load is decreased. Thus if $(\Delta P/P_1)_g$ controls at full load the total loss will remain fairly constant rather than have an undesirable rising characteristic with decreasing load (7).

Heat-Transfer Surfaces

Only four types of surfaces will be considered in this paper: (1) flow inside circular tubes, (2) flow normal to circular-tube bundles, and (3), (4) two plate-fin surfaces, Fig. 1. However, each surface is susceptible to considerable variation as by changing fin and plate spacing and tube diameter. The specific variations in this respect are summarized in Table 2 as 1*a*, 2*b*, etc.

For the circular tube surfaces, in all cases specifically considered here, the hot gas flows normal to the tubes and the cold air within the tubes, as this arrangement results in a minimum weight and volume regenerator. The effect of interchanging the flows, on the shape of the core, will be considered later.

The basic heat-transfer and flow-friction data for each of the four surfaces are presented using the usual dimensionless plots of $N_{St}N_{Pr}^{2/3}$ and f versus Reynolds number, **R**, in Fig. 4. Only for circular tube surfaces, Nos. 1 and 2, Fig. 1, is exact geometrical similarity maintained for all the variations. Nevertheless, for surfaces 3 and 4, even though complete geometrical similarity is not maintained, the use of a single $N_{St}N_{Pr}^{2/3}$ versus **R** and a single f versus **R** characteristic for each surface does not introduce serious error. This has been demonstrated in references (3, 4, 5) which show an excellent heat-transfer correlation for the different fin spacing with Reynolds number based on the flow hydraulic radius, r_h. The f correlation is not as good but the departure from the average characteristics shown in Fig. 4 is less than 15 per cent.

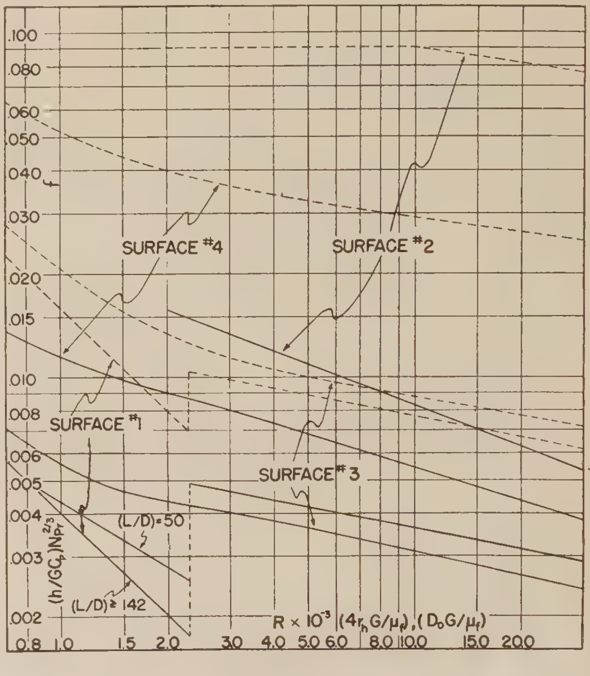

Fig. 4 Basic Heat-Transfer and Flow-Friction Data for the Surfaces of Fig. 1

– – – – – – denotes f characteristic; ———— denotes $N_{St}N_{Pr}^{2/3}$ characteristic.

[Data for surfaces Nos. 3 and 4 from references (2, 3), and for surfaces 1 and 2 from reference (10)].

Gas-Turbine Cycles

Four distinct gas-turbine cycles are included in this regenerator design survey:

1 Cycle (A) is an open cycle with a 9:1 pressure ratio, 90 per cent intercooling and 75 per cent regeneration with $(\Delta P/P_1)_{\text{total}} < 3$ per cent. Such a system, designed for central-station power generation, is described in reference (8).

TABLE

STAGGERED TUBE ARRANGEMENTS

$X_t = 2$
$X_l = 1$

Material of Density 490 lbs./ft.^{3} and
Thermal Conductivity 12 Btu/(hr.ft^2°F/ft.)

ARRANGEMENT	1a	2a	1b	2b
Outside Tube Diameter, in......	1	1	1/4	1/4
Side	inside	outside	inside	outside
Surface	1	2	1	2
$4\ r_h$, ft..........	0.075	--	0.01872	--
D_o, ft............	--	0.0833	--	0.0208
δ, ft............	0.00417		0.00104	
σ	0.318	0.414	0.318	0.414
α, ft.^{2}/ft.^{3}	16.96	18.85	67.9	74.3
Specific Wt., lbs./ft.^{3}.........	36.3		36.3	

PLATE-FIN ARRANGEMENTS

Fin Thickness: 0.010 in.; Plate Thickness: 0.015 in.

ARRANGEMENT	3a	3b	3c	3d	3e	3f	4a	4b	4c
Plate Spacing, in.	1/4	1/4	1/4	1/2	1/2	1/2	1/4	1/4	1/4
Fins per inch	6	9	12	6	9	12	6	9	12
Louver Length, in.	--	--	--	--	--	--	3/8	3/8	3/8
Louver Gap, in.	--	--	--	--	--	--	0.055	0.055	0.055
Surface	3	3	3	3	3	3	4	4	4
r_h, ft.	0.00402	0.00300	0.00236	0.00497	0.00350	0.00266	0.00402	0.00300	0.00236
δ, ft.	0.000833	0.000833	0.000833	0.000833	0.000833	0.000833	0.000833	0.000833	0.000833
a, ft.	0.00125	0.00125	0.00125	0.00125	0.00125	0.00125	0.00125	0.00125	0.00125
b, ft.	0.02083	0.02083	0.02083	0.04167	0.04167	0.04167	0.02083	0.02083	0.02083
β, ft.^{2}/ft.^{3}	234.0	303.3	373.0	189.2	260.0	330.8	234.0	303.3	373.0
Fin Area/Total Area ...	0.600	0.693	0.750	0.750	0.818	0.857	0.600	0.693	0.750
Specific Weight, lbs./ft.^{2} area	0.2448	0.2354	0.2295	0.2295	0.2227	0.2187	0.2448	0.2354	0.2295

TABLE 3 REGENERATOR OPERATING CONDITIONS

	CYCLE A		CYCLE B		CYCLE C		CYCLE D	
Inlet to Regenerator Properties	Air	Gas	Air	Gas	Air	Gas	Air	Gas
P_1, #/in^2	132	14.9	528	59.6	70.0	15.1	45	15.2
T_1, °F.....................	347	805	347	805	422	812	330	1540
v_1, ft^3/lb	2.27	31.4	0.567	7.85	4.65	31.2	6.50	48.7
Average Properties								
c_p, Btu/lb °F	0.248	0.251	0.248	0.251	0.248	0.254	0.257	0.265
μ_f, lbs/hr ft	0.070	0.073	0.070	0.073	0.070	0.075	0.082	0.087
N_{Pr_f}	0.67	0.67	0.67	0.67	0.67	0.67	0.66	0.66
Specific Flow Rate, lbs/1000 shp-hr	38,600		38,600		58,000		71,000	
Capacity Rate Ratio, C_a/C_g........	0.97		0.97		0.96		0.96	

CYCLE A: Open cycle, 9:1 pressure ratio, 90% intercooling, 75% regeneration, $(\Delta P/P_1)_{total} \cong 2.5\text{-}3.0\%$

CYCLE B: Closed cycle, " " " , " " , " " , with 4 atm. base pressure

CYCLE C: Open cycle, 4.8:1 pressure ratio, 60% regeneration, $(\Delta P/P_1)_{total} \cong 5\%$

CYCLE D: Exhaust combustion open cycle, 3:1 pressure ratio, 75-80% regeneration, $(\Delta P/P_1)_{total} \cong 6.5\text{-}7.0\%$

2 Cycle (B) is a closed cycle identical with cycle (A) except that the pressure levels are increased by a factor of four.

3 Cycle (C) is an open-cycle system designed for a locomotive application with a 4.8:1 pressure ratio, no intercooling, and about 60 per cent regeneration with $(\Delta P/P_1)_{\text{total}} < 5$ per cent. A similar system is described in reference (9).

4 Cycle (D) is an open "exhaust-combustion" cycle of 3:1 pressure ratio with 75 to 80 per cent regeneration and $(\Delta P/P_1)_{\text{total}} < 7$ per cent. This system (11) is of possible interest in the coal-burning-locomotive application. All the thermal energy provided to the turbine working substance after leaving the compressor comes from heat transfer in the regenerator. The turbine exhaust air is combusted with the requisite amount of fuel and is then fed into the regenerator before exhausting to the atmosphere. The basic advantage of this cycle for the coal-fueled plant is that the turbine working substance is clean air and not the products of combustion with attendant fly-ash erosion and fouling problems.

The operating conditions for the regenerator for these cycles are summarized in Table 3, giving the inlet state for hot and cold gases—pressure, temperature, and specific volume; the nominal average gas properties used in the heat-transfer friction calculations—viscosity, unit heat capacity, and Prandtl's number, N_{Pr}; and the capacity rate ratio, C_a/C_g, together with the specific air-flow rate, W_a lb/(1000 shp-hr).

GEOMETRICAL RELATIONS

As a preliminary to the consideration of the results of the analysis for core shapes for the different regenerator applications, certain readily derivable geometrical relations first will be established. These equations relate core dimensions and volume, the free flow:frontal area ratios for the two sides, the flow mass velocities, and the specific flow rate, W lb of air or gas/1000 shp-hr. The air and gas-flow dimensions are independent of the plant rating but the nonflow dimension (or dimensions for true counterflow) is, of course, directly dependent on plant rating. The more obvious relations for single-pass crossflow, 2-pass cross-counterflow, and true counterflow are summarized in Fig. 5. This illustration also defines the nomenclature specifying over-all core geometry. From these relations follow directly

For any number of air-passes, n, in a cross-counterflow arrangement (single-pass on gas side)

$$\left.\begin{aligned} a &= \left(\frac{nW^2}{V}\right)\frac{1}{\sigma_a\sigma_g G_a G_g} \\ b &= \left(\frac{V}{W}\right)\sigma_g G_g \\ c &= \left(\frac{V}{nW}\right)\sigma_a G_a \end{aligned}\right\} \quad \ldots\ldots\ldots\ldots\ldots [7]$$

For a true counterflow arrangement

$$\left.\begin{aligned} a\cdot b &= \frac{W}{\sigma_a G_a}\frac{W}{\sigma_g G_g} \\ c &= \left(\frac{V}{W}\right)\sigma_a G_a = \left(\frac{V}{W}\right)\sigma_g G_g \end{aligned}\right\} \quad \ldots\ldots\ldots\ldots [8]$$

The conclusions to be drawn from these relations are as follows:

1 Counter and single-pass crossflow cores will have about the same air-flow dimension, c.

2 Counterflow cores can be designed for any nonflow dimensions, a or b, only satisfying the (ab) product requirement given by the first of Equations [8].

3 For any number of passes in cross-counterflow, as long as all the passes are on the air side, the gas-flow dimension is invariant with n, but the air-flow dimension varies inversely and the nonflow dimension directly with the number of passes, n.

4 If the nonflow dimension tends to be too large for a particular regenerator application, counterflow will give the best shape with single-pass crossflow next.

5 For the crossflow arrangements, the nonflow dimension may be reduced by (a), reducing the number of passes, $a \propto n$; (b), reducing the specific flow rate, $a \propto W^2$; (c), *increasing* the volume, $a \propto 1/V$; (d), maximizing the mass velocities G_a, G_a; (e), maximizing the $\sigma_g \cdot \sigma_a$ product.

In this last respect, 5(e), not too much can be accomplished directly inasmuch as $\sigma_g + \sigma_a \cong 0.9$. Consequently, σ_a can vary from 0.3 to 0.6 with no marked change in the $\sigma_a \cdot \sigma_g$ product. However, for the extended surfaces in particular, the σ magnitudes can have an important influence on transfer area per unit volume, hence on total volume, V, and as a result, indirectly on the nonflow dimension a.

As crossflow cores tend to be better adapted to machinery arrangements as compared to counterflow, and since the plate-fin surfaces to be considered are more readily formed into crossflow cores, no further consideration of counterflow will be attempted in this paper. Additionally, since the air-flow length tends to be considerably greater than the gas-flow length because of the great differences in density, in the specified n-pass arrangements all the passes are on the air side. It is possible to arrange for multipasses on the gas side as well, without a fundamental change in the relative flow geometry, as pictured in Fig. 5, for a core with two passes on both gas and air sides. However, this expedient just results in a further increase in the nonflow dimension with the somewhat doubtful advantage of a decrease in an already small gas-flow dimension.

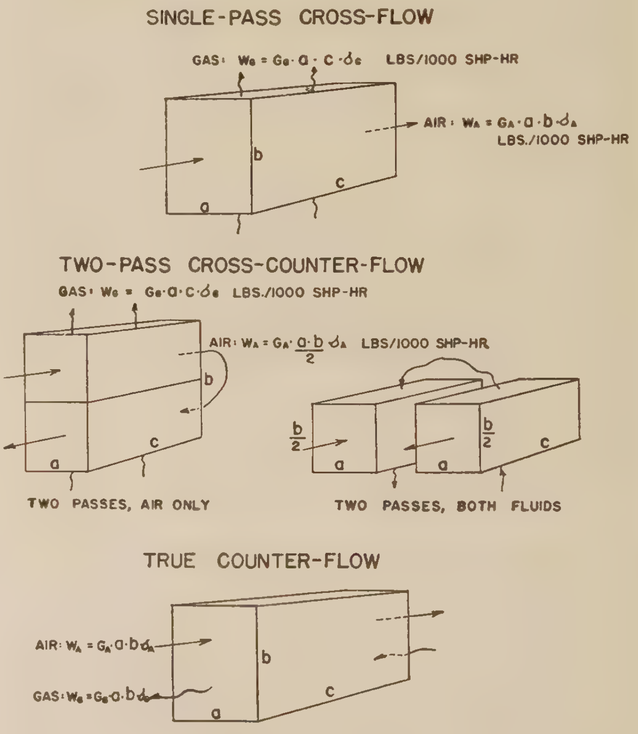
SINGLE-PASS CROSS-FLOW
GAS: $W_G = G_G \cdot a \cdot c \cdot \delta_G$ LBS/1000 SHP-HR
AIR: $W_A = G_A \cdot a \cdot b \cdot \delta_A$ LBS./1000 SHP-HR
b
c
a
TWO-PASS CROSS-COUNTER-FLOW
GAS: $W_G = G_G \cdot a \cdot c \cdot \delta_G$ LBS./1000 SHP-HR
AIR: $W_A = G_A \cdot \frac{a \cdot b}{2} \delta_A$ LBS/1000 SHP-HR
b
c
a
$\frac{b}{2}$
a
a
$\frac{b}{2}$
c
TWO PASSES, AIR ONLY
TWO PASSES, BOTH FLUIDS
TRUE COUNTER-FLOW
AIR: $W_A = G_A \cdot a \cdot b \delta_A$
GAS: $W_G = G_G \cdot a \cdot b \delta_G$
b
c
a

FIG. 5 DESCRIPTION OF CORE GEOMETRY
(See Equations [7] and [8].)

REGENERATOR CORE SHAPES

The foregoing considerations together with the data for the

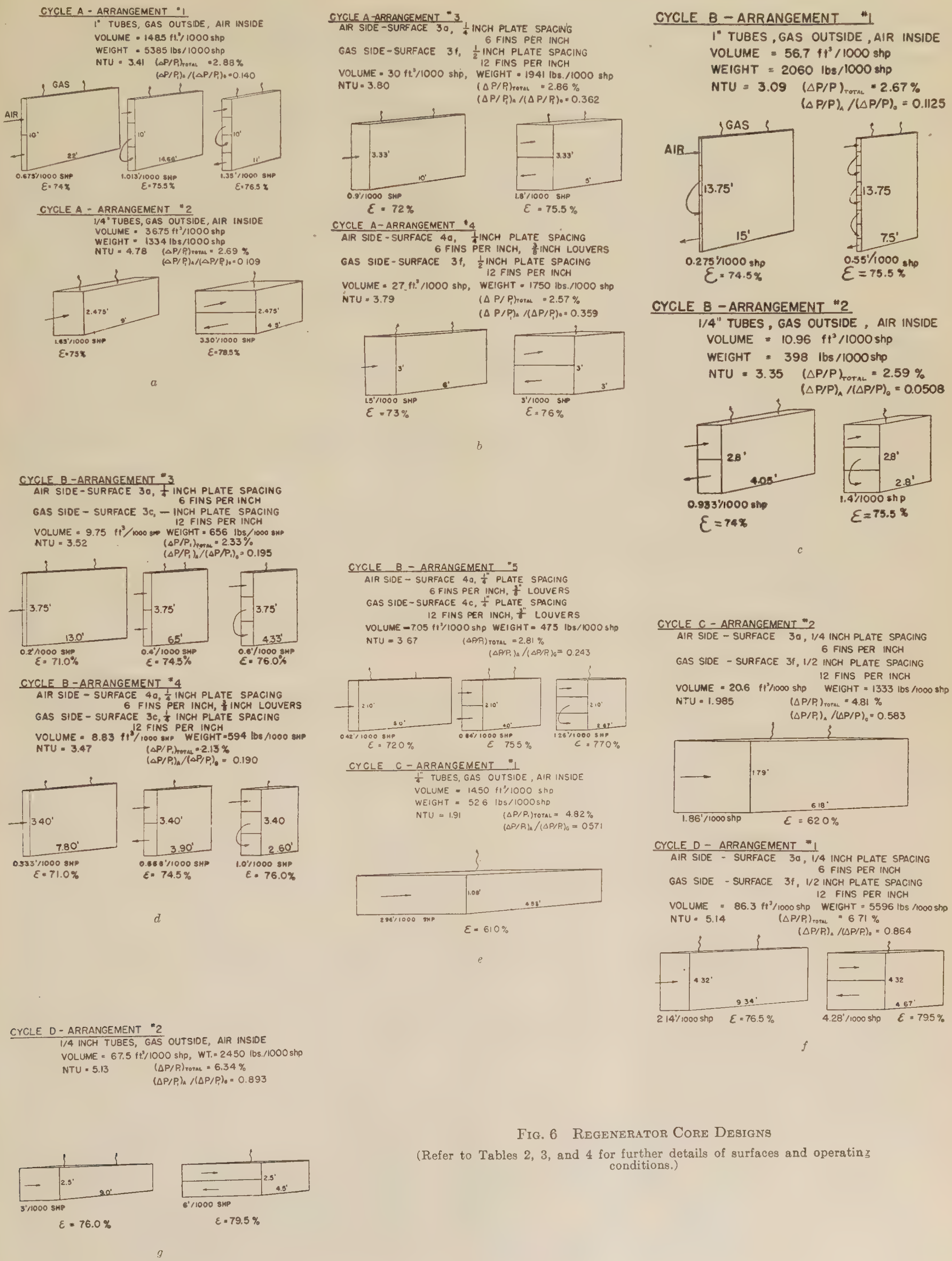
CYCLE A - ARRANGEMENT #1
1" TUBES, GAS OUTSIDE, AIR INSIDE
VOLUME = 148.5 ft³/1000 shp
WEIGHT = 5385 lbs/1000 shp
NTU = 3.41 (ΔP/P₁)TOTAL = 2.88 %
(ΔP/P₁)A /(ΔP/P₁)G = 0.140
GAS
AIR
10'
22'
0.675'/1000 SHP
ε = 74 %
10'
14.66'
1.013'/1000 SHP
ε = 75.5 %
10'
11'
1.35'/1000 SHP
ε = 76.5 %
CYCLE A - ARRANGEMENT #2
1/4" TUBES, GAS OUTSIDE, AIR INSIDE
VOLUME = 36.75 ft³/1000 shp
WEIGHT = 1334 lbs/1000 shp
NTU = 4.78 (ΔP/P₁)TOTAL = 2.69 %
(ΔP/P₁)A /(ΔP/P₁)G = 0.109
2.475'
9'
1.65'/1000 SHP
ε = 75 %
2.475'
4.5'
3.30'/1000 SHP
ε = 78.5 %
a
CYCLE A - ARRANGEMENT #3
AIR SIDE - SURFACE 3a, 1/4 INCH PLATE SPACING
6 FINS PER INCH
GAS SIDE - SURFACE 3f, 1/2 INCH PLATE SPACING
12 FINS PER INCH
VOLUME = 30 ft³/1000 shp, WEIGHT = 1941 lbs./1000 shp
NTU = 3.80 (ΔP/P₁)TOTAL = 2.86 %
(ΔP/P₁)A /(ΔP/P₁)G = 0.362
3.33'
10'
0.9'/1000 SHP
ε = 72 %
3.33'
5'
1.8'/1000 SHP
ε = 75.5 %
CYCLE A - ARRANGEMENT #4
AIR SIDE - SURFACE 4a, 1/4 INCH PLATE SPACING
6 FINS PER INCH, 3/8 INCH LOUVERS
GAS SIDE - SURFACE 3f, 1/2 INCH PLATE SPACING
12 FINS PER INCH
VOLUME = 27 ft³/1000 shp, WEIGHT = 1750 lbs./1000 shp
NTU = 3.79 (ΔP/P₁)TOTAL = 2.57 %
(ΔP/P₁)A /(ΔP/P₁)G = 0.359
3'
6'
1.5'/1000 SHP
ε = 73 %
3'
3'
3'/1000 SHP
ε = 76 %
b
CYCLE B - ARRANGEMENT #1
1" TUBES, GAS OUTSIDE, AIR INSIDE
VOLUME = 56.7 ft³/1000 shp
WEIGHT = 2060 lbs/1000 shp
NTU = 3.09 (ΔP/P)TOTAL = 2.67 %
(ΔP/P)A /(ΔP/P)G = 0.1125
GAS
AIR
13.75'
15'
0.275'/1000 shp
ε = 74.5 %
13.75
7.5'
0.55'/1000 shp
ε = 75.5 %
CYCLE B - ARRANGEMENT #2
1/4" TUBES, GAS OUTSIDE, AIR INSIDE
VOLUME = 10.96 ft³/1000 shp
WEIGHT = 398 lbs/1000 shp
NTU = 3.35 (ΔP/P)TOTAL = 2.59 %
(ΔP/P)A /(ΔP/P)G = 0.0508
2.8'
4.05'
0.933'/1000 shp
ε = 74 %
2.8'
2.8'
1.4'/1000 shp
ε = 75.5 %
c
CYCLE B - ARRANGEMENT #3
AIR SIDE - SURFACE 3a, 1/4 INCH PLATE SPACING
6 FINS PER INCH
GAS SIDE - SURFACE 3c, — INCH PLATE SPACING
12 FINS PER INCH
VOLUME = 9.75 ft³/1000 SHP WEIGHT = 656 lbs/1000 SHP
NTU = 3.52 (ΔP/P₁)TOTAL = 2.33 %
(ΔP/P₁)A /(ΔP/P₁)G = 0.195
3.75'
13.0'
0.2'/1000 SHP
ε = 71.0 %
3.75'
6.5'
0.4'/1000 SHP
ε = 74.5 %
3.75'
4.33'
0.6'/1000 SHP
ε = 76.0 %
CYCLE B - ARRANGEMENT #4
AIR SIDE - SURFACE 4a, 1/4 INCH PLATE SPACING
6 FINS PER INCH, 3/8 INCH LOUVERS
GAS SIDE - SURFACE 3c, 1/4 INCH PLATE SPACING
12 FINS PER INCH
VOLUME = 8.83 ft³/1000 SHP WEIGHT = 594 lbs/1000 SHP
NTU = 3.47 (ΔP/P₁)TOTAL = 2.13 %
(ΔP/P₁)A /(ΔP/P₁)G = 0.190
3.40'
7.80'
0.333'/1000 SHP
ε = 71.0 %
3.40'
3.90'
0.666'/1000 SHP
ε = 74.5 %
3.40
2.60'
1.0'/1000 SHP
ε = 76.0 %
d
CYCLE B - ARRANGEMENT #5
AIR SIDE - SURFACE 4a, 1/4" PLATE SPACING
6 FINS PER INCH, 3/8" LOUVERS
GAS SIDE - SURFACE 4c, 1/4" PLATE SPACING
12 FINS PER INCH, 3/8" LOUVERS
VOLUME = 7.05 ft³/1000 shp WEIGHT = 475 lbs/1000 shp
NTU = 3.67 (ΔP/P₁)TOTAL = 2.81 %
(ΔP/P₁)A /(ΔP/P₁)G = 0.243
2.10'
8.0'
0.42'/1000 SHP
ε = 72.0 %
2.10'
4.0'
0.84'/1000 SHP
ε 75.5 %
2.10'
2.67'
1.26'/1000 SHP
ε = 77.0 %
CYCLE C - ARRANGEMENT #1
1/4" TUBES, GAS OUTSIDE, AIR INSIDE
VOLUME = 14.50 ft³/1000 shp
WEIGHT = 526 lbs/1000 shp
NTU = 1.91 (ΔP/P₁)TOTAL = 4.82 %
(ΔP/P₁)A /(ΔP/P₁)G = 0.571
1.08'
4.53'
2.96'/1000 SHP
ε = 61.0 %
e
CYCLE C - ARRANGEMENT #2
AIR SIDE - SURFACE 3a, 1/4 INCH PLATE SPACING
6 FINS PER INCH
GAS SIDE - SURFACE 3f, 1/2 INCH PLATE SPACING
12 FINS PER INCH
VOLUME = 20.6 ft³/1000 shp WEIGHT = 1333 lbs/1000 shp
NTU = 1.985 (ΔP/P₁)TOTAL = 4.81 %
(ΔP/P₁)A /(ΔP/P)G = 0.583
1.79'
6.18'
1.86'/1000 shp
ε = 62.0 %
CYCLE D - ARRANGEMENT #1
AIR SIDE - SURFACE 3a, 1/4 INCH PLATE SPACING
6 FINS PER INCH
GAS SIDE - SURFACE 3f, 1/2 INCH PLATE SPACING
12 FINS PER INCH
VOLUME = 86.3 ft³/1000 shp WEIGHT = 5596 lbs/1000 shp
NTU = 5.14 (ΔP/P₁)TOTAL = 6.71 %
(ΔP/P₁)A /(ΔP/P₁)G = 0.864
4.32'
9.34'
2.14'/1000 shp
ε = 76.5 %
4.32
4.67'
4.28'/1000 shp
ε = 79.5 %
f
CYCLE D - ARRANGEMENT #2
1/4 INCH TUBES, GAS OUTSIDE, AIR INSIDE
VOLUME = 67.5 ft³/1000 shp, WT. = 2450 lbs./1000 shp
NTU = 5.13 (ΔP/P₁)TOTAL = 6.34 %
(ΔP/P₁)A /(ΔP/P₁)G = 0.893
2.5'
9.0'
3'/1000 SHP
ε = 76.0 %
2.5'
4.5'
6'/1000 SHP
ε = 79.5 %
g

FIG. 6 REGENERATOR CORE DESIGNS

(Refer to Tables 2, 3, and 4 for further details of surfaces and operating conditions.)

TABLE 4 SUMMARY OF DESIGN DATA

	CYCLE A				CYCLE B					CYCLE C		CYCLE D	
	1	2	3	4	1	2	3	4	5	1	2	1	2
Surface:													
Gas	2a	2b	3f	3f	2a	2b	3c	3c	4c	2b	3f	3f	2b
Air	1a	1b	3a	4a	1a	2a	3a	4a	4a	1b	3a	3a	1b
Weight/1000 shp, lbs	5285	1334	1941	1750	2060	398	656	594	475	526	1333	5596	2450
Volume/1000 shp, ft^3	148.5	36.8	30.0	27.0	56.7	10.96	9.75	8.83	7.05	14.5	20.6	86.3	67.5
Flow Lengths, ft:													
Air	44.0	9.00	10.0	6.00	55.0	8.40	13.0	7.80	8.00	4.53	6.18	9.34	9.00
Gas	10.0	2.48	3.33	3.00	15.0	2.80	3.75	3.40	2.10	1.08	1.79	4.32	2.50
Non-flow, 1-pass	0.3375	1.650	0.90	1.50	0.06875	0.4670	0.200	0.333	0.420	2.960	1.860	2.140	3.00
$(\Delta P/P_1)_g$, %	2.53	2.42	2.10	1.89	2.40	2.46	1.98	1.79	2.26	3.07	1.77	3.60	3.35
$(\Delta P/P_1)_a$, %	0.35	0.27	0.76	0.68	0.27	0.13	0.38	0.34	0.55	1.75	3.04	3.11	2.99
$(\Delta P/P_1)_{total}$, %	2.88	2.69	2.86	2.57	2.67	2.59	2.36	2.13	2.81	4.82	4.81	6.71	6.34
h_g, Btu/(hr ft^2 °F)	19.4	34.2	13.1	13.1	42.2	75.5	43.2	43.2	68.7	47.1	14.6	13.9	39.3
h_a, Btu/(hr ft^2 °F)	32.5	36.6	42.9	56.6	89.8	91.5	92.7	113.5	134.5	61.9	54.3	31.3	39.6
η_g	----	----	0.775	0.778	----	----	0.827	0.827	0.765	----	0.758	0.767	----
η_a	----	----	0.864	0.848	----	----	0.777	0.750	0.729	----	0.839	0.893	----
U, Btu/(hr °F ft^2 of Ag)	11.7	16.8	5.72	6.36	27.7	39.4	19.8	21.4	28.4	25.5	6.55	5.13	18.7
A_g, ft^2	2800	2732	6360	5720	1069	815	1713	1552	1240	1077	4365	18310	5020
A_a/A_g	0.900	0.900	0.353	0.353	0.900	0.900	0.628	0.628	0.628	0.900	0.354	0.353	0.900
NTU	3.41	4.78	3.80	3.79	3.09	3.35	3.52	3.47	3.67	1.91	1.985	5.14	5.13
G_g, lbs/(hr ft^2)	6270	6275	7610	7610	22620	23730	35800	35800	27600	10440	8950	6290	6350
V_g, ft/sec	48.0	48.0	58.2	58.2	43.3	45.4	68.5	68.5	52.8	84.8	72.8	65.7	66.3
G_a, lbs/(hr ft^2)	35950	29700	42750	28500	128500	92800	115800	76700	98700	57000	57800	25530	29750
V_a, ft/sec	27.8	23.0	33.0	22.0	24.9	18.0	22.4	14.9	19.1	83.1	84.3	75.3	87.8
R_g	7150	1787	1110	1110	25820	6760	4630	4630	3570	2900	1270	768	1519
R_a	38500	7940	9800	6540	137700	24830	26400	17630	22650	15250	13280	5000	6790

specified surfaces were employed to design thirteen regenerator cores. Four heat-transfer surface variations were used for Cycle (A), the 9:1 pressure ratio central-station-type plant. Five surfaces were considered for the closed-cycle plant (B). Two surface variations were selected for each of the locomotive-plant cycles, (C) and (D). All designs for a particular cycle were made for approximately equal heat-transfer effectiveness and total per cent pressure drops as specified in Table 3. Deviations from uniformity in this respect arise from the necessary trial-and-error successive approximation method of calculation characteristic of heat-exchanger design. The tedium of attaining exact equivalence was considered not to be worth the effort.

These thirteen designs are shown in Fig. 6. More detailed information with respect to film coefficients, mass velocities, Reynolds numbers, temperature effectiveness of extended surfaces, etc., are summarized in Table 4.

From these comparisons the following factors are most strikingly evident:

1 One-inch tube regenerators weigh 3 to 5 times as much as $^1/_4$-in. tube or extended plate-fin surface regenerators.

2 One-inch tube designs have the smallest nonflow dimension for a given number of cross-counterflow passes. However, the other dimensions are so large that the volumes are 4 to 8 times as great as the other designs.

3 For small flow frictions, i.e. $(\Delta P/P_1)_{\text{total}} < 3$ per cent, the plate-fin surfaces have the following advantages relative to the $^1/_4$-in. tube surface: (*a*) smaller volume, by 10 to 15 per cent, (*b*) smaller nonflow dimension, by 10 to 60 per cent. However, the weight is greater by 20 to 60 per cent.

4 For large flow frictions, i.e. $(\Delta P/P)_{\text{total}} > 5$ per cent, the $^1/_4$-in. tube surface has the advantage of (*a*) smaller volume by 30 per cent, (*b*) smaller weight by 20 to 50 per cent. However, even here the nonflow dimension is substantially poorer by 20 to 30 per cent as compared to the plate-fin surface.

5 Low-effectiveness regenerators, i.e., cycle (C), although of considerably smaller volumes, tend to have large nonflow dimensions. Reference to Equation [7] will demonstrate the reasons. The combination of smaller volume and the characteristically higher specific flow rate, W, combine to give a larger nonflow dimension in spite of larger mass velocities permitted by the higher friction allowance.

6 In the exhaust combustion cycle (D), as the effectiveness ϵ must be high and since the specific flow rate is large, the volume of the exchanger is inherently quite large, e.g., 70 to 90 cu ft/1000 shp as compared to 30 to 40 cu ft/1000 shp for cycle (A). To fit the requisite exchanger into a locomotive cab for ratings greater than 2000 shp will necessitate the use of small tubes ($^1/_4$ in.) or extended surfaces.

7 The regenerator volume in the closed-cycle plant (B) is only 25 to 30 per cent of that for the comparable open cycle (A). Most of this reduction of volume is realized by a much smaller nonflow dimension. In turn this means much better regenerator shapes for the large-capacity closed cycle as compared to the open-cycle system.

8 Contrary to general opinion, the extended surfaces of the plate-fin type, even when made of thin sheet (0.010 in.) and low thermal conductivity material (k = 12 Btu/(hr sq ft deg F ft) characteristic of high-temperature alloys), will have a fairly high temperature effectiveness on the order of 70 to 80 per cent, that is, the plate-fin surface per unit area will transfer 70 to 80 per cent as much heat as a prime or direct surface operating with the same temperature and film coefficient conditions. This conclusion also holds for the closed-cycle plant even with the much higher film coefficients, h_g, h_a.

These designs, Fig. 6, are not necessarily of "optimum" shape for the particular surface selected, because optimum conditions depend on the machinery arrangement and rating of the plant in question. However, it is believed that the geometries shown will yield a qualitative idea of what can be accomplished with the different surfaces considered.

For the circular tube surfaces with interchanged flow, i.e., gas inside and air flow normal to the tubes, calculations for several examples yielded the following comparisons with the comparable gas-inside-of-tube systems: (1) volume is increased by 20 per cent, (2) the nonflow dimension is essentially unchanged, (3) the gas-flow dimension is almost exactly doubled, (4) the air-flow dimension is almost exactly halved, and (5) the gas-side velocities are increased two and a half fold and the air-side velocities are reduced three and a half fold.

Fouling Characteristics

The foregoing designs incorporated no allowance for fouling. Until more is known about this behavior for the different surfaces, to include such a factor might be conservative but would be very much guesswork. Cognizance was taken of the problem, however, to the extent that for all the gas-side plate-fin surfaces of the open-cycle plants (A), (C), and (D), plain fins were used in preference to louvered fins, the opinion being that louvered surfaces would provide edges for the accumulation of soot deposits.

The plate-fin surfaces on the gas side operate with somewhat higher average and maximum velocities than the tube surfaces with air flow inside the tubes. Also, there are no low-velocity regions except of course for the boundary layer. Consequently, it is believed that the plate-fin surfaces will have a reduced fouling tendency. In fact, the high velocities (50 to 70 fps) and the smooth passage walls may provide a continuous soot-blowing action. In any event, mechanical cleaning of the gas side will not be feasible for either $^1/_4$-in. tube surfaces or for the plate-fin surfaces. In all probability water or chemical washing methods must be employed.

One advantage of interchanging the flow for the circular tube surfaces, which may outweigh the cost of increased volume, is that for gas flow inside the tube the gas velocities are on the order of 120 fps as compared to 50 fps for gas flow normal to the tubes. These high velocities in smooth tube passages, as in the case of the plate-plain-fin surface, should provide for a very effective self-cleaning action.

Manufacturing Costs

The plate-fin surfaces have several advantages in principle from the point of view of labor and material costs, provided that suitable high-temperature furnace brazing and/or automatic production-welding techniques can be developed.

1 High-temperature alloys in sheet form have a substantially lower cost because of the high cost of the die-drawing procedure used for tubing.

2 The $^1/_4$-in. tube surface regenerator of Cycle (A) requires 4650 9-ft tubes/1000 shp for the single-pass crossflow arrangement. For the n-pass arrangement a proportionately greater number of tubes of shorter length are required. On this basis it would appear that the hand labor involved in providing for more than 9000 tube-sheet joints per 1000 shp rating would be prohibitive. In the case of the plate-fin surface, the tube-sheet periphery requiring sealing is greatly reduced, and possibly furnace-brazing techniques could completely obviate the necessity of hand labor in this respect.

Conclusions

The conclusions and opinions that may be formed from the foregoing discussion are as follows:

1 In order that circular tube surfaces can become competitive with extended surfaces of the plate-fin type with respect to volume, weight, and shape, it is necessary to resort to small diameters of the order of $^1/_4$ in. Even then the plate-fin surface will have the advantage of a smaller nonflow dimension.

2 Units fabricated from small-diameter tubular surfaces in high-alloy material will probably have a higher material and labor cost than the plate-fin surface, provided that methods of furnace-brazing fabrication can be developed for the latter.

3 If compact regenerators have to be realized, mechanical cleaning methods cannot be employed. In this respect the plate-fin-type of surface appears to be more cleanable and will probably show less tendency to foul as compared to $^1/_4$-in. tube or similar surfaces.

4 It is believed that these conclusions justify a considerable developmental effort devoted to plate-fin surface fabrication for high-temperature service.

5 The geometric advantages of true counterflow as compared to *n*-pass cross-counterflow arrangements in many cases may warrant the difficulties of header design.

6 Conceivably, other superior types of compact surfaces are available or can be developed. Firm conclusions regarding each surface can be made only after their basic heat-transfer and flow-friction characteristics are determined. The lack of such data has tended to restrict current regenerator thinking to the shell-and-tube-type surface.

7 In all probability experience will demonstrate that there is no one best surface for the regenerator application and that the designer will need information on a number of surfaces so that the best solution may be made for the particular cycle and machinery arrangement.

ACKNOWLEDGMENT

The Office of Naval Research, the U. S. N. Bureau of Ships, and the U. S. N. Bureau of Aeronautics are currently sponsoring a heat-transfer research program for compact surfaces at Stanford University. The authors prepared this paper on this program and express their appreciation to the sponsoring organizations.

BIBLIOGRAPHY

1 "Test Results of High-Performance Heat-Exchanger Surfaces Used in Aircraft Intercoolers and Their Significance in Gas-Turbine Regenerator Design," by A. L. London and C. K. Ferguson, Trans. ASME, vol. 71, 1949, p. 17.

2 "Gas-Turbine Plant Regenerator Surfaces," by A. L. London and C. K. Ferguson, Bureau of Ships Research Memorandum 2–46, NavShips (250-338-3), July, 1946.

3 "An Investigation of the Effect of Fin Spacing on the Performance of Louvered Plate-Fin Heat Exchanger Surfaces," by W. M. Kays, Tech. Rpt. No. 3, Navy Contract N6-ONR-251, Task Order VI (NR-035-104) Stanford University, December 15, 1948.

4 "Basic Heat-Transfer and Flow-Friction Data for Gas-Turbine Plant Regenerator Surfaces," by John J. Dinan, U. S. N. Engineering Experiment Station Report No. C-2171-D, August, 1947.

5 "Basic Heat-Transfer and Flow-Friction Data for Gas-Turbine Plant Regenerator Surfaces," by John J. Dinan, U. S. N. Engineering Experiment Station Report No. C-2171-E, 1948.

6 "Basic Heat-Transfer and Flow-Friction Data for Gas-Turbine Plant Regenerator Surfaces," by John J. Dinan, U. S. N. Engineering Experiment Station Report No. C-2171-F, 1948.

7 "A Marine Gas-Turbine Plant," by C. R. Soderberg, R. B. Smith, and A. T. Scott, Transactions of the American Society of Naval Architects and Marine Engineers, vol. 53, 1945, pp. 249–289.

8 "A 5000-Kw Gas Turbine for Power Generation," by A. Howard and C. J. Walker, 1948 ASME Annual Meeting paper No. 48–A-83. See digest in *Mechanical Engineering*, vol. 71, 1949, p. 38.

9 "Construction of a Gas Turbine for Locomotive Power Plant," by William B. Tucker, *Mechanical Engineering*, vol. 70, 1948, p. 877.

10 "Heat Transmission," by W. H. McAdams, McGraw-Hill Book Company Inc., New York, N. Y., second edition, 1942.

11 Personal Communication, J. I. Yellott; and "The Exhaust-Heated Gas-Turbine Cycle," by Donald L. Mordell, Trans. ASME, vol. 72, 1950, p. 17.

12 "Gas-Turbine Regenerator-Design Studies," by W. M. Kays and A. L. London, Tech. Rpt. No. 8, Navy Contract N6-ONR-251, Task Order VI (NR-035-104) Stanford University, December 15, 1949.

Discussion

D. ARONSON.[4] A realistic comparison between tubular heat exchangers and extended-surface plate-fin types is extremely difficult to make. The characteristics of tube-and-shell design have been established as a result of years of experience, and manufacturing costs are readily estimated. In so far as this writer knows, only three models of a large-size plate-fin extended-surface exchanger for high-temperature service have been built. The cost of manufacturing these three pioneer models is several times higher than a tubular design for the same service due partly to high cost of development. However, there are no cost data on operations comparable to those involved in the fabrication of extended-surface regenerators to encourage the view that they will be cheaper than tubular units. Engineers have a tendency to look more favorably upon new designs whose full assortment of hobgoblins have not yet made an appearance.

There is a special field of application for each type. For small installations it is possible to obtain better performance with small-diameter tubing or with closely spaced fins than with larger-size tubing. As the size of the gas turbine increases, the need for small diameters diminishes. This arises from the fact that the effectiveness of a regenerator is a function of the length-to-diameter ratio of passages. In small units either length must be obtained by a multipass arrangement or small diameter must be employed. A comparison such as made by the authors on the basis of dimensions per shp is not strictly valid.

The need for further development of plate-fin surface fabrication is very real as regards brazing techniques, end connections, thermal stresses, fin effectiveness, and resistance to oxidation.

The superiority of plate-fin-type surface for minimum weight and volume mentioned in the text of the article is not borne out by the authors' own calculations as shown in Table 4. In every instance the weight and surface are least for $^1/_4$-in. tubes and in most instances the volume is just a little less for the tubular design. The comparison is as follows:

	Weight, lb	
	$^1/_4$-in. tubes	Best design plate-fin extended surface
Cycle A	1050[a]	1750
Cycle B	436[a]	475
Cycle C	526	1333
Cycle D	2450	5996
	Volume, cu ft	
Cycle A	29.3[a]	27.0
Cycle B	12.0[a]	7.05
Cycle C	14.5	20.6
Cycle D	67.5	86.3
	Surface, sq ft (total of both passages)	
Cycle A	4170[a]	8050
Cycle B	1705[a]	2150
Cycle C	2060	6250
Cycle D	9600	25,700

[a] The figures for the tubular design have been modified proportional to the ratio of the *NTU* of the tubular design to that of the extended surface so that the comparison will be somewhat closer to a fair picture.

The advantage of the plate-fin surface in having a smaller nonflow dimension is not quite clear from the authors' remarks. The virtue of the plate-fin surface can perhaps be better expressed in a different way. It possesses a greater degree of design flexibility in that the proportion of surface on the hot side to that on the cold side can be varied over a wide range. This flexibility makes it possible to fit the regenerator into any particular geometry with maximum effectiveness for a given pressure drop. Where volume of regenerator is the sole criterion the non-flow dimension should be made as large as possible.

---

[4] Elliott Company, Jeannette, Pa. Mem. ASME.

The dimensions of a tubular unit often result in an inefficient ratio of heat-transfer coefficients on the cold side to that on the hot side, and since the surface areas on the two sides are related directly as the diameter ratios, there is no opportunity for improving the utilization of surface. As a result, it will often be found that for a particular geometry of available space for the regenerator the plate-fin design can give a higher effectiveness for the same pressure drop. The price to be paid for this better performance will be a greater surface area, possibly a greater weight, and a greater cost.

The writer of this discussion presented at the ASME Annual Meeting, December, 1949, a method of designing for optimum performance, which includes consideration of some of the foregoing factors.

AUTHORS' CLOSURE

The authors agree with Mr. Aronson that a realistic comparison of general validity between tubular and extended surface gas-turbine regenerators is next to impossible to make. Even for a particular application, a comparison made now would not be valid at some later time because of rapidly changing conditions with respect to costs, methods of fabrication, and the development of new surfaces. Nevertheless, if limited comparisons can be made they should be made with as complete a realization as possible of the limitations. These are the "hobgoblins" referred to by Mr. Aronson. If engineers fail to look ahead, that is, "look favorably on new designs," the gas-turbine development will not overcome the advantage of the entrenched position now occupied by the conventional prime mover systems.

The comparison of regenerator geometry on the basis of nonflow dimension per 1000 shp will allow ready visualization of the size of heat exchanger required for any plant capacity, large or small. Mr. Aronson's objection to this basis is not clear to the authors.

There is no disagreement between the authors' text and the comparisons presented by the discusser regarding the "superiority of plate-fin-type surfaces." However, it was perhaps not emphasized that $^1/_4$ in. tubes probably represents the most compact circular tube surface that is practical while it is quite probable that more compact and more effective plate-fin surfaces exist or can be developed. As a matter of fact, current studies (12) confirm this view.

It is obvious from the first of Equations [7] that an increase of volume brought about by a change of surface will tend to decrease the nonflow dimension. It should be pointed out, however, that for a *given surface* the minimum volume design will also be very close to the minimum nonflow-dimension design. The increase of volume which produces a smaller nonflow dimension comes about from the use of a less compact surface. Thus the use of compact heat-transfer surfaces tends to yield small-volume heat exchangers but with large nonflow dimensions, as can be seen by an examination of the various designs for Cycle (A). If small volume is the only criterion then a large nonflow dimension will have to be accepted; as Mr. Aronson points out. It seems to the authors, however, that both "good" shape and "small" volume and "high" effectiveness are criteria which have to be in some measure mutually compromised in the usual design.

A Perforated-Plate Heat Exchanger

By H. O. McMahon,[1] R. J. Bowen,[1] and G. A. Bleyle, Jr.[1]

Performance data of heat transfer and flow resistance are presented for the continuous heating of air in several experimental variations of a new type of perforated-plate heat exchanger. These exchangers consisted of sections built up by stacking multiple units of a perforated aluminum plate and a neoprene gasket, to form parallel channels perpendicular to the plate faces. Tests were conducted by causing air to flow countercurrently through these passages. The effects of hole diameter, plate thickness, and gasket thickness (or plate separation) are indicated. Results are presented jointly in the form of a pressure-drop efficiency factor versus Reynolds number for portions of the range between 800 and 4300.

Nomenclature

The following nomenclature is used in this paper:

a = numerical coefficient, dimensionless
A_1 = surface area inside holes of one set of channels, sq ft
A_2 = total heat-transfer surface on both faces of plates of one set of channels, sq ft
A_3 = effective heat-transfer surface on both faces of plates of one set of channels, sq ft
A_w = mean area of cross section of fins in one set of channels, sq ft
b_c = distance between centers of adjacent holes, in.
b_f = length of fin (i.e., channel width), ft
b_L = channel height, ft
b_w = gasket ligament width (i.e., metal path between channels), ft
c = specific heat of air, Btu/(lb) (deg F)
D = diameter of holes in plates, in.
f_L = friction factor based on plate thickness, defined by Equation [5], dimensionless
g_c = gravitational conversion factor, (lb) (ft)/(sec²) (lb force)
$G_{\max}$ = mass velocity, based on hole diameter, lb/(hr) (sq ft)
h_1 = average heat-transfer coefficient of fin, arbitrarily based on A_1, Btu/(hr) (sq ft) (deg F)
h_2 = actual local heat-transfer coefficient, based on A_2, Btu/(hr) (sq ft) (deg F)
h_3 = actual local heat-transfer coefficient, based on A_1, Btu/(hr) (sq ft) (deg F)
j = heat-transfer factor for fluid flow, dimensionless $j = \left(\dfrac{h_1}{cG_{\max}}\right)\left(\dfrac{c\mu}{k}\right)^{2/3}$
k, k_w = thermal conductivity of air and fin material, respectively, (Btu) (ft)/(hr) (sq ft) (deg F)
L = plate thickness, in.
L_g = gasket thickness, compressed, in.
L_s = length of exchanger section, ft
n = numerical exponent, dimensionless
N_L = number of plates per exchanger section
N_{Re} = Reynolds number, based on hole diameter, dimensionless $\left(N_{\mathrm{Re}} = \dfrac{DG_{\max}}{12\,\mu}\right)$
ΔP_{avg} = averaged pressure difference across warm and cool channels of exchanger, lb force/sq in.
q_{avg} = rate of heat transfer, averaged for the warm and cool channels, Btu/hr
$scfm$ = volumetric flow rate, std cu ft/min
T_1 = cool-side inlet-gas temperature, deg F
T_2 = cool-side outlet-gas temperature, deg F
T_3 = warm-side inlet-gas temperature, deg F
T_4 = warm-side outlet-gas temperature, deg F
T_5 = gas temperature after rotameter, deg F
ΔT_0 = temperature difference between root of fin and gas stream, deg F
ΔT_m = length-mean temperature difference between fin and gas stream, deg F
ΔT_w = temperature difference in metal between channels (i.e., between roots of adjacent fins), deg F
ΔT_{lm} = log-mean temperature difference for exchanger, deg F
U = over-all heat-transfer coefficient, based on A_1, Btu/(hr) (sq ft) (deg F)
V = gas velocity in holes, ft/min
$\eta = \dfrac{\Delta T_m}{\Delta T_0}$ = fin effectiveness, dimensionless
ρ = gas density at average exchanger conditions, lb/cu ft
μ = gas viscosity at average exchanger gas stream temperature, lb/(hr) (ft)

Introduction

During the past decade, and particularly since the end of the war, several industrial processes have been developed which entail the handling of large volumes of gases and depend for commercial feasibility on a high degree of heat economy with a small to moderate capital investment. For example, there are the proposed techniques for tonnage production of oxygen (1)[2] as well as various specialized applications of the gas turbine. However, in none of these cases can the prime requisites of large effective surface area per unit volume of equipment and high efficiency of heat transfer with low flow resistance be satisfactorily met by the use of conventional designs of gas-to-gas heat exchangers. Consequently, process planners have been paying close attention to each promising new design of extended-surface exchanger.

Since the appearance of the definitive paper by Norris and Spofford (2), there have appeared in the technical and patent literature descriptions of many apparently practical design variations of extended-surface heat exchangers. Generally they consist of enclosures of separate, adjacent, fluid-flow channels formed from concentric piping or parallel sheets of highly conductive metal, the free spaces of which are partially occupied by some form of extended surface bonded to the channel-defining walls. Some fin-forming materials which have aroused considerable interest are the edge-wound helixes of copper ribbon devised by Collins (3, 4), louvered or smooth crimped metal plates (5), pin-fins formed from square helixes of wire (6) and stacked, louvered sheet-metal stampings (7), fin-base continuity being obtained in

---

[1] Arthur D. Little, Inc., Cambridge, Mass.

Contributed by the Heat Transfer and Gas Turbine Power Divisions and presented at the Annual Meeting, New York, N. Y., November 27–December 2, 1949, of the American Society of Mechanical Engineers.

Note: Statements and opinions advanced in papers are to be understood as individual expressions of their authors and not those of the Society. Paper No. 49—A-92.

[2] Numbers in parentheses refer to the Bibliography at the end of the paper.

each case by means of brazed or soldered contacts at the channel walls.

The ideal heat exchanger would appear to have the following characteristics: Simplicity of manufacture from low-cost materials; adaptability of the basic design for varying conditions of use; the possibility of effecting repairs to the interior of the unit without total replacement; a relatively simple manifolding problem, particularly for switch or reversing service; the ability to carry fairly large differential pressures in adjacent channels; a minimum effect of longitudinal heat conduction; interchannel heat conduction through "parent" metal without the use of thermal bonding, together with the basic considerations of large heat-transfer capacity and low resistance to flow.

It is the purpose of this paper to present a range of performance data of heat transfer and flow resistance for the heating of air in several variations of three basically similar experimental models of a unique perforated-plate type of extended-surface heat exchanger designed particularly for air separation. Exchangers of this type possess a great many of the characteristics of an ideal heat exchanger, particularly those of large heat-transfer capacity with moderate frictional losses. In recognition of this a patent application has been filed. The data presented are not comprehensive in the sense that they cover only a limited range of variation of the numerous parameters at the control of the designer. It is felt, however, that the range covered is sufficiently broad to include most of the probable engineering applications.

Description of Exchanger

It will become evident that the dimensions and materials of construction of perforated-plate exchangers can vary widely and that the optimum specifications cannot yet be considered as definitely determined for any specific application. For this reason, the present description will be confined to a presentation of the essential details and properties of the particular experimental units studied in this investigation, some sample components of which are shown in Fig. 1. However, it should be noted that commercial-size units are being fabricated, the basic design of which is similar to that of the Groups I-II runs. (See Table 1.)

The experimental exchanger section was $3^1/_2$ in. square and from 1.5 to 3.5 ft in length, completely insulated externally, the only outside connections being the inlet and outlet pipes and two pressure taps at each end. Such a section was built up in the form of a stack of units, each consisting of a thin square plate of precision-punched 2-S aluminum sheet placed on a thin die-cut neoprene gasket to form four individually gastight, parallel, narrow, longitudinal flow channels of matched metal openings, each approximately $^1/_2$ in. wide × 3 in. high. The complete stack, together with a cast aluminum header at each end, was held together by means of steel tie rods bolted to the periphery of $^1/_4$-in-thick steel end plates. Piping connections were provided in the end plates.

The circular punched holes in the plates were spaced evenly along rows parallel to a side and offset from each other in the perpendicular direction at the vertexes of equilateral triangles to form a series of horizontal unit fins, as indicated in Fig. 2.

Gases could thus pass in countercurrent turbulent motion along two sets of adjacent flow passages, transferring heat by conduction through the perforated metal. Actually, the cool and warm gas streams were each divided by the headers, allowing the cooler incoming gas to flow in the two outer channels, while the warmer gas passed in the opposite direction through the inner channels. The center passage was blocked off and served as a dead space.

This design of heat exchanger has certain obvious advantages. The turbulence of flow induced by the presence of the gasket spacers, together with the high proportion of exposed fin surface, provide for a favorable rate of heat transfer. The perforated-plate construction enables the attainment of very high fin efficiencies, by proper choice of fin length and flow conditions. The

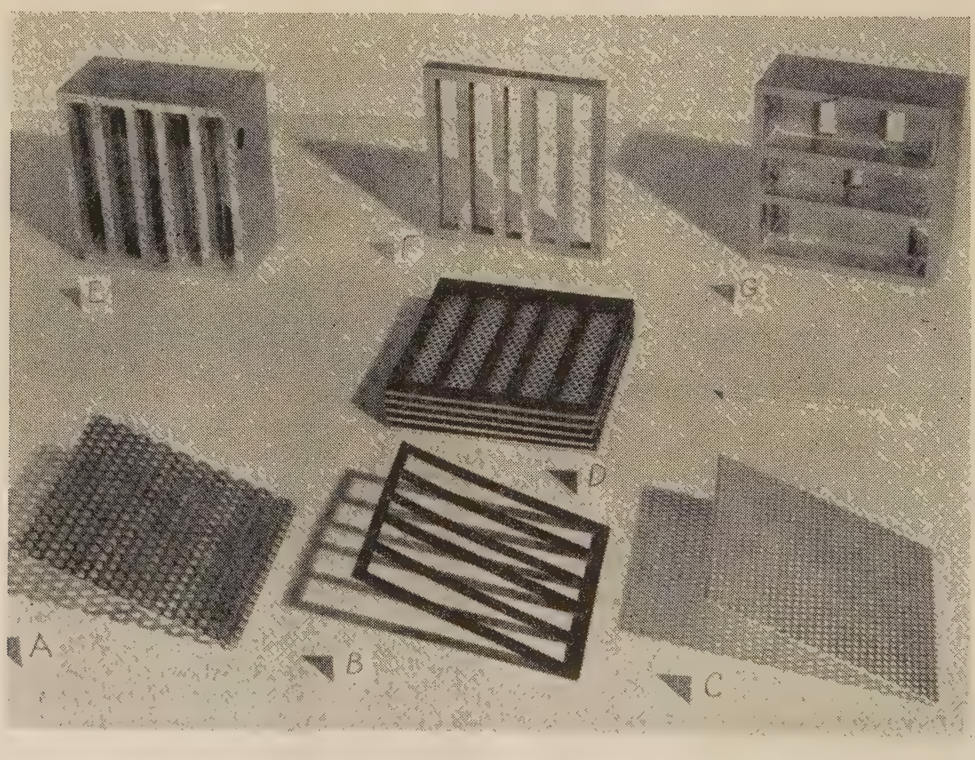

Fig. 1 Some Heat-Exchanger Components

[(A) Plate with $^1/_8$-in. holes on $^3/_{16}$-in. staggered centers; (B) typical neoprene gasket; (C) plate with $^1/_{12}$-in. holes on $^1/_8$-in. staggered centers; (D) portion of stacked exchanger; (E) inner face of header, note pressure taps; (F) center spacer; (G) outer face of header.]

TABLE 1 PHYSICAL DETAILS OF EXCHANGERS

RUN	L_g(in.)	D(in.)	L(in.)	b_c(in.)	b_f(ft.)	b_L(ft.)	b_w(ft.)	L_s(ft.)	N_L	A_1(sq.ft.)	A_w (sq.ft.)
A.											
Group 1											
1	.013	.0833	.0625	.125	.0417	.250	.0130	1.59	246	6.32	0.237
2	.022	"	"	"	"	"	"	1.77	240	6.17	0.231
3	.046	"	"	"	"	"	"	2.20	"	"	"
4	.069	"	"	"	"	"	"	2.66	"	"	"
5	.081	"	"	"	"	"	"	2.13	"	"	"
6	.102	"	"	"	"	"	"	3.36	"	"	"
B.											
Group II											
1	.022	.0833	.125	.125	.0417	.250	.0130	2.98	240	12.35	0.463
2	.047	"	"	"	"	"	"	1.77	120	6.17	0.231
3	.070	"	"	"	"	"	"	2.00	120	6.17	0.231
4	.078	"	"	"	"	"	"	1.75	100	5.15	0.193
5	.093	"	"	"	"	"	"	1.88	100	5.15	0.193
C.											
Group III											
1	.027	.125	.0625	.1875	.0364	.244	.0156	1.58	208	2.91	.199
2	.060	"	"	"	"	"	"	2.13	160	2.24	.153
3	.078	"	"	"	"	"	"	2.23	186	2.60	.178
4	.123	"	"	"	"	"	"	1.67	104	1.45	.099

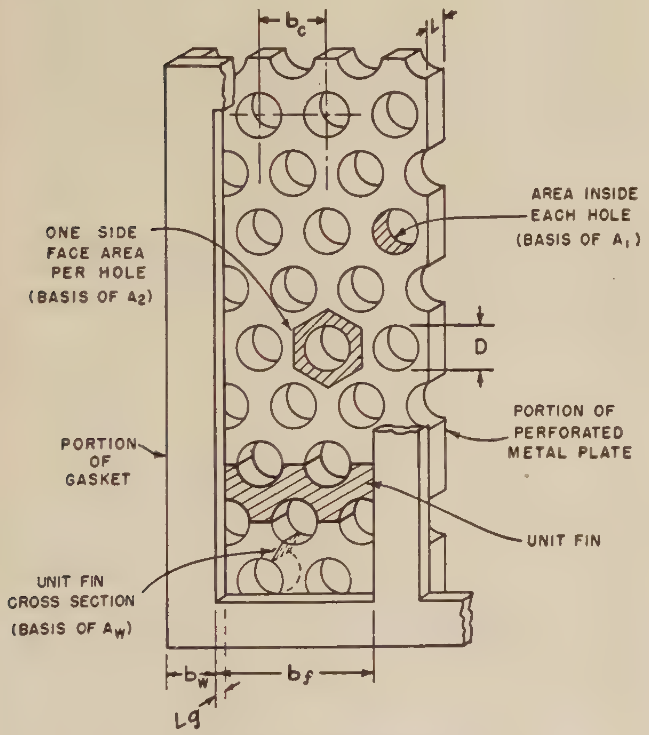
b_c
L
AREA INSIDE EACH HOLE (BASIS OF A_1)
ONE SIDE FACE AREA PER HOLE (BASIS OF A_2)
D
PORTION OF PERFORATED METAL PLATE
PORTION OF GASKET
UNIT FIN
UNIT FIN CROSS SECTION (BASIS OF A_W)
b_w
b_f
Lg

FIG. 2 SCHEMATIC REPRESENTATION OF FIN

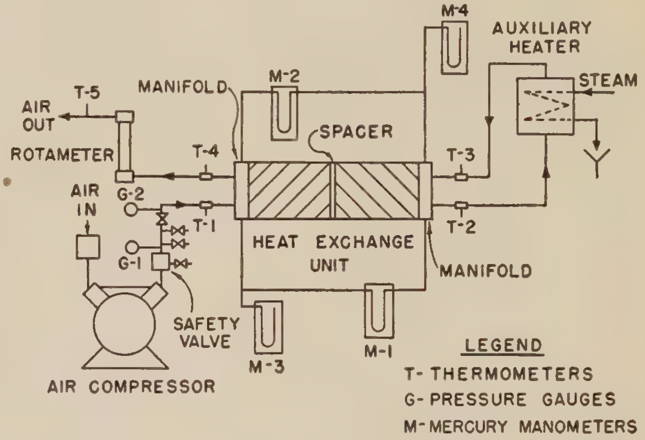

FIG. 3 EXPERIMENTAL INSTALLATION

employment of aluminum makes use of the usually higher ratio of thermal conductivity to cost per unit mass of that material compared to the value for other more conventional heat-transfer media, an important consideration for oxygen plants. The simplicity of construction is evident, as is the fact that an exchanger of this type can be disassembled plate by plate and reconstructed to meet new situations. Also, where necessary, several materials of construction or techniques of assembly can be used in a single section. Through the use of neoprene gaskets, heat conduction along the length of an exchanger is effectively eliminated. The use of neoprene also affords a very tight locked-in-place seal between plates, which can be maintained almost indefinitely, even at the temperatures of liquid air. Finally, it is possible by regulation of the hole diameters, spacing of centers, channel width, and gasket and plate thicknesses to vary the amount and type of induced turbulence as well as the fin efficiency, thereby to obtain the optimum values of heat transfer and friction losses for specific conditions of operation. As will be shown later in this paper, save for certain technical difficulties involved in the preparation of adequate low-cost gaskets, this design seems to offer possibilities of great utility to the field of gas-to-gas heat transfer. Indeed, the results of preliminary tests of furnace-brazed construction employing aluminum gasket spacers have indicated already that the economic position of this exchanger design can be improved greatly with little sacrifice of intrinsic performance characteristics.

TEST INSTALLATIONS

A schematic representation of the arrangement of the equipment used in this investigation is shown in Fig. 3.

Filtered test air was drawn into the system through a compressor of 30 cfm capacity. The air was then moved through the outer cool channels of the exchanger, through a small steam coil heater, and out through the inner warm channels of the exchanger, before being exhausted to the atmosphere.

Gages G-1 and G-2 were used to indicate the approximate inlet air pressure. Temperatures were measured by means of mercury thermometers. Static pressures and pressure drops were measured by means of mercury manometers. Flow rates were measured by means of a rotameter.

The complete exchanger, including manometer taps and thermometer wells, was thermally insulated with 6 in. of closely packed mineral wool.

Because of the simplicity of construction, few difficulties were encountered in the operation of these installations.

PROCEDURE

Experimental: The greatest installation problems were encountered during the assembly of the first exchanger section Finally, a technique was developed to insure uniformity of procedure and freedom from interchannel leaks. For this purpose a U-shaped metal frame was constructed, in which were stacked, in order, a face plate with two $^1/_2$-in. pipe connectors, a heavy neoprene gasket, and a rough-cast-aluminum header, Fig. 1 (G), and then, alternately, gaskets and perforated plates to form half of a unit. A $^3/_8$-in-thick cast-aluminum spacer, Fig. 1 (F), was then added and the second half of the exchanger completed, with the exception that the aluminum plates in this half were reversed as to the direction from which they had been punched. This latter expediency was considered necessary after preliminary tests of frictional effects had demonstrated a certain variation of pressure drop with direction of fluid flow through these plates caused by the difference in roughness of the hole ends. To assure uniformity of alignment still further, the precaution was taken to index the plates as to the direction from which they had been punched. Compared with examples of mill-run punched sheets which have been observed, these plates were quite accurately punched. The exchanger sections were held together by means of tie rods passing along the sides and bolted to the face plates. By taking up on the tie-rod nuts, the thickness of the gaskets could be varied over a range of about 30 per cent. The assemblies were then tested for leaks with air at 200 psig. In the only case of failure, the gasket between a manifold and a face plate gave way under a hydrostatic pressure of 1000 psig. It was observed that the gaskets between plates were actually locked into place by the expansion of the neoprene into the perforations. This same assembly technique was used with good success for the three groups of runs. The auxiliary test equipment was assembled with pipe fittings in a conventional manner. The rotameter was calibrated with a standard orifice.

Three separate groups of runs were carried out, using a different design of perforated plate for each group. The gasket thicknesses were varied as noted in Table 1. It should be pointed out that in the runs of Group II, the $^1/_8$-in. plate thickness was achieved by the use of units consisting of two $^1/_{16}$-in. plates cemented together. In this case an effort was made to assure that the direction of perforation was the same for each $^1/_{16}$-in. plate, but it is not certain that this was always achieved. In any case, the juxtaposition of two slightly conically tapered holes, $^1/_{16}$ in. in length, varying in diameter from end to end by as much as 5 per cent, certainly introduced a complication of the friction situation in comparison to the single-plate installations of Groups I and III.

The capacity of the compressor limited the range of flow rates to between 5 and 29 scfm. The use of mercury manometers necessitated approximations of uncertain precision in the case of pressure drops at the lowest flow rate. The static pressure of the air was kept at about 5 psig.

In the conduct of a run, inlet air was heated from approximately 70 to 220 F in the outer cool channels of an exchanger. This air was then passed through an auxiliary heater, after which it passed back through the warm channels in which it cooled from about 250 to 100 F. Actually, the log mean temperature difference in the exchanger varied from run to run between 11 and 35 F. A typical run to obtain a single series of flow data points required 6 hours for completion. Two extra hours were consumed in obtaining steady temperatures and smooth operation. At least three check values were obtained for each piece of data at 6 points in the range of flow rates for each plate design and gasket thickness.

Treatment of Data: The various temperatures, pressures, pressure differentials, and flow rates measured experimentally were combined with the data on the physical characteristics of the exchangers given in Table 1, to provide values of the heat-transfer coefficients, heat-transfer factors, friction factors, and heat-transfer efficiency factors, some of which are presented in Table 2, together with some of the important lesser variables.

As a matter of convenience, all reported values of heat-transfer coefficients have been based arbitrarily on A_1, the area inside the holes of the aluminum plates. It is recognized that the actual effective area for heat transfer must also include a portion of the face surfaces of each plate, the amount being strongly influenced by the value of the gasket thickness employed, especially when that value approaches the thickness of the plate.

The Reynolds numbers have been based on the hole diameters. In other words, the effect of gasket thickness on heat transfer has been treated as in the nature of a controlled nonconducting artificial roughness or interruption on the surface of otherwise smooth small metal tubing.

Over-all heat-transfer coefficients have been calculated from averaged values of warm- and cool-side heat-transfer rates by means of mass flow rates and air temperatures, as follows

$$U = \frac{q_{\text{avg}}}{(A_1)(\Delta T_{lm})} \quad \ldots\ldots\ldots\ldots \quad [1]$$

Utilizing the fact that the temperature difference between the fin roots of the warm and cool channels was small, it was possible to calculate the values of the effective heat-transfer coefficient (ηh_1) by means of the following expression

$$\eta h_1 = \frac{2}{\dfrac{1}{U} - \dfrac{b_w A_1}{k_w A_w}} \quad \ldots\ldots\ldots\ldots \quad [2]$$

and check them against the equivalent equation

$$\eta h_1 = \frac{2 q_{\text{avg}}}{A_1(\Delta T_{lm} - \Delta T_w)} \quad \ldots\ldots\ldots\ldots \quad [3]$$

The average of the foregoing values of (ηh_1) was solved simultaneously with the definition of fin-effectiveness (2) by trial and error, to give values of η and h_1, as follows

$$\eta = \frac{\Delta T_m}{\Delta T_0} = \frac{\tanh \sqrt{\dfrac{h_1 A_1 b_f}{k_w A_w}}}{\sqrt{\dfrac{h_1 A_1 b_f}{k_w A_w}}} \quad \ldots\ldots\ldots\ldots \quad [4]$$

Values of h_1 are presented versus N_{Re}, for the Group III runs in Fig. 4, from which can be seen their advantage in comparison to the smooth tube coefficients.

Utilizing the foregoing values of h_1, heat-transfer factors were calculated from the following

$$j = \frac{3.30\, h_1}{G_{\max}} \quad \ldots\ldots\ldots\ldots \quad [5]$$

thereby providing a function of h_1 which is only slightly influenced by the mass velocity. Values of j are presented versus N_{Re} in Fig. 5*a*, *b*, and *c*.

TABLE 2 (A) SUMMARIZED DATA AND CALCULATIONS

GROUP I RUNS

D = 1/12 in., L = 1/16 in., b_c = 1/8 in.

DATA	Lg = .013 in.						Lg = .022 in.						Lg = .046 in.					
SCFM	6.05	10.16	14.65	19.16	23.95	28.34	6.23	10.23	15.21	19.82	24.92	29.03	6.24	10.27	15.25	19.94	25.05	29.51
ΔP_{ave} lb/sq.in.	.084	.185	.270	.445	.638	.840	.080	.209	.430	.706	1.01	1.28	.070	.220	.427	.813	1.17	1.40
T-1 °F.	79.3	79.3	79.3	79.0	79.0	78.7	65.2	67.2	64.2	65.5	66.5	63.8	64.0	63.3	64.1	63.0	63.2	64.2
T-2 °F.	234.0	238.7	241.3	243.3	243.3	242.0	191.3	192.3	194.2	193.8	193.2	191.8	201.0	201.7	202.0	201.7	200.3	199.5
T-3 °F.	263.7	273.0	276.0	277.7	278.3	277.7	212.0	214.0	215.0	215.0	214.5	214.7	217.7	219.7	220.0	220.0	220.0	219.7
T-4 °F.	101.3	107.3	108.0	108.3	108.7	109.3	78.8	82.8	81.2	83.5	84.8	83.2	76.5	78.8	79.5	78.9	80.3	81.5
G lb/(hr.)(sq.ft.)	3353	5640	8124	10608	13284	15708	3483	5663	8410	10985	13825	16078	3414	5688	8436	11028	13884	16446
N_{Re}	469	788	1136	1483	1857	2196	509	833	1234	1605	2030	2258	509	839	1240	1625	2041	2405
ρ lb./cu.ft.	.065	.068	.072	.078	.085	.093	.068	.071	.075	.081	.088	.094	.068	.071	.076	.082	.088	.096
$f_{L/2}$	.042	.033	.025	.026	.025	.026	.040	.028	.039	.039	.039	.039	.034	.040	.038	.046	.045	.047
q B.t.u./hr.	1102	1897	2779	3674	4598	5401	928	1509	2306	2958	3678	4332	998	1648	2443	3206	3986	4640
ΔT_{lm} °F.	25.62	31.08	31.61	31.77	31.77	33.11	16.83	18.61	18.68	19.61	19.84	21.06	14.47	16.73	16.71	17.08	18.43	18.86
U B.t.u./(hr.)(sq.ft.)(°F.)	6.81	9.66	13.91	18.30	22.93	25.82	8.94	13.14	20.01	24.46	30.05	33.32	11.18	15.97	23.70	30.43	35.05	39.87
$\frac{\Delta T_w}{b_w}$ °F./ft.	.478	.825	1.21	1.60	2.00	2.35	.413	.672	1.03	1.32	1.64	1.93	.444	.734	1.09	1.43	1.78	2.07
h_1 B.t.u./(hr.)(sq.ft)(°F.)	14.45	21.10	31.44	43.27	56.88	66.09	19.34	29.61	48.04	61.60	79.72	91.62	24.80	37.10	59.17	81.52	98.43	118.02
j	.0142	.0124	.0128	.0135	.0141	.0139	.0184	.0172	.0188	.0185	.0190	.0188	.0236	.0215	.0231	.0244	.0234	.0237
V ft./min.	692	1162	1676	2192	2740	3242	713	1171	1742	2270	2855	3321	714	1175	1744	2281	2865	3376
$j/\frac{f_L}{2}$	.350	.378	.502	.523	.556	.528	.518	.459	.488	.480	.488	.482	.700	.542	.607	.530	.521	.511
η	.96	.94	.92	.89	.86	.84	.95	.92	.88	.85	.82	.80	.93	.90	.86	.81	.79	.76

TABLE 2(A) (*Continued*)

GROUP I RUNS (cont.)

D = 1/12 in., L = 1/16 in., b_c = 1/8 in.

DATA	Lg = .069 in.						Lg = .082 in.						Lg = .102 in.					
SCFM	6.29	10.38	15.46	20.07	25.22	29.77	6.23	10.26	15.24	19.76	24.83	29.04	6.30	10.43	15.54	20.14	25.30	29.51
ΔP_{ave} lb./sq.in.	.095	.305	.660	1.06	1.66	2.17	.106	.368	.782	1.18	1.70	2.20	.122	.466	1.03	1.80	2.34	2.86
T-1 °F.	61.5	61.0	60.2	60.8	61.8	60.1	66.0	65.5	65.3	65.7	67.0	66.0	61.8	60.5	60.2	61.5	60.8	61.0
T-2 °F.	201.7	203.3	203.0	202.7	201.3	200.0	205.3	208.0	207.3	205.3	203.3	198.7	207.5	209.0	209.5	208.5	207.0	205.0
T-3 °F.	215.3	218.3	218.7	218.7	218.7	217.7	225.7	227.7	227.3	227.0	227.3	226.3	224.0	226.0	226.0	226.0	225.5	225.0
T-4 °F.	71.5	72.3	73.6	75.2	76.2	75.7	76.8	78.5	79.8	83.2	85.2	83.8	68.8	70.0	70.8	73.0	74.5	75.0
G_{max} lb./(hr.)(sq.ft.)	3484	5736	8580	11136	13968	16512	3450	5688	8448	10944	13764	16104	3494	5760	8622	11178	14022	16344
N_{Re}	513	847	1261	1638	2057	2430	506	835	1243	1608	2023	2368	514	851	1267	1640	2062	2403
ρ lb./cu.ft.	.069	.071	.076	.082	.091	.098	.068	.072	.076	.083	.090	.099	.068	.072	.078	.085	.093	.101
$f_{L/2}$	.046	.056	.058	.059	.064	.065	.052	.069	.071	.069	.068	.070	.056	.085	.092	.104	.094	.090
q B.t.u./hr.	1026	1701	2559	3263	4089	4823	1030	1720	2536	3220	3974	4593	1090	1827	2720	3472	4323	4986
ΔT_{lm} °F.	11.73	13.67	14.50	15.12	15.79	16.58	15.73	16.09	17.11	19.69	20.96	22.35	11.08	12.88	13.26	14.28	16.02	16.81
U B.t.u./(hr.)(sq.ft.)(°F.)	14.18	21.10	28.60	35.70	41.97	47.16	14.76	24.04	33.36	36.76	42.61	46.19	15.95	22.98	33.25	39.40	43.76	48.08
$\frac{\Delta T_w}{b_w}$ °F/ft.	.458	.758	1.14	1.48	1.82	2.15	.635	1.06	1.56	1.99	2.45	2.83	.486	.814	1.22	1.54	1.92	2.23
h_1 Bt.u./(hr.)(sq.ft.)(°F.)	32.30	51.29	75.01	101.36	128.10	152.28	33.68	60.01	92.14	105.60	130.15	147.86	36.82	56.95	92.00	115.93	134.82	157.19
j	.0306	.0295	.0288	.0300	.0302	.0304	.0322	.0348	.0360	.0318	.0312	.0302	.0348	.0326	.0352	.0342	.0318	.0317
V ft./min.	719	1188	1769	2296	2885	3405	712	1173	1743	2260	2840	3322	721	1193	1778	2303	2894	3376
$j/\frac{f_L}{2}$	.681	.526	.497	.508	.472	.470	.631	.506	.508	.465	.460	.434	.619	.388	.384	.328	.344	.353
η	.91	.87	.83	.78	.74	.71	.91	.86	.80	.77	.74	.71	.90	.86	.80	.76	.74	.70

TABLE 2(B) (*Continued*)

GROUP II RUNS

D = 1/12 in., L = 1/8 in., b_c = 1/8 in.

DATA	Lg =.022 in.						Lg = .047 in.						Lg = .070 in.					
SCFM	6.26	10.33	15.42	20.11	25.40	29.36	6.26	10.31	15.36	19.93	25.02	29.09	6.22	10.25	15.06	19.72	24.89	28.73
ΔPave lb./sq. in.	.140	.387	.795	1.34	1.93	2.38	.120	.412	.872	1.38	1.98	2.49	.162	.524	1,08	1.74	2.44	3.01
T-1 °F.	62.3	61.7	62.7	62.8	64.0	63.5	62.5	62.2	62.0	62.5	63.0	62.2	67.2	67.0	69.0	68.0	70.0	70.7
T-2 °F.	206.7	208.0	207.7	208.7	207.7	207.0	207.5	208.5	208.5	207.0	206.0	203.0	214.3	216.0	216.0	214.3	212.7	211.7
T-3 °F.	223.0	224.3	225.0	225.0	224.7	224.5	227.0	229.5	230.0	230.0	230.0	229.5	235.0	236.3	238.0	237.3	237.0	236.3
T-4 °F.	70.5	71.7	72.7	73.3	74.5	74.8	74.2	76.0	77.0	79.0	80.5	79.5	77.3	79.5	82.2	82.8	85.7	87.7
G_{max} lb./(hr.)(sq.ft.)	3472	5708	8556	11160	14064	16272	3468	5724	8514	11052	13878	16110	3445	5688	8352	10932	13836	15912
N_{Re}	511	841	1259	1640	2071	2395	511	841	1253	1625	2042	2373	508	836	1229	1608	2037	2343
ρ lb./cu.ft.	.068	.072	.077	.083	.092	.098	.068	.072	.077	.084	.092	.100	.068	.071	.077	.084	.093	.100
$f_{L/2}$	.034	.036	.036	.038	.038	.037	.058	.077	.079	.081	.079	.080	.078	.099	.102	.105	.100	.100
q B.t.u./hr.	1068	1775	2635	3439	4289	4948	1072	1777	2644	3384	4207	4861	1089	1800	2621	3410	4219	4783
ΔT_{lm} °F.	11.78	12.91	13.33	13.20	13.49	14.13	15.30	17.11	18.04	19.56	20.60	21.54	14.77	16.13	17.04	18.62	19.67	20.79
U B.t.u/(hr.)(sq. ft.)(°F.)	7.36	11.13	16.05	21.10	25.74	28.35	11.36	16.84	23.74	28.05	33.10	36.59	11.93	18.10	24.95	29.70	34.78	37.31
$\frac{\Delta T_w}{b_w}$ °F./ft.	.237	.390	.580	.757	.944	1.09	.478	.791	1.18	1.50	1.87	2.17	.486	.804	1.17	1.52	1:88	2.14
h_1 B.t.u./(hr.)(sq. ft.)(°F.)	15.75	24.68	37.15	5148	65.82	74.03	25.20	39.20	59.02	73.14	90.91	104.77	26.60	42.76	62.97	78.80	97.57	107.38
j	.0150	.0143	.0143	.0152	.0154	.0150	.0240	.0226	.0228	.0218	.0216	.0214	.0255	.0248	.0248	.0238	.0233	.0223
V ft./min.	716	1181	1764	2300	2905	3358	716	1180	1757	2279	2862	3327	711	1172	1723	2256	2947	3286
$j/\frac{f_L}{2}$	.447	.401	.405	.409	.413	.412	.417	.296	.292	.272	.277	.271	.326	.256	.249	.231	.239	.227
η	.95	.93	.90	.87	.84	.83	.93	.90	.86	.83	.80	.78	.93	.89	.85	.82	.79	.77

TABLE (2B) (*Continued*)

GROUP II RUNS (cont.)

D = 1/12 in., L = 1/8 in., b_c = 1/8 in.

DATA	Lg = .078 in.						Lg = .093 in.					
SCFM	6.14	10.10	15.10	19.47	24.41	28.95	6.16	10.14	15.02	19.40	24.34	28.68
ΔPave lb./sq. in.	.150	.440	.847	1.32	1.90	2.42	.128	.418	.838	1.32	1.85	2.44
T-1 °F.	71.3	70.5	71.2	718	72.5	73.7	66.0	66.0	67.0	68.5	68.2	69.5
T-2 °F.	229.0	230.7	229.0	226.7	224.3	220.7	267.0	269.5	269.0	267.0	263.0	260.5
T-3 °F.	250.7	253.3	252.7	252.3	250.7	249.7	295.5	298.0	299.0	299.0	297.5	295.5
T-4 °F.	85.8	88.3	90.8	93.0	95.2	97.2	84.5	87.2	90.0	95.8	97.5	101.0
G_{max} lb./(hr.)(sq.ft.)	3405	5592	8376	10800	13524	16056	3414	5634	8334	10746	13500	15894
N_{Re}	501	825	1232	1584	1992	2362	502	826	1225	1583	1986	2340
ρ lb./cu.ft.	.066	.070	.074	.080	.088	.096	.064	.067	.073	.078	.085	.094
$f_{L/2}$	.088	.100	.092	.092	.092	.092	.072	.090	.089	.090	.088	.090
q B.t.u./hr.	1138	1889	2774	3514	4312	4982	1459	2414	3538	4480	5523	6356
ΔT_{lm} °F.	17.84	20.16	21.43	23.32	24.49	26.15	23.21	24.68	27.06	29.54	32.04	33.24
U B.t.u./(hr.)(sq. ft.)(°F.)	12.39	18.19	25.14	29.27	34.19	37.03	12.21	18.99	25.39	29.44	33.48	37.12
$\frac{\Delta T_w}{b_w}$ °F./ft.	.605	1.01	1.48	1.88	2.30	2.66	.778	1.28	1.89	2.39	2.95	3.39
h_1 B.t.u./(hr.)(sq. ft.)(°F.)	27.68	42.97	63.43	77.54	95.43	106.55	27.16	45.22	64.52	78.06	92.69	107.33
j	.0268	.0253	.0250	.0237	.0233	.0219	.0262	.0264	.0255	.0240	.0226	.0222
V ft./min.	703	1156	1727	2226	2793	3312	705	1160	1717	2219	2784	3281
$j/\frac{f_L}{2}$	.307	.254	.273	.261	.256	.244	.372	.294	.289	.268	.263	.248
η	.93	.89	.85	.82	.79	.77	.93	.88	.84	.82	.80	.77

TABLE 2(C) (*Continued*)

GROUP III RUNS

D = 1/8 in. , L = 1/16 in. , b_c = 3/16 in.

	(Lg = .027 in.)						(Lg = .060 in.)						(Lg = .078 in.)						(Lg = .123 in.)					
SCFM	6.14	10.07	14.79	19.40	24.39	29.06	6.12	10.07	14.95	19.25	24.25	28.75	6.13	10.09	14.98	19.42	24.35	28.73	5.98	9.79	14.53	18.80	23.56	28.01
ΔP_{ave} lb./sq.in.	.074	.362	.760	1.21	1.76	2.31	.110	.307	.622	1.02	1.44	1.96	.119	.483	.913	1.46	2.02	2.64	.113	.355	.707	1.13	1.60	2.10
T-1 °F.	68.5	69.0	70.3	70.3	70.7	70.3	68.8	68.7	69.7	70.0	70.8	71.3	71.3	71.3	71.0	71.7	72.8	73.8	77.7	77.7	77.0	76.8	76.8	76.8
T-2 °F.	230.5	229.3	228.3	226.0	223.3	219.7	220.0	220.0	220.7	218.0	216.0	213.0	237.3	237.3	234.7	231.0	227.7	224.7	236.7	237.0	234.0	230.3	226.3	221.0
T-3 °F.	257.5	257.0	257.0	255.3	253.7	252.3	248.3	250.7	250.0	250.0	249.7	249.0	261.0	262.7	262.0	261.0	258.7	257.7	272.0	274.0	274.0	272.7	271.0	268.7
T-4 °F.	88.0	91.3	93.7	95.2	97.0	96.3	88.3	91.5	94.7	97.5	100.0	100.7	86.0	88.7	91.8	94.5	96.8	99.2	104.3	108.7	111.7	115.0	117.7	120.3
G_{max} lb./(hr.)(sq.ft.)	4248	6972	10224	13428	16884	20112	4236	6948	10344	13320	16776	19884	4236	6972	10356	13440	16860	19872	4128	6744	10044	12984	16296	19356
N_{Re}	880	1444	2120	2781	3498	4167	888	1443	2173	2761	3476	4177	879	1447	2148	2785	3492	4119	858	1400	2083	2695	3379	4013
ρ lb./cu.ft.	.066	.070	.075	.081	.089	.097	.066	.070	.074	.080	.087	.096	.066	.069	.075	.081	.088	.097	.065	.068	.073	.079	.086	.095
$f_{L/2}$	.037	.071	.075	.074	.074	.075	.075	.082	.080	.085	.082	.086	.067	.105	.098	.100	.096	.098	.125	.154	.148	.152	.146	.150
q B.t.u./hr.	1179	1887	2714	3521	4337	5099	1094	1810	2611	3330	4102	4758	1200	1947	2859	3636	4432	5118	1123	1826	2667	3362	4101	4708
ΔT_{lm} °F.	23.05	24.91	25.93	27.01	28.35	29.17	23.63	25.64	27.12	29.72	31.27	33.46	18.87	21.45	23.92	26.64	27.36	28.99	30.82	33.92	37.21	40.34	42.75	45.62
U B.t.u./(hr.)(sq. ft.)(°F.)	17.58	26.03	35.97	45.02	52.59	60.11	20.68	31.52	42.98	50.02	58.56	62.86	24.46	34.93	45.96	52.54	62.31	67.91	25.13	37.12	49.43	57.48	66.16	71.18
$\frac{\Delta T_w}{b_w}$ °F./ft.	.930	1.49	2.14	2.78	3.42	4.02	1.12	1.86	2.68	3.42	4.21	4.88	1.06	1.72	2.52	3.20	3.91	4.51	1.78	2.89	4.22	5.33	6.50	7.47
h_1 B.t.u./(hr.)(sq. ft.)(°F.)	39.20	61.56	90.50	121.05	151.02	181.56	47.03	77.13	114.08	139.50	174.76	194.39	56.93	87.21	124.82	149.33	191.66	219.48	58.61	94.44	137.71	170.27	211.16	236.75
j	.0304	.0291	.0292	.0297	.0295	.0298	.0366	.0365	.0364	.0345	.0344	.0322	.0443	.0413	.0397	.0367	.0375	.0364	.0468	.0462	.0452	.0432	.0427	.0403
V ft./min.	880	1444	2121	2782	3499	4168	877	1444	2145	2761	3477	4123	879	1447	2149	2785	3493	4121	858	1403	2084	2697	3379	4017
$j/\frac{f_L}{2}$	.823	.411	.392	.402	.396	.398	.491	.446	.458	.405	.421	.374	.670	.394	.408	.366	.392	.374	.380	.301	.326	.285	.292	.269
η	.94	.90	.87	.83	.79	.77	.92	.88	.84	.81	.77	.76	.91	.87	.82	.80	.76	.73	.91	.86	.81	.78	.74	.72

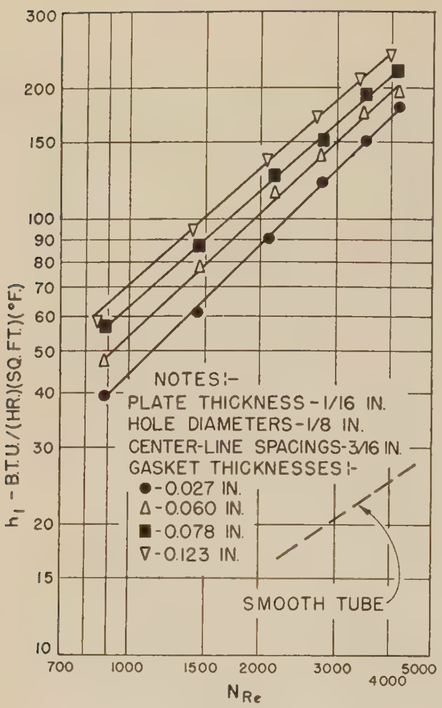

Fig. 4 Heat-Transfer Coefficient, h_1, Based on Hole Area Versus Reynolds Number for Group III Runs

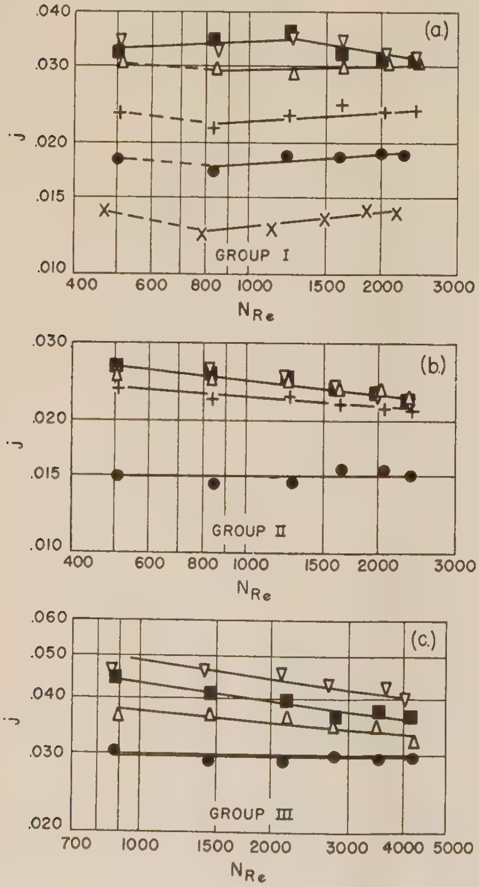

Fig. 5 (*a*, *b*, *c*) Heat-Transfer Factor Versus Reynolds Number

[(*a*) Group I runs, (*b*) Group II runs, (*c*) Group III runs.]

The effects of friction losses were calculated from net pressure drops averaged across the warm and cool channels, by means of the Fanning equation for turbulent flow, as follows

$$f_L = \frac{(72)\,(\Delta P_{\text{avg}})\,(\rho)\,(g_c)\,(D)}{(N_L)\,(L)\,(G_{\max})^2} \quad \ldots\ldots\ldots\ldots [6]$$

Values of $f_L/2$ are presented versus L_g in Fig. 6.

The final results of the heat-transmission and frictional-resistance calculations are presented in terms of the pressure drop efficiency factor $j/(f_L/2)$ versus N_{Re} in Fig. 7.

Discussion of Results

Heat Transfer: From theoretical considerations it can be postulated that the transfer of heat from a stream of gas to the metal of a perforated plate through which it is flowing, should be viewed as the resultant of two simultaneous actions. If, for a given mass flow rate, attention is focused on the events transpiring along the length of a single series of matched holes in a channel of an exchanger section, one plate and gasket of which are shown schematically in Fig. 2, certain predictions can be made concerning the probable variation in the heat-transfer process as the gasket thickness is changed. For a zero gasket thickness and a stipulated 100 per cent fin efficiency, the amount of heat transferred will be small and essentially identical to that for a smooth tube of the same diameter. As the gasket thickness is increased and assumes small finite values, the heat-transfer coefficient, h_1, based on the area A_1 inside of the holes, will rise rapidly because of the interruption and periodic destruction of the laminar-flow boundary layer near the tube walls and the resultant turbulence. As gasket thickness is increased somewhat beyond a moderate fraction of plate thickness, no further improvement in h_1 occurs, presumably because turbulence already is fully developed. This primary effect is shown clearly in the lower portions of the two curves of h_1 versus L_g in Fig. 8, where the cases of $N_{\text{Re}} = 1000$ and 2000 for the Group I runs are presented. But as the spacing is further increased, portions of the total surface, A_2, on the faces of the plates become available for heat transfer, approaching a maximum of availability when the gasket thickness approximates a small multiple of the width of face area per hole, $(b_e/2) - D$, as indicated by the upper portions of the curves of Fig. 8. Thus the actual conditions of heat transfer might perhaps be more realistically represented in the following manner

$$h_1 = h_2 \frac{(A_3)}{(A_1)} + h_3 \quad \ldots\ldots\ldots\ldots [7]$$

Unfortunately, sufficient data were not available from this investigation to do more intergroup correlation than to indicate the general agreement between the results of the Groups I and III runs and the predicted curve shapes. It was not felt advisable to attempt a comparison of the Group II results with those of the other runs, because of the uncertain nature of the surfaces of the hole interiors and the probability that they were not reproducible.

It should be emphasized that the average values of h_1, some of which are presented in Fig. 4, are based on only the surface area inside the holes, and are somewhat higher than the true local fin coefficients. However, even if one allowed for a liberal correction factor of 50 per cent, the point values would still be considerably higher than those estimated for smooth tubes at the same fluid-flow rates. Probably it would have been more realistic to base the heat-transfer coefficients on an average value of surface, such as $A_1 + (A_2/2)$. However, the present values will serve for design calculation purposes. When more data become available, it should be possible to determine with accuracy the point values of

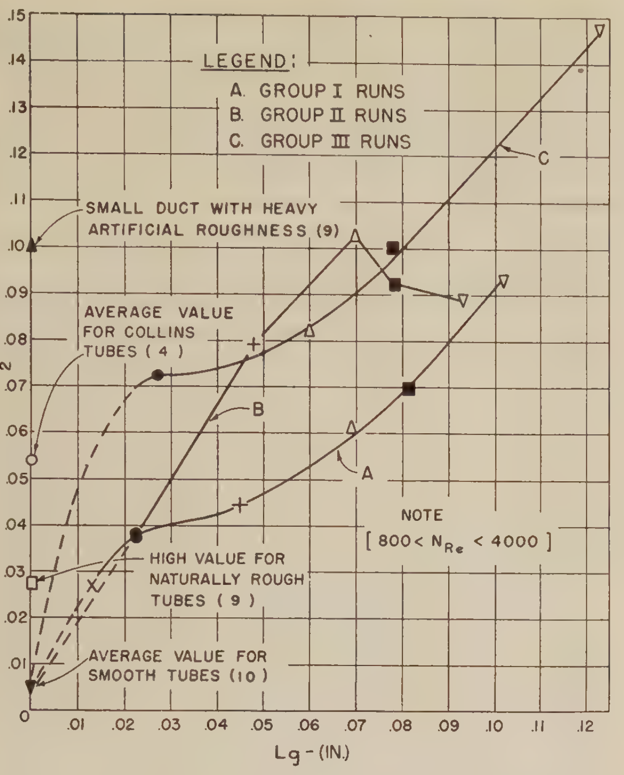

Fig. 6 Half Friction Factor Versus Gasket Thickness

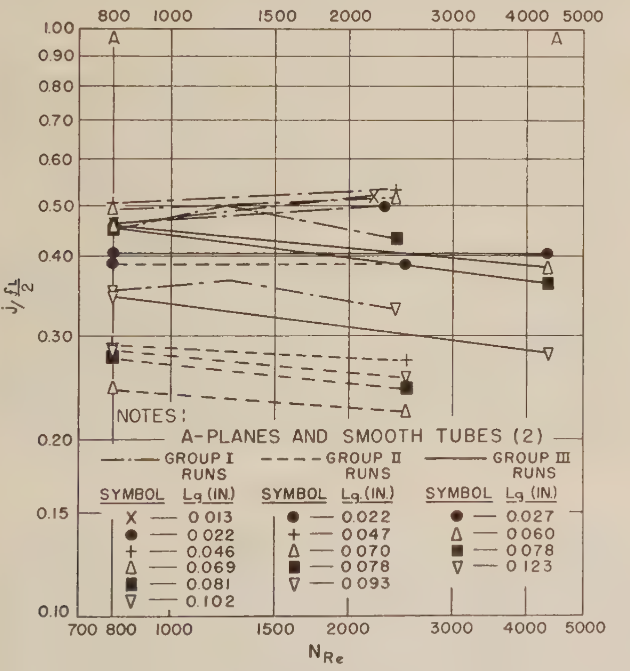

Fig. 7 Pressure-Drop Efficiency Factor Versus Reynolds Number for All Runs

h or, better still, to effect an exact correlation of average h_1's with exchanger dimensions.

Save for the case of the lowest values of Reynolds number in the Group I runs, which may indicate a transition region, the variation of h_1 with N_{Re}, was found to be a simple power function, as follows

$$h_1 = a\ (N_{Re})^n \dots\dots\dots\dots\dots\dots\dots\dots [8]$$

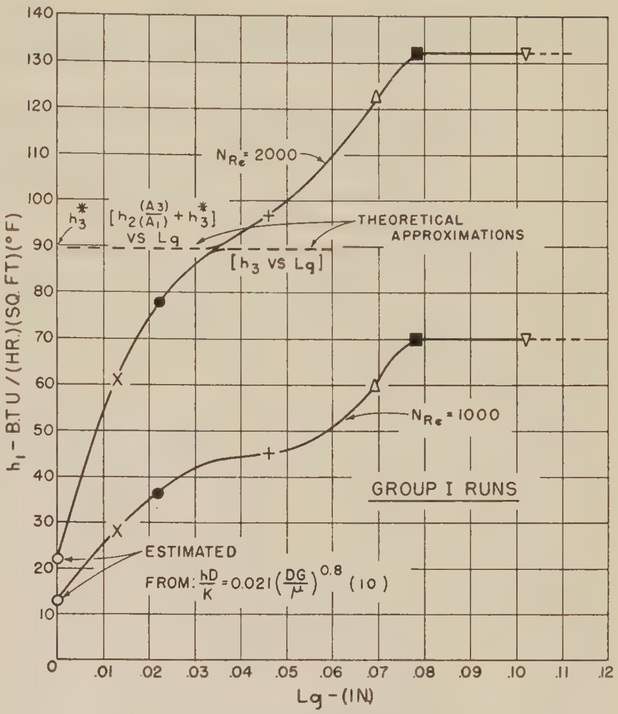

Fig. 8 Heat-Transfer Coefficient h_1, at Constant Mass Flow Rate Versus Gasket Thickness

In the range of N_{Re} covered here, the value of n varied with increasing gasket thickness from approximately 1.14 to 0.88. Since normal turbulent-flow heat exchange inside tubes varies as the 0.8 power of N_{Re}, it seems apparent that even at the lowest values of N_{Re} encountered here, normally considered to be in the region of streamline flow or transition, turbulent conditions prevailed. This was also borne out by the friction results. The fact that h_1 varied to lower powers of N_{Re} as gasket thickness increased may be attributable to a change in the nature of the turbulence. At low values of L_g, but greater than a certain minimum, the constant boundary-layer interruption would not permit normal smooth-tube turbulence. However, conceivably, normal turbulence can exist if gasket thickness is great enough.

The dependence of the heat-transfer factor j, on N_{Re} is shown to be slight in Fig. 5(a, b, and c). The fact that the slopes of these curves vary from positive to negative as gasket thickness is varied is unusual, but depends on the variation of the exponent n just noted.

The values of fin effectiveness, η, presented in Table 2, are generally high, varying between 0.70 and 0.96. From Equation [4] it is seen that any variable which can influence the value of (h_1A_1), such as mass flow rate or plate and gasket dimensions, will change η. The greatest control was exerted by the mass flow rate in these experiments.

Flow Resistance: Plate thickness was chosen as the unit of length for friction factors. It is interesting to note that in comparing values of $f_L/2$ versus N_{Re}, in Table 2, save for the runs at lowest flow rates where pressure-drop data were of uncertain precision, the friction factors are essentially independent of the mass flow rate, but a strong function of the gasket thickness. This relationship is shown in Fig. 6. The curve for the Group I runs can be seen to possess a shape similar to that for the h_1-versus-L_g curves in Fig. 8. The somewhat erratic nature of the results obtained by use of doubled $^1/_{16}$-in. plates in the Group II runs is evident from the shape of the $f_L/2$ versus L_g plot. For this reason, straight lines were used between points.

9 "A Study of the Data on the Flow of Fluids in Pipes," by E. Kemler, Trans. ASME, vol. 55, paper no. HYD-55-2, 1933.

10 "Heat Transmission," by W. H. McAdams, McGraw-Hill Book Co., Inc., New York, N. Y., second edition, 1942, pp. 170–171.

That the friction factor should be greatly influenced by the gasket thickness is obvious if one thinks in terms of tubes with controlled roughness, as mentioned earlier. Indeed, in smooth tubing several inches in diameter, the resistance to a moderately turbulent air-flow rate is raised severalfold by the presence on the pipe wall of a band of paper tape a few thousandths of an inch in thickness (8). This phenomenon bears out the laminar-boundary-layer interruption theory and forms the basis of our proposed explanation for the h_1 versus N_{Re} results of this investigation. There is some evidence from previous work with artificially roughened pipes (9) to indicate the independence of friction factor from Reynolds number in the range covered by this work. At least one author presents values of $f_L/2$ in excess of 0.10. While these previous artificial roughnesses did not begin to approach that of the plate exchangers, the agreement in principle is satisfactory.

In general, then, the results of this series of experiments have indicated that for plate exchangers, friction losses rise with mass flow rate, hole diameter, plate thickness, and gasket thickness.

The plate-exchanger friction when compared to the average Collins tube value (4), shown in Fig. 6, or to the correlations for the various fin constructions of Norris and Spofford (2), is seen to be more satisfactory than the former and to compare somewhat less favorably, even for the optimum plate design of this work, with the most efficient fin systems presented by the latter.

Efficiency Factor: Following the device used by Norris and Spofford, a "pressure-drop efficiency factor," $j/(f_L/2)$, is plotted versus Reynolds number. According to Reynolds analogy this factor is unity for forced convection over a single infinite plane and is less than unity for all other surface types. It is to be noted that the values for the perforated-plate exchangers compare favorably with those for most other forms of extended surface.

It is to be observed that the pressure-drop efficiency factor varies somewhat with Reynolds number, as would be expected from the similar variation of the heat-transfer factors.

These pressure-drop efficiency factors, regardless of the basis of N_{Re}, can be compared approximately with those for the Collins tube and for the single-plane and the finned surfaces presented by Norris and Spofford. In the case of the best values for the plate exchanger, i.e., Group I runs, the efficiencies are somewhat higher than for the Collins tube and more than 80 per cent those of most of the extended-surface designs. They are better than pin fins by about 20 per cent, averaging about 50 per cent of the value for smooth single planes and tubes.

Thus the highest efficiency factors for these plate exchangers were obtained with the smaller hole diameter, the thinner plate, and the smallest gasket thickness.

CONCLUSIONS

From this investigation of three basically similar designs of aluminum perforated-plate exchangers, the following specific conclusions are indicated:

1 In the range of flow rates, $800 < N_{\mathrm{Re}} < 4300$, the average-heat-transfer coefficient, based on the area inside of the holes, is a simple power function of N_{Re}, exponent variations with increasing gasket thickness of from 1.14 to 0.88 having been observed. The highest value of these film coefficients was 237 Btu/(hr) (sq ft) (deg F), obtained in the Group III runs.

2 Heat-transfer and flow-resistance phenomena can be explained on the basis of a two-function theory. The gasket thickness is considered to cause turbulence by the interruption of the laminar-flow layers at the walls of the tube portions, as well as by making available heat-transfer area on the faces of the plates.

3 The influence on fluid friction and heat transfer of increasing hole diameter is to increase them. The influence of increasing plate thickness is to increase fluid friction and to decrease heat transfer somewhat. (This comment is subject to the limitation mentioned previously concerning reproducibility of the Group II plate design.)

4 In the range of flow rates studied, for a given gasket thickness, the fluid friction factor is independent of the mass velocity.

5 Pressure-drop efficiency factors for these exchangers are substantially independent of mass flow rate, the absolute values varying from a low of 0.22 in the case of the Group II runs to a high of 0.53 in the Group I runs. In general, the influence of an increasing gasket thickness was, first, to increase and then to decrease this efficiency factor. Increase of hole diameter or plate thickness lowered the value of the factor. It is apparent that the type of turbulence produced by the frequently interrupted flow passages is quite efficient as a promoter of high heat transfer with only a moderate amount of fluid friction.

6 While much remains to be learned concerning the properties of perforated-plate exchangers, and the problem of gasket economics also requires additional attention, it can be stated that this type of unit possesses very attractive operational characteristics for large-scale gas-to-gas heat exchange. At the present time full-scale commercial units are being constructed in connection with a special assignment in the field of liquid-oxygen production. It is planned to publish information regarding cost analysis and plant performance in the near future.

ACKNOWLEDGMENTS

It is a pleasure to acknowledge the valuable assistance and advice of many of the staff members of Arthur D. Little, Inc., particularly that of Messrs. R. B. Hinckley and A. Latham, Jr. The kind interest and co-operation of Profs. S. C. Collins and A. H. Shapiro of the Mechanical Engineering Department of the Massachusetts Institute of Technology are also gratefully acknowledged.

[AUTHORS' NOTE: Following presentation of this paper, a question was raised concerning the observed small differences between the temperature changes of the fluid in adjacent channels. The temperature drops in the warm channels were consistently greater than the rises in the cool channels. Calculation showed this to be attributable to heat leak to the surroundings. Thus, for practical purposes, it was possible to eliminate the effect by using temperature changes averaged, between channels.]

BIBLIOGRAPHY

1 "Air Separation Principles and Technology," by the editors, *Chemical Engineering*, vol. 54, 1947, pp. 126–134.

2 "High-Performance Fins for Heat Transfer," by R. H. Norris and W. A. Spofford, Trans. ASME, vol. 64, 1942, pp. 489–496.

3 "Reversing Exchangers Purify Air for Oxygen Manufacture," by S. C. Collins, *Chemical Engineering*, vol. 53, 1946, p. 106.

4 "The Design of Ribbon-Packed Exchangers for Low-Temperature Air Separation Plants," by P. R. Trumpler and B. F. Dodge, *Chemical Engineering Progress*, vol. 43, 1947, pp. 75–84.

5 "Basic Heat Transfer and Flow Friction Data for Gas Turbine Plant Regenerator Surfaces," Report No. EES-C-2171-E, U. S. Naval Engineering Experiment Station, June 11, 1948.

6 Same title, Report No. EES-C-2171-F.

7 "New Commercial Tonnage Oxygen System," by B. H. VanDyke, *Steel*, vol. 123, 1948, p. 103.

8 Personal Communication, A. H. Shapiro.

Effect of Size on the Design and Performance of Internal-Combustion Engines

By C. F. TAYLOR,[1] CAMBRIDGE, MASS.

The importance of the problem is outlined and size effects isolated from other effects. Three similar engines were tested at the Sloan Laboratories at M.I.T. Mechanical stresses, volumetric efficiency, heat losses, and wall temperatures are explained as a function of cylinder size. The effects of cylinder size on combustion and fuel requirements are pointed out.

Introduction

A BASIC problem in the production of power, and indeed in many other fields of machine technology, is involved in the question of unit size. At an early stage in the planning of any engineering enterprise the following question should be asked: "To accomplish the required work, is it better to use few units of relatively large size, or a larger number of smaller units?" On the success in arriving at the correct answer to this question may well depend the success or failure of the whole enterprise.

In a broad sense, the discussion which follows can be taken to apply to most types of machinery dealt with by the mechanical engineer. However, since it is the author's chosen field, and since it is an excellent example of the problems involved, from this point on the discussion will be confined to the reciprocating internal-combustion engine. It would be disappointing, however, if the broader implications were entirely forgotten, especially as they apply to other types of power-producing machinery such as turbines, generators, etc.

Reciprocating Internal-Combustion Engines

Similar Engines. In order to study properly the question of unit size, it is necessary to eliminate differences in shape and differences in structural material. This process leads to the following definition of "similar engines." Similar engines are engines of different size in which each linear dimension describing the design has the same ratio to a basic linear dimension, l, which may be conveniently taken as the cylinder bore. In addition, corresponding parts in such engines must be constructed from the same material. The geometry of a series of such engines can be described by the following notation

$$(R_1, R_2, R_3, \ldots\ldots R_n)$$

where R stands for the ratio of the length of a certain part to the length of the basic dimension, and enough R's are included to describe the design completely. Any engine in the series is then completely specified by the R series, by a list of materials used in the various parts, and by the magnitude of the dimension l.

Similar Cylinders. In so far as the cylinders of a reciprocating engine are independent of each other, they can be considered as separate similar machines. Excluding the influence of other cylinders through the crankshaft, crankcase, and manifolding, this discussion can be applied with equal force to the question of whether or not an engine should have few large or many small cylinders to furnish the required power.

Weight of Similar Engines. There are certain characteristics of a series of similar engines which can be predicted from mathematical considerations alone. For example, it is obvious that weights will be proportional to l^3 and areas to l^2. Less obvious, perhaps, are certain important stress relations in such a series.

Stresses in Similar Engines. If it be assumed that the output end of each crankshaft turns with a constant angular velocity, Ω, and that deflections are negligible, it is easy to show that all "inertia" stresses, that is, stresses due to the mass and motion of the parts, will be the same at corresponding points in all engines when the values of $(l\Omega)$ and the crank angle, θ, are the same.

In most practical cases, however, there are cyclic variations in angular velocity, and deflections under load, which cannot be ignored from a stress point of view. The deflections set up vibratory stresses which may be exceedingly important. In order to deal with vibratory stresses it is necessary to assume equal damping due to friction at the rubbing surfaces and to assume that the apparatus driven by the output shaft is similar in the same sense as the engines, or else that the engines are dynamically isolated from the driven apparatus. Under these circumstances, if the pressure cycles in all the engines are the same, the variation of angular velocity with crank angle will again be the same when the values of $(l\Omega)$ at a given point in the cycle are equal. Appendix 1 indicates how this relation may be proved.

If the cycles of cylinder pressure versus crank angle are all the same, it is obvious that the stresses directly attributable to gas pressure will be the same at the same crank angle. The question of the circumstances under which pressure cycles will be the same is discussed in a later section.

Since the product $(l\Omega)$, together with the necessary design ratios and the angle θ, describe the linear velocity of a given point in any one of the engines, it can be said that, under the limitations just stated, the stress-versus-crank-angle cycle caused by gas pressure and by inertia forces will be the same in each engine of the series if the linear velocities of corresponding parts are the same. The implications of this statement for turbines, electrical machinery, etc., are obvious. In reciprocating engines, a convenient measure of linear velocity is the "mean piston speed."

It should be noted that the similitude in stress pattern at a given value of $(l\Omega)$ includes stresses due to vibration in any mode of the system. This conclusion follows not only from considerations of dimensional analysis, but because in similar structures natural frequencies of vibration are inversely proportional to the characteristic linear dimension. Thus, at a given value of $(l\Omega)$ the ratio of forcing frequencies to natural frequencies will be the same in each engine of the series, provided the gas-pressure cycles and the damping are the same and the connected equipment is isolated or is dynamically similar.

Such conditions would be fulfilled by a series of engines connected to a series of similar generators or propellers. These conditions will also be present in the case of motor vehicles, where the driven system is virtually isolated from the engine, dynamically, on account of the great torsional flexibility of the shafting between engine and wheels.

---

[1] Professor, Massachusetts Institute of Technology.

Contributed by the Oil and Gas Power Division and presented at the Annual Meeting, New York, N. Y., November 27–December 2, 1949, of The American Society of Mechanical Engineers.

Note: Statements and opinions advanced in papers are to be understood as individual expressions of their authors and not those of the Society. Paper No. 49—A-116.

Although stresses due to the force of gravity are seldom of much importance in reciprocating engines, it is interesting to note that in a series of similar engines these stresses increase in proportion to the linear dimension. A proof of this statement is given in Appendix 1. The practical conclusion to be drawn from this relation is that gravitational stresses will become important if unit size is made sufficiently large. Evidence of this trend is indicated by the fact that in studying the balance and vibration of very large engines, gravitational forces are usually considered.

The remaining type of stress to be considered is that due to temperature differences. In structures of similar geometry made of the same materials, it can be shown that such stresses will not be the same unless temperatures at corresponding points are the same. This question is more fully discussed in a subsequent section.

A point to be noted in connection with stress considerations is that, in the absence of resonance effects, stresses due to inertia increase with the square of the linear velocity. It may be predicted, therefore, that inertia stresses are likely to constitute a most important limitation on linear velocities. A corresponding limitation is even more obvious in the case of turbines.

M.I.T. Similar Engines. The foregoing relations are capable of mathematical proof which leaves little doubt of their general validity. When it comes to the more complicated questions of fluid flow, heat flow, combustion, etc., theory does not give the complete answer.

In order to afford opportunity for experiment in this highly important field, there have been constructed at the Sloan Laboratories of the Massachusetts Institute of Technology, three single-cylinder engines which fulfill with considerable exactness the definition of similitude on which the foregoing discussion is based. Fig. 1 is a cross section of these engines. One drawing serves for all three, with only a change in scale. The bores are $2^1/_2$, 4, and 6 in., respectively, and the strokes are 3, 4.8, and 7.2 in. All details are in proportion, including bearing clearances, wall thicknesses, and screw threads. As installed for test, inlet and exhaust systems are similar.

At present these engines are arranged for four-stroke spark-ignition operation using a premixed gaseous charge. Later they can be converted to Diesel operation, or, with new cylinders, to operate on the two-stroke cycle.

Similar Operating Conditions. For internal-combustion engines the important independent operating variables include inlet-air pressure and temperature, exhaust pressure, fuel-air ratio and coolant-supply temperature. These variables are controlled primarily by factors other than size, and they will be considered to be held the same for all engines in a similar series, unless otherwise noted. Also, the ignition or injection timing will be taken as optimum in each case. Test results presented for the M.I.T. similar engines have been made under these circumstances. The remaining important independent variable, rotational speed, is limited by size considerations as already indicated.

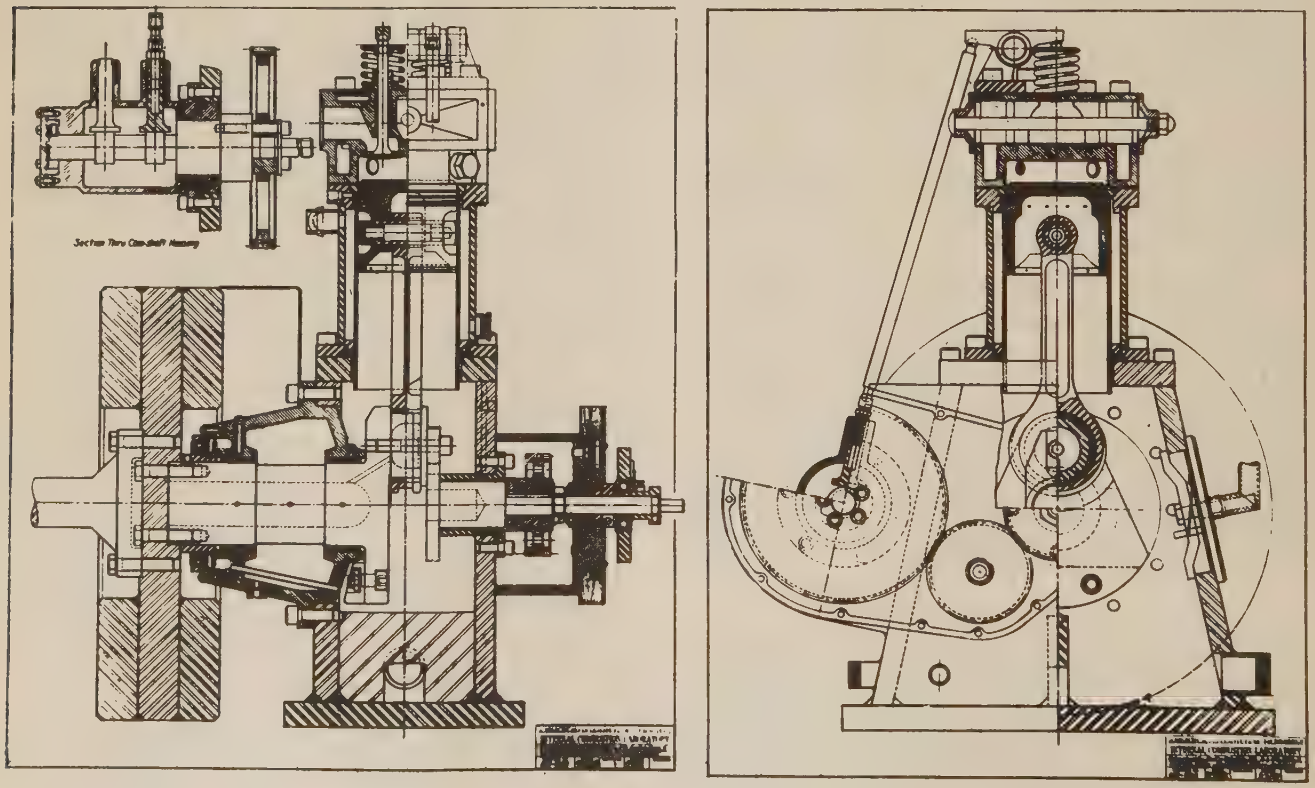

	Bore in.	Stroke in.	Piston Area in.^{2}	Displ. Vol. in.^{3}
Small	2.500	3.000	4.91	14.71
Medium	4.000	4.800	12.57	60.35
Large	6.000	7.200	28.27	203.54

Fig. 1 Cross Sections of the Three M.I.T. Geometrically Similar Engines
(Single-cylinder, water-cooled, compression ratio, r = 5.74.)

Air Flow in Similar Engines. One interesting relation here is quite obvious. Since the speed of sound is the limiting gas velocity at the smallest cross section of a flow system, when pressures and temperatures on the upstream side of this section are the same (and shapes are the same), maximum mass flow will be proportional to the square of the typical dimension. We are used to this relation in turbines, where critical flow through the nozzles is customarily considered. In the case of reciprocating engines the inlet-valve opening is usually the smallest cross section. It is thus easy to see that, under similar operating conditions, the maximum mass rate of air flow, and hence the maximum possible power output, is proportional to an area rather than a volume. For flows less than critical, the foregoing considerations suggest that a Mach index, that is, an index defining the relation of flow velocity to sound velocity, will be of great importance.

In dealing with questions of mass flow of air in reciprocating engines, it is convenient to use the parameter called "volumetric efficiency," which will be defined here as the ratio of the actual mass flow to a mass flow equal to the displaced volume multiplied by the air density in the inlet manifold of the engine.

Appendix 2 shows that, for a series of similar engines operating under similar conditions, volumetric efficiency is a function of the two nondimensional parameters

$$s/c \text{ and } sl\rho/g_0\mu$$

where s is mean piston speed, c is speed of sound in air at inlet conditions, ρ is inlet-air density, μ is viscosity of air at inlet conditions, l is the typical dimension, and g_0 is the coefficient relating force and mass.

It will be noted that the first fraction in the series is in the nature of a Mach index and the second has the characteristics of a Reynolds index. The same system of parameters applies to a gas turbine by substituting rotor tip velocity for mean piston speed.

Volumetric Efficiency Versus Mach Index. It might be inferred that, in reciprocating engines, variations in viscous forces and in heat-transfer coefficients, which depend on the Reynolds number, will be of considerably less importance in this particular case than the forces due to inertia of the gas, which are dependent upon the Mach number. If this be the case, the curve of volumetric efficiency versus Mach index should be the same for similar engines under similar operating conditions. Fig. 2, constructed from tests on the M.I.T. similar engines, shows this assumption to be valid within the size range employed and within the accuracy of the measurements.[2]

There is evidently no discernible trend on the basis of cylinder size, which would not be the case if the Reynolds index had an important influence on volumetric efficiency.[3]

The foregoing statement is not intended to imply that heat transfer is an unimportant factor in connection with volumetric efficiency, or in other aspects of engine performance. As a matter of fact, heat transfer to the inlet gases accounts for a considerable portion of the difference between the actual and ideal volumetric efficiencies of most engines.[4] What appears to be unimportant, from the M.I.T. tests, is the effect of size on the part which heat transfer plays in determining volumetric efficiency.

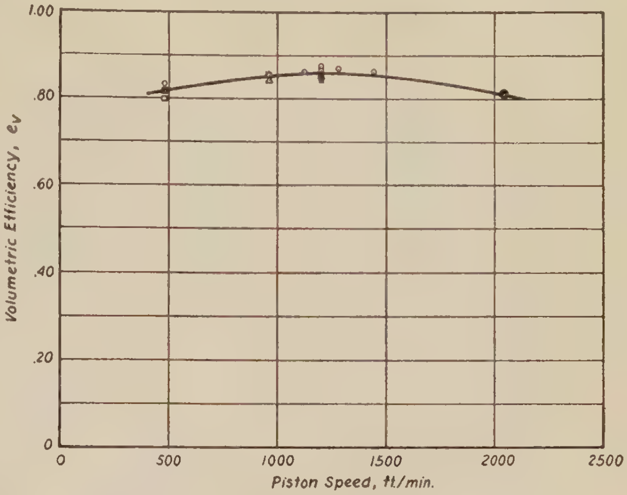

Range of rpm

Piston Speed ft/min. →	480	960	1200	2040
□ Small	960	1920	2400	4080
○ Medium	600	1200	1500	2550
△ Large	400	800	1000	1700

FIG. 2 VOLUMETRIC EFFICIENCY VERSUS PISTON SPEED OF M.I.T. GEOMETRICALLY SIMILAR ENGINES

($r = 5.74$; $F = 0.073$; optimum spark advance; $p_i = 28$ in. Hg, $p_e = 32$ in. Hg absolute; $T_i = 150$ F.)

Another important item to be noted is that the volumetric efficiency versus piston-speed relation will not be the same for similar engines unless the connected inlet and exhaust systems are similar. Without such similitude, pressure-wave patterns in the inlet and exhaust piping will not be the same at the same piston speed.

A third point to be noted is that the foregoing discussion applies to supercharged engines, provided the superchargers and their connections are similar. This conclusion follows, because the theory has placed no limitations on design detail.

Since it has been common practice to regard "rpm" as an important parameter of engine performance, the curve in Fig. 2 has been plotted versus rpm in Fig. 3. Obviously, rpm is a poor index where cylinder size is not the same.

Heat Losses. The coefficient of heat transfer between a fluid and a solid surface depends on geometry, and on the local Reynolds number and Prandtl number.[5] Assuming the same fluids and gases in our system of similar engines, the Prandtl numbers will be the same. Assuming internal Reynolds numbers to be a function of the Reynolds index, $sl\rho/g_0\mu$, with the same inlet conditions and at the same piston speed, heat-transfer coefficients will evidently vary with size. Dimensional analysis, together with existing knowledge of less complicated heat-transfer systems indicates that, under the conditions specified:

1 Heat-transfer coefficients grow less as cylinder size increases, because of the increasing local Reynolds numbers both inside the cylinder and in the cooling system.

2 In spite of the decreasing coefficients, mentioned in (1), temperature differences across the cylinder walls, piston, valves, etc., increase with increasing size, due to the longer heat-flow paths.

3 Heat loss per unit wall area decreases with increasing size.

Fig. 4, taken from the M.I.T. similar engines under similar operating conditions, confirms the second statement. These temperatures were taken by means of thermocouples embedded at corresponding points in the cylinder heads, close to the inner surface of the wall.

---

[2] Since inlet temperature was the same, the value of the speed of sound c was the same for all engines, and volumetric efficiency has been plotted against s rather than against s/c.

[3] Only a limited amount of testing has been completed as yet with the M.I.T. engines. The accuracy of measurement and reproducibility of results are, therefore, not yet as good as is hoped for later.

[4] "Rise in Temperature of the Charge as It Passes Through the Inlet Valve. . .," by J. E. Forbes and E. S. Taylor, Technical Note No. 839, National Advisory Committee for Aeronautics, January, 1942.

[5] "Heat Transmission," by W. H. McAdams, McGraw-Hill Book Company, Inc., New York, N. Y., 1942.

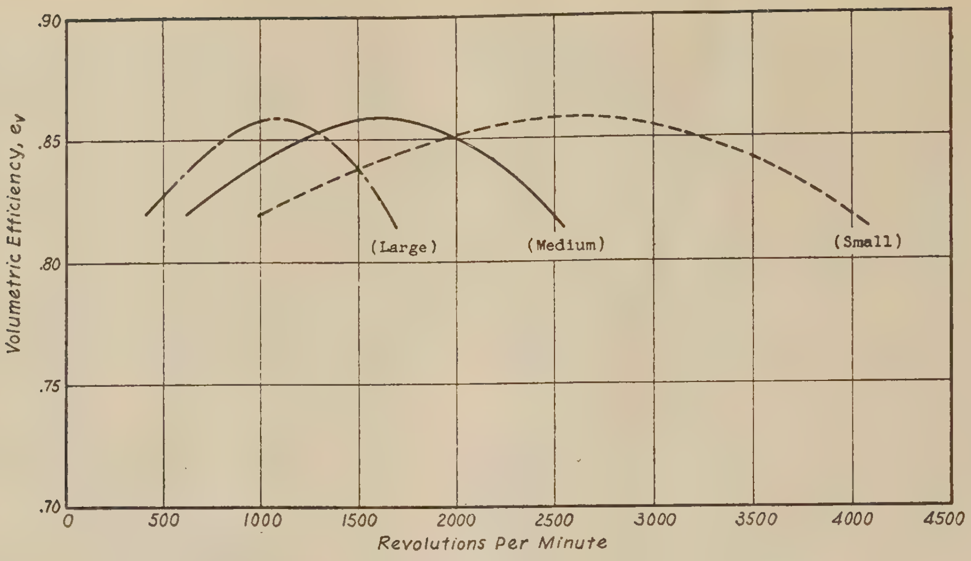

Fig. 3 Volumetric Efficiency Versus Rpm of the M.I.T. Geometrically Similar Engines
(Same operating conditions as in Fig. 2.)

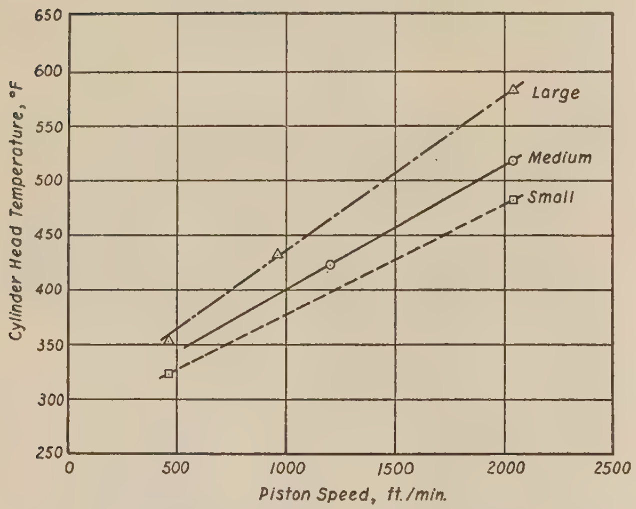

Fig. 4 Cylinder-Head Temperature Versus Piston Speed of M.I.T. Geometrically Similar Engines
(Same operating conditions as in Fig. 2. Temperatures were taken at corresponding points near inside surface of cylinder heads.)

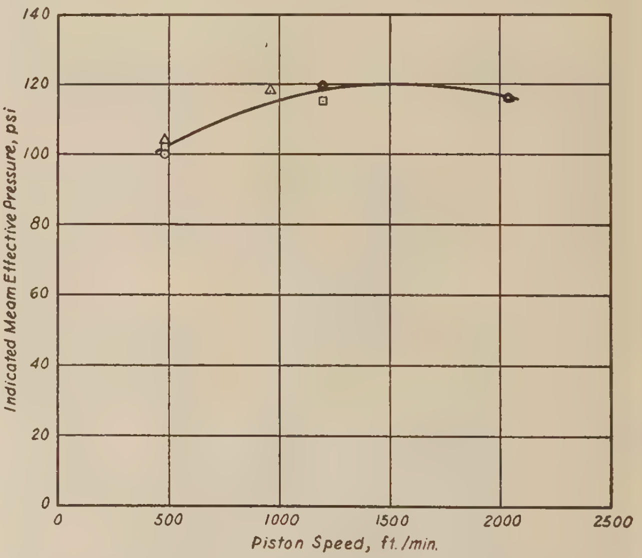

Fig. 5 Indicated Mean Effective Pressure Versus Piston Speed of M.I.T. Geometrically Similar Engines
(Symbols and operating conditions same as in Fig. 2)

The implications of the second conclusion are highly important. It follows that, for similar engines run under similar operating conditions and at the same piston speed, stresses due to temperature differences will increase with cylinder size. In practice, this results in departures from similitude in the direction of more effective cooling as cylinder size increases. Oil or water circulation within the pistons and exhaust valves of large cylinders is an example.

Indicated Mean Pressure. At the same volumetric efficiency and fuel-air ratio, indicated mean effective pressure will be the same, provided thermal efficiency is the same. This statement is simply a matter of accepted definitions.

At the same piston speed and fuel-air ratio, therefore, indicated mean pressure will be proportional to thermal efficiency. Due to the smaller heat losses of the larger cylinder one would expect its thermal efficiency to be higher. Fig. 5 shows, however, that within the range of size of the M.I.T. engines, the differences in efficiency are smaller than the uncertainties of measurement, and the imep versus piston-speed curves are the same.

Figs. 6 and 7 show indicator diagrams made from the three engines at the same piston speed and under similar operating conditions. The diagrams are the same within the accuracy of measurement. At the same rpm the diagrams are quite different. Figs. 6 and 7 lend further confirmation to the foregoing theory, including the predominant influence of the Mach index on volumetric efficiency.

Following up this subject further, the author has plotted, Fig. 8, indicated thermal efficiency versus bore for a number of commercial Diesel engines, based on manufacturers' data. If the data for large bores are representative, a trend in the expected direction is indicated.

Fuel and Combustion. In spark-ignition engines, flame speed tends to be proportional to piston speed, regardless of cylinder size. This being the case, the time required for the flame to cross the combustion chamber of similar engines running at the same piston speed increases in proportion to the bore. The time required for autoignition of the end gas, however, remains constant

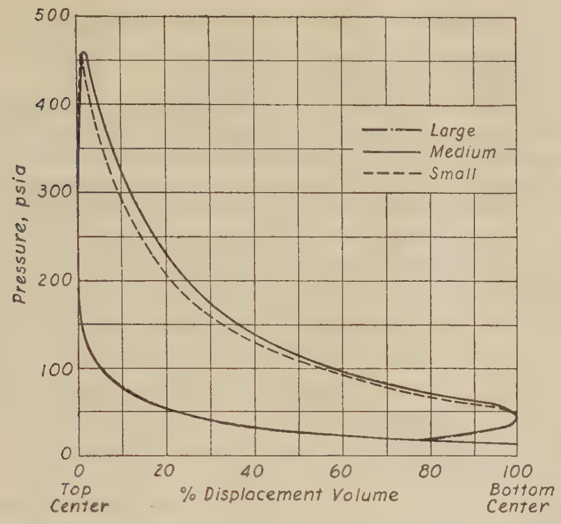

FIG. 6 INDICATOR DIAGRAMS OF M.I.T. GEOMETRICALLY SIMILAR ENGINES

(Piston speed = 2040 fpm; other operating conditions same as in Fig.2.)

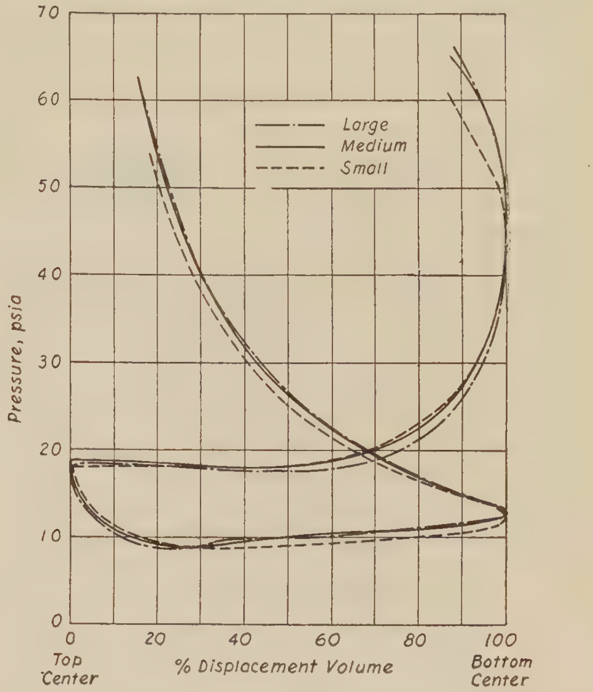

FIG. 7 LIGHT-SPRING INDICATOR DIAGRAMS OF M.I.T. GEOMETRICALLY SIMILAR ENGINES

(Piston speed = 2040 fpm; other operating conditions same as in Fig. 2.)

with a given fuel and fuel-air ratio. Thus there is an increasing tendency toward autoignition of the end gas, causing detonation,[6] as cylinder bore increases. Another way of stating this relation is that the detonation-limited indicated mean effective pressure increases with decreasing bore. Fig. 9 shows this increase to be very rapid, although the slope of the curve may vary with the fuel used. This relation would tend to make small cylinders very desirable for aircraft engines, or in other services where supercharging may be used and very high specific output is desirable. Without supercharging and with a given fuel, compression ratio may be raised as cylinder size decreases, thus increasing indicated mean effective pressure and decreasing fuel consumption. If compression ratio is not changed, a fuel more resistant to detonation will be required as the bore increases. It is considerations of detonation which, perhaps more than any other factor, have tended to limit the bore of spark-ignition engines to a maximum of 6 or 7 in. for most purposes.

In Diesel engines, on the other hand, most of the difficulty in securing satisfactory combustion rates centers around the "delay angle," that is, the crank angle between the start of injection and the beginning of rapid combustion. The larger this angle, the more difficult it is to avoid excessively high rates of pressure rise. At the same piston speed, as cylinders get larger the time to traverse a given crank angle grows correspondingly longer. Thus fuels with longer ignition delays can be tolerated as the bore increases, which is of great practical advantage. In the other direction, as bore gets smaller and rpm increase, either fuels with better ignition quality are required, or the design must be changed to incorporate prechambers designed to limit the rate of pressure rise over the piston.

From these considerations it is easy to see why engines with very large cylinders are invariably Diesels.

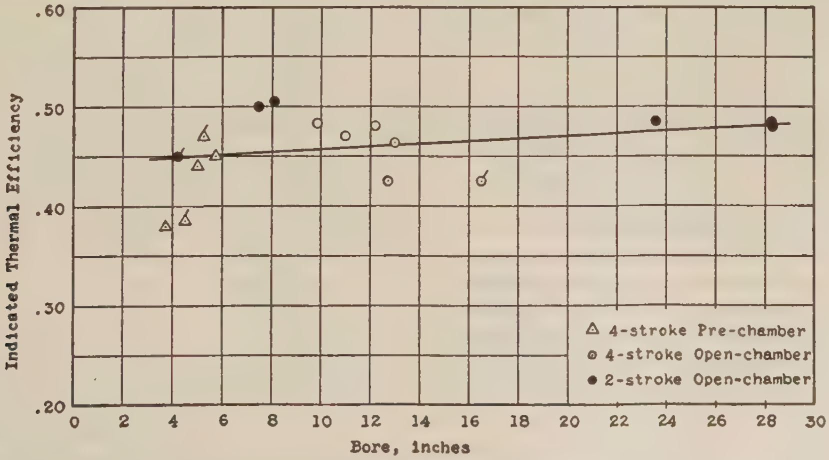

FIG. 8 INDICATED THERMAL EFFICIENCY OF DIESEL ENGINES AT 0.60 × CHEMICALLY CORRECT FUEL-AIR RATIO

(From manufacturers' performance data, 1949.)

---

[6] For definitions of "detonation," "end gas," and for a more complete discussion of this whole subject see "The Internal Combustion Engine," by C. F. Taylor and E. S. Taylor, International Textbook Company, ed. 1948, chapt. 6.

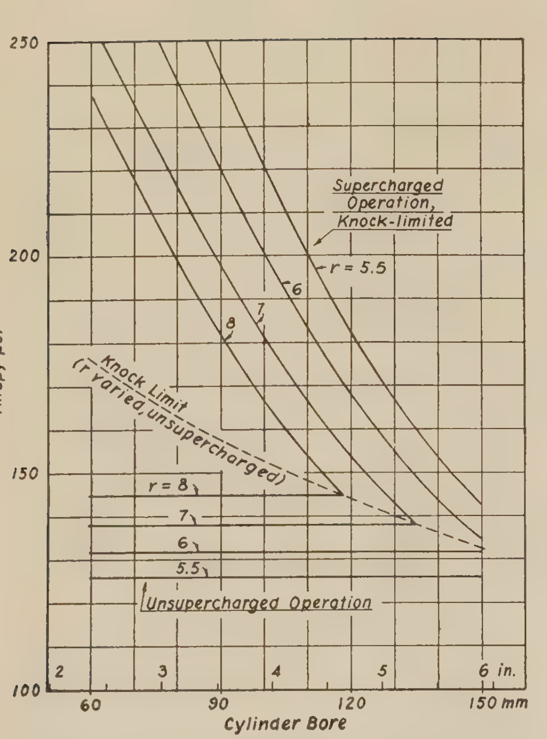

FIG. 9 EFFECT OF SIZE ON KNOCK-LIMITED IMEP IN SIMILAR CYLINDERS

(Piston speed = 2170 fpm, adapted from Kamm, *Schriften der Deutschen Akademie der Luftfahrforschung*, March 3, 1939, r is compression ratio.)

Friction. It is well known that the coefficient of friction of well-lubricated bearings of similar design is a function of the parameter ($\mu N/p$), in which μ is the oil viscosity, N is the angular velocity, and p is the unit load. We have shown that in similar engines running at the same piston speed and under similar operating conditions, p will be the same; N, obviously, will be inversely proportional to the dimension, l, so that for the friction parameter to be the same for all engines of the series, μ/l must be the same. In other words, oil viscosity must be proportional to the characteristic dimension. Similar considerations lead to the same conclusion for sliding bearings under conditions of fluid-film lubrication.

There remains the question of bearings operating under conditions of partial lubrication. Less is known about this type of friction, but since it constitutes only a very small fraction of the total friction, the assumption that all the coefficients of mechanical friction will be the same if oil viscosity is proportional to bore, seems justified.

Since unit bearing pressures in our similar engines under similar operating conditions will be the same at the same piston speed, unit friction forces should be the same, which means that the mean effective pressure to overcome friction should be the same.

Experiments on the M.I.T. similar engines have not borne out this theory, the mechanical friction mep being smaller as engine size increases, Fig. 10. The differences are larger than expected, especially in view of Fig. 11 which shows nearly equal values of friction mep versus piston speed for two engines of enormously different size. Further investigation of the causes for the wide differences in friction mep of the M.I.T. similar engines is indicated.

Brake Mean Effective Pressure. With equal indicated mep and equal friction mep, brake mep obviously will be the same. Even if friction mep is not the same, it is generally small enough compared to indicated mep so that the resulting differences due to engine size should be small. Thus it is not surprising that engines for similar service tend to be rated at the same brake mep and piston speed, as indicated by Fig. 12.

Power Output and Weight. Since power output is proportional to the product of piston area, brake mean effective pressure, and piston speed, the output of similar engines running at the same piston speed will be nearly proportional to l^2, that is, nearly proportional to the "piston area" rather than the piston displacement. Since weight is obviously proportional to l^3, or to displacement, the weight per unit output increases with the linear dimension. In spite of wide differences in design, this trend is indicated by Fig. 13. This relation constitutes one of the strongest arguments for the use of small units or small cylinders, where feasible.

Wear and Life. While the mechanism of wear and how to control it is not yet clearly understood, there seems good basis for the following assumptions:

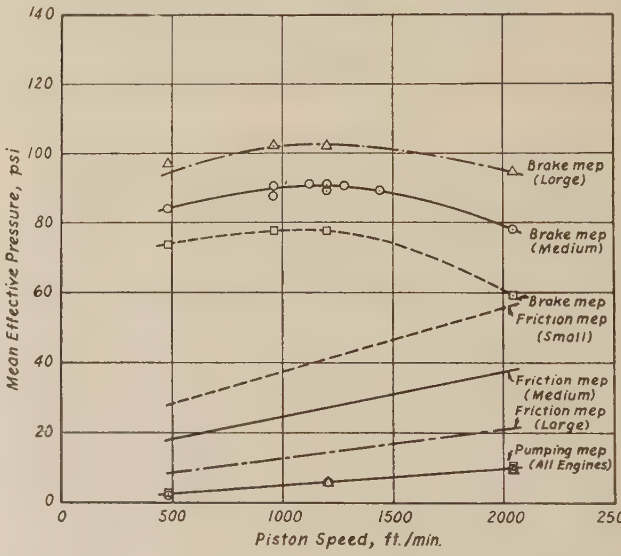

FIG. 10 BRAKE, FRICTION, AND PUMPING MEAN EFFECTIVE PRESSURE VERSUS PISTON SPEED OF M.I.T. GEOMETRICALLY SIMILAR ENGINES

(Same operating conditions as in Fig. 2. Friction mep includes pumping cycle. For mechanical friction only, subtract pumping mep.)

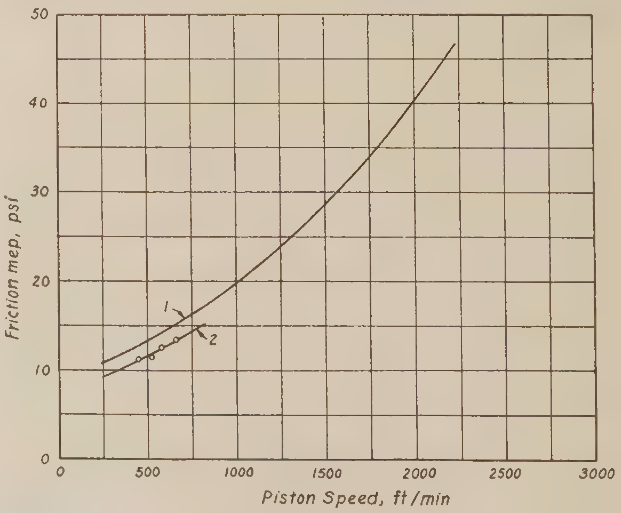

FIG. 11 FRICTION MEAN EFFECTIVE PRESSURE OF TWO ENGINES

(Curve 1 from motoring test of G-M 6-cylinder two-stroke Diesel engine, 4.25 in. × 5 in., single-acting, with scavenging pump. Curve 2 from indicator cards of Sulzer 8-cylinder two-stroke Diesel engine, 19.6 in. × 35.3 in., single acting, with scavenging pump.)

(*a*) Depth of corrosive wear per unit time should be independent of size.

(*b*) With the same materials, same unit pressures, depth of contact wear should be proportional to distance traveled. Therefore depth of contact wear per unit time should be the same for similar engines running at the same piston speed.

Wear "damage" should be measured by depth of wear divided by the dimension of the worn part. Therefore, if (*a*) and (*b*) be true, wear damage per unit time varies in proportion to the reciprocal of the bore. In other words, the "life" of similar engines, as limited by wear, increases as the cylinder bore increases. This conclusion is in line with common experience.

Costs of Manufacture. These depend on weight of materials, size of parts, and on the number and character of machine operations. The small unit would appear to have the advantage in respect to weight and size, but of course requires more parts for the same power output. However, small parts lend themselves to mass-production methods better than do large ones. The following figures apply to two engines with cylinders of nearly similar design:

Engine	No.cyls.	Bore, in.	Stroke, in.	Rpm	Hp	Weight, lb/hp	Retail price, $/hp
GM 6-71.	6	$4^1/_4$	5	1800	180	12.1	28
GM 16-278	16	$8^1/_2$	$10^1/_2$	750	1600	17.5	31

NOTE: Prices include d-c generator, were quoted in Boston, Mass., 1949. Other figures from *Diesel Power*, April, 1949.

It is known that the cost per horsepower of Diesel engines with very large cylinders is much higher than the figures given.

American Diesel Engines. Maximum rated brake mean effective pressure and the piston speed at maximum rating are shown for U. S. Diesel Engines in Figs. 14 and 15, respectively.

Mean effective pressures and piston speeds, on the average, decrease slightly with bore, partly due to considerations of increasing temperature stresses, and partly to the fact that as engines get larger there is less opportunity for development work and ratings must, therefore, be conservative.

A Contrast. Fig. 16 shows a composite view of a Nordberg 29-in. × 40-in. two-stroke Diesel engine and an Arden 0.495-in. × 0.516-in. model airplane engine, also a two-stroke compression-ignition type. In spite of the considerable difference in size and field of these two engines, the last three figures in Table 1 show their basic similarity.

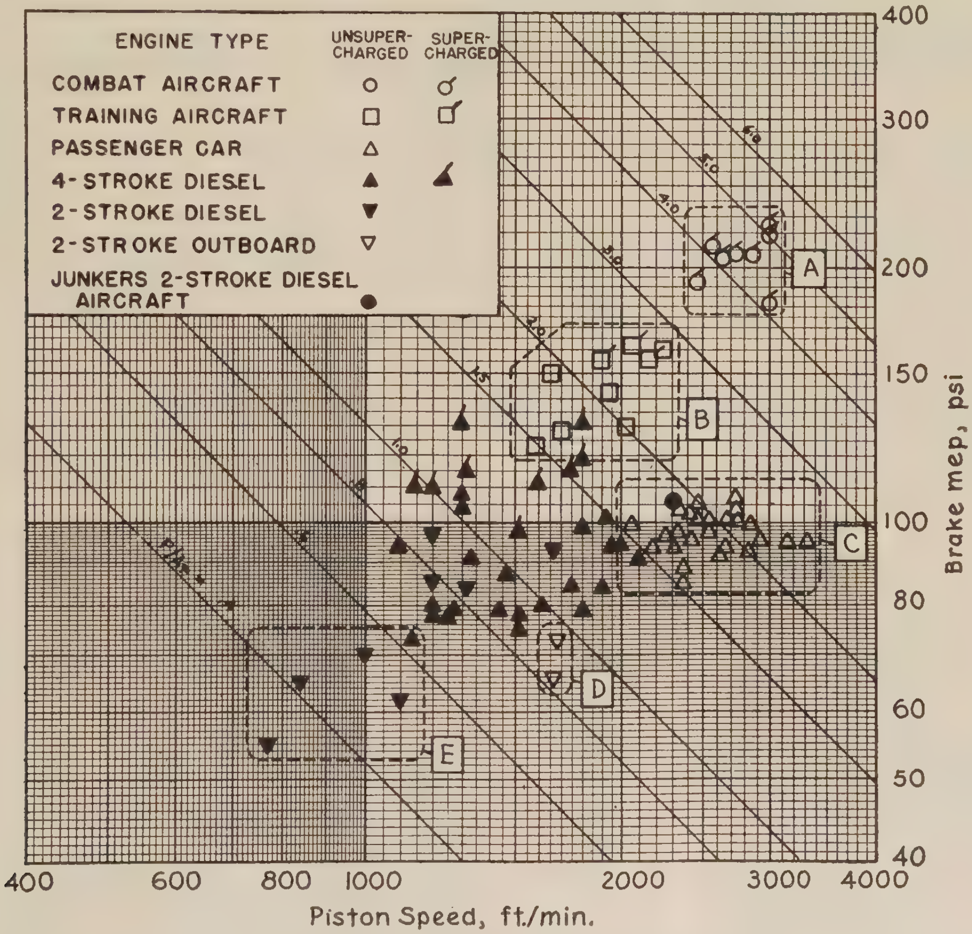

FIG. 12 RATED BRAKE MEAN EFFECTIVE PRESSURE, PISTON SPEED AND POWER PER SQUARE-INCH PISTON AREA OF VARIOUS TYPES OF ENGINES

(Published ratings, 1945; Combat aircraft-engine ratings are at sea-level take-off with 100-octane gasoline, without water injection; P/A_p lines are constant ratios of horsepower to piston area in sq in. for 4-stroke engines: multiply by 2 for 2-stroke engines.

Group A, Combat aircraft engines
Group B, Training aircraft engines
Group C, Passenger-car engines
Group D, Outboard marine engines
Group E, Heavy-duty Diesel engines

Remaining points are for miscellaneous Diesel engines including automotive and locomotive types.)

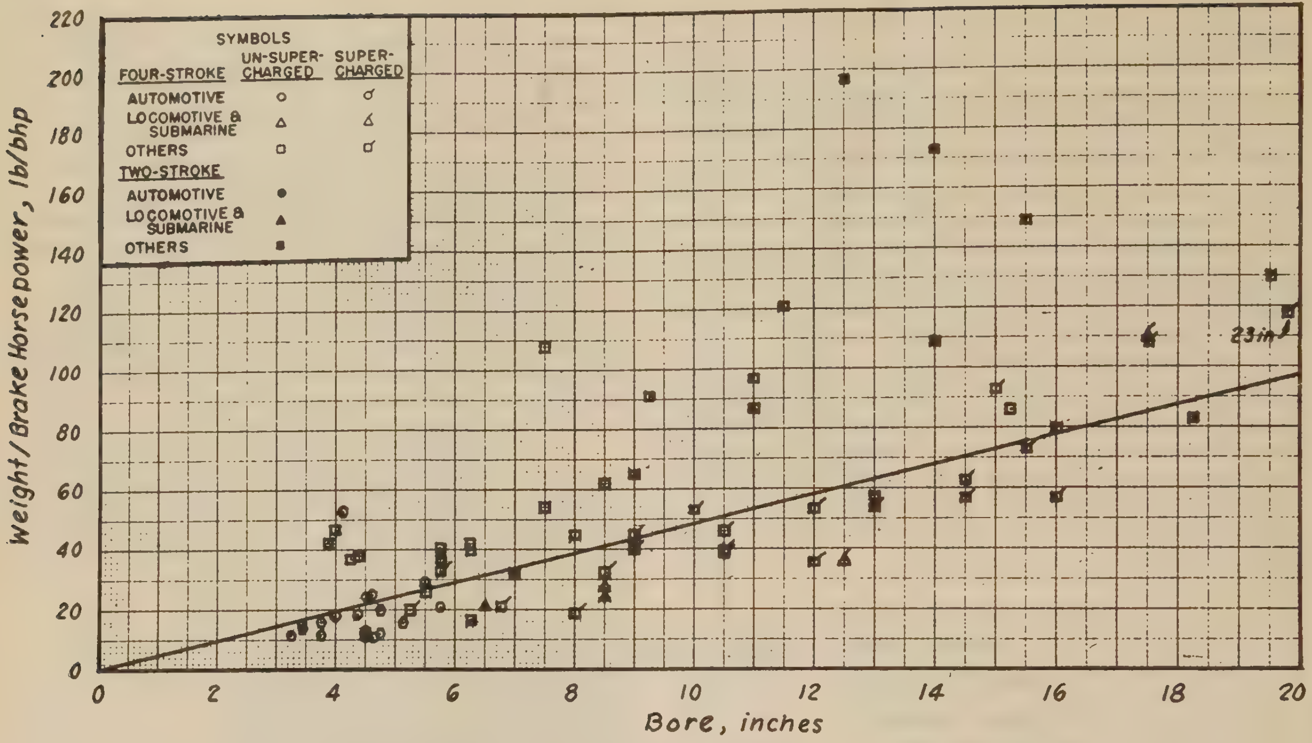

Fig. 13 Weight Per Rated Brake Horsepower Versus Bore of Representative U. S. Compression-Ignition Engines
(Data from *Diesel Power and Diesel Transportation*, April, 1947.)

TABLE 1 ENGINE DETAILS

	Arden	Nordberg
Bhp per cylinder	0.136	710
Rpm	11400	164
Cylinder displacement, in.^{3}	0.10	26500
Piston speed, fpm	980	1100
Bmep, psi	47	66
Weight ÷ bore^3, lb/in.^{3}	3.1	3.2

The performance figures for the Arden were obtained by test at M.I.T. at maximum output. Those for the Nordberg are the manufacturer's ratings. The weight of the Arden has been corrected on the assumption that the aluminum parts are changed to cast iron, to correspond with the materials used in the larger engine.

CONCLUSION

Table 2 has been prepared to summarize the practical aspects of the foregoing discussion.

TABLE 2 SUMMARY OF ENGINE DATA DISCUSSED

	For a given output and for:	Unit size should be	Cylinder size should be
1	Smallest weight	small	small
2	Smallest volume	small	small
3	Lowest first cost	small	small
4	Lowest fuel consumption, Diesel	...	large
5	Cheapest fuel, Diesel	...	large
6	Lowest fuel consumption, spark ignition	...	small
7	Cheapest fuel, spark ignition	...	small
8	Longest life (wear)	large	large

Appendix 1

Similar Engines. These will be taken as engines in which all corresponding length ratios are the same and in which the same materials are used in corresponding parts. Such engines can be completely described by the following notation:

Typical dimension	l
Design (length) ratios	$(R_1, R_2, R_3 \ldots R_n)$
A bill of materials	

Basic properties of the materials can be specified by the value for a given material. For example:

All moduli of elasticity will be proportional to a characteristic modulus, E.

All densities of material will be proportional to a characteristic density ρ.

The same can be said for heat conductivities, etc.

Fundamental Dimensions

For purposes of this discussion, the fundamental dimensions are taken as follows:

Length	L
Force	F
Time	t
Mass	M
Absolute temperature	T

Inertia and Gravitational Stresses. In so far as stresses due to inertia and gravity are concerned, only the following properties will be important:

Name	Symbol	Dimension
Characteristic length	l	L
Design ratios	$(R_1 \ldots R_n)$	0
Characteristic density	ρ	ML^{-3}
Characteristic modulus of elasticity	E	FL^{-2}
Angular velocity	Ω	t^{-1}
Crank angle	θ	0
Damping coefficient[a]	C	$FL^{-3}t$
Acceleration of gravity	g	Lt^{-2}
Dimensional constant connecting force, mass, and acceleration	g_0	$MLT^{-2}F^{-1}$

Introducing the typical stress σ, which has the dimensions FL^{-2} we can write the dimensionless equation

$$\phi_1 \left(\frac{\rho l^2 \Omega^2}{\sigma g_0}, \frac{\rho l^2 \Omega^2}{E g_0}, \frac{g \rho l}{\sigma g_0}, \frac{C g_0}{\rho l \Omega}, \theta, R_1 \ldots R_n \right) = 0$$

---

[a] The damping coefficient here referred to is the damping force per unit area and per unit velocity between rubbing surfaces. The internal damping coefficients of the materials will of course be the same in similar engines.

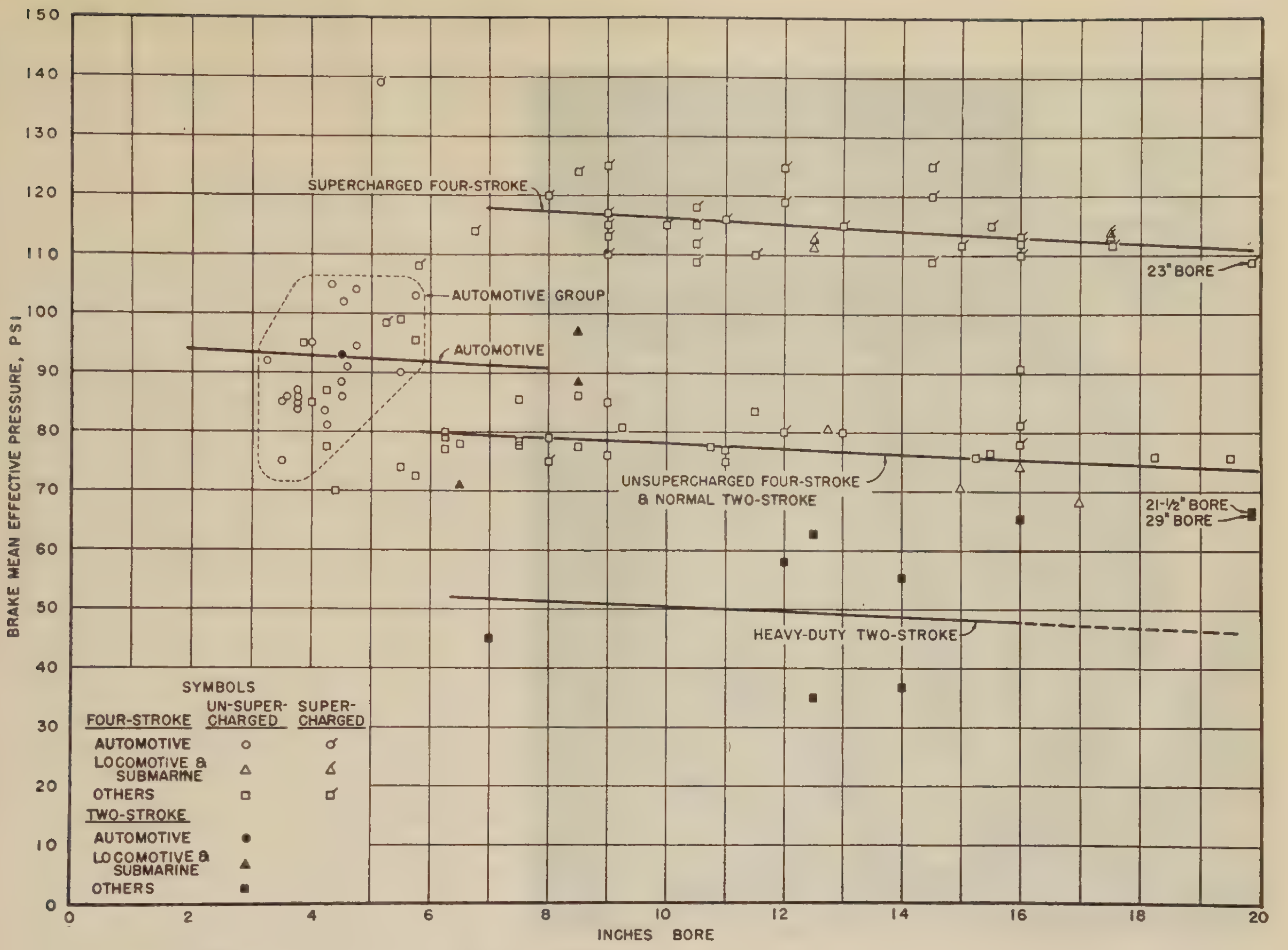

Fig. 14 Rated Brake Mean Effective Pressure Versus Bore of Representative U. S. Compression-Ignition Engines
(Data from *Diesel Power and Diesel Transportation*, April, 1947.)

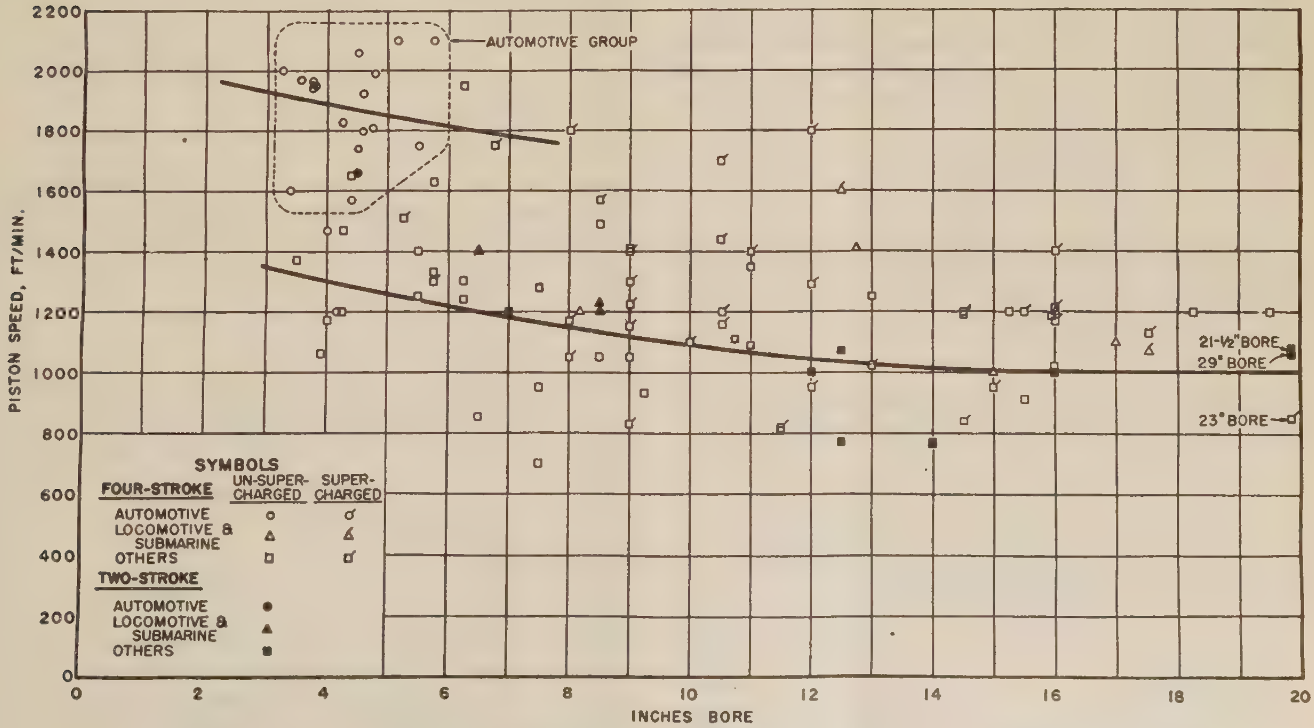

Fig. 15 Piston Speed at Rated Power Versus Bore of Representative U. S. Compression-Ignition Engines
(Data from *Diesel Power and Diesel Transportation*, April, 1947.)

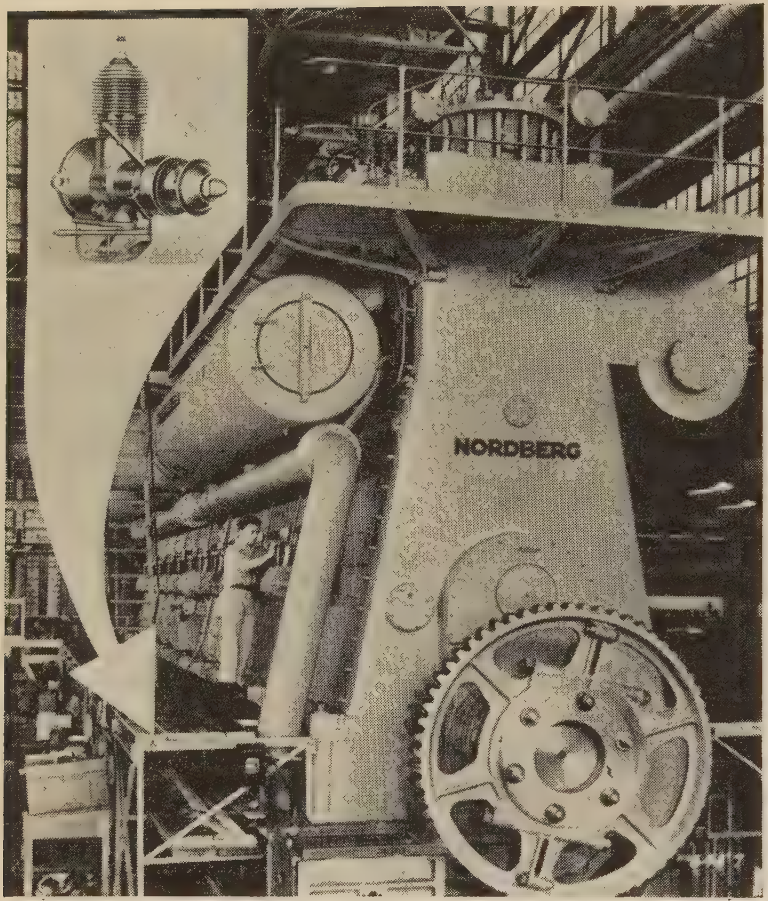

Fig. 16 Comparison of a Nordberg Diesel Engine and an Arden Model Airplane Engine

	Arden	Nordberg
Bore, in.	0.495	29
Stroke, in.	0.516	40
Cylinder displacement, in.^{3}	0.10	26500
No. of cylinders	1	10
Bhp per cylinder	0.136	710
Rpm	11400	164
Piston speed, fpm	980	1100
Bmep, psi	47	66
Weight ÷ bore^3, lb/in.^{3}	3.1	3.2

where ϕ_1 indicates a function of what follows. This notation means that if values are assigned to all but one of the terms in the parentheses, the value of the remaining term is determined. The third term in parentheses describes a parameter controlling stresses due to gravity. It is evident that these stresses vary with the typical length, l. Assuming such stresses to be negligible, and omitting all constant terms gives

$$\phi_2 \left[\frac{\rho(l\Omega)^2}{\sigma g_0}, \frac{\rho(l\Omega)^2}{E g_0}, \frac{C g_0}{\rho l \Omega}, \theta \right] = 0$$

C will be the same in similar engines provided the oil viscosity is proportional to the bore. Assuming this to be the case, and eliminating all constant quantities, we can write the following equation, no longer dimensionless

$$\sigma = \phi_4(l\Omega, \theta)$$

This equation indicates that corresponding stresses will be the same at the same values of mean piston speed and crank angle.

Appendix 2

Volumetric Efficiency of Similar Engines. Assuming similar design, the independent engine variables which affect volumetric efficiency can be taken as follows:

Variable	Symbol	Dimensions
Typical length	l	L
Angular velocity	Ω	t^{-1}
Inlet pressure	p_i	FL^{-2}
Exhaust pressure	p_e	FL^{-2}
Inlet temperature	T_i	T
Coolant temperature	T_j	T
Fuel-air ratio	F	0
Inlet-gas characteristics:		
Density	ρ	ML^{-3}
Viscosity	μ	$FL^{-2}t$
Speed of sound	c	Lt^{-1}
Ratio of specific heats	k	0
Prandtl number	π_p	0

Since the Prandtl number is the same for real gases, it can be omitted from further consideration. Adding volumetric efficiency, e_v, which is the dependent variable under consideration, we can write

$$\phi_1 \left(e_v, \frac{l\Omega}{c}, \frac{\rho l^2 \Omega}{g_0 \mu}, \frac{p_e}{p_i}, F, \frac{T_j}{T_i}, k \right) = 0$$

Let it be assumed that similar engines all use the same inlet gas (air), and that the fuel-air ratio, pressures, and temperatures are held constant. Omitting the constant arguments yields

$$\phi_2 \left(e_v, \frac{l\Omega}{c}, \frac{\rho l^2 \Omega}{g_0 \mu} \right) = 0$$

omitting all constant quantities

$$e_v = \phi_3 \,(l\Omega, l)$$

The function indicated by ϕ_3 now contains constants which are not dimensionless. It indicates that, under similar running conditions, the volumetric efficiency of similar engines is a function of piston speed ($l\Omega$) and of the bore (l). The presence of the term (l) comes from the Reynolds index. If viscous forces and variations in heat-transfer coefficient are considered to have a negligible influence, volumetric efficiency becomes a function of piston speed alone.

Discussion

L. E. Johnson.[7] The thesis Professor Taylor has presented has been carefully developed in two ways: analytically as a problem involving mechanics, hydraulics, and empirically other sciences; and by testing and studying the actual performance of products that are essentially similar.

In any discussion of the effect of engine size on volumetric efficiency, the effect of the residual or unscavenged gases on the effectiveness of the succeeding induction stroke should not be overlooked. Because of lower heat transfer from gases to the cylinder wall with increase in cylinder bore, as pointed out in the paper, these residual gases are measurably higher in enthalpy per cubic inch of displacement than in the smaller-size cylinders. The hotter gases, undoubtedly, tend to reduce the volumetric efficiency of larger engines. However, as a matter of experience, we know that the volumetric efficiency is essentially identical for the same piston speed in cylinders of varying size. We may conclude that the heating effect of residual gases is balanced out by the reduced heat transfer to the incoming air in the manifolds of the larger bore engines, a factor which the author points out but adjudges insignificant. Thus, while the conclusion drawn by the author regarding volumetric efficiency is still essentially correct, for a full understanding of the phenomena these two balancing factors should not be overlooked.

In general, the experience of engine manufacturers with the effect of engine size on friction horsepower is in line with the experience cited in the paper and contrary to the conclusion arrived at analytically, that fmep should remain constant. In general, smaller engines have higher fmep and, as a result, higher fuel consumption at a given bmep than do larger bore engines. In trying to determine where the extra losses occur, we have stripped our smaller engines part by part and have found that most of the difference results from greater heat losses which make available for recovery a smaller percentage of the work of compression. The indicator card may not be accurate enough to show this but motoring tests certainly do.

Perhaps the difference may be explained by the difference in rate of heat transfer per cubic inch of displacement to the cylinder walls during the compression and expansion strokes with varying bore. Presuming that greater heat transfer in the smaller engines does alter cylinder pressures, then the determination of friction horsepower by computing the difference between bhp and card indicated horsepower would not reveal the loss to the cylinder walls whereas friction determined by motoring would. However, a comparison of very accurate indicator diagrams obtained on different sizes of similar engines should reveal lower pressure levels on the smaller bore engines, providing compression ratios and timing events are identical. This difference in friction is not a pumping loss in the normal sense, to be measured by analyzing the indicator diagram during the intake and exhaust stroke, but is a loss of a portion of the energy stored during compression, which cannot be returned to the crankshaft during expansion. In this regard it should be pointed out that the two engines compared in the paper, namely, the GM 671 and the large Sulzer two-stroke cycle Diesel are quite dissimilar in design. The former has a stroke to bore ratio of 1.18 and operates on fast-burning fuels, whereas the latter has a stroke to bore ratio of 1.8 and undoubtedly is operated on bunker C or other heavy fuel.

In general, bearing friction is a very small proportion of engine friction at normal operating temperatures. While the conclusion drawn is that bearing friction will be an identical fraction of output in similar engines, the inference that the large engine should be supplied with a heavier oil than the small engine may be in question. Certainly for equal unit friction, oil viscosity must be greater in the bearings of the larger engine, However, due to the longer leakage path across the bearing of the larger engine with the same average hydrodynamic pressure as in smaller engines, the larger bearing must run with greater clearance. This in itself results in a lower rate of shearing per unit volume of lubricant which in turn produces less bearing temperature rise within the engine. This results in less reduction in viscosity, requiring still more flow clearance and still less heating, sufficient to establish the required balance of pressure and viscosity. Thus automatically the oil is more viscous due to less heating in the bearing of the large engine to a degree which may eliminate completely any difference in viscosity grade of oil required.

Any manufacturer concerned with engine design for wide customer acceptance, is concerned with production and maintenance costs. Some analysis of the relation between the costs of similar engines of different sizes would be intensely interesting. This analysis would be complicated by the wide spread in unit costs for parts made in different quantities per year. This is particularly significant in analyzing the cost of wear. While the smaller part may have to be discarded in a shorter period of time due to less capacity for wear, the replacement cost is often so much less due to the combined factors of size of part and use of mass-production tooling, that replacement cost per horsepower-hour is competitive. The labor involved in installing the smaller part is also less as is also the cost of invested capital that is tied up during the life of the engine and during nonproductive time.

Perhaps the tendency of manufacturers to operate large-bore engines at lower bmep is not because of the inherently poor capabilities of the larger cylinders, but rather because of the different nature of the applications to which the different engine sizes are applied. It is our experience with similar engines in similar service that the opposite is true, that the larger cylinder can operate at higher bmep, providing that piston temperatures which tend to be higher are controlled.

On the other hand, the trend to lower piston speeds for large-bore engines has several practical explanations: Piston temperature drops at a greater rate through reduction in piston speed than it does from reduction in bmep so that lowering speed is a more desirable method of controlling piston temperatures than is lowering of bmep. In fact, it is possible, by lowering piston speed and increasing bmep, to reduce piston temperatures without reducing horsepower output of a given-size cylinder. Another consideration is that the slower-burning heavy fuels have their widest use in the larger engines and are more completely burned at lower piston speeds.

An analysis of the effects of bmep and piston speed on piston temperatures indicates that piston speed should not be held as a constant factor for similitude in rating similar engines. However, the product of piston speed and bmep will be constant for equal service life of similar engines provided piston speed is adjusted downward with increase in cylinder bore sufficiently to maintain piston temperature constant.

The effect of Diesel-engine speed on ignition delay varies from one type of Diesel combustion system to another. In some engines the conclusion drawn in the paper that ignition delay in crank-angle degrees increases with speed may be true. However, ignition-delay time in precombustion-chamber engines tends to vary inversely with engine speed in similar engines, undoubtedly because of increased turbulence at increased speed. It is interesting in this regard to point out that supercharging reduces ignition lag in Diesel engines to an insignificant interval, from a practical standpoint.

---

[7] Staff Engineer, Research Department, Caterpillar Tractor Co., Peoria, Ill.

T. C. Tsu.[8] The author has attacked a basic problem with clarity, both by theoretical analysis and by experimental investigation. The paper contributes greatly toward making engine design more of a science than an art.

In connection with the curves of friction mep versus piston speed, Fig. 10 of the paper, the writer would like to ask whether or not the three similar engines were made with the same degree of surface finish, particularly on the pistons, piston rings, and cylinder walls.

To be exactly geometrically similar, of course, the engines should have different degrees of surface finish. If they were made with the same degree of finish, then, relatively speaking, the small engine would be rougher than the medium engine, and the medium engine rougher than the large engine. In this event the friction mep naturally would increase with decreasing size, in view of the fact that lubrication between the pistons and cylinder walls is relatively poor.

E. T. Vincent.[9] The paper under discussion is of some theoretical interest but seems to the writer to be of minor practical importance since no design criteria for any particular type of application is involved in the analysis. True, it is shown that, given the correct parameters, a number of similar engines have similar characteristics, but this does not mean that any one of such a series is of special application to any particular job. It is the engine least suited to its own particular application that has the least chance of success.

Again by employing data from a large number of engines the author draws a series of straight lines from which he infers that an average engine fulfills his theoretical approach. It is true that the average line, in some cases, does so indicate. However, as an example, if one has not formed an opinion as to how the line should be drawn, the automotive engines in Fig. 14 of the paper lie along a line with a slope of about 45 deg up toward the right much better than the approximately horizontal line drawn by the author.

Again comparison is made between engines of small bore and high speed, and large-bore slow-speed engines. Is not the rating of the latter deliberately held down in order to achieve long life?

The question of rating is peculiar to the application. The writer knows of a comparison, somewhat similar to the author's, made many years ago, of engines for a particular duty in which the assumed conditions were somewhat different. Not only was a specific requirement laid down, but a given space was prescribed at the same time. This was a submarine application where space is of vital importance. The result of these differing assumptions was a totally different answer to that of the author. In this case, for a given output and space limitation the largest cylinder that could be employed, coupled with the fewest number of cylinders was proved, in an equally satisfactory manner as that of the author's, to result in the smallest weight for the required maximum power output. It will be observed that these results are in direct opposition to those in the paper under discussion, illustrating the great effect the initial assumptions can have on the final results.

The writer would differ from the author's conclusion that the lowest fuel consumption for a spark-ignition engine is attained in the small cylinder. This is contrary to practice where it is well known that a fairly large cylinder is required for good fuel consumption, e.g., the work at Studebaker during the last war to develop the most economical engine. This was not done in small bores.

In practice it is well known that high speeds are conductive to high frictional losses which is confirmed by the results observed from the M.I.T. similar engines. The mean-piston-speed comparison in Fig. 11 is not considered to cover a wide enough range to bring out any effective result, since comparison over about 400 to 700 fpm is out of range for the high-speed engine of, say, 300 to 2500 fpm.

While on the subject of frictional losses, the author states that *the friction mep is, in general, such a small quantity compared with the imep.* The writer would hardly consider 30 per cent of the imep a small quantity that could be neglected in the comparison; and that is the value to be expected in many high-speed small-bore engines which are unsupercharged.

Some figures of interest regarding the comparison in Table 1 of the paper are given as follows:

	Four-cycle locomotive engine	Two-cycle locomotive engine
Bhp per cylinder	50	65
Rpm	800	1400
Bmep	80	82
Weight bore^3	0.965	1.35

Both of the Diesel engines listed have considerable life, the first having operated on railroads for many millions of miles. Comparing these figures with the author's seems to indicate that the comparison in the paper was somewhat accidental.

The writer would like to suggest another reason for the similarity of the various engines in some of the different groups, viz., competition. The manufacturer cannot afford to produce an outstanding engine and sell it in a certain field against competition with a cheaper unit that will perform with a reasonable degree of satisfaction, the result being that each type of application has very similar engines built by different manufacturers. If the trade would stand for a better engine, there are many cases where great improvements can be made at some increase in cost, etc., and the result would be that most of this data would not plot near the author's lines and would tend to make curves in place of straight lines.

Author's Closure

In replying to Mr. Johnson, let us assume that the residual gases fill the clearance space at exhaust pressure when the inlet valve opens. Then the temperature of the residual gases has little direct effect on volumetric efficiency because the volume of residuals plus fresh mixture is not altered appreciably by the mixing process. The chief thermal effect on volumetric efficiency is due to heat transferred to the fresh mixture from the engine parts, and this would tend to be less with the larger cylinder, as stated in the paper. The author sees no effect which would tend to balance this one out as bore increases.

With regard to engine friction, indicator diagrams taken both before and since writing the paper show both light-spring and heavy-spring diagrams to be identical at the same piston speed. The differences in "friction" are, therefore, truly frictional and are not connected with heat losses from the gases. Further testing since the paper was written shows that the motoring friction mep is substantially the same at the same piston speed for all three engines, but that the difference between indicated and brake mep is substantially the "friction mep" shown in Fig. 10 of the paper. At present we are inclined to agree with Mr. Johnson that these differences in friction are characteristic of the differences in cylinder size, but the explanation is not yet obvious. One reason might be the higher wall temperature of the larger cylinder, which reduces oil viscosity below proportionality with bore.

---

[8] Research Associate, The Pennsylvania State College, State College, Pa. Mem. ASME.

[9] Professor, Mechanical Engineering, University of Michigan, Ann Arbor, Mich. Mem. ASME.

With regard to bearing friction, the author does not agree that the larger bearing with proportionately larger clearance will have less temperature rise in the oil at the same value of $(\mu N/p)$. Bearing wall temperatures will be higher in the large bearing, due to the longer path for heat conduction from the bearing, so that at the same nominal value of $(\mu N/p)$ the actual value may be lower.

The author is in agreement with Mr. Johnson regarding the importance of production and maintenance costs, and hopes that more study will be given to the effect of cylinder size on such costs. With regard to the effect of cylinder size on engine ratings, Figs. 14 and 15 of the paper show that, on the average, both bmep and piston speed fall off with increasing bore at about the same rate. Apparently manufacturers, in general, have not appreciated the possibility of holding temperatures down by raising bmep and lowering piston speed as the bore increases.

In reply to Mr. Tsu, the surface finish in the three engines is approximately the same, and therefore is not geometrically similar. However, within the usual limits, surface finish has negligible effect on engine friction. The effect of surface finish on wear, however, may be quite important.

Referring to Professor Vincent's comments, the author's experience is that the relations expressed in this paper are of the greatest practical importance, especially in design, and that they have been unconsciously recognized and used for a long time. Of course each design must be made to meet its particular needs, but in recognizing the limitations common to all machines of a given type, an excellent basis is laid for the necessary modifications for a particular case.

With regard to the drawing of the curves in Figs. 14 and 15, it is obvious that the lines for the automotive group were drawn parallel to those indicated by groups which cover a much wider range of cylinder size.

In answer to Professor Vincent's third question, it is agreed that ratings for large cylinders tend to be held down for long life as well as for the other reasons stated in the paper. The author's only surprise is that the average bmep and piston speed of large engines are so little smaller than those of small engines of the same class. It might be expected that the average curves in Figs. 14 and 15 would fall off more rapidly with increasing bore than they actually do.

In the case of the submarine engine quoted as an example by Professor Vincent, the author would be interested to learn what the assumptions were and whether or not this installation is still current. Perhaps the assumption of direct propeller drive was used, in which case the rpm was set by the propeller, and the largest cylinder, which would give a reasonable piston speed, would be the logical choice.

With regard to the effect of cylinder size on fuel consumption of spark-ignition engines, the small cylinder has a lower fuel consumption only if the compression ratio is allowed to rise to hold the knock limit the same. The conclusion reached from the Studebaker tests was, if the author remembers correctly, that the large cylinder had no poorer fuel consumption than the small one. Since both cylinders had the same compression ratio, the larger one could be expected to have a slightly better fuel consumption at the same piston speed, owing to smaller heat losses and friction losses.

With regard to Fig. 11 of the paper, it is to be regretted that the points for curve No. 2 cover such a small speed range. Professor Vincent can be assured, however, that the curve of friction mep versus piston speed of this engine would not flatten out, but would follow essentially the path of the other curve. He states: "High speeds are conducive to high friction losses." The author agrees with this statement entirely, but when cylinders of different sizes are being compared, the speed must be piston speed in order to make the statement accord with reality.

The author fails to see the relevance of the table of figures given by Professor Vincent. Table 1 of the paper refers to a pair of two-stroke loop-scavenged engines whereas his table compares a four-stroke and a two-stroke engine. No claim is made that similitude can be stretched to cover both types. However, although the Arden and Nordberg engines were chosen for comparison before their performance data were available, we could hardly expect such close agreement on weight/bore,^{3} except by chance.

With regard to the last statement of Professor Vincent's comment, the author is in total disagreement. As engines are improved toward optimum design for a given service, they correlate better and better on the basis of rated mep and piston speed. This trend can easily be verified by plotting a graph, similar to that of Fig. 12, for the year 1910, or by leaving obsolescent engines out of Fig. 12 of the paper.

In conclusion, the theory of similitude is offered not as a panacea, but as a tool which can be of great assistance toward rationalization of the design process, which is all too empirical at best. Its validity, at least in many respects, is shown by the performance of the M.I.T. similar engines. Since commercial engines are not similar, they can be expected to follow the laws of similitude only in a general way with wide departures in individual cases. Such wide departures usually indicate either a mistake in rating or some unusual feature. If the departure is below the average there should be an immediate investigation by the producer, and if above the average, by his competitors. Used in this way, the theory, intelligently applied and with a full appreciation of its limitations, can result in significant improvements in the art of engine design.

Previous Work on Similitude. It should have been stated in the paper that the general theory of similitude in engines, and particularly the importance of piston speed as a limiting factor, is not new. A list of references on the subject follows; the paper is simply an attempt to explain and extend the theory and to compare its predictions with the behavior of actual engines.

"Design Limitations of Aircraft Engines," by E. S. Taylor, *Aero Digest*, vol. 26, January, 1935, pp. 22–27 and 45.

"Diesel Engine Design," by H. F. P. Purday, D. Van Nostrand Company, Inc., New York, N. Y. (Constable and Company, Ltd., London, England), 1937; revised, 1948. See especially chapt. 5.

"Ergiebennisse von versuchen mit geomitrischerenlich Gebauten Zylindern verschiedener Grösse und Folgerungen für die Flugmotorentwicklung," by W. Kamm, *Schriften der Deutschen Acadamie der Luftfahrtforschung*, vol. 12, March 3, 1939, 33 pp.

"Dynamic Similitude in Internal Combustion Engines," by O. Lutz, NACA Technical Memorandum No. 978, May, 1941.

"Heat Transfer in Geometrically-Similar Cylinders," by P. Riekert and A. Held, NACA Technical Memorandum No. 977, May, 1941.

"Die Dynamik der Verbrennungskraft-Maschine," by H. Schrön, Julius Springer-Verlag, Vienna, Austria, 1942.

Influence of Compressibility on Cylindrical Pitot-Tube Measurements

By L. W. THRASHER[1] and R. C. BINDER[2]

In the cylindrical Pitot tube, an opening at the critical angle with the flow gives the static pressure. For small-diameter tubes this critical angle is 39¹/₄ deg for incompressible fluids in a certain range of turbulent flow. Using a wind tunnel, the distribution of pressure was measured on the surface of ¹/₈-in. and ³/₁₆-in-diam cylinders at Mach numbers ranging from 0.13 to 0.87. The change in the pressure distribution on the surface of the cylinders was small in the range of Mach numbers up to 0.25. In this range the critical angle was constant, and a simple cylindrical Pitot tube would be convenient for direct measurements of static pressure. At the higher Mach numbers, particularly above 0.4, the critical angle increases above that for incompressible flow. The directional accuracy of the cylindrical Pitot increases as the Mach number increases.

THE measurement of velocity in a gas stream is of basic importance in fluid mechanics, both in research and industrial applications. The cylindrical Pitot tube, or the so-called "direction-finding" Pitot tube, is one device of several for measuring velocity. This tube has advantages in certain cases. It can be used for the measurement of both magnitude and direction, and it is convenient for various mountings, as in surveys in pumps, fans, and compressors.

Consider the two-dimensional flow around a circular cylinder whose axis is perpendicular to the stream some distance ahead of the cylinder. Let p_1 represent the upstream static pressure, and p the pressure at some point on the surface of the cylinder. As illustrated in Fig. 1, the pressure difference $(p - p_1)$ decreases with angle on each side of the stagnation point *B* until the difference is zero at points *A* and *C*. If pressure taps were placed at *A* and *C*, the pressure transmitted to a gage would be the static pressure p_1. The critical angle θ_c is defined as the angle between the stagnation point on the cylinder and the point on the cylinder at which the surface pressure is equal to the static pressure.

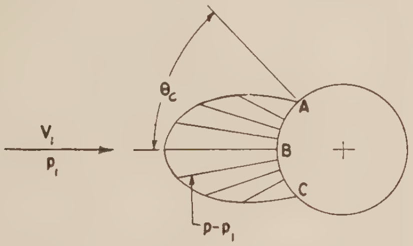

Fig. 1 Pressure Distribution on Surface of Cylinder

If the critical angle for a flow range is known, then for that range a Pitot tube can be constructed for measuring velocity in both magnitude and direction. Various constructions are possible. In one type, a hollow cylinder can be arranged with two holes; each hole leads to a separate compartment connected to a suitable gage. The angle between the holes is twice the critical angle, as the angle between *A* and *C* in Fig. 1. The tube in a stream of unknown direction can be rotated about its axis until the pressure at each hole is p_1. In this position the bisector of the angle between the holes gives the flow direction. If the tube is rotated about its axis so that an opening is in line with V_1, this opening will give the stagnation pressure.

The foregoing discussion indicates the use and importance of experimental data on the critical angle. Information is useful particularly for small-diameter tubes, because it is desirable to minimize disturbances of the flow.

Previous Work

Various data for incompressible flow have been reported. For example, Dryden (1)[3] was one of the first to present measurements of critical angle. A critical angle of 39¹/₄ deg for ³/₁₆-in. and ¹/₄-in-diam tubes at a tube Reynolds number of 1.2×10^4 was the result of a large number of tests with air reported by Fechheimer (2). Binder and Knapp (3) used a critical angle of 39¹/₄ deg on ³/₁₆-in. and ¹/₄-in-diam tubes. These tests were made in water at a Reynolds number approximately that of Fechheimer's tests.

There is a definite need for further experimental information on the cylindrical Pitot tube, particularly for compressible flow around small tubes. The following presentation gives the results of measurements designed to help fill the gap in present literature.

Experimental Investigation

Using a wind tunnel, the distribution of pressure was measured on the surface of ¹/₈-in. and ³/₁₆-in-diam cylinders at Mach numbers ranging from 0.13 to 0.87. Fig. 2 shows a diagrammatic sketch of the tunnel. Atmospheric air entered the bell inlet and

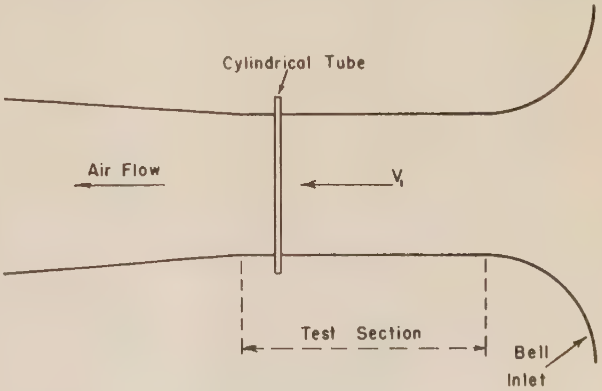

Fig. 2 Diagrammatic Sketch of Wind Tunnel

---

[1] Engineering Department, Arabian-American Oil Company, San Francisco, Calif. Jun. ASME.

[2] Professor of Mechanical Engineering, Purdue University, West Lafayette, Ind. Mem. ASME.

Contributed by the Research Committee on Fluid Meters and presented at the Annual Meeting, New York, N.Y., November 27–December 2, 1949, of The American Society of Mechanical Engineers.

Note: Statements and opinions advanced in papers are to be understood as individual expressions of their authors and not those of the Society. Paper No. 49—A-31.

[3] Numbers in parentheses refer to the Bibliography at the end of the paper.

passed through the test section. In the test section the area normal to the flow was a square 5 in. on each side. The diffuser at the end of the test section was connected to the inlet of a compressor. A screen and an egg-crate type of straightener were mounted at the bell inlet. The flow through the test section was parallel and uniform.

Each cylinder was placed in the test section as indicated in Fig. 2. Each cylinder was a seamless brass tube with a No. 80 (0.0135-in.) hole. Care was taken to have a radial hole, a hole free from burrs, and a smooth tube surface free from scratches. The pressure p at the tube hole was measured by water and mercury manometers. The reference static pressure p_1 was measured at tunnel-wall pressure taps, in a test plane normal to the flow and passing through the cylinder.

For the type of tunnel used, assume that there is no heat transfer through the tunnel walls. As the air expands from the atmosphere to the test plane, a tube placed at the test plane will then measure a stagnation pressure p_2 equal to the atmospheric pressure. Tests showed this assumption to be accurate.

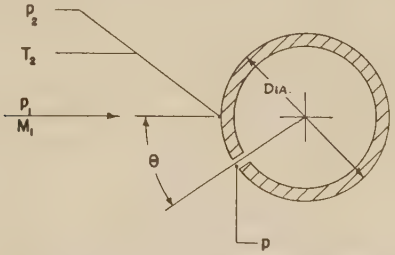

Fig. 3 Notation for Measurements

Let M_1 represent the Mach number of the flow just upstream from the Pitot; $\mathsf{M}_1 = V_1/c_1$, where c_1 is the acoustic velocity. Fig. 3 illustrates the notation. Let $k = c_p/c_v$, where c_p is the specific heat at constant pressure, and c_v is the specific heat at constant volume. In the test section, the energy equation for an isentropic process applied between the undisturbed flow and the stagnation point on the Pitot can be arranged in the form

$$\frac{p_2}{p_1} = \left[1 + \frac{(k-1)}{(2)}\mathsf{M}_1^2\right]^{\frac{k}{k-1}} \qquad [1]$$

In Equation [1], p_2 and p_1 are absolute pressures. From the adiabatic relation between pressure and temperature, we can write

$$\frac{T_2}{T_1} = 1 + \left(\frac{k-1}{2}\right)\mathsf{M}_1^2 \qquad [2]$$

where T_2 is the absolute stagnation temperature, and T_1 is the absolute static temperature. The stagnation temperature was taken as the temperature of the atmospheric air. For an ideal gas, $c_1 = \sqrt{kgRT_1}$, where g is gravitational acceleration, and R is the gas constant. Thus from measurements of pressures and temperature, it was possible to determine M_1, c_1, and V_1.

Fig. 4 shows typical pressure-distribution curves at low Mach numbers. The pressure difference $(p - p_1)$ is plotted as a function of angle. The critical angle θ_c for the $^1/_8$-in-diam tube at both Mach numbers of 0.13 and 0.25 was $39^1/_4$ deg. Fig. 5 shows a plot of a dimensionless pressure ratio versus angle for a range of Mach numbers. At the low Mach numbers the curves are close together. As the Mach number is increased, the critical angle increases.

The solid line in Fig. 6 shows a plot of Mach number versus critical angle for a $^1/_8$-in-diam tube. For Mach numbers up to about 0.25, the critical angle is constant. For higher Mach numbers, the critical angle increases. For the Mach number range from 0.1 to 0.9, the corresponding tube Reynolds number varies from about 0.7×10^4 to 5.9×10^4.

For incompressible frictionless flow, the critical angle is 30 deg. This result can be shown by a purely theoretical study. For real fluids the critical angle is always higher than 30 deg. In Fig. 6 the dashed curve marked "theory" was calculated from a theoretical analysis by Kaplan (4) for frictionless, subsonic flow. The experimental curve follows a trend similar to that of the theoretical up to a Mach number of about 0.6 (a constant difference of roughly 19 deg between the two curves).

Fig. 7 shows a plot of Mach number versus critical angle for a $^3/_{16}$-in-diam tube. The trend for the $^3/_{16}$-in-diam tube was

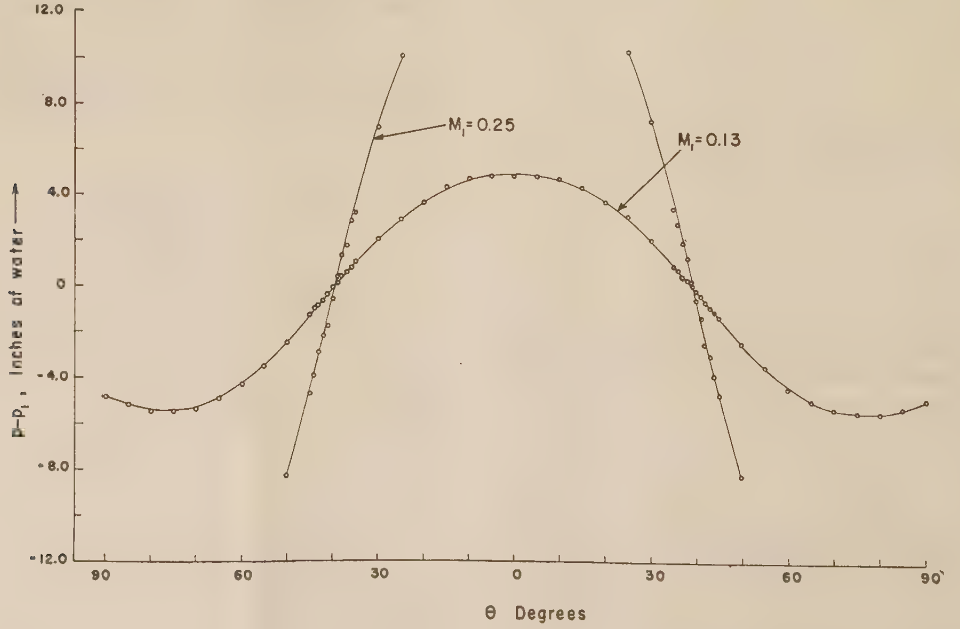

Fig. 4 Pressure Distribution on $^1/_8$-In-Diam Cylinder

(The stagnation-point pressure p_2 was 29.62 in. of mercury abs, and the stagnation-point temperature 74 F.)

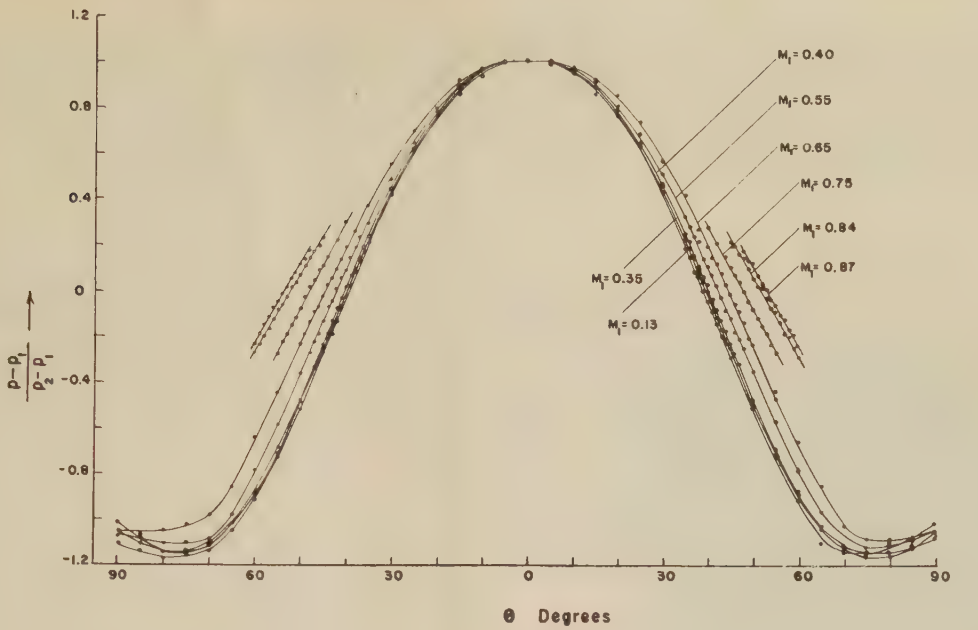

Fig. 5 Pressure Distribution on $^1/_8$-In-Diam Cylinder for Different Mach Numbers

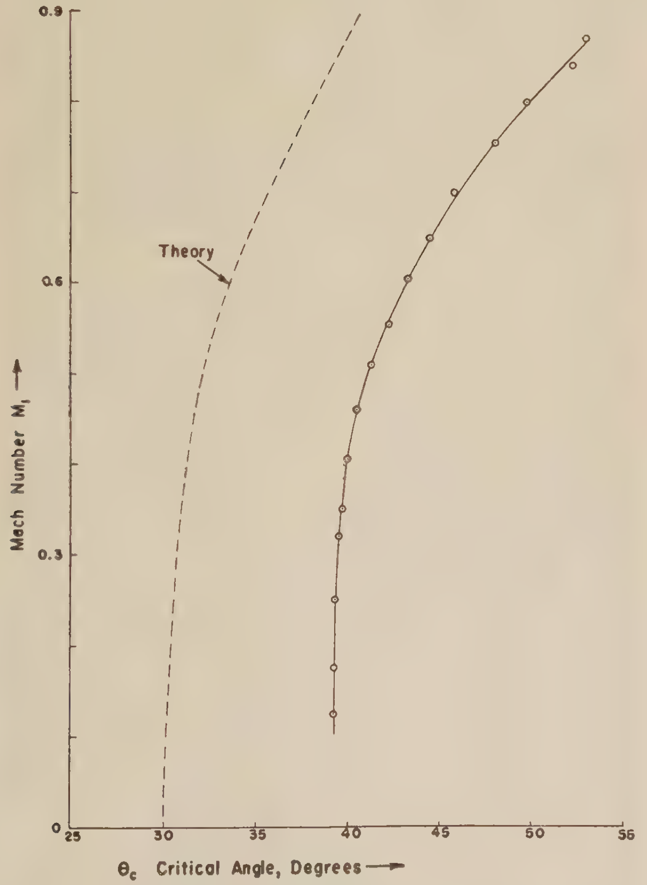

Fig. 6 Plot of Mach Number Versus Critical Angle for $^1/_8$-In-Diam Cylinder

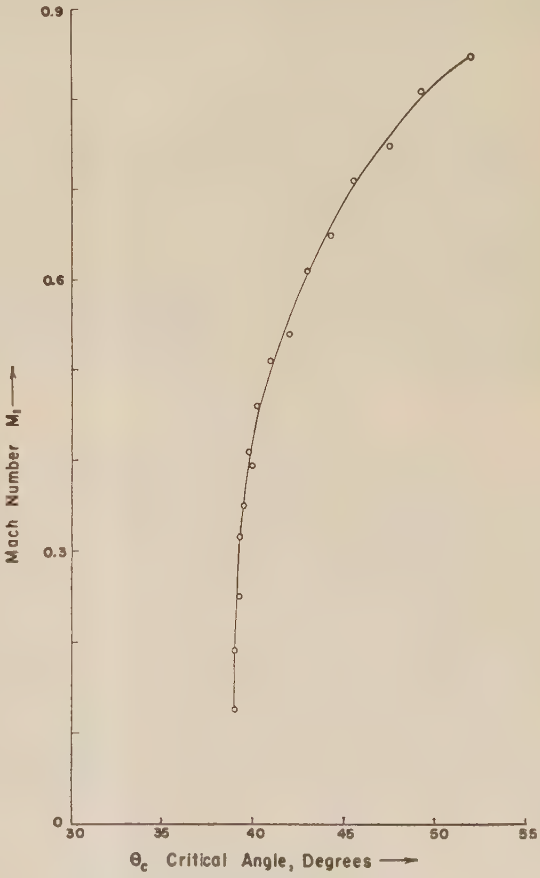

Fig. 7 Plot of Mach Number Versus Critical Angle for $^3/_{16}$-In-Diam Cylinder

the same as that for the $^1/_8$-in-diam tube. The critical angles for the $^3/_{16}$-in. tube were slightly lower ($^1/_4$ deg lower in the Mach number range up to 0.25), than the critical angle for the $^1/_8$-in. tube. This small difference may be due to a wall effect. For the Mach-number range from 0.1 to 0.9 for the $^3/_{16}$-in-diam tube, the corresponding tube Reynolds number varied from about 1.0×10^4 to 8.8×10^4.

Conclusions

The change in the pressure distribution on the surface of the circular cylinders was small in the range of Mach numbers up to 0.25. In this range the critical angle was constant. A simple cylindrical Pitot tube in this range would be convenient for accurate, direct measurements of static pressure. At the higher Mach numbers, particularly above about 0.4, the critical angle increases above that for incompressible flow. At the higher Mach numbers, the static-pressure measurement is more indirect, and requires a calibration over a range of Mach number.

Typical plots, as in Fig. 4, show that the pressure gradient (pressure difference per degree) increases as the Mach number increases. Thus the directional accuracy of the cylindrical Pitot tube increases as the Mach number increases.

Acknowledgment

The authors are grateful to Dean A. A. Potter, Dean of Engineering, and Prof. H. L. Solberg, Head of the School of Mechanical Engineering, both of Purdue University. These gentlemen made possible the facilities for these tests. This paper includes material adapted from a master's thesis (5).

BIBLIOGRAPHY

1 "Air Forces on Circular Cylinders," by H. L. Dryden, Scientific Paper No. 394, U. S. Bureau of Standards, vol. 16, Sept. 4, 1920.

2 "Measurement of Static Pressure," by C. J. Fechheimer, Trans. ASME, vol. 48, 1926, p. 965.

3 "Experimental Determinations of the Flow Characteristics in the Volutes of Centrifugal Pumps," by R. C. Binder and R. T. Knapp, Trans. ASME, vol. 58, 1936, p. 649.

4 "Two-Dimensional Subsonic Compressible Flow Past Elliptic Cylinders," by C. Kaplan, NACA Technical Report No. 624, 1938.

5 "Influence of Compressibility on Cylindrical Pitot Tube Measurements," by L. W. Thrasher, MS thesis, Purdue University, February, 1949.

Discussion

L. J. Hooper.[4] Some work along the lines of that reported in this paper was done at the Alden Hydraulic Laboratory in 1932. This test work was conducted just below the throat of a 36-in. × 16-in. Venturi meter operating with water. Several factors were studied which had an influence on the registration of a cylindrical Pitot tube.

Fig. 8 of this discussion shows the results of tests to determine the effect of piezometer size on the angle of zero impact pressure. These tests were made at a constant Reynolds number of 69,000. On the curve sheet the piezometer size is presented as a ratio to the size of the rod in which it was installed. The actual rod diameter was $1^5/_{16}$ in., and the piezometer diameters were varied successively from $^1/_{16}$ to $^7/_8$ in. It is seen that the angle for zero impact pressure varied from 37 to 56 deg for the range of piezometer sizes tested.

In Fig. 9 herewith the angle required to secure zero impact pressure was determined as a function of Reynolds number. It is seen that for the limited range of the tests (5 to 30 fps), the variation in the angle for zero impact pressure plotted as a straight line between 39.6 and 37.1 deg.

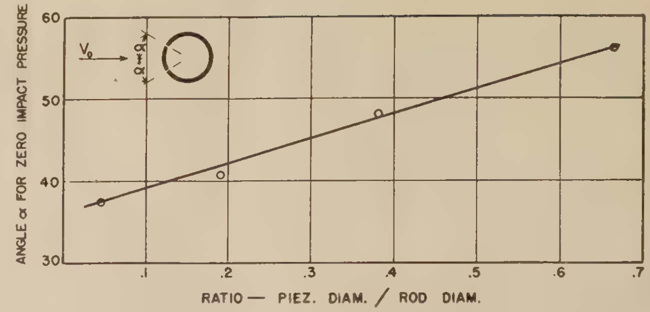

Fig. 8 Effect of Piezometer Size on Position of Zero Impact Pressure on a Cylindrical Tip

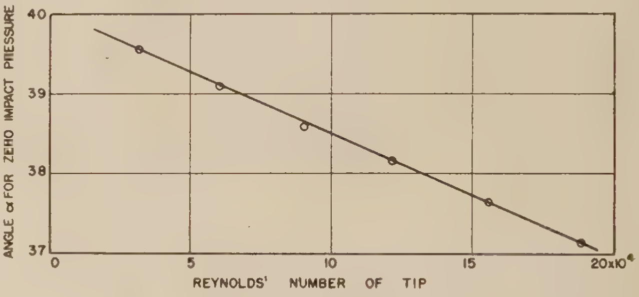

Fig. 9 Effect of Reynolds Number on Position of Zero Impact Pressure on a Cylindrical Tip

These tests indicate that other factors besides Mach number might have been affecting the results quoted in the paper. It would seem that tests in a water tunnel as well as in a wind tunnel would offer a very convenient way of separating the Reynolds and Mach number effects.

Authors' Closure

It is of interest and value to have available the data presented by Professor Hooper. Care should be exercised, however, in comparing the authors' data with those presented by Professor Hooper.

Note that in the authors' tests the tube diameters were $^1/_8$ in. and $^3/_{16}$ in., and the channel was 5 × 5 in. In Professor Hooper's tests the tube, $1^5/_{16}$ in. diam, was a larger portion of the channel size than the tube in the authors' tests. Thus Professor Hooper's data may show a large variation due to a wall effect; this large effect was not present in the authors' tests.

Note also in the authors' tests that the diameter of the pressure hole was 0.0135 in., whereas in Professor Hooper's tests the hole size varied from $^1/_{16}$ to $^7/_8$ in. The variation of pressure over the surface of the cylinder is not linear. An opening of $^1/_2$ in. diam or $^7/_8$ in. diam subtends a relatively large angle. The data in Fig. 8 are open to question. There is a question as to interpretation. What is the meaning of the "angle for zero impact pressure?" The angle indicated in Fig. 8 may not be the actual angle at which the pressure is the static pressure of the stream.

In the authors' tests the wall effect was small. The small pressure opening covered a relatively small angle. The experimental trend, as indicated by Fig. 6, followed the general trend indicated by an analysis of the compressibility effects. We feel, therefore, that the authors' test data indicates clearly the influence of compressibility.

---

[4] Professor, Hydraulic Engineering, Worcester Polytechnic Institute, Worcester, Mass. Mem. ASME.

Determination of ASME Nozzle Coefficients for Variable Nozzle External Dimensions

By R. G. FOLSOM,[1] BERKELEY, CALIF.

Specifications for ASME long-radius nozzles do not include external dimensions. A series of tests have been made in an 8-in. pipe to determine the influence of the external nozzle diameter on pressures measured at several points downstream from the nozzle flange. The results are expressed in terms of per cent of the differential head measured at the standard corner tap locations.

INTRODUCTION

THE internal geometrical configuration and pressure-tap locations for long radius (ASME) flow nozzles are specified in reports of the ASME Special Research Committee on Fluid Meters.[2] Nozzle discharge coefficients are available for several standard pressure-tap locations. Since the nozzle external dimensions have not been specified, the change in discharge coefficient with different widths of the annulus or clearance between the outside contour of a nozzle and the pipe wall are unknown. The experimental investigations reported here are part of a study to determine the preferable location for the outlet pressure tap to be used with the standard long-radius flow nozzles.

EXPERIMENTAL EQUIPMENT

Four 8-in. pipe nozzles with approximate throat diameters of $7^{1}/_{8}$ in., $6^{1}/_{8}$ in., $5^{5}/_{8}$ in., and $5^{1}/_{16}$ in. were tested. The external surface of the nozzle was formed by a wire-mesh-reinforced "Hydrostone" sleeve cast around the nozzle and turned on a lathe to the desired constant external diameter. A clear synthetic resin was applied to the machined surface of the Hydrostone to prevent deterioration by water during the test period. Successive cuts to smaller external diameters and treatment with the resin were used to provide a series of finite widths of annulus between the nozzle outer surface and the pipe inner wall. Fig. 1 shows a test nozzle with the Hydrostone sleeve and ready for insertion into the test pipe.

The test station consisted of 60 diam of straight upstream pipe from a header to the test flange, followed by 30 diam of straight pipe to a 90-deg elbow. Centrifugal pumps driven by induction motors discharged into the header. A downstream control valve and about 20 diam of pipe discharging 1 ft above the elevation of the test section completed the circuit. The pipe was 8-in. nominal diam standard new galvanized iron pipe with standard extra-heavy flanges to hold the test nozzle. The upstream pipe was smooth to the edge of the thin circumferential slit between the end of the pipe and the upstream nozzle face. The flanges were machined to provide a special slit both upstream and downstream of the nozzle for corner-tap pressures. Measurements of the pipe on eight diameters at three sections upstream from the nozzle showed the following:

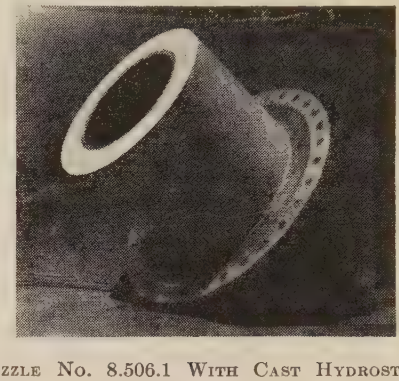

FIG. 1 NOZZLE NO. 8.506.1 WITH CAST HYDROSTONE SLEEVE FINISHED TO MAXIMUM DIAMETER

Pipe end	$3^{1}/_{2}$ in. upstream	$10^{1}/_{2}$ in. upstream
$8.066\text{ in.}\left\{\begin{matrix}+0.026\\-0.049\end{matrix}\right.$	$8.069\text{ in.}\left\{\begin{matrix}+0.074\\-0.056\end{matrix}\right.$	$8.077\text{ in.}\left\{\begin{matrix}+0.123\\-0.085\end{matrix}\right.$

Centering pins were provided in the flanges to place the nozzle concentric with the pipe.

Pressure taps were made at several points downstream and near the nozzle on the underside of the pipe. The longitudinal position of the taps is shown in Table 1. The circumferential spacing of the downstream holes was such that no one hole was directly in line downstream from another. The pressure connection was made by drilling a $^{3}/_{16}$-in-diam hole radially into the pipe and brazing a $^{1}/_{8}$-in. standard coupling to the outside of the pipe.

TABLE 1 PRESSURE TAP LOCATIONS

Tap no.	Longitudinal location, in.	Type of pressure tap
2′	8.1[a]	Hole ($^{3}/_{16}$ in. diam)
1′	0.0[a]	Slit (width less than 0.15 in.)
1	0.0	Slit (width less than 0.15 in.)
2	2.2	Hole ($^{3}/_{16}$ in. diam)
3	3.2	Hole ($^{3}/_{16}$ in. diam)
4	4.2	Hole ($^{3}/_{16}$ in. diam)
5	5.2	Hole ($^{3}/_{16}$ in. diam)
6	6.2	Hole ($^{3}/_{16}$ in. diam)
7	7.2	Hole ($^{3}/_{16}$ in. diam)
8	8.2	Hole ($^{3}/_{16}$ in. diam)
9	9.2	Hole ($^{3}/_{16}$ in. diam)

[a] Measured upstream from the upstream face of the nozzle; all other measurements downstream from the downstream face of the nozzle flange. Thickness of nozzle flange was $^{5}/_{8}$ in. and a metal-to-metal fit was obtained between the nozzle face and the holding flanges.

Plastic or rubber tubes were used as connecting lines from the couplings to the manometers. Since petcocks can be closed without displacement of fluid, all petcocks in the connecting lines were operated by a single lever linkage to function simultaneously and allow corresponding instantaneous observations to be made. Other petcocks were installed to bleed air from the high points in the upstream and downstream piping.

Air-water differential manometers (length of 8 ft) were used to measure pressure differences between taps 2′ and 4 (approximate

---

[1] Professor and Chairman, Division of Mechanical Engineering, University of California. Mem. ASME.

[2] "Fluid Meters, Their Theory and Applications, Part 1," Reports of the ASME Special Research Committee, ASME, 1937.

Contributed by the Research Committee on Fluid Meters and presented at the Annual Meeting, New York, N. Y., November 27–December 2, 1949, of THE AMERICAN SOCIETY OF MECHANICAL ENGINEERS.

NOTE: Statements and opinions advanced in papers are to be understood as individual expressions of their authors and not those of the Society. Paper No. 49—A-110.

standard radius tap locations) and taps 1′ and 1 (standard corner-tap locations). The remainder of the pressure taps were connected to vertical open-end 2-in-diam plastic tubes with point gages mounted to determine the water elevation at the center of the tube. The point gages had a least count of 0.001 ft. Water and air temperatures were recorded, and the manometers were shielded from the sun.

TESTING PROCEDURES

Flow was established in the circuit, all air bled, and equilibrium conditions checked. The petcock linkage was closed and all manometer readings recorded. After opening the petcock linkage and checking equilibrium, the linkage was closed and the manometer readings recorded again. This procedure was repeated to obtain from four to six sets of readings. The manometer zero positions were checked before and after a series of runs.

Clearances of the annulus at the pressure taps were measured with the aid of a machinist micrometer before or after the series of tests on a specific nozzle external diameter. Since the pipe is out of round, the clearances varied. Typical values are shown in Table 2. Curves and data are reported in terms of the average clearances.

TABLE 2 CLEARANCE (ANNULUS) FOR NOZZLE NO. 8.506.1

essure tap no.		2	3	4	5	6	Average
Nominal clearance	$^1/_{16}$ in.	0.084	0.075	0.060	0.033	0.056	0.062
	$^3/_{32}$ in.	0.120	0.103	0.092	0.067	0.085	0.093
	$^1/_8$ in.	0.145	0.132	0.121	0.098	0.126	0.124
	$^5/_{32}$ in.	0.174	1.163	0.150	0.126	0.148	0.152
	$^9/_{32}$ in.	0.295	0.291	0.275	0.245	0.272	0.276
	$^{13}/_{32}$ in.	0.424	0.413	0.396	0.370	0.396	0.400

[a] Clearance magnitudes in inches.

RESULTS

Following the general methods applied by Bean and Beitler,[3] test results are expressed in terms of dimensionless ratios. The pressure loss coefficient is defined as

$$k_n = \frac{100\delta_n}{\Delta_c}$$

where δ_n is the pressure difference between a downstream pressure tap at position n and the downstream corner tap, Δ_c is the differential pressure across the corner taps. The positive value of δ_n indicates a reduction in pressure at the downstream tap with respect to the corner tap. At Reynolds numbers greater than some minimum value, the pressure-loss coefficient should be independent of the flow rate. The experimentally determined values of k_n are given in Table 3. This table includes values of Δ_c and Δ_R (the differential pressure across the approximate radius taps), as well as the Reynolds number based on the throat-diameter conditions. Table 4 presents the average k_n-values for the normal nozzles (as supplied without sleeves). The pressure-tap locations are expressed in terms of pipe diameters X/D, where the distance X is measured from the upstream or the downstream face of the nozzle flange as indicated.

Fig. 2 presents the data of Table 4 in graphical form. The values of k_n have been plotted as positive in the downward direction of the ordinate due to the definition of k_n. The shape of the curve represents the relationship of static pressures measured at the wall with respect to the distance along the pipe axis. The curves in Fig. 2 show a decrease in static pressure as one passes downstream for the range of the experiments, except for the last point on the $\beta = 0.79$ curve (β = ratio of nozzle throat diameter to pipe diameter). When the X/D-values are less than about 0.8, all nozzles show similar characteristics for k_n. Beyond the end of the nozzle and at the larger area ratios, appreciable differences in k_n exist over the region of the tests.

The range of values measured for k_n for nozzle No. 8.506.1 is indicated in Fig. 3. The area designated as "range of all normal nozzle tests" is bounded by the minimum and maximum magnitudes given in Table 3 under clearance of 1.080 in. (as supplied). Thus this area includes all test results over the limits of flow rates investigated for the normal nozzle. The other area in Fig. 3 is bounded by the minimum and maximum average values at a given tap for all other clearances and flow rates as tabulated

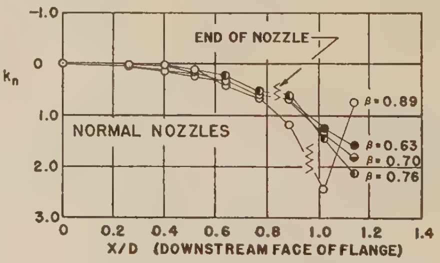

FIG. 2 COEFFICIENTS (k_n) FOR THE ALL NORMAL ASME NOZZLES "AS SUPPLIED"

TABLE 3 SUMMARY OF EXPERIMENTAL RESULTS

Nozzle No. 8.506.1; Clearance = 0.062 in.

Δ_r	$Re \times 10^{-5}$	Δ_e	k_2	k_3	k_4	k_5	k_6	k_7	k_8	k_9
1.04	3.2	1.10	0.09	0	0.09	0.46	0.64	1.36	2.09	2.54
2.50	4.9	2.67	0.04	0	0.08	0.45	0.71	1.31	2.21	2.66
3.27	5.6	3.48	0.06	0.03	0.12	0.55	0.92	1.47	2.41	3.04
4.04	6.2	4.30	0.05	0.04	0.14	0.58	1.05	1.53	2.63	3.14
4.96	7.5	5.30	0.06	0.04	0.15	0.59	1.11	1.57	2.68	3.15
6.87	8.1	7.33	0.06	0.07	0.19	0.61	1.25	1.62	2.93	3.18
Average			0.06	0.03	0.13	0.54	0.95	1.48	2.49	2.95

NOTE: Space did not permit publication of the complete table which consists of 26 sections similar to the one presented. . The complete table is on file at ASME Headquarters, 29 West 39th Street, New York, N. Y., for reference.

TABLE 4 k_n FOR NORMAL NOZZLES (AS SUPPLIED)

Pressure tap no.		1	2	3	4	5	6	7	8	9
X/D	(a)	0	0.27	0.40	0.52	0.64	0.77	0.89	1.02	1.14
	(b)	0.09	0.35	0.47	0.60	0.72	0.85	0.97	1.09	1.22
Nozzle										
8.506.1			0.09	0.17	0.25	0.36	0.60	0.74	1.25	1.59
8.562.1			0.06	0.15	0.20	0.35	0.59	0.72	1.38	1.81
8.615.1			0.06	0.08	0.15	0.24	0.54	0.63	1.44	2.11
8.715.1			0.03	0.03	0.10	0.42	0.63	1.16	2.44	0.74

(a) X/D expressed in terms of X measured from downstream face of flange.
(b) X/D expressed in terms of X measured from upstream face of flange.

---

[3] "Some Results From Research on Flow Nozzles," by H. W. Bean and S. R. Beitler, Trans. ASME, vol. 60, 1938, pp. 235–244.

in Table 3. Within the accuracy of the test results, it is impossible to discover a trend of k_n with clearance at taps before the end of the nozzle.

The average values of k_n given in Table 3 are plotted in Figs. 4, 5, and 6 for three nozzles, the results for a specific nozzle being plotted in a single figure. The general shape of the curves is similar to those in Fig. 2, with separate curves applicable to each sleeve clearance investigated. In general, consistent and definable changes with sleeve clearance appear only at points downstream from the end of the nozzle. The region of $\pm^1/_2$ per cent deviation from the normal nozzle magnitudes is indicated for the tap locations before the end of the nozzle. Although this deviation is small (less than $^1/_2$ per cent for all points in Figs. 4 and 5), it increases as the diameter ratio increases. Fig. 6, for the largest nozzle, shows four points outside the $^1/_2$ per cent deviation limits, these points being at the smaller sleeve clearances. For points beyond the end of the nozzle, the deviation of points for smaller sleeve clearances reduces as the diameter ratio increases. In Figs. 4 and 5 all clearances show k_n magnitudes greater than those for the normal nozzles, a $1^1/_2$ per cent range for Fig. 4, and a 1 per cent range for Fig. 5. In Fig. 6 all results except one point are within $^1/_2$ per cent of the normal nozzle characteristics.

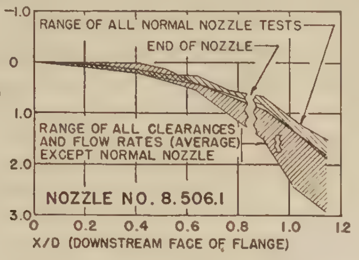

FIG. 3 VARIATION IN COEFFICIENTS (k_n) AS DETERMINED FOR THE TEST RANGE IN REYNOLDS NUMBERS

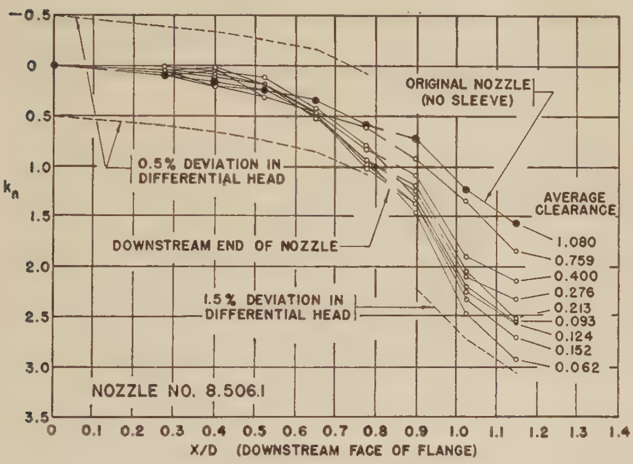

FIG. 4 SUMMARY OF TEST RESULTS ON NOZZLE NO. 8.506.1

The magnitudes of k_n indicate the per cent difference in heads due to measurements at different pressure taps. The corresponding difference in calculated rate of flow (if no change in nozzle coefficient is considered) is one half the per cent difference in head. The test results show that for any pressure-tap location upstream from the downstream end of the nozzle, an error of less than $\pm^1/_4$ per cent in calculated flow rate results from changes in nozzle external diameters, as compared to results with the normal external contours of the standard test nozzles.

No experimental investigation was made of the change in nozzle coefficient for the corner taps when the nozzle external dimensions were changed.

Fig. 7 has been included to demonstrate the change in k-values of pressure for No. 4 as the clearance increases. Data from three nozzles are included. Since this tap is near the location of the standard downstream radius tap, the magnitudes of variables in Fig. 7 correspond approximately to conditions for radius taps.

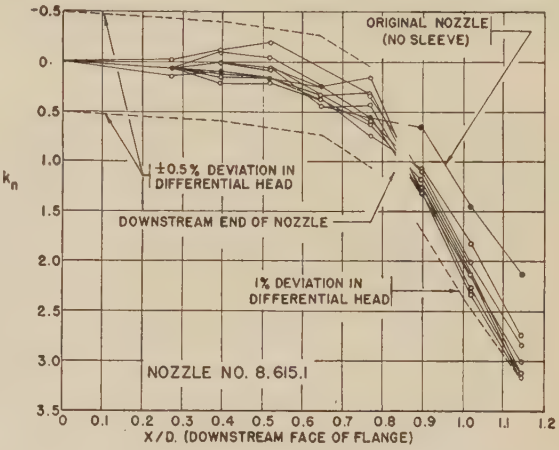

FIG. 5 SUMMARY OF TEST RESULTS ON NOZZLE NO. 8.615.1

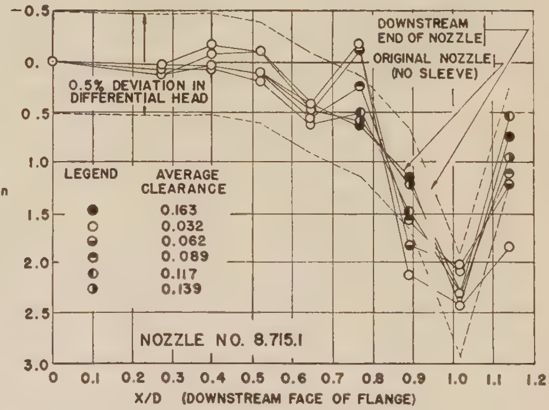

FIG. 6 SUMMARY OF TEST RESULTS ON NOZZLE NO. 8.715.1

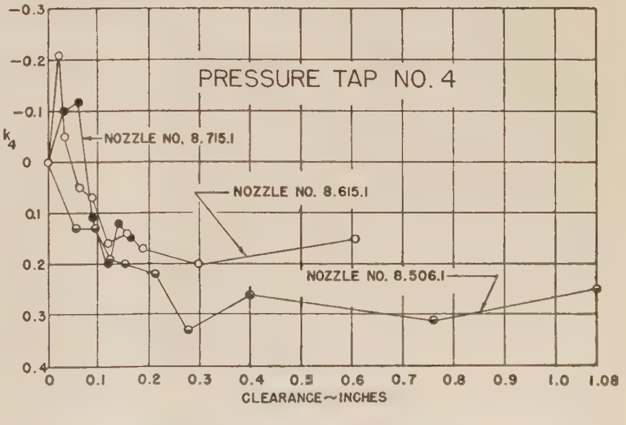

FIG. 7 CHANGE IN COEFFICIENT (k_4) AT NO. 4 PRESSURE TAP WITH CHANGE OF CLEARANCE IN ANNULUS

Conclusions

The discharge coefficients for standard ASME long-radius nozzles are almost independent of the clearance in the annulus between the pipe wall and the nozzle external diameter at all pressure-tap locations between the holding flange and the end of the nozzle. At pressure-tap points downstream from the end, appreciable changes in the coefficient with clearance exist with larger differences corresponding to smaller diameter ratios.

The tabular and graphical results are expressed in terms of per cent of the differential pressure across the corner taps. The maximum difference in heads (pressure at downstream corner tap minus pressure at given downstream tap) at a given downstream tap between the nozzle with reduced clearance in the annulus and the normal nozzle (as supplied) was $1^1/_2$ per cent for the range of the conditions tested in this investigation.

Acknowledgments

The author gratefully acknowledges the co-operation of the ASME Special Research Committee on Fluid Meters in making the standard nozzles available for testing, and the assistance of L. Gray, W. C. Shepherd, and K. J. Bermel in making the tests and reducing the data.

The Response of Thermocouples to Rapid Gas-Temperature Changes[1]

By M. W. CARBON,[2] H. J. KUTSCH,[3] and G. A. HAWKINS[4]

This paper presents practical data which were taken from the main results of a research program dealing with the response of thermocouples to changing gas temperatures. Experimental and theoretical data for the response time of thermocouples ranging in wire size from 0.01 to 0.0005 in. are presented. The experiments were performed over a range of temperatures from 70 F to 950 F, and for air velocities ranging from 0 to 125 fps. All of the experiments were carried out in such a way that the hot junction of the thermocouple was always cooled. An equation is presented for computing the response time for thermocouples fabricated from fine wires and subjected to sudden air-temperature changes. Heat transfer by conduction and radiation were negligible in the experiments performed.

Introduction

A THERMOCOUPLE placed in a gas stream, the temperature of which suddenly changes, will usually indicate a temperature different from that of the true value at any given time before the equilibrium condition has been attained. Due to the fact that the measurement of instantaneous gas-temperature changes is becoming increasingly important in the fields of heat transfer and thermodynamics, this particular part of the main investigation was undertaken to obtain and correlate data on the response time of thermocouples fabricated from fine wires.

One of the purposes of this investigation was to study the response of a thermocouple made from fine wires, by suddenly subjecting it to a low-temperature air stream. The research program consisted of the design and construction of suitable apparatus, development of a satisfactory welding technique, and the collection and analysis of experimental data. Thermocouples composed of platinum and platinum 10 per cent rhodium with wire sizes of 0.01, 0.002, 0.001, and 0.0005 in. were used in the experiments. All of the work was carried out at approximately atmospheric pressure. The temperature range was 70 F to 950 F.

Before undertaking the experimental part of the program, a survey of the literature available to the authors was undertaken. Many of the contributions and suggestions made by previous investigators, as reported in the technical literature, were incorporated in the program. Space limitation does not permit the inclusion of the many references studied, hence only a short Bibliography[5] is included. However, the authors are cognizant of the value of the work of previous investigators.

Description of the Apparatus

Welding Apparatus. Before the actual experimental investigation could be undertaken, it was first necessary to develop suitable apparatus and a technique for welding the fine wires. Many different methods were tried before a satisfactory technique was developed. Finally a satisfactory method was obtained whereby the wires were electrically welded between graphite electrodes. The wires were joined by first crossing the ends and placing the intersection of the wires on the surface of a horizontal graphite rod. A second graphite rod was placed at right angles to the first and then rolled over the intersection of the two wires. A satisfactory weld was obtained when the rods were connected to a 3-volt d-c source. After welding, the excess material was removed carefully from the junction of the thermocouple.

Recently Hammel (1)[5] described a butt-welding technique based on the use of a special jig. By means of this apparatus successfully butt-welded thermocouples have been constructed from wires as small as 0.003 in. diam. If the same apparatus may be used for fabricating thermocouples of even smaller diameter, this procedure may prove to be more effective than the method used by the authors.

Recording Apparatus. Since the object of this phase of the work was to study the response of thermocouples during very rapid temperature changes, it was not possible to use standard laboratory equipment. As a result a large amount of time was spent in constructing suitable recording apparatus.

The thermocouple voltage change was finally recorded by means of an apparatus consisting of an interrupter, alternating-voltage amplifier, oscilloscope, and a rotating-drum camera equipped with a modulator tube for placing timing marks on the photographic paper. Due to unstable operation of the direct-current amplifiers, it was finally decided to use a voltage interrupter in the circuit and a stable alternating-voltage amplifier. The rotating-drum camera was found to be very satisfactory for recording the trace on the oscilloscope. The apparatus was designed on the basis of the idea previously advanced by Champion and Brokaw (2).

Test Apparatus. Two devices were used to subject the thermocouples to a sudden decrease in temperature. The first apparatus consisted of a *T*-shaped section of aluminum mounted in such a way that it could be moved instantly a short distance in a horizontal direction. In the normal operating position a jet of high-temperature air passed through a slot in the aluminum section and flowed over the test thermocouple. Horizontal displacement of the section shut off the high-temperature air stream, and a second slot allowed a cold-air stream to pass over the thermocouple. Whenever the *T*-section was moved, the hot-air stream was suddenly replaced by a cold-air jet which subjected the thermocouple to an instantaneous air-temperature change.

The second method consisted of placing a thermocouple in a low-temperature air stream and raising the temperature of the

---

[1] Based on a PhD thesis, Purdue University, 1949, by one of the authors.[2]

[2] Engineer, Pile Technology Division, General Electric Company, Richland, Wash. Jun. ASME.

[3] Instructor, School of Mechanical Engineering, Purdue University, Lafayette, Ind.

[4] Westinghouse Research Professor of Heat Transfer, Purdue University; Visiting Professor, 1949–1950, Division of Engineering, University of California, Los Angeles, Calif. Mem. ASME.

Contributed by the Heat Transfer Division and presented at the Annual Meeting, New York, N. Y., November 27–December 2, 1949, of The American Society of Mechanical Engineers.

Note: Statements and opinions advanced in papers are to be understood as individual expressions of their authors and not those of the Society. Paper No. 49—A-148.

[5] Numbers in parentheses refer to the Bibliography at the end of the paper.

wire by passing a current through it. After a desired temperature had been reached, the current was cut off, and the couple allowed to cool rapidly in the air stream.

In all tests the thermocouples were placed in a horizontal position, the wires extending in opposite directions from the junction. The horizontal thermocouple was mounted at right angles to the air stream. In this way the thermocouple resembled a very thin cylinder placed at right angles to the air flow.

EXPERIMENTAL PROCEDURES

Before undertaking the main part of the experimental program, calibration tests and preliminary calculations and experiments were conducted.

Experiments were conducted to ascertain as to whether or not conduction of heat along the lead wires of the thermocouples was of large enough magnitude to merit consideration. The results obtained indicated that the heat loss by conduction was negligible.

Calculations indicated that for the experimental range of the apparatus, the transfer of heat by radiation from the junction of the thermocuple to the surroundings was very small in comparison with the convective heat transfer; hence it could also be neglected.

Several experiments were carried out in an effort to determine the maximum air velocity which the couples could withstand without breaking. The results obtained indicated that the couples could be used for velocities up to 400 fps.

Considering only convective heat transfer to or from the couple, a heat balance was written and the final result written in a form similar to that used by Rhodes (3), Harper (4), Fiock (5), and Bailey (6), which follows

$$(t_i - t) = (t_i - t_a)(1 - e^{-\tau/\beta}) \quad \ldots\ldots\ldots\ldots [1]$$

$$\beta = \frac{\rho Dc}{4h} \quad \ldots\ldots\ldots\ldots [2]$$

where

t_i = initial temperature as indicated by thermocouple before temperature change occurs

t = temperature indicated by thermocouple τ millisec after change occurs

t_a = temperature of air stream after temperature change occurs

ρ = density of thermocouple material

c = specific heat of thermocouple material

h = coefficient of heat transfer

D = diameter of thermocouple wire

τ = time elapsed after temperature change occurs

If the time elapsed τ is selected equal to β, then Equation [1] reduces to the following

$$(t_i - t) = 0.632\,(t_i - t_a) \quad \ldots\ldots\ldots\ldots [3]$$

when $\tau = \beta$. This means that if τ is equal to β, then the temperature change $(t_i - t)$ is 63.2 per cent of the total change $(t_i - t_a)$.

Therefore it was decided to measure on the records obtained the time elapsed τ, when the temperature change had reached a value of 63.2 per cent of the total. The average experimental values obtained for τ are recorded in Table 1. The averages are based on 103 individual experiments.

In order to check the experimental values, a mean coefficient of heat transfer was considered during 63.2 per cent of the change and was computed by means of the following correlation given by McAdams (7)

$$\frac{hD}{k_f} = 0.32 + 0.43\left(\frac{DV\rho}{\mu_f}\right)^{0.52} \quad \ldots\ldots\ldots\ldots [4]$$

In order to determine the values for the thermal conductivity, viscosity, and density of the air for use in Equation [4], a mean temperature was used as found by use of the following equation

TABLE 1 EXPERIMENTAL AND COMPUTED DATA

Thermocouple number	Diam of wire, in.	Initial temp of thermocouple t_i, deg F	Air temp, t_a, deg F	Average air velocity, fps	Average for 63.2 per cent response time obtained from photographic records, millisec	Calculated Reynolds number N_{Re}	Calculated time for 63.2 per cent response, millisec
701	0.0005	776	84	24.5	3.6	3.18	3.4
701		794	83	47.1	2.8	6.05	2.6
711		665	87	22.5	4.5	3.17	3.5
711		677	86	49.4	3.5	6.92	2.6
711		667	83	106.8	2.4	15.15	1.9
700	0.001	834	99	49.4	8.0	12.04	7.7
700		840	103	28.8	11.0	6.93	9.7
701		867	104	28.9	12.7	6.83	9.6
701		852	102	48.4	10.8	11.72	7.7
703		814	91	29.2	11.5	7.29	9.6
703		821	90	50.7	9.7	12.62	7.6
703		795	88	118.0	6.5	30.19	5.2
704		580	74	27.3	9.2	8.43	9.9
704		580	70	48.9	7.9	15.22	7.7
500	0.002	908	104	18.2	34.3	8.32	34.8
500		916	100	27.9	31.1	12.77	29.1
500		915	96	50.4	24.9	23.24	22.4
500		910	93	73.8	22.3	34.32	18.7
500		913	91	98.3	20.1	45.70	16.3
500		902	90	124.8	18.2	58.90	14.6
501		853	99	11.1	34.9	5.32	42.5
501		860	93	23.6	31.5	11.40	31.4
501		870	90	49.0	24.8	23.55	22.5
501		886	89	98.8	18.9	47.00	16.3
502		803	104	11.9	35.0	5.93	41.4
502		807	98	26.2	27.2	13.02	29.9
502		818	97	48.9	21.5	24.23	22.6
502		843	92	102.0	16.0	49.95	16.1
542		429	64	25.4	26.4	18.20	30.2
542		372	64	48.9	21.1	37.00	22.3
501		531	80	25.5	28.8	16.07	30.8
501		520	80	48.9	22.3	31.50	22.5
543		417	62	23.7	27.5	17.24	30.9
543		574	84	24.1	26.1	14.73	30.8
542		815	81	21.6	31.4	10.97	32.4
542		830	80	48.9	24.0	24.53	22.6
705	0.01	570	66	54.5	237.0	171.8	246.0
705		574	63	107.4	180.0	340.1	178.0

$$t_f = \frac{\dfrac{t_i + t}{2} + t_a}{2} \quad \ldots\ldots\ldots\ldots\ldots\ldots \quad [5]$$

The symbols have the same significance as previously mentioned.

In the development of Equation [4], the Prandtl number was considered constant, which is a satisfactory assumption for the temperature range used in this investigation.

Using the value for h, together with the density, specific heat, and diameter, the theoretical values for τ were determined for 63.2 per cent of the total time by means of Expression [2] since τ is equal to β under the condition specified.

Results and Conclusions

The values for the theoretical response for various sizes of couples for the range of temperatures and velocities covered in the experiments are shown by the solid lines in Figs. 1 and 2. The points represent the experimental values obtained. From the results it may be concluded that the relations developed may be used to predict the time required for a thermocouple to cool to a value of 63.2 per cent of the total impressed temperature difference for the temperature and air-velocity ranges covered during the investigation. The air velocity was varied from approximately 0 fps to 125 fps. The temperature range was 70 F to 950 F.

Although the experimental data have not been evaluated for other response times, it is felt that other values for the response interval may be calculated by using different relationships for τ and β, such as the following:

Relation between τ and β	Value for ratio $\dfrac{t_i - t}{t_i - t_a}$
$\tau = \beta$	0.632
$\tau = 2\beta$	0.865
$\tau = 3\beta$	0.95

or by evaluating β by use of Equations [2] and [4] and solving for τ in Equation [1].

Acknowledgment

The authors wish to express thanks to E. I. duPont de Nemours and Company for financial assistance and encouragement during the course of the main project. One of the authors[2] held the duPont Company Postgraduate Fellowship in Mechanical Engineering at Purdue University for the 1948–1949 academic year. The authors wish to thank Dr. Max Jakob for valuable suggestions and advice given during the course of the investigation.

BIBLIOGRAPHY

1 "Method for the Preparation of Butt-Welded Thermocouples Using 3-Mil Diameter Wire," by E. F. Hammel, Documents Distribution Subsection, Publication Section, Technical Information Branch, AEC, P. O. Box E, Oak Ridge, Tenn., Reference MDDC 776, LADC 393.

2 "A High-Speed Multiple-Temperature Recorder," by A. R. Champion and G. K. Brokaw, Temperature—Its Measurement and Control in Science and Industry, American Institute of Physics, Reinhold Publishing Corporation, New York, N. Y., 1941.

3 "Industrial Instruments for Measurement and Control," by T. J. Rhodes, McGraw-Hill Book Co., Inc., New York, N. Y., 1941.

4 "Thermometric Lag," by D. H. Harper, 3rd, *Bulletin of the Bureau of Standards*, vol. 8, 1912, p. 664.

5 "Development of Thermocouple Pyrometers for Gas Turbines," by E. F. Fiock and associates, National Bureau of Standards, Reference III-2/ITPU (3225), Washington, D. C.

6 "The Response of Thermocouples," by N. P. Bailey, *Mechanical Engineering*, vol. 53, 1931, pp. 797–804.

7 "Heat Transmission," by W. H. McAdams, McGraw-Hill Book Co., Inc., New York, N. Y., second edition, 1942, p. 220, Equation 4.

8 "The Platinum Metals and Their Alloys," edited by E. M. Wise, The International Nickel Company, Inc., New York, N. Y.

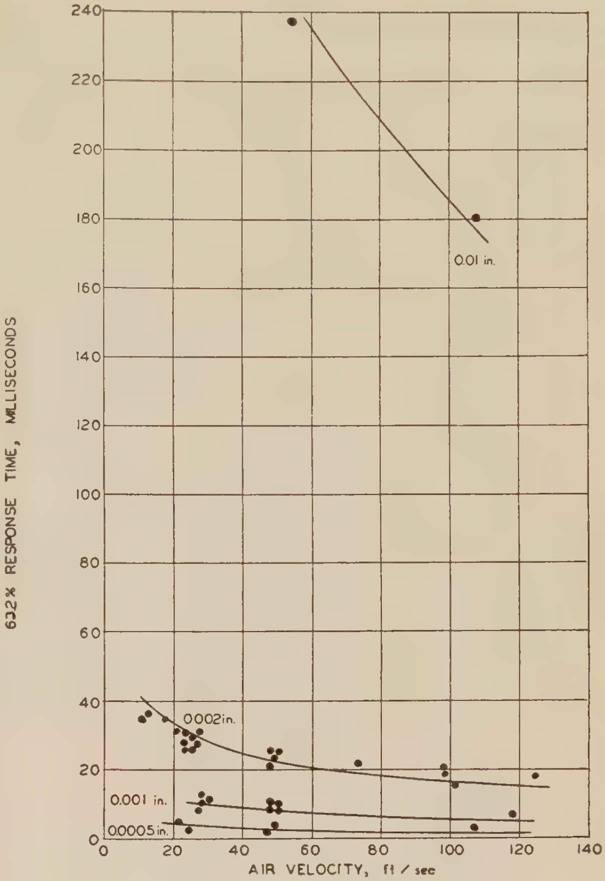

Fig. 1 Response Time Versus Air Velocity

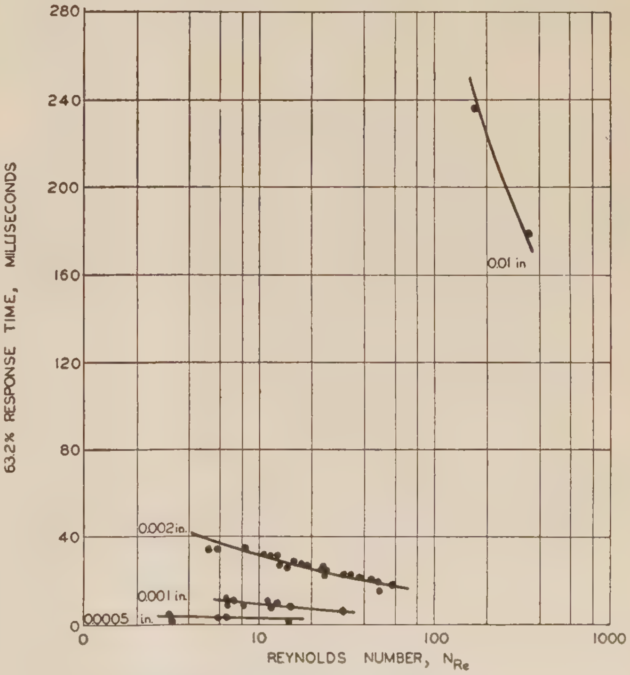

Fig. 2 Response Time Versus Reynolds Number

Crude-Oil Flow Characteristics Experienced in Large-Diameter Lines

By L. E. ANDERSON,[1] TULSA, OKLA.

Characteristics of crude-oil flow in large-diameter lines have been investigated by gathering data on lines under normal operating conditions. A description of these tests, and a summary of the results obtained are discussed in this paper. From these tests, an exponential equation has been derived to determine capacity or pressure drop for all trunk lines pumping crude oil in the turbulent-flow region. In connection with these flow tests, an investigation was made into the effect of pressure on viscosity in the range of normal pipe-line operating pressures. This effect, which in the past has been assumed to be a negligible one, is shown to be of definite importance.

With the advent of larger-size lines for crude-oil transportation, the question has arisen as to the flow characteristics encountered in these larger lines. The term "large diameter" is of course a comparative one, but in this discussion will refer to lines with outside diameter of 16 in. and larger, as prior to the last few years there were few crude-oil pipe-line systems of any appreciable length composed of lines with a nominal diameter greater than 12 in. The increased laying of larger lines has paralleled the development of higher-strength steel, permitting higher station operating pressures, together with improved methods of laying line. A further parallel has been the increased use of technical data for the design of new systems rather than rules of thumb formerly used. Since the pumping rates through these larger lines are much greater, the need for an accurate knowledge of available throughput is gaining in importance so that the optimum-size line will be used in the design of new facilities, and the length of loops required to enlarge on present facilities can be determined accurately.

Basic Hydraulic Formulas

In hydraulic calculations involving crude oil, it has been found that the basic formula as introduced by Darcy in 1857, is the most applicable of the various flow formulas. This equation is a familiar one to all engineers and in its basic form is

$$h_f = \frac{f\,l\,v^2}{2gd}$$

In this form the equation is solvable if the various quantities are expressed in foot-pound-second units, giving the value of h_f in feet. This form is rather cumbersome, however, as units required in the foregoing equation are not commonly used in pipe-line terminology.

This equation, after conversion to a more practical form, can be expressed as

$$P = \frac{34.87\,fB^2s}{D^5} \quad \text{[1]}$$

where each of the terms has the following significance:

P = pressure drop, psi per mile.
B = line throughput, bbl per hr
s = specific gravity of oil pumped
D = internal diameter, in.
f = friction factor

In Equation [1] it is possible to measure physically all quantities, with the exception of the dimensionless friction factor which must be determined experimentally.

The customary means of expressing f is to plot its value against the corresponding value of Reynolds number **R**, which is in existence in the line at that particular time. It is not necessary to dwell at length on this number as it also is familiar to all engineers. In its basic form it is expressed as

$$\mathbf{R} = \frac{dv\rho}{\mu} \quad \text{[2]}$$

where

d = diameter of pipe
v = velocity of fluid
ρ = density of fluid
μ = absolute viscosity

Any consistent set of units can be used such that the value of **R** will be dimensionless. This equation also can be expressed in a form more readily used and remembered by engineers. This converted form is

$$\mathbf{R} = \frac{2214 \times B}{D \times \nu} \quad \text{[3]}$$

where B and D have the same significance as previously given, and ν is the kinematic viscosity of the oil moving through the line, expressed in centistokes. To clarify the formula further, the relationship between centistokes and Saybolt Universal seconds (SUS), a more common way of expressing viscosity, can be set forth by a simple equation

$$\text{Centistokes} = 0.22t - \frac{180}{t} \quad \text{[4]}$$

where t represents Saybolt Universal seconds.

A basic relationship between f and **R** has been established for streamline flow and verified by many experimenters so will be valid for the lines here investigated. This relationship can be expressed by the equation $f = 64/\mathbf{R}$ which when substituted in Equation [1] gives

$$P = \frac{1.008\,B\mu}{D^4} \quad \text{[5]}$$

where μ is the absolute viscosity in centipoises.

---

[1] Stanolind Pipe Line Company. Jun. ASME.

Contributed by the Petroleum Division and presented at the Petroleum Mechanical Engineering Conference, Oklahoma City, Okla., October 2–5, 1949, of The American Society of Mechanical Engineers.

Note: Statements and opinions advanced in papers are to be understood as individual expressions of their authors and not those of the Society. Paper No. 49—PET-13.

Research on Fluid Flow

Experimental work done by Stanton and Pannell on fluid flow through pipes embraced a wide set of flow conditions and has been recognized as one of the most authoritative pieces of work on this subject. Their experiments were carried out using air and water moving at different rates through smooth drawn brass pipe varying in diameter from 0.361 cm to 2.855 cm. The curve propounded by these authors is shown in Fig. 1, plotted in double logarithmic form. This shows the two distinct regions of flow, streamline and turbulent.

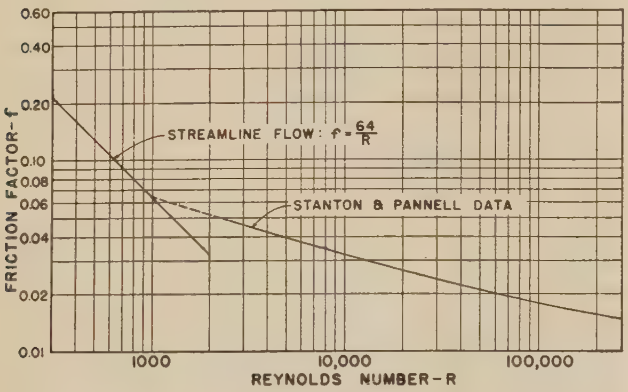

Fig. 1 Plot of Friction Factor Versus Reynolds Number Showing Basic Equation for Streamline Flow and Stanton and Pannell Data for Turbulent Flow

It is the purpose here to describe tests run recently for the evaluation of the friction factor *f* in large-diameter lines in the turbulent-flow region and to express the results obtained from these tests. The intent in carrying out this investigation was to secure data that would be of direct use in hydraulic calculations on commercial pipe lines rather than procuring data that would be of academic interest only. Numerous papers such as that of Stanton and Pannell have been written on the value of *f*, as determined by laboratory experimentation, using various fluids such as water and air in small-diameter lines. Our purpose was to determine which data, if any, obtained from these laboratory experiments would be confirmed by results secured from large-diameter lines moving crude oil. Various authors concur with the reasoning that their results obtained from smaller lines may not hold true for larger lines.

To get information such as was desired, sections of line in our system were utilized as test sections, thus providing the best large-scale laboratory possible. The friction factor was determined in each of a series of test runs on each section of line. This was done by using Equation [1], measuring the four quantities, *P*, *s*, *B*, and *D*, and solving for the unknown friction factor.

To measure the pressure drop *P*, recording pressure gages were normally used. One was installed at each end of the test section of line and calibrated in place by means of a dead-weight tester. For the measurement of specific gravity, periodic samples were taken from the line, and the gravity determined by means of a hydrometer. The gravities of the crude in the lines tested varied from 32 deg API to 44 deg API. For any one test, the gravity remained essentially constant. An accurate measurement of the volume of oil pumped through the line was necessary in order to obtain the pumping rate, *B*. This was done by pumping decrease out of one tank so that the actual volume was determined from hourly tank gages. The internal diameter used was the nominal internal diameter of the line with no allowance being made for manufacturing tolerances. Just prior to the running of a test, a pig-type scraper was run through the line to remove any wall deposits which would have the effect of reducing the internal diameter, which in turn would give a higher value for the calculated friction factor.

To compute the value of **R** to correlate with the value of *f*, it is necessary to determine the viscosity of the oil being pumped, this value then being used in Equation [3]. The ordinary method of measuring viscosity is by use of a commercial viscosimeter, such as the Saybolt type of instrument, which measures the time of efflux of a prescribed amount of liquid through a calibrated orifice.

These tests run at atmospheric pressure, however, do not give the true viscosity of the oil while moving through the line under pressure. It was known that viscosity increased with pressure, but a perusal of available literature on the subject yielded nothing that was specific enough to be applicable for our use. The effect of pressure on viscosity is gaining in importance due to the trend toward higher operating pressures.

To obtain information on conditions existent in our system, tests were run to determine how viscosity varied with pressures normally encountered in pipe-line operation. Fig. 2 shows the results obtained from two crudes analyzed in this manner by means of a falling-ball type of viscosimeter. The East Central Texas crude is one of the lightest common stream crudes handled in our system, and the Wyoming crude is the heaviest common stream crude moved through our lines. An examination of Fig. 2 shows that the relationship between pressure and viscosity is apparently a straight-line function. At higher temperatures, the

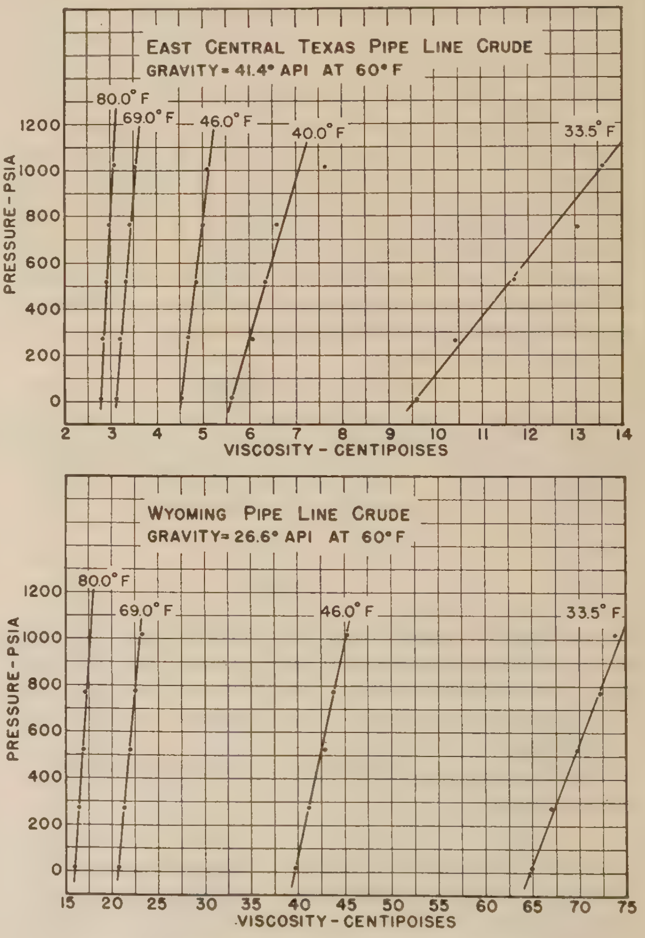

Fig. 2 Effect of Pressure on Viscosity of Two Crude Oils in Ranges of Pressure and Temperature Normally Encountered in Actual Operation

per cent increase in absolute viscosity per 1000 psi is about the same for the two crudes, but at lower temperatures the effect of pressure is much greater on the lighter crude than on the heavier Wyoming crude. Also, for either of the particular crudes, the increase in viscosity due to increased pressure is a greater percentage at lower temperatures. From the trend indicated on the curves, it appears that if the temperature is increased sufficiently, there may be a point at which pressure will have no effect on viscosity. However, this supposition would have to be proved or disproved by actual tests.

Viscosity in Flow Calculations

It is obvious now that using viscosity determined at atmospheric pressure by means of commercial viscosimeters will give erroneous values. With this added information, our problem now is to seek to utilize this information in a simple manner. As realized from past experimentation and evidenced by this investigation, the science of turbulent flow is not an exact one such as is experienced under streamline-flow conditions. Instead, the basic equation includes the empirical term f which is dependent on many variables and which will itself vary over a certain range for the same type of pipe. Because of the inability of measuring f quantitatively, it is proposed to make its value dependent on one more variable—the change in viscosity due to pressure. Since the operating pressures of most trunk-line stations do not vary widely, this effect will be a fairly consistent one, so it is proposed not to use a viscosity correction factor, but instead to plot the values of f determined against the apparent value of $\mathbf{R}$. The apparent value of $\mathbf{R}$ will be the value of this term based on the viscosity determined at atmospheric pressure.

Although the effect of viscosity change in turbulent flow is an indirect one, by reference to Equation [5] it is seen that in streamline flow, the pressure drop is directly proportional to the absolute viscosity. Therefore, using the correct viscosity is of major importance. Normally, crude-oil flow is in the turbulent region, but there are cases where streamline flow is encountered such as in winter months in lines moving the heavy Wyoming oil shown in Fig. 2. Since pressure versus viscosity gives a straight line, the viscosity determined at atmospheric pressure can be corrected by using a correction factor based on the average line pressure. It is difficult to determine the average line pressure exactly because of ground profiles being very irregular, but, for most cases, the average line pressure in a section of line can be assumed to be one-half the station discharge pressure. No investigation has been made into streamline flow in actual operations to determine how closely theoretical conditions will be approximated.

As a counteraction to the effect of pressure on viscosity, some crudes are of a thixotropic nature, i.e., their apparent viscosity decreases as the shear rate increases. The shear rate in any one size line would increase as the pumping rate increases. This characteristic is noticed especially in high-paraffin-base crudes, such as those produced in southwestern Wyoming. On one pipeline system operating in this area, normal operating pressures as high as 2000 psi are encountered, thus resulting in a large throughput and a corresponding high shear rate. In expressing the viscosities of these crudes, viscosities determined by an efflux-type viscosimeter will give a false indication of the viscosity of the oil moving through the line. Instead, a viscosity-temperature curve should be used showing apparent viscosities determined from a study of actual operations.

Most crude oils are of the Newtonian type, however, as their apparent viscosity at any certain temperature is constant regardless of shear rate. For this type of crude, a normal temperature-viscosity curve, as determined by means of an efflux viscosimeter, can be used for determining uncorrected line viscosities.

Results of Tests

The section of the Stanton and Pannell f versus $\mathbf{R}$ curve between Reynolds numbers of 30,000 and 240,000 has been reproduced in Fig. 3, and the author's experimentally determined values for f have been plotted against the apparent $\mathbf{R}$. As shown on the graph, these points were obtained from tests run on lines of 16 in., 20 in., and 30 in. diam. An examination of the graph shows that the author's points determined from the 16-in. lines approximate the Stanton and Pannell curve very closely. The average of the points from the 20-in. line fall slightly above the curve, and the three points representing the 30-in. line are still higher above the curve.

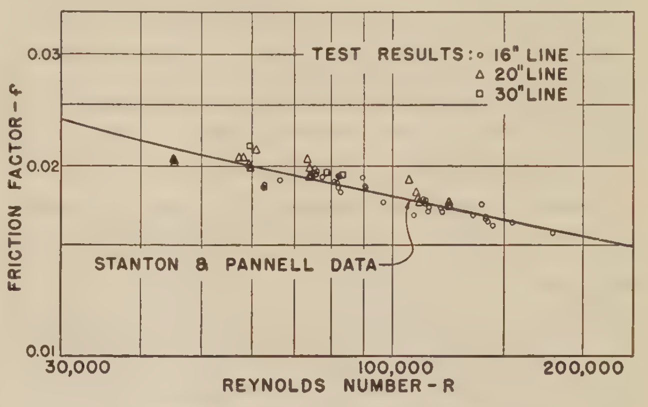

Fig. 3 Plot of Experimental Points Determined From Crude-Oil Lines in Actual Operation, as Compared to Data of Stanton and Pannell

The values of f from the 16-in. and 20-in-diam lines were determined in all cases from sections of trunk line many miles in length, which in most cases included very few valves and no junctions, making the values representative of straight pipe. Much of the 16-in. line has been in West Texas sour-crude service for a period of over 5 years. The 20-in. sections tested have been used for both sour and sweet crude, and have been in service for from 1 to 2 years.

The values shown for the 30-in-diam line were obtained from a section of tank line approximately one-half mile in length. This line was just recently laid and is used for sour West Texas crude. Because of its short length and corresponding small pressure drop, it was necessary to measure the pressure differential by means of a manometer installed at each end of the line. Due to insufficient data on the 30-in. line, no definite conclusions can be reached, but it is felt that in trunk-line service, the friction factor for this size line will be somewhat lower than shown here. The 30-in. tank line tested was $^{1}/_{4}$-in. wall pipe and was laid above ground so was probably not perfectly round, as the pressure in the line did not exceed 15 psi. In addition, the test section included an expansion joint which would have the effect of increasing the pressure drop slightly, resulting in a higher apparent friction factor.

Moody[2] has drawn a family of friction-factor curves based upon different relative roughnesses. The lowest curve in this family is for smooth pipe and approximates the Stanton and Pannell curve. The relative roughness, ϵ/D, as given by Moody for commercial steel pipe in the range of sizes here discussed, is low enough that it can be considered as smooth pipe in the range of Reynolds numbers normally encountered.

---

[2] "Friction Factors for Pipe Flow," by L. F. Moody, Trans. ASME, vol. 66, 1944, pp. 671–684.

Drew, Koo, and McAdams[3] made a survey of work done on determination of the friction factor to ascertain if Lees' equation, which was based upon the data of Stanton and Pannell, gave values for f that were representative of smooth pipe. Their investigation showed that the majority of experimental work, up to a Reynolds number of 500,000, validated Lees' equation. These authors also studied work done on commercial iron and steel pipe and, as a result of this study, presented a curve for f somewhat higher than that for smooth pipes. The work they reviewed was all carried out on small-diameter pipe, and they state that smaller-size pipes generally give higher values for f.

Other experimental work has been done by Heltzel[4] at lower Reynolds numbers on lines of 6 to 12 in. diam in crude-oil service, and the validity of the Stanton and Pannell curve for this use has been verified by him. It is believed the test data accumulated here are sufficient confirmation of this curve to warrant using it for large-diameter lines. Although these tests did not cover the entire range of **R** encountered in these lines, the range covered includes the majority of normal flow conditions.

Determining Trunk-Line Capacity

Because the Stanton and Pannell curve has thus been substantiated for a wide range of pipe sizes, an expedient equation based on this curve will be developed for determining directly trunk-line capacity. The use of Equation [1] for determining line capacity is rather laborious, as it is necessary to use a cut-and-try method for determining the value of f to use in the equation. The range of **R** normally encountered in our crude-oil lines does not exceed 200,000 with the majority of flow conditions giving a value of **R** less than 100,000.

Our problem now is to develop a relationship between f and **R** which will give fairly consistent results over the entire range of turbulent-flow conditions encountered in our work. To do this, a straight line is drawn between points on the Stanton and Pannell curve corresponding to **R** of 6000 and 130,000, as shown in Fig. 4. It can be seen that this straight line does not vary widely from the curve at any point. By simple mathematics, the equation of this line is calculated to be

$$f = \frac{0.3305}{\mathbf{R}^{0.252}} \qquad [6]$$

but

$$\mathbf{R} = \frac{2214 \times B}{D \times \nu}$$

which substituted in Equation [6] gives

$$f = \frac{0.0474\ D^{0.252}\ \nu^{0.252}}{B^{0.252}} \qquad [7]$$

This in turn is substituted in Equation [1] and the resultant form is

$$P = \frac{1.653\ B^{1.748}\ \nu^{0.252} s}{D^{4.748}} \qquad [8]$$

Solving this equation for B gives the following

$$B = \frac{0.750\ P^{0.572}\ D^{2.716}}{\nu^{0.144}\ s^{0.572}} \qquad [9]$$

While this is unwieldy to use, it does give a direct means of solving for the capacity of a line. The greatest value of this type of equation lies in its adaptability to logarithmic charts or a logarithmic slide rule, providing a convenient means of solution.

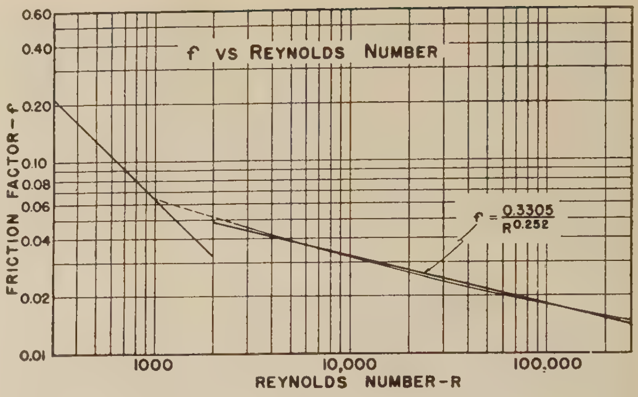

Fig. 4 Straight-Line Relationship Between Friction Factor and Reynolds Number for Turbulent Flow, Based Upon Stanton and Pannell Curve

Practical Verification

It is felt that the choice of the straight line for f versus **R** above the Stanton and Pannell curve will approximate actual conditions very closely as the use of a higher friction factor will give a greater pressure drop than encountered in a straight pipe line. This higher pressure will compensate for certain factors not now considered which have the effect of increasing the operating pressure. Under our present method of calculating, no provision is made for the additional pressure loss through valves, fittings at junctions, and station manifolds. The basis of our calculations is the actual distance of line between stations with the correction for elevation head being taken as the difference in elevation between the station floors. Though most of our stations operate with a tank floating on the line, there are times when they pump their entire stream into a tank at the next station. This would have the effect of increasing the discharge pressure at the pumping station due to the additional pressure drop through the tank line. No correction is made for these operating conditions although the tank lines are one-half mile in length at some stations.

An additional factor that will be corrected for, by using a higher line for f, is the decrease in effective internal diameter between the running of scrapers. As the lines grow older, the value of f experienced may increase due to internal corrosion in some lines, although past performance has shown this factor to be a negligible one in trunk lines where velocity is sufficient to prevent the settling out of water, the primary cause of internal corrosion.

Considering the effect on capacity, the maximum difference encountered is 2.7 per cent less capacity when using the straight line for f instead of the Stanton and Pannell curve for f.

Conclusion

While it is realized that the data presented here are not all-inclusive, it is felt that it is a realistic addition to the field of pipe-line hydraulics. The accumulation of data such as included here is time-consuming as well as costly, but it is hoped that further study can be made of flow conditions in commercial pipe-line systems, for information gathered in this manner will be of definite aid to the pipe-line engineer.

Acknowledgments

The author wishes to acknowledge the help of members of the Engineering Department of the Stanolind Pipe Line Company, and particularly the aid of Messrs. L. E. Tomlinson and W. E.

---

[3] "The Friction Factor for Clean Round Pipe," by T. B. Drew, E. C. Koo, and W. H. McAdams, Trans. AIChE, vol. 28, 1932, pp. 56–72.

[4] "Fluid Flow and Friction in Pipe Lines," by W. G. Heltzel, *The Oil and Gas Journal*, vol. 29, June 5, 1930, pp. T203–T224.

Roads, who assisted in some of the test work and offered helpful suggestions in compiling the data here presented.

Discussion

F. M. Van Deventer.[5] The author has demonstrated that actual operating data on 16-in., 20-in., and 30-in. lines indicate a friction factor versus Reynolds number relationship which closely confirms the Stanton and Pannell data, and that within the normal operating range for oil lines, a straight line may safely be used. From that straight line, he establishes his Equation [9]. This discussion will show that the author's formula is entirely consistent with the D'Arcy general flow formula and friction factors, delineated by the most recent revisions of the friction-factor relationship. Reference will also be made to mechanical calculators, the use of which eliminates the necessity of calculating exponentials of the author's formula.

The writer's Fig. 5 is a graph of the friction factor versus Reynolds number relationship based upon the Colebrook function and has been delineated by Prof. L. F. Moody.[6] This form, prepared by the writer, is considered to be an improvement over Moody's chart, inasmuch as scales are appended for steel, cast iron, and drawn materials. Hence it is unnecessary to refer to a separate chart or table from which the value ϵ/D is obtained; that value being entered on the friction-factor chart.

The writer includes a scale ϵ/D so that solution may be made for materials other than the three referred to.

A series of five circles in the Reynolds-number range between 60,000 and 150,000 are shown in Fig. 5. This is the range covered by the author's tests. It will be noted that if the chart is entered on lines representing 16-in., 20-in., and 30-in. steel pipes, these lines converge so as to become almost indistinguishable in the range under discussion. That line in turn conforms closely with the Stanton and Pannell line, and hence with the author's test data. It is also interesting to observe that this line corresponds to a hydraulic efficiency of about 98 per cent.

A word of caution is in order concerning the limitation of the author's formula if used for Reynolds numbers too far outside the limits covered by the Stanolind tests. This may be demonstrated by observing the spread of friction factors for pipes of 16 in. to 30 in. diam, operating with Reynolds numbers of the order used in natural-gas transportation. (It is recognized that the author's formula is not intended for such use, but this comparison will serve to illustrate the point.)

Modern natural-gas transport lines operate at Reynolds numbers in the range of 8 million to 16 million. The spread of friction factors in this range is represented by the group of small circles plotted on the friction-factor chart. It will be noted that for 16-in. pipes the expected friction factor is 0.012, and for 30-in. pipes, 0.011. In this range there is a particular friction factor corresponding to each pipe size. In comparing this group of points with the oil group, it is interesting to observe that the hydraulic efficiency of the 16-in. and 30-in. pipes would be about 80 per cent and 90 per cent, respectively.

In the interest of labor and timesaving, the writer recommends the use of "mechanical brains" for the solution of most problems concerning the flow of fluids. Some such devices are based upon crude approximations or empirical data, hence satisfactory accuracy may not be obtained. On the other hand, some of them are based upon a formula of the D'Arcy type, means being provided whereby the friction factor may be compensated so as to represent the pipe size and material actually used.

The writer's Fig. 6 is a graphic comparison of the results obtained from (1) the author's formula; (2) the D'Arcy formula; (3) the Polyflo computer. The following assumptions were

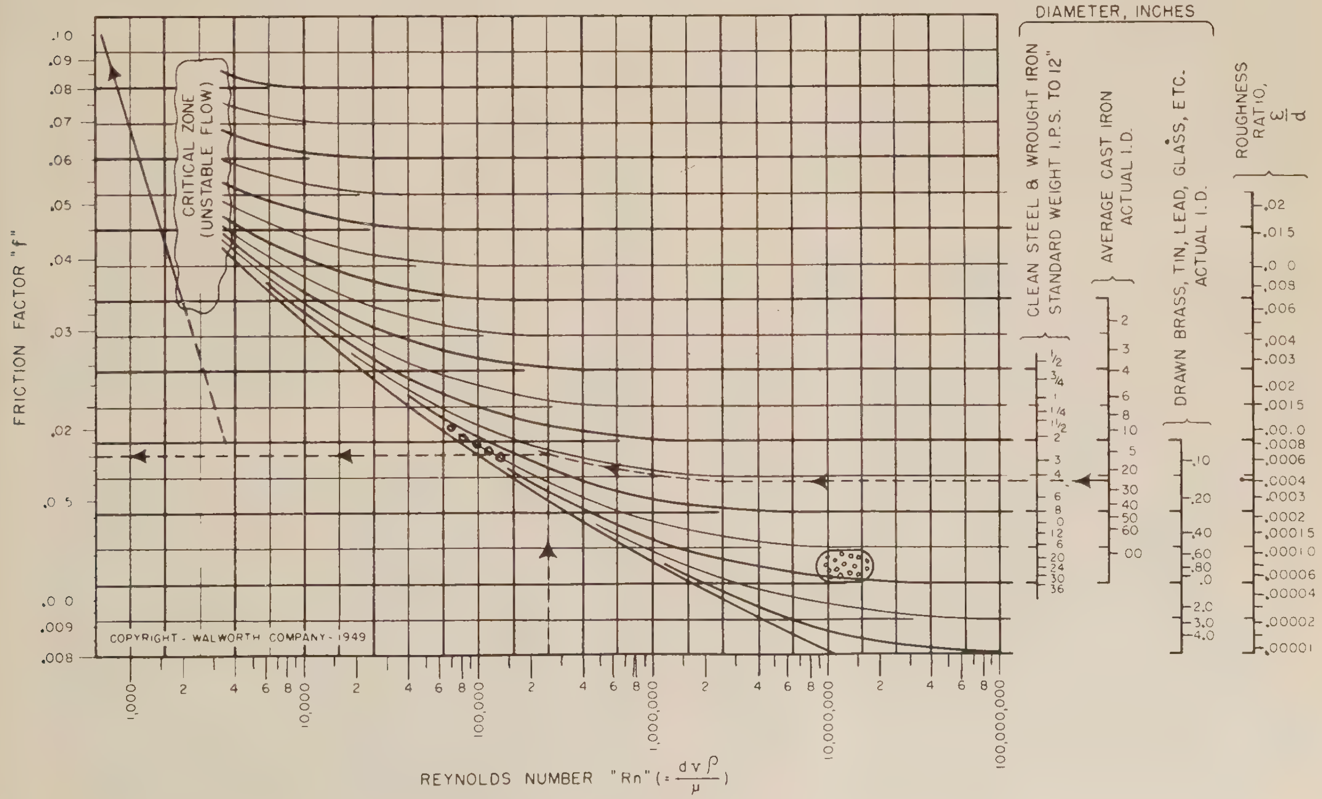

Fig. 5

---

[5] Assistant Chief Engineer, Walworth Company, Inc., New York, N. Y. Mem. ASME.

[6] Author's reference 2.

made: ID of pipe, 20 in.; specific gravity, 0.90; viscosity, 10 centistokes.

Values of 4, 8, 13, and 22 psi per mile were assumed. Barrels per hour was calculated by the author's formula and plotted as shown.

A second set of values for pounds per square inch per mile was computed by the D'Arcy formula, using friction-factor values from the writer's Fig. 5, and the results plotted.

A third set of calculations was solved by the Polyflo computer and plotted. It will be noted that a single line fairly represents the results from all three methods.

It is true that the exponent representing the relation between rate of flow and pressure loss is slightly different for each of the three methods. Hence it is analytically deduced that there should be three separate lines in Fig. 6. However, it may also be shown that within the range of this chart, the difference between any two of these three methods would be in the order of 2 to 3 per cent. Inasmuch as the spread of plotted points in the author's Fig. 4 is plus or minus 5 per cent, it seems reasonable to conclude that a mechanical calculator such as the Polyflo has a degree of accuracy consistent with the solution of most flow problems.

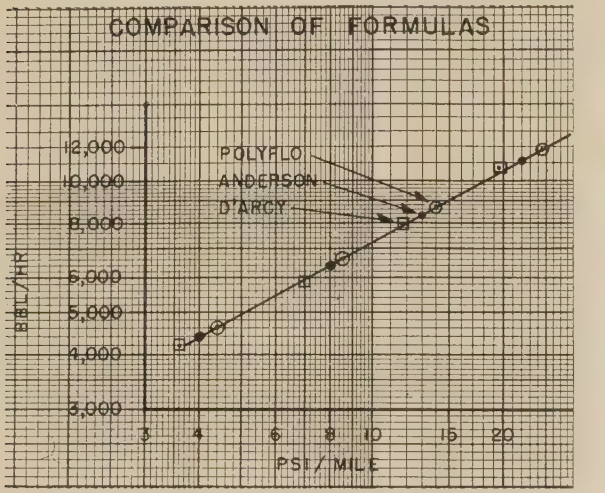

FIG. 6

W. G. HELTZEL.[7] The writer suggested in a paper:[8] "In view of the trend to higher operating pipe-line pressures it would be worth while having some information on the viscosity of crude oils under pressures usedin pipe-line operation." In so far as is known, the data in the present paper are the first to be presented on this subject. It is noteworthy that there is a 50 per cent increase in the viscosity of the East Central Texas crude oil at 33.5 F, corresponding to an increase in pressure from atmospheric to 1000 psi. Likewise, an increase of only 10 per cent for the viscous low-gravity Wyoming crude oil under similar conditions is interesting.

Because pressures up to 1400 psi are used for pumping operations, and since temperatures as low as 32 F are experienced, this subject should be studied further. It is of sufficient importance that the industry should undertake an extensive investigation through the API or one of the engineering societies for the purpose of confirming the author's data and to determine what the relationship is between pressure and viscosity of crude oils. At the same time, a study of the crude oils of a "thixotropic" nature should be made so that a pipe-line engineer will have some way of identifying such a crude oil—and for the purpose of developing suitable means of obtaining a true viscosity. The pipe-line engineer needs more reliable means than those at his disposal now for determining accurately the viscosity of very viscous crude oils.

It would be interesting if the author would report any observations on the pipe line system, referred to in his paper, that is, transporting a thixotropic crude oil at 2000 psi. It is presumed that this is the La Barge Wyoming crude oil. How do the operating results compare with the theoretical calculations for the line, using the viscosities obtained from both the Saybolt and Brookfield types of viscosimeters at atmospheric pressure? In this case can the author give any information as to what extent the increased shear rate offsets the viscosity?

Are there any operating results to compare with theoretical calculations in the case of the 50 per cent increase in the viscosity of the East Central Texas crude oil at 33.5 F, as shown in Fig. 2?

The pipe-line engineer will be interested in knowing more about the manner of conducting the viscosity tests under pressure.

That the author's data for the coefficient of friction fall along the Stanton-Pannell curve is what might be expected. The results for the 16-in. line fall very close to the Stanton-Pannell curve; perhaps these data are the most reliable because, as the writer understands, they were obtained from a long 16-in. pipe line. One would expect the results for the 20-in. and 30-in. lines to be as low or lower than those for the 16-in. line. However, the results are rather consistent for data obtained from operating pipe lines; the shortness of the 30-in. line probably accounts for the higher values obtained in that case. It would be helpful if the author would define in some detail the pipe lines for which the data were obtained, particularly the length of the sections and the period of observations. The author makes reference to some data reported by the writer in 1926, showing that the coefficients of friction for lines in sizes as small as 8 in. and 12 in. lie near the Stanton-Pannell curve. These tests were made on a 12-in. screw-joint line in Wyoming in 1923. The data were obtained by recording the pressure and temperature at $^1/_2$-mile intervals for about 8 miles, and at some longer intervals outside of this stretch. The tests covered about 180 successive days, using 24-hr recording instruments.

The Moody curves show coefficients of friction higher than the Stanton and Pannell curve. There is no reason for doubting the dimensionless analysis expressed by the Colebrook function; however, we should recognize that the absolute coefficient of roughness cannot be determined too accurately. The author's data and other information on the operation of large-diameter crude-oil lines that is gradually coming to light, indicate that the relative roughness of these large-diameter lines approximates that for the small smooth brass tubes used in Stanton and Pannell's experiments. This factor is of such importance in the design of large-diameter lines that the industry should endeavor, through a joint effort, to determine these coefficients for the practical design of crude-oil pipe lines.

It is the writer's opinion now that the empirical formula, as developed in the paper, can be used safely for the design of crude-oil pipe lines. The results probably will be as accurate as those obtained by trying to be precise. It is doubtful if the factors entering into the calculations can be determined accurately enough to warrant striving for precision beyond the results that would be obtained by this formula. In a paper written in 1930, the writer offered two formulas developed in a manner similar to the present method. One covered a range from 3000 to 57,000 for Reynolds number, and another for the region beyond 57,000. Now one formula for the whole range is adequate for practical purposes. The design of many miles of crude-oil pipe lines over the past 26 years, using the Stanton and Pannell curve, has, in general, and for all practical purposes proved satisfactory.

---

[7] Consulting Engineer, Tulsa, Okla. Mem. ASME.

[8] Author's reference (4).

AUTHOR'S CLOSURE

The author wishes to express his appreciation to Messrs. Van Deventer and Heltzel for the foregoing discussions submitted by them.

As Mr. Van Deventer states, and as brought out in the text of this paper, the turbulent-flow formula is not applicable for all values of Reynolds numbers. The formula was derived with the intent of using it for crude-oil flow problems only; it is sufficiently accurate for values of **R** from the lower turbulent-flow region to a maximum **R** of approximately 150,000. This range includes the majority of crude-oil flow conditions encountered in the turbulent-flow region.

With reference to transporting the thixotropic La Barge crude, only a limited amount of data have been obtained from a study of daily reports on operations. Apparent viscosities were determined from these data by using the author's derived equation. These apparent viscosities at low temperatures are lower than the viscosities obtained from the temperature-viscosity curve for this crude oil. The values for the temperature-viscosity curve were determined from viscosity tests run at atmospheric pressure by means of the Saybolt viscosimeter at high temperatures and by the Brookfield viscosimeter in the lower-temperature range.

No data are available from actual operations on the transporting of the East Central Texas crude oil at 33.5 F since our lines transporting this crude in its pure form reach a minimum line temperature in the winter months of only 50 F.

The viscosities under pressure were determined by use of the Humble viscosimeter which is a falling-ball type of viscosimeter designed to measure the viscosity of a small subsurface oil sample under actual reservoir conditions. It is equipped with a water bath to permit viscosity determinations at different temperatures.

Mr. Heltzel suggested that additional information on the lines tested would be helpful. Two different sections of 16-in. line were utilized, a 40-mile section in West Texas and a 15-mile section in Oklahoma. Tests on each of the lines were run over a period of about three weeks with data secured from as wide a range of flow rates as was conveniently possible. The tests conducted on the 20-in. lines were carried out for about the same length of time. Two sections of 20-in. line were also used: one section in Missouri was 74 miles in length, and the other section, which was in Oklahoma, consisted of 57 miles of pipe.

Surge Problems in Pipe Lines—Oil and Water

By S. LOGAN KERR,[1] PHILADELPHIA, PA.

This paper outlines the work done by the Water Hammer Committee of the Society, outlining the publications involved. A general review and summary are given of water-hammer studies as they can be applied to the petroleum pipe-line surge problem.

IN OUR Society, The Hydraulic Division is concerned with the flow of water and other fluids and their use in hydraulic machinery, turbines, pumps, valves, and conduits. The Division is likewise interested in the behavior of flowing fluids under varying conditions where cavitation or water hammer is present. It is to this latter phenomenon that attention is now directed.

In the years from 1920 to 1930 it was increasingly apparent that there was a great dearth of reliable and accurate information on water hammer. Only a few articles had been published in American engineering literature prior to 1930, but many different approximate formulas had found their way into textbooks and handbooks and were widely used by designers, sometimes with serious results.

A preliminary survey indicated the need of some continuing activity by the Hydraulic Division, to remedy this situation. In 1931 the Committee on Water Hammer was set up to continue the survey, to sponsor programs, solicit articles, prepare reports on the state of the art, and to stimulate interest in this subject. A committee of six was appointed, consisting primarily of those who had contributed articles on water hammer in the preceding 10 years.

The membership of the Committee[2] was not restricted to members of the Society, but included some who were members of the American Society of Civil Engineers, and one member who did not belong to any society. At least two members of the committee belonged to both The American Society of Mechanical Engineers and the American Society of Civil Engineers, as well as to The Engineering Institute of Canada. Great stress was laid on the desirability of co-operation between all groups interested in surges and water-hammer problems. The committee membership also was independent of company affiliations and included representatives of the hydraulic-turbine manufacturers, a university professor, and two representatives of one of the largest power companies operating hydroelectric equipment in the United States and Canada.

As the survey continued, and committee reports were prepared, it was felt desirable to hold a series of technical sessions where a carefully selected group of papers could be presented, covering the various aspects of water hammer and thus make available in English a comprehensive treatise on water hammer. Field test data to substantiate the theory were to be made available wherever possible.

Two years of preparation resulted in the first Symposium on Water Hammer, held at the time of the Century of Progress Exposition in Chicago, June, 1933, when several national engineering societies were having conventions, and a maximum attendance could be expected. It was sponsored jointly by The American Society of Mechanical Engineers, Hydraulic Division, and the American Society of Civil Engineers, Power Division, with other societies co-operating.

A comprehensive committee report and seven papers were privately published as a 90-page booklet, in advance of the meeting, and were widely distributed to promote active discussion. These discussions were included in a 60-page supplement which later was combined in a single publication and two editions were rapidly exhausted.

In February, 1949, the Symposium on Water Hammer, 1933, was republished by this Society, and once more is available to engineers and students for study and reference.

1 STATE OF THE ART—1933

The committee report (1)[3] outlined the historical development of surge wave theory, beginning with the experiments by Joukovsky in Moscow in 1897, described in an article (2), published in 1904 by the American Water Works Association. Subsequent treatises were analyzed and evaluated as this fundamental research was extended and amplified by many engineers in Europe and America, the best known being the work by Allievi (3) in Italy and translated into many languages. The English version by E. E. Halmos was published in 1925, under the sponsorship of this Society and the American Society of Civil Engineers, with funds supplied by the late John R. Freeman.

An annotated bibliography was prepared as a part of the committee report, together with a tabulation of symbols used by different authors in their treatises on water hammer. The committee also recommended a uniform nomenclature and symbol system in an attempt to avoid confusion in terminology.

An appendix to the report evaluated the various theories and the approximate formulas in general use prior to 1933. Some of these formulas were derived analytically, some from piecemeal translations of European authors, notably Allievi, and were frequently tagged with his name as the source. These partial abstracts reached American engineering literature by devious routes. The original Allievi treatises were published in Italian, translated into German or French by Swiss engineers, and subsequently, translated from German into English by others. There were many opportunities for substantial departures from the original concept during this process, since the use of formulas alone without full understanding of their limits of accuracy or the assumptions upon which they are based may give results that are frequently in error.

Fig. 1 gives a comparison of the computations of a specific surge problem by several approximate formulas in current use at

---

[1] Consulting Engineer, and President, S. Logan Kerr & Company, Inc.; Chairman, Committee on Water Hammer. Mem. ASME.

[2] Norman R. Gibson, Eugene E. Halmos, Lewis F. Moody, Ray S. Quick, Earl B. Strowger, and S. Logan Kerr.

Contributed by the Petroleum Division and presented at the Petroleum Mechanical Engineering Conference, Oklahoma City, Okla., October 2–5, 1949, of The American Society of Mechanical Engineers.

Note: Statements and opinions advanced in papers are to be understood as individual expressions of their authors and not those of the Society. Paper No. 49—PET-9.

[3] Numbers in parentheses refer to the Bibliography at the end of the paper.

NAME OF FORMULA	FORMULA	MAXIMUM PRESSURE RISE (FT.)	PERCENT OF MAXIMUM BY ELASTIC WAVE THEORY
VENSANO	$h = \frac{2LV}{gT}$	285.0	129.6
WARREN	$h = \frac{LV}{g(T - \frac{L}{a})}$	162.3	73.8
JOHNSON	$h = \frac{LV_0}{2g^2H_0T^2}\left[LV_0 + \sqrt{4g^2H^2T^2 + L^2V_0^2}\right]$	216.0	98.3
FANNING	$h = \frac{LV}{gT}$	142.5	64.8
TALBOT	$h = 2.31\,V\sqrt{\frac{1}{1 + \frac{Kd}{Ee}}}\ \sqrt{\frac{wK}{144g}}$	1175.0	535.0
REDUCES TO:	$h = \frac{aV}{g}$		
de SPARRE (CASE 3)	$h = \frac{2LV_0}{gT}\ \frac{1}{2\left[1 - \frac{LV_0}{2gTH_0}\right]}$	251.0	114.2
ELASTIC WAVE THEORY (a) DETAILED CALCULATION EQUATIONS OF ALLIEVI, GIBSON, QUICK AND GIBSON ARITHMETIC INTEGRATION		219.88	100.0
(b) CHARTS BY QUICK, ALLIEVI		219.9	100.0

FIG. 1

(Example: Length L, 820 ft; velocity, V, 11.75 fps; head, H_0 165 ft; time, T, 2.1 sec; wave velocity, (a), 3220 fps; critical time $2L/a$, 0.509 sec.)

the time. Similar computations were made by the elastic-wave theory, following different mathematical procedures. This example was based upon a hypothetical hydraulic-turbine penstock with flow gradually cut off at a uniform rate. None of the approximate formulas agrees exactly with computations based on the elastic-wave theory, nor do they allow for nonuniform rates of flow cutoff or permit the determination of the wave shape. The wide variations in results show clearly the risk in using such short-cut methods.

One of the most valuable contributions to this first Symposium was made by A. W. K. Billings (4) of Sao Paulo Railway, Light and Power Company, and his associates in Brazil. This covered both theoretical and practical aspects of water hammer and reported extensively on the field tests which were made on a penstock for one of the large impulse-turbine units installed at the Serra plant in Brazil.

The agreement between the theoretical analysis and the actual pressure-time diagrams, Fig. 2, recorded during tests was remarkable, and showed dramatically that all factors affecting water hammer could be taken into account during the design of a project and in advance of construction. It also showed that full and complete reliance could be placed in such theoretical studies when these factors had been included properly in the analysis.

Variations in thickness, diameter, or material of construction of the pipe itself, branch pipes, dead ends or parallel conduits were discussed, and methods shown for computing their effect on the shape of the surge wave and the intensity of the surge pressures above normal working levels.

Their treatment of the subject is applicable to any type of pressure conduit and offers one of the classic contributions to the knowledge of surges in pipe lines. Later developments, described in Section 2 of this paper, offer simplifications in the solution of such problems, but are based upon the same fundamental theory and are just as valid as the methods used by Mr. Billings and his associates.

Other papers in the first Symposium include two analytical derivations of basic water-hammer equations, using the elastic-wave theory; one by Moody (5), and the other by Glover (6). In the discussion by F. Knapp (7), additional theoretical treatments are presented, and Strowger (8) derives the fundamental equations of Allievi and treats further the factors related to partial and complete reflection of surge waves.

Two papers (9, 10) deal with surge problems in discharge lines from motor-driven centrifugal pumps when the power supply is cut off abruptly. A series of field tests is described in detail and a method of counteracting surges, applicable to water lines, is shown.

Certain significant conclusions were reached as a result of this first Symposium:

1 The elastic-wave theory developed by Joukovsky and amplified by Allievi, was valid for simple conduits of uniform thickness and uniform diameter, where friction of flow could be neglected.

2 Studies indicated that the elastic-wave theory could be extended to account for the effect of branch pipes, dead ends, changes in thickness, diameter, and material of construction. The variations in wave form and the magnitude of surge pressures resulting from these factors could be computed.

3 The effect of nonlinear valve movement in either the opening or closing direction, and the behavior of relief valves could be included in any theoretical analysis.

4 The means were available to determine theoretically the surge conditions at any point in a hydraulic system at any time during or after closure or opening of a control valve or other mechanism causing a change in velocity of flow.

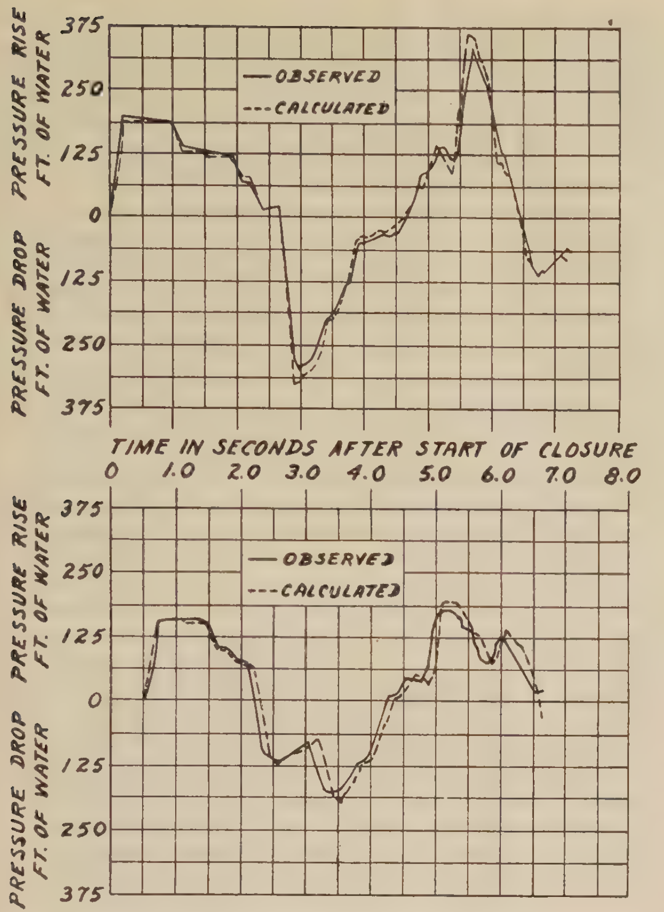

Fig. 2 Comparison of Theoretical and Field Test Pressures

(Serra penstock No. 1, 4550 ft long, of which 663 is 61 in. diam; 527 ft of 55 in. diam; 1872 ft of 49.2 in. diam, and 2071 ft of 43.3 in. diam. Thickness varied 0.375 in. at top to 1.688 in. at bottom. 15.5 cfs stopped in 0.22 sec.)
(a) Pressure-time curves at control valve
(b) Pressure-time curves at lower end 49.2-in. section, 0.455 L from valve

5 Approximate formulas, short cuts and general assumptions, were a source of great potential error and should be eliminated from use, unless the formula itself was accompanied by a statement of its limitations, and the range of application within it agreed reasonably well with the elastic-wave theory.

6 Field-test programs had confirmed the accuracy of the theoretical approach.

Expanded Activities

So successful was this first endeavor that two additional steps were authorized as follows:

1 To invite representatives from other societies in the United States and Canada to serve as associate members of The American Society of Mechanical Engineers' Water Hammer Committee.

2 To broaden its activities to include representatives of engineering societies in other countries, or to designate individuals to serve as associate members of the committee in other countries.

Within a year representatives were designated by the American Society of Civil Engineers, the American Water Works Association, The Engineering Institute of Canada, and The Institution of Mechanical Engineers of Great Britain.

Engineers in other countries were invited to become associate members to represent their own countries, and such delegates were designated in France, Switzerland, Germany, Austria, Brazil, and Australia.

With this broadened scope of activities, The American Society of Mechanical Engineers' Committee on Water Hammer became, to a large extent, the clearing house for accumulating publications on water hammer throughout the world. Many interesting contributions were being received from abroad and much investigation and development work was being carried out in the United States and Canada.

The second Symposium was planned for December of 1937, and the papers presented at that time were published in the November, 1937, issue of Transactions, ASME, and were available for study in advance of the meeting.

The international flavor which this committee had acquired was apparent in the author representation at this second Symposium. While the first Symposium was confined to engineers in the United States and Brazil, the second program in 1937 included contributions from engineers in Canada, Great Britain, Switzerland, Italy, and Brazil, in addition to those from the United States.

The onset of the European war, with its extension to World War II, naturally curtailed the activities of the committee and, while representation of other engineering societies in the United States and in Canada was maintained, the associate memberships from other foreign countries were discontinued until some future time when this very valuable world-wide program of technical co-operation could be resumed.

One major factor in the success of the committee in carrying out its objectives of placing in American and Canadian engineering literature, accurate and authoritative treatises on water hammer, has been the spirit of cordial relationship among engineers who are interested in this subject.

The free interchange of technical information in the form of articles submitted to the committee for possible presentation and publication, the interchange of information by correspondence or by personal visits, have brought about a friendly co-operative situation that could not help but bring success to the program.

Discussion of papers was carried out in an unbiased manner, and there is not on record a single case where personal animosity, personal ambition, or company policies or attitudes were allowed to interfere with constructive progress in this highly technical field. The publication of articles was not confined to the journals of any one society. Outstanding contributions can be found in Transactions, ASME; Proceedings, American Society of Civil Engineers; the Journal of the American Water Works Association; the Journal of The Engineering Institute of Canada, and the Proceedings of The Institution of Mechanical Engineers of Great Britain. Discussions were received from all over the world, and abstracts or republications of many of the symposium articles appeared in technical publications of France, England, Switzerland, Germany, and Italy.

2 STATE OF THE ART IN 1949

In the year 1949, some 18 years after the formation of the Committee on Water Hammer, many of the original objectives have been attained. There are now available, in English, a number of reliable articles dealing with practically every phase of water hammer and surges, as applied to water flowing in closed conduits. A selected list of such papers is included in the Bibliography, that, with few exceptions, are all available in engineering reference libraries.

Graphical methods of solution of the complex surge-wave equations have been developed and are proving most useful in analyzing complex problems (12, 13, 14).

Nonlinear valve characteristics can be accounted for simply. The effect of motor-driven centrifugal pumps on surge pressures during sudden shutdown can be predetermined. The performance of relief valves and their behavior in reducing surges can be related to control-valve operation.

Much progress has been made in applying surge-wave theory to analyses during the design of installations and in advance of construction. It is now possible to predict with a great degree of accuracy the magnitude of surge pressures in any given installation, and thus to design remedial devices with assurance that they will function as desired.

There is a growing interest in water-hammer and surge-wave theory. In several engineering schools, graduate research projects include theses on water hammer.

Some typical examples are included to demonstrate such methods of solving surge problems.

Graphical Solution of Example in Fig. 1

The example used for the comparison of the various approximate formulas, Fig. 1, can also be solved by the graphical method. If the hydraulic characteristics of a given system are plotted on rectangular co-ordinates, Fig. 3(a), it is possible to show along the vertical axis the head or pressure, and along the horizontal axis the velocity of flow in the conduit.

Under any steady-state condition with fixed valve opening, the relationship between velocity and head will be given by a curve (B_0) which follows the square-root relationship between head and discharge. If friction is neglected in this particular example, the static head can be represented as a horizontal line through the vertical axis at a point corresponding to 165 ft.

The static-head line and the steady-state head-velocity relationship intersect at point 1, which represents the normal operating point. Assume that the rate of cutting off flow is uniform with respect to time, and the closure takes place in 2.1 sec. The length, diameter, and material of construction of the pipe give a velocity of the pressure wave of 3220 fps. The critical time ($2L/a$ sec) for a surge wave to travel from the valve to the intake and return is approximately 0.51 sec, and hence the closure will be in slightly over 4 such intervals.

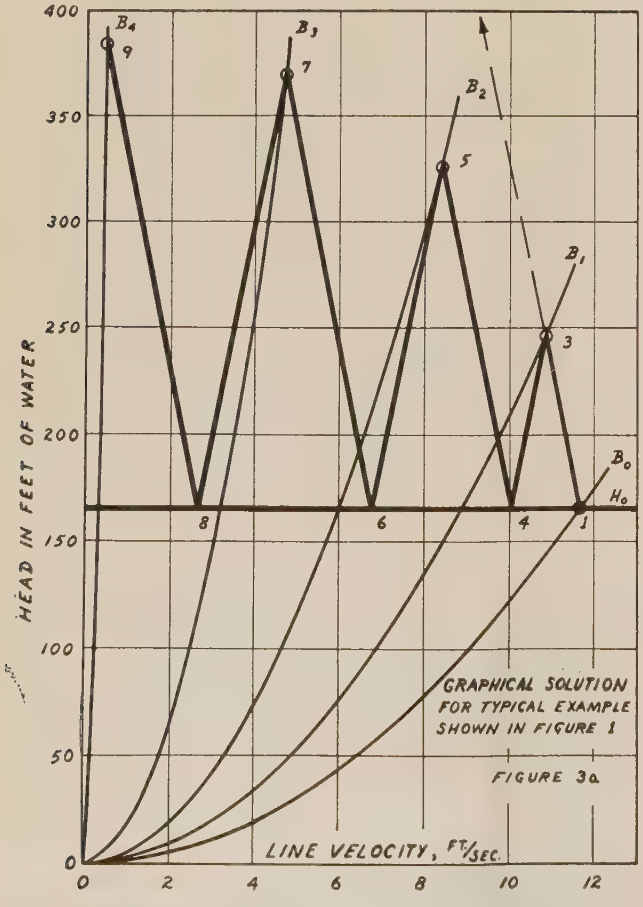

Fig. 3(a) Graphical Solution for Typical Example Shown in Fig. 1

Additional curves which represent the intermediate steady-state condition of the control valve at each unit of critical time can be drawn (B_1, B_2, B_3, and B_4).

A further relationship exists between head and velocity, namely, that the surge pressure is equal to aV/g, whenever the closure rate is in a time equal to or less than the critical time of the conduit.

This becomes a straight line when represented graphically and has a slope of a/g, either plus or minus, depending on whether it is a wave of positive pressure or negative pressure.

If the closure is made instantaneously, then this straight line, having its origin at the initial steady-state condition, point 1, will intersect the zero-velocity line at some point 2 (not shown on diagram), and will result in a surge of 1175 ft above normal.

If the closure is made in a time greater than $2L/a$ sec, then the valve stroke can be assumed to be made in a series of increments each equal to $2L/a$ sec. In this case, the line would start at point 1 and would intersect the next steady-state condition at point 3. It would then be reflected to point 4 along the line drawn with a downward slope, until it intersected the normal head line. Here again, it would be reflected until it reached the point corresponding to two intervals opening under a steady-state condition, shown as point 5. This is continued until the valve is closed.

It will be noted that points 1, 3, 5, 7, and 9 represent the pressures at time increments of $2L/a$ sec. If they are drawn as shown in Fig. 3(b), a curve of pressure rise above normal with respect to time will result, and the shape of the surge wave can be determined. After the valve is closed, the oscillations of pressure, unless damped, will continue above and below the normal head line and can be represented on the diagram accordingly. The maximum pressure as indicated from the graphical solution, is identical with that obtained by the use of the elastic-wave-theory equations, and no new element of theory has been introduced.

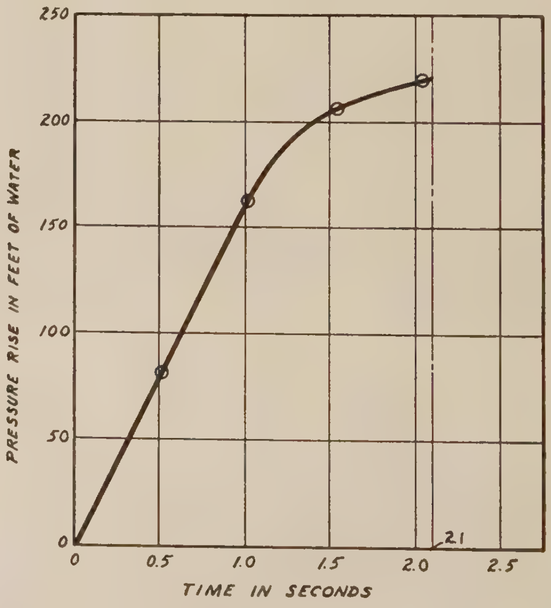

Fig. 3(b) Pressure-Time Diagram for Example, Fig. 3(a)

NONLINEAR VALVE MOVEMENT

In making surge analyses, it is essential to have all of the data on the hydraulic characteristics of the system, including the behavior of the valves or of other devices which may be controlling flow.

The usual assumption of uniform rate of flow reduction is based on the following fallacies:

(*a*) That the stroke of the valve stem cuts off area at a uniform rate.

(*b*) That the flow through a valve is in direct proportion to area and hence to stem travel.

In a given system, with an initial flow of 5 fps, and a shutoff rate of 5 intervals of time ($2L/a$ sec), the uniform rate of flow reduction could be represented as curve A in Fig. 4(*a*). The rate of change of velocity (dv/dt) would be 0.50 fps per sec. The graphical solution is given in Fig. 4(*b*), and pressure-time curve A, Fig. 4(*d*), shows a rise of 60 ft above normal.

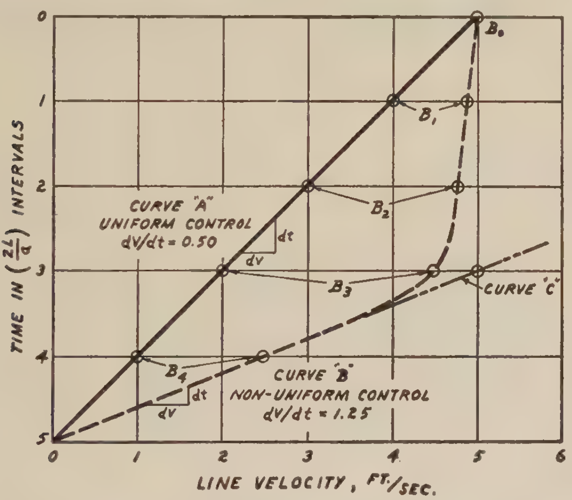

FIG. 4(*a*) COMPARISON OF UNIFORM AND NONUNIFORM RATES OF VELOCITY CONTROL WITH RESPECT TO TIME

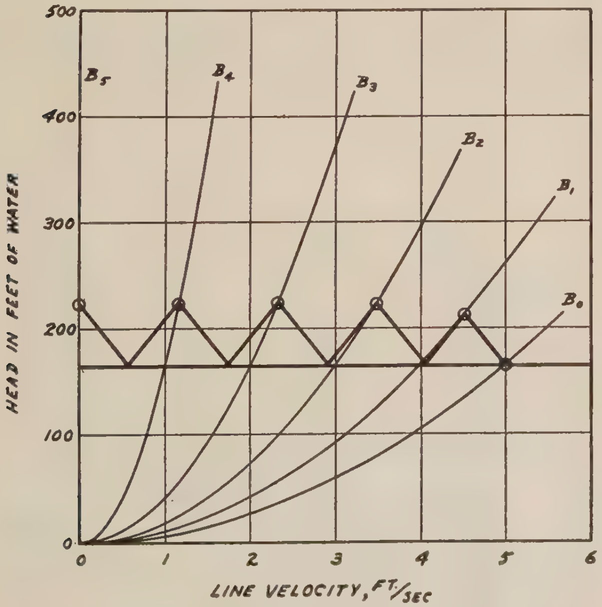

FIG. 4(*b*) GRAPHICAL SOLUTION FOR UNIFORM VARIATION OF VELOCITY WITH RESPECT TO TIME, CURVE A, FIG. 4(*a*)

By contrast, in actual practice, when an ordinary gate valve is closed, there is little or no effect upon the discharge until a point is reached about one half to one third of the full valve opening. The flow then begins to be reduced far more rapidly as the valve continues on toward the seat. Fig. 4(*a*) shows such a typical relationship for an ordinary gate valve, curve B. It will be seen that the maximum rate of change of flow (dv/dt) is $2^1/_2$ times that for uniform closure assumptions, reaching a value of 1.25 fps per sec.

The graphical method can account for variable rates of change of flow by taking the steady-state velocity relationship from curve B, Fig. 4(*a*), at each interval of time. The *B*1, *B*2, etc., points, as shown in Fig. 4(*c*), give the corresponding relationships, and the solution follows the same procedure as with uniform flow cutoff. The pressure rises very slowly until the valve begins to

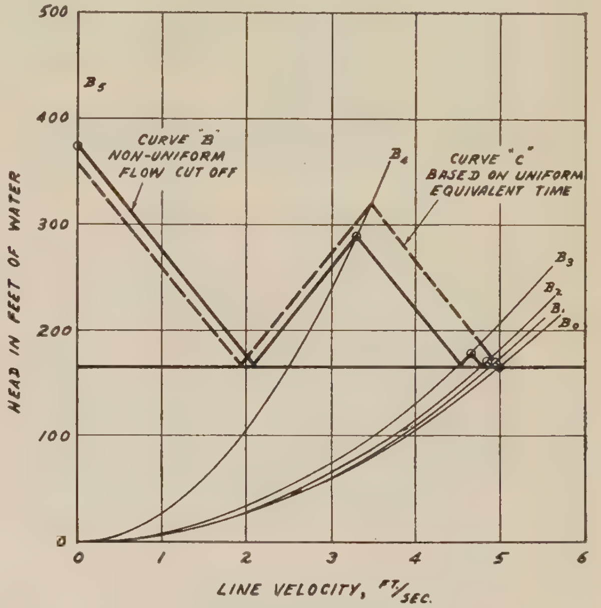

FIG. 4(*c*) GRAPHICAL SOLUTION FOR NONUNIFORM VARIATION OF VELOCITY WITH RESPECT TO TIME, CURVE B, FIG. 4(*a*) AND CURVE C (EQUIVALENT TIME)

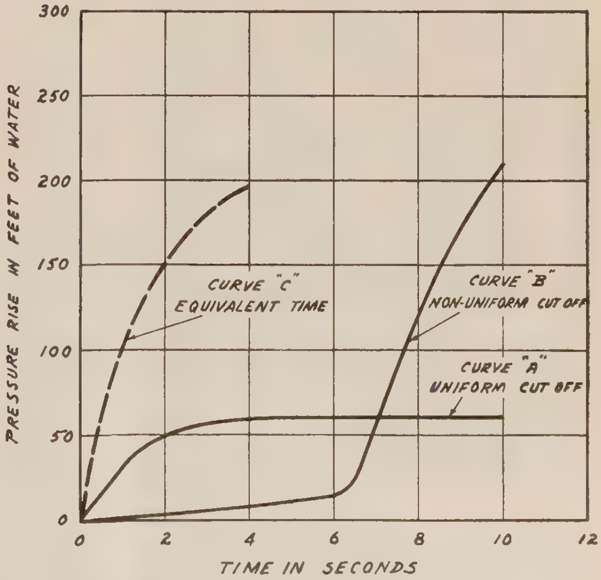

FIG. 4(*d*) PRESSURE-TIME CURVES FOR FIGS. (4*a*), (4*b*), AND (4*c*) cut off flow, then after three intervals of time the pressure rise is very much greater than it would have been if the flow rate had been cut off uniformly throughout the whole stroke.

Fig. 4(*d*) shows the difference in pressure-time curves for these two cases. The rise above normal for nonuniform cutoff, curve B, is about 210 ft, as compared with 60 ft for uniform closure, or $3^1/_2$ times as great. Such differences can explain many pipe-line failures.

In the water-works and hydroelectric fields, a reasonably valid short cut is used to approximate the effect of nonuniform flow-rate cutoff. Since it is the maximum rate of change of flow that determines the maximum rise in pressure, a line tangent to this maximum cutoff rate can be drawn, curve C, Fig. 4(*a*), and a so-called "equivalent time" is secured.

In the present case the equivalent uniform rate would be two intervals of time rather than five. The dash line in Figs. 4(*c*), and (*d*) give the graphical solution of this case. A rise above normal of 195 ft results, as compared with 210 by the more precise method, in an error of only 7 per cent, as compared with 250 per cent by the assumption of curve A.

Using this so-called short cut, the required total time of travel to limit surge pressures to permissible maximum values can be obtained.

Effect of Initial Valve Opening

It is also interesting at this time to analyze the effect of the initial starting point of valve closure upon the magnitude of surge pressures obtained.

Closure from some intermediate point down to zero may give a much higher surge value than closing at the same uniform rate from the wide-open valve position down to zero. Fig. 5(*a*) shows, for the same example (Fig. 4, curve A), the graphical solution which indicates this relationship. It will be seen that higher surge pressures result when closure is initiated from 60 per cent or from 20 per cent flow rates than when full flow is interrupted. Fig. 5(*b*) gives the pressure-time curves and shows the change in wave shape as well.

When the closing rate is greater than $2L/a$ sec, there will be some intermediate point from which the valve can be closed to zero in exactly $2L/a$ sec, and this will result in instantaneous water hammer for that smaller flow. Nonuniform valve operation can aggravate this effect.

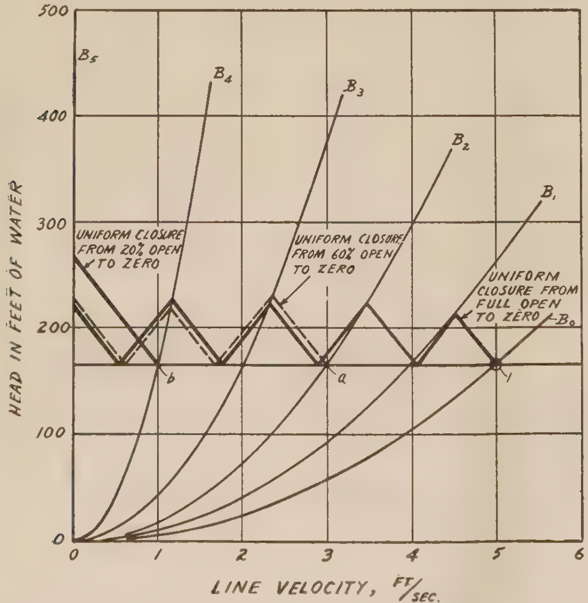

Fig. 5(*a*) Graphical Solution for Uniform Variation of Velocity With Respect to Time, Curve A, Fig. 4(*a*), With Different Initial Valve Positions

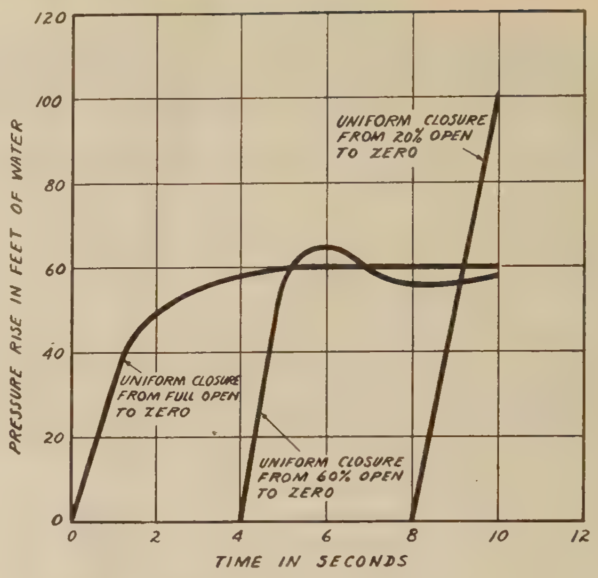

Fig. 5(*b*) Pressure-Time Curves for Fig. 5(*a*)

Variation in Surge Pressure Along Conduit

It is interesting to note the variation in wave form at the control gate and at intermediate points along the pipe line for different rates of closure. If closure is made instantaneously, then aside from any natural damping of the wave due to internal friction, compressibility of the fluid, or expansion of the pipe walls, this wave will travel undiminished from control valve to the point of origin of flow and the distribution of pressure along the line will be *ABFC*.

If the closure is in $2L/a$ sec or over, the surge pressure will diminish uniformly between the control valve and the point of origin of flow and will appear as shown in Fig. 6, as line (*ABD*).

If the closure is made at some intermediate time, between zero and one interval of $2L/a$, the wave will travel undiminished up the line a distance *BF* corresponding to the proportion of time that the closure is less than time $2L/a$ sec, and from that point (*F*)

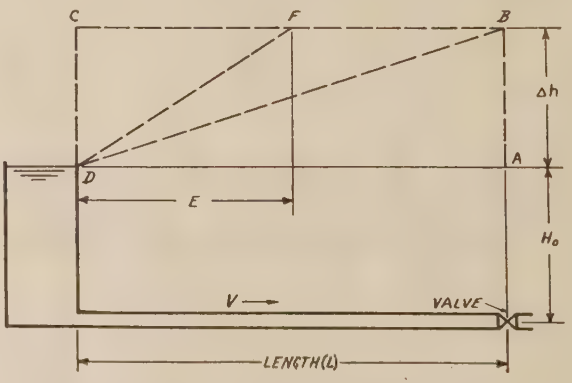

Fig. 6 Distribution of Surge Wave Along Pipe Line When

Time $(T) = 0$, Line $\overline{ABC}$

Time $(T) = \dfrac{2L}{a}$, Line $\overline{ABD}$

Time $(T) > 0 < \dfrac{2L}{a}$, Line $\overline{ABFD}$, with $E = \dfrac{Ta}{2}$

will gradually diminish to zero at the point of origin of flow *ABFD*.

Comparative tests have been made to measure this characteristic and demonstrate very clearly that surge waves, resulting from closures greater than $2L/a$ sec, diminished uniformly in proportion to the distance from control valve to the point of origin of flow.

These same conclusions can be arrived at from an analysis of the graphical solution of the conditions at the control valve by taking intermediate increments of valve movement and tracing through the wave pattern step by step. It is necessary to have the number of increments of valve movement in proportion to the distance from the control gate to the intermediate point where it is desired to investigate pressure variations.

EFFECT OF CENTRIFUGAL PUMPS

It is also possible with the graphical method to take into account centrifugal-pump characteristics, as shown in Fig. 7.

If the head-velocity curves of a centrifugal pump are superimposed on the graphical diagram, a new series of steady-state operation points results. The line friction also can be indicated, and throttling-valve or control-valve characteristics added if desired.

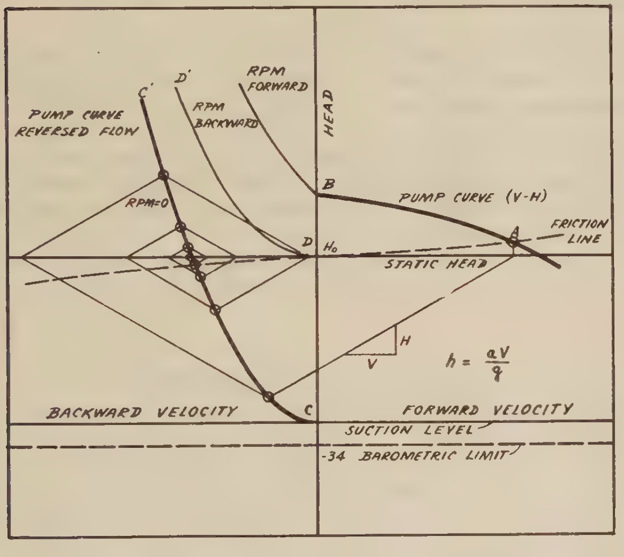

FIG. 7 GRAPHICAL SURGE DIAGRAM FOR PUMPING SYSTEM WITHOUT VALVE

If an analysis is needed of the surge conditions following the power failure to a motor-driven centrifugal pump, the usual sloped lines, showing the transient surge-wave relationship can be drawn, and the step-by-step variation in velocity and pressure determined.

If the flywheel effect of the rotating element of the pump and motor is known, the average pressure can be estimated over given time increments, and the approximate increments of speed reduction for each interval of time computed. The new speeds at such time intervals can be used to secure a head-velocity characteristic of the pump at each of those times.

The successive computations will give the "run-down time" of the pump, and a fairly complete record of what occurs under such conditions. The example in Fig. 7 is based upon a typical water-works installation where the pipe friction was small as compared to the normal operating pressure. It was also assumed that no check valve was present, and the pump was allowed to reverse its rotation.

COMPLETE CHARACTERISTICS OF PUMPS

As an added refinement in complex surge studies, the complete characteristics of centrifugal pumps can be considered. This is important if slow-closing check valves or control valves are to be used. Tests have been made and the results published by R. T. Knapp (11) and others, giving the head, flow, and torque curves at various speeds of pump rotation, both forward and in reverse.

In the example, Fig. 7, two such curves of head-velocity are shown, *CC'*, for backward flow with the rotor stopped, and *DD'* for backward flow with the pump rotating at full speed in the reverse direction. There will be intermediate points between these curves and the full-speed-forward curve which permit the calculation of the speed of the pump and the surge pressures until the system reaches a point of stability and the speed of the pump stays constant.

ANALYSIS OF A PUMPING SYSTEM WITH IRREGULAR PROFILE

It is possible also in these graphical diagrams to determine the pressures at any intermediate point on the line and evaluate the effect of pipe-line profile. In some instances this may prove to be a critical factor. Where the line is level and both the inlet and outlet are at the same elevation as the pumps, the problem is less complex.

When pumping down hill, the liquid column may "run away" from a closed valve, leaving a vapor pocket, which must be refilled at a safe rate to avoid sudden surges when the pumps are restarted and the oncoming liquid column meets the column at rest.

When pumping uphill, the liquid column may come to rest and reverse rapidly, causing the pumps to run backward at a high rate of speed. Check valves can be slammed shut under such conditions and heavy surges experienced.

In some cases a variable gradient is followed where high points in the line may become critical. If a down surge, following pump failure, passes such a point, the internal pressure could be reduced far below the vapor pressure of the fluid and the liquid column would part. Upon rejoining, the two sections may have their relative velocities changed abruptly and a severe surge can result.

It may be of interest to follow one such complete study which had this further variable included, namely, the parting and rejoining of the water column in the discharge line of the pump, upon emergency trip-out or loss of driving power.

The general layout of the conduit is shown in Fig. 8(*a*), together with its characteristic of length, diameter, and velocity. A master diagram was prepared, showing the characteristics of the hydraulic system, including the operation of one, two, or three pumps simultaneously, with and without check valves.

The point at which the column parted and rejoined was approximately one eighth of the distance from the pump house to the discharge basin, and intervals of time equal to one eighth of $2L/a$ sec were utilized in analyzing this diagram.

Fig. 8(*b*) shows the conditions with two pumps tripped out and very gradual check-valve closure. The slowing down and reversal of the pump with the approximate steady-state conditions with the pump operating backward are all shown. The check-valve closure was at a rate sufficiently slow to keep from cutting off the backward flow abruptly and causing the pressure to exceed a predetermined value.

At a point of about 1500 ft beyond the pump house, the subnormal pressure fell below the barometric limit, and the water column parted at this point, the upper portion gradually slowed down, coming to rest and reversing, while the lower portion of the

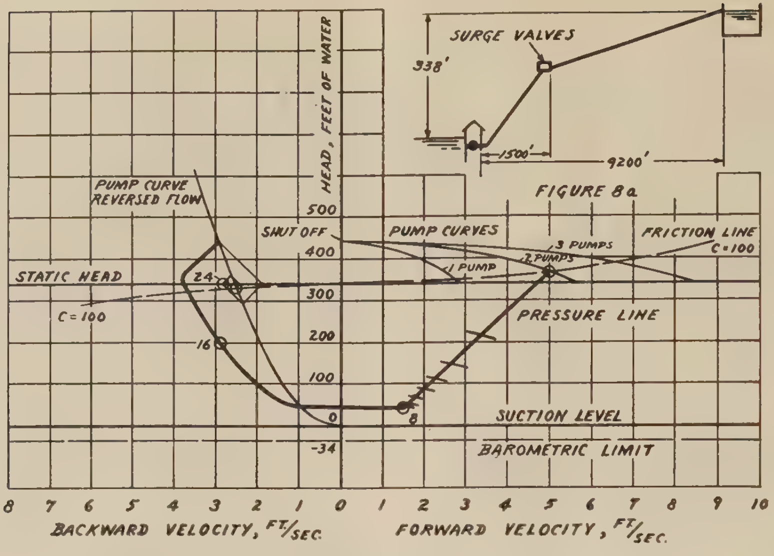

Figs. 8 (*a*) (*b*) Graphical Analysis, Long Lac Pipe Line
(9200 ft long, 36-in-diam pipe, two pumps tripped out, no check valve in operation.)

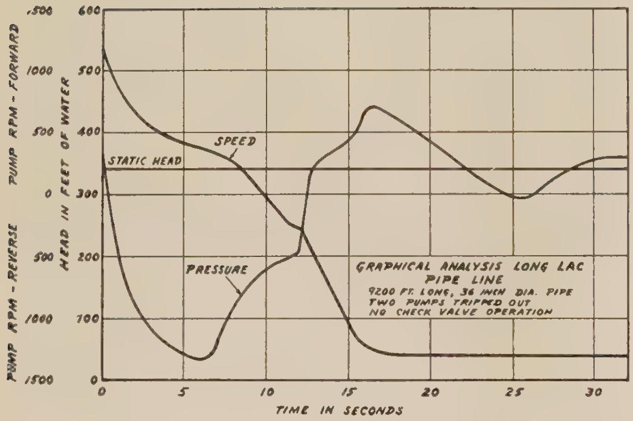

Fig. 8(*c*) Pressure-Time Diagram for Long Lac Pipe Line

column continued to flow back through the pump after having reversed at a much more rapid rate. The upper column gradually picked up momentum and rejoined the lower column, resulting in an instantaneous surge pressure which was much greater than that due to check-valve closure. A resultant surge pressure, upon rejoining the water column, of about 250 lb above normal would be experienced if no remedial devices were installed.

On this installation, some quick-opening, slow-closing air valves were utilized at the crest of the hill, to admit air to act as a cushion to slow up the rate at which the two columns were rejoining.

An analysis in advance of design indicated that a surge pressure of about 70 psi would be experienced and would be within a safe limit of design based on the stress in the thin-wall pipe. The actual tests made in the field, when one pump was tripped-off, showed a surge pressure of 65 psi. While only the operating gages were available for this check test, such readings as were secured indicated an extremely close agreement between the theoretical design values obtained nearly a year previously, and the actual test values recorded under service conditions.

Basic Relations

It may be well at this point to restate a few of the fundamental relationships in surge-wave theory which determine the magnitude of the pressure rise and its distribution along a conduit. These comments relate to gravity flow or discharge lines from centrifugal pumps only.

1 The pressure rise for instantaneous closure is directly proportional to the fluid-velocity (V) cutoff, to the magnitude of the surge-wave velocity (a), and is independent of the length of the conduit. Its value is

$$h = aV/g \text{ ft of water}$$

or

$$p = aWV/144g = (a/g)\ (\text{sp gr}/2.3)\ V \text{ psi}$$

where

$$a = 12 \Bigg/ \sqrt{\frac{W}{g}\left(\frac{1}{k} + \frac{d}{Ee}\right)} \text{ fps}$$

and

$2L/a$ = critical time of conduit, sec
T = closing time, sec
N = number of intervals of $2L/a$ for closing time T
L = length of conduit, ft
h = pressure rise above normal, ft of water
p = pressure rise above normal, psi
V = velocity of flow, fps
W = weight per cu ft of fluid, lb
sp gr = specific gravity of fluid (water = 1.0)
k = bulk modulus of compressibility of liquid, psi
E = Young's modulus of pipe-wall material, psi
d = inside diam of conduit, in.
e = thickness of conduit wall, in.
g = acceleration due to gravity (32.2 fps per sec)

2 When the flow rate is changed in a time greater than zero but less than or equal to $2L/a$ sec, the magnitude of the pressure rise is the same as with instantaneous closure, but the duration of the maximum value decreases as the time of closure approaches $2L/a$ sec.

3 Under the conditions in paragraph 2, the pressure distribution along the pipe line varies as the time of closure varies. The

pressure decreases uniformly along the line if closure is in $2L/a$ sec. The maximum pressure at the control valve exists the full length of the line with instantaneous closure, and for slower rates travels up the pipe a distance equal to $(L\text{-}Ta/2)$ ft, then decreases uniformly.

4 The surge-pressure distribution along the conduit is independent of the profile or ground contour of the line so long as the total pressure remains above the vapor pressure of the fluid.

5 For closing times greater than $2L/a$ sec, the maximum pressure rise will be a function of the maximum rate of change in flow with respect to time (dv/dt).

6 Nonlinear closures can be investigated, and the proper valve timing determined to hold the maximum pressure rise to any desired limiting value.

7 The effect of centrifugal pumps and quick-closing check valves or control valves can be investigated using the graphical method of analysis.

8 The profile of the conduit leading away from a pumping station may have a major influence upon the surge conditions. The minimum effect will be found when the line is level, the maximum when the line is steep, or when high points occur along the line.

9 Parting and rejoining of the liquid column can produce extremely high pressures and may cause failure of the conduit.

10 The effect of friction can be accounted for graphically in any surge problem, and, when such losses are less than 5 per cent of the normal static or working pressure usually can be neglected.

11 The greater the degree of accuracy desired for the results of a surge analysis, the more must be known about the various hydraulic and physical characteristics of the system.

12 The agreement between theoretical analyses and actual field-test results has confirmed the accuracy of the elastic-wave theory in water conduits.

3 APPLICATION TO PETROLEUM SYSTEMS

With this broad knowledge and practice of surge-wave theory applied to water conduits, it has been possible to design projects with complete assurance that the limit set for maximum pressure rise will not be exceeded in actual operation. Behavior under emergency conditions can be predicted, and remedial or alleviating devices utilized to protect the installation.

How, then, can this broad base of knowledge be applied to petroleum pipe lines and their associated apparatus?

1 In either case, there exists a basic physical-hydraulic-mechanical system subject to analysis by the elastic-wave theory.

2 The differences in behavior between dissimilar fluids in the same mechanical system can be accounted for by the differences in the physical properties of the fluids themselves.

3 There may be differing requirements in handling certain fluids as compared with others. This does not represent a departure from established fundamental theory, but merely places limitations on the design of the installations.

By examining the things that are the same in both systems it is possible to select the few factors that are different and concentrate our attention upon them.

The pipe itself, the thickness, diameter, and material of construction, its length, the profile of the country through which it passes, the branches, dead ends, parallel conduits, all these are unchanged by the fluid within a given system.

Centrifugal pumps, differing slightly in details of construction, but driven by electric motors as they are in water systems do not introduce new factors as between oil and water, nor do they control valves, check valves, shutoff valves, relief valves, or other auxiliary devices for regulating flow.

The only basic difference between water systems and petroleum systems is the fluid itself, and possibly the trend today toward lowered factors of safety in crude-oil pipe-line designs, as compared with water-supply systems.

The velocity of the pressure wave a, is a fundamental factor in any surge study, as the surge pressures are directly proportional to its value. The velocity of surge wave is dependent upon the diameter, thickness, material of the pipe walls, and the density and compressibility of the fluid in the pipe.

Our knowledge concerning the physical characteristics of the pipe material is fairly complete. Young's modulus for steel lines can be taken at 30,000,000 psi as an average between 29,000,000 to 31,000,000 psi. If the ratio of diameter to thickness is known, it is necessary to know only the density and the compressibility of the liquid within the pipe to determine the value of a.

Within the range of ordinary operating temperature for water, 32 to 100 F, and for pressures from 0 to 1000 psi, the specific gravity can be taken at 1.00.

In the same range the modulus of compressibility or "bulk modulus" has been measured and checked by field tests to be approximately 300,000 psi with a variation of plus or minus 3 per cent.

For other pipe-wall materials, cast iron, asbestos cement, or concrete, the physical factors are sufficiently well known that a chart, Fig. 9, can be used to determine the value of a when the inside diameter and wall thickness are known.

For crude oil the variations in density and compressibility are greater than with water. Composition of the crude varies from field to field, and the presence of more or less of the highly volatile components may change these two factors at standard conditions.

It is important to know just how these factors vary with pressure and temperature in the ranges encountered in pipe-line pumping, so that such variations can be accounted for in surge investigations. A variation in the bulk modulus will vary the velocity of the pressure wave and thus change the surge intensity by an appreciable amount.

Fig. 10 has been prepared to show the change in surge-wave velocity for different values of specific gravity and compressibility. The range of values has been taken to cover as fully as possible all commonly known crudes.

In a proposed installation it was found that there could be as much as 10 per cent variation in surge-wave velocity due only to variations in compressibility between the terminal pressure at the suction of one pumping unit, as compared with the initial pressure in the discharge of the station.

Where fluid temperatures also vary between pumping stations or between seasons, an additional correction may be necessary, if the value of the surge-wave intensities is to be determined within limits of 2 per cent.

If the limits are not closer than 10 per cent of the actual surge magnitude, then this refinement may be eliminated, and an average surge-wave velocity may be utilized for a given installation.

Where accuracy is needed in determining surge pressures, it is highly desirable to obtain a sample of crude and make a compressibility determination at several different temperatures throughout the range of pressures which may be experienced. Published literature references now available are not dependable for bulk modulus values as applied to surge studies.

It is obvious that the greater the compressibility of a given fluid the more damping effect there will be present and hence the more rapid dying away of the after waves and the lowering of the maximum surge pressures.

When pumping refined products, similar data are needed and the problem is rendered more complex when several different

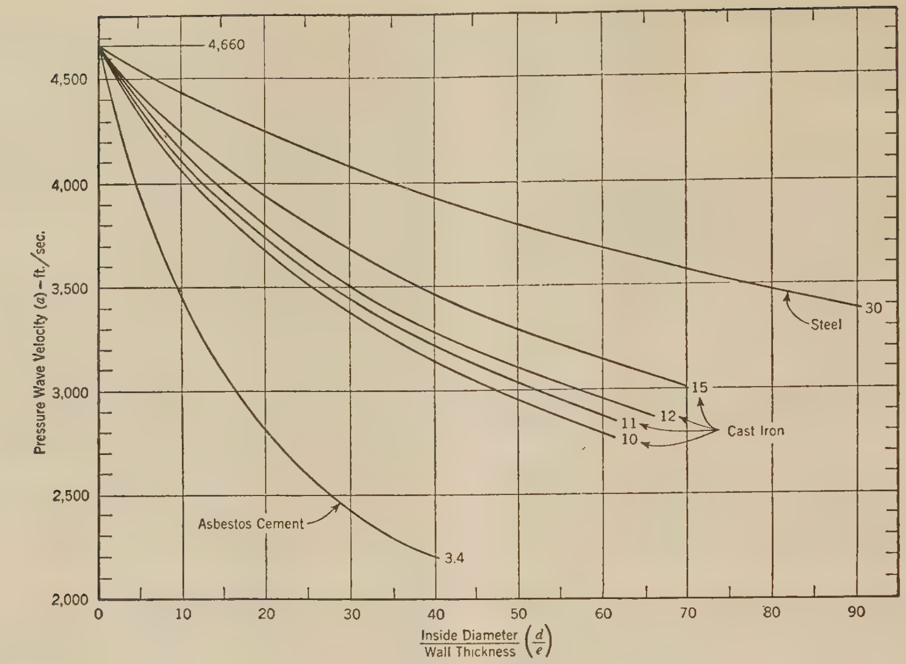

FIG. 9 SURGE-WAVE VELOCITY CHART FOR WATER

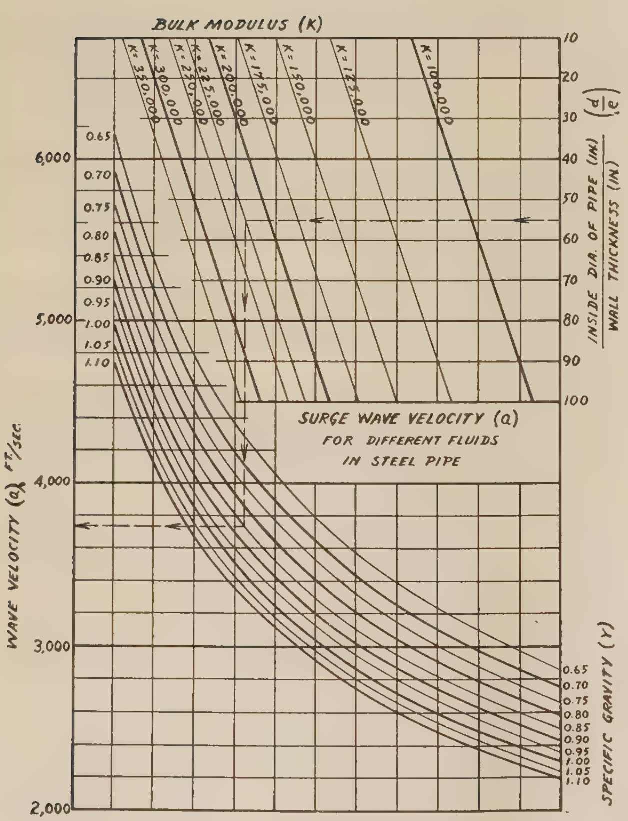

FIG. 10 SURGE-WAVE VELOCITY FOR DIFFERENT FLUIDS IN STEEL PIPE

products are in a given line at one time. The interfaces probably will act as points of partial reflection, in a manner similar to a change in diameter or thickness of the pipe wall.

Once these physical characteristics of the fluid have been determined, the solution of any surge problem (exclusive of positive-displacement pumping), can be obtained by the proper application of the elastic-surge-wave theory developed for water problems.

POSITIVE-DISPLACEMENT PUMPING

The analysis of surges occurring in positive-displacement pumping of fluids has been described in great detail in the classic work of Diederichs and Pomeroy (15), presented before the Petroleum Division in 1929. In 1936 DeJuhasz published two excellent papers (16, 17), extending such analyses to the injection systems of Diesel engines using graphical methods.

In the Diesel-engine field it is well known that the degree of compressibility of Diesel fuel oils will have an effect on the performance of the engine. As the fuel pumps force the liquid into the engine, they store up energy within the system and the pressure wave is slightly delayed in reaching the spray nozzle. When the fuel pump stops delivering oil, this locked-up energy is dissipated, causing the spray nozzle to continue to discharge for a relatively short period of time after the fuel flow is supposed to be cut off.

Analyses have been made using the elastic-wave theory to establish adjustments in the crank-angle setting for fuel injection in the cylinders which are remote from the fuel pumps. Improved performance has resulted from this timing adjustment as it compensates for the surge effect within the fuel lines and makes the torque applied to the crankshaft more uniform.

With positive-displacement pumps on petroleum pipe-line service, harmonic surges can be set up if the impulses from the individual cylinders of two or more pumps get into step with each other. Still another factor enters, namely, the design of station piping and the arrangement of headers, manifolds, branch pipes, and dead ends which may have natural periods of surge-wave oscillations and could aggravate further any "in-step" harmonics between pumping units.

The magnitude of such harmonic surges can be many times the value calculated from the mere starting and stopping of a liquid column by a control valve.

General solutions for the problem have not been too successful, and more detailed studies are usually required to arrive at a means of correcting harmonic surges.

Joint Surge Conference

In connection with the design of large crude-oil pipe lines for the Middle East, and in the United States and elsewhere, it was felt necessary to acquire a more thorough knowledge of the pressure surges that might be experienced.

Since several large lines are now under construction, or are in the design stage, a Joint Surge Conference was organized in October, 1948, to make investigations, conduct field tests, and prepare reports on the subject. The major program has been completed and will doubtless be reported upon in greater detail at other technical meetings in the near future.

Some very interesting results were obtained which can be mentioned briefly. Three sets of field tests were carried on as follows:

(*a*) Gravity series to check the fundamental correlation between so-called "water-hammer" theories and the actual behavior of crude oil in a pipe line, under field conditions where friction was less than 15 per cent of the static pressure.

(*b*) Gravity and pumping series in an actual operating line, some 20 miles long, where friction amounted to 80 to 90 per cent of the pressure available.

(*c*) Operating tests of 50 odd miles of products line, under normal and emergency starting and stopping of the pumping units when operating as a closed system.

It was found that, in every case, the field-test results checked closely with theoretical studies, using the elastic-wave theory and taking into account the differences in bulk modulus and specific gravity of the particular oil or refined product in the line at the time of the test.

There was complete confirmation of the elastic-wave theory as applied to petroleum lines.

Conclusions

As has been found in the water-supply and hydroelectric field over a period of many years, there is no simple quick and easy formula to solve surge problems. Surge conditions can be calculated and predicted during the design stage of a project by proper application of the elastic-wave theory using the graphical method.

The results obtained have been well worth the time and expense of making such analyses, and the practice is increasing in the water-supply and hydroelectric fields of carrying out detailed studies on surges for any proposed installation before construction starts.

As the knowledge of surge-wave theory of "liquid" hammer becomes more widely disseminated in the petroleum-pipe-line field, then, as in the water field, it will be used more and more with assurance. Designs can be based on more accurate advance knowledge of surge conditions, and better designs always lead to better performance of the finished project.

BIBLIOGRAPHY

1 "Report of Committee on Water Hammer," Symposium on Water Hammer, ASME, vol. 55, 1933 (republished 1949), pp. 3–24.

2 "Water Hammer," by Olga Simin, Proceedings of the American Water Works Association, 1904, pp. 336–424.

3 'Theory of Water Hammer," by Lorenzo Allievi, translated by Eugene E. Halmos, 1925, distributed by the ASME.

4 "High Head Penstock Design," by A. W. K. Billings, O. H. Dodkin, A. Santos, Jr., and F. Knapp, Symposium on Water Hammer, published by ASME, 1933 (republished 1949), pp. 29–61.

5 "Simplified Derivation of Water-Hammer Formula," by L. F. Moody, Symposium on Water Hammer, published by ASME, 1933, pp. 25–28 and reprinted, 1949, pp. 1–152.

6 "Computation of Water-Hammer Pressures in Compound Pipes," by R. E. Glover, Symposium on Water Hammer, published by ASME, 1933, pp. 64–71.

7 Ibid., discussion F. Knapp, pp. 128–133.

8 Ibid., discussion E. B. Strowger, pp. 133–139.

9 "Surge Control in Centrifugal Pump Discharge Lines," by R. S. Quick, Symposium on Water Hammer, published by ASME, 1933, pp. 81–83.

10 "Water-Hammer Tests in Croton Lake Pumping Plant," by S. L. Kerr, Symposium on Water Hammer, published by ASME, 1933, pp. 84–87.

11 "Complete Characteristics of Centrifugal Pumps and Their Use in the Prediction of Transient Behavior," by R. T. Knapp, Trans. ASME, vol. 59, 1937, pp. 683–689.

12 "Water Hammer in Pipes, Including Those Supplied by Centrifugal Pumps; Graphical Treatment," by R. W. Angus, Proceedings of The Institution of Mechanical Engineers, London, England, vol. 136, 1937, pp. 245–291.

13 "Methods of Calculating Water-Hammer Pressures," by F. M. Dawson and A. A. Kalinske, *Journal, AWWA*, vol. 31, November, 1939, pp. 1835–1864.

14 "Elements of Graphical Solution of Water-Hammer Problems in Centrifugal-Pump Systems," by A. J. Stepanoff, Trans. ASME, vol. 71, 1949, pp. 515–534.

15 "The Occurrence and Elimination of Surge or Oscillating Pressures in Discharge Lines From Reciprocating Pumps," by H. Diederichs and W. D. Pomeroy, Trans. ASME, vol. 51, 1929, PET-51-2, pp. 9–49.

16 "Graphical Analysis of Transient Phenomena in Linear Flow," by K. J. DeJuhasz, *Journal of The Franklin Institute*, vol. 223, 1937, pp. 463–493, 643–654 and 751–778.

17 "Hydraulic Phenomena in Fuel-Injection Systems for Diesel Engines," by K. J. DeJuhasz, Trans. ASME, vol. 59, 1937, pp. 669–677.

Discussion

F. M. Van Deventer.[4] The author has described one hydraulic line which was periodically shut off by the manual operation of a valve. During this operation an expansion joint failed on several occasions, and this despite his instructions to spread the closing operation over a 5-min interval. His investigation disclosed the fact that, although the full time was used, the operator had divided the time into ten $^1/_2$-min periods. He then rotated the valve handwheel one tenth of full travel every 30 sec. It

---

[4] Assistant Chief Engineer, Walworth Company, Inc., New York, N. Y. Mem. ASME.

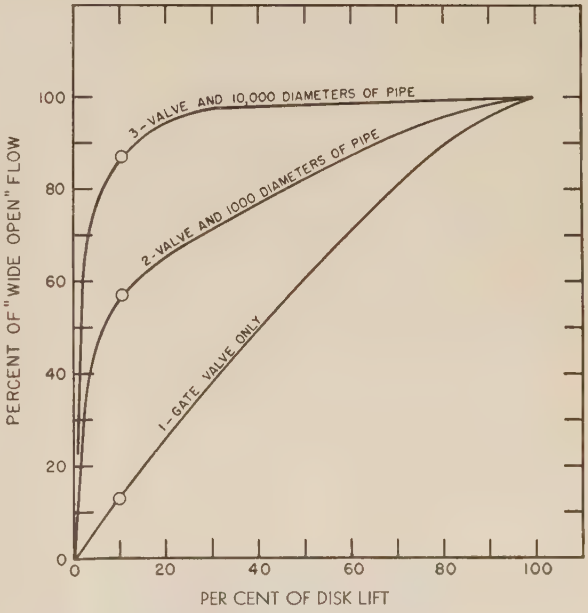

Fig. 11 Curves of Per Cent of Wide-Open Flow Plotted Against Per Cent of Disk Lift

was observed that the joint failed during the final increment of stem travel. Gradual and continuous closing eliminated the trouble.

It seems appropriate to present here an interpretation of valve-closing characteristics, often overlooked, and which may explain the experience reported by the author.

Fig. 11, herewith, presents three curves of per cent of wide-open flow plotted against per cent of disk lift.

Curve 1 represents a typical gate valve with a round disk sliding over a round port. The valve is attached directly to the reservoir, has free discharge, and hence functions as a variable orifice. The characteristic approximates a straight line; hence uniform disk travel during the closing operation would be accompanied by a nearly uniform velocity decrease.

Now, if a length of pipe equal to 1000 or 10,000 pipe diam be connected to the discharge side of the valve, then the flow characteristic will be determined by the resistance of the valve and pipe as a system, rather than by the restraining influence of the valve alone.

Curves 2 and 3 represent those conditions.

Referring to curve 3, it will be noted that if the valve disk be moved 90 per cent of its closing travel, the flow will still be at about 86 per cent of wide-open capacity. (Compares to 14 per cent for valve without pipe.) In this case, most of the flow control takes place during the last small increment of stem travel.

The obvious conclusion is that either manual or mechanical control of valves should be scheduled so as to reduce the rate of stem travel gradually as the closed position is approached. The extent to which this adjustment should be applied will depend upon the characteristic of the pipe and conduit considered as a whole.

AUTHOR'S CLOSURE

Mr. Van Deventer has raised a most interesting question concerning the relative effect of valve operation when controlling flow in long conduits. These factors can be related with reasonable accuracy by using a calibration of the valve where the pressure drop and discharge capacity at various positions of the valve, from wide open to closed position, has been established. It is possible to co-ordinate this data with the friction factor of the lines being controlled and thus secure the net effect of the valve. This will then give the rates at which flow is cut off as the valve travels through its stroke.

It would appear from Fig. 11 that the gate valve acting alone showed almost a uniform rate of change of flow, which is rarely found in any control valve. The normal characteristics of a gate valve operating at free discharge or in a pipe line usually looks more like curve *B* in Fig. 4*a* in the author's paper. The same comment would apply to some degree to the curve in Fig. 11 with the valve in combination with various lengths of pipe. It would be interesting to know whether the curves in this illustration were developed from actual tests or whether it was assumed that flow varied uniformly with the area through the valve, neglecting changes in the discharge coefficient.

Pressure Losses in Tubing, Pipe, and Fittings

By R. J. S. PIGOTT,[1] PITTSBURGH, PA.

This paper is a continuation of the second half of the problem involved in the writer's 1933 paper on pipe flow and Prof. Lewis F. Moody's 1944 paper. The pipe-flow situation is shown to be in satisfactory condition; the main attention is on bends and fittings.

It has been customary in the past to rate the losses in bends and fittings as a function of velocity head. Another old method, less used, was to rate the loss in equivalent length of pipe. In the case of bends and fittings two types of loss are superposed, i.e., skin friction or pipe-loss type, and bend loss. The methods of test are less accurate than for pipe as they involve getting the difference between two much larger readings. Consequently the test data are much poorer than for pipe, for several reasons: one given above; another that the pipe fittings are not geometrically similar; and the test data are very much less than those on pipe. It seems clear that a rational formulation, however, could be attempted if we can establish some picture of the factors involved in the losses. Up to the present time bend and fitting losses have been taken from a range of factors unconnected with size, roughness, or velocity of flow. This formulation, on the basis of the tests, endeavors to show that there is a true bend loss for smooth fittings underlying the superposed losses due to roughness and Reynolds number. The final formulation involves an evaluation of the true bend loss and an evaluation of the roughness and Reynolds number effects paralleling the friction factor in pipe. The final conclusion is that the equivalent pipe length is by all means the most reliable and convenient method of tabulating losses in different kinds of fittings and bends. The final formulation is $\zeta = \zeta_1 + \zeta_2 = 0.106 \left(\frac{r}{d}\right)^{-2.5} + 2000f^{2.5}$. This formulation has been checked against the test results and while it is obvious that the factors will be both plus and minus over a considerable range, the general correlation of the test data appear to be as good as our present test information will permit.

SINCE Osborne Reynolds' development of the Reynolds criterion $dv\rho/\mu$, a great variety of empirical and limited-range formulations for the variation of pressure drop with flow rate continued in use because the effect of surface roughness is not covered in *Rn*. In 1931 and 1932, the author and Dr. Emory Kemler undertook analysis of all published data on flow test of water, oil, air, and steam, the results of which were published by Dr. Kemler (1)[2] in 1933. This study was the groundwork on which the author's hypothesis that roughness had the same effect as reduction of diameter was based (2).

Since 1933 this formulation of friction factor has received rather general adoption, and there is now ample proof of its advantages and much more general application over the earlier formulations. For example, extensive tests on commercial crude-oil pipe lines by W. B. Heltzel (Stanolind) and by Standard Oil of New Jersey, 6-in. to 12-in. sizes, and tests on gasoline in drawn aluminum tubing by CRC (Dr. O. C. Bridgeman, Bureau of Standards) both corroborate the corresponding curves in the formulation.

In 1944 Prof. Lewis F. Moody made a further valuable improvement (3). By the use of the Colebrook equations (4), he established smooth curves for f versus *Rn* for each relative roughness, and also confirmed the important fact that at some Reynolds number for each relative roughness, the friction factor ceased to vary with *Rn* and became a constant. This condition had been uncovered 30 or more years ago by Prof. W. S. Pardoe to be the case for Venturi-meter coefficients. Since the reduction of coefficient from a value of 1.00 in a properly designed Venturi is due to skin friction, it acts like a pipe, and the evidence of hundreds of highly accurate Venturi tests is that for each size and roughness, at some Reynolds number and above, the coefficient becomes constant. A similar behavior is also found for long-radius nozzles (ASME Special Research Committee on Fluid Meters).

The formulas for pipe flow are given again in the following:

Viscous or laminar flow

$$\text{Round pipes, } \Delta p = \frac{0.00691\ \mu l v}{d^2} \qquad [1]$$

For pipes or conduits not circular, the following formula for shapes where the maximum diameter is not more than 25 per cent greater than minimum diameter, is

$$\text{Approximately circular or rectangular } \Delta p = \frac{0.000432\ \mu l v}{M^2} \qquad [2]$$

For shapes greatly different from circles or squares, such as capillary slits or bearing clearances, it has been demonstrated by J. M. Cunningham that Equation [2] is not exact; in fact, for the capillary slit, such as a bearing clearance, the value of Δp correctly calculated, is just 1.5 Δp calculated by Equation [2].

Viscous flow, that is, flow below the critical velocity where $Rn = 1200$ to 2500, is likely to be found in heavy crude-oil pipe lines, most oil lines between oil tank and engine, internal lubrication passages such as drilled crankshafts, oil galleries, drilled connecting rods, and all bearing clearances. It will also be found in drill pipe and hole when handling mud in oil-well drilling, in cement slurries, and heavy sewage.

Turbulent flow will be found in practically all cases involving water, air, natural and manufactured gas, and steam.

Turbulent flow, $Rn > 2500$

$$\text{Round pipes } \Delta p = \frac{0.000108\ fl\rho v^2}{d} \qquad [3]$$

$$\text{Other shapes } \Delta p = \frac{0.000027\ fl\rho v^2}{M} \qquad [4]$$

In the case of turbulent flow, there is no limitation on Equation [4] as to shape, and the mean hydraulic radius is a fully satisfactory criterion which was not the case in viscous flow.

---

[1] Chief Engineer, Gulf Research and Development Company. Fellow ASME.

[2] Numbers in parentheses refer to the Bibliography at the end of the paper.

Contributed by the Petroleum Division and presented at the Petroleum Mechanical Engineering Conference, Oklahoma City, Okla., October 2–5, 1949, of THE AMERICAN SOCIETY OF MECHANICAL ENGINEERS.

NOTE: Statements and opinions advanced in papers are to be understood as individual expressions of their authors and not those of the Society. Paper No. 49—PET-22.

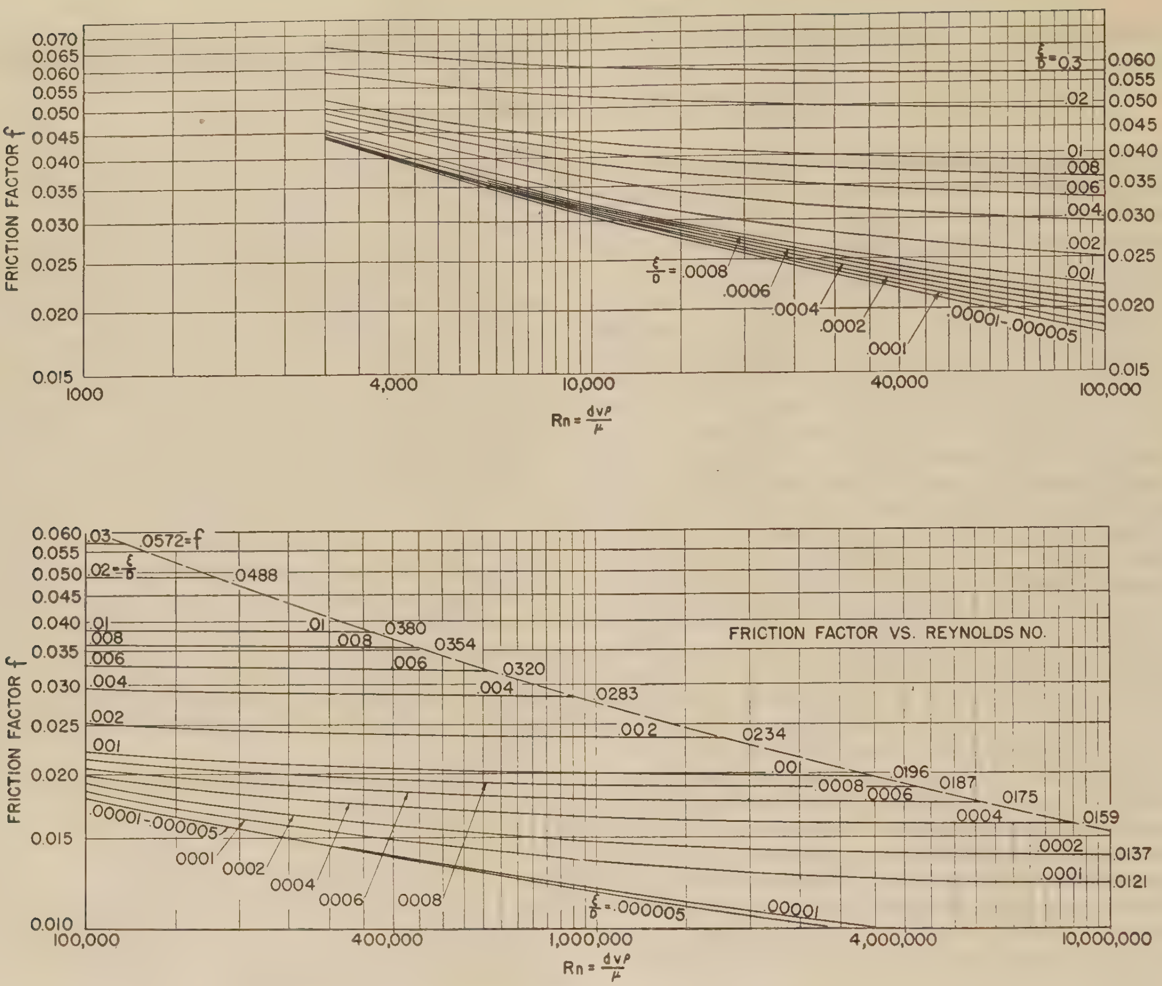

FIG. 1

Professor Moody's plot of f versus Rn was arranged with different log scales for f and Rn; this gives a convenient sized plot for compactness, but the f lines at each value of ϵ/r are quite sharply curved. The original-type plot, Fig. 1, with equal coordinates gives no higher accuracy, but the f lines are so nearly straight over large ranges that generally the whole range of flow likely to be of interest in any particular case can be conveniently predicted by the relation

$$\Delta p \propto v^{2-n} \quad \text{[5]}$$

where n is the slope of the f line for the particular roughness. This procedure offers the convenience that only one flow rate need be calculated by Equation [2]; all other values may be obtained from this value by using Relation [5]. Table 1 gives the roughness for the commonly used materials.

It is of interest to note that, within the ordinary design range, the values in the author's 1933 plot and Professor Moody's 1944 improved plot do not differ over ±2.5 per cent, and this is well within the limits of accuracy even for smooth pipe (±5 per cent). Our selection of ϵ/d for the rougher pipes such as old cast-iron, concrete, or riveted pipe is open to still wider errors.

We have for the past decade been in a satisfactory position in so far as calculating pipe friction with sufficient accuracy is concerned; but the other half of the task, the losses in bends and pipe fittings, has hitherto not been covered in any consistent manner.

TABLE 1 RELATIVE ROUGHNESS ϵ/d

	Brass and Tubing	Galv. Air Duct	Steel Pipe	Asphalted Cast Iron	Galv. Steel	Cast Iron	Concrete Smooth	Concrete Average
1/2	.000107		.0032		.0120	.0204		
3/4	.000076		.0022		.0080	.0136		
1	.000057		.0017		.0060	.0102		
1-1/4			.0014		.0050	.0081		
1-1/2	.000046		.0012		.0040	.0068		
2	.000029	.00015	.00090		.0030	.0051		
2-1/2	.000023	.00012	.00070		.0024	.0041		
3	.000020	.00010	.00060	.00160	.0020	.0034	.0040	.016
4	.000015	.000075	.00045	.00120	.0015	.0026	.0030	.012
6	.000010	.000050	.00030	.00080	.0010	.0017	.0020	.0080
8		.000038	.00023	.00060	.00075	.0013	.0015	.0060
10			.00018	.00048	.00060	.0010	.0012	.0050
12	.000005	.000025	.00015	.00040	.00050	.00085	.0010	.0040
16			.00013	.00030	.00029	.00064	.00075	.0030
20			.000090	.00024		.00051	.00060	.0024
24		.000013	.000075	.00020		.00042	.00050	.0020
36			.000050	.00013		.00028	.00033	.0013

	Rivetted Light	Rivetted Heavy; Brick
3	.0120	
4	.0090	
6	.0060	
8	.0045	.045
10	.0036	
12	.0030	.030
16	.0023	.023
20	.0018	.018
24	.0015	.015
36	.0010	.010
72		.0050
144		.0025

NOTE: The 12-in-diam values are also the absolute roughness, ft.

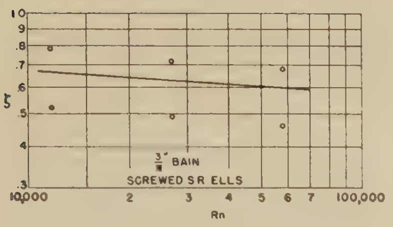

FIG. 2

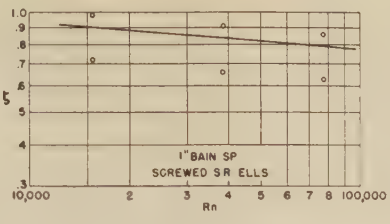

FIG. 3

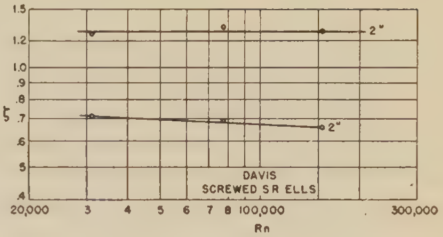

FIG. 4

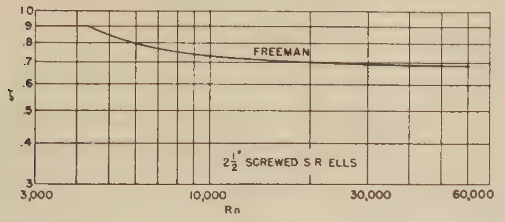

FIG. 5

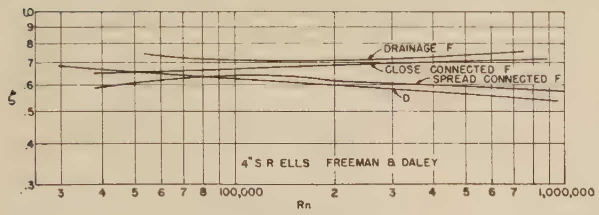

FIG. 7

PREDICTING LOSSES IN BENDS AND FITTINGS

The problem of predicting losses in bends and fittings is much more uncertain than for pipe for the following reasons:

1 The mechanism of flow is not clearly defined; at least two types of loss are superposed—skin friction (pipe loss), and bend loss.

2 The dimensions of fittings, particularly screwed fittings, vary both in the actual body diameter and the ratio of diameter to radius of bend r/d, as commercially produced.

3 The method of test involves taking differences between relatively much larger readings, and the disturbances in flow occasioned by the fitting are not usually completely eliminated at the outlet thereof. In pipe flow, consistency between tests on brass tubing varies ±5 per cent, clean steel ±10 per cent, and for the rougher materials, up to ±30 per cent. Furthermore, for fittings, the variations between tests by different experimenters, and different fittings by the same experimenter, may vary more than 300 per cent.

4 There are very much less test data for fittings and bends than for pipe.

Probably the most extensive and accurate test data on fittings are those by J. R. Freeman (5), covering a range from $2^1/_2$ in. to 8 in. diam, several r/d values, and both screwed and flanged types. With this range of sizes, Freeman's work could be supplemented by the work of others, down to $^3/_4$ in., with some assurance that the correlation would be good enough to furnish a base for rationalization.

The test data have first been plotted ζ versus Rn.

NOMENCLATURE

The nomenclature used is given as follows:

d = pipe diameter, ft

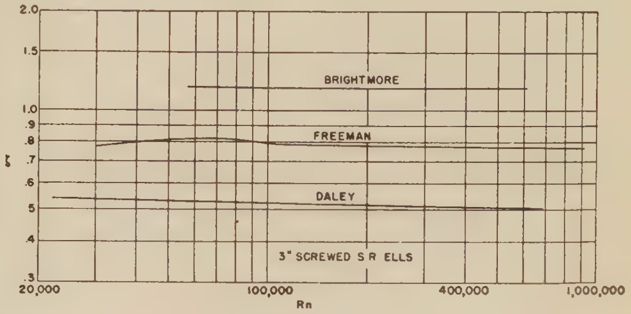

FIG. 6

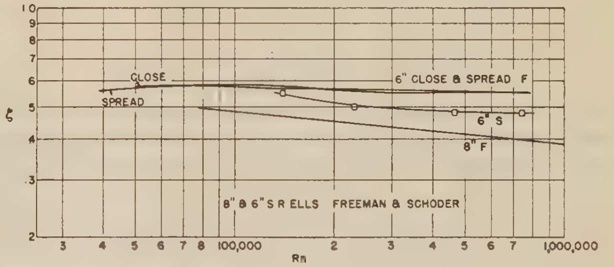

FIG. 8

v = average velocity, fps $\left(\dfrac{Q}{(\pi/4d^2)}\right)$

Q = volume flow, cfs

ρ = density of fluid, lb per cu ft

μ = absolute viscosity, ft-lb-sec units, (= 0.000672 × centipoises)

f = friction factor, a number

l = length of pipe, ft

l_e = equivalent length of pipe for ζp_v

l_f = length of fitting flow path, ft

M = mean hydraulic radius $\left(\dfrac{\text{area}}{\text{wetted perimeter}}\right)$ = ($d/4$ for round pipe)

ϵ = absolute roughness, ft

$\dfrac{\epsilon}{d}$ = relative roughness, a number

ζ = bend loss factor, a number; does not include pipe friction; fraction of velocity head

ζ_1 = true bend loss factor, a number

ζ_2 = Rn and roughness factor, a number

p = pressure, psi

Δp = pressure loss, psi, for length l

Rn = Reynolds number $\dfrac{dv\rho}{\mu}$ or $\dfrac{4Mv\rho}{\mu}$

r = radius of bend, ft

In all cases the values of ζ are for bend loss only. The pipe friction for the length l_f of the fitting path is eliminated; this has been the customary method of handling.

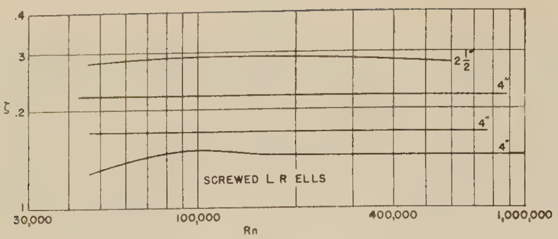

FIG. 9

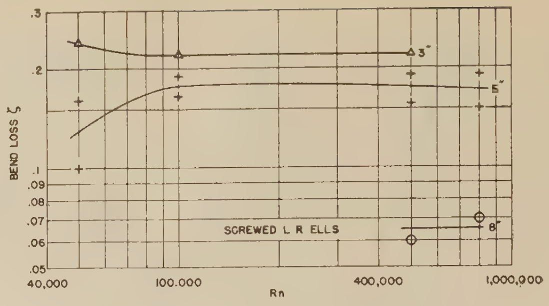

FIG. 10

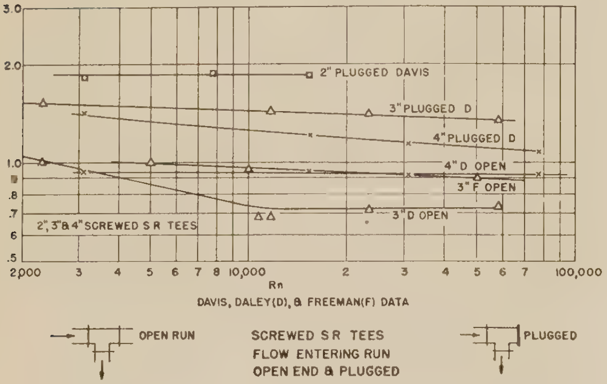

FIG. 11

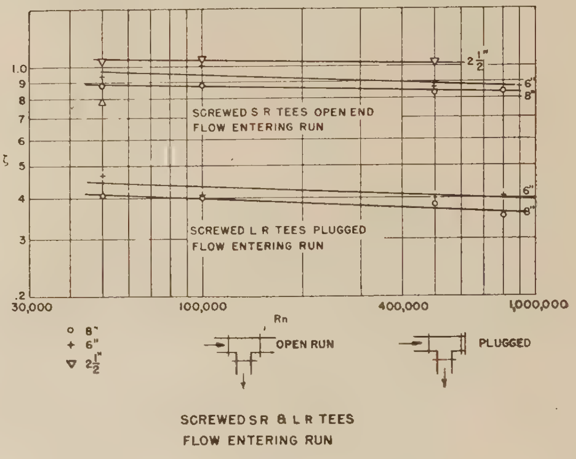

FIG. 12

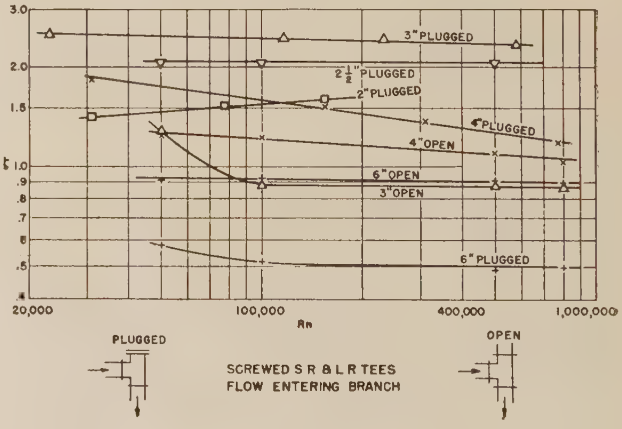

FIG. 13

TEST DATA

Figs. 2 to 8, inclusive, show test data for short-radius (SR) screwed elbows. Test points have been omitted for all Freeman data as there are from 15 to 20 or more points for each, and the curves are simply replotted from the Freeman report (5).

For all other investigators except Hofmann, the experiments were much less extensive, usually 2 or 4 points for each fitting. The scatter is so great as to render any combination of the curves on a single sheet too confusing to read.

Figs. 9 and 10 show long-radius elbow tests (Freeman). Fig. 11 shows SR tees, flow entering run, with the leaving end of the run both plugged and open. Plugging the run end of these tees shows a higher loss than when opening free into the pipe. Plugging in this case is equivalent to converting the tee into a very rough miter bend, and is not a normal use of the tee.

Fig. 12 shows three other sizes of SR tees and two sizes of long radius. Plugging in the case of the long-radius tees does not affect the turn loss, as there is a sufficient length of water between the turning point and the plug, and it behaves the same as if open to the line.

Fig. 13 shows five sizes of short-radius tees, flow entering the branch, and one size of long-radius tee.

An examination of these curves, Figs. 2 to 13, inclusive, discloses some facts likely to be of use in spite of bad scatter.

1 Generally the curves show a decrease of ζ with increase of *Rn* at the lower values of *Rn*, and are flat at higher values of *Rn*. One or two which show apparent increase of ζ with *Rn* are for few test points and probably due, therefore, to experimental error.

2 There is a definite reduction of ζ with size at the same value of *Rn*. Since cast iron has the same absolute roughness for all sizes, this means that ζ varies with relative roughness independently of *Rn*.

3 There appears to be no difference in ζ for screwed and flanged fittings.

From Figs. 1 and 2 we may infer that the variation of ζ is rather similar to f for pipe flow; at low *Rn* values ζ decreases with increase of *Rn* and then becomes constant for further increase.

In so far as can be determined from the relatively small amount of data and bad scatter, for the rougher surfaces (cast iron in small sizes), the value of ζ becomes constant at about the same *Rn* as f in the Moody chart for pipe. In the smoother materials, ζ becomes constant at lower values of *Rn*, than f.

Fig. 14 shows the test results on bends, mostly steel pipe (7, 8, 9, 11,12). In this figure are plotted some screwed and flanged (S and F) cast-iron ells; likewise some small aluminum tubing and Hofmann's (6,10) two sets of tests on machined brass bends, both smooth and artificially roughened with sand and varnish coating. The scatter is again bad, but again there is a general decrease of ζ with roughness.

Fig. 15 shows test results on 3-in., 12-in., and 33-in. air duct. Even for 12-in. square, on which most of the data were taken, the

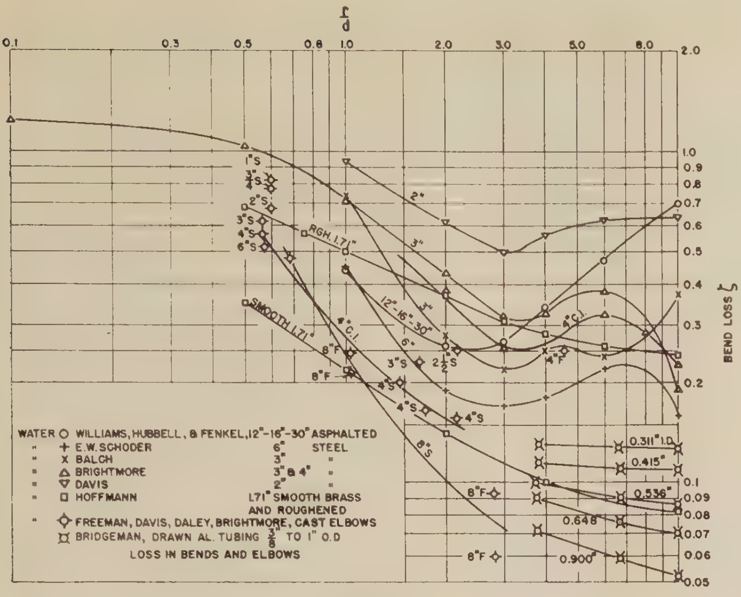

FIG. 14

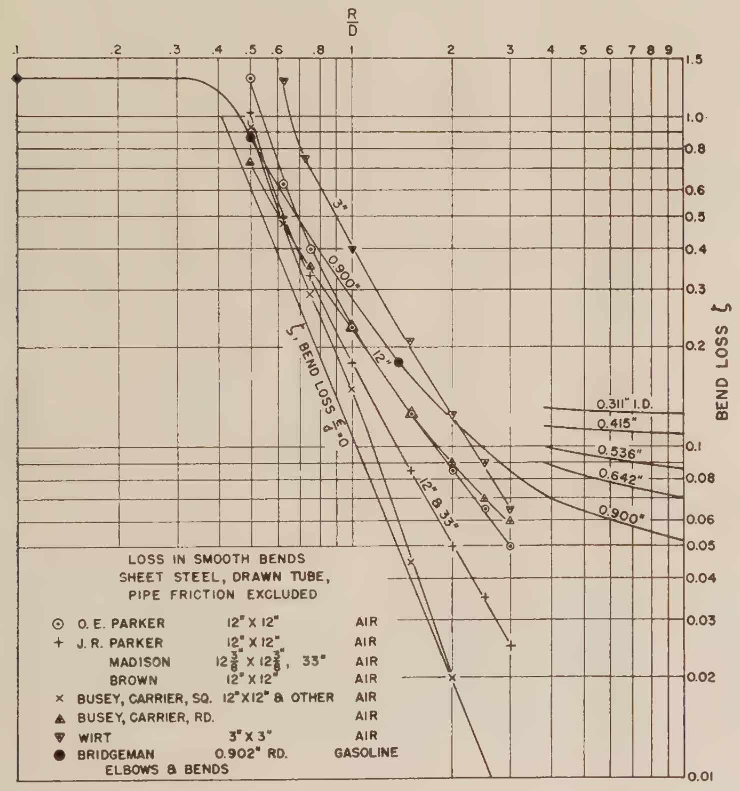

FIG. 15

scatter is considerable as r/d increases; this could be expected, as the value of ζ is a very small difference between two relatively large values (total loss — pipe friction).

Both Fig. 14 and Fig. 15 were plotted on data at the higher values of Rn, where ζ had become substantially constant. In these curves, therefore, variation of Rn is eliminated, leaving only r/d and ϵ/d variation.

The foregoing figures comprise substantially all of the reliable data and we can attempt correlation.

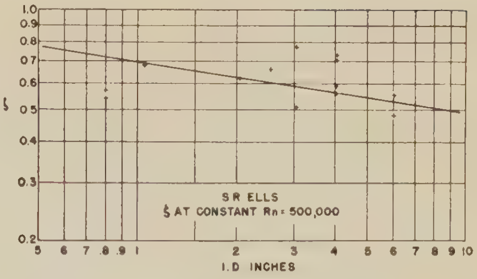

FIG. 16

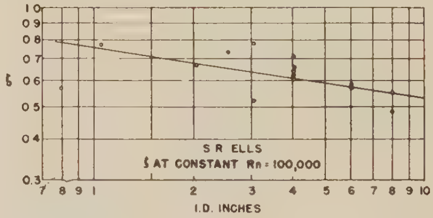

FIG. 17

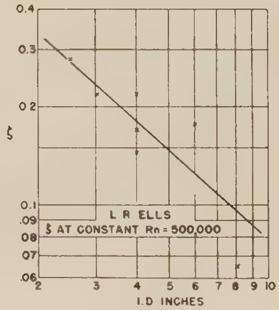

FIG. 18

CORRELATION OF DATA

Fig. 16 shows the values of ζ with size, for cast-iron, short-radius elbows, at $Rn = 100,000$; and Fig. 17 the same, at $Rn = 500,000$. Fig. 18 shows the same for long-radius, cast-iron elbows at $Rn = 500,000$.

These three curves show the nature of the ζ variation with size in a single material, and, consequently, with relative roughness. The rest of the curves for tees, steel bends, and air ducts are not given, as the sample curves are enough to establish the nature of the variation. Using the same plots for tests of SR tees, it was found that the average ζ for flow entering the run, leaving the branch (same size) averaged 1.48 times that for the corresponding elbow. For flow entering the branch, leaving the run, 1.95 times that for the ell. Factors of 1.50 and 2.00 seem satisfactory. The plugged short-radius-tee runs are disregarded as they uniformly show high values, and in any case, are not the normal use of the tee, practically converting it into a rough miter elbow. The value for long-radius tees is correspondingly 2.50 times that for short-radius elbows for both cases of flow entry through run and through branch.

We may now, with the foregoing data, attempt to find some formal relationship.

Inspection of Figs. 14 and 15 shows quite plainly that there is the expected reduction of ζ with increase of r/d; an obvious variation of ζ with ϵ/d; and since the values of ζ are all high at low values of r/d, roughness alone cannot account for all the variation in ζ and there is likely to be an underlying true bend loss for dead smooth materials (which of course do not exist) that is dependent only on r/d.

TEST PLOTS OF VARIOUS MATERIALS

The first move was to plot tests of each kind of material (same absolute roughness) on several kinds of co-ordinate paper to indicate trends. The plot chosen was relative roughness (ϵ/d) versus ζ. The semilog plot proved the most useful as the intercept at $\epsilon/d = 0$ should be the approximate value of the dead smooth pipe-bend loss. These plots are not given since they are merely the working means of approximately the quantities we want. At this point it appeared that the total loss in an elbow or bend is likely made up of three elements:

1 The ordinary pipe friction.

2 A minimum true bend loss for dead smooth conduit, depending only on r/d.

3 A turbulence loss due to the relative roughness of the pipe and affected by Reynolds number and roughness.

Since we are dealing with ζ in the more usual way, pipe friction for the fitting or bend is eliminated (calculated separately with the rest of the pipe friction), and we need only deal with the items 2 and 3.

From the ζ versus ϵ/d plots, it was found that the value of ζ_1, the zero roughness loss, was between 0.40 and 0.50 at $r/d = 0.58$; and 0.02 to 0.09 for $r/d = 1.78$, except for some of the steel pipe bends which are higher.

Using the range just given, the line for ζ_1 was drawn in Fig. 15, corresponding to the equation

$$\zeta_1 = 0.106(r/d)^{-2.5} \qquad [6]$$

This line shows a satisfactory slope referred to the test curves, and leads us to the next step. Subtracting the values of ζ_1 from the test value of ζ, yields ζ_2, the roughness and Reynolds-number factor.

Since in pipe friction f covers both Reynolds number and roughness, and since the value of ζ seems to vary in much the same way as f, with Rn, it appeared that a good plot would be ζ_2 versus f. The value of f is taken for the fitting or bend roughness. The correlation was closest for

$$\zeta_2 = 2 \times 10^3 f^{2.5} \qquad [7]$$

Of course it must be admitted that other power correlations fit nearly as well, since the scatter of test points for ζ_2 is several hundred per cent. The correlation was tried for both ζ_1 and ζ_2 at powers of 2, 2.5, and 3.

Comparing with other methods of estimating ζ, most of these have been based upon a straight velocity-head relationship, no variation with Rn or ϵ/d. Examination of all the test data compels one to recognize that ζ does vary with both Rn and ϵ/d, the same as f, and not alone with $(v^2)/(2g)$.

The Tentative Standards of the Hydraulic Institute, which are probably the latest collection of data from many sources, have been checked against this present formulation

$$\zeta = \zeta_1 + \zeta_2 = 0.106\left(\frac{r}{d}\right)^{-2.5} + 2000 f^{2.5} \qquad [8]$$

For example, the range of values given in the Hydraulic Institute standards for short-radius screwed elbows corresponds to $1^1/_4$ in. to 6 in. by Equation [8]. For flanged short-radius elbows, the Hydraulic Institute range of values covers the 3-in. to 12-in. range by Equation [8].

The formulation also agrees well with the air-duct tests, but is considerably lower than the test data for steel bends, except for one case. There appears to be a reason: With the exception of Freeman, Bridgeman, and Hofmann, most investigators took fitting or bend loss close to the fitting or bend. This procedure can give erratic results, which are quite evident in Fig. 14. It is clear that the up and down variation with r/d is completely inconsistent for various sizes. It does not seem possible for the resistance of a bend, less the pipe friction, to increase to a higher value at $r/d = 10$ than at $r/d = 1$. The air-duct and smooth-tubing experiments do not show any such inconsistent behavior. One other point—the tests on steel bends are generally relatively old, made at a time when steel pipe was rolled considerably rougher than now; much of present production is from smooth rolled plate, or seamless. The greater roughness undoubtedly raised the ζ-values. Moreover, in some cases, cast-iron bends were included with steel, of course raising the averaged results.

The Hofmann tests on a surface as rough as cast iron bear out this view. It seems quite unreasonable to suppose that cast-iron fittings, both short and long radius, should be considerably below steel, a smoother material. The author has given the most weight to Freeman's work, after that to Hofmann's, and the investigators of air-duct bends. These are much more consistent between different experimenters than the steel-pipe tests. The formulation also yields results agreeing quite well with the drawn aluminum-tube tests by CRC (Bridgeman) and fairly well with Hofmann's smooth-tube data. However, the latter gives values for ζ below the true bend loss at values of r/d from 0.5 to 1.0; and higher than Bridgeman at values of r/d greater than 1.0.

PRESENT-DAY STEEL-PIPE VALUES

Therefore it would seem reasonable to assume, since Equation [8] gives results in good agreement with tests on the roughest material, cast iron, and with the smoothest materials, drawn tube and air duct, that the values calculated from Equation [8] for present-day steel pipe are probably nearer the truth than the older steel-pipe tests on a material definitely rougher than now and including some cast iron. This formulation attempts a consistent, rationalized expression for ζ to overcome the rather haphazard and wholly unrelated values hitherto used. This formulation is thought to be justified by the following:

1 ζ has hitherto been treated as corresponding to velocity head and r/d only. Tests show (particularly the more recent work) a definite variation of ζ with Rn and ϵ/d.

2 The use of a formulation covering Rn, ϵ/d and r/d renders results consistent and eliminates the use of range of values, to be selected on judgment alone.

3 The older simple method of equivalent pipe-loss computation may be developed safely.

Referring to item 3, it becomes clear that since ζ_2, involving f, is always a substantial fraction of ζ, the old method of representing fitting and bend loss by length of equivalent pipe is not only likely to give good accuracy, but eliminates all the work of calculating the power formula, Equation [8], if tables are set up. The friction loss for equivalent length of pipe is

$$\Delta p_e = (0.000108\,\rho v^2)\,\frac{fl_e}{d} \qquad [9]$$

The bend loss, not including pipe friction, is

$$\Delta p_b = \zeta(0.000108\,\rho v^2) \qquad [10]$$

Therefore the value of ζ in terms of feet of pipe of the same roughness is

$$l_e = \frac{\zeta d}{f} \qquad [11]$$

The calculated values of ζ for cast-iron elbows are given in

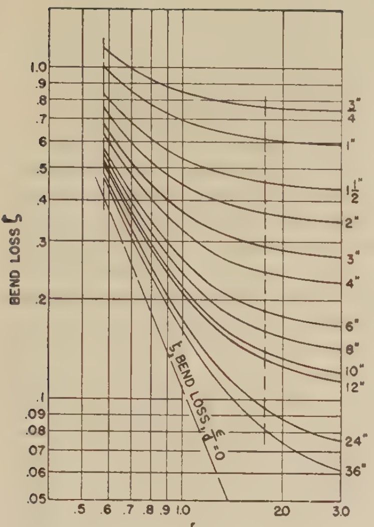

FIG. 19

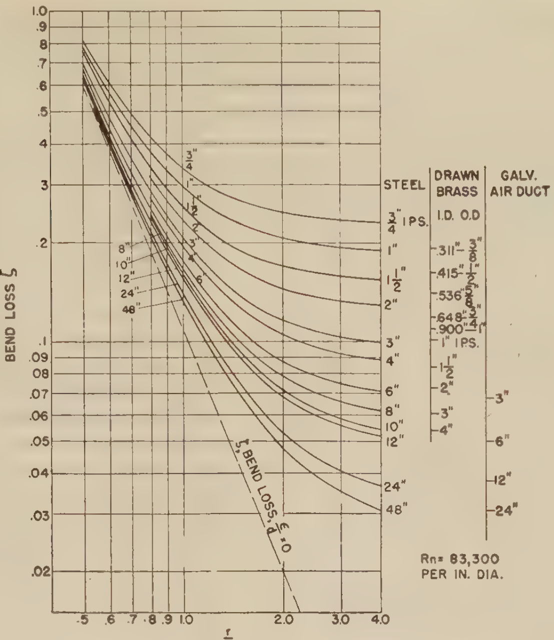

FIG. 20

Fig. 19. Those for drawn tubing, steel pipe, and galvanized-sheet air duct are given in Fig. 20. Table 2 gives the calculated values by Equation [8], from which these curves were plotted.

Applying Equation [11] to this table gives the equivalent feet of pipe; but we use both cast-iron and steel pipe with cast-iron and steel fittings, and brass pipe with cast-brass fittings. Therefore we need three sections, for the three line materials, using the *f* for maximum design flow for cast-iron, steel, and drawn tube for the three cases. The values are given in Table 3. For bends, the bend and the line material will be the same. Table 4 gives the equivalent pipe length; since galvanized air duct is near to drawn tube in roughness, the equivalent lengths come out so nearly alike that they could be combined in one set of figures. All of these tables have been based on the values of ζ after *Rn* was great enough to become constant, and this is near enough to the usual design maximum flow to be satisfactory. To make sure of the values of ζ at lower flows, in which we are occasionally interested, the calculated values were checked for lower *Rn* values. Since they are affected by *f*, they follow the test curves, Figs. 2 to 15, quite reasonably.

TABLE 2 CALCULATED ζ

$$\zeta = 0.106\,\frac{r}{d}^{-2.5} + 2000f^{2.5}$$

	$\frac{r}{d}$ = 0.5	$\frac{r}{d}$ = 0.58	$\frac{r}{d}$ = 1	$\frac{r}{d}$ = 1.78	$\frac{r}{d}$ = 2	$\frac{r}{d}$ = 3	$\frac{r}{d}$ = 4
C.I. Pipe							
3/4		1.158	.850	.769	.763	.753	.749
1		1.002	.694	.613	.607	.595	.591
1-1/2		.844	.536	.455	.449	.437	.433
2		.754	.446	.365	.359	.347	.343
3		.678	.370	.289	.283	.271	.267
4		.633	.325	.244	.238	.226	.222
6		.575	.267	.186	.180	.168	.164
8		.550	.242	.161	.155	.143	.139
10		.528	.220	.139	.133	.121	.117
12		.521	.213	.132	.126	.114	.110
24		.483	.175	.094	.088	.076	.072
36		.469	.161	.080	.074	.062	.058
Steel							
3/4	.829	.644	.336	.255	.248	.236	.232
1	.788	.603	.295	.214	.207	.195	.191
1-1/2	.752	.567	.259	.178	.171	.159	.155
2	.726	.541	.233	.152	.145	.133	.129
2-1/2	.706	.521	.213	.132	.125	.113	.109
3	.697	.512	.204	.123	.116	.104	.100
4	.686	.507	.193	.112	.105	.093	.089
6	.668	.483	.175	.094	.087	.075	.071
8	.659	.474	.166	.085	.078	.066	.062
10	.652	.467	.159	.078	.071	.059	.055
12	.649	.466	.156	.075	.068	.056	.052
16	.642	.457	.149	.068	.061	.049	.045
20	.638	.453	.145	.064	.057	.045	.041
24	.634	.449	.141	.060	.053	.041	.037
Air Duct							
3	.664	.479	.171	.090	.084	.072	.068
6	.646	.461	.153	.072	.066	.054	.050
12	.634	.449	.141	.060	.054	.042	.038
24	.627	.442	.134	.053	.047	.035	.031
Drawn Tubing, Brass or Other							
.311	.789	.603	.296	.214	.209	.197	.193
.415	.760	.575	.267	.186	.180	.168	.164
.536	.737	.552	.244	.163	.157	.145	.141
.648	.715	.536	.222	.147	.135	.123	.119
.900	.706	.521	.213	.132	.126	.114	.110
1 I.P.S.	.698	.513	.205	.124	.118	.106	.102
1-1/2	.680	.495	.187	.114	.100	.088	.084
2	.669	.484	.176	.095	.089	.077	.073
3	.657	.472	.164	.085	.077	.065	.061
4	.650	.465	.157	.076	.070	.058	.054

TABLE 3 EQUIVALENT FEET OF STRAIGHT PIPE

Cast 90-deg Elbows

CAST 90 DEG. ELBOWS

	C.I. Pipe		Steel Pipe		Brass Pipe	
	$\frac{r}{d}$ = 0.58	$\frac{r}{d}$ = 1.78	$\frac{r}{d}$ = 0.58	$\frac{r}{d}$ = 1.78	$\frac{r}{d}$ = 0.58	$\frac{r}{d}$ = 1.78
3/4	1.8	1.2	2.9	1.9	3.9	2.5
1	2.2	1.4	3.5	2.1	4.7	2.7
1-1/4	2.7	1.5	3.6	2.3	4.3	3.1
1-1/2	3.2	1.7	4.9	2.6	6.2	3.3
2	4.2	2.0	6.2	2.9	7.8	3.7
2-1/2	5.1	2.2	7.6	3.3	9.4	4.1
3	6.1	2.5	8.8	3.5	11.0	4.4
4	8.1	2.9	11.5	4.2	14	5.1
6	12.4	3.8	17	5.3	20	6.3
8	17	4.7	23	6.5		
10	22	5.6	30	7.7		
12	27	6.4	37	8.9		
24	58	11.1				
36	93	16				

TABLE 4 EQUIVALENT FEET OF STRAIGHT PIPE

90-deg Bends

	Brass Tub. & Pipe, Sheet Steel Ducts				Steel Pipe			
OD ID	$\frac{r}{d}$ = :5	$\frac{r}{d}$ = 1	$\frac{r}{d}$ = 2	$\frac{r}{d}$ = 3	$\frac{r}{d}$ = .5	$\frac{r}{d}$ = 1	$\frac{r}{d}$ = 2	$\frac{r}{d}$ = 3
3/8 - .311	.82	.31	.22	.20				
1/2 - .415	1.1	.39	.27	.24				
5/8 - .536	1.5	.49	.32	.28				
3/4 - .648	1.9	.59	.36	.32				
1 - .900	2.7	.81	.47	.41				
3/4 I.P.S.	2.3	.72	.43	.38	2.0	.81	.59	.55
1	3.2	.93	.53	.45	2.8	1.0	.71	.65
1-1/4	4.1	1.2	.62	.52	3.6	1.2	.83	.76
1-1/2	5.1	1.4	.71	.59	4.3	1.4	.94	.86
2	6.9	1.8	.88	.71	6.0	1.9	1.2	1.0
2-1/2	9.1	2.2	1.1	.84	7.6	2.3	1.3	1.2
3	10.9	2.7	1.2	1.0	9.3	2.7	1.5	1.3
4	15	3.6	1.6	1.2	13	3.5	1.9	1.6
6	24	5.4	2.2	1.9	20	5.2	2.6	2.1
8					29	7.1	3.3	2.6
10					37	8.9	3.9	3.0
12	146	11	4.2	2.9	46	11	4.6	3.4
16					64	15	5.7	4.2
20					82	18	6.9	5.0
24	117	24	8.0	4.8	102	22	8.2	5.7

CONCLUSIONS

It has been believed generally that screwed fittings of given r/d offered higher resistance than the corresponding flanged fittings. The test evidence, mostly Freeman, does not support this view. The reason is that all the screwed fittings average approximately 12 to 15 per cent larger diameter of body than the inside pipe diameter; this circumstance lowers the turbulence effects sufficiently to offset the loss due to enlargement of section leaving the pipe at entry of the fitting, and the subsequent contraction at exit from the fitting to the line again.

This formulation (Equation [8]), cannot of course be considered final, and it must be admitted it takes an optimist to take the necessary risks with such scattering data.

With regard to gate and globe valves, check valves, unions and couplings, it is thought that skin friction has little part, and that the sharp turns, changes of section, contractions and expansions are the principal cause of loss. Therefore in these cases ζ can be treated as largely varying with velocity head only.

BIBLIOGRAPHY

1 "A Study of the Data on the Flow of Fluids in Pipes," by Emory Kemler, Trans. ASME, Hydraulics Institute, HYD-55,2, vol. 55, 1933, pp. 2–22.

2 "The Flow of Fluids in Closed Conduits," by R. J. S. Pigott, *Mechanical Engineering*, vol. 55, 1933, pp. 497–501 and 505.

3 "Friction Factors for Pipe Flow," by L. F. Moody, Trans. ASME, vol. 66, 1944, pp. 671–678.

4 "Turbulent Flow in Pipes, With Particular Reference to the Transition Region Between the Smooth and Rough Pipe Laws," by C. F. Colebrook, *Journal of the Institution of Civil Engineers*, London, England, vol. 11, 1938–1939, pp. 133–156.

5 "Flow of Water in Pipe and Pipe Fittings," by J. R. Freeman, ASME, New York, N. Y., 1941.

6 "Loss in 90-Degree Pipe Bends of Constant Circular Cross-Section," by Albert Hofmann, Transactions of Munich Hydraulic Institute, Bulletin No. 3; authorized translation published by ASME, vol. 57, 1935, pp. 29–41.

7 "New Data for the Design of Elbows in Duct Systems," by Loring Wirt, *General Electric Review*, vol. 30, 1927, pp. 286–296.

8 "Loss of Pressure Due to Elbows in the Transmission of Air Through Pipes or Ducts," by F. L. Busey, Trans. ASH&VE, vol. 19, 1913, pp. 366–376.

9 "Pressure Loss in Rectangular Elbows," by R. D. Madison and J. R. Parker, Trans. ASME, vol. 58, 1936, pp. 167–176.

10 "CRC Reports on Loss in Aluminum Tubing, Elbows and Fittings, 1939–1940," by O. C. Bridgeman (not published).

11 "Pressure Losses for Fluid Flow in 90° Pipe Bends," by K. Hilding Beij, R. P. 1110, Bureau of Standards, vol. 21, July, 1938.

12 "*Tube Turns*, by J. E. Busher, Bulletin 3002, 1937.

Discussion

S. LOGAN KERR.[3] The author has demonstrated in a very interesting manner the application of the friction-flow theory for pipe lines to the determination of losses in fittings, tubes, and pipes. The comparisons between the various theories are most interesting and confirm the contributions which Prof. Lewis F. Moody made in 1944.

The validity of experimental work in the field of pressure losses in pipes, valves, and fittings is dependent entirely on the methods that are used for measuring pressures and flow. It is well known that pressure taps immediately downstream from obstructions to flow do not give an accurate indication of the head loss. It is necessary to have a series of piezometers above and below the valve or fitting to be investigated, establish from them the normal slope of the pressure loss versus length in straight pipe, then project these lines to the upstream and downstream limits of the fitting or valve, and measure the difference between them in this manner. These multiple piezometers should be located over a distance of not less than 5 diam upstream and downstream from the valve under test. In some cases, 10 to 15 diam will be necessary in order to develop a uniform straight line of pipe loss with respect to length of pipe.

The use of multiple piezometers also aids in detecting errors due to the improper design of piezometers and of their position with respect to the pipe wall which may affect the readings.

There is some question as to the practice of reporting losses through valves and fittings, and it is important that an accurate definition of gross loss and net loss be included in any test reports or studies of friction loss through valves and fittings.

It is the practice of certain manufacturers of valves and fittings to deduct from the gross pressure drop the amount of friction that would occur in a straight piece of pipe of the same length as the face-to-face dimensions of the valve or fitting. This gives a net pressure loss over and above that in straight pipe. On large valves with high velocities through them, it is essential that a careful designation be made as to whether or not the equivalent straight-pipe loss has been deducted, or whether the loss as reported is for the valve itself without adjustment.

The condition of flow entering the test section is also of great importance, as whirling or eddying of the fluid will affect the piezometer readings. It has been found frequently in larger conduits that the presence of a bend or transition section ahead of the test section will distort the results and make them meaningless. It has also been found that repeat runs at the same velocities will not check each other, due to a so-called "rolling-flow" condition which is not identical in the two series of observations.

Mr. Floyd Nagler reported a number of tests made at the University of Iowa on large rectangular conduits with 90 and 180-deg bends. The variation of test results from one run to another indicated a rolling flow, and visual observations made of the flow pattern showed this very clearly. The roughness factor also must be considered in proportion to the size of the conduit. In analyzing the results of pressure-loss investigations, it is essential to have full data on this factor.

F. M. VAN DEVENTER.[4] In the author's 1933 paper[5] he presented the friction-factor relationship using straight lines. The writer is one of the multitude who accepted and used that paper for precise calculations.

The use of that chart involved a supplementary table of pipe sizes and roughness values. That combination of chart and table did not permit smooth interpolation since any reading was taken from one or another of the 18 lines. Thus a comparison of two successive pipe sizes could be quite misleading.

The writer prepared a chart using Pigott's basic data, but with scales appended for steel, cast iron, and drawn tubes. Thus, for most problems, reference to a supplementary table was avoided and smooth interpolation obtained. That chart was published in the general catalog 1937, 1942, and 1947 editions of the writer's company.

As the author has reported, Professor Moody, in his 1944 paper,[6] faired the curves in accordance with the Colebrook equation. He also spaced the plotted lines to correspond to preferred values of relative roughness ϵ/D, and appended a chart from which values of ϵ/D are obtained for known diameter and roughness.

Smith and Shebeko, in designing the "Polyflo" computer, also used the Colebrook data.

The author's present contribution likewise embraces the Colebrook principle and, therefore, yields results commensurate with

---

[3] Consulting Engineer, Philadelphia, Pa. Mem. ASME.

[4] Assistant Chief Engineer, Walworth Company, Inc., New York, N. Y. Mem. ASME.

[5] Refer to author's bibliography (2).

[6] Refer to author's bibliography (3).

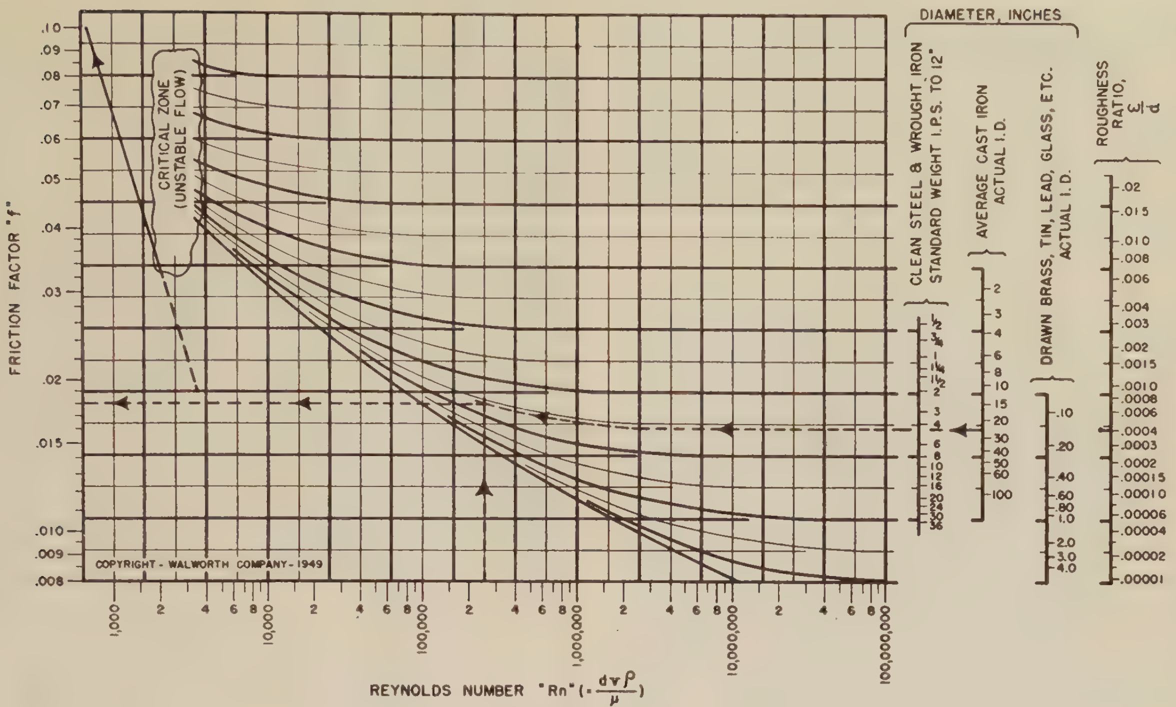

FIG. 21 FRICTION-FACTOR CHART

Moody's. He has adopted ϵ/D in plotting, but again uses a supplementary table from which values of ϵ/D are obtained.

The writer's Fig. 21 is a revision of his 1937 edition, using the Moody and Pigott faired curves. Again, scales are provided directly on the chart for steel, cast iron, and drawn tubes. A fourth scale of ϵ/d values permits solutions involving other materials, provided the absolute roughness is known. Thus reference to supplementary tables or charts is avoided. The use of a uniformly spaced grid also facilitates following the guide lines with a minimum of confusion.

The following statement from the paper requires clarification: "... within the ordinary design range, the values of the author's 1933 plot and Professor Moody's 1944 improved plot do not differ over ±2.5 per cent..." At Reynolds numbers in the range 100,000 to 1,000,000, the old and new plots cross. At lower *Rn*, the old values were high, and at higher *Rn*, the old values become increasingly deficient, e.g., at $Rn = 40{,}000{,}000$, the old values were 50 and 40 per cent low for $^1/_2$-in. and 2-in. steel, respectively. The author implies that this is not in the "ordinary design range." Albeit, the writer is presently concerned with design problems running the gamut of Reynolds numbers from 500 to 50,000,000. Oil transport lines operate in the 40,000 to 200,000 range, natural-gas transport lines 1,000,000 to 20,000,000, and flow channels feeding supersonic wind tunnels and jet-propulsion devices may exceed 50,000,000. The sooner the author's 1933, and the writer's 1937 friction-factor charts are definitely replaced by the more accurate Moody 1944,—Pigott and Van Deventer 1949 versions—the better.

The author has presented in Figs. 2 to 12, graphs for pipe fittings plotting lambda versus *Rn*. This nomenclature (lambda) has been used by foreign writers, while most American authors have used *K*. Either lambda or *K* is the number of velocity heads lost, or the coefficient *K* in the formula

$$h = K \times \frac{v^2}{2g}.$$

This is not made clear in the paper, though loosely implied in the explanation of symbols.

In the several graphs, only upper and lower limits are plotted. One must still use judgment in selecting a datum between these limits. Such being the case, the same end is attained by tabulating the high and low values as has been done by other authors.

To facilitate the use of lambda or *K* values the writer offers the following formulas for the evaluation of velocity pressure

$$\text{Fitting turbulence loss, psi} = K \times VP \quad \text{.........} [12]$$

$$VP \text{ for any liquid} = \frac{0.00116 \times \overline{\text{gpm}}^2 \times G_w}{d^4} \quad \text{.....} [13]$$

$$VP \text{ for any gas} = \frac{0.00113 \times \overline{\text{cfm}}^2 \times G_a \times Z}{P \times d^4} \times \frac{T}{520} \quad \text{...} [14]$$

$$VP \text{ for steam} = \frac{0.28 \times 10^{-6} \times \overline{\text{lb/hr}}^2 \times V}{d^4} \quad \text{.....} [15]$$

where

psi = loss, psi
K = fitting factor, or number of velocity heads lost
VP = velocity pressure, psi
gpm = gallons per minute
cfm = cubic feet per minute measured under standard condition, 14.7 psia and 60 F
lb/hr = pounds per hour, for steam
d = inside diameter, in.
G_w = specific gravity relative to water
G_a = specific gravity relative to air
P = absolute pressure of flowing gas, psia
Z = compressibility factor, if gas deviates from Boyles law
V = specific volume of steam, cu ft per lb

The only objection to the use of the D'Arcy formula is that it is slower and more cumbersome than most of the less precise empirical formulas for specific fluids. It is necessary to obtain from tables, viscosity and density data for the fluid in question. Then two separate solutions must be accomplished: First for Reynolds number, then the basic flow formula. In the interest of time-saving and facility, several forms of special slide rules or "mechanical brains" have been devised. Some of these are eminently satisfactory. The Polyflo type, for example, is based upon a modification of the D'Arcy formula and yields compatible results. Friction factor is easily compensated for correct ϵ/d. Gage points are provided covering almost any fluid met in general engineering practice; hence reference to viscosity tables is unnecessary. The writer, after extended use of this device, recommends it as a general purpose, time-saving tool.

AUTHOR'S CLOSURE

The author is glad to get Mr. Kerr's support of the idea that for testing of hydraulic elements such as fittings, bends, and valves, great care must be used in placing and instrumenting the readings. It must be admitted that much of the early test data lacks a perception of some of these conditions and therefore has added to the difficulties by giving greater scatter to the results.

In preparing this paper the author was preoccupied chiefly with the task of the ordinary designer of a power or industrial plant where the relatively smaller sizes of materials are much in use. In the line in which Mr. Kerr is most interested, the subject covers, as a general rule, by far the largest sizes of piping with which we are concerned and it is readily agreed both that irregularities of flow, such as rolling flow, and other velocity distortions may take a more prominent part than they are likely to do in smaller sizes. The reason is that we are generally dealing with water (low viscosity) and, in these large sizes, cast iron and concrete have very low relative roughness, and therefore the irregularity of the flow plays a considerably greater part. Almost the only man who widely investigated the difference between close-coupled and spread-fitting configurations was John Freeman and there was no consistency even in his results.

The author feels sure that there are some deviations from average results even in the smaller size of piping which can be produced by piping configuration, such as, for example, two short-radius elbows in planes at right angles to each other. We have not enough data to decide upon what increase of loss would occur from such an arrangement, nor indeed do we know how it might vary with Reynolds number or roughness. It is quite agreed that since the pipe loss per foot of length is small, fitting and bend losses will vary more in the large-sized equipment used in hydraulic plants. The present information we have on valves is relatively unsafe for the large valves used in such plants, particularly where the valves are of special design to reduce loss, for example, the Johnson valve.

Referring to Mr. Van Deventer's discussion, in the author's original 1933 paper[7] the roughness table was prepared from a chart of exactly the same nature as Professor Moody's in his 1944 paper (see Fig. 2 of 1933 paper), but both in his own plots as well as Professor Moody's it was found that many kinds of pipe have a range of values which overlap each other and it gets quite confusing to read the chart without error. It should be borne in mind also that the author spent little time in making *convenient* charts, but only in getting one idea across, i.e., that the loss in bends and fittings is, in general, not proportional to $V^2/2g$ only, but is affected by Reynolds number, roughness, and a true bend loss; therefore equivalent length of pipe turns out to be both convenient and more accurate. It is felt that it was wiser in a paper such as this to keep the matter purely on the basis of the original argument and to take up the question of plotting for greater convenience separately. The author feels that Mr. Van Deventer's form of plot is going to be very useful.

With regard to his comment on the "ordinary design range," it should be borne in mind again that this paper is in terms of designing so far commonly done in power plants and industrial plants in which the design habits that have been used are something around 80,000–85,000 *Rn* per in. diam and this applies pretty well both for air and gas, or liquids. In the example which Mr. Van Deventer gave at the meeting, using, if recollection is right, 2 in. pipe on gas, he was dealing with velocity rather close to the acoustic and this is certainly not yet ordinary design. Of course it is true that in the near future, with our ideas opened up during the war period, we may be changing design ranges very considerably.

The author is thankful for the comments by Mr. Kerr and Mr. Van Deventer and wants to reiterate his statement that this was a first crack at the subject. He feels that the values given are not the final ones because there is certainly need of a great deal more testing of elbows and bends than we have had hitherto. It is felt, however, that the use of this method of approach tends to reduce the amount of judgment required of the designer in selecting the values of ζ for any given circumstance. There is not much to be gained by carefully selecting a value by judgment when the variation between tests is in some cases greater than the whole range over which judgment is to be exercised. The writer believes he would rather use a curve which automatically gives better *probability* in accuracy from a single value.

---

[7] "Flow of Fluids in Closed Conduits," by R. J. S. Pigott, *Mechanical Engineering*, vol. 55, 1933, p. 497.

Attenuation of Oscillatory Pressures in Instrument Lines[1]

By A. S. IBERALL,[2] WASHINGTON, D. C.

A theoretical investigation has been made of the attenuation and lag of an oscillatory pressure variation applied to one end of a tube, when the other end is connected to a pressure-sensitive element. An elementary theory based upon incompressible viscous fluid is first developed. The elementary solution is then modified to take into account compressibility; finite-pressure amplitudes; appreciable fluid acceleration; and finite length of tubing (end effects). Account is taken of heat transfer into the tube. The complete theory is derived in an appendix.[3] The results are summarized in eight graphs in a form convenient for use in computing the lag and attenuation of a sinusoidal oscillation in a transmission tube.

NOMENCLATURE

The following nomenclature is used in the paper:

A = tube area
C = velocity of sound
D = inside diameter of tube
E = elastic modulus
L = tube length
M = mass flow
Q = volumetric flow
T = absolute temperature
V = instrument volume
b = compressibility factor for liquid
c = any arbitrary constant
k = compressibility of a liquid
m = exponent of "polytropic" expansion in instrument volume
n = exponent of polytropic expansion in tube
p = pressure
s = tube-wall thickness
t = time
x = axial distance along tube
z = dimensionless parameter of fluid regime
γ = ratio of specific heats
δ = phase angle
η = density ratio
λ = time constant
μ = fluid viscosity
ν = kinematic viscosity
ξ = fractional pressure excess
ρ = fluid density
χ = attenuation factor
ω = angular frequency

INTRODUCTION

In many industrial processes it is necessary to know or to utilize the pressure at one or more points in a fluid conduit. It is not always possible to connect an instrument directly into the conduit at those points. Instead, recourse must be had to remote indication or control. In the case that a fluid is used for transmitting the pressure, it is often of interest to the designer or user of such systems to know their response to variations in pressure. At the present time, the only solution easily available to the engineer is generally based on an elementary theory which considers the system as equivalent to an R-C electrical network.[4] The main defect of the theory is that it does not provide criteria for the limits of its applicability.

In the present paper a relatively complete treatment is given for the transmission of oscillatory pressures in tubing. Primary consideration is given to simplifying the design of high-quality transmission systems for relatively low frequencies.

The elementary solution is derived, and then extended to apply for oscillatory pressures that are an appreciable fraction of the absolute mean pressure, for appreciable frequencies of oscillation, and for tubing short enough to require end corrections. The effect of heat transfer in modifying the oscillatory response of the tube is also discussed.

The chief utility of knowing these corrections is that it permits the designer to choose the size of tubing for specific applications with greater confidence than can otherwise be generally done.

In this paper the elementary theory of transmission lags is developed, and the corrections are discussed. The complete theory is presented in graphical form for the convenience of the designer. A number of examples of the use of the design charts are also given. All mathematical symbols used in this paper are defined in the nomenclature, and also when they are first used.

The theory is developed and more exact results are given in a mathematical appendix,[3] here omitted but included in the complete paper.

ELEMENTARY THEORY

Fig. 1 is a schematic drawing of the system that will be discussed throughout the paper. A tube transmits fluid pressure from a conduit to a pressure-sensitive instrument. The conduit

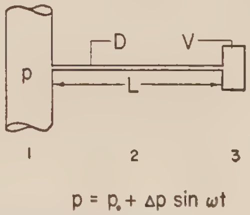

FIG. 1 SCHEMATIC DIAGRAM OF A FLUID TRANSMISSION SYSTEM
(1, conduit. 2, transmission tube. 3, pressure instrument.)

---

[1] This work was supported by the Office of Naval Research under a project on "Basic Instrumentation for Scientific Research."

[2] Physicist, Mechanical Instruments Section, National Bureau of Standards.

[3] This paper with a mathematical appendix is also to be published in the *Journal of Research* of the National Bureau of Standards, Washington, D. C.

Contributed by the Industrial Instruments and Regulators Division of THE AMERICAN SOCIETY OF MECHANICAL ENGINEERS and presented at the National Instruments Conference, September 12–16, 1949, at St. Louis, Mo.

NOTE: Statements and opinions advanced in papers are to be understood as individual expressions of their authors and not those of the Society. Paper No. 49—IIRD-5.

[4] "Pressure Drop in Tubing in Aircraft Instrument Installations," by W. A. Wildhack, NACA Technical Note 593, 1937.

applies an oscillatory (sinusoidal) pressure to the entrance of the transmission tube. The tube, which transmits the pressure, is characterized by a constant cross-sectional area, and its length. The pressure-sensitive instrument, which receives the pressure, is characterized by its enclosed volume. It is assumed that if the walls enclosing the instrument volume are flexible (either elastic or pistonlike), the enclosed volume can be replaced by a larger equivalent rigid volume that will store the same mass of fluid per unit pressure change. It is further assumed that the pressure-sensitive instrument will be so chosen that its indication is independent of the frequency of expected pressure oscillations.

In deriving the elementary theory, it is assumed that Poiseuille's law of viscous resistance holds at each point in the tube; that the fluid is incompressible in the tube; that the sinusoidal pressure oscillations at the beginning of the tube are of small amplitude compared to the mean absolute pressure; and that, if the fluid is a gas, it expands and contracts isothermally in the instrument volume.

The same assumptions applied to an incompressible fluid (e.g., a liquid) lead to the conclusion that there is no loss in amplitude or lag in a liquid-filled system, since a liquid would not expand or contract in the instrument volume.

We may write

$$\frac{\partial p}{\partial x} = -\frac{128}{\pi}\frac{\mu_0}{D^4}Q \qquad [1]$$

for Poiseuille's law, and

$$\frac{\partial M}{\partial x} = -A\frac{\partial \rho}{\partial t} \qquad [2]$$

for the equation of continuity. Here

p = instantaneous pressure at any point in tube
x = distance along tube measured from its entrance
μ_0 = mean fluid viscosity
D = tube diameter
Q = volumetric flow at any point in tube
ρ = instantaneous density at any point in tube
M = the mass flow at any point in tube
A = cross-sectional area of tube
t = time

We infer from the equation of continuity and the assumption that the fluid is incompressible in the tube, (i.e., $\partial\rho/\partial t = 0$) that the mass flow, and, therefore, the volumetric flow does not vary along the tube, but at most varies only with time (the fluid motion is pistonlike).

By differentiating Equation [1], we then obtain

$$\frac{\partial^2 p}{\partial x^2} = 0 \qquad [3]$$

along the tube.

Our boundary conditions are that at $x = 0$

$$p = p_0 + \Delta p e^{j\omega t} \qquad [4]$$

a sinusoidal pressure variation about the mean pressure, and that at $x = L$

$$\left.\begin{aligned} Q &= \frac{V}{p_0}\frac{\partial p}{\partial t} \\ \frac{\partial p}{\partial x} &= -\frac{128}{\pi}\frac{\mu_0}{D^4}Q \end{aligned}\right\} \qquad [5]$$

The first line of Equation [5] expresses the rate at which a compressible fluid entering a rigid volume builds up pressure, while the second line of Equation [5] states that the flow into the volume is limited by the pressure gradient at the end of the tube. Here

p_0 = mean pressure at entrance
Δp = amplitude of pressure oscillation applied at conduit
V = instrument volume
ω = angular frequency of pressure oscillation
L = length of tube

It is convenient to introduce a new variable ξ, the fractional pressure excess, defined as

$$\xi = \frac{p - p_0}{p_0} \qquad [6]$$

so that Equations [3], [4], and [5] become, respectively

$$\frac{\partial^2 \xi}{\partial x^2} = 0 \qquad [7]$$

at $x = 0$

$$\xi = \xi_0 e^{j\omega t} \qquad [8]$$

and at $x = L$

$$\left.\begin{aligned} \frac{\partial \xi}{\partial x} &= -\frac{128}{\pi}\frac{\mu_0}{p_0}\frac{V}{D^4}\frac{\partial \xi}{\partial t} \\ &= -\frac{\lambda_0}{L}\frac{\partial \xi}{\partial t} \end{aligned}\right\} \qquad [9]$$

where

$$\left.\begin{aligned} \lambda_0 &= \frac{128}{\pi}\frac{\mu_0}{p_0}\frac{L}{D^4}V \\ &= 32\frac{\mu_0}{p_0}\left(\frac{L}{D}\right)^2\frac{V}{AL} \end{aligned}\right\} \qquad [10]$$

Here

ξ = fractional pressure excess
ξ_0 = amplitude of fractional pressure excess at origin (= $\Delta p/p_0$)
λ_0 = time constant of system

It is of further convenience to separate the pressure excess into a part that varies with x and one that varies with t.

Let

$$\xi = \tilde{\xi} e^{j\omega t} \qquad [11]$$

where $\tilde{\xi}$ is the maximum amplitude of the pressure excess at any point of the tube.

Our equations then become

$$\frac{d^2\tilde{\xi}}{dx^2} = 0 \qquad [12]$$

at $x = 0$

$$\tilde{\xi} = \xi_0 \qquad [13]$$

and at $x = L$

$$\frac{d\tilde{\xi}}{dx} = -\frac{\lambda_0\omega}{L}j\tilde{\xi} \qquad [14]$$

The solution of Equation [12] which satisfies Equations [13] and [14] is

$$\tilde{\xi} = \xi_0\frac{1 + \lambda_0\omega\left(1 - \dfrac{x}{L}\right)j}{1 + \lambda_0\omega j} \qquad [15]$$

The ratio of the amplitude of the pressure excess at the end of the tube to that at the beginning of the tube is then given by

$$\left.\begin{aligned}\frac{\tilde{\xi}_L}{\xi_0} &= \frac{1}{1+\lambda_0\omega j}\\ &= \frac{1}{1+\chi_0 j}\end{aligned}\right\} \quad \text{[16]}$$

where

$$\chi_0 = \lambda_0\omega \quad \text{[17]}$$

Here

$\tilde{\xi}_L$ = maximum amplitude of pressure excess at instrument volume

χ_0 = attenuation factor

The real part of Equation [16] is the attenuation in amplitude of the pressure excess, while the imaginary part is the phase lag, or

$$\left.\begin{aligned}\left|\frac{\tilde{\xi}_L}{\xi_0}\right| &= \frac{1}{[1+\chi_0^2]^{1/2}}\\ \tan\delta_0 &= \chi_0\end{aligned}\right\} \quad \text{[18]}$$

where δ_0 is the lagging phase angle.

We will regard Equation [18] as the elementary solution of our problem.

It indicates that a transmission system is characterized by a time constant λ_0, which can be computed from a knowledge of the dimensions of the tube, the effective internal volume of the end device, and the average conditions of the gas in the tube; and an attenuation factor χ_0, for each angular frequency, from which one can compute the attenuation and phase lag in a tube. The tube dimensions and the instrument volume furnish the analog to the resistance and capacitance of an electrical network.

In principle, although difficult in practice, from a knowledge of the response to a sine wave, one can obtain the response to square waves, step functions, etc., by Fourier analysis.

DISCUSSION OF CORRECTIONS

The assumptions made in the elementary theory are restrictive, and in the appendix[3] these are modified, one at a time, until finally we arrive at a complete solution that accurately takes into account all first-order phenomena, and partially takes into account second-order phenomena. Complete results are presented in convenient graphical form in Figs. 2 to 9, inclusive.

The factors that must be taken into account are as follows:

Compressible Flow in Tube. The effect of fluid compressibility is to introduce a time constant and corresponding attenuation factor (λ_T, χ_T) depending on the tube volume in addition to the ones depending on the instrument volume. (The time constant and attenuation factor depending upon the instrument volume will be referred to as λ_I and χ_I henceforth instead of λ_0 and χ_0.) In terms of the electrical analog, the tube volume represents a distributed capacitance in addition to the equivalent capacitance of the instrument volume.

Finite Pressure Excess. The effect of the application of a finite pressure excess to a compressible fluid in a transmission tube is to introduce harmonic distortion and to modify the mean pressure. However, the attenuation of the fundamental is essentially independent of the magnitude of the pressure excess. The percentage of distortion is approximately proportional to the applied pressure excess.

Fluid Acceleration. The effect of fluid inertia is to modify the time constants of the system. Both the attenuation of the fundamental and the magnitude of harmonic distortion are affected. A dimensionless parameter z, analogous to the Q of an electrical system, characterizes the fluid regime and determines whether fluid inertia may or may not be neglected.

When fluid inertia is negligible, a transmission tube acts like a highly damped system; when fluid inertia is large, a transmission tube acts like an undamped system, and elementary acoustic theory is applicable.

Finite Length of Tubing. The effect of fluid acceleration at the ends of the tube results in further distortion of wave form, which must be taken into account in short tubes.

Heat Conduction. If there were no heat transfer from outside the tube to inside, the oscillatory processes would take place adiabatically; if there were perfect heat transfer into and through the tube, the processes would take place isothermally. The effect of finite heat conduction is to make the real process occur in between these extremes, although in a rather complicated fashion. At low frequencies the process may be regarded as isothermal.

Although an exact result is given in the appendix,[3] it is advantageous to utilize the thermodynamic equation of condition, discussed in the following section, for elucidating the problem of attenuation in tubing.

THERMODYNAMIC EQUATION OF CONDITION

In the case of an oscillatory variation of fluid flow, the equation relating the thermodynamic parameters of the fluid lies between the adiabatic and the isothermal equations of condition. For high frequencies, as in sound waves, it is well known that the adiabatic equation holds. However, for viscously damped motion, the adiabatic relation is not, in general, attained.

For a gas, we assume and justify in the appendix[3] that the processes can be described as "polytropic," that is, characterized by a constant exponent n, in the expression

$$\left.\begin{aligned}p &= c\rho^n\\ 1+\xi &= \eta^n\end{aligned}\right\} \quad \text{[19]}$$

with

$$1 \leqq |n| \leqq \gamma$$

where

n = exponent of polytropic expansion in tube

γ = ratio of specific heats

η = density ratio (ρ/ρ_0)

ρ_0 = average density in tube

c indicates any constant

The viscosity of gases is independent of the pressure, and, as an approximation, proportional to the absolute temperature. (The more rigorous approximation is that the viscosity is proportional to $(T)^{1/2}/(1+c/T)$, but over a small range this can be approximated by the temperature to a power close to 1. For example, for air at room temperature, a power of 0.8 fits experimental data quite well. The difference from unity is unimportant for our purpose.)

Therefore

$$\left.\begin{aligned}\mu &= cT\\ \frac{\mu}{\mu_0} &= (1+\xi)^{\frac{n-1}{n}}\\ \frac{\mu}{\mu_0} &= \eta^{n-1}\end{aligned}\right\} \quad \text{[20]}$$

follows from the gas laws and Equation [19]. Here

μ = instantaneous fluid viscosity

T = absolute temperature

Equations [19] and [20] thus express the variation of viscosity, density, and pressure, respectively, in a polytropic process in a gas. At low frequencies, the polytropic exponent may be regarded as equal to unity.

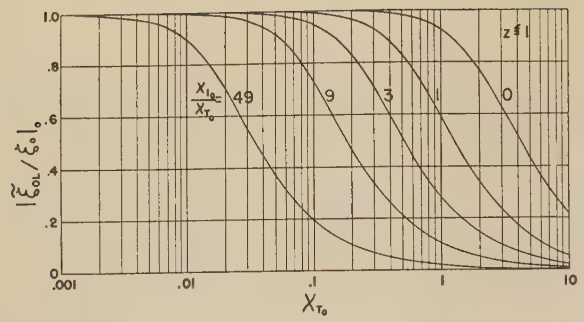

Fig. 2 Amplitude Ratio of Fundamental $|\tilde{\xi}_{OL}/\xi_0|_0$ in a Volume-Terminated Tube as a Function of a Parameter Proportional to Frequency (χ_{T0}) for Various Ratios of Instrument Volume to Tube Volume (χ_{T0}/χ_{T0}) With Large Damping ($z \leq 1$)

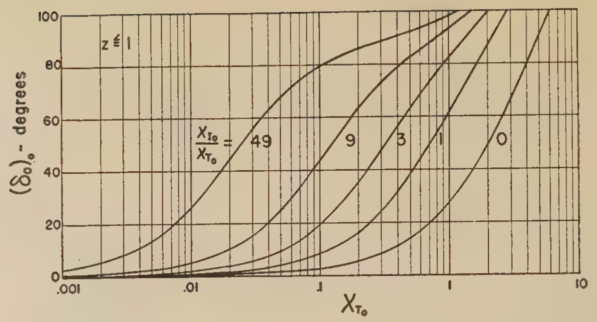

Fig. 3 Phase Lag of Fundamental $(\delta_O)_0$ in a Volume-Terminated Tube as a Function of a Parameter Proportional to Frequency (χ_{T0}) for Various Ratios of Instrument Volume to Tube Volume (χ_{I0}/χ_{T0}) With Large Damping ($z \leq 1$)

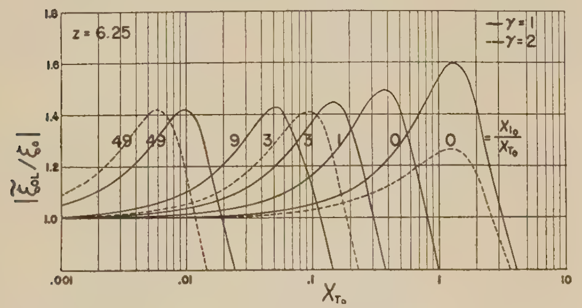

Fig. 4 Amplitude Ratio of Fundamental $|\tilde{\xi}_{OL}/\xi_0|$ in a Volume-Terminated Tube as a Function of a Parameter Proportional to Frequency (χ_{T0}) for Various Ratios of Instrument Volume to Tube Volume (χ_{I0}/χ_{T0}) and for Two Values of Specific Heat Ratio (γ) With Intermediate Damping ($z = 6.25$)

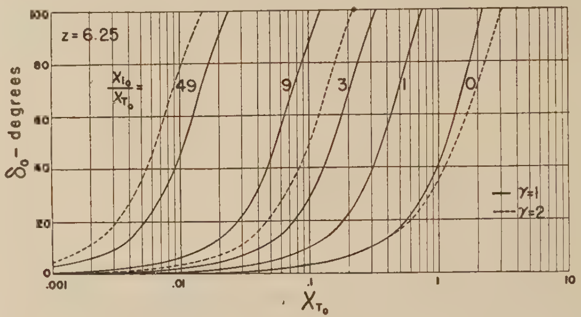

Fig. 5 Phase Lag of Fundamental (δ_O) in a Volume-Terminated Tube as a Function of a Parameter Proportional to Frequency (χ_{T0}) for Various Ratios of Instrument Volume to Tube Volume (χ_{I0}/χ_{T0}) and for Two Values of Specific Heat Ratio (γ) With Intermediate Damping ($z = 6.25$)

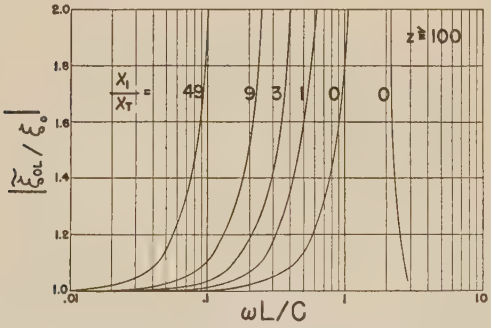

Fig. 6 Amplitude Ratio of Fundamental $|\tilde{\xi}_{OL}/\xi_0|$ in a Volume-Terminated Tube as a Function of a Parameter Proportional to Frequency ($\omega L/C$) for Various Ratios of Instrument Volume to Tube Volume (χ_I/χ_T) With Little Damping ($z \geq 100$)

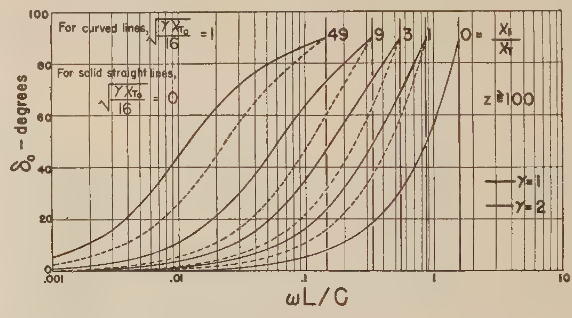

Fig. 7 Phase Lag of Fundamental (δ_O) in a Volume-Terminated Tube as a Function of a Parameter Proportional to Frequency ($\omega L/C$) for Various Ratios of Instrument Volume to Tube Volume (χ_I/χ_T) Indicating the Difference Between No Damping $[\gamma\chi_{T0}/16]^{1/2} = 0$, and Small Damping $[\gamma\chi_{T0}/16]^{1/2} = 1$, for Two Values of Specific Heat Ratio (γ) With Small Damping ($z \geq 100$)

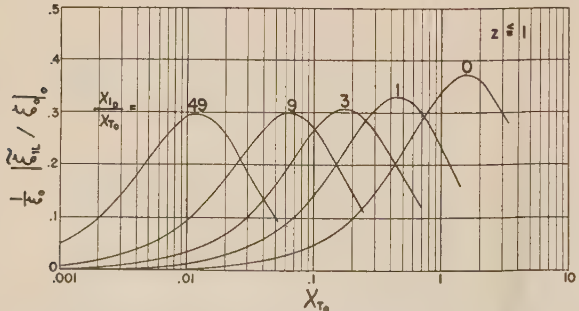

Fig. 8 Relative Amplitude of Double Harmonic Distortion $(|\tilde{\xi}_{1L}/\xi_0|_0/\xi_0)$ in a Volume-Terminated Tube as a Function of a Parameter Proportional to Frequency (χ_{T0}) for Various Ratios of Instrument Volume to Tube Volume (χ_{I0}/χ_{T0}) With Large Damping ($z \leq 1$)

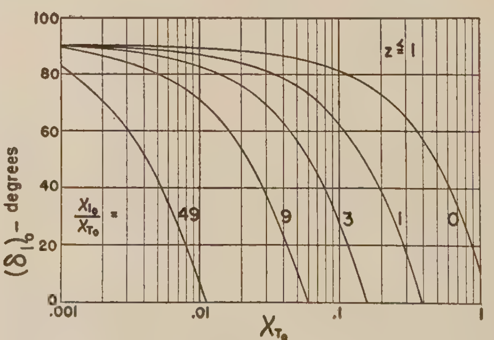

Fig. 9 Phase Lead, as Measured on Fundamental Time Scale, of Double Harmonic Distortion $(\delta_1)_0$ in a Volume-Terminated Tube as a Function of a Parameter Proportional to Frequency (χ_{T0}) for Various Ratios of Instrument Volume to Tube Volume (χ_{I0}/χ_{T0}) With Large Damping ($z \leq 1$)

For liquids, we assume that the equation of condition in a polytropic process is given by

$$\rho = \rho_0 + cp^n \quad [21]$$

where

$$1 \leqq |n| \leqq \gamma$$

For liquids, however, γ lies so close to unity that we may satisfactorily assume $n = 1$.

Equation [21] can then be written in the form

$$\eta = 1 + b\xi \quad [22]$$

where

b = compressibility factor $(= k_0 p_0)$
k_0 = liquid compressibility at average conditions in tube

The variation in viscosity of a liquid over a small range of temperature can be neglected, so that in a polytropic process

$$\mu = \mu_0 \quad [23]$$

Actually, the implication in Equations [22] and [23] is that in a liquid-filled transmission line, the effect of conditions appreciably different from isothermal is negligible.

It is also necessary to take into account heat exchange at the instrument.

For an isothermal process with a gas in the instrument volume, we previously assumed that

$$Q = \frac{V}{p_0} \frac{\partial p}{\partial t} \quad [5]$$

represents the influx of fluid. If, instead, we assume a polytropic process in the instrument, characterized by an exponent m (the heat exchange may differ in the tube and instrument volume so that m is not necessarily equal to n), then Equation [5] should be modified to

$$\left.\begin{aligned} Q &= \frac{V}{mp} \frac{\partial p}{\partial t} \\ Q &= \frac{n}{m} \frac{V}{\rho} \frac{\partial \rho}{\partial t} \end{aligned}\right\} \quad [24]$$

in the case of gases; or to

$$Q = \frac{Vb}{p_0} \frac{\partial p}{\partial t} \quad [25]$$

in the case of liquids.

If the fluid is regarded as a spring, the exponent of the polytropic process for a gas, or the small compressibility of a liquid may be viewed as quantities which make the fluid spring stiffer in the case of gases, or almost infinitely stiff in the case of liquids. It is shown in the appendix[3] that these polytropic exponents modify the time constants of the tube and volume.

General Procedure, With Examples, for Computing Transmitted Pressure

The computation of the attenuation and phase lag at one end of a transmission tube of a sinusoidal pressure variation imposed at the other end can be carried out with the aid of Figs. 2 to 9. These figures are based upon the theory largely developed in the appendix. The computations are made primarily for the attenuation at the fundamental frequency. An estimate of the distortion arising from finite input amplitudes with high damping is made in the appendix.[3] The computation for the first harmonic in the distorted output can be made with the aid of Figs. 8 and 9. An outline of procedure for making computations follows:

1 Compute

$$z = \frac{D^2}{4} \frac{\omega}{\nu_0} \quad [26]$$

a dimensionless parameter of the fluid regime which characterizes the amount of damping present. When this parameter is less than one (large damping), use Figs. 2 and 3; when greater than 100 (small damping), use Figs. 6 and 7. For intermediate values of this parameter, use Figs. 4 and 5 as an aid to interpolation.

2 Compute the attenuation factors

$$\chi_{T0} = \frac{32\mu_0\omega}{p_0} \left(\frac{L}{D}\right)^2 \quad [27]$$

$$\frac{\chi_{I0}}{\chi_{T0}} = \frac{1}{m} \left(\frac{V}{AL}\right) \quad [28]$$

for a gas, or

$$\chi_{T0} = 32\mu_0 k_0 \omega \left(\frac{L}{D}\right)^2 \left(1 + \frac{p_0 - p_a}{p_0} \frac{1}{k_0 E} \frac{D}{s}\right) \quad [29]$$

$$\frac{\chi_{I0}}{\chi_{T0}} = \frac{V}{AL} \frac{1}{\left(1 + \frac{p_0 - p_a}{p_0} \frac{1}{k_0 E} \frac{D}{s}\right)} \quad [30]$$

for a liquid. These quantities χ_{T0} and χ_{I0} are factors based on the tube volume and instrument volume, respectively. The zero subscript means that they are values for the case of large damping.

3 Compute the input pressure excess

$$\xi_0 = \frac{\Delta p}{p_0} \quad [31]$$

4(*a*) For values of z less than 1, enter Fig. 2 with χ_{T0} and χ_{I0}/χ_{T0} to find the amplitude ratio $|\tilde{\xi}_{OL}/\xi_0|_0$, and enter Fig. 3 to find the lagging phase angle $(\delta_O)_0$.

4(*b*) The output pressure excess is then computed from

$$|\tilde{\xi}_{OL}|_0 = \xi_0 \left|\frac{\tilde{\xi}_{OL}}{\xi_0}\right|_0 \quad [32]$$

5(*a*) For values of z greater than 100, compute

$$\frac{\omega L}{c} = \left[\frac{z\chi_{T0}}{8\gamma}\right]^{1/2} \quad [33]$$

$$\frac{\chi_I}{\chi_T} = \gamma \frac{\chi_{I0}}{\chi_{T0}} \quad [34]$$

For liquids, assume $\gamma = 1$.

The quantities χ_I and χ_T are the attenuation factors for the case of low damping. With low damping, it is convenient to use the dimensionless parameter $\omega L/C$ which is proportional to frequency, as the independent variable. The quantity C represents the velocity of sound.

5(*b*) Enter Fig. 6 with $\omega L/C$ and χ_I/χ_T to find the amplitude ratio $|\tilde{\xi}_{OL}/\xi_0|$ and enter Fig. 7 to find the lagging phase angle δ_O. It is necessary to estimate the phase angle by interpolation. For very small values of χ_{T0} compared to 1, the lagging phase angle is zero up to the first resonance. In Fig. 7 curves have been presented to indicate the phase angle for $(\gamma\chi_{T0}/16)^{1/2} = 0$ and $(\gamma\chi_{T0}/16)^{1/2} = 1$. One may linearly interpolate for values lying between 0 and 1.

6(a) For values of z lying between 1 and 100, one may interpolate between the values of amplitude ratio and lagging phase angle obtained in step 4(a) and those obtained in step 5(b) by the use of Figs. 4 and 5. Enter Figs. 4 and 5, with χ_{T0} and χ_{I0}/χ_{T0} to find the amplitude ratio $|\tilde{\xi}_{OL}/\xi_0|$ and lagging phase angle δ_0. These are the values for $z = 6.25$. In order to interpolate, plot a logarithmic graph with z as abscissa and the amplitude ratio or phase angle as ordinate. Plot the values from step 4(a) at $z = 1$, from step 6(a) at $z = 6.25$, and from step 5(b) at $z = 100$, draw a curve through these three points, and interpolate on this curve for the intermediate value of z.

COMPUTATION OF DOUBLE-FREQUENCY DISTORTION

This computation represents only an estimate of the double-frequency distortion, and is strictly only valid for values of z less than 1.

Compute χ_{T0} and χ_{I0}/χ_{T0}. Enter Figs. 8 and 9 to obtain the relative amplitude ratio $|\tilde{\xi}_{1L}/\xi_0|_0/\xi_0$ and leading phase angle $(\delta_1)_0$ for the double-frequency wave. The leading phase angle is measured on the time scale of the fundamental where the input is a cosine term.

Compute the pressure excess of the double frequency $|\tilde{\xi}_{1L}|_0$ from

$$|\tilde{\xi}_{1L}|_0 = \left(\frac{1}{\xi_0}\left|\frac{\tilde{\xi}_{1L}}{\xi_0}\right|_0\right)\xi_0^2 \ldots\ldots\ldots\ldots\ldots [35]$$

Compute the mean pressure at the instrument volume which is larger than the mean pressure at the tube entrance by $\xi_0 \Delta p (1 - |\tilde{\xi}_{OL}/\xi_0|_0^2)/4$.

The various quantities in this section are defined as follows:

μ_0 = mean fluid viscosity
ν_0 = mean kinematic viscosity
p_0 = mean fluid pressure
p_a = ambient pressure external to tube
Δp = amplitude of applied sinusoidal pressure
ξ_0 = applied fractional pressure excess
ξ_{OL} = pressure excess of fundamental at instrument volume
ξ_{1L} = pressure excess of double frequency at instrument volume
δ_O = lagging phase angle of fundamental at instrument volume
δ_1 = leading phase angle of double frequency at instrument volume
k_0 = mean fluid compressibility
V = equivalent rigid internal volume of instrument
A = internal cross section of tube
D = internal diameter of tube
s = wall thickness of tube (assumed small compared to diameter)
E = elastic modulus of tube material
L = length of tube
C = velocity of sound in fluid
γ = ratio of specific heats of fluid (assumed to be 1 for liquids)
m = coefficient of polytropic process in instrument volume. (In lieu of other information, it may be assumed to be 1.)
z = dimensionless parameter characterizing fluid regime
ω = angular frequency applied
χ_T = attenuation factor based on tube volume
χ_I = attenuation factor based on instrument volume

Subscript T refers to parameters based on tube volume.

Subscript I refers to parameters based on end volume.

Subscripts O or 1 adjacent to a letter denote fundamental or first harmonic.

An end subscript of 0 denotes a value for case of large damping.

The attenuation of the fundamental may be computed validly from the formulas developed in this paper when

$$\left.\begin{array}{l}\dfrac{\nu_0}{CD} < 1 \\[2ex] \dfrac{\nu_0 \omega}{C^2} < 1\end{array}\right\} \ldots\ldots\ldots\ldots\ldots [36]$$

The second harmonic distortion, which was only estimated approximately, may be validly computed from the formulas developed when

$$z = \frac{\omega D^2}{4\nu_0} < 1 \ldots\ldots\ldots\ldots\ldots [37]$$

and for applied pressure amplitudes small enough to guarantee laminar flow.

EXAMPLES OF COMPUTATIONS

The calculation of attenuation by the General Procedure outlined will be illustrated by a number of examples.

(a) What is the longest length of $^3/_{16}$-in-ID tubing that can be used to transmit air pressure to a Bourdon-type pressure gage (equivalent internal volume assumed negligible) up to a frequency of $^1/_2$ cycle per sec (cps) with a loss in amplitude not greater than 25 per cent? What will be the double-frequency distortion? For air, assume $\mu_0 = 2 \times 10^{-4}$ poise, $\nu_0 = {}^1/_6$ stokes, $m = 1$, $\gamma = 1.4$, $p_0 = 10^6$ dynes/cm² (atmospheric pressure), angular frequency $\omega = \pi$.

Using Equation [26], $z = 1.1$ (computed in consistent units). This value is sufficiently close to unity to permit the use of Figs. 2 and 3.

Enter Fig. 2 with $|\tilde{\xi}_{OL}/\xi_0|_0 = 0.75$ and $\chi_{OI}/\chi_{T0} = 0$, since the instrument volume is negligible, to find $\chi_{T0} = 2.1$. Compute L in Equation [27] to be 160 ft.

Enter Fig. 3 with $\chi_{T0} = 2.1$, to find that the maximum phase lag will be 53 deg.

Enter Fig. 8 to find that the relative amplitude of the double frequency $|\tilde{\xi}_{1L}/\xi_0|_0/\xi_0 = 0.35$. For initial pressure excesses of 0.1, 0.3, and 1, respectively, the double-frequency amplitude, relative to the input amplitude, will be $3^1/_2$, $10^1/_2$, and 35 per cent, respectively.

(b) What lengths of 0.1-in-ID tubing (nominally $^3/_{16}$-in-OD tubing) can be used for quality transmission of air pressure for frequencies up to 1, 10, 100, 1000 cps into pressure instruments with equivalent rigid volumes of 0.1 cu in. and 1 cu in.?

We will define quality transmission as that in which there is no more than ±5-per cent change in fundamental amplitude or more than ±30-deg phase shift (whichever is more stringent).

Assume that $\mu_0 = 2 \times 10^{-4}$ poise, $\nu_0 = {}^1/_6$ stokes, $m = 1$, $\gamma = 1.4$, $D = 0.1$ in., $A = 0.0079$ sq in., $p_0 = 10^6$ dynes/cm², $\rho_0 = 0.0012$ g/cm³.

We will calculate for each frequency separately.

Let $f = 1$ cps:

Using Equation [26], $z = 0.61$, therefore use Figs. 2 and 3.

Assume $AL = \infty$, therefore, by Equation [28], $\chi_{I0}/\chi_{T0} = 0$.

Enter Fig. 2 for $|\tilde{\xi}_{OL}/\xi_0|_0 = 0.95$ to find $\chi_{T0} = 0.80$.

Enter Fig. 3 for $(\delta_O)_0 = 30$ deg to find $\chi_{T0} = 1.1$; use 0.80 since more stringent.

Calculate L from Equation [27] to be 450 in.

Calculate AL to be 3.5 cu. in.

Compute χ_{I0}/χ_{T0} from Equation [28] to be 0.029 for $V = 0.1$ cu in.; to be 0.29 for $V = 1$ cu in.

In Fig. 2, χ_{T0} is modified negligibly for $V = 0.1$ cu in.

Therefore $L = 450$ in. $= 37$ ft for $V = 0.1$ cu in.

Re-enter Fig. 2 for $|\tilde{\xi}_{OL}/\xi_0|_0 = 0.95$, $\chi_{I0}/\chi_{T0} = 0.29$ to find $\chi_{T0} = 0.5$.

Calculate L to be 350 in. = 29 ft for $V = 1$ cu in.

Let $f = 1000$ cps:

Using Equation [26], $z = 610$, therefore use Figs. 6 and 7.

Assume $\chi_I/\chi_T = 49$ (the line volume will probably be small).

Enter Fig. 6 for $|\tilde{\xi}_{OL}/\xi_0|_0 = 1.05$ to find $\omega L/C = 0.031$.

Calculate L from Equations [33], [26], and [27] to be 0.066 in.

Calculate AL to be 0.00052 cu in.

Using Equation [34], it is seen that χ_I/χ_T is greater than assumed so that $\omega L/C$, and therefore L is less than the previous estimate. One may note that the estimated length will be so small that the theory essentially predicts that no transmission tubing at all may be used. In fact, the acoustic impedance of the entrance orifice into the pressure instrument, or the mechanical impedance of the pressure instrument itself will probably govern the response at this high frequency.

Let $f = 10$ cps:

Using Equation [26], $z = 6.1$, therefore use Figs. 4 and 5.

Assume $AL = \infty$, therefore $\chi_{I0}/\chi_{T0} = 0$.

Enter Fig. 4 with $|\tilde{\xi}_{OL}/\xi_0| = 1.05$, and $\gamma = 1.4$ to find $\chi_{T0} = 0.12$.

Compute L from Equation [27] to be 58 in.

Compute AL to be 0.45 cu in.

Compute χ_{I0}/χ_{T0} from Equation [28] to be 0.22 for $V = 0.1$ cu in.; = 2.2 for $V = 1$ cu in.

In Fig. 4, χ_{T0} is modified to about 0.07 for $V = 0.1$ cu in.

Therefore L is reduced to about 4 ft for $V = 0.1$ cu in.

Enter Fig. 4 for $|\tilde{\xi}_{OL}/\xi_0| = 1.05$, and $\chi_{I0}/\chi_{T0} = 2$ to find $\chi_{T0} = 0.018$.

Compute L to be 22 in. for $V = 1$ cu in.

Compute AL to be 0.17 cu in.

Compute $\chi_{I0}/\chi_{T0} = 6$.

Enter Fig. 4 to find $\chi_{T0} = 0.007$.

Compute L to be 14 in.

Compute AL to be 0.11 cu in.

Compute $\chi_{I0}/\chi_{T0} = 9$.

Enter Fig. 4 to find $\chi_{T0} = 0.004$.

Compute L to be 11 in.

Compute AL to be 0.09 cu in.

Compute $\chi_{I0}/\chi_{T0} = 11$.

In Fig. 4, χ_{T0} is modified negligibly. Therefore L = about 1 ft for $V = 1$ cu in.

To check the phase angle, enter Fig. 5 with $\chi_{I0}/\chi_{T0} = 11$, and $\chi_{T0} = 0.005$, to find 4 deg.

Let $f = 100$ cps:

$z = 61$ (interpolation is necessary).

First estimate from Figs. 6 and 7.

Assume $\chi_I/\chi_T = 9$.

Enter Fig. 6 to find $\omega L/C = 0.068$.

Compute L to be 1.5 in.

Compute AL to be 0.011 in.

Compute $\chi_I/\chi_T = 9.1$ for $V = 0.1$ cu in.; = 91 for $V = 1$ cu in.

By Fig. 6, $\omega L/C$ is negligibly modified for $V = 0.1$ cu in.

Therefore $L = 1.5$ in. for $V = 0.1$ cu in. is our first estimate.

For $V = 1$ cu in., we find again that an extremely small tube is predicted, so that the impedance of the entrance orifice will probably govern.

For $V = 0.1$ cu in., and $L = 1.5$ in., estimate $(\gamma\chi_{T0}/16)^{1/2}$ to be 0.01.

From Fig. 7 we find that the phase lag is negligible.

Compute $\chi_{T0} = 0.0009$, from Equation [27] for $\omega = 200\ \pi$.

Enter Fig. 4 for $\chi_{I0}/\chi_{T0} = 9$, to find $|\tilde{\xi}_{OL}/\xi_0| = 1.00$.

Interpolating between $|\tilde{\xi}_{OL}/\xi_0| = 1$ at $z = 6.25$ and $|\tilde{\xi}_{OL}/\xi_0| = 1.05$ at $z = 100$ for $z = 61$, we find that $|\tilde{\xi}_{OL}/\xi_0|$ is negligibly affected.

Therefore $L = 1.5$ in. for $V = 0.1$ cu in.

Long-Time Tension and Creep Tests of Plastics

By C. E. STAFF,[1] H. M. QUACKENBOS, Jr.,[2] and J. M. HILL,[1] BLOOMFIELD, N. J.

Thermosetting and thermoplastic materials have been maintained under constant load at 25 C and 75 C for periods ranging from 1000 to 14,500 hr. Creep was measured with electric strain gages and, from its course, an estimate has been made of the maximum stresses that can be sustained for 5 years by the thermosetting materials. Both creep and crazing govern the maximum stresses for the thermoplastics, and these have been estimated for 1 year. An examination has been made of the accuracy and precision of the electric strain gage in measurements of creep. It is believed that the results are not confined to use in potential structural applications but have their greatest value in many current problems.

INTRODUCTION

OVER the past 8 years more than a dozen papers have appeared on the creep of rigid plastics and yet our knowledge is far from complete. The common laminates have been fairly well covered, but tests on thermosetting products have not exceeded 1000 hr (1, 2, 3)[3] with one exception (4), and of the thermoplastics only cellulose acetate and polymethylmethacrylate have been investigated (5, 6). It is the aim of this paper to provide more information about the thermoplastic and thermosetting plastics.

Creep tests for plastics have usually been justified in the past for two reasons: (*a*) The results were thought to be connected with fundamental physical properties. In the present paper this aspect will be neglected, although the physical chemist is not excluded from making his own interpretation. (*b*) Plastics were on the threshold of light structural uses. Good creep data, of course, will always find use in structural design, but this study was pursued mainly with the conviction that the results relate to many present applications.

It is not generally recognized that two practical aspects of creep, namely, sustained stress and continuing deformation, affect so many common molded parts. Examples are fan blades resisting centrifugal stresses, material around metal inserts under stresses that have arisen from differential contraction, parts under stress from differential water absorption, objects bearing direct load (e.g., coat hangers and bottle caps screwed tight), and moldings shrinking under the influence of high ambient temperature. Under such circumstances creep may either change tolerances or cause weakening and even fracture. The period of stress or deformation may easily be several years, and in order to avoid undue extrapolation from laboratory to field, the creep test here was usually continued 5000 hr while a few tests lasted 14,500 hr.

Creep usually has been measured with optical devices except in one laboratory (1, 2, 3), where the value of electric strain gages has been demonstrated. Such a gage was preferred here because of its economy and simplicity. The reliability of an electric gage over a long period of time has been questioned, and a secondary objective of this study was to resolve this doubt.

PROCEDURE

The thermosetting materials examined were all commercial combinations of a filler and a two-step resin polymerized from phenol and formaldehyde. The percentage and type of resin varied from one material to another. These materials were compression-molded. The thermoplastics were injection-molded with the exception of vinyl copolymer which was cut from sheet. Fifty bars of each material were prepared at the same time and kept at 25 C and 50 per cent RH until used; for periods ranging from 1 month minimum to 2 years maximum.

The procedure for most creep tests was as follows: The specimen bearing two SR-4 gages connected in series was put into the grips and hung in the rack. (These SR-4 gages, supplied by Baldwin-Southwark, have been described before, reference 1). The gages were balanced electrically, as shown by an SR-4 meter, against two other ("dummy") gages on a similar specimen, or on a steel bar, hanging nearby under no load. Specimens and clamps are shown in Fig. 1. Ten-point switches designed for use with thermocouples were found satisfactory in allowing several specimens and their dummies to be connected to the SR-4 meter in turn. Load was applied directly with iron or lead weights to a pan hooked to the lower grip. Ten 20-lb weights gave a stress of about 3200 psi in the specimen. Strain was observed for each increment of load during loading, in order to determine modulus of elasticity. After loading, strain was observed every one, two, or three days, depending on the duration of the test. Elastic and delayed recovery on unloading were also observed when desired.

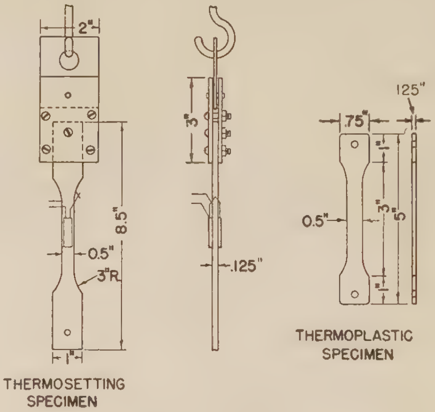

Fig. 1 Specimens, One Grip and Hook for Loading in Creep Tests

Two ambient conditions were maintained; 25 C and 50 per cent RH in a conditioned room, and 75 C and uncontrolled low relative humidity in an ordinary air-circulating oven. Holes were drilled in this oven, and it was supported so as to surround only the specimen and grips. The weights and frame were outside.

---

[1] Research and Development Department, Bakelite Corporation.

[2] Research Engineer, Bakelite Corporation. Jun. ASME.

[3] Numbers in parentheses refer to Bibliography at end of paper.

Contributed by the Rubber and Plastics Division and presented at the Annual Meeting, New York, N. Y., November 27–December 2, 1949, of The American Society of Mechanical Engineers.

Note: Statements and opinions advanced in papers are to be understood as individual expressions of their authors and not those of the Society. Paper No. 49—A-61.

At 25 C and at 75 C the dummy gages were cemented to a specimen resembling that under test. Such a practice is supposed to eliminate fluctuations arising from minor variations in temperature. At 75 C, in addition, the dummies were carried on steel bars.

Tensile tests were made at 25 C and 75 C in a testing machine, and strain to failure was measured usually with a mechanical extensometer at 75 C and SR-4 gages at 25 C. The specimens for tensile tests at 75 C were first exposed for 100 days at that temperature. Details of procedure appear in the Appendix.

Discussion

Creep of Thermosetting Materials. Creep curves are of most value when they are linear and so can be extrapolated if wished. Four of the six materials tested at 25 C followed a course that was linear on logarithmic co-ordinates. These four had fillers, respectively, of woodflour, floc, kraft paper, and fabric. Two of them are illustrated in Figs. 2 and 3. Note that the ordinate is total deformation, the sum of the initial elastic deformation, which occurs immediately on loading, and creep which accumulates with time.

With a filler of asbestos, the creep curve eventually becomes a straight line on rectangular rather than logarithmic co-ordinates, Fig. 4. When the filler is mica, the creep is so small, Fig. 5, that it might be interpreted as linear on almost any kind of plot.

The original points usually have been omitted, in order to make the diagrams more effective. The points were first plotted on rectangular co-ordinates and the best smooth curve was drawn through them, as illustrated for one curve in Fig. 4. Where the co-ordinates are rectangular, the diagrams in this paper show this curve alone, and where logarithmic, the few points shown have been taken from this original curve.

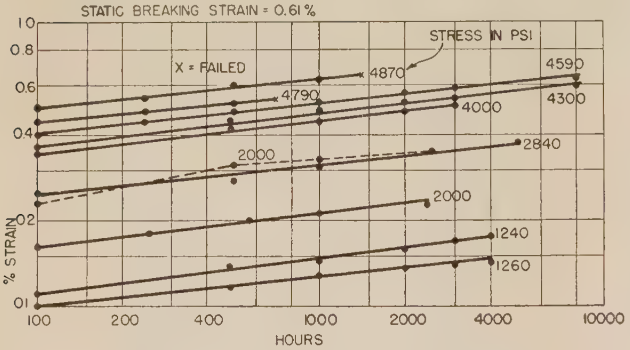

Fig. 2 Creep at 25 C for Combination of Woodflour and Phenolformaldehyde Resin

(Strain shown includes initial elastic deformation which was 0.078 per cent per 1000 psi. Lines not straight in this and in Fig. 3 are dotted.)

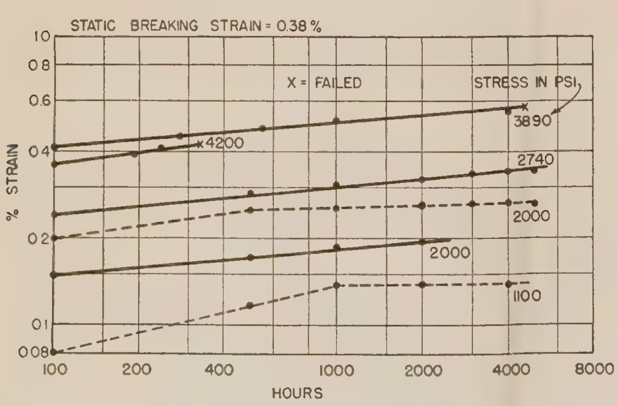

Fig. 3 Creep at 25 C for Combination of Macerated Fabric and Phenolformaldehyde Resin

(Not shown are two tests at 4450 and 4830 psi which ended in failure in 1–3 days with total deformations of 0.42 per cent and 0.44 per cent, respectively. Strain shown includes initial elastic deformation which was 0.067 per cent per 1000 psi.)

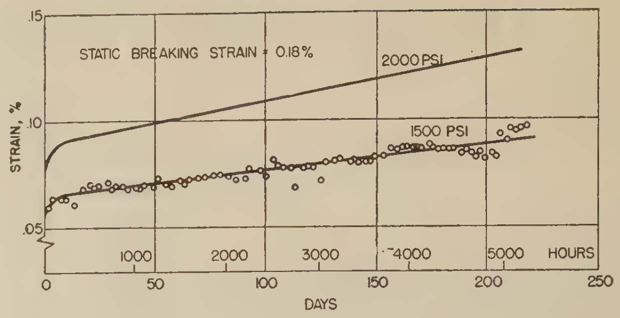

Fig. 4 Creep at 25 C for Combination of Asbestos and Phenolformaldehyde Resin

(Strain at zero time represents initial elastic deformation.)

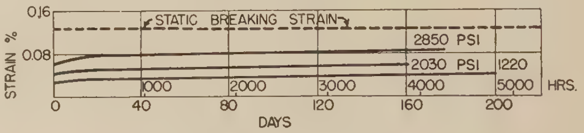

Fig. 5 Creep at 25 C for Combination of Mica and Phenolformaldehyde Resin

(Strain at zero time represents initial elastic deformation.)

At 75 C creep and shrinkage go on together. Creep itself is measured by comparing the stressed specimen with an unstressed one at the same temperature. Figs. 6 and 7 show the same tendency to linearity as at 25 C. The net strain was given by reference to a steel bar at 75 C, and shrinkage was taken as creep minus net strain. Shrinkage itself follows a linear course on a semilogarithmic plot, Fig. 8, and was found independent of stress.

In introducing the subject of creep, it was mentioned that continuing deformation is of practical importance. Figs. 2 to 7, inclusive, inform us of deformation under stress, and Fig. 8 is of interest in connection with operation at an elevated temperature under no stress. All the lines may be extrapolated to longer times if wished.

Sustained stress is also of importance, and one often wishes to know the maximum stress that can be borne without failure for, say, 5 years. In this connection consider Fig. 3. Four tests ended in failure in a period of 180 days, and in each the total deformation (elastic plus creep) was somewhat in excess of that measured in failure in the short-time tensile test. A similar tendency at 25 C was noted in Fig. 2. At 75 C one failure for each of three materials occurred at the corresponding level of deformation.

Thus the 5-year strength is established by finding a stress such that the creep line extrapolated to 5 years does not quite reach the level of tensile breaking strain. Strengths predicted in this way are presented in Table 1. The estimates are conservative, especially at 75 C where the creep data are rather incomplete.

In order to fortify these predictions, one specimen of each material was kept loaded for 19 months (14,500 hr) at 25 C, Fig. 9. The woodflour and asbestos materials, under higher stresses than those predicted, almost reach the dangerous levels, and the lower stresses of Table 1 are more appropriate. The others withstand comfortably the predicted stresses.

There are two points of practical importance about these long-time strengths; (*a*) they are quite low in relation to the tensile strengths, (*b*) they hold only for unnotched specimens. If a sharp notch (or equivalent) is present in the specimen or in a

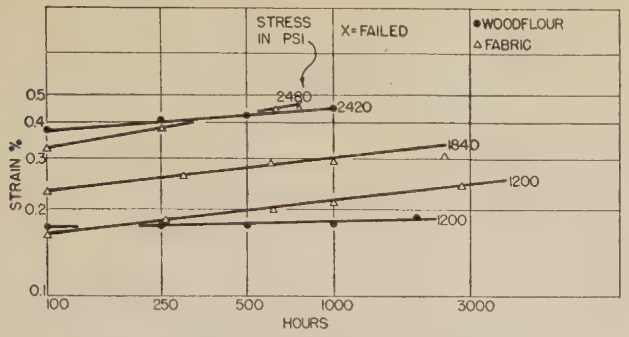

FIG. 6 CREEP AT 75 C FOR PHENOLFORMALDEHYDE RESIN COMBINED WITH FILLERS INDICATED

(Strain shown includes initial elastic deformation, which was about 0.098 per cent for each 1000 psi woodflour and 0.084 per cent fabric, but excludes shrinkage.)

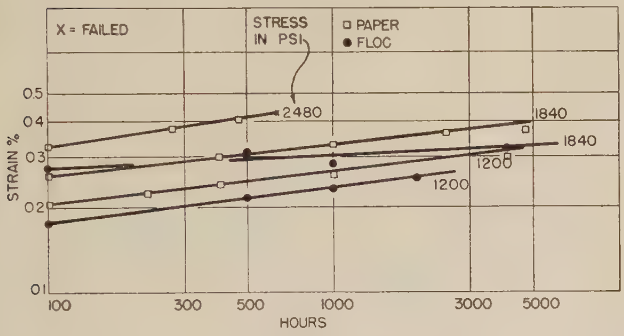

FIG. 7 CREEP AT 75 C FOR PHENOLFORMALDEHYDE RESIN COMBINED WITH FILLERS INDICATED

(Strain shown includes initial elastic deformation, which was about 0.090 per cent for each 1000 psi with both materials, but excludes shrinkage.)

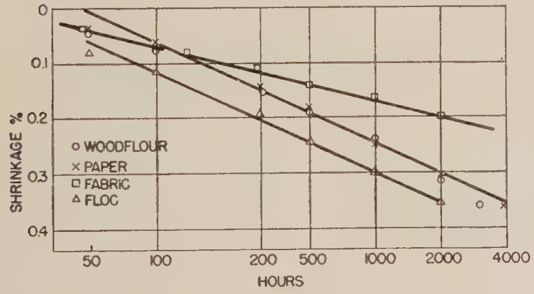

FIG. 8 SHRINKAGE AT 75 C FOR PHENOLFORMALDEHYDE RESIN COMBINED WITH FILLERS INDICATED

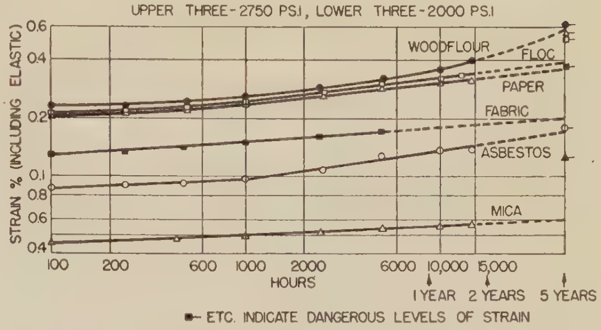

FIG. 9 CREEP TESTS LASTING 14,500 HR AT 25 C FOR SEVERAL THERMOSETTING MATERIALS

(Elastic deformations as in Figs. 2–5.)

molded object, the figure should be divided by the "notch sensitivity" of Table 1.

A quantitative relation between creep and stress is usually of interest. It is remarkable that one equation covers the four materials having fillers of woodflour, fabric, paper, and floc, namely

$$\log_{10}\left(\frac{\epsilon}{\sigma}\right) = 0.103 \log_{10} t + 0.713 \ldots\ldots\ldots\ldots [1]$$

where

t = time, hr
ϵ = per cent strain (elastic plus creep) $\times 10^5$
σ = stress, psi

Within ±20 per cent, this line describes the results for Figs. 2, 3, and 9, and for the data not illustrated for the flock and paper fillers—at four stresses for each, ranging from 1180 to 2750 psi maintained for 2500 to 5000 hr. The exceptions are the three curves in Figs. 2 and 3 that are not linear, and the curve which begins to curve upward at longer times. The equation is not valid for times less than 50 hr.

At 75 C a similar equation correlates the results except that creep is about 1.5 times greater at any given time. The results are more scattered, reflecting some instability of the electric circuit at that temperature.

In several papers, one of Findley's, for example (5), appear graphs relating stress versus time to fracture. For four materials here, Equation [1] can be manipulated, in conjunction with the constant level of critical breaking strain, to demonstrate that such a graph would be linear on logarithmic co-ordinates.

Relaxation, or the decline of load necessary to maintain constant strain, is sometimes of interest. Usually the greater the creep the greater the relaxation. A closer connection has not been evolved except for thermoplastics under high temperature. One relaxation curve is shown in Fig. 10.

No extensive measurements were taken of creep recovery after unloading. Instantaneous elastic recovery at 25 C is equal to the

TABLE 1 PREDICTED LONG-TIME (5-YEAR) TENSILE STRENGTHS OF PHENOL-FORMALDEHYDE MATERIALS

	25 C				75 C		
Filler	Tensile strength, psi	Tensile modulus psi × 10⁻⁶	5-year strength, psi	Notch sensitivity	Tensile strength, psi	Tensile modulus, psi × 10⁻⁶	5-year strength, psi
Woodflour	7800	1.28	2000	2.0	8000	1.30	1200
Asbestos	4400	2.47	1500	1.7	4800	2.3	...
Chopped kraft paper	7700	1.42	2700	1.3	6500	1.39	1200
Macerated fabric	5600	1.49	2000	1.0	5600	1.45	1200
Cotton floc	7500	1.40	2700	1.4	6100	1.48	1200
Mica	5700	4.5	2000	1.3	6000	...	...

NOTE: Products are commercial. Type and content of resin varied. They were all virtually linear to failure in tension and strain to failure can be found by dividing strength by modulus of elasticity. Notch sensitivity is the ratio of the breaking load in flexure for an unnotched bar 0.4 in. deep to the breaking load for a bar 0.5 in. deep containing the standard ASTM notch (0.1 in. deep, 0.01 in. radius) in the lower face.

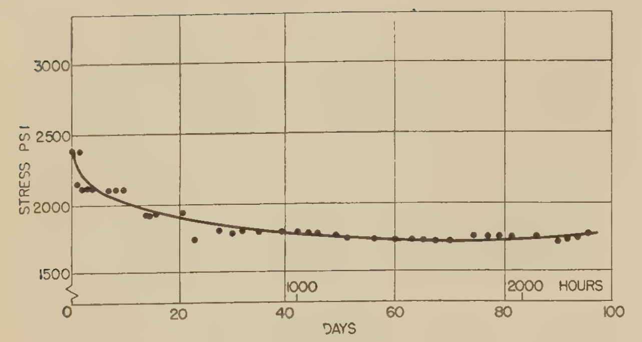

Fig. 10 Relaxation—Constant Strain—at 25 C of a Thermosetting Material With a Filler of Kraft Paper
(Initial stress was 2400 psi.)

original elastic deformation. In thirteen instances the difference between these two elastic deformations averaged 0.004 per cent only. After the usual exposure to 75 C for 1 hr before a creep test was started, the modulus of elasticity was about 20 per cent lower than at 25 C. The instantaneous recovery on unloading after several hundred hours at 75 C was always lower than the initial elastic deformation, because the modulus had risen about 20 per cent in that time.

Few other results exist for comparison. The several materials exposed for 1000 hr by Telfair, Carswell, and Nason (1), and the one material for several thousand hours by Findley (4) resemble the ones in this paper. The curves are not linear on rectangular or semilogarithmic co-ordinates but might become linear on logarithmic co-ordinates. The creep deformation is of the same order. The several authors of the one paper predict, by a procedure not described, a "stress below which no practical danger of failure exists." The predictions agree with those of Table 1. In spite of this apparent success of forecasts based on 1000 hr, it is suggested that a new material be run at least 5000 hr. Lower times might be sufficient for a product resembling quite closely one already tested.

It has been suggested (2) that elevated temperatures promote further curing and hence shrinkage in molded thermosetting specimens. Another possibility is that such shrinkage is connected with the loss of water by diffusion. Under conditions when further curing is probably absent (vacuum desiccation at 25 C), a woodflour-filled material shrinks about 0.20 per cent for each per cent of weight lost.

Measurements of the weight for a woodflour material at 75 C showed a loss of 2.4 per cent at 250 hr. At 1000 hr the loss reached 3 per cent and remained constant for longer times. If these losses are assumed to be all water, they are far too large to account for the shrinkage observed, assuming a shrinkage of 0.2 per cent for each per cent lost. It is not permissible to assume that other volatiles were lost and that the water alone would account for the shrinkage, because shrinkage continues after 1000 hr, although weight loss ceases. It is probable that shrinkage at 75 C is caused both by loss of water and by further curing.

Creep of Thermoplastics. The curves relating deformation and time generally become linear when plotted in the same way as the thermosetting materials, Fig. 11, 12, and 13. The cellulose plastics are exceptions, and their curves are shown on rectangular co-ordinates, Fig. 14. A comparison of creep alone for several thermoplastics is given in Fig. 15.

The data are not comprehensive enough to allow stress to be correlated with creep as in Equation [1]. Judging from results at two stresses, deformation increases out of proportion to stress. Temperature has a tremendous effect on creep. For example, between 24 hr and 2400 hr, polystyrene creeps 0.6 per cent under 3600 psi at 25 C, and at 75 C creeps the same amount under 400

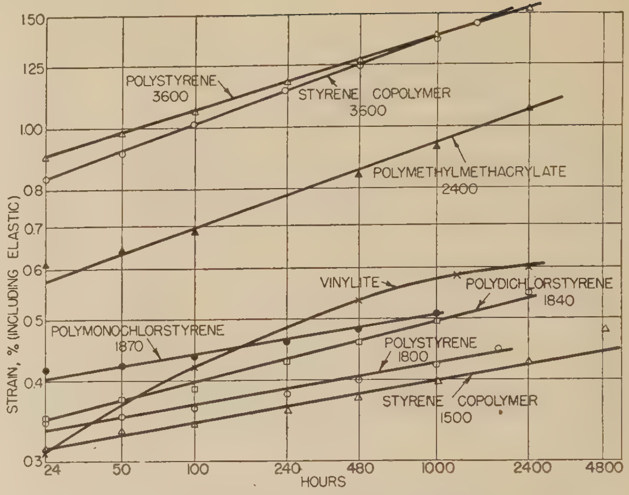

Fig. 11 Creep at 25 C for Various Thermoplastics
(Figure against each line represents stress in pounds per square inch. Initial elastic deformation included in strain shown may be calculated from moduli of Table 2.)

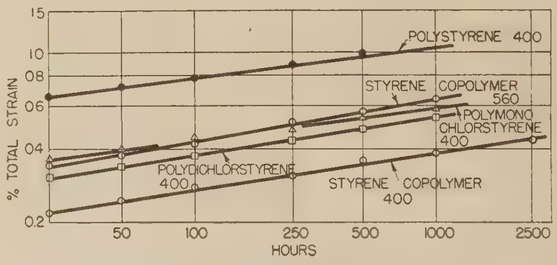

Fig. 12 Creep at 75 C for Various Thermoplastics at Stresses Shown in Pounds per Square Inch
(Strain shown includes initial elastic deformation but excludes shrinkage.)

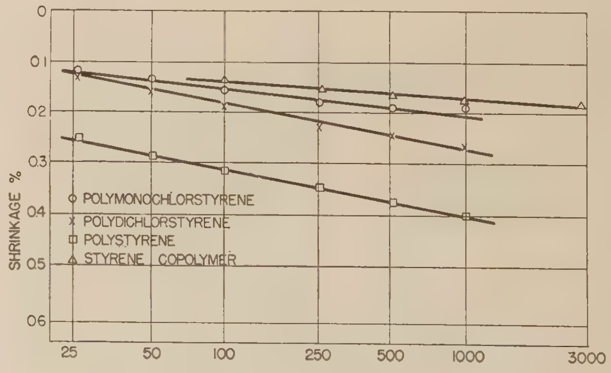

Fig. 13 Shrinkage of Thermoplastics at 75 C

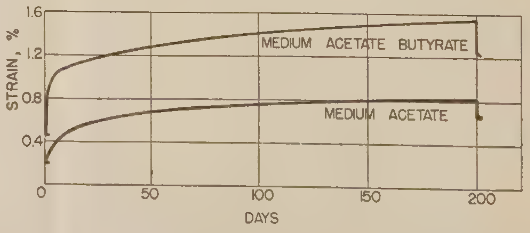

Fig. 14 Creep of Cellulosic Plastics at 25 C Under 640 Psi
(Strain at zero time represents initial elastic deformation.)

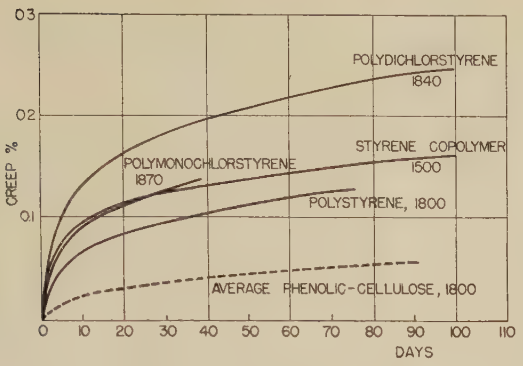

Fig. 15 Creep Alone of Thermoplastics at 25 C
(Figures represent stresses in pounds per square inch.)

psi. The ratio of nine (3600/400) for polystyrene is lower for the other styrene polymers.

Several thermoplastics differ from other thermoplastics, and from thermosetting and laminated products, in that they can soon exhibit crazing or internal cracking under sustained load. Such crazing promotes premature failure. For example, polystyrene under 1800 psi at 25 C exhibits quite low creep, Fig. 11, and yet separation into two parts occurred in one test after 5700 hr. At a lower stress, 1200 psi, there is no danger of failure under 10,000 hr but definite craze marks were observed in 5 to 10 days. The user of polystyrene probably would feel uneasy or dissatisfied if craze marks did appear, and their appearance can be considered as defining failure.

This phenomenon of crazing under stress was observed with polystyrene from several sources, with annealed polystyrene, with a copolymer of styrene and acrylonitrile, and with polychlorstyrenes. Crazing occurred when SR-4 gages were not applied and therefore it cannot have arisen because of chemical attack by the cement. There was no crazing under the low stresses used at 75 C, and a limiting deformation provides the criterion of failure, as described in the following.

Crazing was not observed at 25 C with the cellulose plastics, with "Vinylite" (a copolymer of vinyl chloride and vinyl acetate), or with polymethylmethacrylate. (Under 3600–5400 psi the last was found to craze by Chasman, reference 6. The stresses exceed those suitable for enduring use.) With these plastics that do not craze, the deformation to failure, whether in a short or a long time, is much in excess of 1 per cent. However, a deformation of 1 per cent is usually the acceptable limit. A bar 8 in. long and 0.5 in. × 0.5 in. in section when clamped at one end would deflect 0.8 in. at the other if the load there caused a strain of 1 per cent at the clamped end. Accordingly, the long-time strength will be such that the total deformation does not exceed 1 per cent. At 75 C the proper curves to which this criterion should be applied are those representing net deformation (total deformation minus shrinkage). However, there is so little knowledge of behavior at 75 C that a factor of safety will be applied by considering total deformation.

With the criteria of failure discussed in the foregoing, one can estimate long-time strengths. The data are less thorough than those for the thermosetting materials, and the predictions of Table 2 are for 1 year. The estimates are conservative. With polymethylmethacrylate at 25 C and polystyrene at 75 C, there are no creep data at the estimated stresses, and the very rough approximation was used that total creep is proportional to stress.

The results of Table 2 may be discussed in several ways. Thermoplastics often have a higher tensile strength but are less satisfactory for service under enduring stress than thermosetting materials. The heat distortion temperatures (ASTM D648-45T) for the four polymers of styrene are polystyrene, 83 C, copolymer of styrene and acrylonitrile, 92 C, polymonochlorstyrene, 100 C, polydichlorstyrene, 106 C. Evidently these values are a poor reflection of the serviceability at 75 C indicated by creep tests.

The problem of cracking around inserts may be analyzed. When a piece containing an insert cools after molding, stresses arise because the plastic shrinks more than the metal. At room temperature a stress will be present of a magnitude depending on the temperature at which the plastic becomes rigid and on the coefficient of expansion. With the four styrene polymers of Table 2, the coefficient of expansion falls as softening point rises in such a way that the expected stress is about the same for all. Their tendency to crack around inserts will be governed, therefore, by their long-time strengths at 25 C. Accordingly, polystyrene would crack most readily around inserts. There has been some practical confirmation of this.

The reason for the shrinkage of thermoplastics at 75 C is not known. The loss in weight of the styrene polymers is quite small. It reaches 0.1–0.5 per cent at 100 hr and remains constant for longer times. Coiling of the polymer chains probably accounts for shrinkage at 75 C.

Reliability of SR-4 Gage. Popular suspicion still attaches to the measurement of creep by electric strain gages. There are questions as to the reliability of the bond between the specimen and the gage, and as to the constancy of the electrical circuit over a period of time. The following experiments were designed to resolve the doubts.

The creep of a vinyl copolymer under 1560 psi at 25 C was measured simultaneously by dial gages, reading to 0.0001 in., and by SR-4 gages cemented with "Duco" cement. The specimen cut from a sheet 0.1 in. thick was made long to increase the accuracy of the dial gages. These gages were supported by the testing frame and were held against the edge of the specimen by the spring of the gage, contact being confined to a small area by means of clips, Fig. 16. The use of two dial gages eliminates any effect arising when the specimen shifts slightly in the upper grip or jaw. The SR-4 gages were applied on both sides in two locations to give a mean result. The creep shown by the SR-4 gages is lower than that given by the dial gages, Fig. 17.

Part of the discrepancy in Fig. 17 may arise because the elec-

TABLE 2 PREDICTED LONG-TIME (ONE YEAR) TENSILE STRENGTHS OF THERMOPLASTICS

	25 C				75 C
Material	Tensile strength, psi	Tensile modulus, psi × 10^{-6}	Strain to failure, %	One-year strength, psi	One-year strength, psi
Polystyrene...	7500	0.48	2.1	800	250
Polymonochlorstyrene........	9500	0.52	2.5	1200	400
Polydichlorstyrene..	5900	0.60	1.0	1500	400
Styrene-acrylonitrile copolymer	9100	0.43	2.2	1500	560
"Vinylite"[a]	...	...	...	1600	...
Cellulose acetate[a]	6700	0.35	5.5	600	...
Cellulose acetate-butyrate[a]...	3900	0.16	9.5	less than 600	...
Polymethylmethacrylate[a].....	10100	0.43	4.2	2000	...

---

[a] Properties can vary with the mode of preparation. This is especially true with the cellulose plastics. "Medium" cellulose acetate and cellulose acetate-butyrate were used here.

tric gages actually stiffen the material in their neighborhood. After the creep experiment the central portion of the specimen in Fig. 16 was cut out and pulled in tension. The electric gages and mechanical extensometers applied to span them showed 15 per cent less elongation at a given load than mechanical extensometers outside the region covered by the electric gages. This means that of the 103 lb applied in the creep test, 15 per cent or 15.5 lb are carried by the SR-4 gages and only 87.5 pounds are taken by the adjacent vinyl copolymer. Outside the sections covered by the electric gages, the total load is of course borne by the plastic. In partial confirmation, one SR-4 gage (coated with Duco cement) when loaded by itself needed about 4 lb to register the initial elastic deformation of 0.248 per cent.

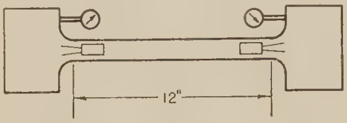

Fig. 16 Measurement of Creep by Electric and Dial Gages on a Piece of Vinylite, 0.1 In. Thick

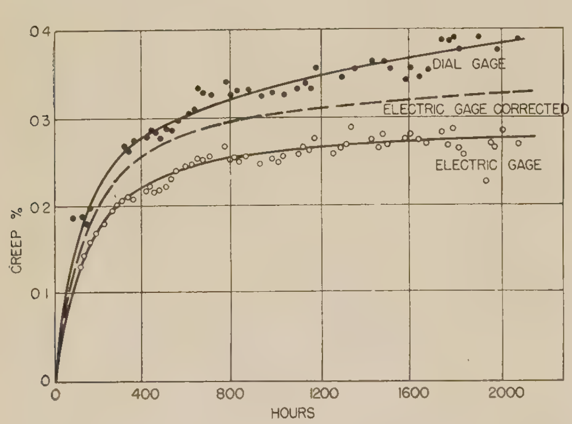

Fig. 17 Creep of Vinylite at 25 C Under 1560 Psi According to Two Kinds of Gage

(Initial elastic deformation was 0.248 per cent according to the electric gages.)

When creep starts, the load carried by the plastic may continue to be 87.5 lb or may change according to the way in which the SR-4 gage and the bond creep under their portion of load. Under the 4 lb just noted, the gage was found to creep (determined by readings on the SR-4 meter) more rapidly at first than the vinyl copolymer in Fig. 16, but after 72 hr settled down to approximately the same rate. When loaded with 7.75 lb (15.5 for two gages) the creep was much more rapid. It is uncertain whether we should prefer the load of 4 lb and the proper initial deformation of the gage, or the 7.75 lb which corresponds with the proper stiffening. It will be assumed that not only during initial loading but also during creep the plastic carries only 87.5 lb, and the adjacent gages 15.5 lb.

Therefore the creep curve using electric gages may be corrected for stiffening by multiplying all ordinates by 103/87.5, where creep is assumed proportional to stress. The corrected curve in Fig. 17 is still low, but it is fair to say that the electric gage gives a good indication of the actual creep in its area.

With several thermosetting specimens $^1/_8$ in. thick, tensile loading was applied with and without electrical gages in the section spanned by a mechanical extensometer. For duplicability it was found necessary to apply the extensometer to each edge in turn rather than to the face of the specimen. The stiffening effect was 11 per cent with fillers of woodflour, floc, and asbestos. The creep of these materials is comparatively low so that the 89 per cent of load borne initially by the specimen tends to increase during creep. If this is neglected the creep curves are about 11 per cent low.

It is easy to show theoretically that the percentage stiffening effect of the gages should be inversely proportional to the stiffness of the specimen (cross-sectional area × modulus of elasticity). On this basis the stiffening effect for the thermosetting products, predicted from the 15 per cent for the vinyl copolymer, should be 4–6 per cent instead of the 11 per cent observed. This theoretical relation brings out that the thinner the specimen the greater the stiffening effect. It is not proper to measure creep on plastic specimens much under 0.10 in. thick. (Further, high sustained strains much exceeding 1 per cent probably cannot be measured reliably.)

The constancy of the electrical circuit over a period of time may be estimated by a method suggested by Tschebotarioff (7). Two pairs of electric gages are affixed to opposite ends of a steel bar, Fig. 18. A first reading is taken with the pairs connected in one way to the SR-4 meter (A → 1, B → 2) and a second with the pairs interchanged (A → 2, B → 1), by means of switches. The meter has been simplified to make the whole circuit a Wheatstone bridge. The same process is repeated daily. Typical readings are as follows:

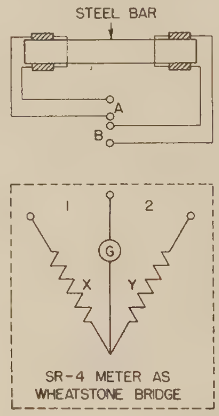

Fig. 18 Measuring Variability of Electric Circuit

	First reading	Δ_1	Second reading	Δ_2	$\frac{\Delta_1 - \Delta}{2}$	$\frac{\Delta_1 + \Delta_2}{2}$
Feb. 1	7-1120	. .	0-940	. .	. .	. .
Feb. 2	7-1080	—40	0-980	+40	—40	0
Feb. 3	7-1070	—50	0-950	+10	—30	—20

Now two kinds of changes occur from day to day in the circuit in Fig. 18. The first is in the circuits of A and B, whether in the leads or switches (gages assumed to remain constant). Let it be a. It appears always as the difference between the changes that have occurred in A and B. The second change takes place in other parts of the circuit, for example, in the fixed resistance X. Let it be x. Therefore

$$\Delta_1 = a + x \qquad [2]$$

$$\Delta_2 = x - a \qquad [3]$$

where the deltas have the meanings in the foregoing tabulation. Hence

$$x = {}^1/_2\,(\Delta_1 + \Delta_2),\text{ and } a = {}^1/_2\,(\Delta_1 - \Delta_2) \qquad [4]$$

The changes x, in the "permanent" part of the circuit for a period exceeding 2 years are shown in Fig. 19. Generally these fluctuations, expressed as strain in microinches/in., are not large, although no special precautions were taken. In the foregoing argument no account was taken of changes that may occur in the switches when A and B are interchanged in the bridge circuit. Such variations in switching are part of the changes in the permanent portion of the circuit. Usually, they are quite small (±10 microinches/in., as shown by repeated switching).

The changes *a*, may vary according to whether the changes in the individual circuits A and B happen to add or subtract. Over a period of 2 years they were usually ±50 microinches/in.

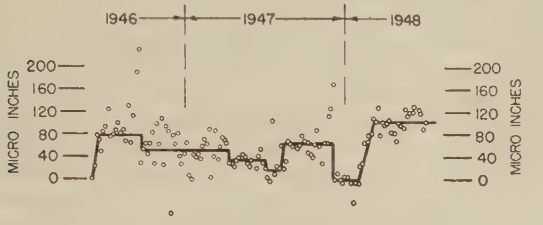

FIG. 19 VARIABILITY OF PERMANENT PART OF ELECTRIC CIRCUIT, EXPRESSED IN MICROINCHES

No check was made of reliability at 75 C. In another paper (1) a steel bar, carrying the AB gage recommended for measurements at 75 C (see Appendix) was bent beyond the elastic limit and held that way for one month at 75 C. The reading on the SR-4 meter did not change in that time, and the bond and circuit were concluded to be good.

BIBLIOGRAPHY

1 "Creep Properties of Molded Phenolic Plastics," by D. Telfair, T. S. Carswell, and H. K. Nason, *Modern Plastics*, vol. 21, February, 1944, pp. 137–144 and 174.

2 "Creep Properties of Molded Phenolic Plastics at Elevated Temperatures," by W. J. Gailus and D. Telfair, *Modern Plastics*, vol. 22, May, 1945, pp. 149–154 and 192.

3 "Creep, Long-Time Tensile and Flexural Fatigue Properties of Melamine and Phenolic-Plastics Materials." by D. Telfair, C. H. Adams, and H. W. Mohrman, Trans. ASME, vol. 69, 1947, pp. 789–793.

4 "Mechanical Tests of Macerated Phenolic Molding Material," by W. N. Findley, *Modern Plastics*, vol. 25, December 1947, pp. 145–150, 218 and 238.

5 "Mechanical Tests of Cellulose Acetate," by W. N. Findley, *Modern Plastics*, vol. 19, September, 1941, pp. 57–62 and 78; vol. 19, August, 1942, pp. 71–73 and 114.

6 "Creep and Time-Fracture Strength of Plastics Under Tensile Stresses," by B. Chasman, *Modern Plastics*, vol. 21, February, 1944, pp. 145–148 and 176.

7 "Use of Electric Resistivity Strain Gages Over Long Periods of Time," by G. Tschebotarioff, *Experimental Stress Analysis*, vol. 3, 1946, pp. 47–52.

Appendix

As an adhesive for electric strain gages, "Duco" cement has been found satisfactory at 25 C for most common plastics except the polymers of styrene. The Duco cement produces a multitude of tiny superficial cracks in these. Such crazing is slight and the bond with the gage is good for the polymers of styrene other than polystyrene. With polystyrene the crazing is bad and the bond is firm only for a few days. Three cements that are effective with polystyrene are a solution of polyvinyl acetate in acetone, a solution of polystrene in benzene and cold-setting glue (resorcinol-formaldehyde) normally used for wood. The latter is good only for small strains up to 1 per cent. When the adhesive is dry, the adhesion should be good enough to allow the gage to withstand prying with the fingernail and flexing of the test specimen by hand. If the gage is firmly attached it will usually give a proper measurement of creep. If the result is unexpectedly low it is advisable to check it with a gage bonded with another adhesive or with dial gages. Finding that initial elastic deformation and instantaneous recovery after creep are equal is no assurance of the bond; it happened with a gage cemented to polystyrene with an aqueous emulsion of polyvinyl acetate whereas the creep under 1800 psi at 25 C appeared to be slightly negative.

For measuring strain at 75 C the special AB gages were applied to the thermosetting specimens. These gages have a special backing and are cemented with a thermosetting glue that must be baked at 100 C. Such a baking cycle rules them out with thermoplastics and so cold-setting glue or Duco cement was used with the ordinary paper gage. The results so obtained were judged reliable because the strains with gages affixed in this way to a thermosetting specimen agreed with those shown by AB gages on the same specimen up to 1000 hr. At that time the paper gage is somewhat charred. Between 1000 and 3000 hr the two curves diverge slightly and the charring becomes serious.

Apart from having the SR-4 gage well cemented, only the following precautions need be observed:

1 At elevated temperatures the dummy must be renewed for each test because it shrinks.

2 Switches should be cleaned every one or two weeks with a solvent and sandpaper to maintain fresh contacts of negligible resistance.

3 In the portable SR-4 meter, the enclosed batteries are small and they may be replaced advantageously with larger, more enduring batteries outside the meter. The sensitivity of the meter falls rapidly as the batteries become exhausted.

Discussion

JAMES BAILEY.[4] The fact that the authors' specimens broke at unusually low stresses and that the cracks started in the interior of the injection-molded test specimens, indicates that the specimens had an inside portion which was under an initial tension due to thermal strains. Test specimens which had been annealed might show substantially higher long-time strength. Were the test specimens annealed?

HARRY MAJORS, JR.[5] The authors have included as a third part of their paper the reliability of a bonded-wire resistance strain gage over long periods of time. It is to be noted that they do not mention what method was used for waterproofing the active gage and the dummy compensating gage. For precision work some system of waterproofing is desirable even though the laboratory conditions are fixed. Zero drift usually accompanies absorption of moisture which is due to the effect between that of the dummy compensating gage and the active gage.

A method of determining the constancy of the SR-4 strain indicator as used by Mr. Ruge and Mr. Tschebotarioff is explained in the paper. It would have been interesting if the method had been extended to determine the constancy of the wire resistance gages mounted on a similar test specimen as the specimen under the creep test, but maintained at "zero stress" near the active specimen throughout the total time of testing. If this had been carried out using wire gages from the same lot and adequately waterproofed, one would have a measure of the constancy of the active measuring gages as well as that of the SR-4 strain indicator.

Fig. 16 of the paper is in conflict with the results in Fig. 17. The dial gages measure not only the uniform strain in the specimen, but also the increase in strain due to the stress concentration at the fillet. One would have been more satisfied if the dial gages were arranged so as to measure the strain in the straight section only, and if the wire gages had been moved just a bit more toward the center.

---

[4] Vice-President and Research Director, Plax Corporation, Hartford, Conn.

[5] Director, Engineering Experiment Station, University of Alabama, University, Ala.

This paper is a further contribution to the correct technique in applying wire gages to the study of plastics.

AUTHORS' CLOSURE

The answer to Mr. Bailey is that the results are for thermoplastics that were not annealed. However, when polystyrene was found to craze at such low stresses, several fresh specimens were annealed and submitted to a sustained stress of 1500 psi. Crazing was observed to appear to the same extent as for specimens that were not annealed. The annealed specimens were free of residual stress according to Mr. Bailey's test (no cracking of the specimen when drilled with holes of $^1/_{16}$ in. diam and immersed in kerosene).

Although Mr. Majors commends waterproofing we did not use it at all. In the first place it seemed unnecessary, in a laboratory maintained at constant temperature and humidity, for the degree of precision needed, and second we wished to avoid complications that would deter routine groups from considering this method. The changes a discussed in the paper include any effects of humidity on the gages and leads. In regard to these changes a and the changes x we seem to have induced a misunderstanding. The changes a ($\pm$ 50 microinches/in.) include changes in the sensitive wires of the gage and in the leads and in the switches outside the SR-4 meter. While these changes were measured for gages on a steel bar they should apply equally well to the active or dummy plastic specimens. Perhaps Mr. Majors is considering changes that we neglected; for example, two ends of a molded bar may gain or lose very slightly different amounts of water in attaining equilibrium with the ambient air, and in consequence may undergo a very slight differential change. This would show up in his proposed extension of the method to a plastic dummy but would not appear in our estimates of a. Fig. 16 is a pictorial representation prepared by a draftsman. The electric gages were actually close to the center of the specimen. The dial gages unavoidably measured the extension of a uniform 12-in. length and the extensions of two flared areas of small effective length.

Even a large error in an estimate of these effective lengths would hardly affect to $\pm$ 5 per cent the over-all length to be used in reducing the extension to a strain.

Accelerated-Cavitation Research

By W. J. RHEINGANS,[1] MILWAUKEE, WIS.

The cavitation-pitting tests described in this paper were made with an accelerated-cavitation machine of the vibratory type. An attempt was made to solve some of the phenomena of cavitation by varying the amplitude of vibration, by varying the depth of submergence of the test specimen in the test liquid, and by using alkalis, acids, and oils for the test liquid. Other tests were made to determine the relative resistance to pitting of recently developed materials and techniques for applying these materials. Results showed that accelerated-cavitation tests can be used to determine some of the mechanics of cavitation, as well as to indicate that some of the newly developed materials might be suitable for use on hydraulic machinery under operating conditions where cavitation occurs.

An accelerated-cavitation machine of the vibratory type was constructed by the Research Laboratory of the author's company in 1948, and was placed in operation in September of that year. It has been in continuous use ever since for making hundreds of tests on a large variety of materials to determine their relative resistance to cavitation and has also been used for investigations of some of the phenomena of cavitation and pitting.

These tests supplement the accelerated-cavitation tests made during the years 1934 to 1937, by J. M. Mousson (1),[2] and S. Logan Kerr (2), who tested almost all of the materials available at that time which were suited for use on hydraulic machinery. The development of new materials and new techniques for the application of materials since 1937, some of which have unusually high resistance to pitting or other advantages when used where cavitation occurs, indicated the necessity for continuous research of this type and resulted in the construction of the accelerated-cavitation machine described in this paper.

History of Cavitation

The following is a brief history of cavitation and the problems which brought about the development of accelerated-cavitation machines.

Cavitation as used throughout this paper is defined as the formation of voids within a body of moving liquid (or around a body moving in liquid) when the particles of liquid fail to adhere to the boundaries of the passageway. This occurs when there is insufficient internal pressure to overcome the inertia of the particles and force them to take sufficiently curved paths along a boundary which has a change or a variation in shape.

Cavitation affects the operation of hydraulic machinery in various ways. It can cause a loss of power and efficiency by increasing resistance to flow. It can produce noise and vibration and it can produce pitting which is defined as the actual erosion of material subjected to cavitation.

The phenomenon of cavitation was anticipated as early as 1754 by Leonhard Euler (3) in his theory on hydraulic turbines, when he noted that an insufficient pressure in a perfect liquid can cause a divergence between theory and experiment and can result in zero resistance.

Some of the practical aspects of cavitation were first noted in connection with ship propellers operating at high speeds. Sidney W. Barnaby and Mr. Thorncroft, in a paper presented to The Institution of Civil Engineers in London in 1895, mentioned the occurrence of a new phenomenon during propeller trials of HMS *Daring* (4). They noted the formation of cavities in water which tended to become filled with water vapor. This condition was held responsible for waste of power and other difficulties. About the same time Charles A. Parsons (5) verified this by tests on the steamship *Turbinia* where loss of power on the first steam-turbine-driven propellers was traced to cavitation.

The first recorded indication that cavitation produced erosion or pitting of materials was in an article published in 1907, by W. Wagenbach (6), in which he described how the Francis turbine runners of the Jaice hydroelectric works in Bosnia failed after a few weeks of operation in 1890. The runners were so badly eroded by cavitation that they had to be replaced. After this there were numerous reports of pitting, both on hydraulic turbine runners and on ship propellers.

However, the wide variation in the resistance of different materials to pitting is a phenomenon that was first discovered during the 1920's. It is probable that prior to this period some engineers may have suspected such variations but there is no record of any published information on actual comparative tests.

J. Ackert, in his handbook published in 1926 (7), reported the relative resistance of cast iron, cast steel, and bronze to erosion or pitting.

In 1924 a cast-iron Francis runner with 15 patch plates of various types of materials fastened to the back sides of the runner blades near the discharge edge was installed at the Isle Malign Plant in Quebec. An inspection of this runner after $3^1/_2$ years of operation showed that patch plates of stainless steel resisted pitting to a remarkable degree as compared to the cast iron in the runner, and as compared to other materials used in the remainder of the patch plates. About this time similar experiments with various materials, including stainless steel, were being made on hydraulic-turbine runners in a number of other power plants. However, it was soon realized that placing different types of material in a hydraulic turbine and then waiting a number of years for an answer was not a very satifactory method of determining the degree of resistance to pitting of these materials. The time interval was entirely too long, and there was no satisfactory method for comparing materials tried in one turbine with those tried in another.

Therefore, starting about 1932, several types of machines were developed which were capable of producing accelerated cavitation whereby the resistance of various metals to pitting could be determined accurately under laboratory control within a reasonable period of time (8).

The earlier machines used the principle of passing water at a high velocity through a restricted area, followed by a sudden enlargement. This was known as the Venturi-tube type of machine.

---

[1] Assistant Manager, Hydraulic Department, Allis-Chalmers Manufacturing Company, Milwaukee, Wis. Mem. ASME.

[2] Numbers in parentheses refer to the Bibliography at the end of the paper.

Contributed by the Hydraulic Division and presented at the Annual Meeting, New York, N. Y., November 27–December 2, 1949, of The American Society Mechanical Engineers.

Note: Statements and opinions advanced in papers are to be understood as individual expressions of their authors and not those of the Society. Manuscript received at ASME Headquarters, December 8, 1949. Paper No. 49—A-140.

In 1935 Dr. J. C. Hunsaker and Dr. H. Peters of the Massachusetts Institute of Technology, developed the vibratory method of accelerated cavitation (9, 10). This is the method used for the tests described in this article.

CAVITATION MACHINE

Fig. 1 shows a schematic layout of the vibratory type of accelerated-cavitation machine. Figs. 2 and 3 are views of the machine as originally built for temporary use, when only a few tests were being planned. However, the results of the tests were so revealing, so many new materials were being developed, and so many new ideas on the phenomena of cavitation were being advanced, that the machine has been in constant operation from the day it was completed. Since many additional tests are scheduled for this machine which may require several years to complete, it is being rebuilt in more permanent form, with cabinets for housing all of the electrical equipment, and with a neater arrangement of supports, connecting wires, and auxiliaries.

The apparatus follows the general description by S. Logan Kerr (2). It consists of a vacuum-tube oscillator which produces an alternating magnetic field through the nickel tube. When the frequency of the magnetic field is the same as the natural longitudinal frequency of vibration of the nickel tube, the tube will vibrate at maximum amplitude in the longitudinal direction.

The test specimen, Fig. 4, is attached to the end of the tube and immersed in the test fluid to a depth of $^1/_8$ in. Since the test fluid heats rapidly during a test run, the beaker containing the test fluid is set in a running-water bath to maintain a constant temperature of 76 plus or minus 1 F.

Since the frequency and amplitude of vibration of the test specimen have considerable effect on the rate of pitting, provisions are made to control these quantities at all times. The frequency of course is determined by the length of the nickel tube. The vacuum-tube oscillator circuit is tuned to the natural frequency of the nickel tube. All tests are made at a frequency of 6500 cycles per second (cps), this being the natural frequency of vibration of the nickel tube 12 in. long, with test button attached.

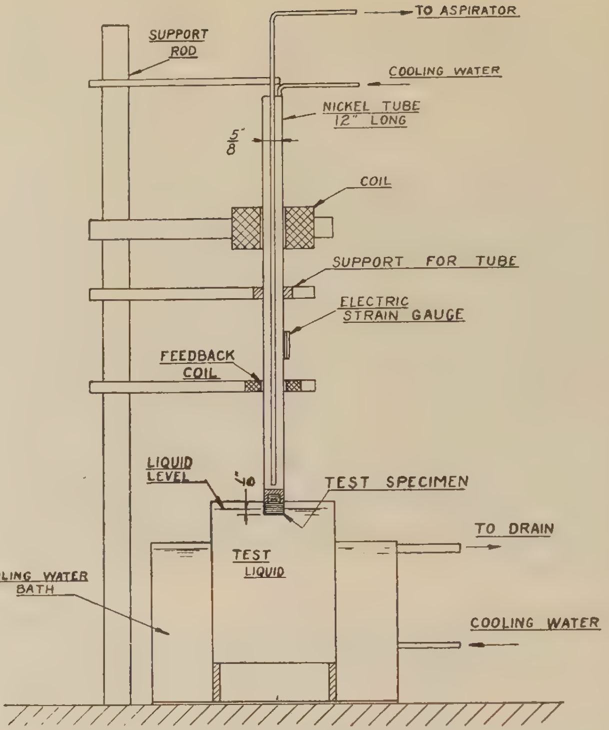

FIG. 1 SCHEMATIC LAYOUT OF VIBRATORY-TYPE ACCELERATED-CAVITATION MACHINE

An electric strain gage is attached to the nickel tube to measure the amplitude of longitudinal vibration. It is calibrated at frequent intervals by measuring the actual movement of the test specimen by means of a stroboscopic light and a microscope with

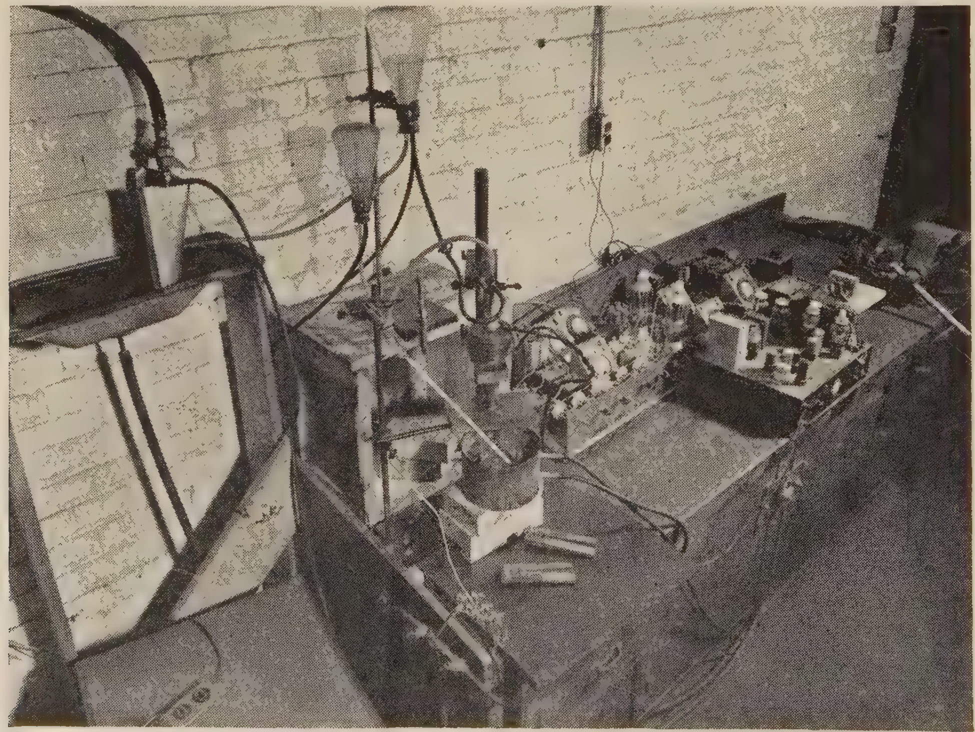

FIG. 2 HIGH-FREQUENCY OSCILLATOR AND ELECTRONIC CONTROL

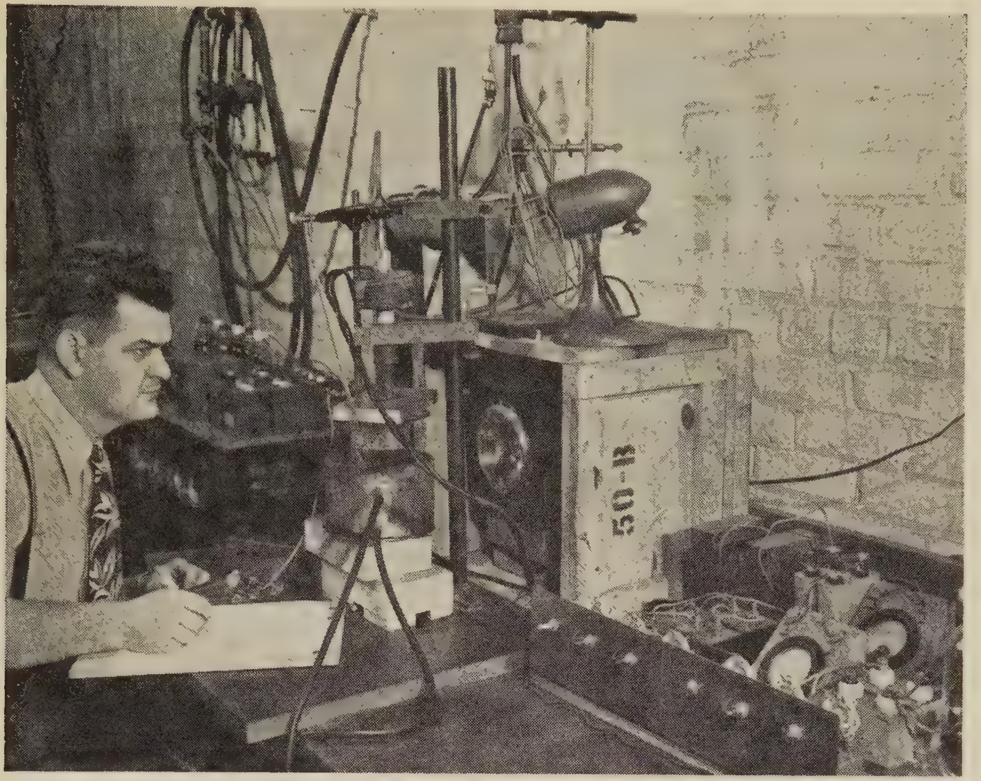

FIG. 3 HIGH-FREQUENCY OSCILLATOR

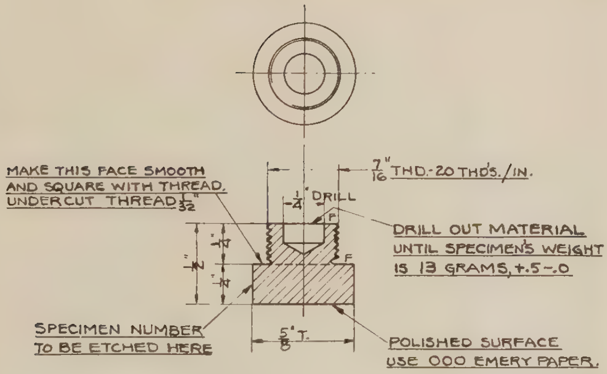

MAKE THIS FACE SMOOTH AND SQUARE WITH THREAD. UNDERCUT THREAD 1/32"
7/16" THD.-20 THD'S./IN.
1/4" DRILL
F
F
DRILL OUT MATERIAL UNTIL SPECIMEN'S WEIGHT IS 13 GRAMS, +.5 -.0
SPECIMEN NUMBER TO BE ETCHED HERE
5/8" T.
POLISHED SURFACE USE 000 EMERY PAPER.

FIG. 4 BUTTONS USED FOR TEST SPECIMENS IN CAVITATION MACHINE

micrometer scale. All tests are made with an amplitude of vibration of 0.0034 in. In this paper the amplitude of vibration refers to the total travel of the test specimen. The criterion for rate of pitting is the loss of weight of the test specimen.

METHOD OF TESTING

As a check on the relative performance of the vibratory machine, it was decided to use a brass test specimen as a standard to be tested at frequent intervals. By comparing the rate of pitting of the various standard specimens, any serious deviation in the relative performance of the apparatus becomes apparent immediately.

At first, cast bronze was used for this purpose. However, it was found that this material would pick up water and actually increase in weight during the first 30 min of testing. The standard test specimen was then changed to rolled brass, ASTM Specifications B-16-44, which gave satisfactory results.

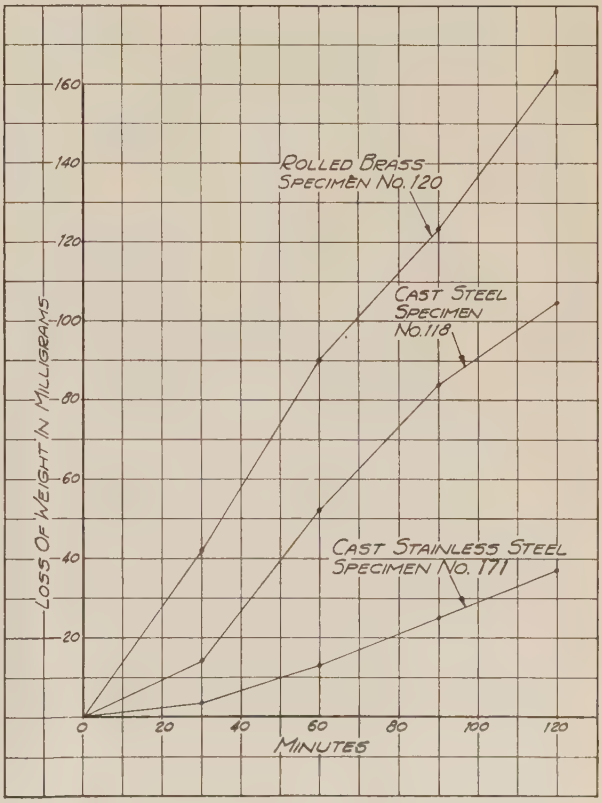

FIG. 5 LOSS OF WEIGHT OF TEST SPECIMENS

However, since most materials, particularly cast materials, have a tendency to pick up some moisture during the course of a 2-hr cavitation test, all of the test specimens are placed in boiling water for 30 min, before being tested and before being weighed.

All of the test specimens are carefully adjusted to the same weight within $^1/_2$ gram. They are all weighed accurately to the nearest $^1/_{10}$ mg in a chemical-balance scale. All specimens are weighed every 30 min during the test. It was found that the rate of loss of some of the metals increases for the first 60 to 90 min, but after that period the loss approaches a fairly constant rate. Therefore the length of each test was limited to 120 min. Fig. 5 shows how the rate of loss of metal varied with time. It was observed in several instances that a highly polished specimen had a slower rate of pitting during the first 60 min of testing than the same material with a dull finish. However, by the end of a 120-min test, the highly polished specimen would be pitting at the same rate as the duller specimen. Therefore, in comparing the relative rate of pitting of various materials, the rate of loss during the last 30 min, as well as the total loss of weight in 120 min, is used as a criterion.

Effect of Amplitude of Vibration

An interesting series of tests were made on several materials to determine the effect on the rate of pitting by changing the amplitude of vibration of the test specimen. The construction of the accelerated-cavitation machine made it possible to control the amplitude of vibration by controlling the power output of the vacuum-tube oscillator. The amplitude was measured by means of an electric strain gage fastened to the nickel tube. This strain gage was calibrated at frequent intervals by means of a microscope micrometer. During these tests the frequency of vibration was the same as for all the tests described in this paper, namely, 6500 cps.

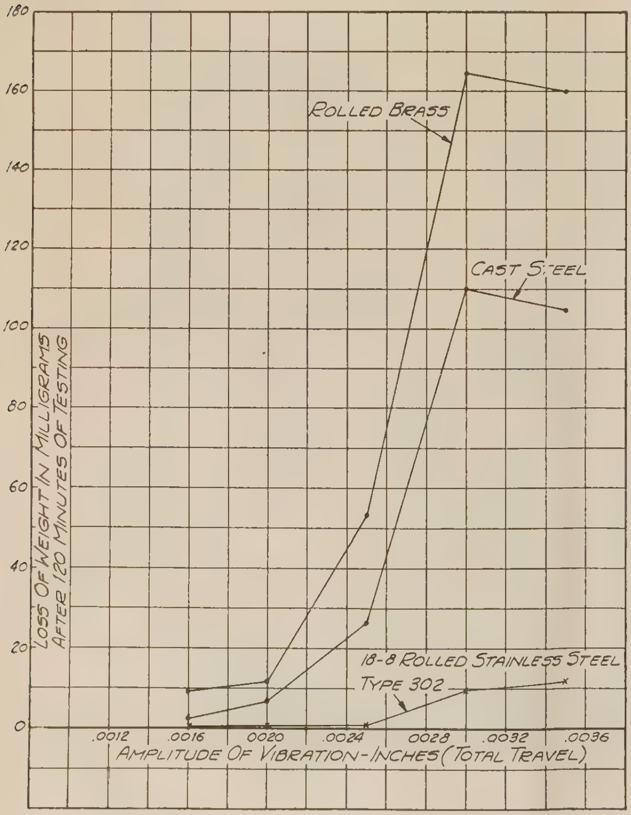

Fig. 6 Effect of Amplitude of Vibration

Fig. 6 shows how the amount of pitting decreased as the amplitude was decreased. There was very little difference in the rate of pitting between 0.0030 in. and 0.0035 in. amplitude. For this reason, an amplitude of 0.0034 in. was selected for all the standard tests made on different materials to determine their relative resistance to pitting. Thus a slight variation in amplitude for different tests had very little effect on the relative rate of pitting of the test specimens.

The results of these tests indicate that a certain amplitude of vibration of the test specimen is needed to produce actual pitting, and that the magnitude of the amplitude required varies for different metals. The 18-8 rolled stainless-steel type 302 required an amplitude of 0.0025 in. before pitting became appreciable. The cast-steel specimen showed very little pitting below 0.0016 in. amplitude, and the brass specimen probably would have stopped pitting below 0.001 in., if the tests had been carried to such low values.

Apparently there is a difference in the minimum force required to produce pitting on different materials, and changing the amplitude of vibration seems to change the forces which produce pitting. This experimental data correspond to some of the field results, where cast iron or cast steel, which pitted rapidly, was replaced with stainless steel, which did not pit at all under the same operating and cavitation conditions.

Just what the forces are that are created by the vibrating specimen and which produce pitting is still open to speculation. The maximum velocity of the test specimen when vibrating at 6500 cps, with an amplitude of 0.0034 in. is only 5.8 fps, as computed from the sine-wave formula

$$V = \pi F A$$

where

V = maximum velocity
F = frequency
A = amplitude (full travel)

This velocity is much too low to produce any impact forces sufficient to cause pitting. However, the acceleration of the test specimen is quite high, as is shown in Fig. 7. At 0.0034 in. amplitude of vibration, the maximum acceleration is 7300 G's or about 235,000 ft per sec per sec. It is possible that this high rate of acceleration is responsible for the forces that produce pitting.

The most logical explanation is the theory by R. T. Knapp and A. Hollander (11) that bubbles form in the cavitation region where the absolute pressure drops below the vapor pressure of the surrounding liquid. They actually demonstrated by high-speed moving pictures that cavitation bubbles form in the liquid and then collapse at velocities up to 800 fps, depending upon the size of the bubble. These extremely high velocities of collapse produce pressures of approximately 50,000 psi, but only over a microscopically small area.

Observation of the test specimens, after having been tested at various amplitudes of vibration, showed that the pitted area on the bottom of the button, and the depth of pitting decreased with a decrease in amplitude. One of the reasons why the depth of pitting decreases with a decrease in amplitude is apparent when observing the test fluid in stroboscopic light. As the amplitude is decreased, the size of the vapor bubbles that form beneath the button also decreases. According to the theory of collapse of a vapor bubble, the smaller the bubble, the smaller the velocity of collapse and, therefore, the smaller the pressure produced.

The reason for the decrease in pitted area with a decrease in amplitude is also apparent from observation of the test fluid under stroboscopic light. As the amplitude decreases, the area covered by vapor bubbles also decreases. This is probably due to the lower vacuums produced under the test button at lower ampli-

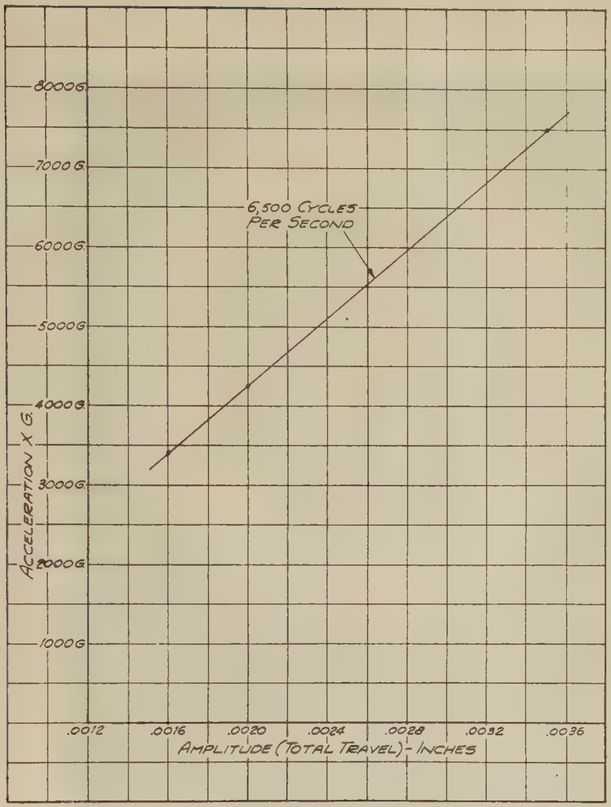

Fig. 7 Acceleration—Displacement Relationship at 6500 Cps

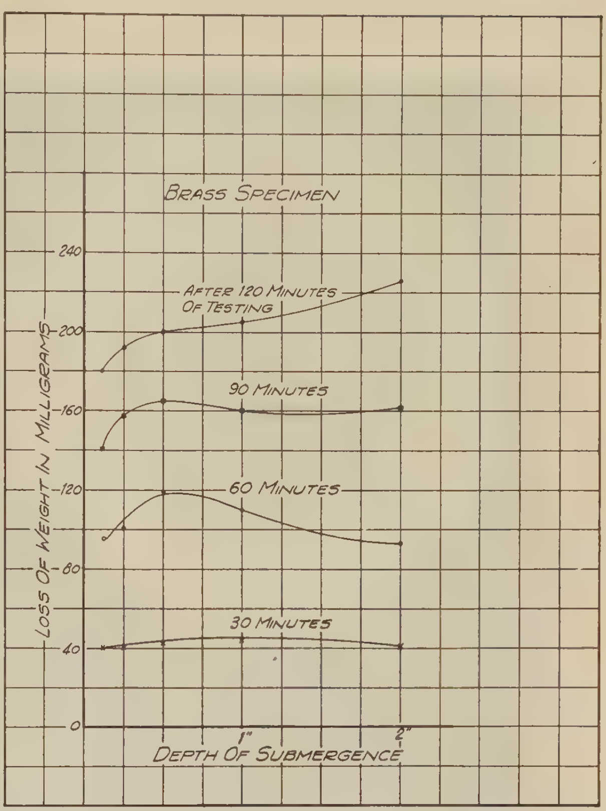

Fig. 8 Cavitation Tests to Determine Effect of Submergence on Brass Specimen

tudes, and therefore the formation of vapor bubbles over a large area is prevented by the surrounding pressure.

Further tests are being made in an attempt to determine what forces are being produced under the vibrating test specimen, or what is actually taking place that produces the pitting.

Effect of Submergence in Test Liquid

Another series of tests were made to determine the effect on the rate of pitting of various depths of submergence of the test specimen in the fluid. Tests were made on brass and on 18-8 cast stainless steel at various depths of submergence from $^1/_8$ to 2 in.

The results of these tests are shown in Figs. 8 and 9. With the rolled-brass specimen, the material removed increased 25 per cent with an increase of submergence from $^1/_8$ to 2 in. With the 18-8 cast stainless-steel specimen, the material removed decreased 60 per cent with an increase of submergence from $^1/_8$ to 2 in.

On both the brass and the stainless steel, the area of the pitted surface on the specimens increased with an increase in submergence. However, on the brass the depth of pitting remained about the same for all depths of submergence, while on the stainless steel the depth of pitting decreased as the submergence was increased. Fig. 10 shows the pitting of brass and stainless steel at $^1/_8$ in. submergence and at 2 in. submergence.

The reason why only the central portion of the specimen is eroded or pitted is apparent when observing the test liquid with stroboscopic light. As the test specimen vibrates, vapor bubbles form near the center of the bottom of the button and flow downward to the bottom of the container in a continuous stream.

Fig. 11 shows this action with a test specimen vibrating in oil. Air bubbles are also visible in the liquid. Apparently air is being drawn down along the side of the test button from the surface of the liquid. This air flows underneath the button to prevent

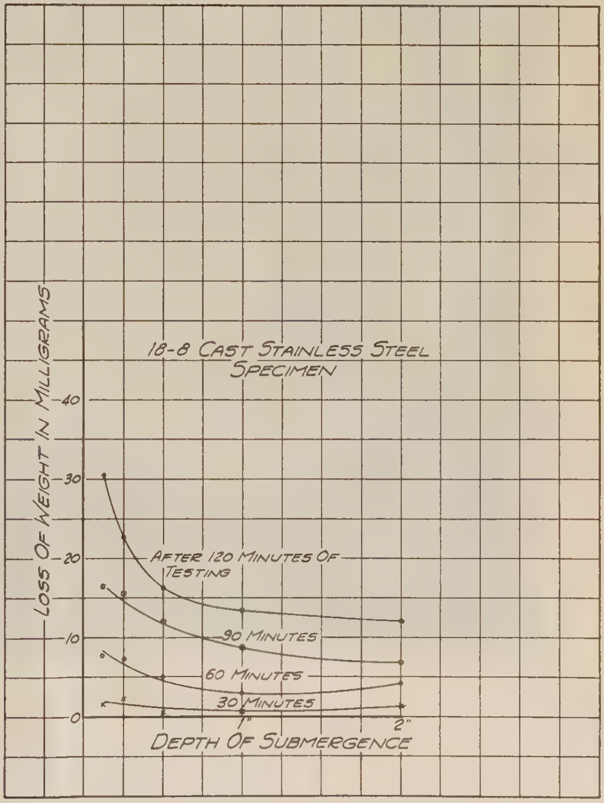

Fig. 9 Cavitation Tests to Determine Effects of Submergence on Stainless-Steel Specimens

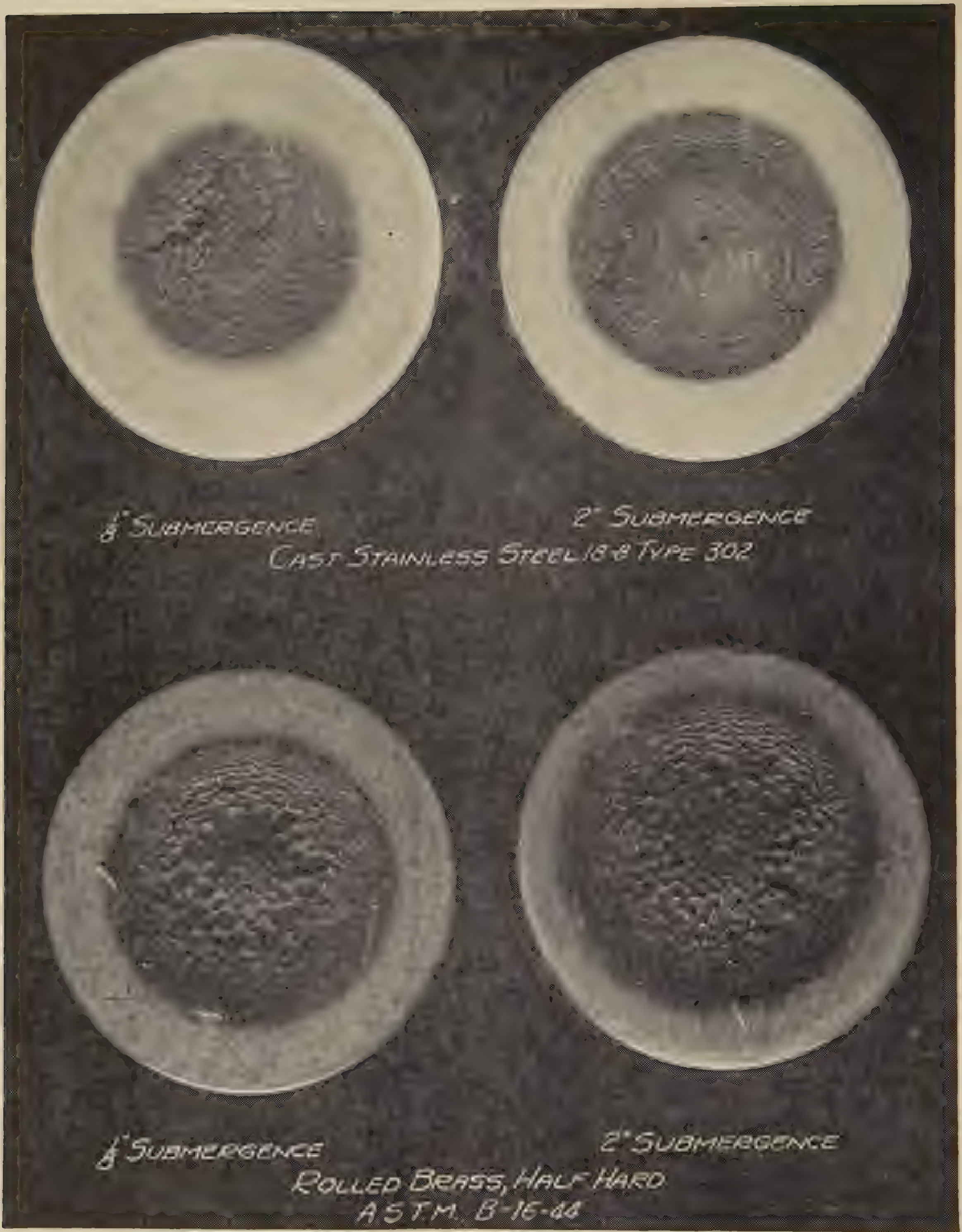

Fig. 10 Brass and Stainless Steel at $^1/_8$ In. and 2 In. Submergence

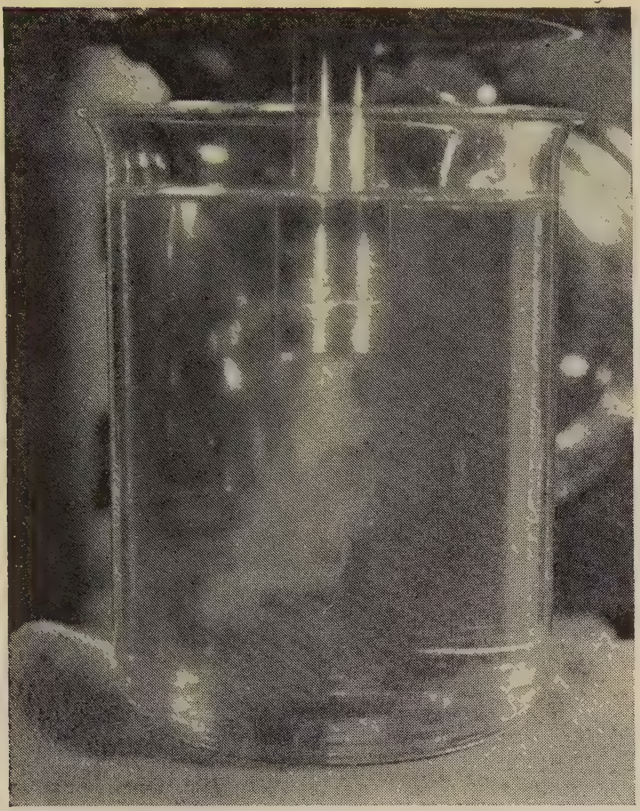

FIG. 11 SPECIMEN VIBRATING IN OIL

formation of the vapor bubbles at the outer edges. As the depth of submergence of the test specimen is increased, the quantity of air drawn from the surface decreases, thereby permitting the formation of larger pitted areas on the test specimen. This flow of air is not visible on any of the photographs, but close observation with stroboscopic light indicates that air is being drawn from the surface of the liquid to the bottom of the vibrating test specimen.

The reason why the brass specimens pitted to the same depth at all depths of submergence, and why the pitting on the stainless steel decreased with an increase of depth, cannot be explained quite as easily. It might be expected that pitting would decrease with increased submergence, because, with increased pressure, the formation of vapor bubbles decreases. It is possible that the severity of cavitation actually did decrease with an increase in submergence, but that the brass specimen was so susceptible to cavitation that it was not very sensitive to a change in the cavitation forces. On the other hand, the stainless steel was probably close to the borderline between pitting and not pitting and therefore was sensitive to any slight differences in the cavitation forces such as would occur due to an increase in the depth of submergence. This is similar to what occurred when the amplitude of vibration was decreased as shown in Fig. 6.

Further tests are being made to determine the effect of submergence on the rate of pitting of other materials. All of the other tests described in this paper were made at $^1/_8$ in. depth of submergence in the test liquid.

EFFECT OF DIFFERENT TEST LIQUIDS

One of the most interesting series of tests was made using different test liquids. Most of the standard tests to determine the relative resistance of different materials to pitting have been made in distilled water. S. Logan Kerr made some tests using salt water (2) which showed very little difference in the rate of pitting as compared to fresh water.

The present series of tests used liquids such as sulphuric acid, hydrochloric acid, oils and water, treated with a chromate inhibitor. The materials tested were brass, stainless steel, cast steel, and special cast irons.

Table 1 lists the results of tests on various cast irons when tested in distilled water and in water treated with chromate ($Na_3\,CrO_4$). The chromate solutions were alkaline, having a pH number of 8.6. The chemical compositions of the five different cast irons tested are shown in Table 2.

The purpose of these tests was to determine whether addition of an inhibitor such as chromate to water would reduce pitting. With the exception of the heat-treated low-alloy cast iron, none of the test results indicated that addition of chromate increased the resistance to pitting any appreciable amount.

However, since the Brinell hardness was determined for all of the test specimens, it was noted that the loss of metal of the various materials after 120 min of testing varied with hardness. This is shown in Fig. 12, and, despite the fact that this curve

TABLE 1 EFFECT OF INHIBITOR IN TEST LIQUID ON RESISTANCE TO PITTING

Material	Test liquid	Rate of loss mg per min during last 30 min of test	Total loss in mg in 120 min
Low-alloy gray iron, as cast, Rockwell A55......	Water (distilled)	0.60	68
Low-alloy gray iron, as cast, Rockwell A55......	0.2% chromate (Na_3CrO_4) 99.8% water, pH = 8.6	0.57	67
Low-alloy gray iron, as cast, Rockwell A55......	0.4% chromate, Na_3CrO_4) 99.6% water, pH = 8.6	0.55	67
Low-alloy gray iron, heat-treated, Rockwell A71..	Water (distilled)	0.67	59
Low-alloy gray iron, heat-treated, Rockwell A71..	0.2% chromate (Na_3CrO_4) 99.8% water, pH = 8.6	0.36	36
Low-alloy gray iron, heat-treated, Rockwell A71	0.5% chromate (Na_3CrO_4) 99.6% water, pH = 8.6	0.32	31
Type no. 1 Ni-Resist, Rockwell A43............	Water (distilled)	0.58	136
Type no. 1 Ni-Resist, Rockwell A43............	0.2% chromate (Na_3CrO_4) 99.8% water, pH = 8.6	0.53	115
Type no. 1 Ni-Resist, Rockwell A43............	0.4% chromate (Na_3CrO_4 99.6% water, pH = 8.6	0.79	122
Type no. 2 Ni-Resist, Rockwell A35............	Water (distilled)	1.03	166
Type no. 2 Ni-Resist, Rockwell A35............	0.2% chromate (Na_3CrO_4) 99.8% water, pH = 8.6	0.99	166
Type no. 2 Ni-Resist, Rockwell A35............	0.4% chromate (Na_3CrO_4 99.6% water, pH = 8.6	1.02	181
Type no. 3 Ni-Resist, Rockwell A42............	Water (distilled)	1.00	133
Type no. 3 Ni-Resist, Rockwell A42............	0.2% chromate (Na_3CrO_4) 99.8% water, pH = 8.6	0.89	130
Type no. 3 Ni-Resist, Rockwell A42............	0.4% chromate (Na_3CrO_4) 99.6% water, pH = 8.6	0.79	115

TABLE 2 CHEMICAL COMPOSITION OF MATERIALS TESTED IN CHROMATE SOLUTION

Material[a]	Tc	Si	Mn	Ni	Cr	Cu	P	S
	———	———	———	Chemical composition, per cent	———	———	———	———
Low-alloy gray iron as cast..........	3.15	2.14	0.64	2.17	..	..	0.08	0.08
Low-alloy gray iron heat-treated.....	3.15	2.14	0.64	2.17	..	..	0.08	0.08
Type 1 Ni-Resist...	2.97	1.82	1.21	13.82	2.24	6.14	0.08	0.08
Type 2 Ni-Resist...	2.74	2.32	1.20	19.98	2.00	..	0.08	0.08
Type 3 Ni-Resist...	2.47	1.81	0.71	29.75	3.00	..	0.08	0.08

---

[a] Furnished by International Nickel Company.

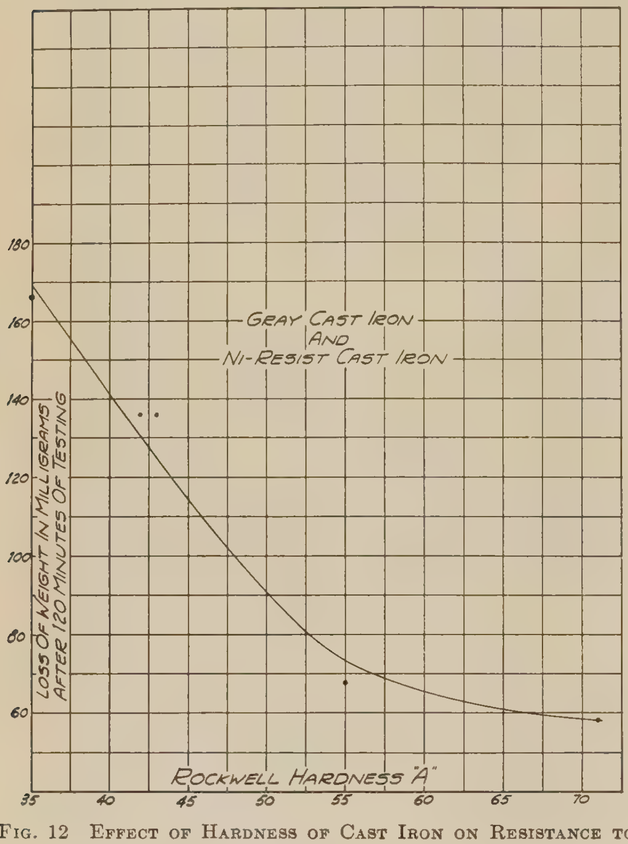

FIG. 12 EFFECT OF HARDNESS OF CAST IRON ON RESISTANCE TO PITTING

represents cast iron with various chemical compositions, there is a definite relation between hardness and resistance to pitting.

Table 3 lists the results of tests on half-hard rolled-brass bar stock using various solutions of sulphuric and hydrochloric acid, and also oils. The first group of tests seemed to indicate that the greater the concentration of sulphuric acid, the greater the resistance to cavitation. In the second series, however, where both the water and the acid solutions were wetted to give approximately the surface tensions of the oils used, there seemed to be very little difference in the resistance to pitting between distilled water and various concentrations of acids. The biggest variation was found when oil was used as the test liquid. The results showed that there was a marked drop in loss of weight of the test specimen when vibrated in either mineral seal oil or transformer oil. A test was also made mixing the mineral seal oil with chloroform to increase the specific gravity and decrease the viscosity, bringing these values closer to that for water. This mixture showed an increase in the loss of weight of the test specimen.

Table 4 lists the results of tests on cast stainless steel, type 302. Again the acid solutions showed no marked increase or decrease, but the test in the seal oil showed a big decrease in pitting.

TABLE 3 ROLLED-BRASS BAR STOCK, ASTM, B-16-44, HALF-HARD

(Cu 60 per cent, Zn 27 per cent, PB 3 per cent, 90 Bhn)

Test liquid	Specific gravity	Viscosity 100 F, centistokes	Surface tension, dynes per cm	Rate of loss mg per min during last 30 min of test	Total loss in mg in 120 min
	———	Properties of liquid	———		
Water (distilled)..	1.00	0.77	76.5	1.37	190
5% H_2SO_4, 95% H_2O..........	1.058	0.83	76.1	1.13	174
25% H_2SO_4, 75% H_2O..........	1.226	1.20	71.2	1.44	154
50% H_2SO_4, 50% H_2O..........	1.424	2.99	65.5	0.73	77
Water (wetted to reduce surface tension)........	1.00	0.77	34.6	1.26	145
25% H_2SO_4, 75% H_2O (wetted)...	1.226	1.20	32.0	1.27	166
5% HCl, 95% H_2O (wetted).......	1.100	0.76	49.1	1.10	156
25% HCl, 75% H_2O (wetted).......	1.057	0.86	41.0	2.36	164
Mineral seal oil...	0.838	4.98	32.3	0.010	1.2
Mineral seal oil and chloroform.....	0.993	1.86	31.5	0.42	39
Transformer oil... (Spec. N-2698, Sun Oil Company T-92304-6199 Sun X 2587)	0.897	10.95	34.7	0.047	4.7

TABLE 4 CAST STAINLESS STEEL, TYPE 302

(18 per cent CR, 8 per cent Ni, 0.11 per cent C)

Test liquid	Specific gravity	Viscosity 100 F, centistokes	Surface tension, dynes per cm	Rate of loss mg per min during last 30 min of test	Total loss in mg in 120 min
	———	Properties of liquid	———		
Water (distilled)..	1.00	0.77	76.5	0.47	35
25% H_2SO_4, 75% H_2O (wetted)...	1.226	1.20	32.0	0.24	25
25% HCl, 75% H_2O (wetted).......	1.057	0.86	41.0	0.48	48
Mineral seal oil and chloroform.....	0.993	1.86	31.5	0.028	2.1

TABLE 5 CAST STEEL, FEDERAL SPECIFICATION QQ-S-681 b CLASS 2 MEDIUM

Test liquid	Specific gravity	Viscosity 100 F, centistokes	Surface tension, dynes per cm	Rate of loss mg per min during last 30 min of test	Total loss in mg in 120 min
	———	Properties of liquid	———		
Water...........	1.00	0.77	76.5	0.75	104.4
25% H_2SO_4, 75% H_2O (wetted)...	1.226	1.20	32.0	1.91	155.5
25% HCl, 75% H_2O (wetted).......	1.057	0.86	41.0	0.99	146.0
Mineral seal oil and chloroform.....	0.993	1.86	31.5	0.073	6.9

TABLE 6 LOSS OF WEIGHT OF TEST SPECIMENS DUE TO CORROSION WHEN IMMERSED STATICALLY IN TEST LIQUID FOR 120 MIN

Material	Test liquid	Loss of weight in mg in 120 min
Rolled brass, ASTM, B-16-44, half-hard..	25% H_2SO_4, 75% H_2O	0.3
Rolled brass, ASTM, B-16-44, half-hard..	50% H_2SO_4, 50% H_2O	2.2
Cast stainless steel, type 302...........	25% H_2SO_4, 75% H_2O	6.5
Cast stainless steel, type 302...........	25% HCl, 75% H_2O	5.2
Cast steel, QQ-S-681 b, Class 2 med	25% H_2SO_4, 75% H_2O	51.8
Cast steel, QQ-S-681 b, Class 2 med	25% HCl, 75% H_2O	67.3

Table 5 lists the results of tests on cast steel. These tests indicate a definite increase in loss of weight with the acid solutions. However, the acid solutions have a definite corrosive effect on cast steel and can cause an appreciable loss of weight due to corrosion alone during the 2-hr test period. This static loss of weight of the test specimens in the acid solutions is shown in Table 6. The brass and stainless-steel losses due to corrosion are negligible. However, when the static loss due to corrosion for cast steel is subtracted from the loss of weight of the test specimens, as determined during the cavitation tests, there again is an indication that the acid solutions do not affect the resistance to pitting.

The general conclusion from all of these tests is that acid solutions do not change the cavitation forces, and there is some evidence that the greater the acid concentration, the smaller the amount of pitting. On the other hand, when the test specimens are vibrated in oil, the weight loss is greatly reduced. The explanation for this phenomenon is not quite clear. However, Dr. W. A. Weyl and F. C. Marbae (12) have suggested that water molecules can be fractured under high negative pressures such as are present where cavitation occurs, and produce a solution of H^+ and OH^- ions. This is comparable to a combination of a strong acid and a strong base, which produces strong corrosion. If this theory is correct it will explain why the pitting of metals decrease as the acid concentration is increased, since the water molecules available to be fractured decrease. It will also explain the exceedingly large decrease in pitting when the metals were vibrated in oil. However, it will not explain the pitting of such materials as glass and rubber. Therefore further investigations along these lines are required before any definite conclusions can be reached.

Tables 7 to 19, inclusive, list practically all of the materials tested in the accelerated-cavitation machine. These materials were tested at a depth of immersion of $^1/_8$ in. in distilled water at 6500 cps with a total travel amplitude of 0.0034 in.

Each specimen was tested for a total period of 120 min, but the loss in weight was determined every 30 min.

Cast and Rolled Stainless Steels

Table 7 lists tests on a number of cast stainless steels, which indicate quite a variation in resistance to pitting. Even cast stainless steels of the same type but cast in different foundries show considerable variation in their resistance to pitting. For example, cast stainless-steel type 302, which contains 18 per cent chrome and 8 per cent nickel, showed losses of 12, 22, and 35 mg, respectively, as furnished by three different foundries. This is a maximum variation of 300 per cent in the resistance to pitting. Some of these variations may be due to the materials being cast for different purposes. Other causes for variations are the carbon content of the steel, where the specifications for a particular type permit a wide variation in carbon. The heat-treatment of the casting and the hardness of the material also affect its resistance to pitting.

TABLE 7 MATERIALS TESTED IN ACCELERATED-CAVITATION MACHINE

Specimen no.	Material	Rate of loss, mg per min during last 30 min of test	Total loss in mg in 120 min
	Cast Stainless Steels		
159...	18% Cr, 8% Ni, 0.12% C, Type 302[a]	0.19	12
103...	18% Cr, 8% Ni, 0.12% C, Type 302[a]	0.18	13
137...	27% Cr, 10% Ni, 0.26% C, Type 312	0.18	13
108...	12% Cr, 0.10% C, Type 410	0.21	22
106...	18% Cr, 8% Ni, 0.10% C, Type 302[b]	0.27	22
107...	17% Cr, 12% Ni, 0.10 C, Type 316	0.25	24
139...	21% Cr, 10% Ni, 0.11% C, Type 307	0.38	31
168...	18% Cr, 8% Ni, 0.11% C, Type 304[c]	0.45	33
167...	18% Cr, 8% Ni, 0.11% C, Type 302[c]	0.47	35
171...	13% Cr, 0.12% C, Type 420[c]	0.40	38
169...	Type 327[c]	0.50	53
170...	13% Cr, 0.12% C, Type 410[c]	0.55	59

[a] Cast by Midvale. [b] Cast by Bonney Floyd Co. [c] Cast by Allegheny Ludlum.

TABLE 8 MATERIALS TESTED IN ACCELERATED-CAVITATION MACHINE; CAST STAINLESS STEELS—EFFECT OF HARDNESS

Specimen no.	Material		Rate of loss, mg per min during last 30 min of test	Total loss in mg in 120 min
	Cr, per cent	Bhn		
182[a]........	12	302	0.20	20
196[b]........	13	302	0.26	25
194[b]........	13	235	0.43	49
195[b]........	13	241	0.39	51
181[a]........	12	225	0.55	54
193[b]........	13	229	0.46	57
192[b]........	13	207	0.51	70
180[a]........	12	167	0.73	141

[a] Cast by Ohio Steel. [b] Cast by Allegheny Ludlum.

Table 8 lists the results of tests on a 12 per cent and a 13 per cent chrome cast steel with varying Brinell hardness. Fig. 13 shows the loss in milligrams during a 2-hr test in the accelerated-cavitation machine plotted against Brinell hardness. For both the 12 per cent and the 13 per cent chrome steels, the test specimens were taken from the same castings, and the variation in Brinell hardness was obtained entirely by changing the heat-treatment of the two materials. These tests show the large effect that hardness of a material has on its resistance to pitting.

The large variations in resistance to pitting of the different cast stainless steels indicate the necessity for constant checks on such material when used in hydraulic machinery to assure that the desired resistance to pitting is being obtained.

Table 9 lists the results of tests on rolled annealed stainless steel. The wide variation in resistance to pitting of the two

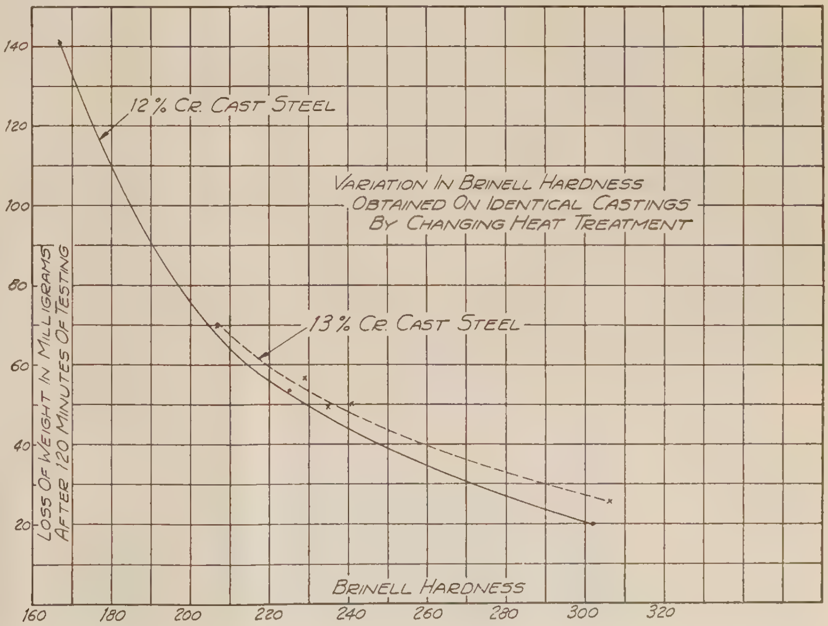

Fig. 13 (*right*) Effect of Brinell Hardness of Cast-Chrome Stainless Steel on Resistance to Pitting

TABLE 9 MATERIALS TESTED IN ACCELERATED-CAVITATION MACHINE; ROLLED ANNEALED STAINLESS STEELS

Specimen no.	Material	Rate of loss, mg per min during last 30 min of test	Total loss in mg in 120 min
105......	18% Cr, 8% Ni, 0.12% C, Type 302	0.107	8.0
157......	18% Cr, 8% Ni, 0.12% C, Type 302	0.33	32

rolled stainless steels of the same type is another reason for the necessity of making careful accelerated cavitation tests on all materials of this type before using them for the purpose of resisting pitting.

WELDED STAINLESS STEELS

Table 10 lists the results of tests on welded stainless steels. These tests also show a wide variation in resistance to pitting, depending upon the type of material used.

TABLE 10 MATERIALS TESTED IN ACCELERATED-CAVITATION MACHINE; WELDED STAINLESS STEELS

Specimen no.	Material	Rate of loss, mg per min during last 30 min of test	Total loss in mg in 120 min
136........	16% Cr, 7% Ni, 2 layers	0.057	9.4
135........	19% Cr, 9% Ni-Cb, 1 layer	0.18	13
15........	Lincoln A5	0.23	27
16........	Stelco 604	0.23	27
134........	19% Cr, 9% Ni-Cb, 2 layers	0.83	36
132........	25% Cr, 12% Ni-Cb	0.43	36
14........	130x Inco Monel	0.36	37
133........	25% Cr, 12% Ni-Cb, 1st layer 19% Cr, 9% Ni-Cb, 2nd layer	0.50	41
17........	Lincoln Aerisweld AE-124K	0.55	55

TABLE 11 MATERIALS TESTED IN ACCELERATED-CAVITATION MACHINE; WELDED STAINLESS STEELS—EFFECT OF PREHEAT ON BASE METAL

Specimen no.	Material	Rate of loss, mg per min during last 30 in of test	Total loss in mg in 120 min
188...	18% Cr, 8% Ni on 12% Cr. Cast steel, preheated to 600 F	0.095	7.6
186...	18% Cr, 8% Ni, on 12% Cr. Cast steel, no preheat	0.099	7.8
187...	18% Cr, 8% Ni, on 12% Cr. Cast steel, preheated to 400 F	0.082	8.0
184...	12% Cr, on 12% Cr. Cast steel, preheated to 400 F	0.15	13
185...	12% Cr, on 12% Cr. Cast steel, preheated to 600 F	0.16	14
183...	12% Cr, on 12% Cr. Cast steel, no preheat	0.18	16.8

Table 11 shows the results of tests on welded stainless steels when welded to 12 per cent chrome, either preheated or not preheated. These tests show that preheating of the base metal has very little effect on the resistance to pitting of the welded deposit.

Table 12 lists the results of tests on various welded stainless steels and on various combinations of welded layers. The chromium and nickel contents refer to the commercial weld-rod designation and do not refer to the chemical analysis of the weld deposit. One object of this series of tests was to determine the resistance to pitting of different types of stainless-steel welds.

Another object was to determine the effect of one and two layers of weld and of various combination of materials on the resistance of pitting. In each case the base metal consisted of cast steel, conforming to Federal specification QQ-S-681b, Class 2, medium.

The results indicate that of the three types of chromium-nickel steels tested, type 301, with 17 per cent chromium and 7 per cent nickel, gave the highest resistance to pitting. There again appears to be a definite relationship between hardness of the material and its resistance to pitting, since type 301 had the highest Brinell.

The tests also show that two layers of type 301 weld are better than one layer, although the single layer had a higher Brinell hardness than two layers. This may be due to other characteristics of the welded material, since it is certain that the first layer is contaminated by the base metal and therefore its characteristics probably change materially while cooling.

An additional indication of such contamination is shown where a first layer of type 309 with a second layer of type 301 had less hardness and considerably less resistance to pitting than two layers of type 301.

The 18 per cent chromium, 8 per cent nickel stainless steel, type 308, did not seem to become contaminated very much by either the base metal or a first layer of type 309, but it had considerably less resistance to pitting than type 301.

One definite conclusion that can be made from this series of tests is that a first layer of type 309 has no beneficial effects on the resistance to pitting and, in the case of type 301, definitely lowers this resistance.

Since a lot of welded stainless-steel repairs and overlays are being made, using type 309 as a first layer, it was decided to determine whether this material had any other beneficial effects. One of the dangers of stainless-steel welds is that they may produce brittleness in either the weld deposit or in the base metal. A measure of brittleness is the bend test. Therefore, in preparing the test specimens for this series of tests, the weld was deposited on cast-steel bars 1 in. wide × 8 in. long × 1 in. thick. The cast steel conformed to Federal specification QQ-S-681b, Class 2, medium, which is a steel commonly used for hydraulic-turbine runners. In making the welds, only standard commercial weld rods were used.

The bend tests showed that in each case two weld layers gave a greater bend angle and therefore greater ductility than a single layer. Use of type 309 as a first layer did not increase the bend angle compared to any of the other two materials. However, two layers of type 308 had a higher bend angle than two layers of type 301.

The conclusion from these tests is that type 309 stainless steel as a first layer does not improve the characteristics of the weld. Although two layers of type 308 had greater ductility than two layers of type 301, this was more than offset by the greater resistance to pitting of type 301.

All of these tests indicate that for all welding repairs and all prewelding of hydraulic-turbine machinery, two layers of stainless steel should be used and, if it is desired to obtain the maximum

TABLE 12 MATERIALS TESTED IN ACCELERATED-CAVITATION MACHINE; WELDED STAINLESS STEELS—VARIATION IN LAYERS

Specimen no.	Material		Bhn	Rate of loss, mg per min during last 30 min of test	Total loss, in mg in 120 min,
	First layer of weld	Second or final layer of weld			
203....	17% Cr, 7% Ni, Type 301	...	308	0.098	10
201....	18% Cr, 8% Ni, Type 308	...	160	0.28	23
198....	25% Cr, 12% Ni, Type 309	...	145	0.36	26
204....	17% Cr, 7% Ni, Type 301	17% Cr, 7% Ni, Type 301	255	0.075	6
199....	25% Cr, 12% Ni, Type 309	18% Cr, 8% Ni, Type 308	145	0.36	31
202....	18% Cr, 8% Ni, Type 308	18% Cr, 8% Ni, Type 308	151	0.35	33
200....	25% Cr, 12% Ni, Type 309	17% Cr, 7% Ni, Type 301	175	0.40	35

resistance to pitting, type 301 stainless-steel weld rods should be used.

Sprayed Stainless Steels

Table 13 lists the tests on various sprayed stainless steels. These tests indicate that although some of the sprayed stainless materials had a resistance about equal to cast steel, others pitted very rapidly. These differences are probably due largely to the method of application of the sprayed metal, which accounts for the variance in field reports as to their effectiveness. Quite a number of the test specimens had to be scrapped before the 2-hr test period was completed, because the sprayed metal would separate from the base. The high acceleration (about 7300 G's) of the vibratory test is a severe test on the adhesion of the metal.

TABLE 13 MATERIALS TESTED IN ACCELERATED-CAVITATION MACHINE; SPRAYED STAINLESS STEELS

Specimen no.	Material	Rate of loss, mg per min during last 30 min of test	Total loss in mg in 120 min
12.....	Metco Metcaloy No. 2	0.57	72
11.....	Metco Metcaloy No. 1	0.50	98
112.....	18% Cr, 8% Ni, Type 302	0.61	187
116.....	13% Cr, Type 420	0.70	192
179.....	Metcaloy No. 2	1.33	216

If the sprayed material is applied carefully it seems to have about the same resistance to pitting as cast steel, but considerably less resistance than a properly welded stainless steel. In general, the application of sprayed metal is cheaper than welding with mild or stainless steel, and it sometimes proves to be a satisfactory means of repair where pitting is not very severe, and where speed of application and low initial costs are a factor.

Cast Steels

Table 14 lists the results of tests on the cast steel most commonly used for hydraulic-turbine runners. The tests on three castings from 3 different foundries do not show any appreciable variation.

TABLE 14 MATERIALS TESTED IN ACCELERATED-CAVITATION MACHINE; CAST STEELS

Specimen no.	Material	Rate of loss, mg per min during last 30 min of test	Total loss in mg in 120 min
178......	Fed. Spec. QQ-S-681 b Class 2 medium	1.09	88
158......	Fed. Spec. QQ-S-681 b Class 2 medium	0.75	104
118......	Fed. Spec. QQ-S-681 b Class 2 medium	0.70	105

Ampco Bronzes

Table 15 lists an interesting series of tests on Ampco bronzes. Ampco is the trade name for a bronze with an aluminum content varying from 10 to approximately 14 per cent. The Brinell hardness increases as the aluminum content increases. The results of the tests on the cast bronzes show that some of them have twice the resistance to pitting compared to the best stainless-steel castings. The welded bronzes also show a remarkable resistance to pitting. Fig. 14 shows cast and welded Ampco bronze test specimens. Fig. 15 shows how the resistance to pitting of these materials varies with hardness. This curve indicates that while the resistance to pitting increases with hardness, there is a maximum point beyond which resistance to pitting decreases with increased hardness.

Unfortunately, there is very little information with reference to how these bronzes, either cast or welded, stand up under field conditions, which is really the final criterion. The author knows of only one instance where Ampco bronze was used on a hydraulic-turbine runner. In this case Ampco bronze patch plates were alternated with ordinary bronze on the back sides of the blades of a hydraulic-turbine runner. After a period of operation the ordinary bronze patch plates had pitted to a considerable extent, while the Ampco bronze showed very little sign of pitting.

TABLE 15 MATERIALS TESTED IN ACCELERATED-CAVITATION MACHINE; BRONZES

Specimen no.	Material	Bhn	Rate of loss, mg per min during last 30 min of test	Total loss in mg in 120 min
	Ampco Rolled Bronzes			
111...	Ampco no. 18 (Extruded)	190	0.15	12
	Ampco Cast Bronzes			
160...	Ampco no. 20	235	0.095	5.8
161...	Ampco no. 21	285	0.080	6.2
162...	Ampco no. 22	340	0.115	9.5
125...	Ampcoloy 46	190	0.113	9.9
124...	Ampco no. 18	170	0.12	12
121...	Ampcoloy A3	130	0.27	22
	Welded Ampco Bronzes			
163...	Ampcotrode 200 on SAE 1010 steel	220	0.062	3.2
164...	Ampcotrode 250 on SAE 1010 steel	260	0.075	5.3
126...	Ampcotrode 160 on SAE 1010 steel	185	0.107	5.2
127...	Ampcotrode 160 on Ampco 18	185	0.093	5.9
165...	Ampcotrode 300 on SAE 1010 steel	320	0.100	9.5
128...	Ampcotrode 160 on Ampcoloy 46	180	0.23	20
123...	Ampcotrode 10 on SAE 1010 steel	140	0.28	24
122...	Ampcotrode 10 on Ampcoloy A3	140	0.39	31

Note: Materials furnished by Ampco Co.

Certainly the tests of the Ampco bronzes in the accelerated-cavitation machine warrant experimenting with this material in field installations.

Colmonoy

Table 16 lists tests made on welded Colmonoy. The tests show that some types of welded Colmonoy have a high resistance to pitting.

Table 17 lists Colmonoy sprayed onto a base and then fused on at a temperature of 1850 F. These tests show that some of these materials also have a high resistance to pitting.

Colmonoy is a trade name for a material consisting primarily of iron, nickel, chromium, borium, silicon, and carbon. Before applying Colmonoy as a spray, the base metal is thoroughly grit-blasted. The Colmonoy is then sprayed uniformly over the grit-blasted area to a thickness of approximately 0.060 in. The sprayed area is then heated with an oxyacetylene flame or in a heat-treating furnace to a temperature of 1850 F. Colmonoy has the property of becoming very plastic at this temperature, thereby fusing itself to a grit-blasted area.

The author knows of no field tests on this material, but based on the results in the accelerated-cavitation machine, it merits consideration. One advantage is the ease of application, whereby the material is sprayed on and then fused with a torch or in an oven. However, the fusing process presents the problem of possible distortion of the base metal. The cost of the Colmonoy material also may be a deterrent to its general use in the prevention of pitting.

Several test buttons were prepared by spraying Colmonoy to a base, but eliminating the fusing process. It was impossible to obtain any pitting data on these specimens because the sprayed material separated from the base during the vibration tests.

Thiokol Rubber

Table 18 lists tests made on Thiokol rubber sprayed on various materials used for a base. The test specimens were prepared by the U. S. Navy. The loss of weight of the test specimens is not a very satisfactory means for determining the relative resistance of rubber because of its low specific gravity compared to metal. However, visual inspection of the test specimens indicated that the rubber overlay gave considerable resistance to pitting. Fig.

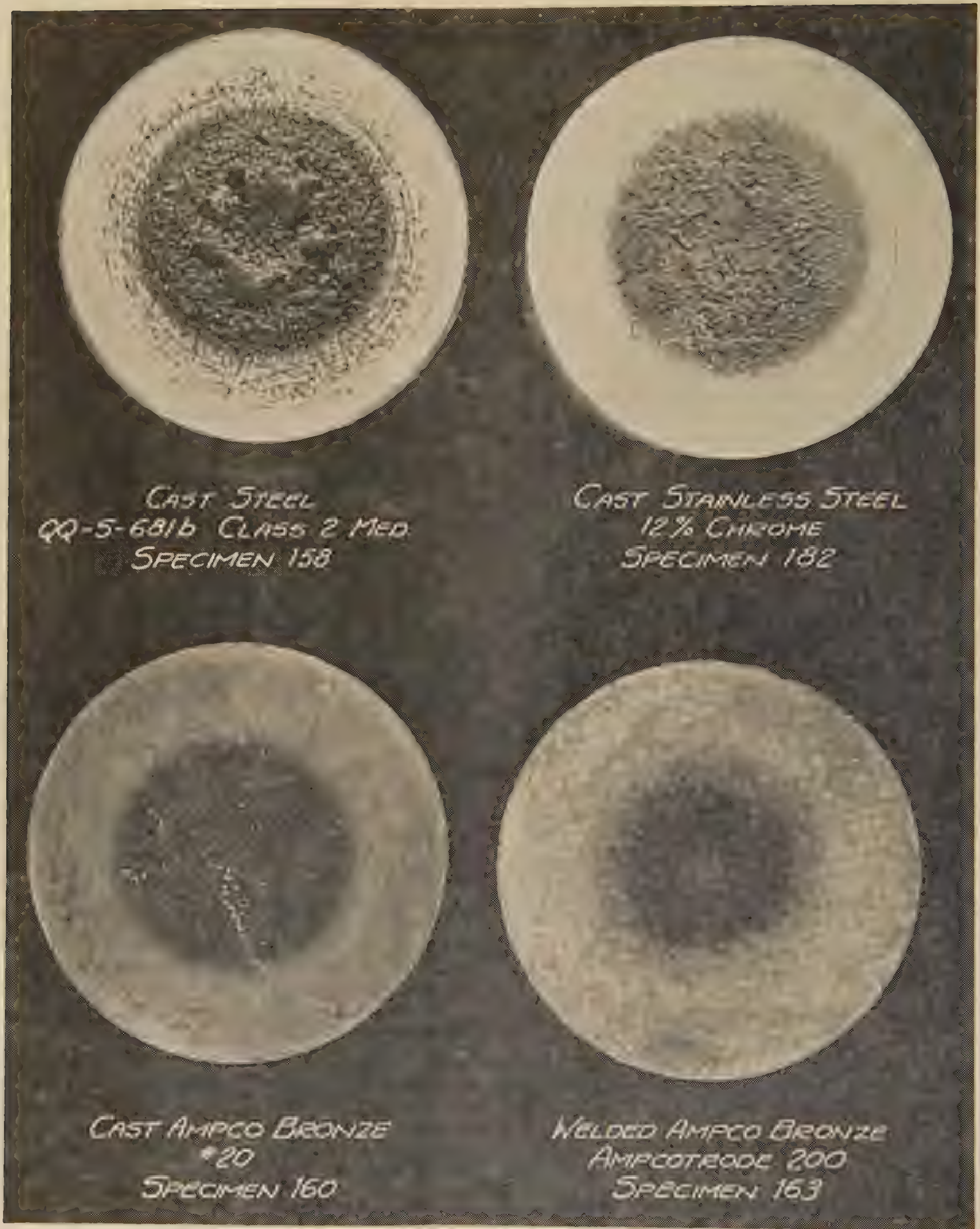

Fig. 14 Cast and Welded Ampco Bronze, Compared to Cast Steel and Cast Stainless Steel

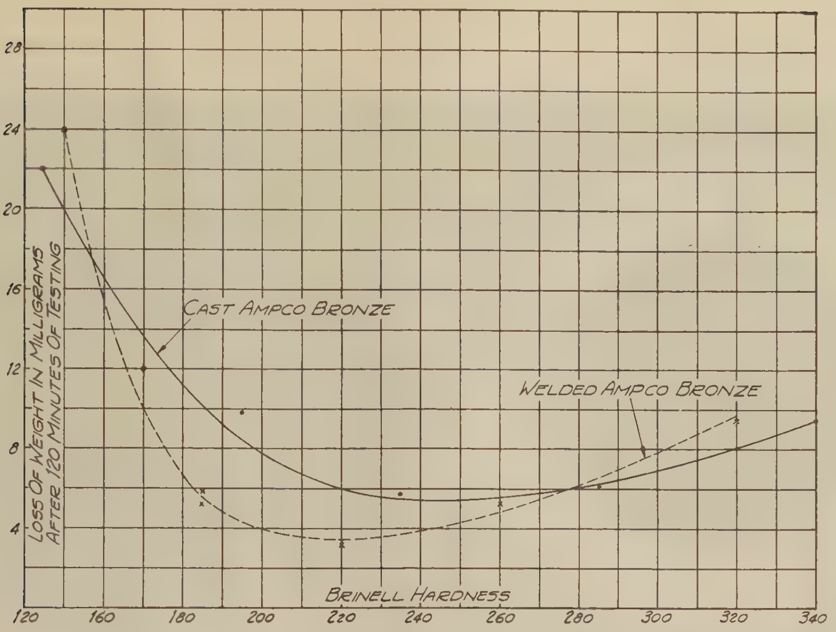

FIG. 15 EFFECT OF HARDNESS OF AMPCO BRONZES ON RESISTANCE TO PITTING

TABLE 16 MATERIALS TESTED IN ACCELERATED-CAVITATION MACHINE; WELDED OVERLAY[a]

Specimen no.	Material	Rate of loss, mg per min during last 30 min of test	Total loss in mg in 120 min
148.....	Colmonoy WER-100, arc-welded	0.043	6.0
145.....	Colmonoy no. 6, arc-welded	0.070	8.4
129.....	Colmonoy—2 layers, gas-welded	0.20	19
130.....	Colmonoy—1 layer, gas-welded	0.24	23
147.....	Colmonoy no. 5, arc-welded	0.18	23
146.....	Colmonoy no. 4, arc-welded	0.21	29

[a] "Colmonoy" furnished by Wall Colmonoy Company.

TABLE 17 MATERIALS TESTED IN ACCELERATED-CAVITATION MACHINE; COLMONOY SPRAYED AND FUSED TO BASE

Specimen no.	Material	Rate of loss, mg per min during last 30 min of test	Total loss in mg in 120 min
144.......	Colmonoy no. 6	0.064	8.0
156.......	Colmonoy no. 6	0.092	9.5
143.......	Colmonoy no. 5	0.19	16
141.......	Colmonoy no. 4	0.31	30
151.......	Colmonoy, sweat-on-paste arc application	0.32	30
150.......	Colmonoy, sweat-on-paste QXI-acetylene application	0.38	34

TABLE 18 MATERIALS TESTED IN ACCELERATED-CAVITATION MACHINE; THIOKOL RUBBER[a]

Specimen no.	Materials	Rate of loss mg per min during last 30 min of test	Total loss in mg in 120 min
Navy no. 2..	Flame-sprayed on stainless steel	0.17	26
Navy no. 4.	Flame-sprayed on stainless steel, weld inlay	0.16	28
Navy no. 10.	Flame-sprayed on manganese bronze	0.18	30
Navy no. 8..	Flame-sprayed on mild welded steel	0.14	31
Navy no. 6..	Flame-sprayed on mild steel	0.16	33

[a] Furnished by U. S. Navy.

16 shows several of the rubber overlays after 2 hr of testing in the accelerated-cavitation testing machine. These illustrations show how the center of the rubber overlay is eroded down to the base metal. The composition of the base metal apparently has very little influence on the resistance of the rubber to pitting, as is indicated in Table 18.

The U. S. Navy has used this rubber overlay with considerable success on propeller shafts, rudders, and struts of naval vessels where pitting was being encountered. One of the important features of the successful use of rubber overlays is proper application. The U. S. Navy sandblasts the base metal to obtain a clean surface. The metal is heated to a temperature somewhat above the surrounding air temperature. The rubber is then sprayed on with a gun, using the powder and gun developed by the Schori Process Corporation.

The results of the tests in the accelerated-cavitation machine, and the results obtained by the Navy under actual operating conditions, indicate that it might be desirable to investigate the performance of this rubber when used for hydraulic-machinery parts subject to pitting.

MISCELLANEOUS MATERIALS

Table 19 lists some miscellaneous materials tested in the accelerated-cavitation machine. These include the base metals used by the Navy in connection with Thiokol rubber overlays. This table shows that stellite has by far the greatest resistance to pitting of all of the materials tested, which agrees with the results obtained in other accelerated-cavitation machines.

The stellite used in the present test was a rolled material consisting of 55 per cent cobalt, 33 per cent chrome, and 6 per cent tungsten, with a Brinell hardness of about 410. The stellite was brazed to the base metal with silver solder. Stellite can be obtained as a casting and also can be applied by welding. Its disadvantage for ordinary hydraulic machinery is its high cost, and

TABLE 19 MATERIALS TESTED IN ACCELERATED-CAVITATION MACHINE; MISCELLANEOUS MATERIALS

Specimen no.	Material	Rate of loss, mg per min during last 30 min of test	Total loss in mg in 120 min
Special.....	Stellite, Haynes no. 6, Rolled, Bhn 410	0.017	0.60
166.....	Nitraloy—Holcomb no. 218	0.07	14
Navy no. 3.	Welded stainless steel	0.35	28
Navy no. 1.	Stainless steel	0.46	47
Navy no. 9.	Manganese bronze	0.70	80
Navy no. 7.	Welded mild steel	0.79	97
Navy no. 5.	Mild steel	0.78	107
119.....	Brass, 70% Cu, 30% Zn	1.17	156
120.....	Rolled brass B-16-44 half-hard bar stock used for standard to check cavitation machine, Cu 60%, Zn 27% Pb 3%, Bhn 90	1.01	162

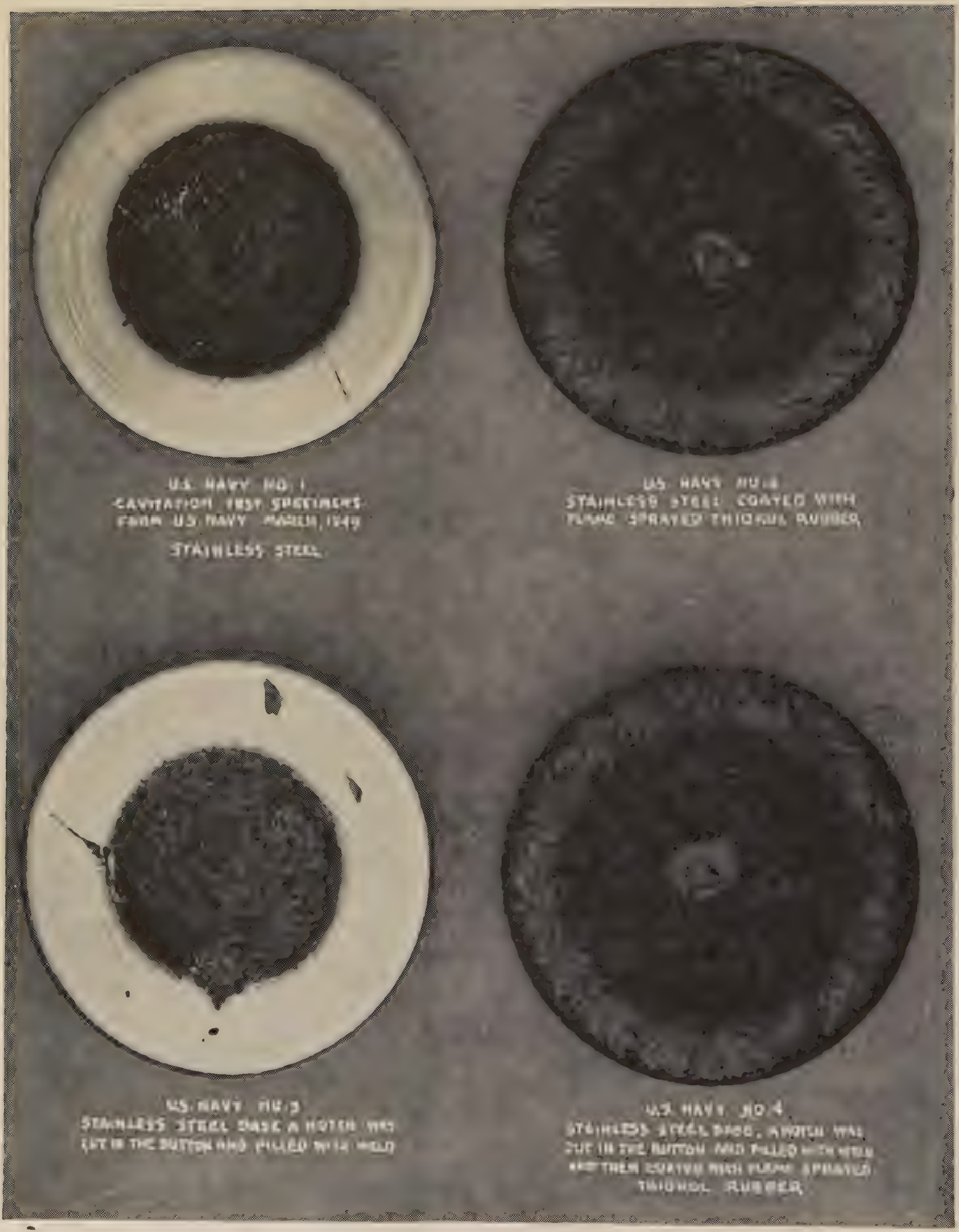
U.S. NAVY NO. 1
CAVITATION TEST SPECIMENS
FROM U.S. NAVY MARCH, 1949
STAINLESS STEEL
U.S. NAVY NO. 2
STAINLESS STEEL COATED WITH
FLAME SPRAYED THIOKOL RUBBER
U.S. NAVY NO. 3
STAINLESS STEEL BASE A NOTCH WAS
CUT IN THE BUTTON AND FILLED WITH WELD
U.S. NAVY NO. 4
STAINLESS STEEL BASE, A NOTCH WAS
CUT IN THE BUTTON AND FILLED WITH WELD
AND THEN COATED WITH FLAME SPRAYED
THIOKOL RUBBER

Fig. 16 Thiokol Rubber Specimens

the difficulty of machining and grinding it because of its extreme hardness. However, it has been used successfully for steam-turbine blading where the erosion problems are somewhat similar to pitting in hydraulic turbines.

CONCLUSIONS

The tests on variation in amplitude of vibration, on variation in depth of submergence and with various liquids, answered some of the questions regarding the phenomena of cavitation. Although these tests were not always conclusive, they indicated the type of additional investigations that should be made.

The standard accelerated-cavitation tests were made mostly on standard trade materials to determine the qualities of materials readily available to the industry. These tests showed the following:

1 That new materials such as the Ampco bronzes, Colmonoy, Thikol rubber, and others, which are constantly being developed, might be suitable for hydraulic machinery and might have a distinct advantage over the materials now in use.

2 That the practical application of the materials, such as number of layers to be used when making repairs by welding or when prewelding, influences the resistance to pitting whereas preheating the base metal has very little effect on the resistance.

3 That hardness has a definite effect on resistance to pitting regardless of the material being used.

4 That it is desirable to make accelerated-cavitation tests on the special materials, particularly stainless steels, to insure obtaining the requisite resistance to pitting.

The results of all of the tests showed that the accelerated-cavitation machine can be used to:

1 Make further investigations on the phenomena of cavitation.

2 Test new materials and new techniques of application of materials for their relative resistance to pitting.

3 Test samples of all special materials to determine their resistance to pitting to avoid the wide variation of these qualities when the materials are obtained from different sources.

Although items 2 and 3 constitute practically a full-time test program for an accelerated-cavitation machine, any suggestions as to how it can be used for advancing the knowledge of the mechanics and phenomena of cavitation and pitting are welcomed.

ACKNOWLEDGMENTS

All of these accelerated-cavitation tests were made possible through funds provided by the Allis-Chalmers Manufacturing Company. The Research Laboratory of this company built the cavitation machine and kept it in operation. The tests were made under the direction of the Hydraulic Department.

The Ampco bronze test specimens were provided by the Ampco Metal Company, Milwaukee, Wis.

The Colmonoy specimens were furnished by the Wall Colmonoy Corporation, Detroit, Mich.

Cast stainless-steel specimens were provided by Allegheny Ludlum Steel Corporation, Brakenridge, Pa., Ohio Steel Foundry Company, Lima, Ohio, and Midvale Company, Midvale, Pa.

The Thiokol rubber specimens were supplied by the Material Laboratory, New York Naval Shipyard, Naval Base Station, Brooklyn, N. Y.

The cast-iron specimens for the tests with the chromate inhibitor were supplied by the International Nickel Company, New York, N. Y.

The author is indebted to these companies for making the facilities available for the tests, for furnishing test specimens, and for permission to publish the test results.

BIBLIOGRAPHY

1 "Pitting Resistance of Metals Under Cavitation Conditions," by J. M. Mousson, Trans. ASME, vol. 59, 1937, pp. 399–408.

2 "Determination of the Relative Resistance to Cavitation Erosion by the Vibratory Method," by S. Logan Kerr, Trans. ASME, vol. 59, 1937, pp. 373–397.

3 "Théorie plus complète des machines qui sont mises in mouvement par la réaction de l'eau" (More complete theory of machines driven by Hydraulic Reaction), by Leonard Euler, *Historie de l'Académie Royale*, Berlin, Germany, 1754.

4 "On the Formation of Cavities in Water by Screw Propellers at High Speeds," by Sydney W. Barnaby, Trans. Institution of Naval Architects, London, England, vol. 39, 1897, pp. 139–143.

5 "The Application of the Compound Steam Turbine to the Purpose of Marine Propulsion," by Charles A. Parsons, Trans. Institution of Naval Architects, London, England, vol. 38, 1897, pp. 232–237.

6 "Beiträge zur Berechnung und Konstrucktion der Wasserturbinen" (Contribution to the Calculation and Construction of Hydraulic Turbines), by W. Wagenbach, *Zeitschrift für das Gesamte Turbinenwesen*, vol. 4, 1907, pp. 273–277.

7 "Kavitation" (Cavitation), by J. Ackert, Handbuch der Experimentalphysik, *Akademische Verlagsgesellschaft*, Leipzig, Germany, vol. 4, part 1, 1926.

8 "Korrosion durch Kavitation in einem Diffusor" (Erosion by Cavitation in a Diffusor), by Hellmut Schröter, *Zeitschrift Verein deutscher Ingenieure*, vol. 76, 1932, pp. 511–512.

9 "A Magnetostriction Oscillator Producing Intense Audible Sound and Some Effects Obtained" by Newton Gaines, *Physics*, vol. 3, 1932, pp. 2-9 and 229.

10 "Progress Report on Cavitation Research at Massachusetts Institute of Technology," by J. C. Hunsaker, Trans. ASME, vol. 57, 1935, pp. 423–424.

11 "Laboratory Investigations of the Mechanism of Cavitation," by R. T. Knapp and A. Hollander, Trans. ASME, vol. 70, 1948, pp. 419–431.

12 "Some Mechano-Chemical Properties of Water," by W. A. Weyl and E. C. Marbae, publication NAVEXOSP-571, Office of Naval Research, Navy Department, Washington, D. C.

Discussion

T. BAUMEISTER.[3] This is the kind of document which adds greatly to our store of knowledge on a problem which is by no means limited to the field of hydraulics, or more particularly, the hydraulic turbine. The hydroelectric engineer probably has recognized the problem of cavitation for a longer period than have most other engineers. Likewise, he has tried to do something about it. He has not stood by waiting for someone to develop a solution.

This whole problem, however, of the aging and wasting of metals is one to which we must address ourselves more aggressively. The design of boilers has been changed radically in the last few years because of fly-ash-erosion problems which were formerly nonexistent or not recognized. Cavitation on waterwheels is one thing, but so is cavitation on (*a*) centrifugal and axial-flow pumps; (*b*) at the entrance to tubes in closed feedwater heaters or surface condensers; or (*c*) on rayon spinnerets. The examples are myriad. The pitting which results from cavitation must be met in a rational, practical way.

The contribution in the author's work is appreciated. His meticulous studies show the many variables which can influence this phenomenon. The accelerated technique should be of value to designers and users of equipment.

Criticism might be directed to the method, because it does not give absolute or thoretical values. It is in somewhat the same category as grindability testing devices; hardness testers; viscosimeters, and numerous other instruments. They all give useful data. The data obtained by the author's method should prove equally valuable, and it is to be hoped that he will continue and extend his researches so that those of us who are concerned with attempting to correct the ill effects of cavitation will have better assurances of success.

---

[3] Professor of Mechanical Engineering, Columbia University; Consulting Engineer, American Gas and Electric Service Corporation, New York, N. Y. Mem. ASME.

R. C. Glazebrook.[4] The writer fears that as written the author's definition of cavitation may cause some confusion in the minds of some readers as to the difference between separation and cavitation. To the writer, cavitation, as defined, sounds more like separation. A more foolproof definition would be to state that it is a phenomenon occurring when the absolute pressure has been reduced to or below the vapor pressure of the liquid being handled so that the liquid flashes into the gaseous form, followed by a subsequent increase in pressure, resulting in a collapse of these cavities, which may be termed an implosion (the opposite of an explosion), a destructive shock phenomenon resulting in reduced performance, noise, and pitting.

The author's results show clearly that resistance to cavitation is definitely affected by the hardness of the materials, the harder materials being appreciably more resistant to cavitation. While not entirely confirmed by test, we have a somewhat conclusive suspicion that this is brought about by the finer grain size of the harder materials. It might be well to offer this as a possible explanation for this increased resistance with the harder materials and draw forth some opinion on the subject which would be mutually helpful to the hydraulic profession in general.

W. R. MacNamee.[5] Another source of damage to hydraulic equipment which frequently combines with cavitation is erosion. This is usually not serious as long as clear water is used, but when water at high velocities also carries in suspension hard material, such as sand, damage can be very rapid and severe.

Such conditions are not uncommon in South America, where the volcanic nature of much of the country, plus a rainy season of heavy and prolonged rainfall, combine to carry off large quantities of very finely divided solids of an abrasive nature.

The writer's company and the Braden Copper Company have been engaged in a program of materials testing to evaluate both standard and new materials under cavitation and erosive conditions.

The test program was carried out at the Pangal Plant of the Braden Copper Company, in Chile, where the nature of the water flow varies from clear water in the dry season to water heavily laden with silt in the rainy season.

By subjecting samples of various materials to a high-velocity jet of clear water, the resulting damage could be considered due to cavitation. During the rainy season, when turbid water was used, the rate of removal of test material was 5 to 10 times as great, and was no doubt due to erosion by the sand particles.

Fig. 17, herewith, shows the arrangement of test equipment, with and without the jet in operation.

A jet of water $^1/_2$ in. diam under 650 psi pressure was directed against the test specimen. The angle between the jet and the test specimen was 15 deg. A hole $^1/_4$ in. diam was purposely placed in each specimen at the point of impingement to produce severe cavitation. The two spots on the specimen downstream from the hole are typical of the patterns produced by cavitation in the clear-water tests. When tests were made with turbid water, the damaged area usually showed a smooth, though irregular surface, quite different from the characteristic pockmarks of cavitation.

For metals, the time of exposure to the jet varied from a few hours for the soft steels to 20 days for the hardest alloys.

As might be expected, the hard, strong materials were most resistant to erosion as well as to cavitation. The Colmonoy alloys, mentioned by the author, were outstanding in their excellent resistance to erosion. In general, materials showing good resistance to cavitation in the clear-water tests also performed well under erosive conditions with turbid water.

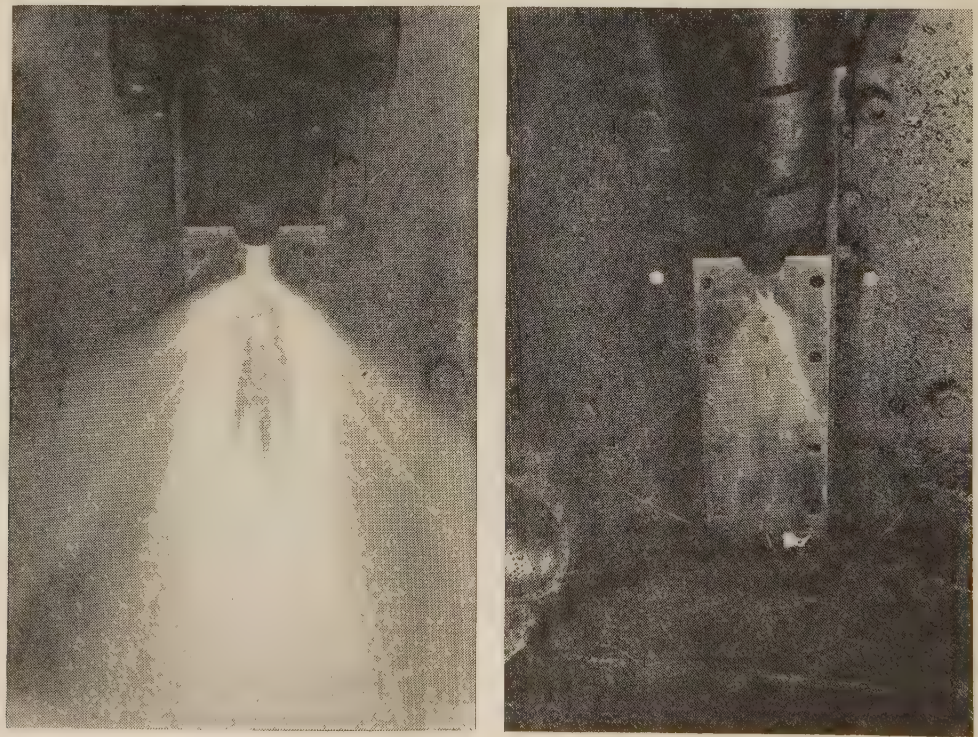

Fig. 17 Arrangement of Equipment for Testing Effect of High-Pressure Jet Impingement Using Clear Water and Turbid Water for Erosive Effect

---

[4] Chief Engineer, Hydraulic Division, Fairbanks, Morse & Company, Beloit, Wis. Mem. ASME.

[5] Assistant Supervising Engineer, Baldwin Locomotive Works, Philadelphia, Pa. Mem. ASME.

It was noted, however, that 18-8 stainless steel, which resisted cavitation far better than mild steel, performed but little better when erosion was combined with cavitation. It may be that the ability of 18-8 to work-harden was an important factor in this result. The repeated blows sustained under cavitation conditions may produce local work-hardening to a much greater degree than the cutting action of sand particles in the water.

The straight chromium steels of about 14 per cent chromium, heat-treated, were especially good in resisting erosion.

As tested here, rubber proved completely disappointing. Two samples, consisting of $^1/_8$-in. rubber, vulcanized to steel plate under factory conditions, were tested with clear water only. Each failed in less than 1 min. Each time a strong odor of burned rubber was noticeable, and bits of rubber in the pit had the appearance of being charred. It appears that impingement of the jet produced sufficient working of the rubber to cause destructive internal heating.

One unexpected variable developed in these tests when it was discovered that the rate of pitting and erosion varied with barometric pressure, low pressure definitely accelerating removal of material.

It would be interesting to know if the author has detected any such correlation in his tests. Variation in barometric pressure would exceed considerably the variation in depth of submergence shown on the author's Fig. 8, although whether the variations shown there are due to the static-pressure change or variations in entrained air is not clear.

It is noted that the author makes no mention of tests of hard steels other than the stainless varieties. Such tests would round out the study in so far as materials commonly available are concerned.

At the present time there exists quite a gap between the existence of highly resistant alloys and their practical use, due not only to cost, but to the difficulty of applying them to the surfaces to be protected. In some cases, the necessity of obtaining a reasonably smooth surface after application is a difficult requirement.

These problems no doubt will decrease as improved techniques in the handling of these materials are developed, leading to longer and more reliable performance of hydraulic machinery.

H. S. Van Patter.[6] It is most interesting to compare the cavitation damage rates reported by the author with those reported in 1937 by S. L. Kerr and J. M. Mousson. The author shows much greater variations than found by Kerr with similar apparatus in the performance of particular materials from different sources. The loss rate for stellite is only 10 per cent of the lowest and about 1 per cent of the highest loss rates for the various stainless steels, whereas Mousson, using Venturi-type equipment, reported losses with stellite to be of the same order as with stainless steel. The author's results for aluminum bronze are somewhat better than reported by Kerr, but the check is quite good, and the excellent performance of type 301 stainless steel checks well with Mousson's findings.

The writer would appreciate some further comments from the author regarding his observation of the vapor bubbles at the specimen surface under stroboscopic lighting. Does one large bubble or a collection of small bubbles form over the area of damage with each upward movement of the specimen? What is the maximum size of these bubbles under the normal test conditions? Can the complete or partial collapse of the bubbles be observed by changing the phase of the light flashes gradually in relation to the movement of the specimen?

The effects of increasing the submergence in the test liquid are rather surprising in degree if not in character. The writer suggests that the increase in damage area with increasing depth is due not to varying air content but to the greater inertia of the greater depth of water surrounding the specimen and supporting tube, which would reduce the rates of vertical and horizontal flow at the periphery of the test surface and allow the pressure over a larger area to drop below the vapor pressure.

With reference to the author's remarks concerning the effect of variation of the amplitude of vibration, it is indicated that tests were made under conditions which showed no pitting on some materials and measurable pitting on others. Has the author been able to determine the amplitude at which pitting begins for the various materials tested? This might give another measure of relative resistance to pitting, possibly bearing a closer relation to the performance under field conditions than the maximum rate of loss.

The author states, "all of these tests indicate that for all welding repairs and all prewelding of hydraulic turbine machinery, two layers of stainless steel should be used and if it is desired to obtain the maximum resistance to pitting, type 301 stainless-steel weld rods should be used." This is a surprising statement considering the excellent results with single-layer 301 stainless, the Ampco bronzes, and stellite.

B. G. Rightmire.[7] The experiments on the effect of amplitude, depth of immersion, and kind of liquid raise a number of interesting questions that the author has discussed qualitatively. In particular, he has suggested that air drawn in from the free surface reduces the damaged area more and more as the depth of immersion decreases. This explanation appears unlikely to the writer, for two reasons: (*a*) The air bubbles, which appear initially under the vibrating specimen, do not continue to form after dissolved gas has been partially removed, as by an extended period of vibration. (*b*) At small depths of immersion the free surface of the liquid near the vibrator is elevated slightly, indicating a mean pressure at the rim of the specimen greater than that at the same depth in the distant liquid.

In the writer's opinion, the flow set up by the vibrator suffices to explain the observed effects of depth of immersion. This flow can be visualized by imagining the vibrating member to be replaced by a pipe which alternately injects and removes liquid. When removing liquid, the pipe acts approximately like a point sink, that is, the flow tends to be radially inward toward the open end of the pipe. On the other hand, when the pipe discharges liquid, a jet is formed, separated by a surface of discontinuity of velocity from the surrounding liquid. The rapid alternation of these two tendencies results in a general circulatory flow exhibiting a high outward velocity along the normal to the vibrating surface, and a low return velocity along the walls of the container, in accordance with the requirements of continuity.

If the depth of immersion is small compared with the diameter of the vibrating member ($^1/_8$-in. immersion), the velocity field of this circulation will be as shown in Fig. 18(*a*) of this discussion. Fig. 18(*b*) shows the velocity field if the depth is large compared with the diameter (2-in. immersion). The chief difference between these two fields is at the rim of the specimen, where the the tendency for separation when the specimen moves upward is obviously greater in Fig. 18(*b*). One would thus expect the damaged area to be greater, the larger the depth of immersion.

Further tests along these fundamental lines can be planned and analyzed more effectively if the independent variables that are suspected to be of greatest importance are listed, and a dimensional analysis made. Thus one may assume here that for a

---

[6] Chief Engineer, Hydraulic Division, Dominion Engineering Works, Ltd., Montreal, Can. Mem. ASME.

[7] Assistant Professor of Mechanical Engineering, Massachusetts Institute of Technology, Cambridge, Mass. Mem. ASME.

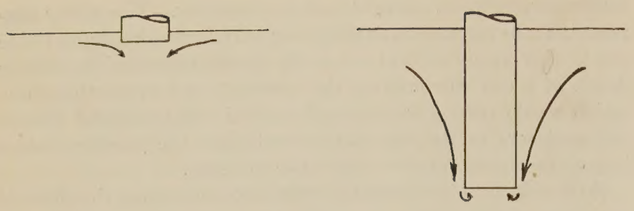

(a) (b)

Fig. 18 Illustrating Effect of Depth of Immersion on Flow Pattern at Specimen

given air content and a given material, the independent variables are as follows:

α = amplitude of vibration, in.
f = frequency of vibration, cps
ρ = density of liquid, lb sec^2/in.^{4}
$p - p_v$ = difference between pressure at specimen and vapor pressure of liquid, psi
ν = kinematic viscosity of liquid, in.^{2}/sec
d = diameter of specimen, in.
h = depth of immersion, in.

The dependent variable may be conveniently taken as the volume loss of the material at the end of a given period of vibration, V. A dimensional analysis shows that one possible arrangement of the variables is

$$\frac{V}{\alpha^3} = \text{function of} \left(\frac{p - p_v}{\rho f^2 \alpha^2}, \frac{f\alpha^2}{\nu}, \frac{d}{\alpha}, \frac{h}{\alpha} \right)$$

Two series of tests probing the effect of the first two dimensionless variables (cavitation number and Reynolds number) were made several years ago at M.I.T. It is hoped that the results will soon be released for publication.

C. G. Southmayd.[8] The test data presented by the author is a welcome supplement to the investigations undertaken by J. M. Mousson and S. Logan Kerr some 12 years ago, in the determination of the resistance of various then available materials to the action of pitting. The advisability of, and necessity for, continual research of this type, particularly in the appraisal of new materials and techniques, cannot be questioned. The fact that it is possible to produce the phenomena of the cavitation in the laboratory, and so closely to parallel field experience is of special interest to the writer. This is particularly so when the apparatus does not in any way attempt to duplicate conditions under which cavitation is encountered in practice and yet affords a means whereby the effect of cavitation can be intensified and the relative resistance of different materials thereto appraised accurately.

For many years it has been suggested that the destructive action of pitting is at least partially due to chemical activity of the gases within the cavities, but the present investigations appear to confirm more recent theories which attribute the destructive action to mechanical forces alone.

In the discussion relative to the effect of the depth of submergence of the specimen in the test liquid, attention is drawn to the tendency for air to be carried down along the side of the test button and prevent the formation of cavities adjacent to the periphery of the specimen. Possibly tests undertaken in a pressurized chamber with constant depths of submergence but variable air pressure above the liquid would maintain a constant pattern of the pitting and so allow the loss of weight determination to give a true index of the benefit attained by increase of pressure at the location of the disturbance.

When tests have been undertaken in the field to appraise the relative resistance of different materials to the destructive forces of cavitation on a single hydraulic turbine runner, it often has appeared that the application of stainless steel to the portions that are most seriously affected has a tendency to shift the position of "the affected area." The apparatus discussed would provide a means whereby it should be possible to apply stainless steel to half of the specimen (a semicircle), and to determine whether or not there is a tendency for a distortion of the pattern of the pitted surface on the parent metal. Probably such is not the case—although the premise is widely held.

In general, the relative resistance of the materials discussed in this paper to the action of cavitation closely corresponds to conditions found during field investigations. The suggestion that "there is a difference in the minimum force required to produce pitting in different materials," is most interesting, and the data supplied in Fig. 6 of the paper explains the apparent inconsistencies of field tests, when in some cases the substitution of rolled stainless steel for cast mild steel entirely eliminates destruction by cavitation in locations where this condition has been quite pronounced and yet in other cases the same stainless steel may be destroyed by this action (although at a considerably lower rate). The relatively small advantage attained by a high surface finish is also worthy of note.

Perhaps one of the greatest contributions is the disclosure of the very pronounced relationship between the resistance of any material to pitting and the hardness of that material. This may account for the wide divergence of much data obtained in the field during tests undertaken on materials of exactly the same chemical composition under comparable operating conditions. The data presented in Fig. 13 are most pertinent.

Wilhelm Spannhake.[9] The consistent tests and their most interesting and practically important results remind the writer of a series of experiments which he initiated at the Technical University of Karlsruhe, Baden, Germany, in 1939. They have been carried through by Dr. Hans Nowotny and were published in 1942.[10] These tests gave similar results for the curves showing the relationship between the loss of weight and the time of exposure of the material to the cavitation attack. However, Nowotny found that the loss of weight distinctly began after a certain "time of incubation," during which no loss of weight could be measured. For instance, with some sort of steel he found that during this incubation time, the material suffered about $6 \cdot 10^6$ hits of collapsing bubbles. He believes that during this time the material changes its properties, especially under the influence of heat created by the numerous blows concentrated on very small areas. He came to the conclusion that it is difficult to establish a general connection between the resistance against cavitation damage and the purely mechanical properties of materials as they are found at room temperature. By the same reason he finds that those high static pressures, which many authors believe to be necessary for an explanation of the cavitation damage, and which they failed to measure by experiments, are actually not necessary.

Nowotny went still further in analyzing the details of the destruction. He applied a very sensitive x-ray method, taking pictures not only of the various samples of material before and after cavitation, but also of the particles broken out of the sample and fished out of the liquid. In this way he found that not only the grain structure was destroyed, but that even the single grains were broken. The grains fished out of the liquid showed a distinct reduction in size.

---

[8] Manager, Hydraulic Division, Canadian Allis-Chalmers Ltd., Lachine, Inc., Canada. Mem. ASME.

[9] Senior Research Scientist, Armour Research Foundation, and Adjunct Professor, Illinois Institute of Technology, Chicago, Ill.

[10] "Destruction of Materials by Cavitation," by Dr. Hans Nowotny (booklet in German), 1942; reprinted by Edwards Brothers, Ann Arbor, Mich., 1946.

These few details out of Nowotny's book have been given in order to demonstrate that the vibratory method is fit not only for practical purposes, but also for a very thorough basic investigation in order to establish a consistent theory of the particular form of wear and tear inherent in the cavitation phenomenon. It might be possible that by means of such a theory we may sometime succeed in "constructing" that material which has the strongest resistance against the cavitation damage.

On the other hand, the writer would recommend not to abandon the other methods of creating cavitation such as that in Venturi tubes or around specially shaped bodies. It is still important to compare the effects of different kinds of cavitation.

At the same time Nowotny made his experiments, the writer succeeded in creating in a high-power Venturi tube with a velocity of 250 fps in the throat, the same primary effects such as discoloring, and the like, after an exposure of the best steel for only 30 sec.

The scientists of both hydrodynamics and metallurgy should combine their efforts to clear this phenomenon of cavitation which has obtained so great an importance since high speeds are being applied more and more in so many fields of modern technique.

Any contribution out of the laboratories of the industry such as the author's should be highly appreciated.

AUTHOR'S CLOSURE

Mr. Baumeister's statement that the accelerated-cavitation method does not give absolute or theoretical values is correct. Up to the present time the test results have all been relative. However, there is a possibility that as our knowledge of the mechanics of cavitation increases, absolute or theoretical results can be obtained. For the time being we have to use the cut-and-try method of selecting materials for highest resistance to pitting.

The author does not agree with the limited definition of cavitation suggested by Mr. Glazebrook. It has been demonstrated experimentally[11] that actual voids or separations can be created in a liquid, and that the threshold of force required to create these voids varies with the gas content of the liquid and other factors. While the author's definition of cavitation could no doubt be improved, it should not be related to the vapor pressure of the liquid nor should it describe the details of some of the resulting phenomena as recommended by Mr. Glazebrook.

Although tests on materials with varying grain size[12] indicate that the finer the grain, the greater the resistance to pitting, there is no definite relationship between the hardness of a material and its grain size. However, fatigue strength is a determining factor in the ability of a material to resist pitting, and since those with a high hardness usually have a high fatigue strength, it may account for the increase in resistance to pitting with increased hardness.

Mr. MacNamee's description of the tests to determine the resistance to erosion of various materials is very interesting. He should have sufficient data to warrant a separate treatise on this subject.

No tests have ever been made to determine the effect of barometric pressure on the rate of pitting. However, there is definite proof that the rate of pitting varies with the temperature of the liquid (1),[13] and it is generally accepted that this variation is due to the change of the vapor pressure with temperature. Therefore it can be assumed that barometric pressure has a similar effect on the rate of pitting.

The results of the tests which were made with different liquids are a further indication of the correlation between the rate of pitting and vapor pressure. These tests are described by the author as having been made with various concentrates of acids, and oils to determine whether the rate of pitting was affected by corrosive liquids. At the time the paper was written there was no good explanation for the results obtained. Recently a calculation was made on the vapor pressure of the liquids used in the tests. Plotting the rate of pitting against the vapor pressure of the liquid showed a definite straight-line relationship. This relationship is similar to the relationship Mousson (1)[13] and Nowotny[10] found in their tests by changing the temperature of the water, Fig. 19, herewith.

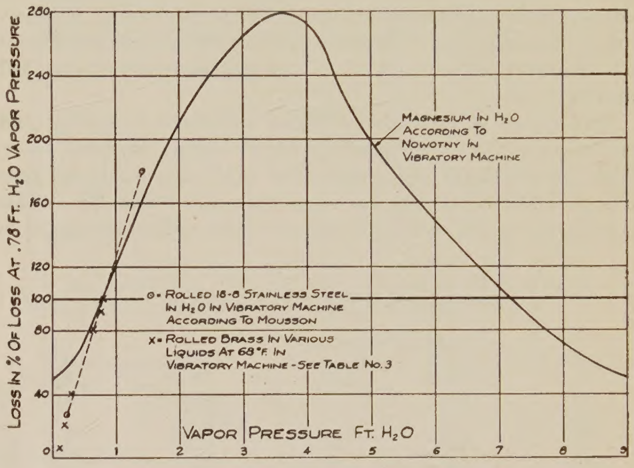

FIG. 19 RELATION BETWEEN VAPOR PRESSURE AND RATE OF PITTING AS MEASURED BY LOSS OF METAL OF TEST SPECIMEN

The experiments by Mousson and the author were confined to the lower temperatures and vapor pressures, whereas Nowotny covered the entire range of temperature of water from freezing to boiling. The author is now conducting experiments with liquids with vapor pressures between 0.2 and 8.0 ft of water for comparison with Nowotny's curve.

The relationship between the rate of pitting and the vapor pressure of various liquids is very significant. It adds to our knowledge as to the nature of cavitation, and also indicates that there is a similarity between the cavitation produced by Mousson with a Venturi-tube type of machine and the cavitation produced with the vibratory machines.

Mr. MacNamee calls attention to the fact that the only hard steels tested were stainless steels. Accelerated-cavitation tests on various alloyed steels were made by both Mousson (1)[13] and Kerr (2)[13] and time did not permit the duplication of all of their tests.

In comparing the relative rate of pitting of stellite to other materials, Mr. Van Patter should take into consideration that there are various types and grades of stellite. The author tested rolled stellite which had shown high resistance to erosion in a special erosion testing machine. Mousson (1)[13] tested both welded stellites and rolled stellites. The welded stellites showed losses from 3.4 to 10.8 cu mm, as compared to 0.9 to 2.8 cu mm for rolled stellites. This showed the large possible variation in the resistance to pitting of this material.

With reference to the formation of vapor bubbles on the test specimen, the stroboscopic light used did not have the high frequency necessary to stop the movement of the specimen, and, therefore, the exact bubble formation could not be observed in detail. The author refers Mr. Van Patter to an article by M. Kornfeld and L. Suvorov,[14] which gives a detailed description of the bubble formation, as observed in connection with a vibratory machine.

---

[11] "Apparatus and Techniques for a Study of Cavitation," by F. G. Blake, Jr., Technical Memorandum no. 12, NR-014-903, Office of Naval Research, Department of the Navy, Washington, D.C.

[12] "Failure of Metal Due to Cavitation Under Experimental Conditions," by H. N. Boetcher, Trans. ASME, vol. 57, 1935, pp. 355–360.

[13] Reference is to author's Bibliography.

No tests have been made to determine at what amplitude pitting begins on various materials. However, this is an interesting subject and is scheduled for future investigation.

The author's statement that two layers of type 301 stainless-steel weld should be used for repairing and prewelding hydraulic turbine machinery, was based largely upon the practical application of weldments. The stellite tested by the author was a rolled plate and not a weldment, and therefore is not particularly suitable for repairs. Welded stellite is not practical because of its cost, and because it is difficult to grind and machine. There is very little information available at the present time on the performance of Ampco bronzes in field installations. Furthermore, the application of Ampco bronze weldments is more difficult and requires greater care than stainless steel and cannot be applied overhead.

Two layers of weld give a higher resistance to pitting and result in a better coverage of the welded surface than one layer. Also the first layer of stainless-steel weld on a mild-steel base has a tendency to become contaminated. Table 20 of this closure shows the chemical analysis of the weldments shown in Table 12 of the paper. This indicates how the use of one layer of weld decreases the chromium content of the weldment. With two layers, the surface of the weldment approaches more closely the chemical composition of the weld rod used.

TABLE 20 CHROME AND NICKEL CONTENT OF STAINLESS-STEEL WELDMENTS[a]

	Type of weld-rod material		Content per cent	
Specimen no.	1st layer of weld	2nd layer of weld	Cr	Ni
203	301	...	12.5	4.9
201	308	...	16.5	7.8
198	309	...	16.9	11.2
204	301	301	15.8	6.5
199	309	308	19.9	10.3
202	308	308	19.6	9.7
200	309	301	19.9	10.3

[a] As shown in Table 12 of paper.

Mr. Rightmire gives a good explanation of the cavitation action at various depths of submergence. It is hoped that the results of the tests to which he refers will be published at an early date.

Mr. Southmayd refers to the tendency for pitting to shift on hydraulic-turbine runners when repairs are made with stainless steel. This can probably be explained by the fact that the material erodes due to fatigue. Repairs are usually made only on the areas that have actually pitted and where the most severe cavitation occurs. However, in the surrounding areas where cavitation is not quite so severe the material has already been weakened due to fatigue and therefore sometimes starts to erode soon after repairs have been made to the other areas.

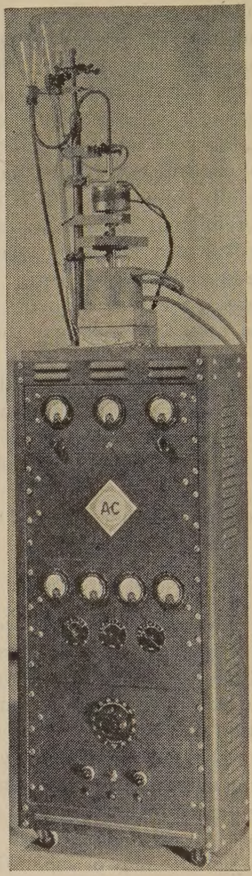

Fig. 20 Accelerated-Cavitation Machine, Vibratory Type, as Arranged for Permanent Use

Mr. Spannhake's reference to Nowotny's experiments is a valuable contribution.

The accelerated-cavitation tests described by the author in the original paper were made with the temporary machine shown in Figs. 2 and 3. Since then this machine has been rebuilt in more permanent form as shown in Fig. 20, herewith.

---

[14] "On the Destructive Action of Cavitation," by M. Kornfeld and L. Suvorov, *Journal of Applied Physics*, vol. 15, 1944, pp. 495-506.